OPTIMISATION OF T CELL RECEPTOR ANTIGEN RECOGNITION FOR TARGETING DISEASE

A Thesis Submitted in Requirement of

Cardiff University for the Degree of Doctor of Philosophy

***

Anna Lissina

2011

School of Medicine

ProQuest LLC
789 East Eisenhower Parkway
P.O. Box 1346
Ann Arbor, MI 48106-1346

To Ivan

ACKNOWLEDGEMENTS

This thesis arose out of 3.5 years of research that I have undertaken since taking up the post of Research Assistant in the T cell modulation group at the Cardiff University School of Medicine. I would like to thank all people who have helped and inspired me during these years. Firstly, I am incredibly grateful to the Wellcome Trust for funding the research documented in this thesis and for making this work possible. I especially would like to thank my supervisor Prof. Andy K. Sewell for offering his guidance and vast knowledge in the area of T cell immunology, whist giving me the opportunity to develop as an independent scientist. I am grateful that despite his hectic schedule of conferences, seminars and grant submission deadlines he was able to find the time to attend to my thesis, at one point sacrificing sleep to proofread four of my thesis chapters within 24 hours of receiving them. His perpetual enthusiasm, passion, and original ideas have inspired me to pursue a career in academic research. I would like to thank Prof. David A. Price for sharing his worldly wisdom encompassing theories on the extraction of true meaning from the patterns of chaos, and for providing me with an alternative perspective on my work. I was also delighted to interact with Dr. Linda Wooldridge, whose friendly leadership, honest advice and readiness to discuss my work is much appreciated. I am grateful to have known Dr. Jonathan Boulter, whom I acknowledge for his help and supervision at the beginning of my studies. Jonathan's contribution to T cell research and his warm personality will be fondly remembered by all his friends and colleagues. I would like to extend my thanks to all my collaborators at Immunocore Ltd, Adaptimmune Ltd, and Immudex Ltd. for allowing me to contribute to some of the most novel and exciting developments occurring in the field of translational immunology today. I have thoroughly enjoyed the work, our discussions and of course the unexpected delivery of chocolates. A big thank you to the members of my lab for providing a fun and friendly atmosphere to work in, and I apologise that the fact that the group has grown so tremendously in the past year prevents me from mentioning them personally one by one. I am also very grateful to everyone within the department of Infection, Immunity and Biochemistry, who has been important to the realisation of this thesis. I have thoroughly enjoyed my time working in the 'blue palace', home to many talented individuals and valued friends. I would like to express a special thank you to my mum and dad for nurturing my interest in science from a very young age, for their support and encouragement, and for giving me the opportunities that I would not have had growing up in post-Soviet Russia. A 'bigger than words' thank you to my brother Ivan, who has been my greatest inspiration and who, despite his short life, has taught me a great deal about its richness and meaning. Finally, I would like to thank my boyfriend Simon for getting me away from the lab bench in search of adventure, to prevent me from turning into a complete science geek.

PREFACE

This thesis is a collection of some of the studies I have undertaken over the last 3.5 years while working as a Research Assistant in the T cell modulation group at the Cardiff University School of Medicine. The work contained within is linked by the common theme of optimising interactions between peptide-Major Histocompatibility (pMHC) molecules, the T cell receptor (TCR), and/or coreceptor that engages these ligands. The work of the T cell modulation group is heavily focused on translational medicine. This aspect of biomedicine is also strongly encouraged by my funding body, the Wellcome Trust. My focus on translational aspects of interactions with pMHC ligands took my work in several different directions. Initially, I examined ways of improving interactions with pMHC that could be used to ameliorate the detection of antigen-specific T cells by flow cytometry. My studies have improved this technology to a point where I can now reliably claim to be able to stain the majority of relevant T cells with their cognate multimeric antigen. The approaches I helped pioneer are now in use all over the world. This work is reported in Chapters 3 and 5, and has resulted in two published primary data papers. A third paper that examines pMHC multimer valency (described in Chapter 4) is in preparation. In addition to the above-mentioned work aimed at improving T cell-related diagnostics using pMHC multimers, I also explored potential ways of improving TCR/pMHC interactions for therapeutic approaches. Specifically, I was interested in exploring whether TCRs displaying enhanced affinities for antigen would be useful in the clinic. These studies necessitated that we establish optimal TCR gene transfer protocols in Cardiff. I took the lead on these optimisation studies (Chapter 6). With the TCR gene transfer technology optimised, I was able to investigate whether increasing functional avidity of TCR-redirected T cells could be achieved by removing defined N-glycosylation sites within the TCR constant domain. This work was based on my observation that the desialylation of T cells improved the surface engagement of pMHC multimers and the recognition of cognate antigen when displayed naturally on a target cell surface. These studies were taken forward in Chapter 7. As part of my work with affinity enhanced TCRs, I was fortunate to test a novel set of TCR-based soluble therapeutic reagents comprising affinity-enhanced TCRs (Chapter 8). The enhanced TCRs were generated by phage display and directed evolution using techniques that were pioneered by my T cell modulation group colleague Jonathan Boulter while working at Avidex Ltd.

DECLARATION

This work has not previously been accepted in substance for any degree and is not concurrently submitted in candidature for any degree.

Signed ..... (candidate) Date 18/08/11

Statement 1:

This thesis is being submitted in partial fulfilment of the requirements for the degree of PhD.

Signed ..... (candidate) Date 18/08/11

Statement 2:

This thesis is the result of my own independent work/investigation, except where otherwise stated. Other sources are acknowledged by explicit references.

Signed ..... (candidate) Date 18/08/11

Statement 3:

I hereby give consent for my thesis, if accepted, to be available for photocopying and for inter-library loan, and for the title and summary to be made available to outside organisations.

Signed ..... (candidate) Date 18/08/11

TABLE OF CONTENTS

ABSTRACT

αβ T cells are some of the most important cells in our bodies as they: (i) orchestrate immunity and are key elements in the control of infection; (ii) are important for the natural eradication of cancer; (iii) hold the key to successful vaccination; (iv) are an important factor in transplant rejection; (v) cause all autoimmune diseases; and, (iv) mediate many allergic reactions. Consequently, T cells sit at the heart of most human pathologies and it is very important that we understand how these pivotal cells operate. αβ T cells recognise short 'foreign' peptides bound to major histocompatibility complex (MHC) molecules; the antigen specificity of T cells is conferred by the highly variable complementarity determining regions (CDRs) of the αβ T cell receptor (TCR) that interact with the peptide-binding platform of the MHC. The CD8 and CD4 glycoproteins on the T cell surface also act as receptors for pMHC class I and II, respectively in concert with the TCR. CD8 and CD4 and have been termed 'coreceptors' to reflect this role. The pivotal role T cells play in pathogen protection, cancer immunity and autoimmunity has ensured that there is a huge interest in the detection, understanding and manipulation of antigen-specific T cells. Recent advances using fluorochrome-conjugated multimeric pMHC molecules in conjunction with flow cytometry have revolutionised the study of antigen-specific T cells by enabling direct visualisation, enumeration, phenotyping and clonotyping of these important cells. In the decade since their initial description such multimeric pMHC molecules have been used in over 7000 published studies and there are now half a dozen commercial enterprises aimed at manufacturing such reagents. My laboratory has described that pMHC multimer staining and the sensitivity of T cells to antigen density are dependent on TCR/pMHC affinity. We have also shown that the interaction affinity required for good pMHC multimer staining can be substantially higher than that required for T cell activation. As a result, current technology does not detect all T cells that can respond to a particular pMHC antigen. This failure represents a significant problem for the detection of anti-cancer and autoimmune T cells which tend to have weaker binding TCRs. In this thesis I describe how the physical detection of T cells with low affinity TCRs can be improved by: (i) enhancing coreceptor binding; (ii) enhancing the valency of pMHC and fluorochrome within pMHC multimers by using a larger multimerization scaffold; and, (iii) the use of the protein tyrosine kinase inhibitor (PKI) dasatinib. These 'tricks' can all be used to detect and isolate antigen-specific T cells that remain undetected by current technologies. I also examine several possibilities for enhancing TCR recognition. First, I optimise a system for stable TCR expression in primary $CD8^+$ T lymphocytes (Chapter 6). Second, I show that the antigen-sensitivity of $CD8^+$ T cells can also be enhanced by the removal of surface sialic acid residues from the sugars that coat glycoproteins on the surface of all mammalian T cells, and I explore this effect in more detail by examining whether the removal of particular N-glycosylation sites on an αβ TCR accounts for the increase in antigen sensitivity observed. Finally, I experiment with a means of using soluble TCRs to redirect lysis by polyclonal $CD8^+$ T cells using TCR-anti-CD3 fusion constructs called Immune mobilising monoclonal TCRs Against Cancer/Virus (ImmTAC/Vs). In summary, my results have uncovered several important 'tricks' for improved physical detection of T cells and these methodologies are already being employed by numerous research laboratories across the globe to identify and characterise antigen-specific T cell responses. Furthermore, I have also shown that enhanced affinity TCRs might provide effective therapeutic reagents either when transferred into recipient host T cells by gene transfer or when used as soluble molecules to recruit polyclonal T cell populations.

ABBREVIATIONS

General

Abs	Antibodies
ACT	Adoptive T Cell Therapy
ALL	Acute lymphoblastic leukaemia
APC	Antigen presenting cell
APL	Altered peptide ligand
7-AAD	7-Aminoactinomycin D
B_2m	B_2 microglobulin
BCR	B cell receptor
CD (number)	Clusters of Differentiation (number)
CML	Chronic myeloid leukaemia
CMV	Cytomegalovirus
CTL	Cytotoxic T lymphocyte
cPPT	central Polypurine tract
DNA	Deoxyribonucleic acid
DTT	Dithiothreitol
EBV	Epstein-Barr Virus
ELISA	Enzyme linked immunosorbent assay
ELISpot	Enzyme linked immunospot
E:T	Effector cell: Target cell
FACS	Fluorescence activated cell sorter/ing
FATAL	Fluorometric Assessment of T lymphocyte Antigen-specific Lysis
FCS	Foetal calf serum
FPLC	Fast protein liquid chromatography
GFP	Green Fluorescent Protein
GOI	Gene of Interest
HAART	Highly Active Anti-Retroviral Therapy
HIV-1	Human Immunodeficiency Virus Type-1
HLA	Human Leukocyte Antigen
HLA A2	HLA A*0201
IFNγ	Interferon gamma

Ig	Immunoglobulin
IL	Interleukin
ImmTAC	Immune mobilising monoclonal TCRs Against Cancer
ImmTAV	Immune mobolising monoclonal TCRs Against Viruses
IPTG	Isopropyl-1-thio-β-D-galactopyranoside
IRES	Internal Ribosome Entry Site
IVT	*In Vitro* Transcribed
K_D	Dissociation constant
KD	Kilodalton
LTR	Long Terminal Repeats
LPS	Lipopolysaccharide
MAGE	Melanoma-associated antigen
MHC	Major Histocompatibility Complex Class I
MIP-1β	Macrophage Inflammatory Protein-1β
MOI	Multiplicity of Infection
mRNA	messenger Ribonucleic acid
NK cells	Natural killer cells
OD	Optical density
ORF	Open Reading Frame
PBL	Peripheral blood lymphocytes
PBMC	Peripheral blood mononuclear cells
PBS	Phosphate buffered saline
PCR	Polymerase chain reaction
PHA	Phytohaemagglutinin
PNA	Peanut Agglutinin
PPI	Preproinsulin
PTK	Protein tyrosine kinase
PTKI	Protein tyrosine kinase inhibitor
pMHCI	peptide Major Histocompatibility Complex Class I
pMHCII	peptide Major Histocompatibility Complex Class II
RANTES	Regulated on Activation, Normal T Expressed and Secreted
RCR	Replication Competent Retrovirus
SDS-PAGE	Sodium Dodecyl Sulphate-Polyacrylamide Gel Electrophoresis

SFFV	Spleen Focus Forming Virus
SIN	Self-Inactivating (vector)
SIV	Simian Immunodeficiency Virus
SPR	Surface Plasmon Resonance
TAA	Tumour-Associated Antigen
TAP	Transporter associated with Antigen Processing
TCR	T Cell Receptor
TGF	Transforming Growth Factor
Th1	Type I helper T cells
Th2	Type II helper T cells
TNF	Tumour Necrosis Factor
WPRE	Woodchuck hepatitis virus Post-transcriptional Regulatory Element
WT-1	Wilms' Tumour antigen 1

Fluorochromes

APC	Allophycocyanin
APC-Cy7	Allophycocyanin Cychrome-7
FITC	Fluorescein isothiocyanate
PB	Pacific Blue
PE	Phycoerythrin
PE-Cy7	Phycoerythrin Cychrome-7
PerCP	Peridinin Chlorophyll Protein

Signal transduction components

ITAM	Immunoglobulin receptor family Tyrosine based Activation Motif
LAT	Linker for Activation of T cells
Lck	Lymphocyte specific protein tyrosine kinase
PI3K	Phosphatidylinositol-3-Kinase
PKC	Protein Kinase C
PTK	Protein Tyrosine Kinase
PTKI	Protein Tyrosine Kinase Inhibitor
SH	Src Homology domain
SMACs	Supramolecular activation clusters

ZAP-70	Zeta Associated Protein of 70 KD

Amino Acids

A	Ala	Alanine
C	Cys	Cysteine
D	Asp	Aspartic acid
E	Glu	Glutamic acid
F	Phe	Phenylalanine
G	Gly	Glycine
H	His	Histidine
I	Ile	Isoleucine
K	Lys	Lysine
L	Leu	Leucine
M	Met	Methionine
N	Asn	Asparagine
P	Pro	Proline
Q	Gln	Glutamine
R	Arg	Arginine
S	Ser	Serine
T	Thr	Threonine
V	Val	Valine
W	Trp	Tryptophan
Y	Tyr	Tyrosine

PUBLICATIONS

Publication resulting from the work in this thesis

Wooldridge L, Lissina A, Vernazza J, Gostick E, Laugel B, Hutchinson SL, Mirza F, Dunbar PR, Boulter JM, Glick M, Cerundolo V, van den Berg HA, Price DA, Sewell AK. 2007. Enhanced immunogenicity of CTL antigens through mutation of the CD8 binding MHC class I invariant region. *European Journal of Immunology* 37, pp. 1323-33.

Melenhorst JJ, Scheinberg P, Chattopadhyay PK, Lissina A, Gostick E, Cole DK, Wooldridge L, van den Berg HA, Bornstein E, Hensel NF, Douek DC, Roederer M, Sewell AK, Barrett AJ, Price DA. 2008. Detection of low avidity $CD8^+$ T cell populations with coreceptor-enhanced peptide-major histocompatibility complex class I tetramers. *Journal of Immunological Methods* 338, pp. 31-9.

Lissina A, Ladell K, Skowera A, Clement M, Edwards E, Seggewiss R, van den Berg HA, Gostick E, Gallagher K, Jones E, Melenhorst JJ, Godkin AJ, Peakman M, Price DA, Sewell AK, Wooldridge L. 2009. Protein kinase inhibitors substantially improve the physical detection of T-cells with peptide-MHC tetramers. *Journal of Immunological Methods* 340, pp. 11-24.

Lissina A, Wooldridge L, Cole DK, van den Berg HA, Price DA, Sewell AK. 2009. Tricks with tetramers: how to get the most from multimeric peptide-MHC. *Immunology* 126, pp. 147-64.

Liddy N, Bossi G, Adams KJ, Lissina A, Mahon TM, Hassan NJ, Gavarret J, Bianchi FC, Pumphrey NJ, Ladell K, Gostick E, Sewell AK, Lissin NM, Harwood NE, Molloy PE, Li Y, Cameron BJ, Sami M, Baston EE, Todorov PT, Paston SJ, Dennis RE, Dunn SM, Ashfield R, Johnson A, McGrath Y, Price DA, Vuidepot A, Williams DD, Sutton DH, Jakobsen BK. Monoclonal TCR-redirected tumour cell killing. *(manuscript accepted for publication at Nature Medicine).*

Lissina A, Dalton G, et al. Detection of low-avidity $CD8^+$ T cells with peptide-MHC dextramers. *(manuscript in preparation)*

Lissina A et al. T cell desialylation as a tool for increasing pMHC multimer-mediated detection of T cells. *(manuscript in preparation)*

Other co-authored publications from my laboratory

Choi EM, Chen JL, Wooldridge L, Salio M, Lissina A, Lissin N, Hermans IF, Silk JD, Mirza F, Palmowski MJ, Dunbar PR, Jakobsen BK, Sewell AK, Cerundolo V. 2003. High avidity antigen-specific CTL identified by CD8-independent tetramer staining. *Journal of Immunology* 171, pp. 5116-23.

Wooldridge L, Hutchinson SL, Choi EM, Lissina A, Jones E, Mirza F, Dunbar PR, Price DA, Cerundolo V, Sewell AK. 2003. Anti-CD8 antibodies can inhibit or enhance peptide-MHC class I (pMHCI) multimer binding: this is paralleled by their effects on CTL activation and occurs in the absence of an interaction between pMHCI and CD8 on the cell surface. *Journal of Immunology* 171, pp. 6650-60.

Green AE, Lissina A, Hutchinson SL, Hewitt RE, Temple B, James D, Boulter JM, Price DA, Sewell AK. 2004. Recognition of non-peptide antigens by human V gamma 9V delta 2 T cells requires contact with cells of human origin. *Clinical Experimental Immunology* 136, pp. 472-82.

Hewitt RE, Lissina A, Green AE, Slay ES, Price DA, Sewell AK. 2005. The bisphosphonate acute phase response: rapid and copious production of proinflammatory cytokines by peripheral blood γδ T cells in response to aminobisphosphonates is inhibited by statins. *Clinical Experimental Immunology* 139, pp. 101-11.

Gostick E, Cole DK, Hutchinson SL, Wooldridge L, Tafuro S, Laugel B, Lissina A, Oxenius A, Boulter JM, Price DA, Sewell AK. 2007. Functional and biophysical characterization of an HLA-A*6801-restricted HIV-specific T cell receptor. *European Journal of Immunology* 37, pp. 479-86.

Wooldridge L, Clement M, Lissina A, Edwards ES, Ladell K, Ekeruche J, Hewitt RE, Laugel B, Gostick E, Cole DK, Debets R, Berrevoets C, Miles JJ, Burrows SR, Price DA, Sewell AK. 2010. MHC class I molecules with Superenhanced CD8 binding properties bypass the requirement for cognate TCR recognition and non-specifically activate CTLs. *Journal of Immunology* 184(7), pp. 3357-66.

Chapter 1

1

INTRODUCTION

Summary

The work contained within this thesis is linked by the common theme of optimising interactions between peptide-Major Histocompatibility complex (pMHC) molecules and the T cell receptor (TCR) and/or coreceptor that engages them. I explore several different translational aspects that touch on a wide range of biomedical topics. I will begin by providing an overview of the mammalian immune system with special emphasis on human T cells and the molecular interactions they use to detect, and remove, threats to the host. In later chapters I will examine how enhanced interactions with pMHC molecules can be used to improve the physical detection of T cell using fluorochrome-conjugated antigens in conjunction with modern polychromatic flow cytometry. I will therefore introduce this technology in this general introduction. Later chapters also examine methodologies for using enhanced TCRs in therapeutic strategies for curing viral disease and cancer. I will introduce these aspect here by examining the role T cells play in clearing the body of infected or dysregulated cells. Finally, I will put my own studies in context by reviewing the current strategies that are in use for harnessing T cells for therapeutic benefit before introducing the aims of the research work I have undertaken as part of my PhD studies.

1.1 Overview of the immune system

Mammals live in a world inhabited by a multitude of pathogenic organisms which are constantly evolving. In order to protect themselves, they rely on a highly sophisticated immune system, that itself evolves to keep pace with the pathogens that threaten the host organism's existence. A fundamental feature of the immune system is its ability to detect structural aspects of the pathogen that distinguishes it from host tissues. The level of discrimination is fine-tuned to eliminate the threat of toxicity without causing damage to the host tissues the immune system serves to protect. In order to deal with the vast number and sophisticated evasion mechanisms displayed by pathogens and their toxins, the immune system employs a division of labour between two types of immune response: innate and adaptive. The innate branch of the immune system is a hard-wired response encoded by genes in the host's germline that specialise in the recognition of molecular

patterns that are a common feature of many microbes and other host-invading organisms (Fraser et al. 1998; Janeway and Medzhitov 2002). Although the innate branch of the immune system is relatively inflexible in terms of the number of pathogenic organisms it can respond to, it has the advantage of acting rapidly once a potentially harmful object is encountered. The fast action of the response is attributed to the broad expression of pattern recognition molecules on a large number of cells. The key players in the innate immune response are phagocytic cells (monocytes, macrophages, and neutrophils), cells that release inflammatory mediators (eosinophils and basophils), natural killer cells and molecular components such as complement (Delves and Roitt 2000a; Delves and Roitt 2000b; Janeway and Medzhitov 2002). The components of the adaptive immune response are encoded by gene elements capable of undergoing somatic rearrangements to generate a vast repertoire of antigen-binding molecules greatly exceeding the number of primitive pattern recognition receptors (PRRs) produced by the innate immune system.

The adaptive immune response relies on B and T lymphocytes, which mediate the humoral (soluble) and cellular arms of the response, respectively (Delves and Roitt 2000a; Delves and Roitt 2000b). Unlike the germline-encoded recognition molecules of the innate immune response, the antigen-specific receptors of the adaptive immune response are encoded by somatically-rearranged gene elements that make up T cell receptor (TCR, of two types: αβ and γδ) and immunoglobulin; Ig (B cell receptor, BCR) genes. It is estimated that the human adaptive immune response is capable of generating approximately 10^{14} BCRs, 10^{18} αβ TCRs and 10^{20} γδ TCRs (Davis and Bjorkman 1988; Venturi et al. 2008). Since each B and T cell expresses a potentially unique antigen recognition receptor (BCR or TCR, respectively), the proportion of cells specific for a particular antigen at any given time is very small. As a consequence, the responding lymphocytes must undergo expansion to reach sufficient numbers before an effective attack on the pathogen is initiated. This need to proliferate explains why the adaptive response takes longer to come into effect than the innate response. Another important feature of the adaptive immune response is 'immunological memory', whereby lymphocytes that have previously encountered antigen enter into an apparently dormant state in which the cells can persist until they are re-challenged with

antigen. These 'memory cells' retain immune memory of a particular antigen for years even decades after their initial encounter (Obar and Lefrancois 2010b). Consequently, memory cells are capable of eliciting a rapid response on repeated encounters with the same antigen. Although, the innate and adaptive branches of the immune response are often seen as completely separate entities, they complement each other; with the innate response acting as the first line of defence allowing the cells of the adaptive response to clonally expand and take over the fight against infection once sufficient numbers of cells have been reached a few days later. The interplay between aspects of the innate and adaptive braches of the immune response is essential in an effective immune system.

1.2 T cell development and selection

In order to recognise the vast universe of pathogenic antigens, T cells must be equipped with a diverse repertoire of TCRs. This incredible level of diversity (up to 10^{18} possible human TCRs) is achieved through the somatic rearrangement of gene elements encoding TCR alpha and beta chains, which are designated: variable (V), diversity (D), and joining (J) gene elements (Schatz et al. 1992). The TCR alpha chain is assembled from V_α J_α, whilst the beta chain comprises all three types of element $V_\beta D_\beta J_\beta$ (Bonilla and Oettgen 2010). Because the segments are rearranged randomly, millions of different TCR specificities are generated, with additional diversity provided by the enzyme terminal deoxynucleotidyl transferase (TdT) which adds additional deoxynucleotides into certain VDJ junctions (Nguyen et al. 2007). Due to its random nature, this process is also responsible for the generation of non-functional TCRs, in addition to TCRs with specificities directed against self-antigens. The selection of T cells carrying only functional and non-autoaggressive TCRs takes place in the thymus (Godfrey et al. 1993). This complex lymphoid organ is subdivided into three compartments, each with a distinct role:

i) Subcapsular zone: The site where immature bone marrow-derived pro-thymocytes proliferate, differentiate, and rearrange their TCR β chains.

ii) Thymic cortex: The site where TCR α chain rearrangement takes place, and the incorporation of some of these α chains into αβ TCRs. The mature αβ TCRs are subsequently tested for functionality through their recognition of self-MHC molecules presented by the cortical epithelium in a process called positive selection (Nitta et al. 2008).

iii) Thymic medulla: The site where mature T thymocytes are screened for autoreactivity, by subjecting their TCRs to an extensive array of self-antigens expressed on specialised thymic medullary epithelial cells. This process is called negative selection.

Thymocytes capable of recognising self MHC molecules progress from the thymic cortex to the medulla (positive selection), whilst those that fail to do so die by neglect. In the thymic medulla, thymocytes that recognise self-antigen with affinities greater than a set threshold undergo deletion by apoptosis (negative selection), and the surviving cells exit into the periphery (Savage and Davis 2001). The stringent selection process ensures that only ~5% of developing T cells are permitted to enter circulation, and those that make it display very weak/ intermediate affinities for self-antigen (Sebzda et al. 1999).

1.3 T cell antigen recognition and effector function

T cells are a major player in the adaptive arm of the immune response. There are two subsets of T cells; αβ and γδ T cells. The majority of human T cells in the periphery express the αβ TCR on their surface. The αβ TCR mediates recognition of short peptide fragments processed within cells and presented on their surface in association with Major Histocompatibility Complex (MHC) molecules (Davis et al. 1998). This requirement for the T cell to recognise antigenic peptides only in the context of MHC molecules permits the T cell to ignore free extracellular antigen, shifting its focus on to the recognition of infected or cancerous cells. There are two classes of MHC molecules; Whereas MHC class I (MHCI) molecules are expressed on all nucleated cells, MHC class II (MHCII) are only expressed by 'professional' antigen presenting cells (APC) such as macrophages, dendritic cells (DCs), B cells, and activated human (but not murine) αβ and γδ T cells. Peptides presented on MHCI

molecules are derived from cytosolic degradation of all the proteins within the cell, permitting the recognition of aberrant proteins as found in virally-infected or malignantly-transformed cells (Janeway 2001). MHCI-associated peptides are typically 8-11 amino acids in length. MHCII-restricted peptides are longer, varying between 13 and 17 amino acids in length, although shorter or longer lengths are not uncommon (Chicz et al. 1992; Sercarz and Maverakis 2003). MHCII-associated peptides are derived from lysosomal degradation of proteins ingested outside the cell (e.g. phagocytosed bacteria).

The differing nature of the two MHC structures and their associated peptides lends itself to recognition by two functionally distinct classes of αβ T cells: $CD8^+$ T cells and $CD4^+$ T cells. The nomenclature and function of $CD8^+$ T cells and $CD4^+$ T cells arises from the type of coreceptor they express in conjunction with their TCR: CD8, and CD4, respectively. The coreceptors CD8 and CD4 are cell surface glycoproteins, which are associated closely with the TCR on the surface of a T cell. The main function of CD8 and CD4 is thought to be enhancing T cell signalling by contacting MHC molecules and by interacting with cytosolic components of the TCR signalling machinery. Peptide-MHCI (pMHCI) is recognised by $CD8^+$ cytotoxic T lymphocytes or 'killer' T cells, which as their name suggests posses the cytotoxic activity to kill infected or neoplastic cells. They do this by releasing a number of cytolytic enzymes such as granzymes (proteases that remain sequestered in lytic granules), and soluble factors such as tumour necrosis factor (TNF), interferon-γ (IFN-γ), and macrophage inflammatory protein 1β (MIP-1β) with wide-ranging anti-pathogenic effects (Kagi et al. 1996; Lieberman 2003). pMHCII molecules are recognised by $CD4^+$ T helper (Th) cells.

1.4 Molecular mechanisms of T cell recognition

1.4.1 MHCI and MHCII structures and antigen processing

The human MHC, designated Human Leukocyte Antigen (HLA), is encoded on the short arm of chromosome 6. HLA class I molecules (designated HLA-A, -B, and -C) are cell-surface heterodimeric glycoproteins consisting of a polymorphic transmembrane α-chain (or class I heavy chain) which is subdivided into α_1, α_2, and α_3 domains and is non-covalently associated

with an invariable β_2-microglobulin (β_2m) (Bjorkman 1997). The α_1, α_2, and α_3 domains come together to form a binding groove for the antigenic peptide that is closed at both ends, allowing for some 'bulging' of the peptide in the middle of the groove. The α_3 domain of the HLA class I heavy chain interacts with the CD8 coreceptor on $CD8^+$ T cells. The composite structure of peptide and MHCI is the target of the MHCI-restricted αβ TCR on the surface of $CD8^+$ T cells (Figure 1.1 A), in a phenomenon called 'MHC restriction' (Zinkernagel and Doherty 1997).

As for HLA class I molecules, there are three classes of HLA class II molecules designated HLA-DR, HLA-DQ, and HLA-DP (Bjorkman 1997). The HLA class II molecule is a complex formed from the non-covalent association of an α and a β domain (instead of the β_2m subunit as in HLA class I), and unlike β_2m both chains span the membrane. Both the α and β chains contain a short cytoplasmic tail, a transmembrane region, and two extracellular domains; α_1 and α_2 for the alpha chain, and β_1 and β_2 for the beta chain. The α_1 and β_1 come together to form the peptide binding groove, not dissimilar in structure from the MHCI α_1-α_2 arrangement (Bjorkman 1997). The α_2 and β_2 subunits provide support for the peptide binding groove, whist the β_2 domain also forms the point of contact for the CD4 coreceptor. The interaction of pMHCII molecules with the CD4 coreceptor restricts pMHCII recognition to $CD4^+$ T helper cells (Figure 1.1 B and (Konig et al. 1996)).

1.4.1a MHCI antigen presentation: endogenous pathway

The process by which intracellular proteins are degraded into peptides suitable for presentation in the context of MHCI molecules is referred to as the MHCI antigen processing pathway. The molecular machinery that generates these endogenous peptide antigens and delivers the peptide-MHCI molecules to the cell surface is outlined in Figure 1.2 A. Essentially, peptide fragments are generated from cellular proteins through the action of a proteolytic machine composed of >25 subunits called the proteasome (Niedermann 2002). The proteasome is constitutively expressed in all cells, where its main role is the degradation of proteins as part of normal cellular homeostasis. However, if a pathogenic threat is detected, release of IFNγ by cells such as macrophages signals a transformation of

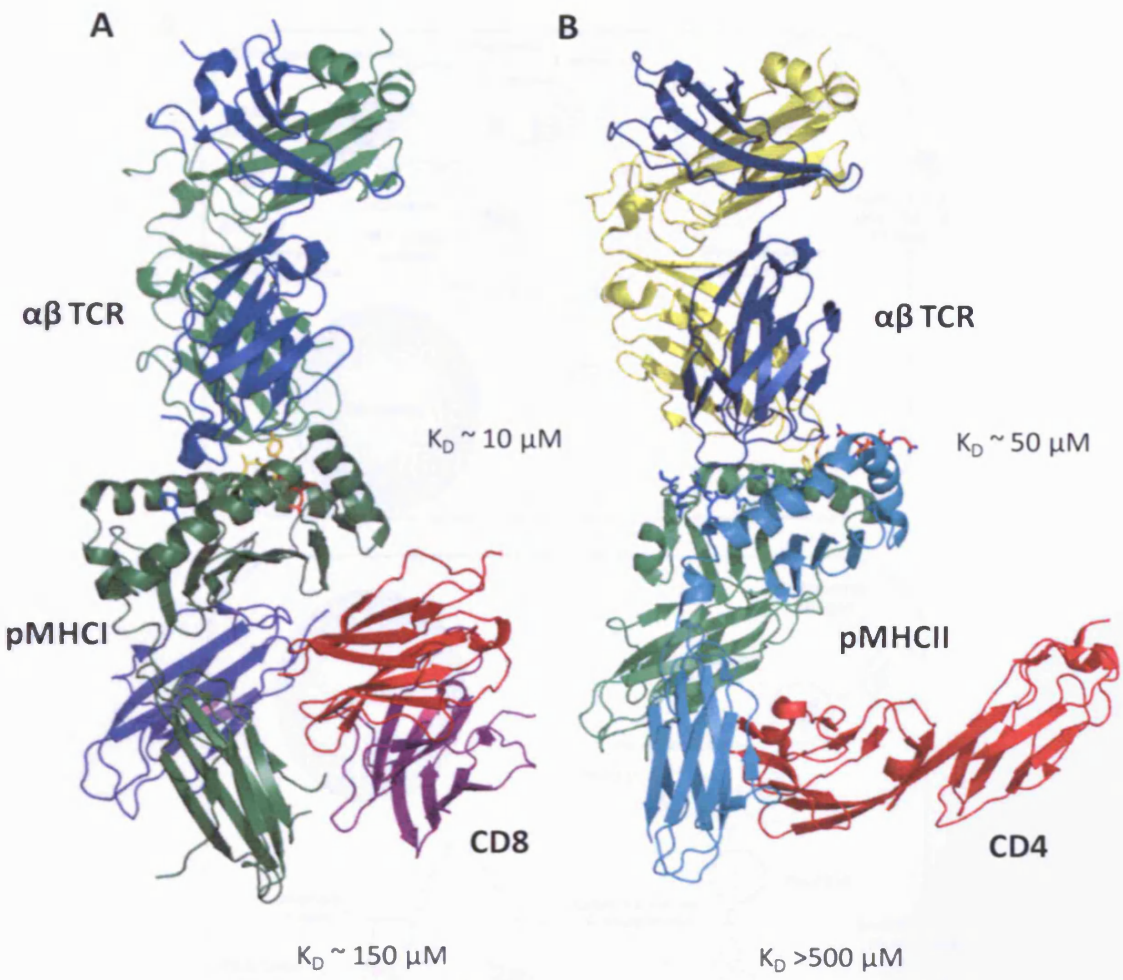

Figure 1.1: The TCR/pMHCI/CD8 and TCR/pMHCII/CD4 interactions. Ribbon diagram representations of crystal structures of αβ TCR/pMHCI/CD8 (**A**) and αβ TCR/pMHCII/CD4 (**B**) complexes. Three dimensional dissociation constants (K_D values) for the TCR/pMHC and the pMHC/coreceptor interactions are indicated. Importantly, the TCR/pMHCII interaction is ~5 fold weaker than the TCR/pMHCI interaction, and pMHCII/CD4 binding is substantially weaker than pMHCI/CD8 association. (Structures kindly provided by D. Cole).

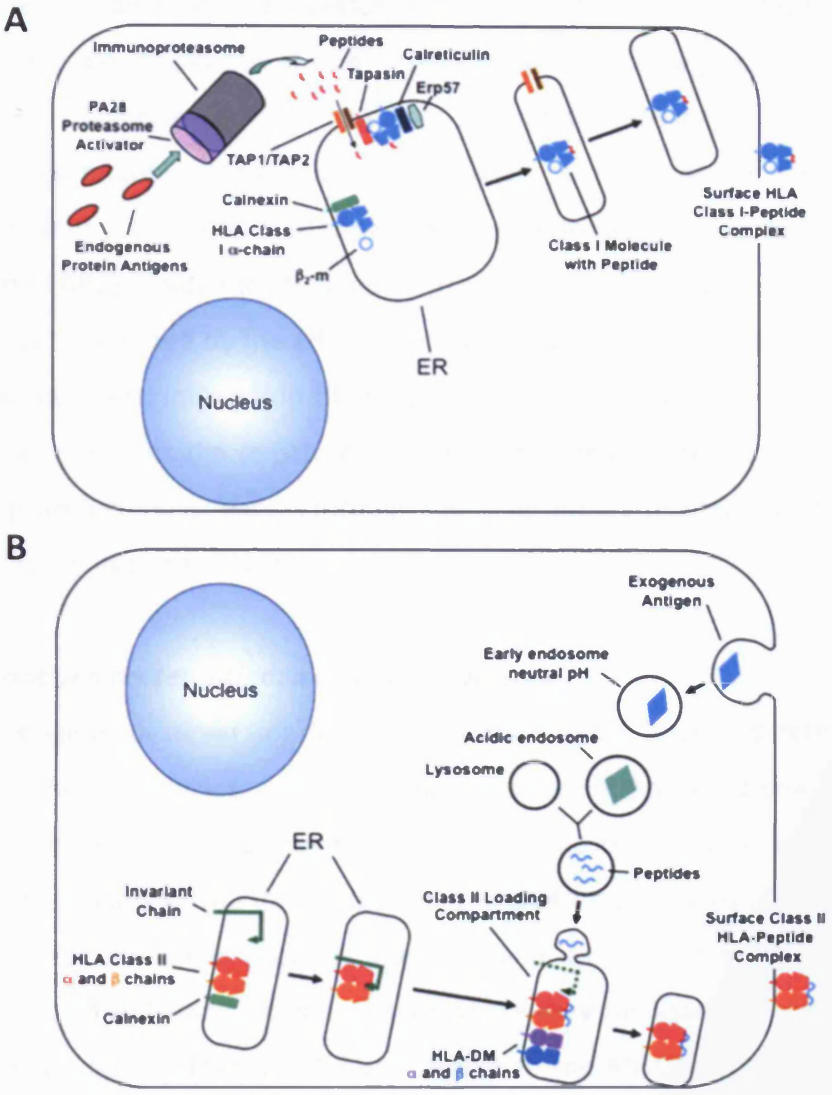

Figure 1.2: T cell antigen presentation pathways. A. Cellular pathway for the processing of endogenous antigens. Antigenic proteins found within the cell are degraded into peptides by the immunoproteasome and transported into the endoplasmic reticulum (ER) by the transporter associated with antigen processing (TAP 1 and 2). Some of these peptides can bind to MHC class I molecules and are transported to the cell surface for immune surveillance by the TCRs of $CD8^+$ T cells. **B.** Cellular pathway for the processing of exogenous antigens. Proteins from outside the cell are taken up by phagocytosis or endocytosis and are degraded into peptides by the action of enzymes and the acidic environment of fusion with lysosomes. Merging of antigen peptide and MHC II -containing compartments and the removal of the invariant chain (Ii) from the MHC II allows binding of peptides, before upregulation to the cell surface for presentation to $CD4^+$ T cells. (Figure adapted from Chaplin 2010).

the proteasome into an immunoproteasome. The role of the immunoproteasome is the production of peptide fragments of appropriate length and charge for binding into the groove of MHCI molecules. On exiting the (immuno)proteasome, the peptides are transported to the endoplasmic reticulum (ER), aided by a transporter composed of two ATP-binding cassette subunits termed the transporter associated with antigen processing 1 and 2 (TAP1 and TAP2). Inside the ER, loading of peptide into the peptide-binding groove of MHCI heavy chain is assisted by the ER protein tapasin with the help of chaperone proteins calreticulin and calnexin. Interaction of the β_2m subunit with peptide-MHCI heavy chain-calnexin complex stabilises the structure and causes the chaperone calnexin to dissociate. The complete pMHCI complex passes through the Golgi apparatus before being transported to the cell surface in exocytic vesicles.

1.4.1b MHCII antigen presentation: exogenous pathway

Extracellular antigens destined for MHCII presentation are imported into the cell for processing in endocytic vehicles, and include proteins derived from bacteria, viral particles, allergens and environmental proteins. Fusion of endosomes with lysosomes causes acidification, which leads to the degradation of the captured proteins (Turley et al. 2000). Once MHCII molecules have been synthesised and assembled in the ER, they are transported to the MHCII loading compartment where they can associate with the peptides generated in acidic late endosomes. To gain access to the MHCII peptide-binding groove, peptides must displace the invariant chain (Ii) that shields the groove. The acidic environment inside the MHCII loading compartment leads to the partial degradation of Ii, and the remaining peptide fragment is exchanged for antigenic peptides with the help of the HLA-DM molecule, which itself is structurally related to MHCII (Sadegh-Nasseri et al. 2008). The complete pMHCII molecules are transported to the cell surface in endosomes. The steps of the exogenous presentation pathway are summarised in Figure 1.2 B.

1.4.1c Cross-presentation

Although the processing of antigen for MHCI and MHCII presentation was thought to occur by the two distinct pathways described above, recent studies have shown that under

certain circumstances antigen from outside the cell can also be presented on MHCI molecules. This phenomenon is designated cross-presentation, and plays an important role in antiviral immunity whereby viral escape mechanisms can inhibit aspects of the endogenous pathway of antigen presentation (Sigal et al. 1999).

1.4.2 TCR/pMHC/CD8 (or CD4)

1.4.2a The TCR/pMHC interaction

Recognition of pMHC complexes by T cells is mediated by the TCR. This cell surface structure is composed of an α and a β chain linked covalently by a disulphide bridge (van der Merwe and Davis 2003). Each chain is subdivided into four regions: a membrane-distal variable region (Vα or Vβ), and a membrane-proximal immunoglobulin-like constant region (Cα or Cβ), a transmembrane region, and a short cytoplasmic region. The TCR Vα or Vβ domains make up the pMHC binding site by each contributing three complementarity-determining regions (CDR1-3) which are characterised by a very high degree of variability. The CDR2 and CDR3 loops of each TCR α and β chain position themselves over the MHC (α_1 and α_2 domains of MHCI, or α_1 and β_1 domains of MHCII), and the CDR3 loops make contact with the antigenic peptide. Based on crystal structures solved for several TCR/pMHC complexes, the αβ TCR is thought to bind pMHC in a diagonal fashion with the Vα domain positioned over the N-terminal of the antigenic peptide and the Vβ positioned over the C-terminal ((Hennecke and Wiley 2001; Rudolph and Wilson 2002) and Figure 1.1). Figure 1.3 depicts the key molecules involved in antigen recognition at the $CD8^+$ T cell/ antigen presenting cell (APC) interface.

1.4.2b The coreceptors CD8 and CD4

The cell surface glycoproteins CD8 and CD4 were initially described as markers of the two T cells subsets: cytotoxic T lymphocytes and T helper cells, respectively (Swain 1983). Their role in T cell activation was proposed nearly ten years later when it was shown that anti-CD8 and anti-CD4 antibodies block T cells activation in response to antigen (Janeway 1992). It is now well established that CD8 and CD4 are important in enhancing T cell sensitivity to

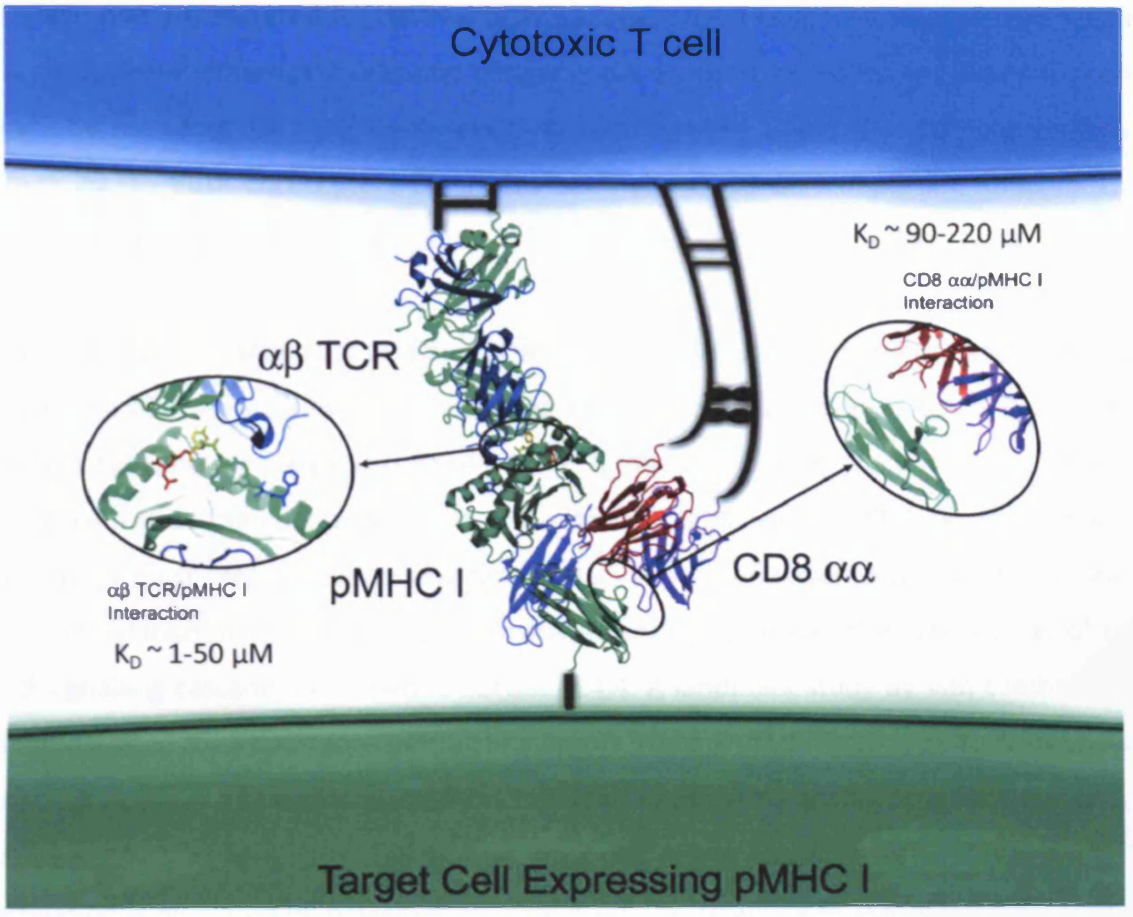

Figure 1.3: The TCR/pMHCI/CD8 interaction: target cell recognition by a $CD8^+$ T cells. Three dimensional dissociation constants (K_D values) for the TCR/pMHC and the pMHCI/CD8 interactions are indicated. (Figure kindly provided by D.C ole).

antigen and are required for optimal activation by most T cells. The level of enhancement varies between different T cells and antigens, but a report by Holler and Kranz suggested that CD8 may enhance $CD8^+$ T cell sensitivity to antigen by as much as 10^6 fold (Holler and Kranz 2003). Both coreceptors have also been shown to play important roles in T cell development (Fung-Leung et al. 1991; Rahemtulla et al. 1991; Van Laethem et al. 2007).

The extracellular domains of CD4 and CD8 coreceptors bind to MHC (Doyle and Strominger, 1987; Norment et al., 1988), whereas their cytosolic domains bind to Lck, a non-receptor protein tyrosine kinase (Marth et al., 1986, Rudd et al., 1988; Veillette et al., 1988). A principal role of the coreceptors is in sequestering Lck. Since the TCR lacks intrinsic kinase activity, it must rely on the coreceptors to deliver the sequestered Lck within its vicinity. Phosphorylation of specific phosphotyrosine motifs by Lck marks the early events of the T cell signalling cascade, described in Section 1.4.4. A landmark study by Van Laethem *et al.* demonstrated the importance of the coreceptors in shaping the T cell repertoire by showing that αβ T cells extracted from CD8/CD4 knockout mice were capable of recognising antigen independently of MHC (Van Laethem et al. 2007). In the absence of the coreceptors, TCR activation is mediated by passive capture of 'free' Lck, resulting in TCR-antigen engagement independently of MHC (Van Laethem et al. 2007). Importantly, these dual coreceptor knockout mice rapidly succumb to autoimmune conditions, highlighting the difficulty of modulating αβ TCR signalling intensity in the absence of CD4 and CD8 (Van Laethem et al. 2007). The Lck-sequestering role of CD8/CD4 functions to ensure that the body only generates T cells that recognise MHC-restricted ligands, thus limiting reactivity with self and promoting interaction of T cells with other cells. As this thesis is primarily concerned with antigen recognition by MHCI-restricted $CD8^+$ T cells, more time will be dedicated to the CD8 coreceptor with some mention of CD4 where relevant.

1.4.2c The structure and function of the CD8 coreceptor

The CD8 coreceptor is assembled from two chains and exists in two different forms on the cell surface: either as an αα homodimer or as an αβ heterodimer (Moebius et al. 1991; Terry et al. 1990). Whilst CD8αβ is exclusively present on the surface of $CD8^+$ T cells, expression of

CD8αα is restricted to γδ T cells, NK cells, memory αβ T cells, or a special subset of intraepithelial lymphocytes (IEL) residing in the gut (Gangadharan and Cheroutre 2004; Madakamutil et al. 2004). Each α and β chain is subdivided into four domains: a membrane distal immunoglobulin-like ectodomain, a heavily glycosylated membrane-proximal extended polypeptide stalk, a transmembrane domain, and a cytoplasmic domain (Gao et al. 2000; Zamoyska 1998). Although the CD8 α and β subunits are topologically similar, they show some differences in the stalk and cytoplasmic regions which reflect their different functions. The CD8α cytoplasmic tail has been shown to associate with signalling molecule Lck, and is involved in mediating efficient signal transduction leading to T cell activation (Veillette et al. 1988). The CD8β cytoplasmic tail is palmitoylated at position C179 and is responsible for the recruitment of the CD8 coreceptor to lipid rafts, which are specialised membrane microdomains rich in sphingolipids, cholesterol and molecules associated with T cell signalling (Arcaro et al. 2000; Viola 2001). The CD8β tail also increases the efficiency of $CD8^+$ T cell signal transduction by crosslinking components of the CD3 machinery with the αβ TCR (Arcaro et al. 2000; Doucey et al. 2003). Briefly, the CD4 coreceptor is a single polypeptide composed of four immunoglobulin-like domains designated D1-D4 (Brady and Barclay 1996; Wu et al. 1997).

1.4.2d The pMHCI/CD8 interaction

An association between the CD8 coreceptor and pMHCI was first postulated by Norment and colleagues, by showing that B cells expressing pMHCI molecules were able to bind cells transfected with high levels of CD8αα even in the absence of a TCR/pMHCI interaction (Norment et al. 1988). Subsequently, a crystal structure of the human pMHCI/CD8αα confirmed that the α chain of CD8 does indeed make contact with the α_3 domain of pMHCI ((Gao et al. 1997) and Figure 1.3). The structure also revealed that the CD8αα binds to non-polymorphic regions distinct from the polymorphic α_1 and α_2 regions which form the peptide-binding groove recognised by the TCR.

1.4.2e The pMHCII/CD4 interaction

A crystal structure of a human CD4 amino-terminal two-domain fragment complexed with the murine MHCII I-A^K has revealed that the D1 domain of CD4 binds to non-polymorphic regions of the MHCII molecule (α_2 and β_2) (Wang et al. 2001). The fact that CD4 contacts the MHCII molecule at a site distinct from the TCR binding site is reminiscent of the MHCI interaction with the CD8 coreceptor. However, whereas both domains of CD8 cooperatively bind MHCI molecules, only one domain (the N-terminal D1 domain) of CD4 makes contact with MHCII, whilst the second tandem CD4 domain remains distal to the interface (Wang et al. 2001).

1.4.3 Kinetics of the TCR/pMHC and the pMHC/coreceptor interactions

1.4.3a Kinetics of the TCR/pMHC interaction

Compared to the strength of most antibody-antigen interactions (dissociation constants (K_D) of <1 nM, (Mason and Williams 1980)), the majority of natural TCR-antigen interactions are extremely weak (Cole et al. 2007; Gao et al. 2000). The K_D for the TCR/pMHCI interaction normally ranges 1-50 μM (Gao et al. 2000). The kinetics of such weak, non-covalent protein-protein interactions can be measured using 3D or 2D technologies. To date, the majority of TCR/pMHC binding interactions have only been analysed three-dimensionally using a technique called surface plasmon resonance (SPR) (Davis et al. 1998; Gascoigne et al. 2001; Stone et al. 2009). In SPR experiments measuring TCR/pMHC binding, the pMHC is immobilised on a 'sensor chip' and the TCR is pumped over the surface of the chip. As the protein in solution binds to the immobilised protein, there is a change in refractive index at the surface of the sensor chip that is detected by the instrument using polarised light. This is related to the mass of protein close to the surface of the chip and thus allows measurement of binding kinetics in real-time. This method for measuring protein-protein interactions is classed as 3D chemistry because the protein present in the soluble phase is free to move about in three dimensions prior to binding its ligand. Although, in general, a good correlation has been demonstrated between the kinetics of binding (in particular the off-rate) and the strength of T cell activation (Davis et al. 1998; Gascoigne et al. 2001; Stone et

al. 2009), some researchers argue that SPR experiments are not an accurate representation of T cell/APC interactions.

In a biological setting, when a T cell encounters its target APC, the TCR and pMHC molecules are tethered to two opposing membranes and are therefore constrained to move in two dimensions. In view of this, 2D chemistry techniques have been developed for the purpose of measuring TCR/pMHC interactions with physiologically-relevant accuracy. A number of different methods have been developed to measure protein-protein interactions in two dimensions. In the fluorescence approach, TCR-expressing cells are placed on a glass-supported bilayer reconstituted with lipid-anchored, fluorescently-labelled pMHC ligands (Dustin et al. 1996; Dustin et al. 1997). TCR/pMHC interactions locally deplete free pMHC, creating a density gradient that drives net diffusion of free ligands into the contact area. This further pushes the process toward formation of more TCR/pMHC interactions and diffusion of more free pMHC into the contact area, leading to ligand accumulation within the contact area, as revealed by the higher fluorescence intensity inside than outside the contact region. Alternatively, 2D affinities can be determined mechanistically, whereby, interacting receptor/ligand complexes physically link two cells or a cell to a surface. The binding kinetics of TCR/pMHC interactions can be quantified by several mechanical methods such as the flow-chamber (Kaplanski et al. 1993), the micropipette (Chesla et al. 1998; Huang et al. 2010) and the centrifugation methods (Piper et al. 1998). The differences in kinetic measurements obtained by 2D and 3D approaches relate to how molecules approach each other. Instead of approaching each other by free diffusion, as in 3D SPR systems, molecules in 2D experiments are brought together (and apart) by membranes to which they are anchored. Furthermore, as molecules are brought in together to interact, more degrees of freedom are lost on binding of soluble molecules in a 3D setting than membrane-anchored molecules in 2D experiments. This greater entropic penalty incurred by free-flowing molecules in SPR experiments is thought to be accountable for the differences in kinetic measurements determined using 2D and 3D systems (Dustin et al. 2001; Huang et al. 2010).

Compared to 3D-derived data, 2D affinities and on-rates of the TCR for a panel of pMHC ligands possess far broader dynamic ranges, which are much more closely matched to that of their corresponding T cell responses (Huang et al. 2010). For instance, the low affinity characteristic of TCR/pMHC interactions in 3D is explained by a slow association rate (K_{on}~ 10^{-2}-10^{-4} $M^{-1}s^{-1}$) rather than a fast dissociation rate (K_{off} ~ 0.5-0.01 s^{-1}) (Davis et al. 1998). The slow association rate is thought to be a consequence of conformational flexibility at the TCR/pMHC interface (Willcox et al. 1999a). The best 3D parameter for TCR/pMHC affinity is however the dissociation rate, with agonist pMHC dissociating the slowest (Davis et al. 1998; Gascoigne et al. 2001; Stone et al. 2009). Contrastingly, in 2D, the affinities between a TCR and its antigenic pMHCs are driven by rapid association rates and rapid dissociation rates (up to 8,300-fold faster than off-rates determined in 3D) (Huang et al. 2010). Evaluation of TCR/pMHC kinetics in 2D therefore proposes a scenario whereby T cells rapidly and serially engage a few agonist pMHCs (via their TCRs) in a large self pMHC background.

It has been shown that the CD8 coreceptor can increase TCR/pMHCI on-rates (Gakamsky et al. 2005; Laugel et al. 2007) and reduce off-rates (Laugel et al. 2007; Wooldridge et al. 2005), at the same time as stabilising the TCR/pMHCI interaction by approximately two-fold (Wooldridge et al. 2005). The ability of CD8 to influence TCR/pMHCI binding kinetics has been attributed to the existence of spatially localised TCR-coreceptor adducts, which are predicted to be substantially better at engaging pMHCI antigen than if the TCR and CD8 were spatially distinct (Arcaro et al. 2001; Doucey et al. 2003; Wooldridge et al. 2003; Wooldridge et al. 2006). The currently proposed models of TCR association with pMHC and how this leads to T cell activation are discussed in section 1.4.5.

1.4.3b Kinetics of the pMHCI/CD8 and pMHCII/CD4 interactions

SPR analysis of the human pMHCI/CD8 interaction has revealed that the affinity of this interaction is very low ($K_D \leq$ 90-220 μM) (Figure 1.3), and is similar for both homodimeric and heterodimeric forms of CD8 (Gao et al. 2000; Garcia et al. 1996; Wyer et al. 1999). However, the pMHCI/CD8 interaction displays some interesting kinetics as the dissociation

of CD8(αα) from the prevalent pMHCI allele HLA A2 is extremely rapid ($K_{off} \geq 18^{-5}$) (Wyer et al. 1999). As a result, the duration of a single TCR/pMHCI interaction can encompass many pMHCI/CD8 association and dissociation events. The MHCII/CD4 interaction is much weaker ($K_D \geq 200$ μM) than the MHCI/CD8 interaction, making its kinetics difficult to measure accurately by SPR (Xiong et al. 2001).

1.4.4 Overview of T cell activation

1.4.4a The immunological synapse

In addition to the coreceptor (CD8 or CD4), the antigen specific αβ TCR is present on the T cell surface in association with the CD3 complex composed of four invariant accessory subunits present in the ratio $\gamma\delta\varepsilon_2\zeta_2$ (van der Merwe and Davis 2003; Weiss and Littman 1994). The main role of the CD3 machinery is to transduce signals to the interior of the cell when the TCR makes contact with cognate pMHC (Salmond et al. 2009). T cell activation also involves a host of antigen independent cell-cell interactions including CD2 (LFA-2), CD40L, LFA-1, and CD28 located on the T cell surface, which contact CD58 (LFA-3), CD40, ICAM-1, and CD80 (B7.1)/CD86 (B7.2) on the surface of APCs, respectively. Collectively, the interactions act to strengthen T cell-APC contact and regulate T cell activation (Bennett et al. 1998; Jenkins et al. 1991). Whereas effector and memory subsets of T cells that have previously come into contact with antigen can become activated relatively independently of the co-stimulatory signals provided by these extra interactions, naïve T cells that have never encountered antigen require costimulation. On encounter of an APC, a T cell initiates a process of cell surface molecular rearrangement culminating in the formation of organised cell-cell interfaces termed 'immunological synapses' or supramolecular activation clusters (SMAC) (Grakoui et al. 1999). The SMAC is organised into: i) a central area (cSMAC) in which the TCR-CD3 complex, its coreceptors CD8/CD4 and the costimulatory protein CD28 are positioned for optimal interaction with pMHC, CD80 and CD86 on the APC; and, ii) a peripheral area (pSMAC) where LFA-1, CD43, CD45, and ICAM-1 are sequestered. These latter molecules located in the pSMAC regulate the activity initiated by the cSMAC members. Although SMACs have taught immunologists a great deal about the mechanisms involved in T cell-antigen recognition, these types of structures are generally only observed

when very high peptide concentration (≥ 100 μM) are presented (Monks et al. 1998). Such antigen densities are unnatural, and 'real' activation *in vivo* occurs at much lower antigen densities (as few as ~ 10 pMHC copies per cell) (Irvine et al. 2002; Purbhoo et al. 2004; Valitutti et al. 1995). Furthermore, the formation of a SMAC can take several hours and requires for the T cell to be stationary in relation to the APC (Iezzi et al. 1998). With the availability of increasingly more powerful imaging techniques, it was observed that T cells interact with their target APCs in a dynamic manner (Miller et al. 2004; Miller et al. 2002). In a process called 'serial triggering', a single T cell is able to sequentially interact with several APCs (Valitutti et al. 1995). This ensures that T cells are highly efficient at recognising and responding to their target APCs even at very low effector to target ratios. As a result of low levels of antigenic peptide presentation and the dynamic and rapid nature of T cells/APC interactions, it is likely that the immunological synapse does not involve the formation of a SMAC, but smaller more transient versions of such structures.

1.4.4b The TCR/CD3 complex

In resting cells, the CD3ζ subunit exists in a partially phosphorylated state. However on productive engagement of pMHC by the TCR and CD4/CD8 coreceptor couple, special tyrosine residues located in regions of the CD3ε and CD3ζ subunits known as the immunoreceptor tyrosine-based activation motifs (ITAMs) become fully phosphorylated by a member of the Src family of tyrosine kinases called Lck (Barber et al. 1989). The phosphorylation of CD3ζ takes place in a series of ordered steps, all of which must be completed for full T cell activation (Kersh et al. 1998). Each step of the phosphorylation process represents a checkpoint, progression through which is related to the ability of a particular pMHC ligand to activate a given TCR. Therefore, any factor that influences the multistep CD3ζ phosphorylation process will affect the outcome of TCR engagement (Kersh et al. 1998).

1.4.4c The protein tyrosine kinase Lck

Early phosphorylation events triggered by TCR engagement of foreign pMHC is mediated by protein tyrosine kinases (PTKs). PTKs are grouped into families: Src or Syk, which differ

structurally (Chan et al. 1994). The aforementioned Lck is a Src PTK, and is expressed abundantly in T cells. Structurally, Lck is similar to other members of the Src family and contains three Src homology (SH) domains designated SH1-3. SH1 is a protein tyrosine kinase domain with intrinsic ATPase activity and an autophosphorylation site at residue 394. Phosphorylation of tyrosine-394 is thought to initiate the phosphorylation events of the T cell signalling cascade (Abraham and Veillette 1990). The SH2 and SH3 domains mediate protein-protein contacts between phosphotyrosine-containing motifs (Fantl et al. 1992). The termini of Lck also have important roles. The amino terminus of Lck remains associated with the plasma membrane (Resh and Ling 1990) and interacts with CD8/ CD4 coreceptors (Shaw et al. 1990), whilst the carboxyl terminus of Lck contains a negative regulatory tyrosine at position 505, the phosphorylation of which inactivates Lck (Veillette et al. 1988; Weiss and Littman 1994). The PTK Csk is responsible for the phosphorylation of the tyrosine-505, and consequently inhibition of Lck (Chow and Veillette 1995). Lck is positively regulated by the tyrosine phosphatase CD45, the most abundant glycoprotein expressed on the surface of T cells (Thomas 1989). CD45 is found associated with Lck in resting T cells (Guttinger et al. 1992). On TCR/pMHC engagement, CD45 releases Lck by dephosphorylating the negative regulatory phosphate on tyrosine-505 (Ostergaard and Trowbridge 1990). Chapter 5 of this thesis investigates how inhibition of Lck by a PTK inhibitor dasatinib can be exploited to improve the detection of low avidity T cells with pMHC tetramers.

1.4.4d T cell signal transduction cascade

A productive engagement of a TCR with its cognate pMHC and an interaction between pMHC and CD8/CD4 coreceptors results in the activation of Src kinases Lck and Fyn (Weiss and Littman 1994). Phosphorylation of CD3ζ ITAM motifs by these kinases provides docking sites for downstream signalling elements (Nel 2002; Nel and Slaughter 2002). The Syk family PTK zeta chain-associated protein of 70 kD (ZAP-70) subsequently binds to the CD3 complex via the phosphotyrosine motifs, and is in turn phosphorylated by Lck (Chan et al. 1995). On activation, ZAP-70 acquires the ability to recruit and activate adaptor proteins which possess no intrinsic enzymatic activity but are responsible for bringing together members of the signalling cascade that would not associate with each other if left unaided (Myung et al.

2000). One of the most important adaptor proteins in the signalling cascade is the linker for activation in T cells (LAT). LAT is an integral membrane-associated protein whose principal function is to recruit downstream signalling proteins including Grb2, PLC-γ1, Cbl, SOS, Vav, and SLP-76, thus linking extracellular TCR/pMHC engagement to intracellular signals. LAT interacts with these signalling proteins via its 10 tyrosine residues, which once phosphorylated by ZAP-70 can bind to SH2 domains of proteins found downstream in the signalling cascade (Zhang et al. 1998). At this stage the signal transduction pathway branches out into secondary pathways, but it ultimately culminates in the nucleus, where transcription factors such as NF-κB, NFAT, and AP-1 are activated (Kuo and Leiden 1999; Myung et al. 2000). Activation of these and other transcription factors elicits novel patterns of gene expression and results in proliferation, differentiation, and effector functions.

1.4.5 TCR triggering and models of T cell activation

Although we are starting to piece together the details about molecular interactions that take place on TCR association with pMHC antigen, we do not yet fully understand how the TCR transduces signals across the plasma membrane, a process referred to as TCR triggering. The central conundrum in TCR triggering is how the engagement of TCR with antigen leads to ITAM phosphorylation. Despite numerous publications on the subject, no unanimous consensus has thus far been reached. However, three basic categories of TCR triggering models have been proposed, the key features of which are outlined below:

1.4.5a Aggregation models

The notion behind this group of models stems from observations that aggregation of TCRs by antibody or pMHC multimer binding is sufficient to initiate TCR triggering (Qian and Weiss 1997; Weiss and Littman 1994). According to aggregation models, TCR triggering is thought to occur by increasing the proximity of the TCR/CD3 complex to signalling molecules such as the Src kinases Lck and Fyn (Boniface et al. 1998; van der Merwe 2001). The models rely on the fact that either specific pMHC molecules exist on the antigen presenting cell in high numbers, or that cognate pMHC are able to form dimers with self-pMHC. Reports that a single specific pMHC is sufficient to induce TCR triggering (Irvine et al.

2002; Purbhoo et al. 2004), and limited evidence for the existence of covalent pMHC heterodimers have put serious doubt on the plausibility of aggregation models. However, a possibility remains that TCR aggregation could amplify triggering initiated by other mechanisms (Minguet et al. 2007).

1.4.5b Conformational change models

Conformational change models propose that on ligation of cognate pMHC, the TCR undergoes a structural conformational change that is propagated to the CD3 complex, initiating the tyrosine phosphorylation events. Although there was some initial evidence for such a conformational change (Gil et al. 2002), analysis of a large number of TCR/pMHC structures has conclusively shown that TCR binding to pMHC is not accompanied by any consistent conformational change within the TCR that could lead to signal transduction (Rudolph et al. 2006). Van der Merwe and colleagues have recently postulated that because pMHC and TCR/CD3 are anchored in the plasma membrane of two distinct cells, the binding of pMHC may exert a pulling force on the TCR, which could change its orientation with respect to the CD3 subunits (Choudhuri and van der Merwe 2007). Although plausible, it is not certain whether the TCR/pMHC interaction is sufficiently strong or long-lived to generate the forces required for this to happen.

1.4.5c Segregation models

Two types of model fall into this category: i) the kinetic segregation model; and, ii) the lipid raft model.

i) Kinetic segregation model

The kinetic segregation model postulates that the immunological synapse is organised into multiple zones, with some zones being devoid of molecules with large ectodomains, such as the inhibitory tyrosine phosphatases. Trapping of TCR/CD3 in these zones results in the constitutive phosphorylation of CD3 ITAMs by Src kinases, potentially leading to TCR triggering (Davis and van der Merwe 1996). The model is supported by a number of key observations including that: i) inhibitory phosphatases segregate from areas of TCR

triggering (Lin and Weiss 2003); ii) truncation of phosphatase ectodomains inhibits TCR triggering (Irles et al. 2003); and, iii) elongation of the pMHC complex inhibits TCR triggering (Choudhuri et al. 2005). However the evidence does not establish whether the environment within these zones is alone sufficient to induce TCR triggering.

ii) Lipid raft model

The lipid raft model proposes that TCR binding to pMHC leads to TCR association with lipid rafts, which are areas of the plasma membrane enriched in molecules associated with TCR signal transduction such as Lck (Kabouridis et al. 1997), Fyn (van't Hof and Resh 1999), LAT (Zhang et al. 1998b), and the coreceptors CD4 (Crise and Rose 1992) and CD8 (Arcaro et al. 2000). A key piece of evidence in support of the lipid raft model of T cell activation is the fact that the CD8 coreceptor β chain is selectively palmitoylated (Arcaro et al. 2000). As a consequence, CD8 αβ (but not CD8 αα) is responsible for recruiting the TCR to the lipid rafts, where it co-localises with Lck. In a similar fashion: i) Fyn has been shown to associate preferentially with CD3 in lipid rafts (van't Hof and Resh 1999); and, ii) the formation of dipalmitoylated CD4/Lck complexes was demonstrated in $CD4^+$ T cells (Maroun and Julius 1994). The recruitment of TCRs to these rafts is predicted to lead to phosphorylation of TCR/CD3 ITAMs and ultimately TCR triggering. Although a substantial body of evidence supporting the role of lipid raft localisation in TCR signalling has been published (reviewed in (Horejsi 2005)), a greater number of studies have challenged these claims (Glebov and Nichols 2004; Zhu et al. 2005).

A number of other models have been proposed to address the important question of how a relatively small number of agonist pMHC molecules can trigger a much larger number of TCRs (Valitutti et al. 1995). The principles behind two favoured models are summarised below:

1.4.5d Serial triggering model

The serial triggering model postulates that each 'foreign' pMHC serially engages many TCRs, one after another (Valitutti and Lanzavecchia 1997). The model is consistent with the short-

lived nature of the majority of TCR/pMHC interactions and dictates a requirement for an optimal half-life for a given TCR/pMHC complex. Interactions with half-lives exceeding this optimum are predicted to be less effective. The serial triggering model therefore predicts that there exists an 'affinity ceiling' for TCR/pMHC interactions beyond which T cell activation will become less efficient (Sewell 2002). Schmid *et al.* have recently tested this hypothesis and concluded that above a defined TCR affinity threshold, T cell avidity and function were not further enhanced (Schmid et al. 2010). These findings imply that TCRs may not need to be optimised beyond a given affinity threshold to achieve best functionality.

1.4.5e Kinetic proofreading model

The kinetic proofreading model proposes that TCR signalling goes through a series of sequential steps, the completion of which is essential for full activation. On dissociation of the antigen, these steps are fully reversed (McKeithan 1995; Rabinowitz et al. 1996). To summarise, despite the extensive amount of research effort dedicated to studying the events that take place following TCR/pMHC engagement and preceding T cell activation, the process of TCR triggering remains poorly understood. And although experimental evidence supports some of the models described here better than others, it is likely that these models are not mutually exclusive. In view of this, the true mechanism of TCR triggering may encompass aspects of several of the models described.

1.5 Glycosylation and T cell antigen recognition

Nearly all mammalian cell surface proteins are terminally modified by glycosylation. These cell surface oligosaccharides have many roles, the importance of which becomes apparent in cases where the glycosylation pathway is disrupted (Schachter and Freeze 2009). Glycans regulate lateral mobility of proteins in the plasma membrane, influence protein-protein interactions, and mediate organisation of proteins into domains (Baum 2002). Glycosylation is also extremely important for cells of the immune system, where carbohydrate interactions can influence lymphocyte development, migration and responsiveness (Daniels

et al. 2002). For instance, early studies with carbohydrate-binding plant lectins have demonstrated that the cell surface glycosylation profile for a T cell changes dramatically during thymocyte development (Despont et al. 1975; Pink 1983; Reisner et al. 1976). More specifically, the maturation of thymocytes coincides with increased expression of terminal negatively-charged sialic acid residues (Baum et al. 1996; Gillespie et al. 1993; Reisner et al. 1976). In addition to the mass restructuring of glycans during T cell development in the thymus, mature T cells experience changes in glycosylation of cell surface proteins during activation and on transition into the memory state (Galvan et al. 1998; Harrington et al. 2000). Thus, the extent of protein modification by glycosylation fluctuates throughout the lifetime of a lymphocyte, and this remodelling of cell surface carbohydrate is accompanied by changes in T cell antigen sensitivity (Brennan et al. 2006; Daniels et al. 2002; Galvan et al. 1998; Garcia et al. 2005; Garcia and Miller 2003; Lowe 2001; Pappu and Shrikant 2004). Chapter 7 of this thesis explores the potential of altering the level of cell surface glycosylation to enhance T cell sensitivity to antigen.

1.6 pMHC multimers as tools for the detection, characterisation and isolation of T cells

The TCR/pMHC interaction is weak and typically lasts only a matter of seconds at physiological temperatures, making soluble pMHC monomers inadequate reagents for the detection and characterisation of specific T cell responses. A pioneering study by John Altman and colleagues presented a means of extending the life-time of the TCR/pMHC interaction by multimerizing soluble pMHC molecules (Altman et al. 1996). These first pMHC 'tetramers' consisted of four pMHC molecules around an avidin-biotin scaffold (O'Callaghan C et al. 1999), and are still the most common form of pMHC multimer used to date. Although different manufacturing techniques are employed by different research groups, pMHC tetramers are essentially assembled from soluble biotinylated pMHC monomers complexed with fluorochrome-conjugated avidin or streptavidin molecules in a 4:1 ratio.

1.6.1 The avidity effect

In physical terms, affinity can be described as the strength of the reaction (or bond) between a single antigen and its specific receptor, comprising the sum of the attractive and repulsive forces operating between these two entities. In contrast, the avidity of a multimeric interaction is a measure of the overall strength of binding between each antigen and its cognate receptor. If affinity describes the strength of a single bond, than avidity equates to the combined synergistic strength of multiple bond interactions, which is greater than the sum of the individual affinities. In the biological setting, avidity is a property of molecules with multiple binding sites, where it refers to the combined affinities of each of the binding sites for their respective ligands. Measurement of monomeric and multimeric TCR/pMHC interactions by surface plasmon resonance (SPR) has demonstrated that the avidity for a set of interactions far exceeds the sum of the contributing affinities (Laugel et al. 2005). This 'avidity effect' arises because the probability of all monomeric interactions dissociating simultaneously is exceedingly small. With respect to pMHC tetramers, three of the four pMHC arms are capable of engaging surface TCRs simultaneously (McMichael and O'Callaghan 1998), greatly reducing the probability of complete pMHC tetramer dissociation even if one of the TCR/pMHC contacts is momentarily disrupted (Figure 1.4). The avidity effect extends the half-life of TCR/pMHC interactions from seconds (as monomer) to several hours (as tetramer), making them extremely useful tools for specific surface staining of T cells in a variety of laboratory and increasingly clinical applications. However, the avidity effect does not come into play for all pMHC multimer binding events as it relies on the duration of the monomeric TCR/pMHC interaction. To take advantage of the avidity effect, the first monomer or 'arm' of the pMHC multimer must associate with a cognate TCR for long enough to enable a second pMHC 'arm' to bind a second TCR. A TCR/pMHCI interaction of $K_D \leq 40$ μM is required to observe good pMHC tetramer staining using standard techniques (Laugel et al. 2007). The on-rate of the initial TCR/pMHC interaction is also critical, as it determines the probability of a second TCR/pMHC interaction taking place. Engagement of two or more pMHC monomers within a given pMHC multimer is believed to determine whether the molecule is captured from solution (Wooldridge et al. 2009; Wooldridge et al. 2005). As described in the next section, the likelihood of a pMHC multimer

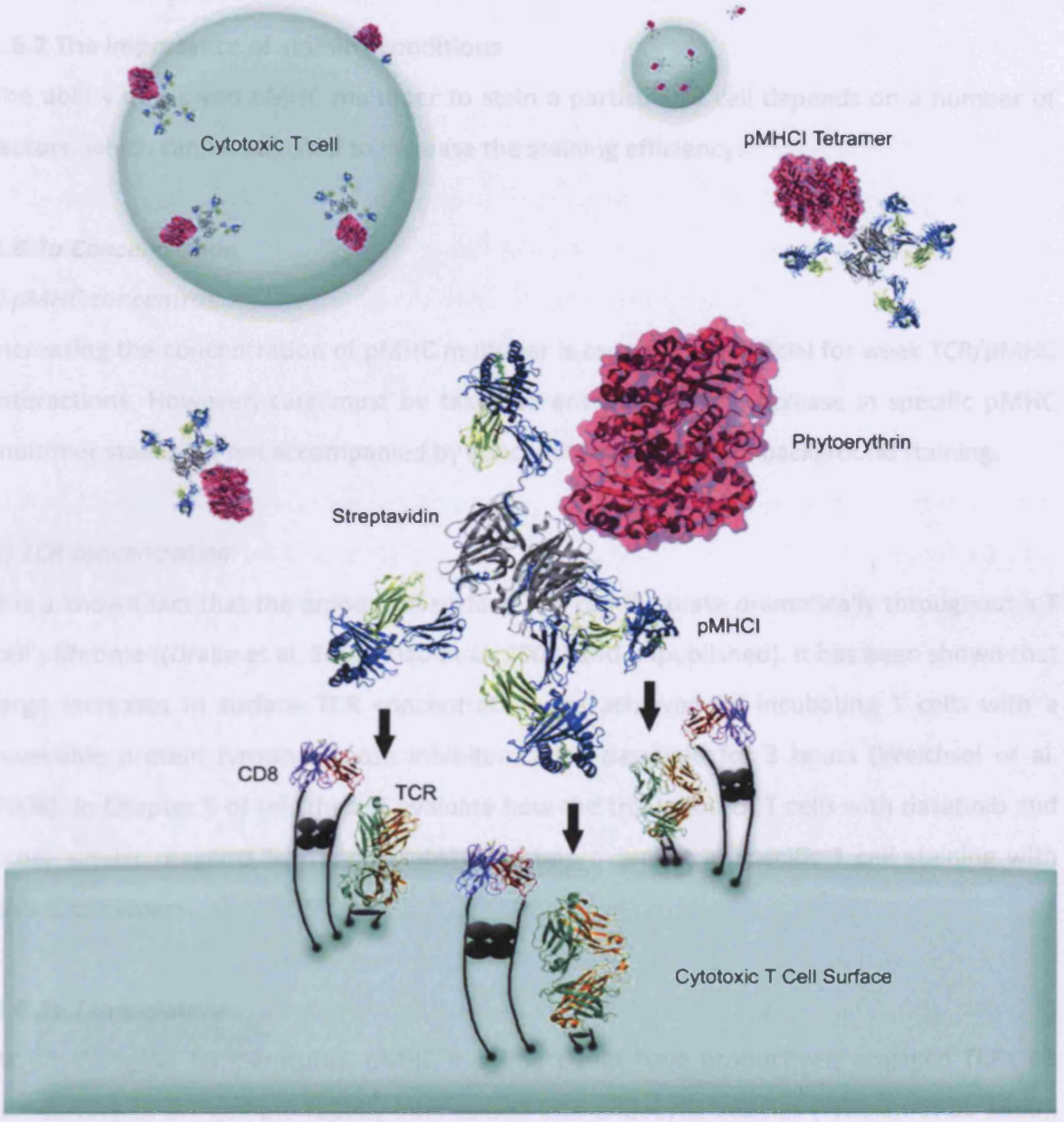

Figure 1.4: A tetramer binding to cognate TCR/CD8 complexes. pMHCI tetramers consist of four biotinylated peptide-HLA complexes bound to a single streptavidin molecule, conjugated to a fluorescent dye. Tetramerisation extends the half lives of TCR/pMHCI interactions from seconds to several hours due to 'avidity'; a multiple of the binding affinities of individual monomers. Avidity arises because the probability of all monomeric TCR/pMHCI interactions dissociating simultaneously is significantly reduced. Each 'arm' of the tetramer will undergo a large number of dissociation/association events before the tetramer eventually drops off the surface of the $CD8^+$ T cell.

binding to the surface of a T cell is greatly dependent on the density of surface TCRs as well as their distribution within the lipid bilayer (Wooldridge et al. 2009).

1.6.2 The importance of staining conditions

The ability of a given pMHC multimer to stain a particular T cell depends on a number of factors, which can be adjusted to increase the staining efficiency:

1.6.2a Concentration

i) pMHC concentration:

Increasing the concentration of pMHC multimer is especially beneficial for weak TCR/pMHC interactions. However, care must be taken to ensure that the increase in specific pMHC multimer staining is not accompanied by concomitant increases in background staining.

ii) TCR concentration:

It is a known fact that the amount of surface TCR can fluctuate dramatically throughout a T cell's lifetime ((Drake et al. 2005; Xiao et al. 2007) and unpublished). It has been shown that large increases in surface TCR concentration are achieved by incubating T cells with a reversible protein tyrosine kinase inhibitor called dasatinib for 3 hours (Weichsel et al. 2008). In Chapter 5 of this thesis I evaluate how the treatment of T cells with dasatinib and other similar reagents leads to a substantial improvement in specific T cell staining with pMHC tetramers.

1.6.2b Temperature

At physiological temperatures, pMHC multimers that have productively engaged TCRs on the surface of a T cell are rapidly internalised into endocytic vesicles (Whelan et al. 1999). The trapped pMHC multimers can no longer dissociate from the T cell surface, meaning that performing staining at 37°C is particularly beneficial for weak TCR/pMHC interactions with short binding half-lives. T cell homeostasis is slower at low temperatures (4°C), which greatly reduced the internalisation of TCR-bound pMHC multimers (Whelan et al. 1999). Thus at low temperatures, the staining intensity depends wholly on the surface-bound

pMHC multimers and consequently the ability of these reagents to remain in association with surface TCR. Since pMHC multimer-induced TCR triggering is toxic to T cells, processes where pMHC multimers are used to isolate or sort cells for culturing or cloning are typically performed at low temperatures (Cebecauer et al. 2005).

1.6.2c Duration of staining

While pMHC tetramers typically display very rapid association kinetics and are able to attain their optimal staining intensity after a few minutes, other pMHC multimeric reagents such as dextramers (see Chapter 4) require longer incubation periods.

1.6.2d Anti-coreceptor antibody

Staining with pMHC multimers is generally performed in conjunction with antibodies specific for various cell-surface markers. Some of these antibodies, and in particular anti-CD8 and anti-CD4 antibodies, have disruptive effects on pMHC multimer staining (Wooldridge et al. 2003; Wooldridge et al. 2006). The hindering effect of certain antibodies can be overcome by staining with pMHC tetramers before the addition of antibodies (Whelan et al. 1999; Wooldridge et al. 2003; Wooldridge et al. 2006), or by using non-blocking/enhancing coreceptor antibodies ((Wooldridge et al. 2003) and Clement et al. submitted).

1.6.3 pMHCI versus pMHCII multimers

The use of pMHCII multimers is less widespread than the use of pMHCI multimers, largely due to the TCR/pMHCII interaction being substantially weaker than TCR/pMHCI binding (Cole et al. 2007). In addition, the CD4 coreceptor does nothing to enhance TCR/pMHCII binding (Boniface et al. 1998; Crawford et al. 1998; Hamad et al. 1998) in contrast to the way CD8 stabilises the TCR/pMHCI interaction (Choi et al. 2003; Laugel et al. 2007; Pittet et al. 2003). Both of these factors explain why the majority of TCR/pMHCII associations fall below the affinity threshold required for tetramer staining.

1.6.4 Higher valency pMHC multimers

Although the pMHC tetramer is the most popular form of pMHC-based reagent, and is considered optimal for the detection of T cells by flow cytometry and fluorescence microscopy, other valencies of pMHC have been explored. The efficiency of lower (dimers) and higher (pentamers, octamers, and pMHC-coated magnetic beads) valencies of pMHC have been demonstrated by a number of groups (Bakker and Schumacher 2005; Buslepp et al. 2001; Ogg et al. 1999). In addition to my work with pMHC tetramers, I evaluate the merits of a novel type of pMHC multimer called a dextramer. Dextramers comprise large numbers of pMHC monomers bound to streptavidin molecules arranged around a dextran polymer scaffold laden with multiple copies of a fluorochrome. Whether the higher valency, the predicted conformational freedom of pMHC molecules, or the large number of fluorochrome moieties per reagent offer some advantage over standard pMHC tetramers in the labelling of T cells is explored in Chapter 4 of this thesis.

1.6.5 Applications of pMHC multimers

1.6.5a Grading T cell responses

It has been shown that T cells within a population primed to respond to a particular antigen display intrinsically different sensitivities to that antigen (Alexander-Miller 2000; Alexander-Miller et al. 1996). Numerous studies have subsequently demonstrated that T cells capable of recognising very low antigen densities are more effective than their less sensitive counterparts at eliminating tumours and virally-infected cells *in vivo* (Alexander-Miller et al. 1996; Dutoit et al. 2001; Sedlik et al. 2000; Yee et al. 1999; Zeh et al. 1999). In view of this, it is becoming increasingly accepted that the quality of T cells responding to an antigen is as important as their quantity. Assessing the quality of a responding T cell population is of outmost significance in adoptive T cell therapy, where the antigen sensitivity and functionality of T cells can greatly influence the outcome of the therapy. pMHC multimers have become invaluable tools for 'grading' the quality of antigen-specific T cell populations for clinical and laboratory applications.

1.6.5b Specific sorting and cloning of T cells

The purity of a T cell population responding to a particular antigen can be increased by sort-cloning pMHC-labelled T cells. However, care must be taken to minimise the toxic effects of pMHCI multimers (Cebecauer et al. 2005a). Most cell sorting protocols recommend reducing staining times in addition to performing the staining at low temperatures (see Section 1.6.2b).

1.6.5c T cell activation

Soluble pMHC multimers have been used to examine the activation requirements of T cells. Importantly, pMHC multimer-induced activation has enabled the study of TCR/pMHC and pMHC/coreceptor interactions in isolation without altering the kinetics of these interactions that is inherent to studies using antibodies targeting these components.

1.6.5d Identification and isolation of anti-tumour, anti-viral, and autoreactive T cells ex vivo

Both adoptive T cell therapy (Section 1.8.2) and TCR gene transfer therapy (Section 1.8.3) rely on the availability of specific T cell populations, which can be isolated from individuals by means of pMHC multimer sorting. The apparent correlation between pMHC tetramer staining and monomeric TCR/pMHC interaction affinity (Laugel et al. 2007) suggests that, in general, it will be more difficult to stain T cells specific for tumour-associated and self-antigens compared to T cells directed against viral antigens. In view of this, improvements in the pMHC multimer staining efficiency are urgently needed. Furthermore, persistent viral infection often results in the exhaustion of T cell populations (Oxenius et al. 2002). In such cases, pMHC multimers allow the identification of T cells that express the antigen-specific TCR but are no longer capable of making an immune response (Barnes et al. 2004). Isolation of these cognate TCR genes and their subsequent transfer to autologous T cells restores their functionality, and constitutes an important aspect of TCR gene transfer therapy.

1.6.5e Manipulation of T cells in vivo

Soluble pMHC multimers might be useful for suppressing unwanted T cell responses or for boosting desirable responses *in vivo*. Published examples of pMHC multimers include: the *ex vivo* removal of alloreactive T cells before transplantation (Kappel et al. 2006), the deletion of autoimmune T cells for the prevention of diseases such as type I diabetes (Casares et al. 2002; Masteller et al. 2003) and arthritis (Zuo et al. 2002), and the priming of beneficial T cell responses *in vivo* (Maile et al. 2001). New generations of 'suicide' pMHC multimers, coupled to radioactive isotopes or biological poisons are also being developed with therapeutic implications (Hess et al. 2007; Yuan et al. 2004).

1.7 The role of $CD8^+$ T cells in the recognition and eradication of virally-infected and tumour cells

The immune system has evolved to respond primarily to foreign pathogens. While $CD8^+$ T cells effectively target and eradicate acute viral infections, the persistence of foreign antigens encountered in chronic viral infection results in a dysfunctional immune response. Furthermore, many pathogens associated with chronic viral infection display variable antigenicity profiles and employ multiple evasion techniques to escape immune detection. In contrast, cancer; a disease of the developed world associated with an increasingly aging population, represents a relatively new challenge for the immune system. The poor immunogenicity of tumour-associated antigens, the immunosuppressive tumour microenvironment, and the low frequency of functional tumour-reactive T cells result in inefficient cancer targeting. In this section, I describe the various challenges faced by the $CD8^+$ T cell response in the eradication of chronic viral pathogens and tumour-transformed cells, while the subsequent section (1.8) deals with the therapeutic methods employed to overcome the immunological barriers presented by these diseases.

1.7.1 Viral infections

The adaptive immune response has developed an elegant strategy for the detection and eradication of host cells infected with pathogenic viruses. The key event in this battle

against infection is the recognition of viral peptide fragments presented in the context of MHC class I molecules, by $CD8^+$ T cells. In response to pressures from the immune response, viruses have in turn evolved ingenious evasion strategies.

1.7.1a Problems associated with viral antigen recognition

The majority of the mechanisms by which viruses are able to trick the host's immune defences involve the mutation of their genomes to prevent or alter the display of viral antigens via the MHCI antigen presentation pathway. Examples of viruses targeting stages of the MHCI antigen presentation pathway are summarised in Table 1.1 (Hansen and Bouvier 2009). Since the work described in this thesis deals primarily with HIV infection, reference to other viral pathogens will be kept to a minimum.

The detection of cells infected with a family of viruses called retroviruses poses a particular challenge for $CD8^+$ T cells. Retroviruses are exemplified by the human immunodeficiency virus (HIV). HIV is responsible for inducing acquired immunodeficiency syndrome (AIDS), one of the most destructive diseases in human history. AIDS develops following depletion of $CD4^+$ T cells as they become infected with HIV. The majority of AIDS patients die due to the inability of the weakened immune system to control opportunistic infection. The devastating nature of retroviruses such as HIV stems primarily from their single-stranded RNA genomes, which are much more prone to spontaneous mutagenesis than the double-stranded DNA genomes of other common viruses that target human cells. Thus, in addition to employing non-mutational strategies of escape such as the Nef-mediated downregulation of MHCI, HIV can mutate to disable or alter presentation of peptide antigen on MHCI molecules. For instance, the virus can mutate epitopes that are normally available for presentation to anti-viral T cells in a way that interferes with recognition by their TCRs. In some cases however, by mutating to escape from a $CD8^+$ T cell response a virus can incur significant structural or functional penalties. With respect to HIV, studies of both the simian immunodeficiency virus (SIV) model and of natural HIV infection have shown that the virus loses 'fitness' whilst attempting to escape from certain $CD8^+$ T cell responses (Crawford et al. 2007; Friedrich et al. 2004; Leslie et al. 2004). Furthermore, HIV-infected individuals

whose $CD8^+$ T cells target the virus through these epitopes show improved viral clearance and have longer life expectancy (Leslie et al. 2004). Such studies have set forth the analogy of viruses such as HIV to 'walking a tightrope' by balancing the need to escape from the host $CD8^+$ T cell response with the need to preserve 'fitness'.

Virus	**Effect on MHCI antigen presentation pathway**
Epstein-Barr virus (EBV)	EBV nuclear antigen 1 (EBNA1) acts as a proteasomal processing inhibitor.
Herpes simplex virus (HSV)	HSV protein ICP47 prevents transport of viral protein into the ER for processing by blocking peptide binding to TAP.
Human cytomegalovirus (HCMV)	HCMV protein US6 prevents transport of viral protein into the ER for processing by inhibiting ATP binding to TAP.
Adenovirus	Adenovirus protein E3-19K retains peptide-loaded MHCI molecules in the ER.
Human cytomegalovirus (HCMV)	HCMV proteins US2 and US11 target MHCI molecules for degradation by the proteasome.
Kaposi's sarcoma-associated virus (KSHV)	KSHV proteins kK3 and kK5 induce rapid endocytosis of cell surface pMHCI molecules into lysosomal vesicles for degradation.
Human immunodeficiency virus (HIV)	HIV protein Nef downregulates pMHCI molecules from the cells surface.

Table 1.1: Examples of viral evasion by targeting the pMHC class I antigen presentation pathway.

Currently, the most widely used treatment for HIV infection is the administration of highly active anti-retroviral therapy (HAART). Modern HAART regimens are combinations (or 'cocktails') comprising at least three anti-retroviral agents; inhibitors targeting reverse transcriptase and protease enzymes, which are essential for retroviral replication. In light of the fact that $CD8^+$ T cells play a vital role in the detection and eradication of virally-infected cells, recent therapeutic developments have focused on supplementing the patients' own immune system with $CD8^+$ T cells targeting HIV-derived epitopes. The numerous means by which this can potentially be achieved are outlined in Section 1.8.

1.7.2 Cancer

Cancer is one of the leading causes of death in industrialised nations, and is likely to become the most fatal disease threatening humanity as our average life expectancy increases in the near future. Cancer arises when the checkpoints monitoring cellular replication, growth, and/or death are no longer properly regulated due to mutations affecting the proteins involved in these key processes. Generally, a healthy cell must accumulate approximately 6 mutations targeting different aspects of cell metabolism, homeostasis and physiology before malignant growth occurs, permitting a cancerous tumour to develop (Hanahan and Weinberg 2000). Curing cancer is a challenging prospect that requires the destruction of every malignant cell whilst minimising the toxicity to the host's healthy tissues. An attractive way of eradicating cancer would be to induce an immune response to selectively target the tumour without inducing autoreactivity.

A functional relationship between cancers and the immune system was proposed as early as 1863, when an infiltration of leukocytes was detected in an excised tumour (Virchow 1863). Since then, our increased understanding of immune cell function has reinforced these initial speculations about the involvement of the immune response in the prevention and clearance of cancer. The recognition and eradication of cancer cells by the immune system is termed cancer immunosurveillance (Smyth et al. 2001). As key mediators and effectors of the adaptive immune response, T cells were proposed to play a critical role in the control of malignant cell growth. Evidence that T cells can help control tumour development was

demonstrated by reports of tumour prevalence in individuals with HIV-induced immunodeficiency (Goedert 2000) and incidence of carcinogen-induced tumours in immunosuppressive mouse models (Shankaran et al. 2001). Further evidence that manipulation of the immune response (and in particular T cells) can cause the regression of established tumours came from a study in which the cytokine interleukin-2 (IL-2) was administered to patients with metastatic kidney cancer or melanoma (Rosenberg et al. 1985). IL-2 is an immune regulator produced by $CD4^+$ T-helper cells, and is responsible for large-scale expansion of effector $CD8^+$ T cells. Since IL-2 has no direct effect on the viability of malignant cells alone, its anti-tumour effect *in vivo* was attributed to the expansion of $CD8^+$ T cells with tumour-lytic activity.

In view of this, the modern approach for the treatment of cancer has attempted to distance itself from systemically toxic conventional treatments such as chemotherapy, in favour of engaging the immune response. Unfortunately, efforts to launch a therapeutic response by the patient's immune system have not been entirely successful. In the recombinant IL-2 administration study for instance, although regression of tumours was observed, the typical response rate was low (~8% complete response, and ~9% partial response in a study of 409 kidney cancer and melanoma patients) (Rosenberg et al. 1998). Furthermore, the magnitude of the response varied from patient to patient (Rosenberg et al. 1998). Since then, better understanding of the molecular basis of tumour-host interactions has provided some explanations for the limitations of the immune system in the fight against cancer.

1.7.2a Problems associated with cancer antigen recognition

Malignant tumours exhibit a variety of highly sophisticated tricks for evading attack from T cells:

1) Establishment of an immunosuppressive tumour microenvironment; the tumour can tolerise T cells to evade T cell recognition by the following mechanisms:

i) Downregulation of some MHC class I alleles for low surface antigen presentation.

ii) Reduction in expression of co-stimulatory signals by the tumour cells, which can result in anergy or deletion of naïve T cells on exposure to antigen.

iii) Manipulation of immune cells by secretion of immunosuppressive chemokines and cytokines such as transforming growth factor-β (TGF-β).

iv) Recruitment of regulatory T cells (Tregs) into the tumour microenvironment.

v) Tissue remodelling; solid tumours can provide a physical barrier for the infiltration of T cells and APC.

vi) Induction of hypoxia (oxygen deprivation) within regions of the tumour has been shown to inhibit $CD8^+$ T cell-dependent cytotoxicity (Hamai et al. 2010).

2) Selection pressure mounted by the immune response can encourage the persistence of malignant cells that have altered their antigenic profile to avoid T cell-mediated recognition (Chouaib et al. 1997).

1.7.2b Thymic deletion of autoreactive T cells during the process of negative selection

A further great concern in tumour immunology is a shortage of suitable candidates to act as tumour antigens and the subsequent lack of T cells that can recognise them. As mentioned previously, tumours arise due to the malignant transformation of healthy cells, meaning that the majority of processed antigen presented in the context of MHCI molecules on the tumour cell surface is identical to self-antigens presented by healthy cells (Rosenberg 2001). Recognition of self-antigens by T cells would result in autoimmunity, a condition that the immune system has developed strategies to minimise. Tolerance to self-antigens is built up by thymic deletion, whereby thymocytes recognising self-peptides undergo apoptosis (Nitta et al. 2008; Surh and Sprent 1994). This process of negative selection is highly dependent on both the strength of the TCR/pMHC interaction and the amount of antigen presented in the thymus (Ashton-Rickardt et al. 1994; Sebzda et al. 1994). These restrictions enable T cells with TCR/pMHC interactions below a certain affinity threshold to leave the thymus and enter the periphery (Liu et al. 1995; Oehen et al. 1994). A T cell repertoire that has been shaped by such a mechanism of self-tolerance contains few tumour-reactive T cells, and those that do graduate into the periphery generally display low affinities for cognate

antigen (Kisielow et al. 1988). For instance, many common tumour-associated self-antigens, including NY-ESO-1- and MAGE-A3-derived epitopes (see Table 1.2), have been found expressed in the thymus (Gotter et al. 2004). Any T cells responding to these antigens are thus subject to thymic tolerance mechanisms, explaining the low frequency of NY-ESO-1- and MAGE-A3-specific T cells in the periphery. Furthermore, there is evidence to suggest that the activity of any self-antigen-reactive T cells that enter the periphery may be hampered by mechanisms of peripheral tolerance induction including clonal deletion (Rocha and von Boehmer 1991), suppression by regulatory T cells (Tregs) (Wing et al. 2008), or anergy (Ramsdell and Fowlkes 1992; Willimsky and Blankenstein 2005).

1.7.2c Which antigens are recognised in human cancers?

With the aim of generating an effective cancer therapy, significant effort has been devoted to the identification of tumour-associated antigens (TAAs) recognised by anti-tumour $CD8^+$ T cells that are shared between individuals. Unfortunately, the majority of these TAAs are non-mutated self-antigens (Rosenberg 2001). Some of the common TAAs dealt with in this thesis are summarised in Table 1.2. However, for the reasons described in the previous paragraph, the endogenous T cell repertoire responding to these antigens is likely to be small in size and activity (Romieu et al. 1998). Consequently, a number of therapeutic approaches have been investigated and developed to address this major issue (Section 1.8).

TAA name:	**Description:**
gp100	A melanocyte differentiation antigen (Adema et al. 1993; Cox et al. 1994).
MAGE-A3	A cancer testis antigen expressed by a wide variety of tumours (Celis et al. 1994; Gaugler et al. 1994).
Melan-A/ MART-1	A lineage-specific antigen expressed by a large proportion of primary and metastatic melanomas (Coulie et al. 1994; Kawakami et al. 1994).
NY-ESO-1	A cancer testis antigen expressed in multiple myeloma, melanoma and a range of other cancers (Chen et al. 1997)

Table 1.2: Four commonly targeted tumour-associated antigens (TAAs).

1.8 Current strategies for manipulation of immune system for targeting disease

1.8.1 Vaccination

Vaccination represents the most cost-effective and successful approach for the prevention of infectious diseases, and is second only to sanitation in terms of the estimated number of lives it has saved. Since the advent of widespread vaccination, the incidence of many diseases such as measles, mumps, diphtheria, poliomyelitis and rubella has dropped significantly. The greatest triumph of vaccination has been the global eradication of smallpox. In the sixteenth century, before Jenner's discovery of vaccination, smallpox was a lethal disease, as widespread as cancer or heart disease are in modern times, but with the difference that the majority of its victims were infants and young children. No endemic cases of the disease have been reported since 1980. Therefore, due entirely to the success of vaccination, smallpox is a disease of the past.

The purpose of vaccines is to prime the recipient's immune response (hence an alternative name for vaccination is immunisation) in order to generate immunological memory in the form of memory T cells. If successful, vaccination will elicit a heightened, more effective immune response on re-exposure to a specific antigen. There are two categories of vaccines: i) prophylactic vaccines, which are administered prior to the exposure to pathogen and aim to offer protective immunity (eg. smallpox vaccine); and, ii) therapeutic vaccines, which are administered following disease diagnosis, and aim to increase the frequency of antigen-specific T cells targeting antigens associated with the disease (eg. cancer vaccines). Over the years, several vaccination strategies have been developed, which use different forms of immunising agent: i) whole organism (attenuated live/dead); ii) purified (subunit) antigen; iii) recombinant antigen; iv) synthetic peptide; v) recombinant vector; and, vi) DNA derived from the pathogen. All these approaches have one thing in common: they elicit a specific immune response to the immunising agent without causing the disease they are designed to prevent.

Despite the fact that vaccination is the most successful medical intervention ever developed, there are two areas where vaccines are not yet particularly effective: i) pathogens of variable antigenicity (such as HIV); and, ii) cancer.

1.8.1a Vaccines targeting pathogens of variable antigenicity (specifically HIV)

Prophylactic vaccination represent the most cost-effective and successful approach for the prevention of infectious disease. However, vaccination against pathogens of variable antigenicity such as HBV (Michel et al. 2001), HCV (Leroux-Roels et al. 2005), and HIV (Oxenius et al. 2002a), has not been entirely promising. Developing a vaccine against a pathogen of variable antigenicity like HIV is problematic. As described in section 1.7.1a, HIV is a retrovirus, capable of undergoing rapid mutagenesis to evade from the immune response. Selecting a suitable antigen for immunisation against this virus presents a veritable challenge. The gravity of the situation is illustrated by the fact that a recent clinical trial conducted in Thailand was hailed as promising after eliciting a mere 30% reduction in HIV infection. Such a low level of efficiency is clearly unacceptable, and there is currently no publicly available vaccine against HIV (Vaccari et al. 2010).

1.8.1b Cancer vaccines

Although a handful of successful cancer vaccines exist, these typically target tumours that have been induced as a result of viral infection: Hepatitis B vaccine (Maugh 1981) and very recently, the human papillomavirus (HPV) vaccine (Frazer et al. 2010). The expression of viral antigens on the surface of these virally-induced tumour cells easily distinguishes them from healthy cells. However, the majority of cancer vaccines fail to induce an effective anti-tumour immune responses. An extensive survey summarising the results of cancer vaccination trials showed that a mere 3% of >600 patients enrolled showed an objective response to the vaccination regimens (Rosenberg et al. 2004). This response rate is within the range for spontaneous remissions. A major reason for the failure of cancer vaccination is the limited repertoire of T cells capable of responding to the tumour antigens concerned (Kisielow et al. 1988). Anti-tumour vaccines are typically designed around epitopes that are over-expressed on tumours but are indistinguishable from the antigens presented by

healthy cells. Thus, any T cells specific for these antigens are likely to have undergone deletion during the process of negative selection in the thymus, or display very low affinities for the target antigen. Other causes of poor anti-cancer vaccine success include rapid degradation of target peptide antigens by proteases, possible immunosuppressive mechanisms restricting the activity of primed T cells (see section 1.7.2a), and the severely weakened immune defences in patients typically enrolled in phase I/II studies (Rosenberg et al. 2004). Improving the efficacy of anti-tumour vaccines would require the identification of TAAs that are restricted to tumour cells and are not presented by healthy tissues.

1.8.2 Adoptive T cell therapy (ACT)

The low frequency of anti-tumour T cells in the periphery has been blamed for the disappointing outcome of anti-cancer peptide vaccination trials. A sensible solution would thus involve increasing anti-tumour T cell numbers by adoptively transferring T cells of a desired specificity to a patient. Adoptive T cell therapy (ACT) aims to do just that, and works by providing an individual with mature antigen-responsive allogeneic or autologous T cell subsets, with the hope that the infused cells would eliminate a tumour or pathogen and prevent its reoccurrence. Figure 1.5 A summarises the main steps involved in the adoptive transfer of lymphocytes.

Primary $CD8^+$ T cells have been selected as the cells of choice for adoptive therapy for their cytotoxicity, and the fact that unlike other cytolytic cell subsets they display a high degree of specificity by recognising antigen in the form of peptide-MHC class I. There are a number of protocols for obtaining $CD8^+$ T cells specific for a desired cancer or viral antigen. The preferred sources of cancer antigen-specific T cell are peripheral blood or tumour specimens, the latter are often enriched for tumour-infiltrating lymphocytes (TILs). Because many patients are already primed to their tumours, the main challenge is improving the quantity and quality of the desired T cell subset (Germeau et al. 2005). The use of pMHC multimers for the *ex vivo* isolation of antigen-specific T cells using fluorescence cell sorting is by far the most effective means of obtaining a pure population of effector cells of a desired specificity. Once isolated, the T cells are expanded using microbeads coated with anti-CD3

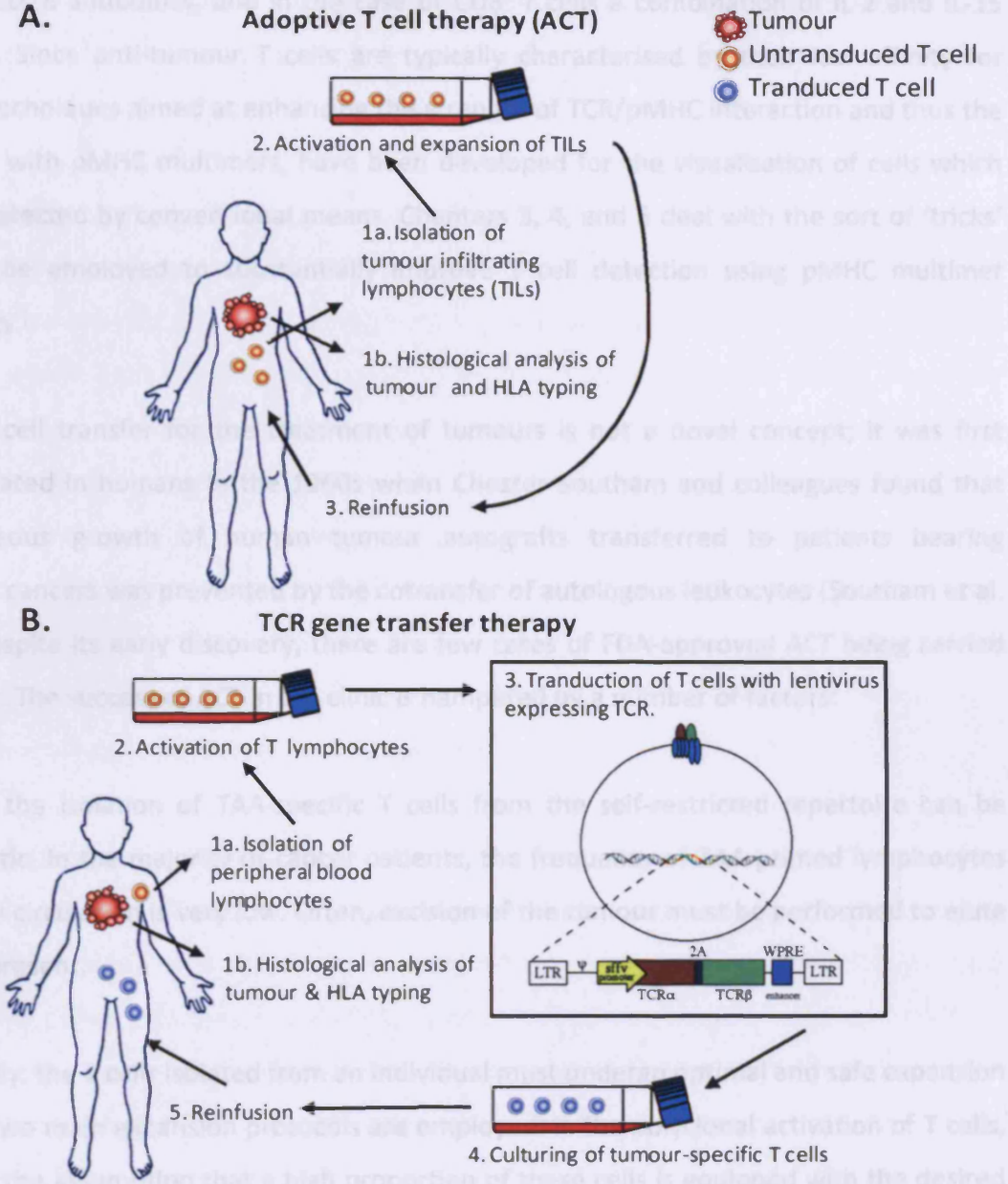

Figure 1.5: Two variations of T cell-mediated immunotherapy. Although the figure illustrates a scheme for tumour eradication, the same procedures are applicable to the treatment of viral disease.

and anti-CD28 antibodies, and in the case of $CD8^+$ T cells a combination of IL-2 and IL-15 cytokines. Since anti-tumour T cells are typically characterised by their low affinity for antigen, techniques aimed at enhancing the strength of TCR/pMHC interaction and thus the detection with pMHC multimers, have been developed for the visualisation of cells which are not detected by conventional means. Chapters 3, 4, and 5 deal with the sort of 'tricks' that can be employed to substantially improve T cell detection using pMHC multimer technology.

Adoptive cell transfer for the treatment of tumours is not a novel concept; it was first demonstrated in humans in the 1960s when Chester Southam and colleagues found that subcutaneous growth of human tumour autografts transferred to patients bearing advanced cancers was prevented by the cotransfer of autologous leukocytes (Southam et al. 1966). Despite its early discovery, there are few cases of FDA-approved ACT being carried out today. The success of ACT in the clinic is hampered by a number of factors:

i) Firstly, the isolation of TAA-specific T cells from the self-restricted repertoire can be problematic. In the majority of cancer patients, the frequency of TAA-primed lymphocytes present in circulation is very low. Often, excision of the tumour must be performed to elute any TILs present.

ii) Secondly, the T cells isolated from an individual must undergo optimal and safe expansion *in vitro*. Two main expansion protocols are employed: i) The polyclonal activation of T cells, based on the assumption that a high proportion of these cells is equipped with the desired TAA specificities; and, ii) The clonal expansion of cells. Although this second approach guarantees antigen specificity without the possibility of coinfusion of hindering regulatory and immunosuppressive T cell subsets, it suffers from being costly and labour-intensive. Following observations that many cancer patients exhibit a substantial T cell response to their tumours, the more rapid cost-effective polyclonal expansion approach has been adopted when conducting randomised clinical trials (Rapoport et al. 2005). This polyclonal

approach is also favoured from an ethical perspective, since it ensures that the treatment is given to all patients and not just the minority that have tumour-reactive TILs.

iii) Thirdly, the ability of a $CD8^+$ T cell clone to expand in culture and respond to a given antigen *in vitro* does not guarantee its success at fighting tumours and infection *in vivo*. Once infused into an individual, the $CD8^+$ T cells must not only target antigen specifically, but also retain effector function, homing potential and persistence *in vivo*. Efforts are being made to ensure that the protocols used to expand T cells in culture retain, or where possible, improve the quality of the immune response once the cells are re-infused into the individual undergoing therapy. In addition, studies with melanoma patients have shown that chemotherapy-induced host conditioning prior to adoptive T cell transfer improves the persistence of adoptively-transferred T cells by providing them with a niche (Dudley et al. 2002; Rosenberg et al. 2004). Under these lymphopenic conditions, approximately 50% of patients receiving adoptive T cell therapy for metastatic melanoma showed reductions in their tumour burden (Rosenberg and Dudley 2004).

iv) Finally, adoptive T cell therapy relies on the presence of tumour-specific T cells within the T cell repertoire, and that these T cells are in turn functional. Since many tumour-reactive T cells are either deleted during thymic development or display pitifully weak affinities for cognate antigen, the availability of suitable T cell candidates for use in ACT is often limited. Furthermore, patients selected to receive ACT (at this early stage of its implementation) suffer from aggressive forms of cancer which become too advanced for treatment by the time sufficient numbers of T cells have been expanded for infusion.

Although I have mainly addressed ACT as an anti-cancer therapy, the same principles and drawbacks apply for the treatment of viral infections. Albeit, the biggest challenge for anti-viral ACT is the identification and isolation of $CD8^+$ T cells capable of successfully targeting viral escape mutants. Nevertheless, a number of studies have demonstrated the effectiveness of adoptive T cell therapy for the protection of bone marrow transplant patients from CMV- and EBV-mediated diseases, which are a major concern during the post-

transplant immunodeficiency period (Haque et al. 2002; Rooney et al. 1995; Walter et al. 1995). As mentioned in the previous paragraph, a limitation of conventional adoptive therapy is the time-consuming (~ 3 months) process associated with the detection, isolation and generation of substantial numbers of autologous antigen-specific $CD8^+$ T cells required to treat a patient. The aggressive nature of many lymphoproliferative disorders means that there is a high likelihood of the condition proving fatal before a treatment is provided. An initiative led by Prof. D Crawford aims to reduce the large time gap between disease diagnosis and treatment by generating a T cell bank comprising hundreds of EBV- and CMV-specific $CD8^+$ T cell lines derived from a wide range of donors with varied HLA profiles. The cell bank ensures that suitable numbers of allogeneic partly HLA-matched $CD8^+$ T cells are readily available for treatment. Adoptive transfer of these antigen-specific banked $CD8^+$ T cells has thus far shown considerable success in the treatment of EBV-associated malignant disorders including CNS lymphomas (Haque et al. 2007; Haque et al. 2002; Wynn et al. 2005).

1.8.3 TCR gene transfer therapy

Given the limitations of the endogenous T cell repertoire specific for tumour-associated antigens, and the inadequacy of anti-viral $CD8^+$ T cells in targeting certain viral escape mutants, the development of adoptive therapies that utilise TCR gene-modified T cells seems an attractive prospect. The concept behind TCR gene therapy is simple, stemming from the fact that the TCR is the only structure on the T cell surface that dictates antigen recognition (Rudolph et al. 2006). Subsequently, the transfer of genes encoding a particular TCR to another T cell should result in a shift in antigen specificity in the recipient cell whilst preserving its effector functions. The main steps involved in TCR gene therapy are outlined in Figure 1.5 B. The proof of principle that the transfer of TCR genes is sufficient to endow recipient T cells with the specificity of donor cells was first shown by Steinmetz and colleagues in 1986 (Dembic et al. 1986). The authors used a cosmid vector to deliver the α and β TCR genes to a cytotoxic T cell hybridoma by means of protoplast fusion. Since this exciting discovery, TCR gene transfer has seen some significant developments: addressing the quality of TCR genes, the various TCR gene delivery methods used, and the efficiency of

exogenous TCR expression on the surface of recipient T cells. These developments are described in more detail in Chapter 6 of this thesis.

1.8.3a Potential risks associated with TCR gene transfer

General risks associated with retroviral vectors

The introduction of a live virus into host cells raises serious issues with regard to safety, especially in cases where the virus is used as a vector for the introduction of therapeutic genes, such as T cell receptors in TCR gene transfer therapy. A theoretical safety concern during vector production is that a replication competent retrovirus (RCR) is generated. This can happen if recombination takes place between the main retroviral vector and genomes of packaging plasmids or the host cell (Temin 1990). The probability of this depends upon the amount of nucleotide sequence homology between the vector and other retroviral or cellular sequences. Measures to reduce the likelihood of RCR formation include separation of the *trans*-acting and *cis*-acting elements required for viral assembly and replication on separate plasmids, and reducing the amount of sequence homology among the constructs.

The ability of retroviruses to integrate into the host genome also raises the probability of insertional mutagenesis and malignant transformation if the promoter elements of the virus become suddenly flanked by genes involved in growth control. The dangers of such an event were illustrated by a study in which 2 out of 10 children receiving retroviral vector therapy for an inherited metabolic disorder went on to develop T cell leukaemia as a consequence of the treatment (Hacein-Bey-Abina et al. 2008; Hacein-Bey-Abina et al. 2003). The introduction of self-inactivating vectors, and a transition to using vectors derived from non-oncogenic lentiviruses with low mitotic indexes has greatly reduced the probability of this happening again (Anson and Fuller 2003).

Specific risks for TCR gene transfer: TCR chain mispairing

A potential problem that arises from the introduction of a T cell receptor into T cells that already express their own native TCR is the mispairing of the endogenous TCR α and β chains with the exogenous TCR α and β chains. If this occurs, a single T cell can theoretically express a total of four different TCRs: native, exogenous, and two mispaired variants. Since

TCRs have to compete for available CD3 molecules for expression at the cell surface, the formation of mispaired TCRs can reduce the expression of relevant TCR αβ heterodimers, resulting in insufficient function of transduced T cells. The generation of TCRs with novel and unknown specificities through chain mispairing carries a potential risk of some of these TCRs being autoreactive. The dangers of TCR mispairing have not as yet been fully assessed, with some groups reporting associated pathology (Bendle et al. 2009; Bendle et al. 2010; van Loenen et al. 2010), whilst others observing no adverse effects (Johnson et al. 2009; Morgan et al. 2006; Robbins et al. 2011). Several strategies have been developed to reduce the level of mispairing and enhance the association of exogenous TCRs with CD3 molecules. Boulter *et al.* engineered a means of encouraging exogenous TCR α and β chains to preferentially pair with each other by mutating defined residues in the constant regions to cysteines, which can participate in the formation of an additional disulphide bond between the transduced TCR chains (Boulter et al. 2003; Cohen et al. 2007; Kuball et al. 2007). Other groups have reported improvements in TCR pairing and enhanced association with CD3 molecules by i) exchanging the human TCR constant regions for murine ones, ii) introducing retroviral vectors encoding small interfering RNA (siRNA) constructs that specifically downregulate endogenous TCR, or by iii) fusing TCR chains to CD3ζ molecules to bypass the need for endogenous CD3 (Cohen et al. 2006; Okamoto et al. 2009; Sebestyen et al. 2008). The 868 TCR used in this investigation lacks any of the above modifications but has undergone codon optimisation for enhanced expression in mammalian cells. Codon optimisation works by minimising some of the problems associated with expressing transgenes in mammalian cells, including transcriptional silencing, low mRNA half-life, alternative splicing events, premature polyadenylation and limited availability of certain tRNAs (Bradel-Tretheway et al. 2003). Altering the GC-content, modifying the secondary structure of the resultant mRNA transcript, and adapting the codon bias with respect to non-limiting tRNA pools of the mammalian cell act to increase the efficiency of transcription, stability of the transcript, and ultimately allow for a high level of protein production within the mammalian host. It is one of the aims of this chapter to determine the extent of TCR chain mispairing when a codon-optimised 868 TCR is transduced into primary $CD8^+$ T lymphocytes.

1.8.3b Advantages of TCR gene transfer therapy over ACT

TCR gene transfer therapy offers several important advantages over adoptive T cell therapy:

i) Firstly, TCR gene therapy is substantially more rapid. If a TCR specific for a particular antigen is known, its genes can be delivered to autologous T cells (derived from the individual receiving the therapy) and the cells expanded in a matter of days.

ii) Secondly, the T cells with the desired specificities may not be naturally present in the T cell repertoire. The potential of introducing TCR genes into T cells, thus endowing them with new specificities represents an attractive solution.

iii) Thirdly, TCR gene therapy offers the prospect of modifying TCRs (in terms of affinity, expression levels, signalling and TCR chain pairing), and thus the functionality of the recipient T cell population.

TCR gene transfer therapy is particularly important in tumour immunology, where the available tumour-reactive T cell repertoire is weakened by thymic selection. Three different approaches can be employed to ensure that the TCRs used for TCR gene transfer have a sufficiently high affinity for the target antigen: i) using xenoreactive TCRs that contain murine sequence elements; ii) using alloreactive TCRs that have not undergone thymic selection; or, iii) subjecting TCRs derived from peripheral T cells to artificial affinity maturation procedures. The use of xenoreactive TCRs for TCR gene therapy is relatively uncommon, due to the 'foreign' nature of murine TCR regions. In contrast, a number of studies have demonstrated the successful application of TCR gene transfer for the treatment of human leukaemias by endowing T cells with a high affinity alloreactive TCR specific for an epitope of the Wilms' tumour antigen 1 (WT1) (Baird and Simmons 1997; Morris et al. 2006; Oji et al. 2003c; Oji et al. 2003b; Oji et al. 2003a). The WT1 antigen is overexpressed in a large number of human cancers but assumes normal expression levels in healthy tissues, making it a good candidate for TCR gene therapy. It will be very interesting to see how the promising results achieved with the WT1-specific alloreactive TCR in the

laboratory translate into the clinical setting. A phase I trial is currently underway to address this.

In cases where high affinity TCRs cannot be extracted naturally from the T cell repertoire either by staining with low avidity pMHC multimers or by priming with low concentrations of antigen, they must be generated artificially. Two developments have helped solve the problem of low TCR affinities: yeast and phage display techniques. Using yeast display, Holler *et al.* were able to increase the K_D of the 2C TCR over 100-fold to 9nM (Holler et al. 2000). The most effective means of generating high affinity TCRs for use in TCR gene transfer is now considered to be TCR phage display (Li et al. 2005). With this approach, TCR genes are displayed on the surface of the M13 bacteriophage, fused to the gene III of the phage. Essentially, a library of phage expressing a surface TCR gene is screened for high affinity TCR/pMHC interactions using immobilised pMHC molecules of interest. Rounds of bacterial re-infection and panning of immobilised pMHC selects for the highest affinity variants. Mutations in the highest affinity CDR sequences are then combined in a single high affinity TCR (Li et al. 2005). This process is described in more detail in section 8.1.2 of Chapter 8. Phage display has the following attributes: i) it can be applied to any TCR; ii) it does not include a mutant selection step with clonotypic antibodies (unlike yeast display); and, iii) it can be used to screen library sizes of $\geq 10^{10}$ variants. This approach has been used to improve the affinity of TCRs by a million-fold to pM affinities (Laugel et al. 2005). More recent unpublished studies have produced TCRs with affinities for cognate antigen in the fM range and that bind with half-lives > 48 hours. Several studies have demonstrated the success of high affinity TCRs generated by phage display in targeting both tumour-associated (Zhao et al. 2007) and viral (Varela-Rohena et al. 2008b) antigens *in vitro* and in murine models. The latter study, documenting how enhancing TCR affinity is beneficial to the clearance of rapidly mutating viruses such as HIV from culture, represents an international collaborative effort involving research groups from the University of Pennsylvania, and Oxford and Cardiff Universities (Varela-Rohena et al. 2008). The ultimate advantage of TCR gene therapy is that it not an entirely personalised approach, and can be used in any individual provided they carry the restricting HLA allele for a particular cognate

TCR/pMHC pair. One can envisage whole libraries of delivery vectors encoding a broad range of TCR genes being compiled to target the most common epitopes associated with cancer and viral infections.

1.8.3c Limitations of TCR gene transfer therapy over ACT

Despite sounding very promising, TCR gene therapy is without its limitations. In a clinical trial involving melanoma cancer patients, the success of conventional adoptive T cell therapy with expanded Melan-A specific TILs (~50% response rate, (Rosenberg and Dudley 2004)) was far greater than the anti-melanoma activity of the TCR-transduced lymphocytes (2/15 patients showed tumour regression, (Morgan et al. 2006)). These observations suggest that the efficiency of TCR gene therapy should be improved to achieve a better clinical outcome. The measures taken to improve the success of TCR gene therapy are discussed in Chapter 6 of this thesis. Whilst optimisation of TCR gene therapy is under way, a number of safety issues must also be considered. The introduction of TCR specificities that lie outside the normal T cell repertoire have the potential to cause autoimmunity. New unknown specificities can theoretically be generated by the mispairing of the introduced and endogenous TCR chains. Although evidence of autoimmunity arising from TCR mispairing has been difficult to produce, a recent murine study has shown some cause for concern (Bendle et al. 2010). A further risk of autoimmunity is posed by transfer of a TCR which is derived from a donor with a different MHC haplotype than the recipient. In such a situation, $CD8^+$ T cells transduced with the donor TCR can potentially react towards allogeneic MHC molecules presenting self-antigen. In view of this, the compatibility between donor TCRs and recipient MHC haplotype profiles should be assessed for each individual receiving TCR gene therapy. Because enhancing the affinity of a TCR is thought to correlate with increased crossreactivity (the property of a single TCR to recognise more than one antigen) (Mason 1998), altering the affinity of a TCR must be treated with caution. The side effects associated with enhanced TCR affinity were demonstrated in a TCR gene transfer clinical trial conducted with patients undergoing treatment for melanoma (Johnson et al. 2009). During the trial period 30% of patients responded to the treatment, but a small number exhibited destruction of healthy melanocytes in the skin, eye and ear, resulting in

the conditions vitiligo, uveitis and hearing loss, respectively. Although this is an extreme and isolated case, this study highlights the importance of rigorous testing of engineered T cells in an *in vitro* setting prior to administering them to patients. It also highlights the need for the identification of TAAs that differ from the self-antigens expressed on healthy tissues. However, in comparison to induction of T cell immunity by vaccination and adoptive T cell transfer, TCR gene transfer is likely to prove itself the most useful in the clinical setting, provided any associated immunopathology issues are rapidly resolved. Periodic vaccination with peptide antigen following T cell transfer may then be relied upon for enhancing the beneficial immune response.

1.8.4 Chimeric Antigen Receptors (CARs)

As described in the previous section, TCR gene transfer therapy has shown considerable promise in redirecting immune recognition to target tumours and virally-infected cells. However, the use of TCRs is this context is limited by a number of factors, namely; i) the requirement for an antigen-restricting HLA allele; ii) the downregulation of pMHCI complexes from the surface of the tumour or virally infected targets; and, iii) the difficulty of finding suitable antigens for TCR recognition. The use of chimeric antigen receptors (CARs) represents an alternative approach to targeted immune therapy, and promises to bypass some of these problems. The concept of CARs originated in the 1980s, when Professor Zelig Eshhar's group first demonstrated that the functional redirection of a T cell to a protein antigen could be achieved by the expression of a receptor consisting of a protein-binding domain fused to a T cell signalling molecule (Gross et al. 1989). The archetypal CAR consists of a single-chain antibody fragment (scFv) capable of binding antigen, fused (either directly or via a spacer) to a component of the T cell receptor complex, which on antigen binding primes the engrafted T cell for cytotoxic activity. The combination of various extracellular, transmembrane and signalling domains has lead to the development of a multitude of different CARs. There appears to be little reported rational strategies for CAR structure design, with many groups simply opting for their favourite structural and functional components. Table 1.4 contains examples of various CAR

structures that have been developed to date, and highlights the preference for CD3ζ, (primarily due to the large number of ITAMs) and FcεRIγ as signalling domains.

1.8.4a Advantages and disadvantages of CAR versus TCR immunotherapy

The use of CARs in immunotherapy has a number of advantages over the use of TCRs. Firstly, the CAR approach bypasses the need for MHC restriction, meaning it is more generic and applicable in all patients, not just those harbouring a particular HLA allele. Secondly, CARs overcome the clever defences of tumours and viruses that can escape from TCR-mediated recognition through the downregulation of MHCI expression (see sections 1.7.1 and 1.7.2). Thirdly, many CAR structures are manufactured using antibody technology, and thus are able to target any antigen for which an antibody is available, thus bypassing the need for MHC-associated antigen. However, the recognition of surface proteins rather than processed peptide carries associated risks. This is especially true for tumour recognition, where the degree of tumour specificity and relative expression of target antigen on normal tissue may be a source of toxicity. A recent *in vivo* murine study reported that T cells engrafted with a CD19-specific CAR bearing a CD3ζ signalling domain resulted in considerable depletion of healthy B cells (Cheadle et al. 2009). Efforts are currently underway to quantify the level of off-target toxicity that is acceptable for CAR-based immunotherapy, and limit damage to healthy tissues accordingly. A further advantage of CARs over TCRs is that they carry their own signalling domains and therefore do not rely on the interaction with components of the CD3 complex for cell surface expression and function. As a result, CARs can be delivered into cells other than T cells, harnessing their different effector functions. Although the development of non-T cell CAR therapy is still at a relatively early stage, a number of studies have successfully demonstrated the suitability of CARs for the transduction of NK cells. Primary $CD3^{-}CD56^{+}$ human NK cells transduced with a retroviral vector encoding a Neu/HER2-specific CD3ζCD28 receptor showed redirected function against cell lines presenting cognate antigen *in vitro* and in short term *in vivo* assays (Kruschinski et al. 2008). NK cells have also been shown to be permissive to RNA-based electroporation with a CD19-specific CAR, following which they gained specificity for transformed B cells (Li et al. 2009). In summary, over twenty years of research has seen the

transfer of CARs into the clinical setting with CAR-transduced T cells now reported in completed trials for the treatment of HIV (Mitsuyasu et al. 2000) and cancer (Kershaw et al. 2006). Going head to head with TCR-based therapies, it remains to be seen whether CARs offer an overall therapeutic advantage in the long term.

Antigen Specificity	Spacer	Transmembrane Domain	Signalling domain	Reference
CEA	-	CD3ζ	CD3ζ	(Gilham et al. 2002)
Neu/HER2	-	CD3ζ	CD3ζ	(Stancovski et al. 1993)
gp120	CD8	CD3ζ	CD3ζ	(Patel et al. 1999)
gp100	CD8	CD8	CD3ζ	(Masiero et al. 2005)
CD19	-	CD3ζ	CD3ζ	(Cheadle et al. 2009)
OKT8	CD8	CD8	CD3ζ (mutated)	(Chae et al. 2004)
TCR	-	H2-Kb	CD3ζ (mutated)	(Geiger et al. 2001)
CEA	-	CD3ε	CD3ε	(Nolan et al. 1999)
DAP10	CD19	CD8	DAP10	(Marin et al. 2007)
CEA	hIgG	FcεRIγ	FcεRIγ	(Heuser et al. 2003)
CEA	hIgG1	FcεRIγ	FcεRIγ	(Hombach et al. 2007)
CEA	CD8	FcεRIγ	FcεRIγ	(Haynes et al. 2001)
Neu/HER2	-	FcεRIγ	FcεRIγ	(Eshhar et al. 1993)
CEA	hIgG1	FcγRI	FcγRI	(Biglari et al. 2006)
TCR	-	H2-Kb	CD3ζLck	(Geiger et al. 2001)
TNP	-	CD4 or CD8	Syk	(Fitzer-Attas et al. 1998)
TNP	-	CD4 or CD8	ZAP-70	(Fitzer-Attas et al. 1998)

Table 1.4: Examples of Chimeric Antigen Receptors (CARs).

1.9 Aims of the thesis

The work contained within this thesis aims to explore diagnostic and therapeutic uses of optimised interactions between peptide-Major Histocompatibility complex (pMHC) molecules and the T cell receptor (TCR) and/or coreceptor that engages them. Specifically, I aimed to:

1) Experiment with a number of 'tricks' to improve the detection of T cells using soluble pMHC multimers;

2) Explore the use of TCRs in TCR gene transfer;

3) Investigate the role of glycosylation in antigen recognition by the TCR and,

4) To assess the therapeutic potential of novel reagents based on high affinity soluble TCRs.

Chapter 2

2

MATERIALS AND METHODS

2.1 Reagents and consumables

2.1.1 Antibodies

2.1.1a Activating antibodies

Anti-CD3 and anti-CD28 unconjugated antibodies were purchased from Pharmingen, BD Biosciences (San Jose, CA).

2.1.1b Fluorescent conjugated anti-human antibodies for detection of cell surface protein expression

Anti-CD3$^{FITC,\ PerCP,\ PECy7}$, anti-CD4$^{FITC,\ PE,\ Cy\text{-}5PE\ PerCPCy5.5,\ APC}$, anti-CD8$^{FITC,\ PE,\ PerCP,\ APC,\ Q\text{-}705}$, anti-TCRαβ$^{FITC,\ PE}$, pan-TCRγδ^{PE}, anti-CD25$^{PE,\ APC}$, anti-CD69$^{FITC,\ APCCy7,\ APC}$, anti-CD19$^{APC,\ APCCy7}$, anti-CD28^{APC}, anti-CD45RA$^{PE,\ PECy7}$, anti-CD45RO$^{ECD\ (Texas\ Red)}$, anti-CCR7^{PECy7}, anti-CD107a^{FITC}, Vivid$^{Pacific\ Blue}$ and Viaprobe^{TM} were purchased from Pharmingen, BD Biosciences (San Jose, CA). Anti-HLA-A2 BB7.2 was purchased from Serotec (Oxford, U.K.). The panel of anti-TCR Vβ$^{FITC,\ PE}$ antibodies (Appendix 5 for a full list) was purchased from Beckman Coulter and Immunotech Coulter (Fullerton, CA). The anti-TCR Vβ5 (a)^{FITC} and anti-TCR Vα2^{FITC} were purchased from Thermo Fisher Scientific.

2.1.2 Cellular dyes

Carboxyfluorescein diacetate Succinimydyl Ester (CFSE)

CFSE powder was purchased from Invitrogen and suspended in ddH_2O to give a 10 mM stock solution, which was sterile filtered, dispensed in to 10 µl aliquots and stored at -20°C. Aliquots were thawed once and not re-frozen.

2.1.3 Peptides

Peptides used in the study were HLA A2 restricted and prepared to >95% purity (for pMHC tetramer refolds) or 50% purity (crude fragments for all other readouts) by PepScan (Netherlands). All peptides were received in powder form and dissolved in DMSO, prior to dilution in RPMI medium to the desired concentration. Peptides were pulsed onto target

cells (all assays apart from ELISpot) by incubating 10^6 CIR cells in 1 ml of R10 media (see section 2.1.5 below) with peptide, for a minimum of 1 hour at 37°C, 5% CO_2.

2.1.4 Protein kinase inhibitors (PKIs)

2.1.4a Dasatinib

N-(2-Chloro-6-methyl-phenyl)-2-(6-(4-(2-hydroxyethyl)-piperazin-1-yl)-2-methylpyrimidin-4-ylamino) thiazole-5-carboxamide (BMS-354825) alternatively known as dasatinib was synthesized as described previously (Lombardo et al. 2004). Biological activity was tested in a cell death titration assay on BA/F3 bcr-abl cells as described in (Magnusson et al. 2002). Dasatinib was dissolved in DMSO to a concentration of 1 mM, and stored in aliquots at -20°C. Once thawed, these stocks were stored at 4°C and used within 3-4 days of thawing as the reagent had a limited stability at this temperature. The 1 mM DMSO stock was diluted 1/10,000 in PBS on the day of experimentation to achieve a working solution of 100 nM. Subsequent 1/2 dilution in cellular assays yielded a final concentration of 50 nM, which was the standard concentration used unless stated otherwise.

2.1.4b Other PKIs

Staurosporine was purchased from Biomol (Exeter, U.K.). Lck inhibitor II, genestein, herbimycin A, PP2 and PP3 were all purchased from Calbiochem (San Diego, CA). The PKIs were dissolved in DMSO and stored at -20°C, prior to being diluted in PBS and tested in assays at concentrations of 1 nM, 3 nM, 5 nM, 10 nM, 20 nM, 100 nM, 250 nM, 500 nM, and 1 μM.

2.1.5 Cell culture media and associated reagents

2.1.5a PSG media (Penicillin, Streptomycin, Glutamine)

Roswell Park Memorial Institute medium-1640 (RPMI-1640) supplemented with 2 mM L-glutamine, 100 units/ml penicillin, and 100 μg/ml streptomycin.

2.1.5b R10 media

PSG supplemented with 10% heat inactivated (at 56°C for 1 hour) foetal calf serum (FCS; Sigma Aldrich, Poole, U.K., and PAA Laboratories Limited, Pasching, Austria).

2.5.1c CK media

R10 supplemented with 2.5% Cellkines (Helvetica Healthcare, Geneva), 200 IU/ml IL-2 (Pharmacy) and 25 ng/ml IL-15 (PeproTech, London, U.K.).

2.5.1d 293 T cell culture media (DMEM-10)

Dulbecco modified Eagle's minimal essential media (DMEM), supplemented with 2 mM L-glutamine, 100 units/ml penicillin, 100 μg/ml streptomycin, 1% sodium pyruvate, and 10% heat inactivated FCS.

2.5.1e Freezer mix

PSG supplemented with 10% sterile domethyl sulfoxide (DMSO; Sigma Aldrich, Poole, U.K.) and 50% FCS, passed through a 0.2 μ filter.

RPMI-1640, DMEM, phosphate buffer saline (PBS), L-glutamine, penicillin, streptomycin, sodium pyruvate, and 0.5% trypsin in HBSS were purchased from Gibco, Invitrogen (Paisley, U.K.).

2.1.6 Bacterial plasmids

The pUC19 plasmid used for all the cloning steps prior to transfer into a lentiviral vector originates from the University of California and can be purchased commercially from a number of suppliers (eg. NEB, Sigma). The plasmid was modified in my laboratory by insertion of a restriction cassette for shuttling TCR alpha and beta fragment in and out of the plasmid. A TCR alpha chain sequence was inserted via Xba I and Xho I restriction enzymes, while the TCR beta chain sequence was Kpn I and Not I restriction enzymes. The pUC19 vector was further modified by insertion of a 2A peptide-encoding sequence and a SGSG spacer sequence in between the insertion sites for TCR alpha and beta genes

(Appendix 1 C). A schematic of the modified pUC19 x-SGSG-2A-γ shuttle vector can be found in Chapter 6 of this thesis (Figure 6.5).

2.1.7 Viral vector and packaging plasmids

The Lenti-SxW lentiviral vector and the packaging plasmids pMD.2G and pΔ8.91 were kindly donated by Qasim Waseem (Molecular Immunology Unit, UCL, London) and are fully documented in (Demaison et al. 2002).

2.2 Mammalian cell lines and clones

2.2.1 Human $CD8^+$ T cell lines

Blood from HLA A*0201 (HLA A2 from hereon) positive donors was used to generate $CD8^+$ T cell lines. $CD8^+$ T cells were initially stimulated by exposure to peptide-pulsed autologous peripheral blood mononuclear cells (PBMCs). $CD8^+$ T cell lines specific for the human telomerase reverse transcriptase $(hTERT)_{540\text{-}548}$ (ILAKFLHWL) and Melan-$A_{26\text{-}35}$ (ELAGIGILTV) epitopes, both restricted by HLA A2, were generated by pulsing $6x10^6$ PBMC from an HLA A2 individual with cognate peptide at concentrations of 1 μM and 100 μM respectively, for 1 hour at 37°C. Cells were subsequently washed and resuspended in R10 only. After 3 days, increasing amounts of Interleukin-2 (IL-2) were gradually added to the media, reaching a maximum concentration of 20 IU/ml by day 14. Expansion of antigen specific $CD8^+$ T cells was assessed by FACS staining with cognate peptide/HLA A2 tetramers and anti-CD8 antibody conjugated to a fluorochrome, as well as by Interferon-γ (IFNγ) enzyme linked immunospot (ELISpot) (section 2.11.1).

2.2.2 Human $CD8^+$ T cell clones

The ILA1 $CD8^+$ T cell clone is specific for the HLA A2 restricted human telomerase reverse transcriptase (hTERT) epitope ILAKFLHWL ($hTERT_{540\text{-}548}$). Mel13 and Mel5 $CD8^+$ T cell clones are specific for the HLA A2 restricted Melan-$A_{26\text{-}35}$ epitope ELAGIGILTV. 3F2 $CD8^+$ T cell clone recognises the HLA A2-restricted epitope of the preproinsulin ($PPI_{15\text{-}24}$; ALWGPDPAAA) antigen, called ALW. $CD8^+$ T cell lines responding to the three epitopes mentioned were

initially expanded by exposure to peptide-pulsed autologous PBMC in R10 and then further stimulated with mixed irradiated allogeneic feeder PBMC from three unrelated donors in PSG media supplemented with foetal calf serum and antibiotics together with phytohemaglutinin (PHA) (4 μg/ml) and T-STIM (10%; BD Biosciences) or Cellkines (2.5%; Helvetica Healthcare, Geneva) instead of T-STIM for clone 3F2. ILA1, Mel13, Mel5 and 3F2 clones were all generated by limiting dilution culture from the peptide-specific T cells lines (section 2.3.5).

2.2.3 Culture of human $CD8^+$ T cell lines and clones

$CD8^+$ T cells were grown from cryopreserved stocks in 24-well tissue culture plates in CK media for two weeks following restimulation using 5 μg/ml PHA with $5x10^6$ irradiated allogeneic PBMC in 2 ml of media per well of a 24 well tissue culture plate. Following this, the cells were maintained in CK media for several months without the need for restimulation with antigen and/or irradiated autologous PBMC feeders. $CD8^+$ T cell clones maintained and cultured in the presence of IL-15 for three months exhibited an identical activation profile in terms of early tyrosine phosphorylation events and effector function (specific lysis of antigen-bearing target cells, production of macrophage inflammatory protein 1β (MIP-1β) and IFNγ) to $CD8^+$ T cells maintained in media supplemented with IL-2 alone.

2.2.4 Human $CD4^+$ T cell lines and clones

The $CD4^+$ T cell clone (Flu2-5) specific for the HLA DR*0101-restricted influenza virus A $HA_{307-319}$ epitope PKYVKQNTLKLAT (PKY) was kindly donated by A. Godkin (Cardiff University, Cardiff). The JF-HA $CD4^+$ T cell line specific for the same Flu epitope was kindly donated by T. Scriba (Oxford University, Oxford). The $CD4^+$ T cell lines and clones were cultured in the same way as $CD8^+$ T cells with the exception that no Cellkines were added to the culture media.

2.2.5 Other cell types

2.2.5a Stable HLA A2-expressing C1R B cell clones

Endotoxin free pcDNA3.1 mammalian expression vectors (Invitrogen) with inserts encoding either full length HLA A2 or one of the following mutants: HLA A2 DT227/8KA, HLA A245V, HLA A2 Q115E or chimeric HLA A2/Kb (where the α3 HLA A2 domain has been substituted with the α3 of murine H-2K^{b}) were generated then linearised before transfection into the C1R cell line by electroporation. The C1R cell line is a Class I negative Epstein-Barr virus (EBV) transformed B cell line cultured in R10 (Storkus et al. 1989; Messer et al. 1992). The transfected C1R cell lines were cloned by limiting dilution (section 2.3.5). The clones were then regularly tested for HLA A2 expression by staining with HLA A2 conformation specific antibody clone BB7.2 conjugated to FITC (Serotec; Oxford, U.K.), and analysed on the FACSCalibur flow cytometer. All clones showed 100% HLA A2 expression, with equal MFIs in the FL1 channel.

2.2.5b T0 cells

A CD4^{+} T cell line typically employed for the study of HIV-1 infection. T0 cells were cultured in R10 media.

2.2.5c T2 cells

A CD4^{+} T cell line typically employed for the study of HIV-1 infection and peptide binding assays. The cells are very similar to T0 cells but are deficient in TAP, and are thus only capable of exogenous peptide presentation. T2 cells were cultured in R10 media.

2.2.5d 293 T (HEK 293) lentiviral packaging cell line

The 293 T cell line was originally derived from human embryonic kidney (HEK) cells by transformation of cultured cells with sheared adenovirus-5 DNA (Graham et al. 1977) 293 T cells were chosen as the packaging cell line for the production of the lentiviral particles due to its ease of transfection. 293 T is an adhesive cell line, and was therefore cultured in specialised tissue culture flasks (T25, T75, and T175) and petri dishes (all supplied by Fisher Scientific), in 293 T cell culture media (DMEM-10). Cultures reaching 100% confluency were

removed from the tissue culture plastic by incubation with 0.5% trypsin in HBSS (Gibco, Invitrogen) washed with 293T culture media (DMEM-10) to remove the trypsin, and split every 2 days to ensure log phase growth. The passage numbers were kept low, as the lentiviral titre from 293T cells decreases after 1 month of continuous culture.

2.2.6 Cryopreservation of cells

2-10 x 10^6 lymphocytes were pelleted at 500 x g (Sorvall RT 6000D centrifuge; Dupont Instruments) for 5 minutes then resuspended in 1 ml freezer mix and transferred to a cryovial (Nunc). Cryovials were stored in polystyrene containers at -80°C for 48 hours before being transferred to liquid nitrogen containers for long term storage. When required, cell stocks were rapidly thawed at 37°C to minimize cell death, washed once in PSG to remove the DMSO, and resuspended in appropriate culture media.

2.3 Mammalian cell-based techniques

2.3.1 Counting cells with Trypan blue

An aliquot of cells was mixed with an equal volume of 0.1% Trypan blue in PBS (w/v) and loaded on to an improved Neubaur haemocytometer (Weber Scientific International Limited, Lancing, U.K.). Viable cells assuming a colourless appearance were counted at 100 times magnification on a light microscope (Olympus CK40 model).

2.3.2 Preparation of peripheral blood mononuclear cells (PBMC)

Typically 50 ml of peripheral blood was collected into a sterile 50 ml Falcon tube (BD Biosciences) containing the anti-coagulant heparin (Unihep Leo) at 1000 units/ml. PBMC were generated by Ficoll-Hypaque density gradient centrifugation. Peripheral blood was gently layered onto an equal volume of Ficoll-Hypaque solution (Lymphoprep, Nycomed) and centrifuged for 15 minutes at 733 x g (Sorvall RT 6000D centrifuge; Dupont Instruments) with the break off. The buffy coat layer was gently removed from the gradient interface using a sterile Pasteur pipette and placed in a 20 ml universal for washing. Cells were

washed twice with PSG by centrifugation at 600 x g for 10 minutes followed by 500 x g for 5 minutes (Sorvall RT 6000D centrifuge; Dupont Instruments), with maximum break. After the final wash, cells were resuspended in R10 and kept in the incubator at 37°C/5% CO_2.

2.3.3 Preparation of cord blood mononuclear cells (CBMC)

Typically 30ml of blood was collected from the umbilical cord of a newborn during an elected caesarean section. Since isolation of cord blood neutrophils had to be performed for other projects in the group, isolation of CBMC employed a different protocol from that used for standard PBMC isolation. Following blood collection, 5 ml of anti-coagulant and calcium-chelator sodium citrate (Martindale Pharma) was added to 30ml of blood, and centrifuged at 500 x g (Sorvall RT 6000D centrifuge; Dupont Instruments) for 20 minutes at RT with no break. All plasma was then gently removed with a Pasteur pipette and placed into a 15 ml falcon tube, before being centrifuged at 833 x g (Sorvall RT 6000D centrifuge; Dupont Instruments) for 20 minutes at RT to give platelet-poor plasma (PPP). PPP and 90% Percoll (Sigma-Aldrich) 10% saline (Sigma-Aldrich) were used make up the gradient in a 15 ml falcon tube:

42%- 0.84 ml 90% Percoll + 1.16 ml PPP (top layer)
51%- 1.02 ml 90% Percoll + 0.98 ml PPP (bottom layer)

Meanwhile, 6 ml of dextran (Pharmacosmos, Holbaek, Denmark) was added to the sodium citrate layer, before making the volume up to the original 30 ml with warm (37°C) saline (Sigma-Aldrich, Poole, U.K.). The cell/saline mixture was left to incubate for 30 minutes in a water bath set to 37°C. The uppermost cell-rich layer was aspirated and centrifuged at 500 x g (Sorvall RT 6000D centrifuge; Dupont Instruments) for 6 minutes at RT, before being resuspended in 2 ml PPP and gently layered onto the Percoll-PPP gradient. The loaded gradient was centrifuged at 433 x g (Sorvall RT 6000D centrifuge; Dupont Instruments) for 13 minutes at RT with no break. The neutrophil (lower layer) and lymphocyte (upper layer) were collected using a Pasteur pipette, washed in PSG, and resuspended in appropriate media. To increase the yield of this procedure, which is not optimal for lymphocyte

isolation, the remaining volume of Percoll-PPP-cell mixture was again separated using the standard lymphocyte isolation protocol (section 2.3.2).

2.3.4 MACS bead isolation

For positive $CD8^+$ T cell selection: 10^7 cells were resuspended in 80 µl of chilled MACS buffer (PBS, 0.5% FCS, 2 mM EDTA; filtered), to which 20 µl anti-CD8 antibody coated microbeads (Miltenyi Biotech) were added. The cells and beads were agitated together for 15 minutes at 4°C. The mixture was washed by adding 1-2 ml MACS buffer and centrifugation at 300 x g for 10 minutes (Sorvall RT 6000D centrifuge; Dupont Instruments). The supernatant was aspirated and the cells resuspended in 500 µl of MACS buffer and administered to a 25 ms MACS separation column (Miltenyi Biotech) equilibrated with 500 µl MACS buffer, held in a MACS magnet (MACS). The CD8 negative cells passed through the column and were discarded with the flow through, or used as feeder cells after irradiation. The column was washed by running 3 x 500 µl MACS buffer through it, and the $CD8^+$ T cells were eluted by application of 1 ml MACS buffer and a plunger. The $CD8^+$ T cells were isolated with 99% purity. This protocol also applies to $CD4^+$, $CD25^+$ selection for isolation of $CD4^+$ T cells and Tregs from PBMC, however the latter procedure also involved an initial depletion of $CD4^-$, $CD127^{Lo}$ cells.

For the anti-Fluorescein isothiocyanate (FITC)/anti-Phycoerythrin (PE) isolations: The protocol was identical to the one above except for the cells being stained with a particular antibody (or pMHCI tetramer) conjugated to FITC or PE fluorochromes, and the beads were coated with anti-FITC and anti-PE secondary antibodies.

2.3.5 Generation of human $CD8^+$ T cell clones by limiting dilution

Cloning mix consisting of $2x10^6$ PBMCs and $2x10^5$ peptide-pulsed allogeneic B cells per ml of R10, supplemented with 10% T-STIM (BD Biosciences) or 2.5% Cellkines (Helvetica Healthcare, Geneva) and 200 IU/ml IL-2 was made and γ-irradiated (30Gy). Cells to be cloned were added to the cloning mix at a concentration of 1 cell per 600 µl mix, then plated out at 200 µl per well of a round-bottom 96 well plate (i.e. 0.3 cells per well). Control

wells at 10 and 100 cells per well were also set up. Plates were cultured at 37°C/5% CO_2 and after 14-21 days examined for clones. Clones were re-stimulated as necessary, transferring them first to a 48 well plate, then at a second restimulation to a 24 well plate. Since the discontinuation of T-STIM in 2007, all $CD8^+$ T cell clones and lines were subsequently cultured in CK media.

2.4 Bacterial cell-based techniques

2.4.1 Bacterial culture media and strains

2.4.1a LB low salt media

1% Bacto-tryptone (Difco), 0.5% NaCl (Sigma Aldrich), 0.5% yeast extract (Difco).

2.4.1b TYP media

1.6% yeast extract (Difco), 1.6% Bacto-tryptone (Difco), 0.5% NaCl, 0.25% K_2 HPO_4 (Sigma Aldrich).

All media was autoclaved on a liquid cycle at 121°C for 60 minutes, and supplemented with 100 μg/ml ampicillin/carbanicillin (Fisher Scientific) prior to use.

2.4.1c Agar plates

15 g Bacto-agar/litre (Fisher Scientific) supplemented with 100 μg/ml ampicillin/carbanicillin (Fisher Scientific).

2.4.1d Bacterial strains

Strain	*Description/Application*	*Antibiotic resistance*	*Supplier*
Top10	Plasmid amplification for transformation, sequencing or transfection.	Ampicillin/Carbanicillin	Invitrogen

BL21 (DE3) pLysS	High stringency expression in bacterial cell culture under the control of the T7 promoter.	Ampicillin/Carbanicillin	Invitrogen

2.4.2 Making competent bacterial cells

Bacterial cells were streaked out onto an LB agar plate and incubated overnight at 37°C. 200 ml of LB low salt media was inoculated with a single colony and grown to an OD_{600} of 0.5-0.7. Cells were pelleted by centrifugation at 1590 x g for 20 minutes in a Beckman J2-MC centrifuge with a JA 10 rotor at 4°C. The pellet was resuspended in 40 ml of ice cold TFB1 (30 mM KOAc, 50 mM $MnCl_2$, 100 mM KCl pH5.8, 10 mM $CaCl_2$, and 15% v/v glycerol). After pelleting by centrifugation as above, the bacterial cells were resuspended in 20 ml ice cold TFB2 (10 mM Na-MOPS pH7, 75 mM $CaCl_2$, 10 mM KCl and 15% v/v glycerol). Cells were then aliquoted into pre-chilled eppendorf tubes and stored at -80°C.

2.4.3 Transformation of competent bacterial cells by heat shock method

Aliquots of competent bacteria, prepared as instructed above were thawed slowly on ice. 50-100 ng of plasmid DNA (quantified by absorbance at 260 nm) was added to 50 µl thawed competent bacteria, kept on ice for 15 minutes, before being transferred to 37°C for 2 minutes, and replaced on ice for 1 minute. Following this heat shock procedure, 100 ml of SOC media (Invitrogen) was added to the bacteria, and the mixture placed in a 37°C shaker set to 220 rpm for 30 minutes. Cells were then streaked out on LB agar plates supplemented with 100 µg/ml ampicillin/carbanicillin (Fisher Scientific) and incubated overnight at 37°C. A negative control tube containing bacteria alone was plated out for every transformation.

2.4.4 Target gene expression in bacterial cell culture

A single colony from a plate of freshly transformed BL21 bacteria was used to inoculate 50 ml of TYP media supplemented with 100 µg/ml ampicillin/carbanicillin and agitated overnight at 220 rpm, 37°C. The following morning 1 litre of TYP media (supplemented with 100 µg/ml ampicillin/carbanicillin) was inoculated with 2-5 ml of the starter culture and agitated at 37°C until the OD_{600} reached between 0.4 and 1 (ideally 0.6). A 1 ml pre-

induction sample was collected, microcentrifuged at 15600 x g (Centrifuge 5415D; Eppendorf) for 1 minute and the pellet stored at -20°C. Protein expression was induced by adding dioxin free isopropyl-1-thio-β-D-galactopyranoside (IPTG; Melford Laboratories) to make a final concentration of 0.5 mM. Flasks were agitated for a further 4-6 hours post induction. A 1 ml post-induction sample was taken and stored as for the pre-induction sample. The remaining culture was centrifuged at 1725 x g for 20 minutes at 4°C in a Beckman JE-6B centrifuge and the supernatant discarded. The bacterial pellet was either resuspended in lysis buffer for immediate inclusion body preparation (section 2.7.1), or in 10-15 ml d.H_2O and stored at -20°C.

2.5 Molecular Biology

2.5.1 DNA-based techniques

2.5.1a Mini-prep of plasmid DNA

A single transformed bacterial colony was grown overnight under agitation at 220 rpm in 5 ml LB media supplemented with 100 μg/ml ampicillin/carbanicillin at 37°C. Bacterial cells were pelleted by centrifugation at 1,333 x g (Sorvall RT 6000D centrifuge; Dupont Instruments) for 10 minutes at RT and the supernatant discarded. Plasmid DNA was extracted using a commercially available miniprep kit (Miniprep 250 kit; Qiagen) based on the alkaline lysis method. Extracted DNA was resuspended in warm (50°C) d.H_2O and stored a -20°C.

2.5.1b Maxi-prep of plasmid DNA

A single bacterial colony previously transformed with plasmid DNA was used to inoculate a starter culture of 5 ml LB media (supplemented with 100 μg/ml ampicillin/carbanicillin) and shaken for 8 hours at 220 rpm at 37°C. 0.5-2 ml of starter culture was used to inoculate 100-200 ml LB media (for high-copy plasmids) and 250-500 ml LB media (for low-copy plasmids), which was subsequently shaken overnight at 220 rpm, 37°C. The cultures were centrifuged at 1,333 x g (Sorvall RT 6000D centrifuge; Dupont Instruments) for 20 minutes at 4°C and the supernatant discarded. The bacterial pellet was treated using a commercial

endotoxin-free maxi-prep kit (Qiagen and Invitrogen) to extract the plasmid DNA. In the final step of the protocol the ethanol precipitated and dried DNA pellets were resuspended in 200-500 µl TE buffer and the concentration of eluted DNA quantified as outlined below. A maxi-prep typically yielded 700 µg of plasmid DNA.

2.5.1c Quantification of DNA

2 µl of DNA eluted following a mini- or maxi-prep procedure was diluted in 198 µl d.H_2O (milliQ). The absorbance of this solution was then measured on a spectrophotometer set to record at 260 nm wavelength. MilliQ d.H_2O was used as a blank reference. An absorbance of 1 at 260 nm was assumed to indicate a DNA concentration of 50 ng/µl (after the extinction coefficient for DNA, and the dilution factor were taken into account).

2.5.1d DNA sequencing

Sequencing was performed after each cloning step or PCR site directed mutagenesis (see sections 2.5.1f) to verify the construct. For a construct containing the final TCR alpha-2A-beta sequence, three sequencing reactions were set up:

1) To check the pUC plasmid-TCR alpha junction.
2) To check the pUC plasmid-TCR beta junction.
3) To check the alpha-2A-beta junction.

500 ng of DNA template, 1 µl forward or reverse primer (MWG) (primer stock at 25 pmol/µl), 1 µl ABI BigDye enzyme and 3 µl of the corresponding sequencing buffer, made up to a final volume of 15 µl. DNA was denatured at 95°C for 15 seconds, primers allowed to anneal at 50°C for 30 seconds, and DNA allowed to elongate at 60°C for 4 minutes for a total of 25 cycles. The sequencing reaction was cooled to 4°C before ethanol precipitation was performed (section 2.5.1e).

2.5.1e Ethanol precipitation

To the 15 µl of the sequencing PCR reaction (above), 35 µl of 100% ethanol (Sigma Aldrich) was added, and the mixture incubated at RT for 10 minutes. The reaction was centrifuged at 13,400 x g (Microcentaur, MSE) for 10 minutes and the supernatant was carefully aspirated and discarded. 50 µl of 70% ethanol was used to resuspend the DNA pellet for washing. The same centrifugation step was repeated and the supernatant again discarded. The pellet was allowed to dry before being sequence analysed at the central biotechnology services (CBS, Cardiff University) facility.

2.5.1f PCR site directed mutagenesis (PCR-SDM)

To perform site directed mutagenesis of the N-glycosylation sites on the HLA A2 restricted SL9 epitope-specific 868 TCR, the alpha-2A-beta construct was supplied in a pUC (University of California) background. Five point mutations were made in the alpha chain and two in the beta chain using oligonucleotide pairs designed to insert the desired mutation. The resulting asparagine to glutamine substitutions alleviated the target sites for enzymes involved in the N-glycosylation process. The PCR reaction (30 ng DNA template, 10 µl forward primer and 10 µl reverse primer (both at 100 pmol/µl; MWG), 1 µl 10 mM dNTPs (Promega), 1 µl Pfu polymerase (2.5 U/µl; Stratagene), 5 µl Pfu 10x buffer (Stratagene), and 22 µl d.H_2O was placed in a sterile 0.2 ml PCR tube. DNA was denatured at 95°C for 30 seconds, primers allowed to anneal at 55°C for 1 minute, and DNA allowed to elongate at 68°C for 14 minutes for a total of 25 cycles. PCR tubes were cooled by placing on ice. The DpnI endonuclease is specific for methylated and hemimethylated DNA (target sequence: 5'–Gm6ATC-3'). The parental DNA template was digested by adding 10 U DpnI endonuclease (Promega) for each tube and incubating at 37°C for 2 hours. Competent DH5α bacteria were transformed with 10 µl of the DpnI treated PCR reaction mix (section 2.5.1f) and the bacteria grown overnight at 37°C. The next day 5 colonies were randomly selected from each plate, grown overnight, and had their DNA extracted (section 2.5.1a). All the constructs were verified to contain the desired mutations by sequencing (section 2.5.1d).

2.5.2 RNA-based techniques

2.5.2a In vitro transcription (IVT)

RNA was synthesized using the mMessage mMachine T7 kit (Ambion) in line with the manufacturer's instructions. One 20 µl reaction required: 1 µg pure linear template DNA, 10 µl 2x NTP/CAP, 2 µl 10x reaction buffer, 2 µl enzyme mix, made up to 20 µl with nuclease free water. The reaction was incubated for 2.5 hours at 37°C, followed by enzyme inactivation (5 minute incubation at 70°C) and DNase treatment to remove the DNA template (15 minute incubation at 37°C with 1 µl TURBO DNase (Ambion), 30 µl nuclease free water, and 30 µl LiCl). The synthesized RNA was precipitated by centrifugation at 13,400 x g (Microcentaur, MSE) for 30 minutes at 4°C. The supernatant was removed and replaced with 1 ml of nuclease free 70% ethanol before another centrifugation step (13,400 x g for 10 minutes at 4°C). The supernatant was again discarded and the pellets dried at room temperature, and resuspended in 20 µl nuclease free water. The polyA tail was made by adding the following components to the 20 µl reaction mixture; 36 µl nuclease free water, 20 µl 5x E-PAP buffer, 10 µl 25 mM $MnCl_2$, 10 µl ATP solution, and finally 4 µl E-PAP enzyme. The 100 µl reaction incubated at 37°C for 15-20 minutes. The RNA was recovered using the RNAeasy kit (Quigen). The concentration of RNA was quantified from absorbance at 260 nm wavelength using a spectrophotometer and on an RNA TBE gel (Invitrogen), and stored at -80°C. A typical 20 µl reaction yielded 20-30 µg RNA.

2.5.2b Transient transfection (Electroporation of IVT mRNA)

Jurkat cells were adjusted to a concentration of $7.5x10^6$/ml in R10. The counted cells, 0.4 cm cuvettes (Biorad), and mRNA were pre-chilled on ice for 5 minutes prior to electroporation. 5 µg of IVT mRNA and 400 µl of cell suspension ($3x10^6$ cells) were applied to one pre-chilled cuvette, while the control cuvette contained cells only. Using the Gene Pulsar II electroporator (Biorad), the cells were electroporated at 0.270 kV and 975 µF. The electroporated cells were immediately transferred to 6 ml of pre-warmed (37°C) R10 into a well of a 6-well tissue culture plate, and incubated for 24 hours at 37°C/5% CO_2 before carrying out flow-cytometric analysis for target protein expression levels.

2.6 Lentiviral technologies

2.6.1 Viral assembly

2.6.1a Initial method[1]

The transfection reagent was prepared by mixing 150 µl $CaCl_2$ and 1300 µl dH_2O, to which the three plasmids were added in the following amounts:

pΔ8.91 15 µg

pMD2G 10 µg

pDNA (containing the construct of interest) 20 µg

The mixture of DNA and diluted 10 mM $CaCl_2$ was then added drop by drop to 1500 µl 2x HEPES pH7.1 (Calcium phosphate transfection kit, Sigma Aldrich), as it was being bubbled using a 5 ml serological pipette to encourage formation of viral particles. The solution was incubated at RT for 20 minutes.

2.6.1b method[2]

174 µl of Express-In transfection reagent (Thermo Scientific) was slowly added to 3 ml of DMEM-10/10 mM HEPES pH7.1 in a 15 ml falcon tube. The tube was inverted 4 times and incubated at RT for 20 minutes. Meanwhile, the DNA mix was prepared by combining the three plasmids in the following amounts:

pΔ8.91 18 µg

pMD2G 7 µg

pDNA (containing the construct of interest) 15 µg

1 ml of the DMEM/Express-In mix was then slowly added to the DNA, mixed and transferred to the remainder of the transfection reagent solution, inverted 4 times to mix and left to incubate for a further 30 minutes at RT.

2.6.2 Transfection of packaging cell line and processing of viral supernatant

2.6.2a Initial method[1]

Following a 20 minute incubation at RT, the transfection reagent was applied directly to 293T cells (ideally 80% confluent), cultured in a T175 flask in 30 ml of DMEM-10 media.

Transfection was allowed to proceed for 48 hours, after which the cell culture supernatant was aspirated, centrifuged at 1,000 x g (Sorvall RT 6000D centrifuge; Dupont Instruments) to remove any cell debris, and loaded onto Ultra-Clear 38.5 ml thin-wall centrifuge tubes (Beckman Coulter) for concentration of the viral supernatant in the ultracentrifuge (Optima L-100 XP Ultracentrifuge, SW 28.1 rotor, Beckman Coulter) at 129463 x g for 2 hours. The supernatant was discarded and the viral pellet resuspended in 500 µl PSG, before being either stored at -80 °C or used in transduction of cell lines.

2.6.2b Revised method[2]

3 ml of the DMEM/Express-In/DNA mix was then applied to 293T cells (just exceeding 50% confluency) in a T175 culture flask, from which all DMEM-10 media has been aspirated. The reagent was left to cover the cells for 1 minute, before 22 ml of fresh DMEM-10 were added to the cells, and the flask was incubated at 37°C, 5% CO_2 for 48 hours. The viral supernatant was harvested and processed as described in the initial method except for the following changes: After centrifugation at 1,000 x g (Sorvall RT 6000D centrifuge; Dupont Instruments) to remove the cell debris, the viral supernatant was syringed through a 0.45 µ nylon filter (Nalgene), and the concentrated virus was resuspended in 2 ml of CK media.

2.6.3 Transduction of lymphocytes

2.6.3a Initial method[1]

For transduction of Jurkat cell line, 1-128 µl of 1/50 diluted viral supernatant were applied to 2x 10^5 cells per well of a 24 well plate, initially to establish the multiplicity of infection (MOI) for a particular virus. 128 µl was typically sufficient to cause 100% transduction of 2x 10^5 Jurkat cells.

For primary $CD8^+$ T cells, the entire 500 µl of the concentrated viral supernatant was administered to 10^6 cells in a well of a 24 well plate, from which all the media was removed. The cells and virus were incubated together for 4 hours, at 37°C, 5% CO_2, before 2 ml CK media was added to the cells, and they were left to express the protein of interest for a further 70 hours.

In both cases, the efficiency of transduction was assessed by following target protein expressing using flow cytometry.

2.6.3b Revised method[2]

24 hours prior to transduction, the $CD8^+$ and $CD4^+$ T cells were isolated from PBMC using anti-CD8, anti-CD4 MACS beads, MACS separation columns and a MACs magnetic cell sorter (all from Miltenyi Biotech) as described in section 2.3.4. 10^6 $CD8^+$ and $CD4^+$ cells were mixed in a 1:1 ratio in CK media, applied to a well of a 24 well tissue culture plate, and stimulated to divide by addition of 6x 10^6 pre-washed (3 times, using R10) anti-CD3/anti-CD28 antibody coated microbeads (Dynabeads T cell expander, Invitrogen) at a 1:3 cell: bead ratio. Following a 24 hour incubation at 37°C, 5% CO_2, 1 of 2 ml of CK media was aspirated and 1 ml of viral supernatant added onto the cell-bead mix. Efficiency of transduction was assessed by flow cytometry after a 72 hour culture period.

[1] *Lentiviral production protocol obtained courtesy of Dr. P. Brennan, Cardiff University, UK.*

[2] *An adaptation of the lentiviral production protocol obtained through a collaboration with the University of Pennsylvania, USA.*

2.6.4 Titering viral supernatant and calculating multiplicity of infection (MOI)

2x10^5 Jurkat cells in 1 ml of R10 were placed in each of 9 wells of a 24 well plate. The concentrated virus supernatant was diluted 1/50 in R10 and the following amounts of diluted virus were added to the Jurkat cell-containing wells; 0 µl, 1 µl, 2 µl, 4 µl, 8 µl, 16 µl, 32 µl, 64 µl, and 128 µl. The cells were then allowed to incubate with the virus for 28 hours at 37°C.

Multiplicity of infection (MOI) is the number of infectious viral particles per number of cells. We have to assume that each particle infects a cell (this of course isn't the case but accurate enough for calculating MOI). For example, if 10 µl of GFP viral supernatant was added to 10^6 Jurkat cells and 26% became infected, 10 µl of viral supernatant would contain 26% of 10^6 (260,000) particles of virus, meaning 1 µl contains 26,000 particles. Plotting the percentage of GFP positive cells at each amount of viral supernatant added against the amount of viral

supernatant added produces a titration curve (Figure 6.8). The MOI is then estimated from values on the linear range of the curve as after the curvilinear and plateau phase the virus saturates the system and MOI estimates become inaccurate. Knowing the average number of cells infected in the linear portion of the titration curve, it is possible to calculate the number of particles of virus per µl assuming each particle infects a single cell. As an example, if 1 µl of viral supernatant contains 792,000 particles we assume it infects 792,000 cells, giving an MOI of 1.

2.7 Protein Chemistry

2.7.1 Inclusion body preparation

Biotin-tagged MHCI heavy chains (wild type and Q115E mutant) and β_2m (wild type and K58E mutant) were expressed under the control of the T7 promoter as insoluble inclusion bodies in the *Escherichia coli* strain BL21 (DE3) pLys (Invitrogen) as described in section 2.4.4. Inclusion bodies were released from IPTG-induced *E. coli* as follows. The bacterial pellet from 1 litre culture was re-suspended in 20 ml of lysis buffer (10 mM Tris pH8.1 (Sigma), 10 mM $MgCl_2$ (Sigma), 150 mM NaCl (Sigma) and lysozyme (Fisher Scientific)) were added both to a final concentration of 0.2 mg/ml. Finally, a cocktail of 5 protease inhibitors: 500 µM AEBSF, 1 µg/ml Aprotinin, 1 µM E-64, 500 µM EDTA and 1 µM Leupeptin (Calbiochem) was added and bacterial suspension stirred at RT for 60 minutes. The bacterial suspension was then transferred to a 50 ml centrifuge tube (Falcon) and lysed by three repeated freeze/thaw cycles or by sonication to release the inclusion bodies. Inclusion bodies were purified by adding 5 volumes of Triton wash buffer (0.5% Triton X-100 (Sigma), 50 mM Tris pH8.1 (Sigma), 100 mM NaCl (Sigma), 10 mM EDTA (Sigma), 2 mM DTT (Sigma)), pelleted by centrifugation at 1,333 x g (Sorvall RT 6000D centrifuge; Dupont Instruments) for 20 minutes at 4°C and the supernatant containing the bacterial cell debris discarded. This step was repeated 2-3 times (a homogenizer was used each time to resolubilise the pellet in the Triton buffer) or until the inclusion body preparation was clean enough on the sodium dodecyl sulphate-polyacrylamide gel electrophoresis (SDS-PAGE) gel. Once clean, the inclusion body pellet was denatured in 8 M urea or guanidine buffer (8 M urea or

guanidine, 50 mM Tris pH8.1, 100 mM NaCl, 10 mM ethylenediaminetetraacetic acid (EDTA) pH8 and 10 mM dithiothreitol (DTT), all from Sigma), the concentration estimated as described in section 2.7.5 and then stored in 1 ml aliquots at -80°C.

2.7.3 Fast protein liquid chromatography (FPLC)

The table on the next page outlines some of the properties of the Amersham Pharmacia columns used in the next section. All the columns were used by attaching them to an automated FPLC system (Amersham Pharmacia). Protein levels were continuously monitored by UV at 280 nm.

Column	Description	Use(s)	Column volume (ml)	Volume of sample added (ml)	Flow rate (ml/min)	Volume of Fractions collected (ml)
Hi Trap Q	Anion Exchange	Purification of pMHCI monomers or TCR	5	500-1000	5	1
Hi Trap Q desalting	Gel Filtration	Removal of salt prior to biotiny-lation	5	0.5	0.5	0.5
Superdex HR 75	Gel Filtration	Removal of excess biotin after bioti-nylation	23	2	0.5	0.5

2.7.3 Production of soluble human biotinylated peptide-MHC class I monomers

For the manufacture of pMHCI monomers, 30 mg of HLA A2 heavy chain with a biotin tag and 30 mg of β_2m inclusion body preparations were denatured separately in 10 ml 8 M urea or guanidine buffer (8 M urea (Sigma), 50 mM Tris pH8.1 (Sigma), 100 mM NaCl (Sigma), 10 mM EDTA pH8 (Sigma) and 10 mM DTT (Sigma)) for 30 minutes at 37°C. Refolding was

initiated by adding (in the order described) 1 ml peptide (4 mg/ml in DMSO), 30 mg denatured β_2m, 30 mg denatured heavy chain in 1 litre of a pre-chilled β-mercaptoethylamine/cystamine redox buffer (100 mM Tris pH8.1 (Sigma), 400 mM L-arginine HCL (Sigma), 2 mM EDTA (Sigma), 6.5 mM β-mercaptoethylamine (Sigma) and 3.7 mM cystamine (Acros organics) at 4°C while stirring vigorously. After stirring for 4 hours at 4°C the refold was transferred into 12 KDa dialysis tubing (Sigma), and dialysed against 12 litres of d.H_2O overnight then against 12 litres 10 mM Tris pH8.1 for 8 hours. Following equilibration of a 5 ml anion exchange column (Hi Trap Q HP; Amersham Pharmacia) with 10 mM Tris pH8.1, the refold was loaded onto the column and the protein eluted with a salt gradient (0-500 mM NaCl in 10 minutes/10 mM Tris pH8.1). Figure 2.1 A shows a typical anion exchange trace where peak 1 contains refolded monomer and peak 2 contains the misfolded protein. The fractions containing peak 1 were collected, protease inhibitors added to prevent biotin tag cleavage, stored at 4°C and analysed by SDS-PAGE. If fractions contained the correctly refolded pMHCI, the SDS-PAGE gel showed two main bands (with some impurities after this ion exchange phase): a band at ~37 KDa (pMHCI heavy chain) and a band at ~12 KDa (β_2m) (Figure 2.1B). The pMHCI band was typically more prominent than the β_2m band. After analysis of the collected fractions on the SDS-PAGE gel, the fractions containing the two correctly folded proteins were pooled, concentrated down to 500 µl using 10 KDa cut off Ultrafree centrifugal filter (Millipore) and desalted using a 5 ml Hi Trap desalting column (Amersham Pharmacia) equilibrated with 10 mM Tris pH8.1 (Sigma). Desalted pMHCI monomer fractions were collected and biotinylated in a 2 ml biotinylation reaction (10 mM Tris pH8.1 (Sigma), 0.1 mM Tris HCl/1 mM biotin (Sigma), 8 mM $MgCl_2$ (Sigma), 5 mM ATP (Sigma), 2.5 µg Bir A enzyme (Invitrogen) (O'Callaghan C et al. 1999) overnight at room temperature. The removal of excess biotin and buffer exchange into PBS was performed by gel filtration (size exclusion) chromatography using a Superdex HR 75 10/30 column (Amersham Pharmacia) equilibrated in PBS. Figure 2.2 shows a typical gel filtration profile, where peak 1 is the biotinylated pMHCI monomer and peak 2 is excess biotin. The excess biotin was concentrated and recycled for use in further biotinylation reactions. The peak 1 fractions were concentrated down to a 300 µl volume and stored at -80°C.

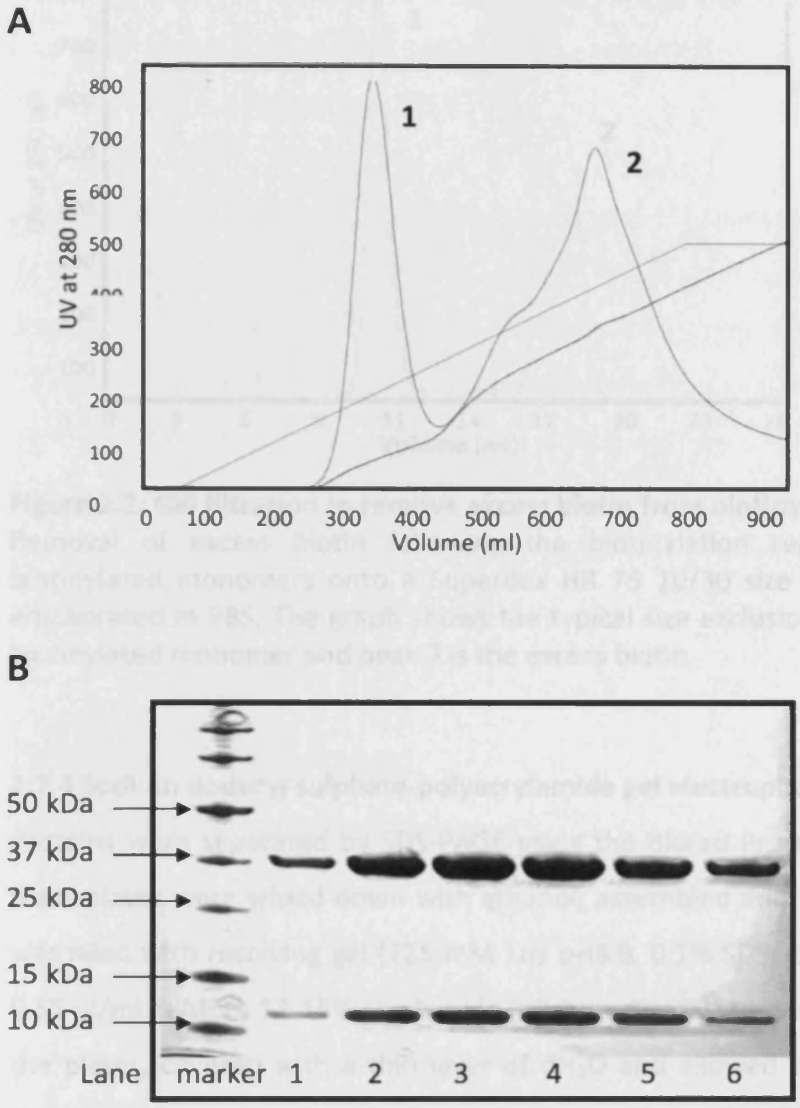

Figure 2.1: Purification of pMHCI monomers by anion exchange. A. A typical anion exchange trace for pMHCI monomer refolds eluted with a salt gradient (the conductivity and concentration of which is shown as green and brown traces, respectively). Peak 1 is the correctly refolded pMHCI monomer and peak 2 is the misfolded protein. Peaks were subsequently analysed by SDS-PAGE analysis. **B.** 1 µg of pMHCI monomer loaded onto each of the six lanes (corresponding to the collected fractions) and separated by SDS-PAGE.

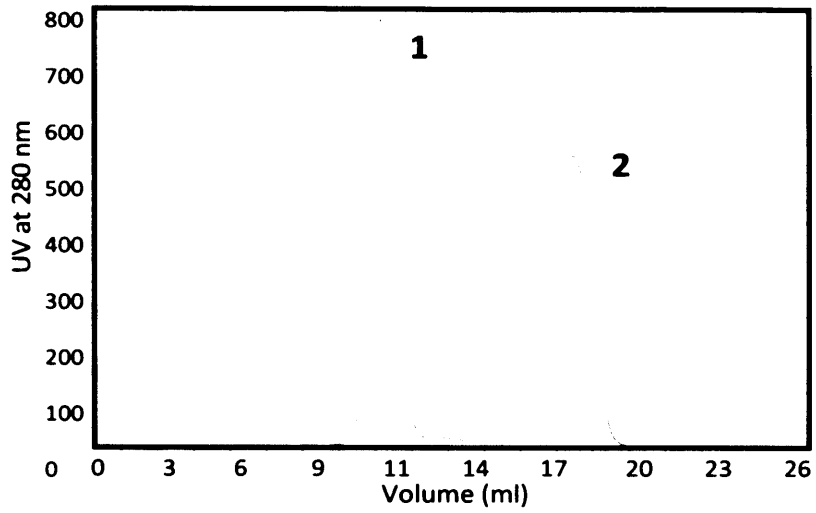

Figure 2.2: Gel filtration to remove excess biotin from biotinylated pMHCI monomers. Removal of excess biotin following the biotinylation reaction involved loading the biotinylated monomers onto a Superdex HR 75 10/30 size exclusion column, previously equilibrated in PBS. The graph shows the typical size exclusion profile, where peak 1 is the biotinylated monomer and peak 2 is the excess biotin.

2.7.4 Sodium dodecyl sulphate-polyacrylamide gel electrophoresis (SDS-PAGE)

Proteins were separated by SDS-PAGE using the Biorad Protean II electrophoresis system. Glass plates were wiped down with ethanol, assembled and the space between the plates was filled with resolving gel (125 mM Tris pH8.8, 0.1% SDS, 2 µl/ml of 25% AMPS solution, 0.55 µl/ml TEMED, 12-15% acrylamide (all from Sigma)) to a height of 1 cm from the top of the plates, covered with a thin layer of dH_2O and allowed to polymerise for 30 minutes. Excess water was removed and the denser stacking gel solution (125 ml Tris pH6.8, 0.1% SDS, 7.5 µl/ml 25% AMPS solution, 0.625 µl/ml TEMED, 6% acrylamide (all from Sigma)) applied gently to the top of the plates. The comb was inserted into the stacking gel, and the gel left to polymerise for a further 40 minutes. After removal of the comb, the gel was transferred into an electrophoresis tank and submerged in running buffer (192 mM glycine, 50 mM Tris pH8.8, 350 µM SDS). Samples were prepared by diluting 1:5 in 6x sample buffer (125 mM Tris pH6.8, 4% SDS, 10% β-mercaptoethanol, 20% glycerol, 20 µg/ml bromothenol blue) and heating to 95°C for 4 minutes. The samples and the molecular weight marker (Seeblue Plus2 marker, Invitrogen) were loaded into separate lanes on the gel. Gels were run at 80 mA for 45 minutes, and stained by agitating them for 1 hour with Coomasie Blue

staining solution (40% methanol (BDH), 7% acetic acid (BDH), 0.025% Brilliant Blue G). The gels were destained by further agitation for a minimum of 1 hour with destain solution (10% methanol (BDH), 10% acetic acid (BDH)).

2.7.5 Estimating protein concentration by UV spectrophotometry

Inclusion bodies were diluted 1 in 100 in either 8 M urea or 6 M guanidine buffer, depending on the original solvent. The refolded pMHCI monomer samples were diluted 1 in 10 in PBS. Using either the urea/guanidine buffers (for inclusion bodies) or PBS (for refolds) as reference blanks, readings at 280 nm wavelength were recorded. Protein concentration was calculated using the extinction co-efficient for each protein previously calculated from the amino acid sequence using Vector NTI suite (Microsoft). For example the extinction co-efficient for monomeric pMHCI is 0.46.

2.8 pMHC multimer technology

2.8.1 Manufacture of pMHCI tetramers

Streptavidin (SA) has four binding sites for biotin therefore pMHCI tetramers can be constructed by adding streptavidin to a solution of biotinylated pMHCI monomers in a 1:4 molar ratio. Tetramers were conjugate to R-phycoerythrin (PE) (Molecular Probes) and Allophycocyanin (APC) (Caltag) for use in flow cytometry, or Alexa Fluor-488 and Alexa Fluor-594 (both from Molecular Probes) for use in fluorescence microscopy. The volume of conjugated streptavidin required for each tetramer preparation was calculated and added in 5 aliquots of equal volume at 20 minutes intervals at 4°C, mixing the contents well each time. By adding streptavidin in aliquots as described the complete saturation of all four biotin binding sites for streptavidin is ensured with each addition. The tetramers were stored at 4°C for a period of up to four weeks, or until the tetramer showed signs of disintegration.

2.8.2 pMHCI tetramer decay experiments

10^6 $CD8^+$ T cells were stained in 100 µl azide buffer (PBS, 0.1% NaN_3/0.5% FCS (Sigma)) for 20 minutes on ice with a concentration of tetramer, previously determined by titration that gave a starting fluorescence intensity (MFI) of 200 (+/- 50). After washing with 1-2 ml of azide buffer, the $CD8^+$ T cells were resuspended in 110 µl azide buffer. A 10 µl aliquot was placed in a separate FACS tube to act as a control without the addition of competing unconjugated HLA A2-specific antibody. To the other tube containing the remaining 100 µl of cell suspension, 10 µl of unconjugated anti-HLA A2 mAb (clone BB7.2, Serotec, UK) at 100 µg/ml was added to block tetramer re-binding. Aliquots of 10 µl were taken at the following time points after addition of the antibody; 0, 2, 5, 8, 10, 15, 18, 20, and 30 minutes, added to FACS tubes containing 100 µl of PBS, and analysed on a FACSCalibur flow cytometer (BD). The control sample without any HLA A2 antibody added was analysed at 30 minutes.

2.8.3 pMHCI tetramer association experiments

10^6 $CD8^+$ T cells were pelleted and resuspended in 200 µl PBS. A specific concentration of pMHCI tetramer was applied to the cell suspension, and 10 µl aliquots were taken out and placed in individual FACS tubes containing 100 µl PBS. The aliquots were removed from the master mix at the following time points; 0, 1, 2, 4, 6, 8, 10, 12, 15, 18, 20, 25, 28, and 30 minutes, and were analysed on the FACSCalibur (BD).

2.8.4 Assembly of pMHC dextramers

Dextramers are composed of a dextran backbone decorated with streptavidin bound to biotinylated pMHC molecules (as in a pMHC tetramer), and several copies of a fluorochrome. The dextran backbones (obtained from Immudex, Denmark) were available with three types of fluorochrome attached: PE, APC, and FITC. The method of dextramer assembly with all three types of backbone was essentially the same, but the ratios of backbone to pMHC varied slightly. To prepare 500 µl (50 tests) of dextramer reagent with pMHCI monomers (Mr≈ 48.5 KDa) if the monomer is for instance at a concentration of 1.95 mg/ml is outlined below:

1) Dextramer-PE: 2 µl of dextran backbone is required for each 10 µl test of assembled dextramer reagent. Therefore for 50 tests, 100 µl of dextran-PE backbone and 7.9 µl of pMHCI monomer (at 1.95 mg/ml) were incubated together for 30 minutes at RT in the dark. The reagent was made up to 500 µl with 392.1 µl assembly buffer (0.05 M TRIS-HCL, 15 mM NaN_3, pH7.2).
2) Dextramer-APC: 100 µl of dextran-APC and 4.4 µl of pMHCI monomer were incubated together for 30 minutes at RT in the dark. 395.6 µl of assembly buffer was added to make up the volume to 500 µl.
3) Dextramer-FITC: Two different types of FITC dextramer were made. For flow cytometry a reagent with 1 pMHC monomer per streptavidin molecule was assembled as follows: 100 µl of dextran-FITC and 5.6 µl of pMHCI monomer were incubated for 30 minutes at RT in the dark. Subsequently, 394.4 µl of assembly buffer was added to the pMHC monomer backbone mix. For microscopy work, a dextramer containing 3 pMHC molecules per streptavidin was made up as follows: 100 µl of dextran-FITC and 16.8 µl of pMHCI monomer were incubated together for 30 minutes at RT in the dark. 383.2 µl of assembly buffer were added to complete the process.

The final concentration of dextramer in the preparations was $3.2x10^{-8}$ M, and a 10 µl volume was typically used per stain. The concentrations of monomeric pMHC in a 10 µl preparation of each type of fluorochrome-conjugated dextramer reagent are outlined below:

1) Dextramer-PE : 6.6 Streptavidin (SA) molecules/ dextramer, 3 pMHC/SA.
   Total pMHC per dextramer : 19.8
   Amount of pMHC (n) = $3.2x10^{-8}/100000$ (for 10 µl)
   = $3.2x10^{-13}$ moles of dextramer in 10 µl
   19.8 MHC per dextramer so 19.8 x ($3.2x10^{-13}$) = $6.33x10^{-12}$ moles (or 0.3 µg)
   Therefore dextramer-PE contains $6.3x10^{-12}$ moles (or 0.3 µg) pMHC monomer per 10 µl staining volume.

2) Dextramer-APC: 2.9 SA/dextramer, 3 pMHC/SA.

Total pMHC per dextramer: 8.7

n = $3.2x10^{-8}$/100000 (for 10 µl)

= $3.2x10^{-13}$ moles of dextramer in 10 µl

8.7 pMHC per dextramer-APC so 8.7 x ($3.2x10^{-13}$) = $2.78x10^{-12}$ moles (or 0.13 µg)

Therefore dextramer-APC contains $2.8x10^{-12}$ moles (or 0.13 µg) pMHC monomer per 10 µl staining volume.

3) Dextramer-FITC (MHC High version): 14.25 SA/dextramer, 3 pMHC/SA.

Total pMHC per dextramer: 42.75

n = $3.2x10^{-8}$/100000 (for 10 µl)

= $3.2x10^{-13}$ moles of dextramer in 10 µl

42.75 pMHC per dextramer so 42.75 x ($3.2x10^{-13}$) = $13.68x10^{-12}$ moles (or 0.65 µg)

Therefore dextramer-FITC contains $13.7x10^{-12}$ moles (or 0.65 µg) pMHC monomer per 10 µl staining volume.

For comparison, the calculation for determining the concentration of monomeric pMHC in each 0.5 µg pMHC tetramer preparation is shown below:

Tetramer-PE/APC/FITC: 1 SA/tetramer, 4 pMHC/SA.

Total pMHC per tetramer: 4

Amount (n) = mass (m)/ Molar mass (M_r)

n = $0.5x10^{-6}$ g/48 KDa (average Mr of pMHCI)

= $1.04x10^{-11}$ moles (or 0.5 µg) of MHC

Therefore 0.5 µg of tetramer preparation contains $1.04x10^{-11}$ moles pMHCI monomer.

2.9 Treatment of cells with dasatinib and neuraminidase

2.9.1 Dasatinib treatment

Dasatinib was synthesized according to the published procedure (Lombardo et al. 2004). After initial optimization, $CD8^+$ T cells were incubated with 50 nM drug for 30 minutes at 37 °C.

2.9.2 Neuraminidase treatment

$5x10^5$ $CD8^+$ T cells were treated with 0.011 U of *vibrio cholerae* neuraminidase in a total volume of 500 µl of PSG medium for 15 minutes at R.T. The cells were subsequently washed with R10, as the FCS also inactivates neuraminidase. The cells were stained with FITC-conjugated peanut agglutinin (PNA) for 20 min at 4 °C to verify the desialylation status of the neuraminidase treated and untreated cells.

2.10 Flow cytometry

2.10.1 pMHC tetramer staining of T cell clones, lines and PBMC

Unless otherwise stated ~10^5 $CD8^+$ T cells specific for an antigen of interest were re-suspended in 50 µl PBS and stained with 1 or 0.5 µg PE (Molecular Probes) or APC (Caltag) conjugated pMHCI tetramer for 15 minutes at 37°C or 20 minutes on ice, washed in PBS and centrifuged at 500 x g (Sorvall RT 6000D centrifuge; Dupont Instruments) for 5 minutes and resuspended in 50 µl PBS. The cells were then stained with 3 µl of an antibody (eg. anti-CD3 FITC, clone SK7; BD) and 5 µl 7-Aminoactinomycin D (7AAD) (Viaprobe; BD) for 30 minutes on ice. After washing in PBS, cells were resuspended in 200 µl PBS or FACSfix (4% formaldehyde), and analysed using a FACSCalibur or a Canto II (both BD) flow cytometer (when using fluorochromes other than FITC, PE, and PerCP).

2.10.2 pMHC dextramer staining of T cell clones, lines and PBMC

Unless otherwise stated ~10^5 $CD8^+$/$CD4^+$ T cells specific for an antigen of interest were re-suspended in 40 µl PBS and stained with 10 µl PE, APC, or FITC-conjugated pMHCI

dextramer (Immudex, Denmark) for 30 minutes at RT. The unbound dextramers were removed by performing three washes with PBS, and the cells resuspended in 50 µl PBS prior to staining with cell surface antibodies as in section 2.10.1 above.

2.10.3 Gating strategy for phenotyping PBMC

When performing flow cytometric analysis it is important to employ a stringent gating strategy to exclude artefacts that may be contaminating the data. This is especially important in experiments when the cells of interest are present in very low frequencies in the sample. Figure 2.3 exemplifies the sort of gating strategy that was employed to phenotype $CD4^+$ T cells from a PBMC sample. In order to get to the final $CD4^+$ population, the following steps were taken: 1) FSC-H vs. SSC-H gating on the live lymphocyte population; 2) FSC-A vs FSC-H to eliminate any doublets; 3) Dead cells and $CD14^+$ and $CD19^+$ cells were excluded in the dump channel, and the gate placed around $CD3^+$ cells; 4) and finally $CD4^+$ cells. The $CD4^+$ population was separated further into effector memory, central memory, and naïve subsets according to their differential expression of CD27 and CD45RO phenotypic markers. Variations of this gating strategy were used for other cells types such as $CD8^+$ T cells, B cells, and γδ T cells. The gating strategy can be made even more stringent by performing a Boolean gating step after the first lymphocyte gate was drawn. Boolean gating serves to eliminate outliers that may occur due to fluorochrome spreading between FL channels.

2.11 $CD8^+$ T cell effector function assays

2.11.1 Enzyme linked immunospot (ELISpot) assay for interferon-γ (IFNγ)

96-well PVDF-backed plates (Millipore) were coated with IFNγ capture antibody 1-DIK (Mabtech) at 15 µg/ml overnight at 4°C. Plates were washed twice in PSG and blocked with RPMI containing 10% FCS for 3 hours at 37°C. For target cell ELISpots: $2.5x10^2$-$5x10^2$ $CD8^+$ T cells/well and $2.5x10^4$ CIR B cells expressing HLA A2/well +/- peptide were applied to duplicate wells of pre-coated plates in a total volume of 200 µl in PSG and incubated for 4-12 hours at 37°C. For tetramer ELISpots: $2x10^3$ $CD8^+$ T cells +/- various concentrations of

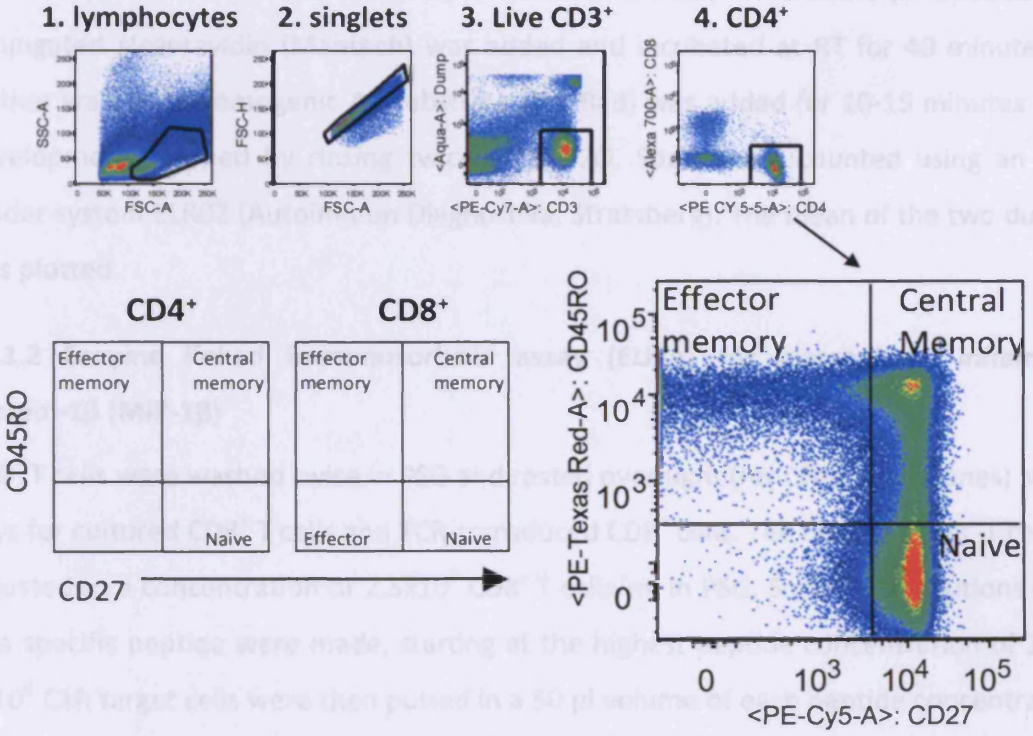

Figure 2.3: Gating strategy for phenotypic analysis of PBMC. In order to eliminate artefacts, variations of this basic gating strategy were adhered to for flow cytometric analysis of PBMC. Gating steps 1-4 in addition to Boolean gating were followed before phenotypic analysis of a specific cell population (in this case $CD4^+$ cells) was performed. Flow plot outlines in the bottom left portion of the figure depict the different phenotypic subsets of $CD4^+$ and $CD8^+$ T cells that can be viewed using a $CD27^-/CD45RO^-$ antibody co-staining.

pMHCI tetramer (starting at 1 µg/ml) were applied to duplicated wells of pre-coated plates in a total volume of 200 µl PSG and incubated for 4-12 hours at 37°C. Plates were washed 6 times with PBS at RT and incubated for 90 minutes with 1 µg/ml anti-IFNγ-mAb-7B6-1 biotin (Mabtech). After 6 further washes, a 1:1000 dilution of alkaline-phosphatase (AP)-conjugated streptavidin (Mabtech) was added and incubated at RT for 40 minutes. After further washes, chromogenic AP substrate (Bio-Rad) was added for 10-15 minutes and the development stopped by rinsing twice with H2O. Spots were counted using an ELISpot reader system ELR02 (Autoimmun Diagnostika; Strassberg). The mean of the two duplicates was plotted.

2.11.2 Enzyme linked immunosorbent assay (ELISA) for macrophage inflammatory protein-1β (MIP-1β)

$CD8^+$ T cells were washed twice in PSG and rested overnight (for $CD8^+$ T cell clones) and for 3 days for cultured $CD8^+$ T cells and TCR-transduced $CD8^+$ cells. The next day $CD8^+$ T cells were adjusted to a concentration of $2.5x10^5$ $CD8^+$ T cells/ml in PSG. Serial 1/10 dilutions (in PSG) of a specific peptide were made, starting at the highest peptide concentration of 100 µM. $1x10^6$ C1R target cells were then pulsed in a 50 µl volume of each peptide concentration for 1 hour at 37°C. After washing with PSG, target C1R cells were counted and adjusted to $2.5x10^5$ cells/ml. $2.5x10^4$ $CD8^+$ T cells were placed into each well of a 96-U bottom plate with or without $2.5x10^4$ pulsed C1R target cells in a final volume of 200 µl/well. Plates were incubated for 4-12 hours at 37°C. Supernatants was removed and assayed for MIP-1β using a Quantikine ELISA kit (R&D systems). Alternatively the supernatant from the ELISA was assayed for other cytokines and chemokines using the cytometric bead assay (CBA) (see section 2.11.3).

2.11.2a MIP-1β ELISA for combinatorial peptide library screening

Background

The measurement of TCR cross-reactivity in a laboratory setting employs the combinatorial library screening technique. Combinatorial peptide libraries consist of all possible peptides of a defined length that can be synthesized from the 20 natural L-amino acids (Figure 2.4). Since the typical αβ TCR recognizes peptides 9-11 amino acids in length, a 9mer library is a

sensible place to begin. For a 9mer library, each mixture contains $1.7x10^{10}$ different 9mer peptides. When used at 100 μg/ml, the concentration of each peptide in each mixture is very low ($5.3x10^{-14}$ M). In order to measure even the slightest $CD8^+$ T cell responses, a highly sensitive MIP-1β ELISA has become the method of choice for assessing TCR cross-reactivity of a human $CD8^+$ T cell line or clone.

Position:	1	2	3	4	5	6	7	8	9
	O	X	X	X	X	X	X	X	X
	X	O	X	X	X	X	X	X	X
	X	X	O	X	X	X	X	X	X
	X	X	X	O	X	X	X	X	X
	X	X	X	X	O	X	X	X	X
	X	X	X	X	X	O	X	X	X
	X	X	X	X	X	X	O	X	X
	X	X	X	X	X	X	X	O	X
	X	X	X	X	X	X	X	X	O

Figure 2.4: A nanomer (9mer) peptide library layout. Libraries are ordered in a position-scanning format. The 9mer library consists of 180 different peptide mixtures, each having one of the 20 L-amino acids in a defined fixed position (O) and all the other amino acids except cysteine at the remaining positions (X). Using this system the amino acids are entered into the fixed position (O) in alphabetical order according to their single letter code, the first mixture would contain peptides that all have an alanine (A) fixed at position one, and all the other possible amino acid combinations in the remaining positions. Whilst, the peptides in mixture 180 would all terminate in a tyrosine (Y).

The assay

The effector $CD8^+$ T cells were 'rested' in R2 media (2% FCS) for three days prior to the date of experiment to reduce the background cytokine levels. 5 μl of each 1 mM (1000 μM) peptide mix was added per well of a 96 well plate to C1R target cells (60,000 cells/well in 45 μl/well volume), giving a final peptide concentration of 100 μM. 5 μl of PSG was added to the zero wells, and 5 μl of the relevant index peptide (at a final concentration of 1 μM) was used as a positive control. The target cells were incubated with the peptides for 2 hours at

37°C, before the addition of effector $CD8^+$ T cells at a concentration of 30,000 cells per 50 µl. The assembled assay was incubated for 12-20 hours at 37°C. 50 µl of supernatant was collected from each well and either diluted 2.4x in assay diluent to be developed according to the standard ELISA protocol (section 2.11.2a) or frozen at -20°C for future analysis. All assays were performed in duplicate and averaged.

2.11.3 Cytometric bead array (CBA)

Peptide-pulsed C1R target cells were incubated with $CD8^+$ T cells (in a 3:1 target: effector ratio) for 4-12 hours at 37°C. The supernatant was assayed using the human Th1/Th2 Cytokine kit (BD) according to the manufacturer's instructions. The sample acquisition was performed on a FACSCalibur (BD) flow cytometer, and the results analysed using standard curves constructed with the aid of CBA software (BD).

2.11.4 TCR/CD8 downregulation assay

HLA A2-expressing C1R cells were either pulsed with 1 µM peptide for 1 hour or incubated in PSG media alone. After two washes with PSG, $6x10^5$ pulsed or unpulsed targets were incubated with $3x10^5$ effector $CD8^+$ T cells for 4-12 hours at 37°C. Following the incubation, the cells were pelleted and the supernatant removed or analysed for cytokines in ELISA or CBA assays. The cell pellets were stained with anti-TCR^{FITC} (Clone BMA 031; Serotec) and anti-$CD8^{APC}$ (clone RPA-T8; BD Pharmingen) for 30 minutes on ice, washed twice, and resuspended in PBS. Data was acquired using a FACSCalibur (BD) flow cytometer and analysed using FlowJo software (Treestar Inc., Ashland, OR, USA).

2.11.5 Intracellular cytokine staining (ICS) for $CD8^+$ T cell effector functions

This procedure enables quantification of various $CD8^+$ T cell effector functions by flow cytometry. The assay set up was identical to a MIP-1β ELISA (section 2.11.2a and b), and the E:T ratio was typically 2:1, but 90,000 (instead of 60,000) $CD8^+$ effectors were used per well of a 96 well plate (100 µl assay volume). Once the effector and target cells were placed in the wells, 1 µl/ml of BFA (stock at 10 mg/ml, Sigma-Aldrich), 0.7 µl/ml Monensin (Golgi-stop, BD), and 3 µl/well anti-CD107a (optional) were added. The assay was incubated for 6-

12 hours at 37 °C, 5% CO_2. After the desired incubation period, the assay plate was centrifuged at 667 x g for 3 minutes (Sorvall RT 6000D centrifuge; Dupont Instruments), and the supernatant discarded. The samples were washed once by application of 200 µl of PBS and centrifuged at 667 x g for 3 minutes (Sorvall RT 6000D centrifuge; Dupont Instruments). Once the supernatant was once again discarded, the pelleted cells were stained with a mixture of surface antibodies (typically binding the surface molecules CD3, CD8, CD4, CD14, and CD19) in a 50 µl volume for 20 minutes at RT. The cells were washed twice using the washing procedure with PBS, and resuspended in 100 µl 1x cytofix/cytoperm solution (BD), and incubated for 20 minutes at RT, protected from light. The samples were then washed twice with 150 µl perm wash buffer (BD) diluted 1:10 with $d.H_2O$ and centrifugation at 733 x g for 3 minutes (Sorvall RT 6000D centrifuge; Dupont Instruments). The cell pellets were subsequently resuspended in 100 µl intracellular antibody mix (typically targeting activation markers IL-2, MIP-1β, TNF, and IFNγ), and incubated for 20 minutes at RT, protected from light. The cells were finally given a further two washes with the perm wash buffer, and resuspended in 100 µl perm wash or PBS. The samples were analysed by flow cytometry using the FACS Canto II (BD) and FlowJo software (Tree Star Inc.).

2.11.6 Infection of T0 and primary $CD4^+$ T cells with HIV-1 and intracellular staining for the HIVgag p24 protein

Intracellular staining for the p24 protein is used to assess the extent of HIV infection by flow cytometry. T0 cells are very permissive to infection with HIV-1. To infect, ~10^6 T0 cells were pelleted by centrifugation at 500 x g for 5 minutes (Sorvall RT 6000D centrifuge; Dupont Instruments) and the pellet incubated with 100 µl HIV-1 (Strain HTLV-IIIB/H9 (NIH), which is CXCR4-dependent T cell-tropic) supernatant for 1 hour at 37 °C, 5% CO_2. The cells were then resuspended in 10 ml R10 media and placed in a T75 flask for culture. The cells were maintained in culture and remained infected with HIV for prolonged periods (up to several months), but the percentage of infected cells generally declined if cells remained in culture in excess of this culture period. Supernatant from the infected T0 cells containing HIV-1 particles and was used to infect new batches of T0 cells, as well as primary $CD4^+$ T cells. For this, $CD4^+$ T cells were MACS-sorted from fresh PBMC isolated from HLA A2 positive blood

donors (see section 2.3.4). 10^6 $CD4^+$ T cells per well of a 24 well plate were stimulated with anti-CD3/anti-CD28 coated microbeads in ratio of 1:3 cells: beads for a period of 48 hours in R10 media containing 200 IU/ml IL-2 (IL-2 media). 1 ml of viral supernatant (depleted of T0 cells by centrifugation at 1,000 x g for 10 minutes (Sorvall RT 6000D centrifuge; Dupont Instruments)) was applied to the pre-activated $CD4^+$ T cells in the presence of 200 IU/ml IL-2 and incubated for 3 days at 37 °C, 5% CO_2. Following this incubation with the virus, the beads were magnetically removed and the cells placed in IL-2 media for further expansion.

Both T0 and primary $CD4^+$ T cells were tested for HIV infection by intracellular staining for the p24 protein, which forms part of the HIV capsid. Cells were pelleted in 5ml FACS tubes and incubated with $Aqua^{Amcyan}$ viability dye, washed 3 times in 1 ml PBS, resuspended in 250 µl cytofix/ cytoperm solution (BD), and incubated for 20 minutes at 4 °C in the dark. The cells were then washed again (3 times with 1 ml perm/wash buffer (BD)) and stained with the following antibodies: CD3 $^{APC\text{-}H7}$, CD8 $^{PE\text{-}Cy7}$, and p24 ^{FITC} for 20 minutes at 4 °C in the dark. Unbound antibodies were washed off (three times with 200 µl perm/wash buffer) and the cells resuspended in 200 µl of PBS. The cells were acquired on a FACS Aria flow cytometer (BD) and the data analysed using FlowJo (Treestar). Figure 2.5 shows the gating strategy typically used to assess the success of HIV infection.

2.11.7 Fluorometric assessment of T lymphocyte antigen-specific lysis (FATAL)-$CD8^+$ T cell killing assay

$3x10^4$ of either pulsed (with antigenic or control peptide, for 1 hour) or unpulsed (incubated in media alone) target cells (typically C1R, T0 or T2 cells) were stained with two different concentrations of CFSE (1 µl/ml and 10 µl/ml of 1/375 pre-diluted 10 mM stock) for 10 minutes (and protected from light) to distinguish the antigen-presenting and internal control populations, prior to application of both population to a well of a 96-well U-bottom plate. $15x10^5$ $CD8^+$ T cells (giving an E:T ratio of 5:1) were applied to the same plate (either specific for the antigenic peptide presented by targets or in conjunction with an ImmTAC/V reagent specific for the peptide) in a final of 200 µl. The assay was incubated for 4-12 hours

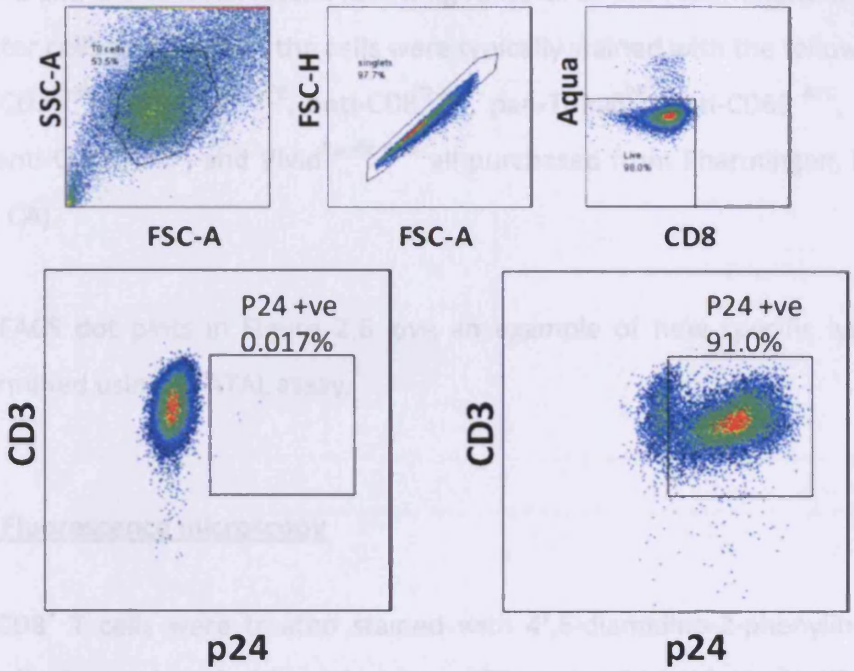

Figure 2.5: Assessment of the extent of HIV infection by intracellular staining for p24 expression. 10^6 HIV-infected (bottom right plot) or uninfected (bottom left plot) T0 cells were treated with the viability dye Aqua followed by an intracellular stain with anti-CD3, -CD8, and -p24 antibodies. Although T0 cells are $CD4^+$, no anti-CD4 stain was included as the HIV infection induced downregulation of the CD4 coreceptor, and an intracellular CD4 stain (unlike intracellular anti-CD3 and anti-CD8 stains) was not effective. The efficiency of T0 cell infection with HIV ranged between approximately 90 and 100%, and a p24 stain was routinely performed prior to using the cells in functional assays.

at 37°C and the cells harvested following removal of the supernatant. If PBMC were used as effector cells in this assay, the cells were typically stained with the following antibodies: Anti-CD3$^{Cy\text{-}PE}$, anti-CD4$^{Cy5\text{-}PE}$, anti-CD8$^{Q\text{-}705}$, pan-TCRγδ^{PE}, anti-CD69 ^{APC}, anti-CD45RO$^{ECD(Texas\ Red)}$, anti-CD19^{APCCy7}, and Vivid$^{Pacific\ Blue}$ all purchased from Pharmingen, BD Biosciences (San Jose, CA).

The FACS dot plots in Figure 2.6 give an example of how specific lysis of target cells is determined using a FATAL assay.

2.12 Fluorescence microscopy

10^5 $CD8^+$ T cells were treated stained with 4',6-diamidino-2-phenylindole (DAPI) nuclear stain (Invitrogen) and either Alexafluor-488 conjugated (Molecular Probes) peptide-MHC tetramers (at a final concentration of 12.5 μg/ml) or FITC-conjugated dextramers (Immudex, Denmark) (at a final concentration of 16.25 μg/ml) for 30 minutes at RT. Following three washes with PBS, each sample was fixed in 2% paraformaldehyde. After fixing, the $CD8^+$ T cells were re-suspended in 100 μl of 2% FCS/PBS and then spun onto a microscope slide at 550 rpm for 5 minutes using a cytospin III centrifuge (Harlow Scientific). Samples were subsequently analysed on a Leica DM LB2 (Leica Microsystems) fluorescence microscope.

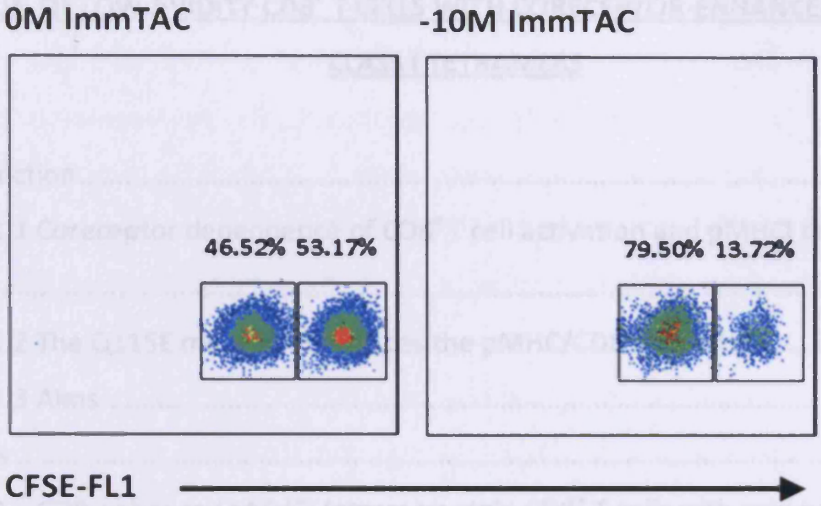

Figure 2.6: An example of a FATAL assay layout. Peptide-pulsed target cells were stained with one concentration of CFSE dye, while unpulsed control cells were stained with a different concentration of the same dye. The target and control populations were combined in the same FATAL assay and can each be identified by flow cytometry by their different CFSE signal intensities in the FL1 channel. In the absence of any peptide-specific ImmTAC reagent and effector $CD8^+$ T cells, both populations remain intact (left panel), while in the presence of sufficient reagent and $CD8^+$ T cells, the peptide-pulsed population disappears as the $CD8^+$ T cells in the assay are being redirected to lyse target cells presenting the cognate peptide.

Chapter 3

3

DETECTION OF LOW AVIDITY CD8$^+$ T CELLS WITH CORECEPTOR-ENHANCED PEPTIDE-MHC CLASS I TETRAMERS

Chapter 3

3.1 Introduction

The interaction between the TCR and peptide-MHC is central to T cell recognition of infected and dysregulated cells. Exploiting the high degree of specificity, afforded by the TCR/pMHC interaction, through the use of soluble pMHC molecules to target T cells bearing cognate TCRs, presents an attractive prospect for the detection of specific T cells in *ex vivo* samples. However, the monomeric TCR/pMHC interaction is classically weak and lasts only a matter of seconds at physiological temperatures, rendering the use of monomeric pMHC inadequate for such purposes. A solution was provided by Altman *et al*, who in 1996 published a landmark paper describing the generation of tetrameric forms of pMHC molecules (Altman et al. 1996). As a result of the avidity effect which arises on multimerization, the half life of the TCR/pMHC interaction was increased from seconds to hours, permitting the use of specific fluorochrome-conjugated pMHC tetramers to detect T cells of interest by flow cytometry. Over a decade later, the uses of pMHC tetramers, still the most favoured form of pMHC multimer, have grown dramatically (see section 1.6 of the main Introduction for a few examples) and with it so too has our knowledge of T cell responses. It is no longer enough to simply highlight a select population of T cells and report its presence. Immunologists, my group included, are increasingly interested in characterising and grading the quality of specific T cell responses. The majority of these T cell responses are studied due to their involvement in diseases such as cancer, chronic infection, and autoimmunity. For the reasons described in more detail in section 1.7 of the Introduction of this thesis, the TCRs on many of these T cells display very low affinities for their cognate antigen. The low affinity of some TCR/pMHC interactions means it is not possible to use conventional pMHC tetramer technology to detect T cells bearing such TCRs. As part of my investigations into optimising TCR/pMHC interactions for targeting disease, I have developed a number of 'tricks' aimed at improving the detection and characterisation of low avidity T cells using multimeric pMHC molecules (Chapters 3-5). In this chapter I report the use of pMHCI tetramers with enhanced CD8 binding. I will begin by laying out key aspects of research generated by members of my group, which have provided a basis for my own studies.

3.1.1 CD8 coreceptor dependence of $CD8^+$ T cell activation and pMHCI tetramer binding

As described in section 1.4 of the main Introduction, the CD8 coreceptor is a key player in the process of antigen recognition by $CD8^+$ T cells. Understanding how CD8 influences the dynamics of the TCR/pMHCI interaction and thus $CD8^+$ T cell function represents a major focus of the 'T cell modulation group'. At the heart of this investigation were two important questions: i) What range of TCR/pMHCI affinities is required for the detection of antigen-specific $CD8^+$ T cells by pMHCI tetramers? and, ii) How does the CD8 coreceptor influence this process? My colleague Bruno Laugel proceeded to address these questions by studying the efficiency of cell staining with a set of altered pMHCI tetramers, assembled from monomeric pMHCI molecules which exhibited impaired CD8 binding (Laugel et al. 2007). These 'CD8-null' pMHCI tetramers were constructed from HLA A2 monomers containing a double D227K/T228A substitution in the α3 domain (Purbhoo et al. 2001), which completely abrogated binding to the CD8 coreceptor whilst leaving the TCR/pMHC interaction unperturbed. Data obtained with these CD8-null pMHCI tetramers indicated that the CD8 coreceptor was required for binding of antigenic ligands that display suboptimal TCR/pMHCI affinities. Furthermore, the extent of coreceptor dependence appeared to be inversely correlated with TCR/pMHCI affinity (Laugel et al. 2007). In order to obtain a quantitative measure of the contribution of CD8 binding to the engagement of soluble tetrameric pMHCI molecules, a $CD8^+$ T cell clone that recognises the HLA A2-restricted human telomerase reverse transcriptase $(hTERT)_{540\text{-}548}$ peptide (ILAKFLHWL, ILA from hereon), called ILA1 (Laugel et al. 2007; Purbhoo et al. 2007), was stained with a panel of pMHCI molecules displaying: i) varying affinities for CD8; and, ii) a number of biophysically characterised altered peptide ligands (APLs). The APLs used in this study were selected from a peptide library of ~50 monosubstituted ILA peptides, based on their divergent abilities to stimulate the ILA1 clone. The activation results, measured by IFNγ ELISpot are summarised in Figure 3.1B. From this initial ILA variant peptide screen, the number of APLs was narrowed down to six: 8E, 5Y, 4L, 3G8T, 3G, and 8Y. The 3G, 3G8T and 8Y high affinity binders can be referred to as 'superagonists' relative to the index peptide, whist 5Y, 8E and 4L represent weak agonists. Together with the index ILA peptide, these ligands span a wide range of binding affinities for the ILA1 TCR. The dissociation constant (K_D), which is determined by surface plasmon resonance (SPR) binding equilibrium experiments, is a measure of TCR/ligand

A

Ligand	8E	5Y	4L	ILA index	8Y	3G8T	3G
Dissociation constant K_D (μM)	>500	242	117	36.6	22.6	4.04	3.7

B

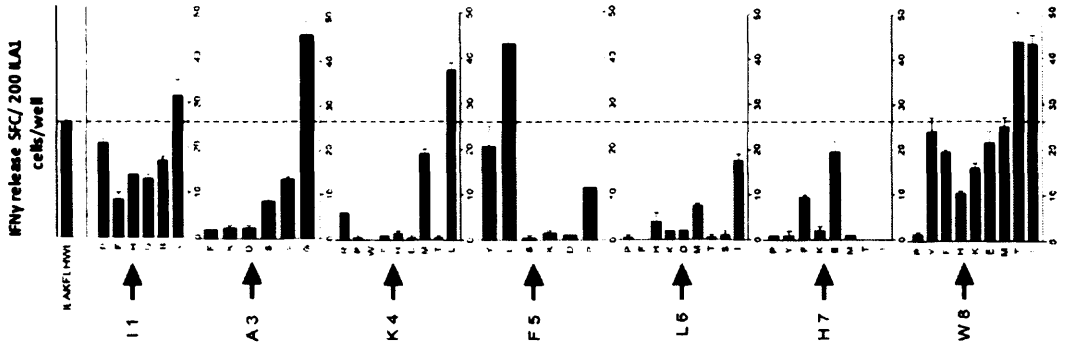

Figure 3.1: Kinetic and functional characteristics of the ILA epitope variants recognized by ILA1 CD8⁺ T cells. A. Table of K_D values calculated from kinetic parameters determined by surface plasmon resonance (SPR). **B.** An IFNγ ELISpot screen of the peptide positions recognized by the ILA1 CD8⁺ T cell clone. The height of the peaks represents the strength of the IFNγ signal quantified as the number of spot-forming cells per 200 ILA1 T cells added per well of the assay. The left-most peak represents the IFNγ response exerted by the ILA index peptide, which was used as a reference. The number labels on the x-axis refer to the positions of the amino acids in the index ILA (ILAKFLHWL) peptide, which are indicated by the single letter code. Positions 2 and 9 are anchor residues and were thus kept the same as in the index sequence. (Data kindly provided by B. Laugel).

affinity. The K_D values for the monomeric ILA1 TCR/APL ligand interactions are summarised in Figure 3.1A. ILA1 TCR-binding to the weakest variant 8E has an estimated K_D value of ~2 mM. However, because the affinity of this ligand lies on the threshold of detection by SPR, we can only confirm its K_D as being > 500 μM with certainty.

To assess the influence of the monomeric TCR/pMHCI affinity and presence of a pMHCI/CD8 interaction on pMHCI tetramer staining of $CD8^+$ T cells, the APLs summarised in Figure 3.1A were complexed with MHCI molecules (either wildtype or CD8-null) and assembled into fluorochrome-conjugated pMHCI tetramers. The two panels of pMHCI tetramers were then tested for their ability to stain the ILA1 clone under different staining conditions (4°C versus 37°C). Figure 3.2 illustrates the differences in brightness intensity of the ILA1 $CD8^+$ T cell clone when labelled with either wildtype (Figure 3.2A) or CD8-null (Figure 3.2B) pMHCI tetramers refolded around several ILA APLs, at 37°C or 4°C (Figure 3.2 C and D, respectively). The results indicate that a functional wildtype pMHC/CD8 interaction is essential for the visualisation of $CD8^+$ T cells in cases where the pMHCI tetramer used to stain these cells incorporated a low affinity APL. From the pMHCI tetramer staining data, it was deduced that under 'normal' staining conditions (staining with 10 μg/ml tetrameric pMHCI at 37°C for ~ 15 minutes) a TCR/pMHCI interaction of $K_D \leq 40$ μM was required for good pMHCI tetramer staining of $CD8^+$ T cells. Importantly, the only variant in these clonal studies is the antigenic peptide used. Thus, the level of TCR and CD8 expression on the T cell surface are constant within any given experiment. The findings from this study set a basis for the work presented in this chapter.

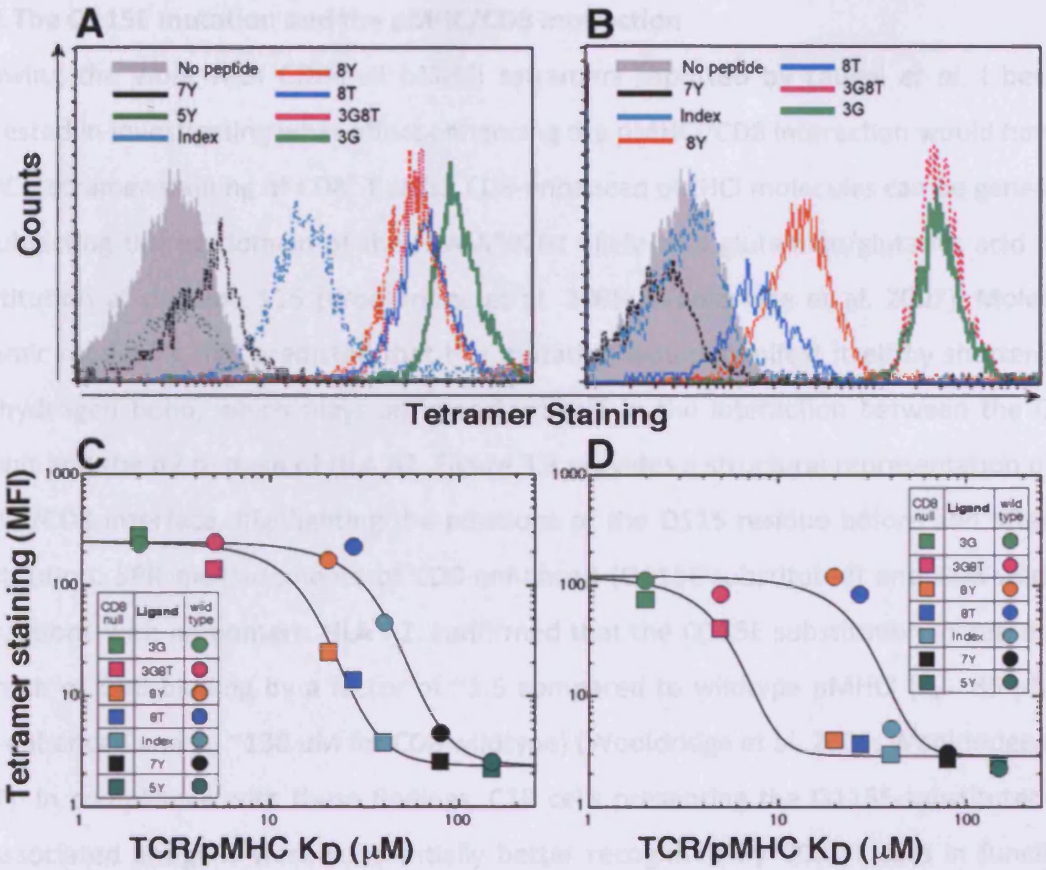

Figure 3.2: Staining of ILA1 CD8⁺ T cell clone with tetramerised cognate pMHCI molecules. The figure shows the staining of the ILA1 CD8⁺ T cell clone with seven different $hTERT_{540–548}$ variants, as indicated, refolded with wildtype (WT) HLA A2 (**A**) or D227K/T228A (CD8-null) HLA A2 (**B**) at 37°C. The mean fluorescence intensity (MFI) values observed with pMHCI tetramer staining were plotted versus the TCR/pMHCI interaction K_D values for experiments conducted at 37°C (**C**) and 4°C (**D**) with WT HLA A2 (circles) and CD8-null HLA A2 (squares) molecules for each variant added at a final concentration of 220 nM (10 μg/ml). Colour codes in C and D correspond to those shown in A and B. Staining with the set of altered peptide ligands refolded with each type of heavy chain was performed at least three times. Representative data are shown. Curves are the best fit of the model described under Experimental Procedures of (Laugel et al. 2007). (Data kindly provided by B. Laugel).

3.1.2 The Q115E mutation and the pMHC/CD8 interaction

Following the work with CD8-null pMHCI tetramers reported by Laugel *et al*, I became interested in investigating what effect enhancing the pMHCI/CD8 interaction would have on pMHCI tetramer staining of $CD8^+$ T cells. CD8-enhanced pMHCI molecules can be generated by subjecting the α2 domain of the HLA A*0201 allele to a glutamine/glutamic acid (Q/E) substitution at position 115 (Wooldridge et al. 2005; Wooldridge et al. 2007). Molecular dynamic modelling had predicted that this mutation would manifest itself by shortening a key hydrogen bond, which plays an important role in the interaction between the CD8α subunit and the α2 domain of HLA A2. Figure 3.3 provides a structural representation of the pMHCI/CD8 interface, highlighting the positions of the Q115 residue before and after the substitution. SPR measurements of CD8-enhanced (Q115E-substituted) and CD8-wildtype interactions with monomeric HLA A2, confirmed that the Q115E substitution increased the strength of CD8 binding by a factor of ~1.5 compared to wildtype pMHCI (K_D ~85 μM for CD8-enhanced and K_D ~130 μM for CD8 wildtype) (Wooldridge et al. 2005; Wooldridge et al. 2007). In compliance with these findings, C1R cells presenting the Q115E-substituted HLA A2-associated antigens were substantially better recognised by $CD8^+$ T cells in functional assays. Furthermore, $CD8^+$ T cells showed vast improvements in antigen-specific activation and cytotoxicity in response to target cells presenting cognate peptide in the context of Q115E HLA A2 molecules (Wooldridge et al. 2005; Wooldridge et al. 2007). Importantly, just like the D227K/T228A mutation, the Q115E substitution was not accompanied by changes in TCR/pMHCI specificity (Wooldridge et al. 2007). This enabled the influence of the CD8 coreceptor on antigen recognition by $CD8^+$ T cells to be assessed independently of TCR/pMHCI binding.

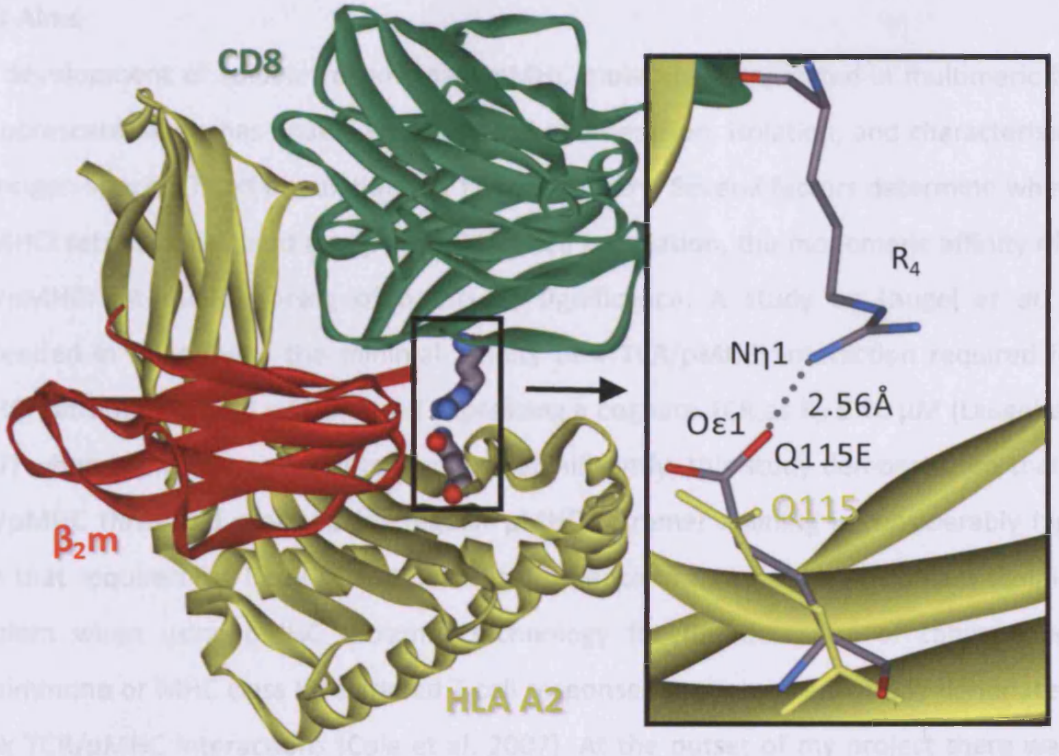

Figure 3.3: The CD8α1R_4 guanidinium moiety forms a stronger electrostatic interaction with the HLA A*0201 Q115E mutant carboxylate than with the wildtype Q residue. HLA-A2 heavy chain is shown in yellow complexed with β2m (red) and CD8 (green). The inset shows the location of the key residues Q_{115} in HLA A2 and R_4 in CD8α1. For clarity, the right-hand-side close up is rotated about the vertical relative to the standard view. The wildtype Q_{115} residue is shown for comparison (yellow). The Q_{115}/R_4 Oε1..Nη1 distance in the HLA A2 CD8αα crystal structure (Gao et al. 1997) is 3.18 Å. This distance is predicted by the molecular dynamics simulation to shorten to an average of 2.56 Å with $Q_{115}E$ (shown as broken line) and enables these moieties to form a strong electrostatic interaction.

3.1.3 Aims

The development of soluble recombinant pMHC molecules conjugated in multimeric form to fluorescent labels has enabled the physical enumeration, isolation, and characterisation of antigen-specific T cell populations by flow cytometry. Several factors determine whether a pMHCI tetramer will bind a cognate $CD8^+$ T cell population, the monomeric affinity of the TCR/pMHCI interaction being of particular significance. A study by Laugel *et al.* had succeeded in quantifying the minimal affinity of a TCR/pMHCI interaction required for a pMHCI tetramer to bind a $CD8^+$ T cell expressing a cognate TCR as $K_D \leq 40\ \mu M$ (Laugel et al. 2007) when using conventional technology. Significantly, this study demonstrated that the TCR/pMHC threshold required for regular pMHC tetramer staining is considerably higher than that required for T cell activation. This difference in threshold represents a significant problem when using pMHC tetramer technology for the detection of cancer-specific, autoimmune or MHC class II-restricted T cell responses as these are typically dominated by weak TCR/pMHC interactions (Cole et al. 2007). At the outset of my project there was an urgent need to address this problem so as to develop technology that could be used to visualise all antigen-specific T cells using pMHC multimers and flow cytometry. The major aim of this work was to address this deficiency and therefore extend the diagnostic use of pMHC multimer technology and make it relevant in other important disease states. Since the CD8 coreceptor is involved in stabilising the TCR/pMHC interaction (Wooldridge et al. 2005), CD8-null pMHCI tetramers, which do not benefit from this stabilisation effect, were only successful in staining $CD8^+$ T cells displaying high affinities for cognate antigen (Laugel et al. 2007). The principle aim of my investigation was thus to determine whether enhancing the pMHCI/CD8 interaction would have the opposite effect of lowering the threshold required for pMHCI tetramer staining of $CD8^+$ T cells, without incurring a loss in TCR/pMHCI specificity. The specific aims of this work were to:

i) Manufacture wildtype and CD8-enhanced HLA A2 monomers refolded around a set APLs, and assemble these into tetramers.

ii) Determine if pMHCI tetramers constructed from CD8-enhanced (Q115E-substitued) peptide-HLA A2 monomers engineered to have ~1.5 fold higher affinity for CD8 are

better able to detect cognate $CD8^+$ T cell populations than wildtype pHLA A2 tetrameric reagents, using the well characterised ILA1 system as a model.

iii) Provide a mechanistic explanation for the observations in ii).

iv) Assess whether the findings with the ILA1 system extend to other systems, by studying the ability of wildtype and CD8-enhanced pMHCI tetramers to stain low avidity $CD8^+$ T cells (displaying a number of different antigen specificities) directly *ex vivo*.

3.2 Results

3.2.1 CD8-enhanced pMHCI tetramers stain $CD8^+$ T cells with avidities for cognate antigen that lie below the threshold of detection with corresponding wildtype reagents

To determine the binding threshold of wildtype and CD8-enhanced pHLA A2 tetramers with respect to monomeric TCR/pMHCI ligand affinity, I constructed two sets of pMHCI monomers specific for the $CD8^+$ T cell clone ILA1. This was done by refolding either wildtype or CD8-enhanced (Q115E-substituted) HLA A2 heavy chains with a set of six ILA APL (8E, 5Y, 4L, 8Y, 3G8T, and 3G) or the ILA index peptide (Figure 3.1 A). The refolding process and pMHCI tetramer assembly are described in Sections 2.7 and 2.8 of Materials and Methods. The two sets of HLA A2 tetramers were used to stain the cognate $CD8^+$ T cell clone, ILA1. To enable direct tetramer staining comparisons limited solely to differences in CD8 binding properties, pMHCI tetramer concentration (10 μg/ml), staining temperature (37 °C), incubation period (15 minutes), and staining volumes were standardised for each staining procedure. As shown in Figure 3.4, the mean fluorescence intensity (MFI) of staining for the ILA1 clone with both sets (wildtype versus CD8-enhanced) of variant MHCI tetramers correlated with the affinity (K_D) of the monomeric TCR/pMHC interaction (Figure 3.1 A). The CD8-enhanced pMHCI tetramers conserved the staining positions of the APLs relative to each other, but resulted in a significant enhancement of tetramer staining when compared to the wildtype reagents (Figure 3.4 A and B). This shift in the recognition spectrum in favour of low affinity ligands is more clearly demonstrated on a mathematically fitted curve of MFI versus K_D values for the two sets of tetramers (figure 3.4 D). According to the curve, coreceptor-enhanced pHLA A2 tetramers refolded with APLs that exhibited low monomeric TCR/pMHCI binding affinities in surface plasmon resonance (SPR) experiments (K_D >100 μM) stained ILA1 $CD8^+$ T cells with greater intensities compared to the corresponding wildtype reagents. This effect was most marked with APLs displaying mid-range K_D values such as the 4L (K_D~117 μM; Figure 3.4 C) and 5Y (K_D~242 μM; Figure 3.4 and (Laugel et al. 2007)) APL/HLA A2 tetramers. No significant staining differences between wildtype and CD8-enhanced tetramers were observed with lower monomeric TCR/pMHCI affinities (K_D> 500 μM, variant 8E) or with high affinity ligands 8Y, 3G8T, and 3G ($K_D \leq 20$ μM) (Figure 3.4). Importantly, since the experiments were conducted using a monoclonal $CD8^+$ T cell system

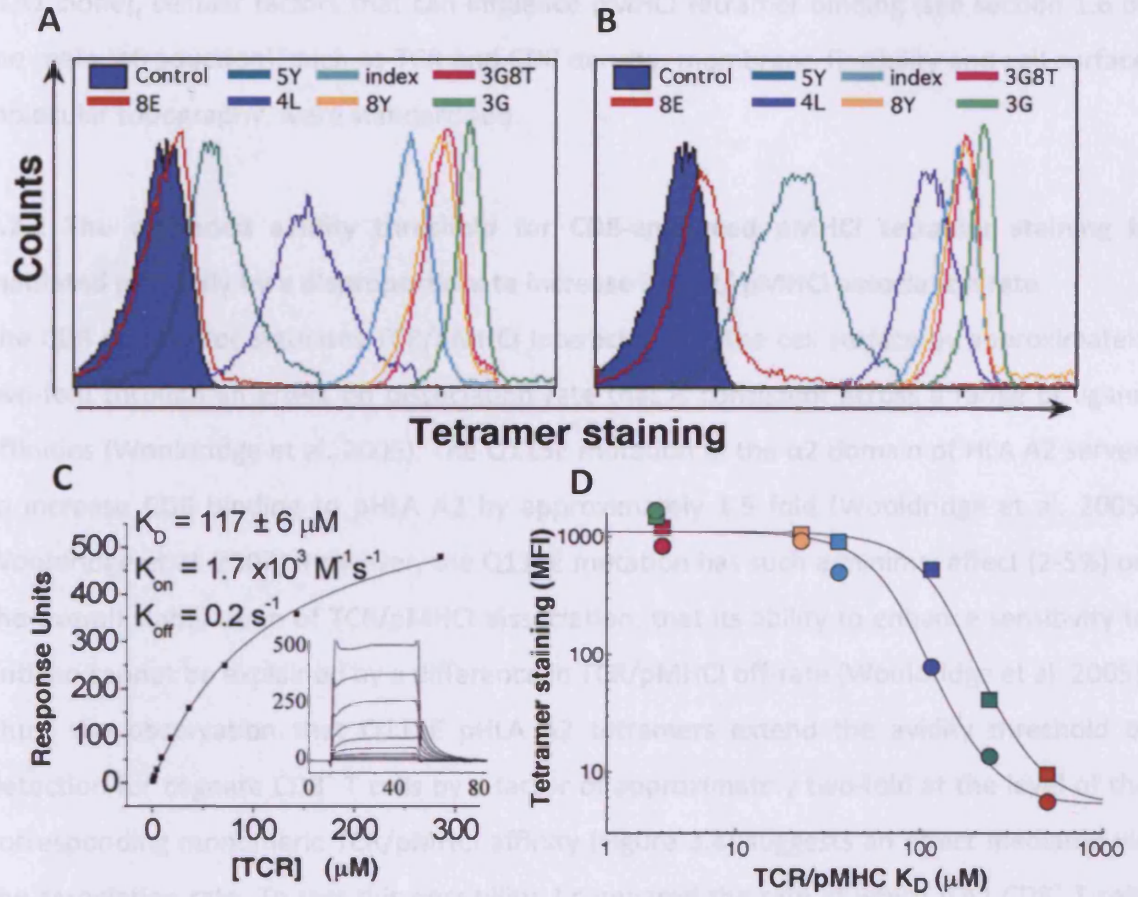

Figure 3.4: Tetrameric complexes of pHLA A2 containing the heavy chain α2 domain Q115E substitution bind low avidity CD8⁺ T cells. The ILA1 CD8⁺ T cell clone was stained with wildtype (**A**) and Q115E-substituted (**B**) pHLA A*0201 tetramers bearing different APL at a final concentration of 10 μg/ml with respect to the monomeric pMHCI component. The TCR/pMHCI affinities measured by SPR for the APL interactions shown are summarised in Figure 3.1 A. **C.** Affinity and binding kinetics of the ILA1 TCR/4L HLA A*0201 interaction; SPR experiments were performed as described previously (Laugel et al. 2007). Standard deviation from the mean dissociation constant (K_D) of 3 separate experiments is shown. **D.** Staining intensities shown in (A) and (B) were plotted against TCR/pMHCI binding affinity (K_D) for wildtype (circles) and Q115E (squares) pHLA A2 tetramers; APL colour codes match those shown in A and B. Curves were fitted as described previously (Laugel et al. 2007). (The data in C was kindly provided by D. Cole.)

(ILA1 clone), cellular factors that can influence pMHCI tetramer binding (see section 1.6 of the main Introduction), such as TCR and CD8 density, membrane flexibility and cell surface molecular topography, were standardised.

3.2.2 The extended avidity threshold for CD8-enhanced pMHCI tetramer staining is mediated primarily by a disproportionate increase in TCR/ pMHCI association rate

The CD8 coreceptor stabilises TCR/pMHCI interactions at the cell surface by approximately two-fold through an effect on dissociation rate that is consistent across a range of ligand affinities (Wooldridge et al. 2005). The Q115E mutation in the α2 domain of HLA A2 served to increase CD8 binding to pHLA A2 by approximately 1.5 fold (Wooldridge et al. 2005; Wooldridge et al. 2007). However, the Q115E mutation has such a minimal effect (2-5%) on the overall stabilisation of TCR/pMHCI dissociation, that its ability to enhance sensitivity to antigen cannot be explained by a difference in TCR/pMHCI off-rate (Wooldridge et al. 2005). Thus, the observation that Q115E pHLA A2 tetramers extend the avidity threshold of detection for cognate $CD8^+$ T cells by a factor of approximately two-fold at the level of the corresponding monomeric TCR/pMHCI affinity (Figure 3.4) suggests an effect mediated via the association rate. To test this possibility, I compared the rate at which ILA1 $CD8^+$ T cells bound identical concentrations of wildtype and Q115E-substitued pHLA A2 tetramers from solution. From the panel of tetramers, three pairs of wildtype and CD8-enhanced tetramers were chosen: i) refolded around a high affinity (3G8T); ii) intermediate affinity (ILA index); and, iii) low affinity (4L) ligands (Figure 3.5 A, B, and C, respectively). In all cases, Q115E pHLA A2 tetramers exhibited more rapid uptake in these association assays (see section 2.8.3 of Material and Methods for assay details). Notably, however, this effect was more pronounced for the 4L APL/HLA A2 complex, which displays low/intermediate monomeric affinity for the ILA1 TCR (Figure 3.5 C), consistent with the staining data in Figure 3.4. Thus, mechanistically, the enhanced detection of low avidity $CD8^+$ T cells afforded by Q115E CD8-enhanced pHLA A2 tetramers is mediated primarily by a disproportionate increase in the TCR/pMHCI association rate.

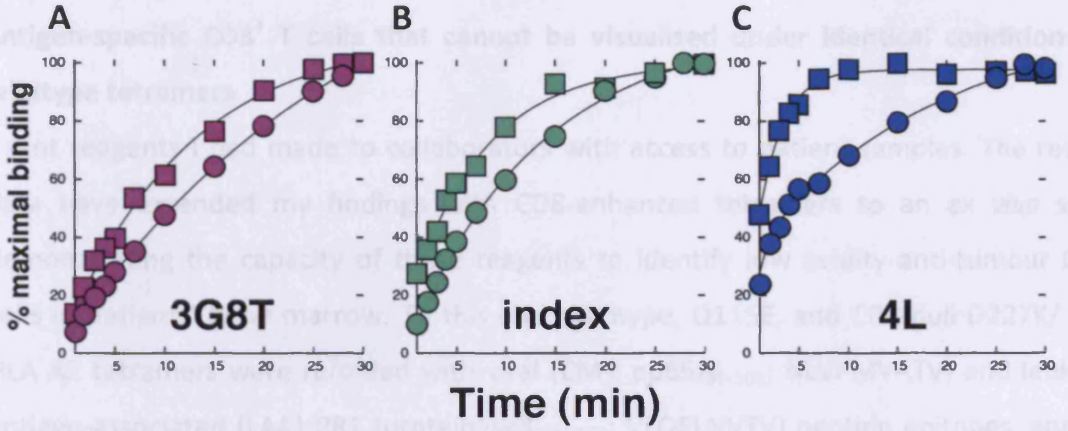

Figure 3.5: WT and Q115E tetramer on-rates for the index ILA peptide and two variants. The figure shows cognate pMHCI tetramer capture from solution by ILA1 $CD8^+$ T cells. Concentrations of tetramer were titrated in an attempt to achieve a maximum fluorescence intensity of ~200. This level of staining could not be achieved for the wildtype 4L ligand, and staining only reached an MFI of ~60 in this case. From left to right, panels show % maximal binding over 30 minutes for ILA1 cells stained with 0.2 µg/ml 3G8T (**A**), 1 µg/ml ILA index (**B**) and 5 µg/ml 4L (**C**) wildtype (circles) and Q115E (squares) tetramers. Representative data of 3 separate experiments shown.C urves represent least squares fit to equation 20 in (van den Berg et al. 2007).

3.2.3 CD8-enhanced pMHCI tetramers enable direct *ex vivo* detection of low avidity antigen-specific CD8$^+$ T cells that cannot be visualised under identical conditions with wildtype tetramers

I sent reagents I had made to collaborators with access to patient samples. The resultant data have extended my findings with CD8-enhanced tetramers to an *ex vivo* setting, demonstrating the capacity of these reagents to identify low avidity anti-tumour CD8$^+$ T cells in patients' bone marrow. To this end, wildtype, Q115E, and CD8-null D227K/ T228A HLA A2 tetramers were refolded with viral (CMV pp65$_{495\text{-}503}$; NLVPMVATV) and leukaemia antigen-associated (LAA) PR1 (proteinase3$_{169\text{–}177}$; VLQELNVTV) peptide epitopes, and were used to stain *ex vivo*-derived PBMC samples. In contrast to pathogen-specific responses, CD8$^+$ T cell populations directed against tumour-derived epitopes generally exhibit low avidities for antigen and bear TCRs with weaker monomeric affinities for cognate pMHCI (Molldrem et al. 2003; Cole et al. 2007). Consistent with these properties, PR1-specific CD8$^+$ T cell populations showed variable staining with different tetrameric reagents (Figure 3.6 A). Thus, while a minute number of high avidity PR1-specific CD8$^+$ T cells could be identified with D227K/T228A pHLA A2 tetramers in some individuals with myeloid leukaemias, larger populations were generally defined with the corresponding wildtype reagents. The number of PR1/HLA A2 tetramer positive cells was larger still when staining was performed with Q115E tetramers. The number of cognate Q115E-substituted cells was consistent with the number of PR1 peptide-responding cells in the sample detected by ELISpot (Melenhorst et al. 2008), thereby indicating the existence of specific CD8$^+$ T cell populations below the threshold of detection with wildtype tetramers (Figure 3.6 A). In contrast, higher avidity anti-pathogen CD8$^+$ T cell populations specific for the CMV pp65$_{495\text{–}503}$ epitope were defined in mononuclear cell preparations at similar magnitudes with all three forms of the corresponding cognate tetramer (Melenhorst et al. 2008). This suggests that the increase in cellular events detected by pMHCI tetramers bearing the Q115E mutation does not simply correlate with an increase in non-specific background staining. However, a small increase in aberrant binding events was detected by performing phenotypic analysis of the cognate tetramer positive population. Figure 3.6 B shows how the majority of 'true' PR1/Q115E HLA A2 tetramer-binding events, which carry the memory phenotype (CCR7$^-$ CD45RA$^-$/CD27$^+$

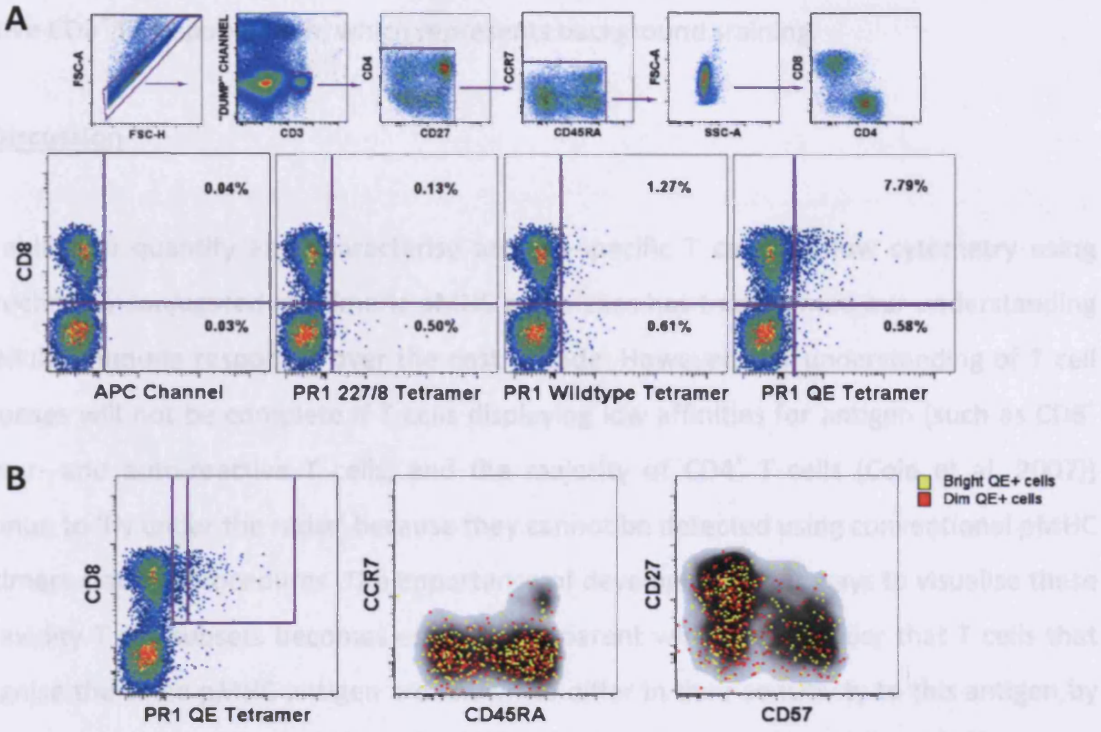

Figure 3.6: Coreceptor-enhanced pHLA A2 tetramers can identify low avidity antigen-specific CD8⁺ T cells that are not visible with the corresponding wildtype tetramers directly *ex vivo*. A. The upper panels show the gating strategy used to identify antigen-specific CD8⁺ T cells. First, doublets were distinguished from single cell events on the basis of their forward scatter-area (FSC-A) vs. forward scatter-height profile (FSC-H). Live CD3⁺ T cells were then distinguished from dead cells (ViVid⁺), monocytes (CD14⁺) and B cells (CD19⁺). Subsequently, fluorochrome aggregates were gated out in two consecutive bivariate plots and lymphocytes were further identified according to forward scatter (FSC) vs. side scatter profile (SSC). Histograms were then transformed at the level of the CD4 vs. CD8 plot. The frequencies of D227K/T228A, WT and Q115E PR1/HLA A2 tetramer-positive and background events, calculated within the CD8⁺an d CD8⁻ populations respectively, are shown as a percentage of the total live CD3⁺ lymphocyte population (lower panels).**B .** Cells staining brightly (yellow) and dimly (red) with the Q115E PR1/HLA A2 tetramer exhibit similar phenotypes based on expression of CCR7, CD27, CD45RA and CD57;t he tetramer-positive events are almost exclusively CCR7⁻ memory cells, although a few naïve events consistent with background staining are apparent as the gate is extended towards the CD8⁺ tetramer-negative population. The phenotypic distribution of these PR1-specific CD8⁺ T cells differs considerably from that of the overall CD8⁺ T cell population (grey density plot). (Data kindly provided by J. Melenhorst)

$CD57^-$) can be differentiated from the naïve ($CCR7^+$ $CD45RA^+/CD27^+$ $CD57^+$) tetramer positive $CD8^+$ T cell population, which represents background staining.

3.3 Discussion

The ability to quantify and characterise antigen-specific T cells by flow cytometry using fluorochrome-conjugated multimeric pMHC complexes has transformed our understanding of cellular immune responses over the past decade. However, our understanding of T cell responses will not be complete if T cells displaying low affinities for antigen (such as $CD8^+$ tumour- and auto-reactive T cells, and the majority of $CD4^+$ T cells (Cole et al. 2007)) continue to 'fly under the radar' because they cannot be detected using conventional pMHC multimers staining procedures. The importance of developing better ways to visualise these low avidity T cell subsets becomes especially apparent when we consider that T cells that recognise the same pMHC antigen are known to differ in their sensitivity to this antigen by several orders of magnitude (Alexander-Miller et al. 1996; Alexander-Miller 2000). In view of this, it is becoming increasingly accepted that the quality of a T cell response may be just as important as its quantity, and that pMHC multimers can be used as invaluable tools for 'grading' the quality of an antigen-specific T cell population. In this chapter I investigated the properties of tetrameric pHLA A2 complexes containing a Q115E mutation in the α2 domain of the heavy chain (Figure 3.3), to engage CD8 with enhanced affinity without affecting the integrity of the TCR binding platform. The principal findings are:

i) CD8 coreceptor-enhanced Q115E pHLA A2 tetramers bind antigen-specific $CD8^+$ T cells with avidities that lie below the detection threshold for wildtype tetramers (Figure 3.4).

ii) This effect is achieved through a disproportionate enhancement of the TCR/pMHCI association rate (Figure 3.5).

iii) The CD8-enhanced tetramers retain their cognate binding properties in direct *ex vivo* applications (Figure 3.6).

iv) Background staining of the $CD8^+$ T cell subset can be distinguished phenotypically as a mixture of naïve and memory cells (Figure 3.6).

By experimenting with Q115E-substituted HLA A2 tetramers presenting a collection of ILA APLs (Figure 3.1), I have quantified the ability of these CD8-enhanced reagents to detect significantly weaker TCR/pMHCI (approximate $K_D \geq 250$ μM) interactions than wildtype reagents (approximate $K_D \geq 80$ μM), without significant increases in background levels. Furthermore, using the well characterised ILA system, I have succeeded in proving that the ability of CD8-enhanced tetramers to stain low avidity T cells arises from a disproportionate increase in TCR/pMHC association rate. So while a single Q115E mutation in the heavy chain of HLA A2 stabilises the cognate TCR/pMHCI by only ~50%, the combined avidity of this effect can substantially increase tetramer on-rate and impact on tetramer staining. Extending the findings from the well characterised ILA system to an *ex vivo* setting highlights a novel use of CD8-enhanced pMHCI tetramers for the physical detection, quantification and characterisation of low avidity antigen-specific $CD8^+$ T cell populations by flow cytometry, a task that would otherwise not be achieved with wildtype reagents. While there are concerns that as the CD8-enhanced tetramers lower the affinity threshold for the TCR/pMHCI interaction, increases in background level of staining would become inevitable for some *ex vivo* specimens, background staining can be reliably distinguished from cognate staining on the basis of phenotypic characteristics. Naive populations displaying a low level of fluorescence are a typical indication of non-specific tetramer uptake. Thus, is it highly recommended that CD8-enhanced pMHCI tetramers are used in conjunction with polychromatic flow cytometric platforms for optimal evaluation of antigen-specific immune responses. In addition, where the staining of intermediate/high avidity T cells is concerned, low concentrations of Q115E HLA A2 tetramers can be used as a substitute for wildtype tetramers in order to conserve reagent.

Chapter 4

4

DETECTION OF LOW AVIDITY CD8$^+$ T CELLS WITH PEPTIDE-MHC DEXTRAMERS

Chapter 4

4.1 Introduction

The low affinity of some TCR/pMHC interactions means it is not possible to use conventional pMHC tetramer technology to detect T cells bearing such TCRs. In the previous chapter I have demonstrated how pMHCI tetramers displaying an enhanced interaction with the CD8 coreceptor are able to stain low avidity T cells, which remain undetected by conventional pMHCI tetramer technology. In this chapter I report the use of an alternative multimerization scaffold (dextran) to increase pMHC and fluorochrome valency, with the ultimate aim of improving the detection of $CD8^+$ and $CD4^+$ T cells bearing low affinity TCRs.

4.1.1 pMHC dextramers

The design of pMHC dextramers arises from the same principles as other pMHC multimers: the multimerization of pMHC allows several pMHC molecules to interact simultaneously with multiple TCRs on a single T cell, greatly prolonging the half-life of interaction, and thus enabling specific T cell detection. Dextramers differ from tetramers in three ways: i) each dextramer contains 8-12 pMHC molecules instead of the four found in a pMHC tetramer; ii) the pMHC molecules are organised around a dextran polymer backbone (instead of a single streptavidin molecule used to make pMHC tetramers) in an orientation that enables optimal TCR/pMHC contact; and, iii) the dextran backbone of dextramers carries a larger number of conjugated fluorochrome molecules than a pMHC tetramer (Batard et al. 2006). Theoretically, these features act to increase the dextramers' avidity for specific T cells and enhance their staining intensity, thereby increasing the resolution and signal to noise ratio. Figure 4.1 shows a schematic of a pMHC dextramer alongside a pMHC tetramer.

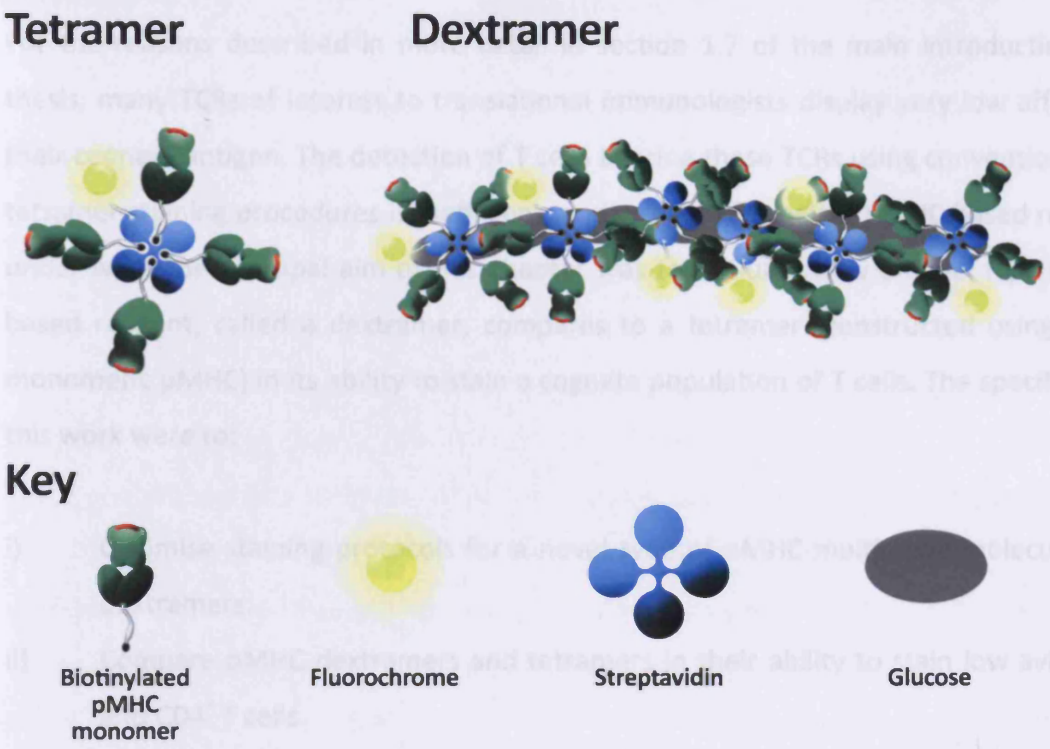

Figure 4.1: Comparison of dextramer and tetramer structures. A pMHC dextramer is composed of a dextran (polymer of glucose) backbone decorated with numerous streptavidin molecules which in turn bind 1-4 pMHC molecules (via their biotin tags), and several fluorochrome molecules.T he numbers of each type of component varies between different dextramers. A pMHC tetramer is composed of a streptavidin molecule, around which 4 pMHC molecules and a fluorochrome are arranged.

4.1.2 Aims

For the reasons described in more detail in section 1.7 of the main Introduction of this thesis, many TCRs of interest to translational immunologists display very low affinities for their cognate antigen. The detection of T cells bearing these TCRs using conventional pMHC tetramer staining procedures is inefficient, and a search for better pMHC-based reagents is under way. The principal aim of this chapter was to evaluate how a novel type of pMHC-based reagent, called a dextramer, compares to a tetramer (constructed using identical monomeric pMHC) in its ability to stain a cognate population of T cells. The specific aims of this work were to:

i) Optimise staining protocols for a novel type of pMHC multimeric molecules called dextramers.

ii) Compare pMHC dextramers and tetramers in their ability to stain low avidity $CD8^+$ and $CD4^+$ T cells.

iii) Provide a mechanistic explanation for pMHC dextramer action based on observations in ii), if time-permitting.

4.2 Results

4.2.1 pMHCI dextramers show improved staining of low avidity $CD8^+$ T cells over corresponding pMHCI tetramers

In addition to my investigation into the influence of the CD8 coreceptor on pMHCI tetramer staining of $CD8^+$ T cells, I was given the opportunity to test a novel type of pMHC multimeric reagent called a dextramer. The well documented ILA system was ideal for the initial part of the investigation into whether pMHCI dextramers would hold an advantage over pMHCI tetramers in staining specific $CD8^+$ T cells. HLA A2 monomers were refolded around the ILA index peptide and four APLs (8E, 5Y, 4L and 3G) displaying a wide range of affinities for the ILA1 TCR (K_D ~2000-3.7 μM, Figure 3.1 A in Chapter 3). An additional HLA A2 monomer was refolded around the $HIV_{309-317}$ epitope (ILKEPVHGV), designed to act as a negative control for monitoring background staining with each type of pMHCI multimeric reagent. The pMHCI monomers were assembled into either tetramers or dextramers (Figure 4.1, and sections 2.8.1 and 2.8.5 of Material and Methods), both conjugated to the same R-phycoerythrin (PE) fluorochrome for detection by flow cytometry. Initially, a titration of tetramers and dextramers incorporating ILA index/HLA A2 and non-cognate HIV epitope/HLA A2 was performed to establish the amount of each type of reagent required to stain the ILA1 clone with the highest signal to noise ratio (Figure 4.2). From this preliminary titration experiment it was decided that the optimal staining amounts for each reagent were: 10 μl for dextramer and 0.5 μg for tetramer. Since tetramers and dextramers are different types of reagents it was possible that by performing a titration, the increase in staining MFI demonstrated by dextramers over tetramers was simply due to a 10 μl dextramer preparation containing more monomeric pMHC than found in 0.5 μg of tetramer preparation. By calculating the amount of monomeric pMHC in 10 μl dextramer and 0.5 μg tetramer preparations I was able to establish the concentration of pMHC monomer present per dextramer or tetramer staining. Because dextramers conjugated to each of three fluorochromes (PE, APC, or FITC) have been optimised to comprise different quantities of streptavidin (SA) or pMHC monomer, the amounts of monomeric pMHC within each type of dextrameric reagent varies (see section 2.8.5 of Materials and Methods). When carried out in a 40 μl final staining volume, each 0.5 μg tetramer-PE stain corresponds to a

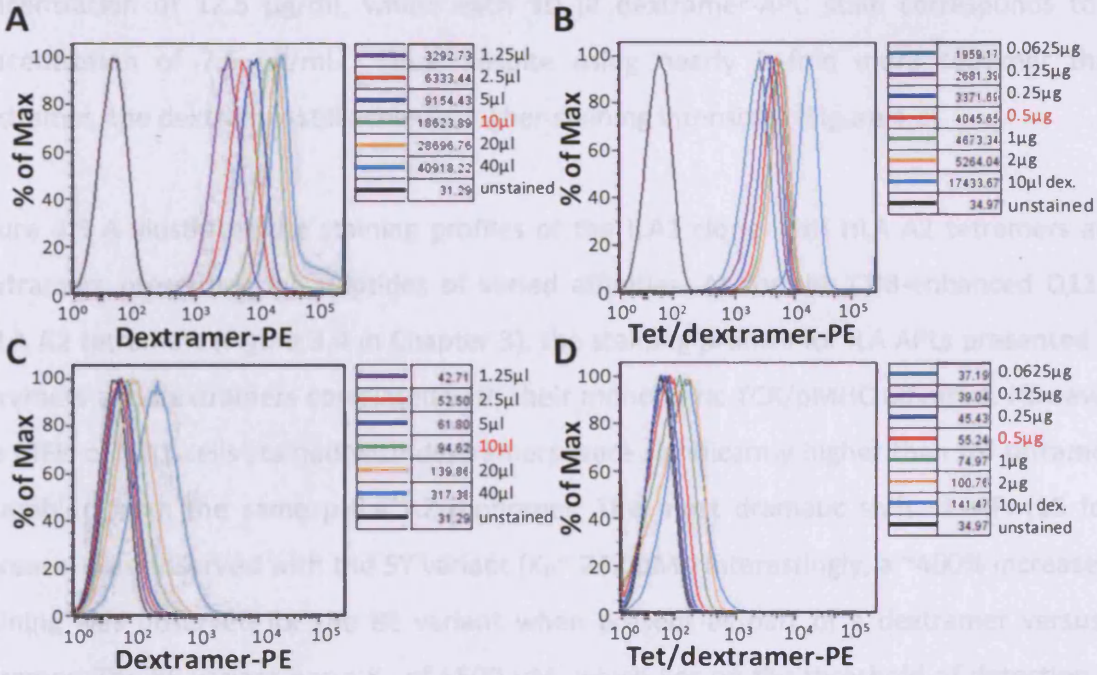

Figure 4.2: Establishing optimal amounts of pMHC tetramer and dextramer reagents to use per test. 10^5 ILA1 cells were stained with different quantities of ILA index/ HLA A*0201 dextramer (**A**) and tetramer (**B**), or a non-cognate HIV epitope/ HLA A*0201 dextramer (**C**) and tetramer (**D**), all conjugated to the R-phycoerythrin (PE) fluorochrome, and recorded by flow cytometry. The histograms show staining mean fluorescence intensity (MFI) obtained with titrated amounts of pMHCI tetramer/ dextramer. The optimal amount of each type of pMHC multimeric reagent (highlighted in red) was determined by looking at staining profiles with the highest signal to noise ratios. The data is representative of 2 separate experiments.

concentration of 12.5 μg/ml, whilst each 10 μl dextramer-APC stain corresponds to a concentration of 7.5 μg/ml. Thus, despite using nearly 2 fold more tetramer than dextramer, the dextramer still achieves higher staining intensities (Figure 4.2).

Figure 4.3 A illustrates the staining profiles of the ILA1 clone with HLA A2 tetramers and dextramers presenting ILA peptides of varied affinities. As for the CD8-enhanced Q115E pHLA A2 tetramers (Figure 3.4 in Chapter 3), the staining profiles for ILA APLs presented by tetramers and dextramers correlated with their monomeric TCR/pMHC affinities. However, the MFIs of ILA1 cells stained with dextramers were significantly higher than for tetramers assembled from the same pHLA A2 monomer. The most dramatic shift in MFI (15 fold increase) was observed with the 5Y variant (K_D~ 242 μM). Interestingly, a ~400% increase in staining was observed for the 8E variant when present as part of a dextramer versus a tetramer. The 8E variant has a K_D of >500 μM, which lies on the threshold of detection by SPR, and does not stain the ILA1 clone when presented by tetrameric HLA A2. If the staining seen with the 8E variant is indeed real, it represents one of the weakest TCR/pMHCI interactions ever detected by a relatively insensitive technique of flow cytometry. Finally, although there was some increase in background staining with non-cognate dextramers over tetramers, this corresponded to a very small percentage of the dramatic increase in specific staining signal and was therefore deemed to be acceptable in terms of signal to noise ratio.

To test how the pMHCI tetramer and dextramer reagents performed in a more physiological setting, I set up a 'spiking' experiment by staining PBMC (isolated directly *ex vivo*) which have been mixed (spiked) with a small percentage (1%) of ILA1 $CD8^+$ T cells. Figure 4.3 B shows the ability of each ILA APL/HLA A2 tetramer (top panel) and dextramer (bottom panel) to pick out the ILA1 population amongst the PBMC. Consistent with the results from ILA1 staining alone (Figure 4.3 A), the 5Y dextramer was able to stain the target ILA1 population, whilst the 5Y tetramer failed to separate the ILA1 clone from the bulk PBMC $CD8^+$ population. Clearer separation of the ILA1 target population (from bulk PBMC) was seen with the 4L dextramers compared to 4L tetramers. Slight increases in MFI were also

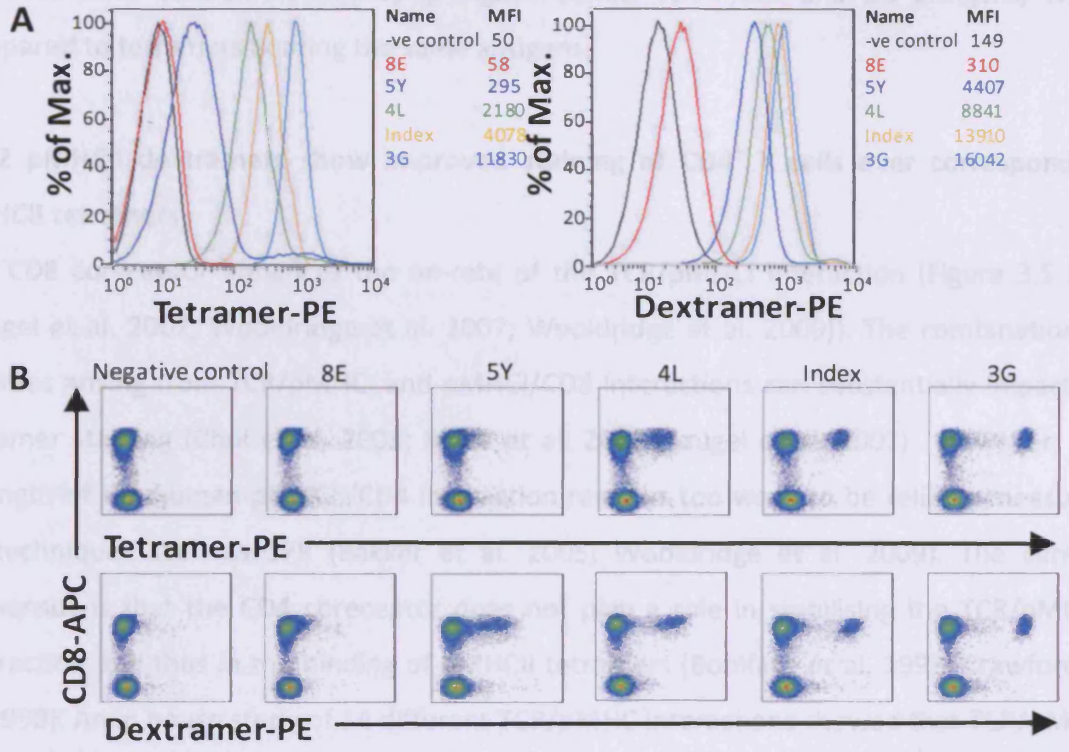

Figure 4.3: Comparison of pHLA A2 tetramer and dextramer staining profiles of ILA1 CD8⁺ T cells and PBMC spiked with ILA1. A. The ILA1 CD8⁺ T cell clone was stained with tetramer (left panel) and dextramer (right panel) reagents made with pHLA A2 monomers bearing different variants of the index $hTERT_{540-548}$ peptide (ILAKFLHWL), or the non-cognate $HIV_{309-317}$ peptide (ILKEPVHGV), conjugated to the R-phycoerythrin (PE) fluorochrome. TCR/pMHCI affinities measured by SPR for the ILA variants has been previously documented (Laugel et al. 2007). **B.** 10^6 human PBMC were spiked with 10^4 ILA1 cells and stained with the ILA variant tetramers (top panel) or dextramers (bottom panel) and a combination of antibodies against the surface markers CD3, CD4, CD8, CD14, CD19, and the viability dye Aqua. Staining with dextramers and tetramers (in A and B) was performed using optimal conditions for each type of reagent (section 2.10 of Materials and Methods). Representative data of 3 separate experiments shown.

observed with dextramers displaying higher affinity ILA index and 3G antigens, when compared to tetramers bearing the same antigens.

4.2.2 pMHCII dextramers show improved staining of $CD4^+$ T cells over corresponding pMHCII tetramers

The CD8 coreceptor enhances the on-rate of the TCR/pMHCI interaction (Figure 3.5 and (Laugel et al. 2007; Wooldridge et al. 2007; Wooldridge et al. 2009)). The combination of avidities arising from TCR/pMHCI and pMHCI/CD8 interactions can substantially impact on tetramer staining (Choi et al. 2003; Pittet et al. 2003; Laugel et al. 2007). However, the strength of the human pMHCII/CD4 interaction remains too weak to be reliably measured by techniques such as SPR (Bakker et al. 2005; Wooldridge et al. 2009). The current consensus is that the CD4 coreceptor does not play a role in stabilising the TCR/pMHCII interaction and thus in the binding of pMHCII tetramers (Boniface et al. 1998; Crawford et al. 1998). An in house study of 14 different TCR/pMHC interactions showed that TCR/pMHCI interactions were of significantly higher affinity than TCR interactions with MHCII-restricted peptides (Cole et al. 2007). In light of this, $CD4^+$ T cells are notoriously more difficult to detect using pMHC tetramer technology. To determine whether the staining advantage of pMHC dextramers over tetramers was true for the MHC class II system, I stained a $CD4^+$ T cell clone (Flu2-5), specific for the HLA DR*0101 (HLA DR1)-restricted influenza virus A $HA_{307-319}$ epitope (PKYVKQNTLKLAT), with tetramers and dextramers assembled from HA/HLA DR1 monomeric pMHCII. The Flu2-5 T cell clone was also stained with non-cognate tetramers and dextramers containing MAGE-$A3_{271-279}$ (FLWGPRALV)/HLA A*0101 (HLA A1) monomeric pMHCI to monitor differences in background staining for the two types of pMHC multimeric reagent. Figure 4.4 (A) shows the MFI profiles for the tetramer- and dextramer-stained Flu2-5 T cell clone. The HA dextramer stained the Flu2-5 clone with 5-fold higher intensity than the HA tetramer, with an insignificant increase in background staining. When the HA tetramer and dextramer reagents were used to stain PBMC which had been 'spiked' with the Flu2-5 clone (comprising 1% of total PBMC), the HA dextramer was able to specifically distinguish the target $CD4^+$ T cell clone from the rest of the PBMC,

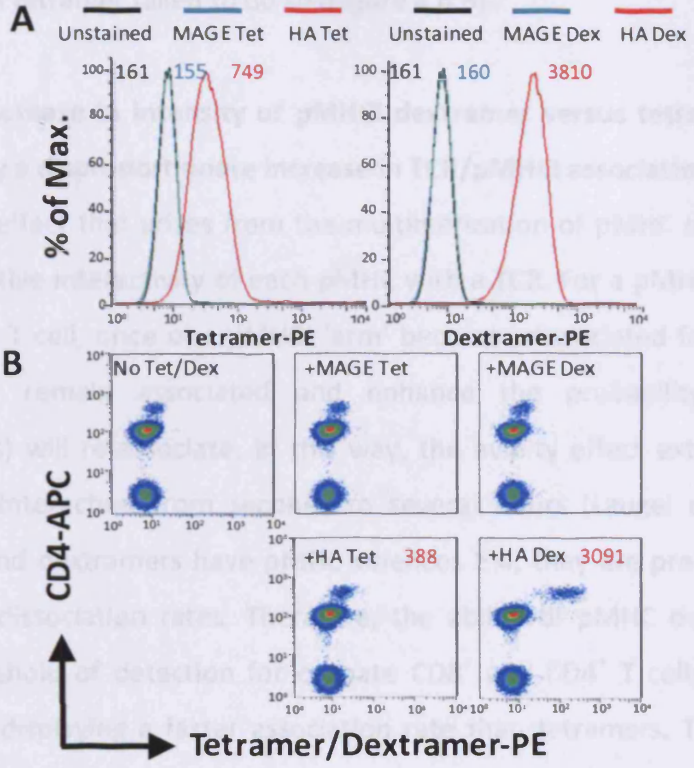

Figure 4.4: Dextramers made with pHLA DR*0101 bind CD4⁺ T cells substantially better than tetramers made with equivalent monomeric pMHC. A. The Flu2-5 CD4⁺ T cell clone was stained with tetramer (left panel) and dextramer (right panel) reagents made with pHLA DR*0101 monomers bearing the cognate influenza virus A $HA_{307-319}$ (PKYVKQNTLKLAT) peptide (red line) and MAGE-$A3_{271-279}$ (FLWGPRALW)/ HLA A*0101 (blue line) as a negative control, all conjugated to the R-phycoerythrin (PE) fluorochrome. The numbers next to each histogram correspond to the staining MFI with each tetramer/dextramer reagent and unstained cells (black line). **B.** 10^6 human PBMC were spiked with 10^4 Flu2-5 CD4⁺T cells and stained with cognate Flu HA or non-cognate MAGE tetramers or dextramers and a combination of antibodies against the surface markers CD3, CD4, CD8, CD14, CD19, and the viability dye Aqua. Numbers in red correspond to the staining MFI of the Flu2-5 T cells population. Staining with dextramers and tetramers (in A and B) was performed using 10 µg/ml of each type of reagent with respect to monomeric pMHC content. Representative data of 2 separate experiments shown.

while the HA tetramer failed to do so (Figure 4.4 B).

4.2.3 The increase in intensity of pMHCI dextramer versus tetramer staining cannot be explained by a disproportionate increase in TCR/pMHCI association rate

The avidity effect that arises from the multimerization of pMHC molecules is the result of the cooperative interactivity of each pMHC with a TCR. For a pMHC tetramer bound to the surface of a T cell, once one pMHCI 'arm' becomes dissociated from its cognate TCR, the other arms remain associated and enhance the probability that the dissociated interaction(s) will re-associate. In this way, the avidity effect extends the half-life of the TCR/pMHC interaction from seconds to several hours (Laugel et al. 2005). Since both tetramers and dextramers have pMHC valences ≥ 4, they are predicted to have very long TCR/pMHC dissociation rates. Therefore, the ability of pMHC dextramers to extend the avidity threshold of detection for cognate $CD8^+$ and $CD4^+$ T cells might be explained by dextramers displaying a faster association rate than tetramers. To test whether this was indeed the case, I compared the rate at which ILA1 $CD8^+$ T cells adsorbed tetramers and dextramers (assembled from 4L/HLA A2 monomers) from solution over a 20 minute period at room temperature (Figure 4.5). Although the 4L-dextramer stained the ILA1 clone with an MFI four times higher than observed with 4L-tetramer (Figure 3.4), surprisingly its association rate was considerably (~ 6 fold) lower than for the corresponding tetramer. And while the tetramer stained the ILA1 population at its maximum fluorescence intensity after only 7 minutes, the dextramer required >20 minutes to reach its maximum level of staining (Figure 4.5). The fact that the efficiency of dextramer staining was not a result of high association rates, proved somewhat surprising. Perhaps the explanation to the dextramers' mode of action was more to do with the structure of these molecules, than with the binding kinetics of the individual pMHCs. When pMHC tetramers are used to stain a specific T cell under physiological temperatures, they are readily internalised into endocytic vesicles (Whelan et al. 1999). Thus, any tetramer that can associate with the T cell surface for just a few minutes at 37°C will be internalised and subsequently unable to dissociate from the cell during an experiment. The endocytosis is a consequence of TCR ligation by its cognate pMHC antigen, and results in the downregulation of TCR/pMHC tetramer complexes from the cell surface. Once inside the endocytic vesicles, the tetramers cannot dissociate

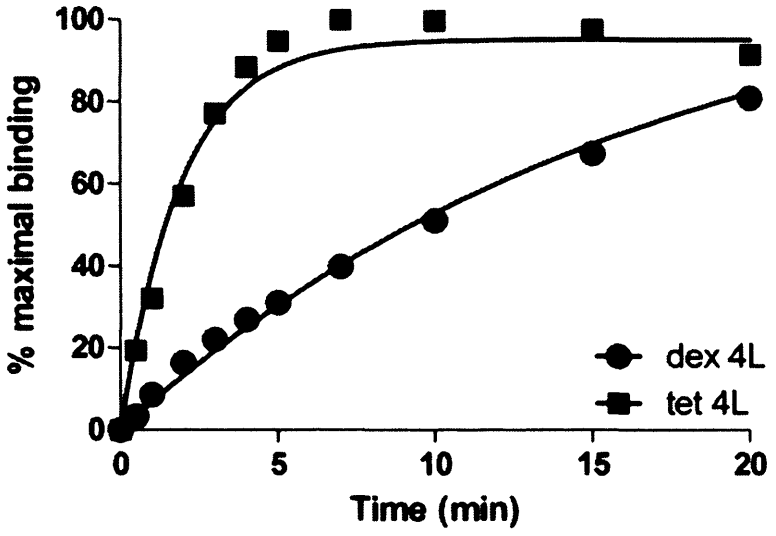

Figure 4.5: A comparison of pMHCI dextramer and tetramer association rates. 4L/ HLA A*0201 dextramer (circles) and tetramer (squares) capture from solution by the ILA1 $CD8^+$ T cell clone over a period of 20 minutes at room temperature. The concentrations of both reagents were titrated to achieve a maximal fluorescence intensity of ~2000. The pMHC association curves are representative of 2 separate experiments.

from the cell during an experiment. Another consequence of TCR/pMHC internalisation into vesicles is that any bound tetramers are enzymatically degraded, which leads to a reduction in the fluorescence signal over time (Whelan et al. 1999). In addition to endocytic degradation, pMHC tetramer-mediated TCR downregulation reduces the TCR concentration on the T cell surface. As described in section 1.6 of the main Introduction, TCR concentration constitutes an important parameter of pMHC tetramer staining efficiency. We hypothesised that the sheer size of dextramers, composed of the bulky dextran backbone in addition to a multitude of pMHC and fluorochrome entities, may simply prevent the internalisation of these molecules into endocytic vesicles following TCR engagement. To this end, I performed fluorescence microscopy with tetramers and dextramers under identical staining conditions (as described in section 2.12 of Materials and Methods) (Figure 4.6 B). ALW/HLA A2 Alexa-488 conjugated tetramers and ALW/HLA A2 FITC-conjugated dextramers were used to stain the 3F2 $CD8^+$ T cell clone, which recognises the HLA A2-restricted epitope of the preproinsulin (PPI_{15-24}; ALWGPDPAAA) antigen, called ALW. The staining intensities for the two types of ALW/HLA A2 multimer were verified by flow cytometry prior to performing microscopy (Figure 4.6 A). The presence of multitudes of small fluorescent vesicles in the microscopy images (Figure 4.6 B) confirmed that dextramers, like tetramers, were being internalised from the T cell surface. The only marked difference was the fact that dextramer staining delivered a consistently brighter fluorescence signal compared to tetramers, when measured by both flow cytometry and fluorescence microscopy (Figure 4.6).

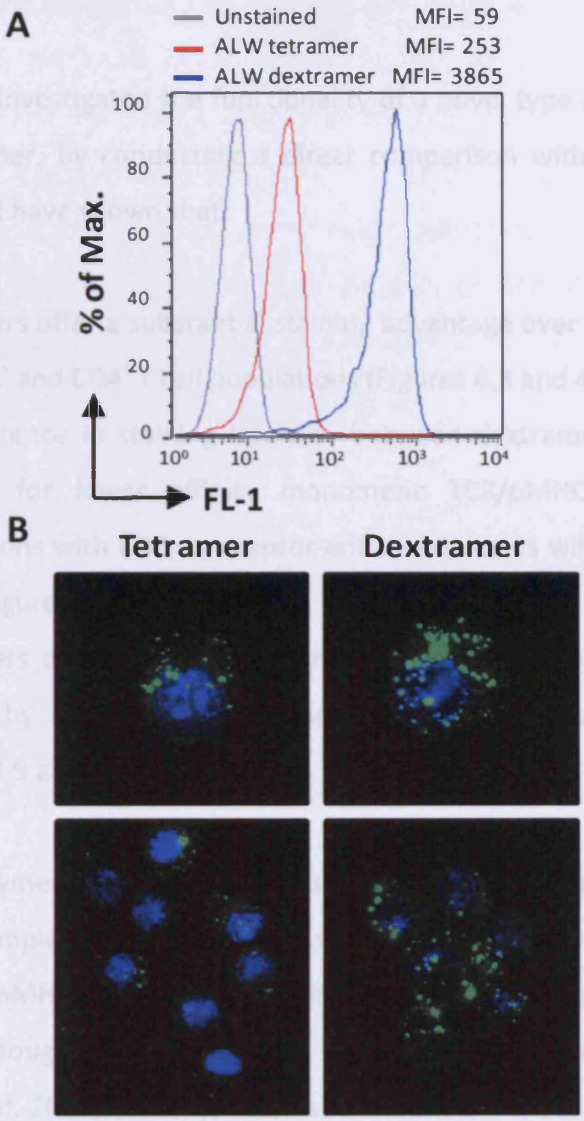

Figure 4.6: pMHC tetramers and dextramers are internalised by T cells at 37°C.A . FACS plot showing the differences in mean fluorescence staining intensities (MFIs) between tetramer- and dextramer-stained $CD8^+$ T cell clone, ALW, specific for the HLA A*0201-restriced epitope of preproinsulin, ALW (PPI_{15-24}; ALWGPDPAAA). The cognate ALW-specific tetramers and dextramers were assembled using ALW/HLA A2 monomers conjugated to the fluorochrome Alexa-488, and FITC, respectively. Both fluorochromes, fluoresce in the same channel (FL-1).**B .** Fluorescence microscopy images of ALW cells stained with cognate ALW/pHLA A2 tetramers (left panels) and cognate dextramers (right panels). The staining was performed at 37°C and as described in section 2.12 of Materials and Methods, and is representative of at least 3 replicates. Nuclei are shown in blue, and the tetramers/ dextramers in green. Although the pattern observed using fluorescence microscopy does not guarantee the presence of pMHC multimer inside cells, evidence for internalisation of tetramer into early-endocytic vesicles at 37°C has previously been documented by Whelan *et al.* 1999 using confocal microscopy.

4.3 Discussion

In this chapter I investigated the functionality of a novel type of pMHC multimeric reagent, called a dextramer, by conducting a direct comparison with tetramers assembled using identical pMHC. I have shown that:

i) Dextramers offer a substantial staining advantage over tetramers in the detection of both $CD8^+$ and $CD4^+$ T cell populations (Figures 4.3 and 4.4).

ii) The difference in staining intensity between dextramers and tetramers was most dramatic for lower affinity monomeric TCR/pMHC interactions, echoing the observations with CD8 coreceptor-enhanced versus wildtype tetramers summarised earlier (Figures 4.3 and 4.4).

iii) Dextramers do not manifest their effects by displaying increased TCR association-rates or by evading internalisation into early endosomes from the cell surface (Figures 4.5 and 4.6).

The dextran polymer backbone stabilises the conformation of the attached proteins, the MHC-peptide complexes and fluorochromes in a way that aims to maximise the number of successful TCR/pMHC contact points. In contrast, only three out of the four pMHC molecules are thought to be capable of engaging a cell-surface TCR in a pMHC tetramer (Wooldridge et al. 2009). Initially, these structural differences pointed towards dextramers manifesting their effects via a faster rate of association. However, dextramers took ≥3 times longer than tetramers to attain their maximum staining potential (Figure 4.5). Confronted with this result, we considered the possibility that perhaps the sheer size of dextramers, compared to the much smaller tetramers, prevented the internalisation of these reagents into endocytic vesicles when the staining was performed under physiological temperatures. My microscopy data showed that this was not the case (Figure 4.6). And although it would have been interesting to provide a mechanistic explanation for the fact that dextramers hold an advantage over conventional tetramers in staining low avidity T cells, it was not a principal aim of this study and was not pursued further. We can however speculate that the size of dextramers is responsible for the slow rates of uptake observed (Figure 4.5). While

compact tetramers can diffuse between cells with relative ease, bulky dextramers may take longer to do so. The most likely reason that dextramers are better than conventional tetramers at staining low avidity T cells may be due to something as simple as dextramers having a brighter signal due to the large number of fluorochrome molecules per reagent compared to tetramers. Irrespective of their mode of action, the data presented in this chapter provide validation of dextramers as a novel and valuable tool for the physical detection of low avidity $CD8^+$ and $CD4^+$ T cell populations by flow cytometry.

Chapter 5

5

PROTEIN KINASE INHIBITORS SUBSTANTIALLY IMPROVE THE PHYSICAL DETECTION OF T CELLS WITH PEPTIDE-MHC TETRAMERS

Chapter 5

5.1 Introduction

5.1.1 What is dasatinib?

Dasatinib is a dual Bcr-Abl/Src kinase inhibitor, which entered the clinic for the treatment of chronic myeloid leukaemia (CML) and acute lymphoblastic leukaemia (ALL), and is a second generation drug designed to benefit cancer patients that have become resistant to its predecessor imatinib (common name Glivec, Novartis)(Shah et al. 2004; Weichsel et al. 2008). Since Src kinases are known to play an important physiological role in T cell activation, Weichsel *et al.* conducted an elegant study into the role of the protein tyrosine kinase inhibitor (PKI) dasatinib on T cell function, to assess its toxicity to the immune system compared to the promiscuous PKI staurosporine. The authors examined the effects of dasatinib and staurosporine on T cells, and discovered that both reagents exerted an inhibitory effect on multiple T cell effector functions including proliferation, activation, cytokine production, and degranulation. Importantly, this was mediated by the disruption of early T cell signal transduction events and was not due to a reduction in T cell viability. Despite reducing T cell functionality, the inhibitory effect of dasatinib (unlike staurosporine) was entirely reversible following withdrawal of the drug. Indeed, T cell clones incubated in 50 nM dasatinib for 24 hours were able to regain responsiveness to antigen within 1 hour of drug removal.

5.1.2 T cell signalling and dasatinib

Many of the inhibitory effects of dasatinib can be attributed to its action on the signalling molecule Lck. Lck is a key player in the TCR-mediated signalling cascade, which is initiated when a T cell makes contact with cognate antigen. Together with another kinase from the Src family, Fyn, Lck is closely associated with coreceptors CD4 and CD8 (Zamoyska et al. 2003). As described in more detail in section 1.4.4 of the main Introduction, recognition of an antigenic stimulus by the TCR results in the activation of Lck and Fyn, which in turn phosphorylate tyrosine motifs located within the ζ chains of the TCR/CD3 complex. The signalling cascade eventually culminates in the activation and proliferation of the T cell. By inhibiting Lck and Fyn kinases, dasatinib is able to shut down signal transduction, resulting in T cells with defective effector functions. Because dasatinib is ~1000 times more potent than

imatinib (dasatinib IC50, 0.5 nmol/L; imatinib IC50, 0.6-0.8 μmol/L), its effect on Lck and Fyn, and ultimately T cell function is likely to be more pronounced (Carter et al. 2005; Weichsel et al. 2008). The T cell modulation group collaborated with Weichsel and colleagues to investigate whether this increase in potency displayed by the new anti-cancer drug was associated with a reduction in T cell activity, and thus immunosuppression that could prove detrimental in a clinical setting. During these studies we noticed that dasatinib treatment of T cells resulted in increased surface expression of both TCR and CD8.

5.1.3 Dasatanib increases levels of TCR and CD8 on the T cell surface

The idea that dasatinib may be used as a reagent to enhance tetramer staining stemmed from the observation by Weichsel *et al.* that dasatinib increased TCR and CD8 expression on the surface of $CD8^+$ T cells (Weichsel et al. 2008). EBV-C, ILA1, and Mel13 $CD8^+$ T cell clones (specific for the HLA A2-restricted: EBV-derived epitope GLCTLVAML; human telomerase reverse transcriptase epitope ILAKFLHWL; and, Melan-A epitope ELAGIGILTV, respectively) were treated with either dasatinib or the promiscuous PKI staurosporine at 0, 2, 10, or 100 nmol/L concentrations for 3 hours. Following incubation with either PKI, cells were stained with anti-αβTCR and anti-CD8 antibodies, and the percentage increase (above untreated $CD8^+$ T cells) in αβTCR and CD8 cell surface expression was recorded. All three $CD8^+$ T cell clones experienced increases in surface TCR and CD8 expression on treatment with dasatinib and staurosporine, predominantly when these reagents were used at 50 nM/L (Figure 5.1). The observation that dasatinib was able to increase the TCR and CD8 concentrations without appearing toxic to T cells at concentrations of <100 nM (Weichsel et al. 2008) opened up the question of whether this anti-cancer drug could be used as a tool for improving pMHC tetramer-mediated detection of T cells. However, since staurosporine was also shown to increase cell surface expression of TCR and CD8, a selection of PKIs on T cells would have to be assessed to determine which PKI had the best effect on pMHC tetramer staining with minimal T cell toxicity. This data is presented in section 5.2.1.

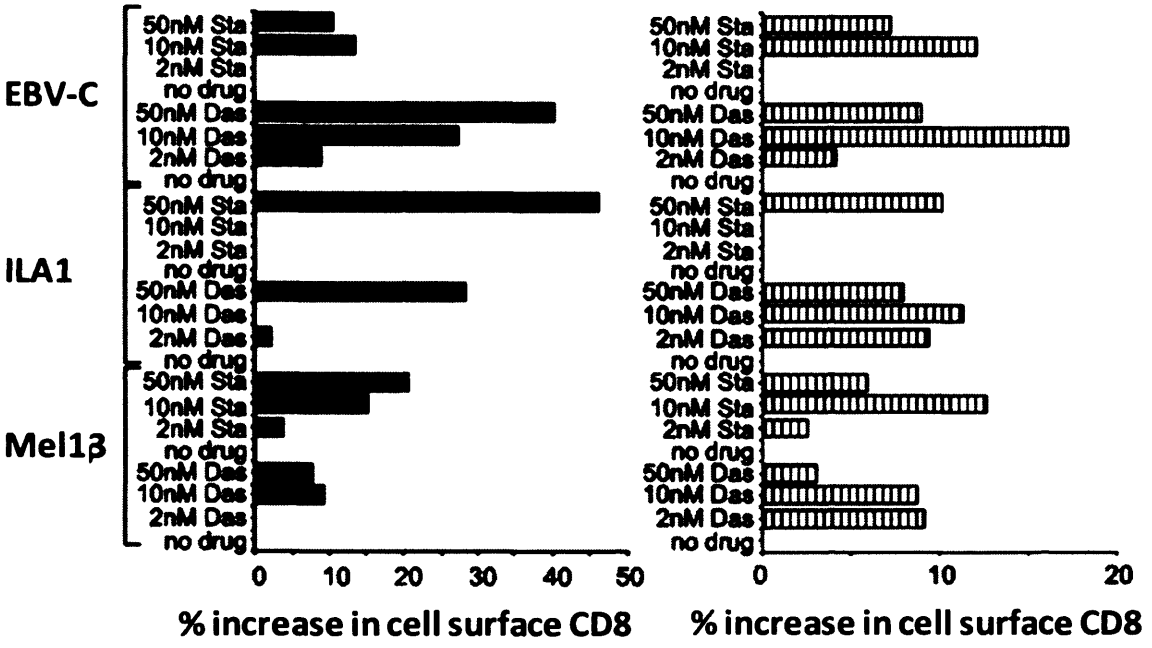

Figure 5.1: Effects of dasatinib and staurosporine on antigen-specific CD8⁺ T cell clones. Cells (1×10^5) of the CD8⁺ T cell clones EBV-C, MEL13, or ILA1 were either left untreated or treated with either dasatinib or staurosporine at concentrations of 2, 10, or 50 nmol/L for 3 hours at 37°C. The samples were analyzed for αβ TCR and CD8 expression by flow cytometry using flurochrome-conjugate surface antibody staining. (Data kindly provided by L. Wooldridge (Weichsel et al. 2008)).

5.1.4 Aims

As described in section 1.6 of the main Introduction, pMHC multimers have transformed the study of antigen-specific T cells by enabling their visualisation, enumeration, phenotypic characterisation and isolation from *ex vivo* samples. However, these reagents are far from ideal for the study of interactions where TCR/pMHC interactions are weak such as those that predominate in anti-tumour and autoimmune T cell responses. Current technology is also rather poor for MHCII-restricted T cells because their TCRs bind with lower affinity than MHCI-restricted T cells (Colf et al. 2007). Furthermore, unlike CD8, the CD4 coreceptor does not help stabilise TCR/pMHC interactions (Wooldridge et al. 2003; Wooldridge et al. 2006; Wooldridge et al. 2009) to mean that over half of pMHCII-restricted T cells fail to stain with cognate pMHCII tetramer using conventional technology. The fortuitous discovery by our laboratory that a short treatment with the non-toxic PKI dasatinib results in increased expression of both TCR and CD8 lead to speculation that we might be able to use this effect for diagnostic benefit by enhancing pMHC tetramer staining. The aims of this work were to:

i) Study the effects of short-term treatment with a selection of PKIs on pMHCI tetramer staining and determine which PKI had the best effects.

ii) Examine whether dasatinib treatment could be used to enhance pMHCII tetramer staining without a concomitant increase in background staining.

iii) Examine if dasatinib treatment could also be beneficial for pMHC tetramer staining of murine T cells.

iv) Explore whether dasatinib could help pMHC tetramer staining where TCR/pMHC affinity was low and 'beyond the reach' of current technologies.

v) Test whether dasatinib treatment could bring autoimmune T cells within the range of pMHC tetramer staining.

vi) Determine whether dasatinib could prevent the problem of pMHC tetramer-induced cell death.

vii) Assess whether dasatinib treatment could improve pMHC tetramer staining of *ex vivo* samples.

viii) Delineate the mechanism by which dasatinib improves pMHC tetramer staining.

5.2 Results

5.2.1 The effect of PKI treatment on pMHC tetramer staining of $CD8^+$ and $CD4^+$ T cells

Initially, the effect of multiple different PKIs on cognate and non-cognate pMHCI tetramer staining was determined by treating ILA1, a $CD8^+$ T cell clone specific for the HLA A2-restricted epitope $hTERT_{540-548}$ (ILAKFHWL), with titrated amounts of each PKI (Figure 5.2). Pre-incubation with the PKI PP2 (Calbiochem) resulted in a moderate increase in tetramer staining; however, no significant enhancement was observed when ILA1 $CD8^+$ T cells were pre-treated with herbimycin, PP3, genestein (Calbiochem) or staurosporine (Biomol) (Figure 5.2). Incubation of ILA1 $CD8^+$ T cells with the PKIs dasatinib or 3-(2-(1H-benzo[d]imidazol-1-yl)-6-(2-morpho-linoethoxy) pyrimidin-4-ylamino)-4-methylphenol (Lck inhibitor II; Calbiochem) resulted in a 3-10 fold increase in pMHCI tetramer staining intensity (Figures 5.2 E and 5.3 A). The variations in pMHCI tetramer staining were likely a result of natural fluctuations in TCR and CD8 expression on the surface of $CD8^+$ T cells during different stages of the grown cycle. Importantly, PKI inhibitor treatment did not enhance staining with non-cognate pMHCI tetramer (Figures 5.2 F and 5.3 B). The enhancement of pMHCI tetramer staining following dasatinib treatment was highly dose dependent (Figure 5.3 C). Maximal effect was achieved by exposing $CD8^+$ T cells to 50 nM dasatinib for 1 hour, which resulted in an 89% increase in pMHCI tetramer staining intensity (Figure 5.3 C). Unexpectedly, pre-incubation of $CD8^+$ T cells with 50 nM dasatinib for as little as 30 seconds resulted in a 60% increase in pMHCI tetramer staining (Figure 5.3 D). Furthermore, incubation with 50 nM dasatinib for 30 minutes significantly enhanced the staining of both ILA1 and Mel13 $CD8^+$ T cell clones over a wide range of pMHCI tetramer concentrations (Figure 5.3 E&F). Pre-incubation with dasatinib also enhanced pMHCI tetramer staining of the naïve murine F5 $CD8^+$ T cells directly *ex vivo* (Figure 5.3 G) and pMHCII tetramer staining of a HLA DR1-restricted $CD4^+$ T cell clone (Figure 5.3 H). Thus, pre-incubation with 50 nM dasatinib for 30 minutes provides a quick and easy way to enhance pMHC tetramer staining efficiency in both human ($CD4^+$ and $CD8^+$ T cells) and murine systems. These effects were highly specific; increased pMHC tetramer binding only occurs in the presence of a cognate TCR/pMHC interaction (Figure 5.3 B&H).

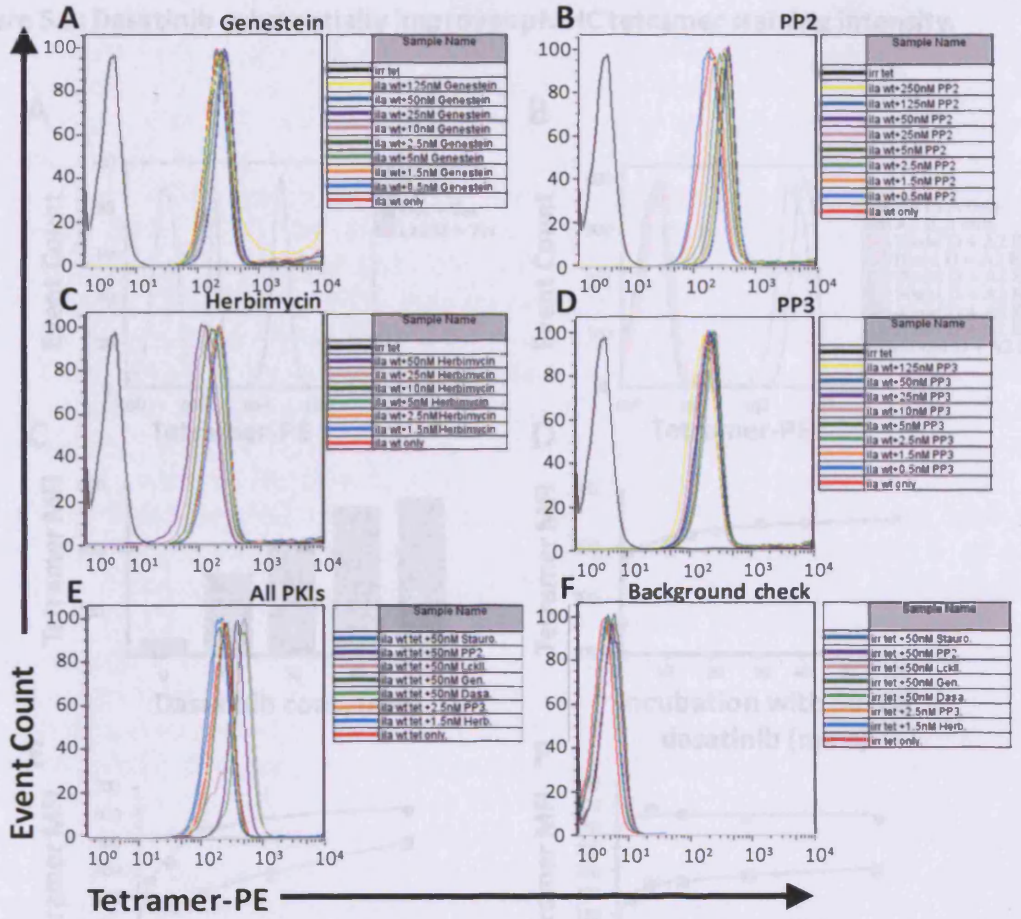

Figure 5.2: Testing the effects of other PKIs on tetramer staining. 10^5 ILA1 $CD8^+$ T cells were re-suspended in 40µl of PBS and pre-treated with various concentrations of protein kinase inhibitors; genestein (**A**), PP2 (**B**), herbimycin (**C**), and PP3 (**D**) prior to staining with cognate HLA A2/ILAKFLHWL-PE (ILA-PE) tetramer at a final concentration of 10 µg/ml for 20 minutes at 37°C. In each case, the mean fluorescence intensity (MFI) of ILA-PE tetramer staining at each concentration of PKI was compared to untreated ILA-PE stained ILA1 $CD8^+$ T cells as a reference. Untreated ILA1 cells stained with a non-cognate tetramer-PE (irr tet) were used as a negative control. **E.** ILA1 $CD8^+$ T cells were treated with optimal concentrations of each PKI (determined from A-D) and 50 nM dasatinib, or left untreated, and stained with ILA-PE tetramer. Dasatinib increased ILA1 $CD8^+$ T cell staining with ILA-PE tetramer by 127%, with the Lck II and PP2 reagents coming second and third, with 125% and 70% enhancement in staining, respectively. The increases in MFI afforded by dasatinib, Lck II inhibitor, and PP2 were determined as significant ($p < 0.001$ for dasatinib and LckII, and $p<0.05$ for PP2). **F.** The same panel of PKIs as in (E) was used to pre-treat ILA1 $CD8^+$ T cells prior to staining with non-cognate tetramer-PE to show no significant increase in background fluorescence.

Figure 5.3: Dasatinib substantially improves pMHC tetramer staining intensity.

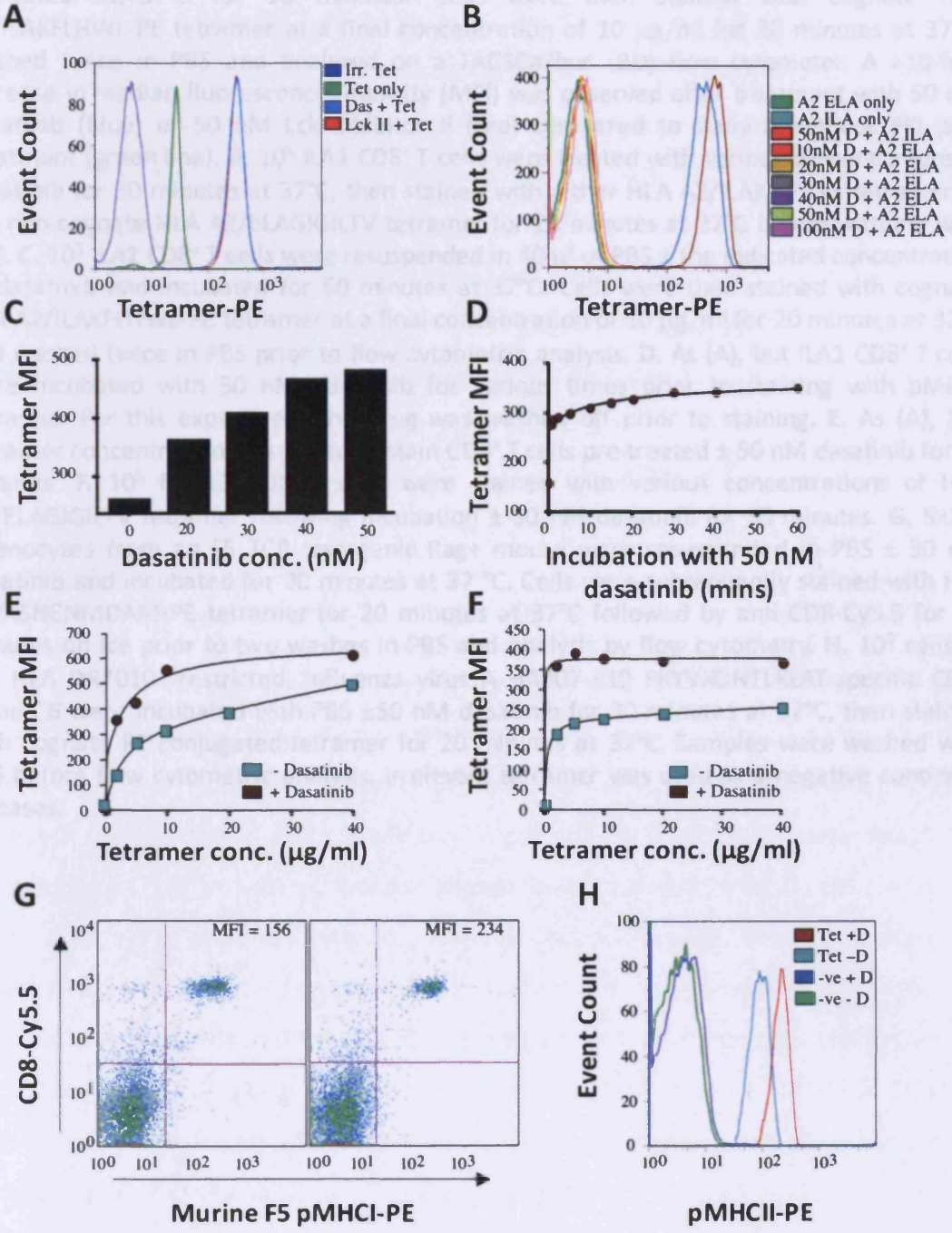

Figure 5.3: Dasatinib substantially improves pMHC tetramer staining intensity. A. 10^5 ILA1 $CD8^+$ T cells were re-suspended in 40 µl of PBS ±50 nM dasatinib or Lck inhibitor II, then incubated at 37°C for 30 minutes. Cells were then stained with cognate HLA A2/ILAKFLHWL-PE tetramer at a final concentration of 10 µg/ml for 20 minutes at 37°C, washed twice in PBS and analyzed on a FACSCalibur (BD) flow cytometer. A >10-fold increase in median fluorescence intensity (MFI) was observed after treatment with 50 nM dasatinib (blue) or 50 nM Lck inhibitor II (red) compared to staining without PKI pre-treatment (green line). **B.** 10^5 ILA1 $CD8^+$ T cells were treated with various concentrations of dasatinib for 30 minutes at 37°C, then stained with either HLA A2/ILAKFLHWL tetramer or the non-cognate HLA A2/ELAGIGILTV tetramer for 20 minutes at 37°C before washing with PBS. **C.** 10^5 ILA1 $CD8^+$ T cells were resuspended in 40 µl of PBS ± the indicated concentration of dasatinib and incubated for 60 minutes at 37°C. Cells were then stained with cognate HLA A2/ILAKFLHWL-PE tetramer at a final concentration of 10 µg/ml for 20 minutes at 37°C and washed twice in PBS prior to flow cytometric analysis. **D.** As (A), but ILA1 $CD8^+$ T cells were incubated with 50 nM dasatinib for various times prior to staining with pMHCI tetramer. For this experiment the drug was washed off prior to staining. **E.** As (A), but tetramer concentration was varied to stain $CD8^+$ T cells pre-treated ± 50 nM dasatinib for 30 minutes. **F.** 10^5 Mel13 $CD8^+$ T cells were stained with various concentrations of HLA A2/ELAGIGILTV tetramer following incubation ± 50 nM dasatinib for 30 minutes. **G.** $5x10^5$ splenocytes from an F5 TCR transgenic Rag+ mouse were resuspended in PBS ± 50 nM dasatinib and incubated for 30 minutes at 37 °C. Cells were subsequently stained with H2-Db/ASNENMDAM-PE tetramer for 20 minutes at 37°C followed by anti-CD8-Cy5.5 for 30 minutes on ice prior to two washes in PBS and analysis by flow cytometry. **H.** 10^5 cells of the HLA DR*0101-restricted, influenza virus A HA307-319 PKYVKQNTLKLAT-specific $CD4^+$ clone C6 were incubated with PBS ±50 nM dasatinib for 30 minutes at 37°C, then stained with cognate PE-conjugated tetramer for 20 minutes at 37°C. Samples were washed with PBS before flow cytometric analysis. Irrelevant tetramer was used as a negative control in all cases.

The best results were observed with the PKIs dasatinib and Lck II. Because the two reagents exhibited such similar functionality, I was interested to see if one of the reagents had an advantage over the other with relation to its stability. To compare the stability of the drugs, dasatinib and Lck II inhibitor, which are typically stored at -20°C and thawed on the day of experiment, were left at room temperature for a maximum period of 14 days. At several time points during this period, both reagents were tested for their ability to enhance staining of ILA1 $CD8^+$ T cell clone with cognate HLA A2 tetramers refolded around ILA peptide variants (Table 5.1). The results are summarised in Figure 5.4. Over the two week period that dasatinib and Lck II inhibitor were kept at RT, both reagents had retained their functionality and were able to enhance tetramer staining with the ILA variant tetramers in each case. On closer observation, dasatinib lost some of its activity after days 7, 10 and 14 at RT. This was especially visible with the low avidity 5Y and 8E ILA tetramers. However, the overall difference in stability was not considered important enough to warrant using one reagent rather than the other.

Compared to the less well characterised (at least with respect to T cell function) Lck II, dasatinib is an FDA approved drug (commercial name Sprycel, manufactured by Bristol-Myers Squibb) and is non-toxic to patients (Lombardo et al. 2004; Weichsel et al. 2008). Furthermore, when tested for stability, Lck II did not perform substantially better than dasatinib (Figure 5.4). In order to avoid an inundation of requests for us to manufacture and provide dasatinib to other laboratories, Professor Sewell informed several drug companies that there might be a new market for the substance as a research reagent. Dasatinib (>99% purity) can now be purchased for £80.00 for 10 mg (Axon Medchem) (pure reagent was not commercially available when I undertook the experiments described herein). 10 mg of dasatinib is sufficient for 10^7 pMHC tetramer stains. Due to the low cost of dasatinib and its low toxicity as evidenced by its use in patients (Lombardo et al. 2004; Weichsel et al. 2008) we decided to take dasatinib forward as our PKI of choice for subsequent studies of pMHC tetramer staining.

LIGAND	8E	5Y	4L	Index	8Y	3G8T	3G
K_D ILA1 TCR Binding (μM)	>500	242	117	36.6	22.6	4.04	3.7

Table 5.1: Affinity measurements of the interaction between the ILA1 TCR and hTERT540-548 pMHCI variants. Summary of the results obtained by nonlinear analysis of surface plasmon resonance binding equilibrium experiments as detailed in (Laugel et al. 2007) and (Melenhorst et al. 2008). K_D values were determined by analyzing the data in nonlinear curve fittings to the equation $AB=BxAB_{max}/(K_D+B)$ assuming 1:1 Langmuir binding.

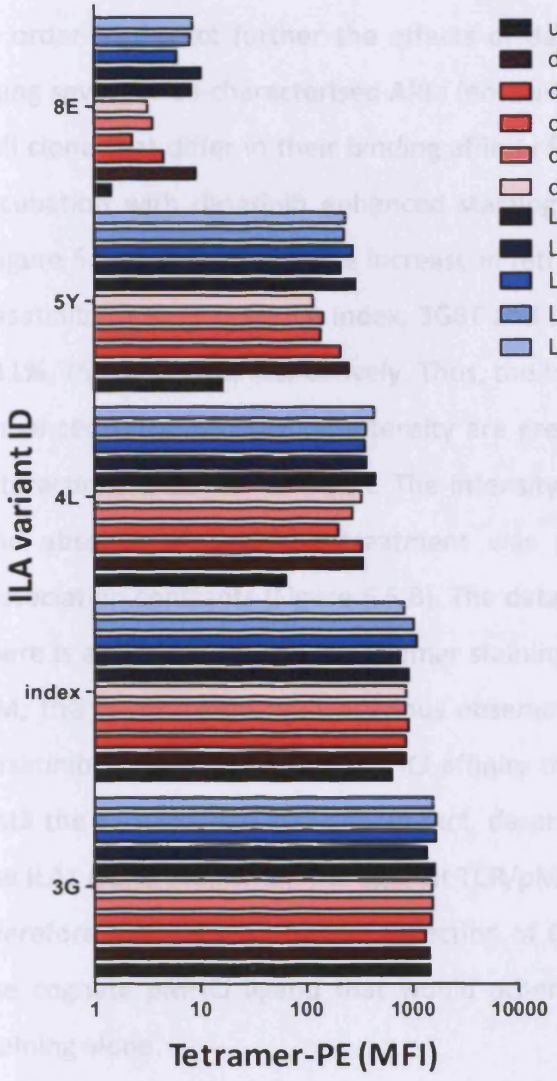

Figure 5.4: The stabilities of dasatinib and Lck II PKIs are closely matched. 10^5 ILA1 $CD8^+$ T cells were re-suspended in 40 µl of PBS and pre-treated with 50 nM dasatinib or 50 nM Lck II inhibitor prior to staining with cognate HLA A2 tetramers refolded around variants of the ILA (ILAKFLHWL) peptide (Table 5.1) at a final concentration of 10 µg/ml for 20 minutes at 37°C.T o test the stability of the PKIs relative to each other, an aliquot of dasatinib and Lck II inhibitor were left at RT for period of 1-14 days (indicated by the fading red and blue bars, respectively). ILA-PE variant tetramer staining of untreated ILA1 $CD8^+$ T cells (black bars) was used as a reference.

5.2.2 Dasatinib preferentially enhances pMHCI staining of T cells bearing low affinity TCRs

In order to dissect further the effects of dasatinib, I examined pMHCI tetramer staining using several well-characterised APLs (encountered in Chapters 3 and 4) for the ILA1 $CD8^+$ T cell clone that differ in their binding affinity for the ILA1 TCR by >100-fold (Table 5.1). Pre-incubation with dasatinib enhanced staining efficiency with all variant pMHCI tetramers (Figure 5.5 A). The percentage increase in tetramer staining afforded by pre-incubation with dasatinib for 8E, 5Y, 4L, ILA index, 3G8T and 3G pMHCI tetramers was 675%, 1825%, 324%, 111%, 75% and 26%, respectively. Thus, the benefits of dasatinib pre-treatment in terms of enhanced tetramer staining intensity are greater for peptide variants that exhibit weaker interactions with the ILA1 TCR. The intensity of pMHCI tetramer staining in the presence and absence of dasatinib treatment was plotted against the monomeric TCR/pMHCI dissociation constants (Figure 5.5 B). The data demonstrate that in the absence of dasatinib there is a sharp reduction in tetramer staining intensity for ligands with TCR/pMHCI K_D >35 μM; this is consistent with previous observations (Laugel et al. 2007). In the presence of dasatinib however, the TCR/pMHCI affinity threshold for this sharp drop-off did not occur until the K_D exceeded 200 μM. In fact, dasatinib treatment allowed detectable staining of the ILA1 clone even when the agonist TCR/pMHCI K_D exceeded 500 μM. Dasatinib treatment therefore enables the physical detection of $CD8^+$ T cells bearing TCRs with low affinity for the cognate pMHCI ligand that would otherwise be undetectable using pMHCI tetramer staining alone.

5.2.3 Dasatinib reduces pMHCI tetramer-induced cell death

Previous studies have shown that soluble pMHCI tetramer-induced signalling can trigger cell death (Purbhoo et al. 2001; Guillaume et al. 2003; Cebecauer et al. 2005). This can reduce the number of live cells that remain after pMHCI tetramer staining. Activation-induced cell death (AICD) represents a huge impediment for pMHC multimer guided sort-cloning of antigen specific T cells. At best, such sort cloning is only ~2% efficient (unpublished observations). This low frequency drops further when TCR/pMHC interactions are of high affinity or for staining times longer than 10 minutes. Consequently, methodologies for preventing pMHC multimer-induced cell death are highly desirable. Since dasatinib blocks

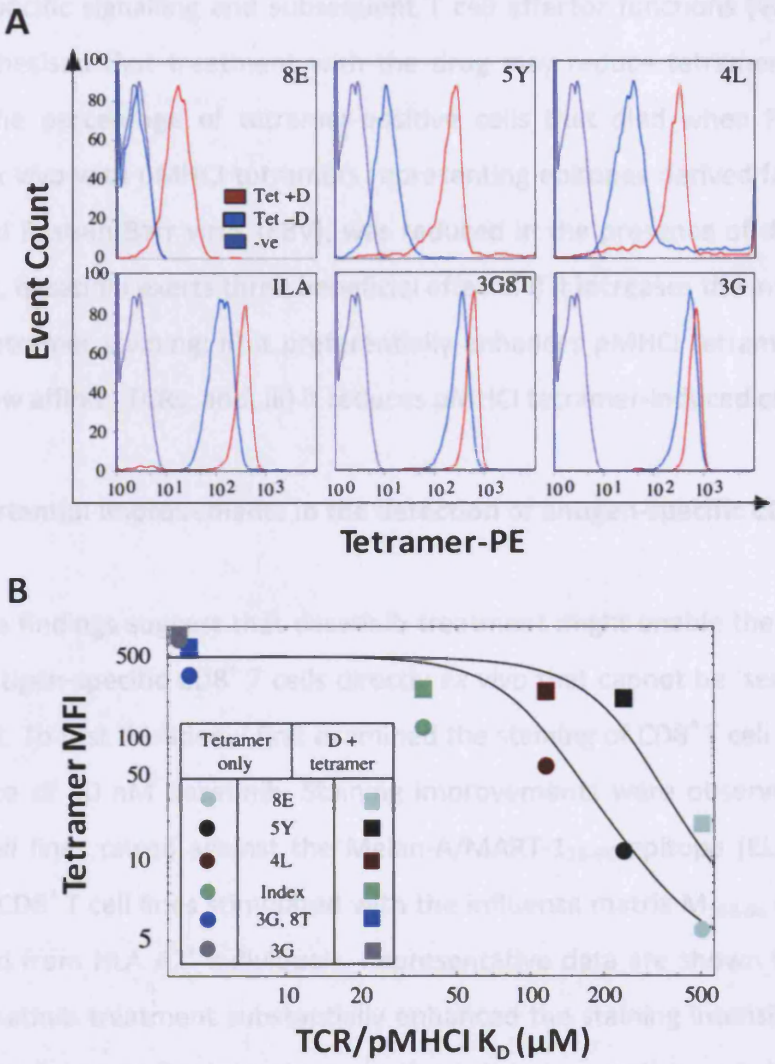

Figure 5.5: Dasatinib treatment preferentially increases the ability of pMHCI tetramers to stain T cells bearing low affinity TCRs. A. 10^5 ILA1 $CD8^+$ T cells were stained with 10 μg/ml PE-conjugated HLA A2 tetramer folded around the 8E, 5Y, 4L, index (ILAKFLHWL), 3G8T or 3G peptides for 20 minutes at 37°C following incubation ± 50 nM dasatinib for 30 minutes at 37°C. For all samples, data were acquired with a FACSCalibur flow cytometer (BD) and analyzed using FlowJo software.Ir relevant tetramer was used as a negative control.**B .** The MFI of tetramer staining for all of the variants in the presence and absence of dasatinib displayed in (A) were plotted against the monomeric affinity of TCR/pMHCI interactions previously measured for each of these variants expressed as the dissociation constant (K_D)(Table 5.1). Curves were fitted as described in the Materials and Methods. FACS staining data is representative of 2 separate experiments.

antigen-specific signalling and subsequent T cell effector functions (Weichsel et al. 2008), we hypothesised that treatment with the drug may reduce tetramer-induced cell death. Indeed, the percentage of tetramer-positive cells that died when PBMCs were stained directly *ex vivo* with pMHCI tetramers representing epitopes derived from cytomegalovirus (CMV) and Epstein-Barr virus (EBV), was reduced in the presence of dasatinib (Figure 5.6). Therefore, dasatinib exerts three beneficial effects: i) it increases the intensity of pMHCI and pMHCII tetramer staining; ii) it preferentially enhances pMHCI tetramer staining of T cells bearing low affinity TCRs; and, iii) it reduces pMHCI tetramer-induced cell death.

5.2.4 Substantial improvements in the detection of antigen-specific $CD8^+$ T cells directly *ex vivo*

The above findings suggest that dasatinib treatment might enable the identification of low avidity antigen-specific $CD8^+$ T cells directly *ex vivo* that cannot be 'seen' in the absence of treatment. To test this idea, I first examined the staining of $CD8^+$ T cell lines in the presence or absence of 50 nM dasatinib. Staining improvements were observed in three different $CD8^+$ T cell lines raised against the Melan-A/MART-1_{26-35} epitope (ELAGIGILTV) and three different $CD8^+$ T cell lines stimulated with the influenza matrix M_{158-66} epitope (GILGFVFTL), all derived from HLA $A2^+$ individuals. Representative data are shown in Figure 5.7 A. In all cases, dasatinib treatment substantially enhanced the staining intensity of cognate $CD8^+$ T cells without concomitant increases in the tetramer-negative population. In accordance with the results above, $CD8^+$ T cells that stained poorly with pMHCI tetramer received the greatest benefit from dasatinib treatment. The staining intensity of all cognate $CD8^+$ T cells increased by at least 2-fold after dasatinib treatment, but T cells that bound tetramer weakly exhibited increases of >20-fold in their fluorescence intensity. In many cases, larger populations of cells that stained with the corresponding pMHCI tetramer were detected after dasatinib treatment. This increase in tetramer-positive cells after dasatinib treatment likely reflects the combined effects of a lower detection threshold in terms of TCR/pMHCI affinity and the fact that dasatinib reduces pMHCI multimer-induced cell death (Figure 5.6). Subsequently, collaborators with access to patient PBMC samples examined whether dasatinib could enhance pMHCI tetramer staining of cognate $CD8^+$ T cells directly *ex vivo* and enable the detection of antigen-specific $CD8^+$ T cells that are 'invisible' with routine

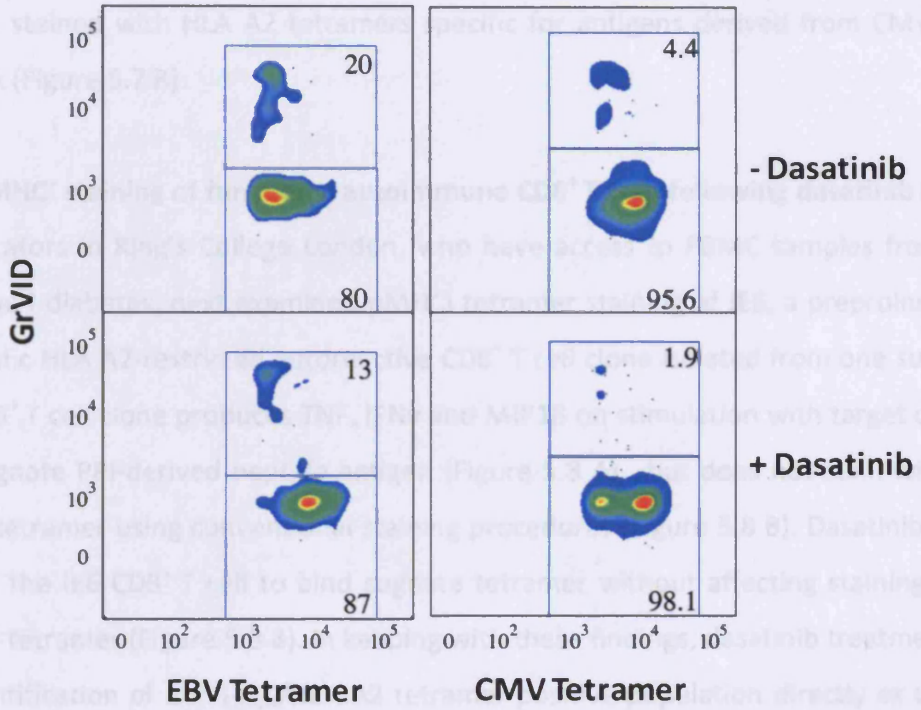

Figure 5.6: Dasatinib reduces pMHCI tetramer-induced cell death. Increased tetramer staining in the presence of dasatinib appears to be due partly to reduced cell death. Cell death induced by tetramer staining was assessed using the amine-reactive viability dye GrViD at the end of the staining procedure, which is spectrally distinct from ViViD. PBMC were stained with ViViD to identify and allow exclusion of dead and dying cells prior to the addition of pMHCI tetramer; GrVID staining was performed after pMHCI tetramer and surface antibody staining. Data were acquired on a BDLSR II flow cytometer and analyzed using FlowJo software. ViViD$^+$, CD14$^+$ and CD19$^+$ cells were excluded from the analysis and the frequency of GrViD$^+$ cells was assessed in the tetramer$^+$C D3$^+$CD8$^+$ T cell populations. Representative flow profiles are shown here for CD8$^+$ T cells specific for the HLA A2-restricted epitopes CMV $pp65_{495\text{-}503}$ (NLVPMVATV) and EBV $BMLFI_{259\text{-}267}$ (GLCTLVAML). The frequencies of dead cells varied depending on the tetramer used, but the frequency of GrViD-positive dead cells within the tetramer$^+$ population was always lower in the presence of 50 nM dasatinib.(Data kindly provided by K. Ladell).

staining procedures. Indeed, a substantial increase in both pMHCI staining intensity and the percentage of antigen-specific $CD8^+$ T cells was observed at both 4°C and 37°C in PBMC samples stained with HLA A2 tetramers specific for antigens derived from CMV, EBV and Melan-A (Figure 5.7 B).

5.2.5 pMHCI staining of functional autoimmune $CD8^+$ T cells following dasatinib treatment

Collaborators in King's College London, who have access to PBMC samples from patients with type I diabetes, next examined pMHCI tetramer staining of IE6, a preproinsulin (PPI_{15-24})-specific HLA A2-restricted autoreactive $CD8^+$ T cell clone isolated from one such patient. This $CD8^+$ T cell clone produces TNF, IFNγ and MIP1β on stimulation with target cells pulsed with cognate PPI-derived peptide antigen (Figure 5.8 A), but does not stain with cognate pMHCI tetramer using conventional staining procedures (Figure 5.8 B). Dasatinib treatment allowed the IE6 $CD8^+$ T cell to bind cognate tetramer without affecting staining with non-cognate tetramer (Figure 5.8 B). In keeping with these findings, dasatinib treatment allowed the identification of a PPI_{15-24}/HLA A2 tetramer-positive population directly *ex vivo* from a type I diabetic patient, consistent with a corresponding IFNγ ELISpot response to PPI peptide of 13 responder cells per 10^6 PBMCs (Figure 5.8 C). Dasatinib did not increase direct *ex vivo* PPI/HLA A2 tetramer staining in healthy HLA A2-matched control subjects (Figure 5.8 C). A seven-fold increase in the percentage of autoreactive $CD8^+$ T cells was observed when short-term lines expanded from two type I diabetic patients were stained in the presence of dasatinib (Figure 5.8 C). Thus, dasatinib treatment allows the detection of functional autoreactive $CD8^+$ T cells that are otherwise undetectable with standard staining conditions.

5.2.6 How does dasatinib exert its beneficial effects on pMHC tetramer staining?

Previous studies have demonstrated that incubation with Src kinase inhibitors results in enhanced TCR and CD8 expression at the cell surface (Luton et al. 1994; D'Oro et al. 1997). Consistent with these observations, Weichsel *et al.* have recently demonstrated that increased levels of TCR and CD8 are seen at the cell surface following incubation with dasatinib for 4 hours (Weichsel et al. 2008). Initially, therefore, I investigated this increase in TCR and CD8 levels as a possible mechanism for the observed effects on tetramer binding.

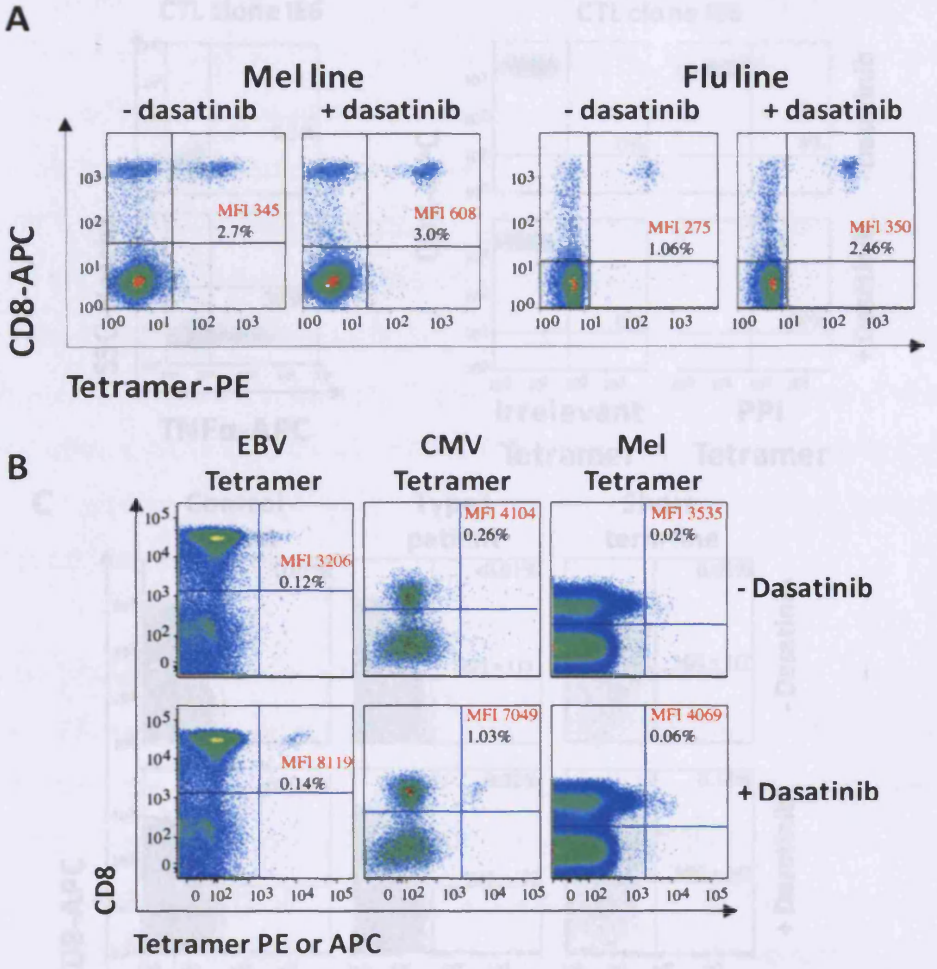

Figure 5.7: Dasatinib enhances the visualization of antigen-specific CD8⁺ T cells in mixed cell populations. A. Staining of HLA A2-restricted CD8⁺ T cell lines expanded from PBMC by one round of stimulation with the influenza matrix $M1_{58-66}$ peptide (GILGFVFTL) or the Melan-A/MART-1_{26-35} peptide (ELAGIGILTV). Lines were stained with cognate tetramer ± pre-treatment with 50 nM dasatinib for 30 minutes at 37°C. **B.** Flow cytometric profiles of live CD3⁺ lymphocytes stained with HLA A2 tetramers folded around the EBV $BMLF1_{259-267}$ (GLCTLVAML), CMV $pp65_{495-503}$ (NLVPMVATV) or Melan-A/MART-1_{26-35} (ELAGIGILTV) peptide epitopes. $2x10^6$ PBMC were stained with the amine-reactive viability dye ViViD, then stained with tetramer (1µ g in minimal staining volume) ± pre-treatment with dasatinib for 30 minutes at 37°C. Cells were then stained with cell surface markers as described in the Materials and Methods; a dump channel was used to exclude dead cells, CD14⁺ and CD19⁺ cells from the analysis. Data were acquired with a BD LSR IIf low cytometer and analyzed using FlowJo software.(D ata in B. kindly provided by K.L adell).

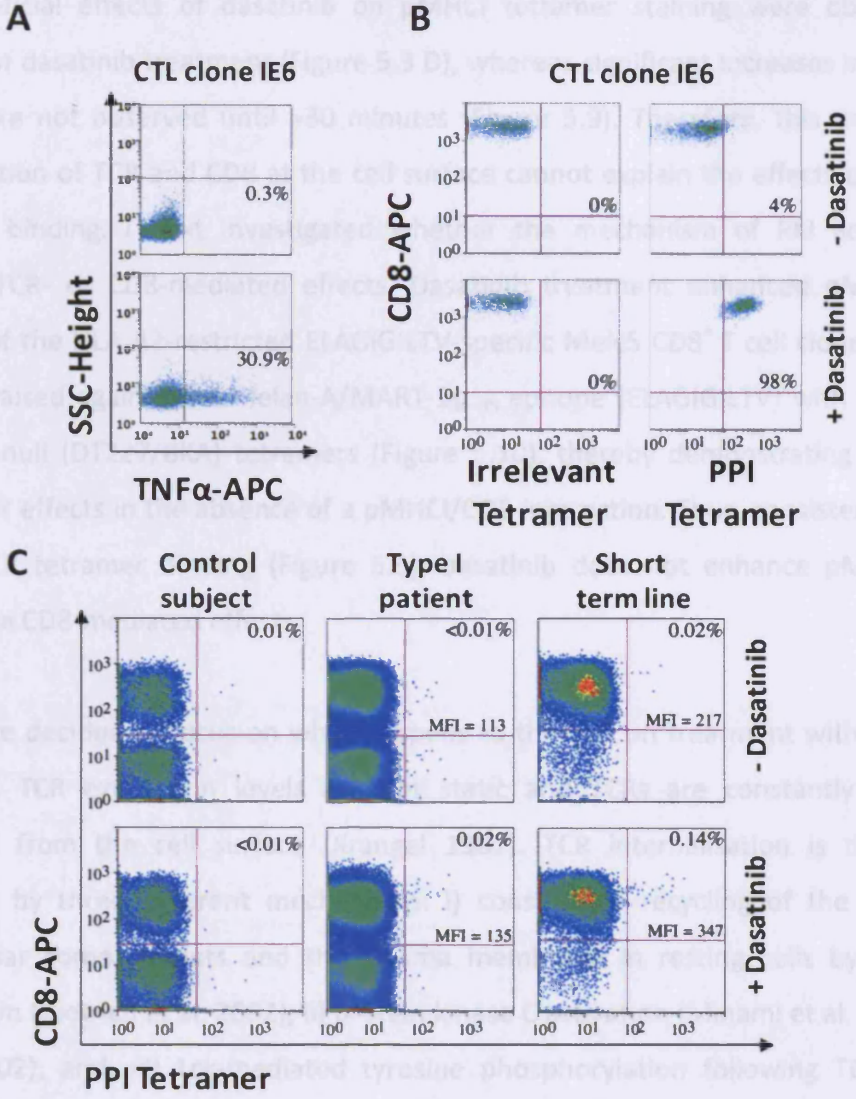

Figure 5.8: Dasatinib allows detection of autoreactive CD8⁺ T cells. A. CD8⁺T cell clone IE6, specific for the HLA A2-restricted epitope PPI_{15-24}, was activated with either $CMVpp65_{495-503}$ or PPI_{15-24} peptide for 6 hours at 37°C and then assayed for TNFα production by intracellular cytokine staining (ICS) as detailed in the Materials and Methods section 2.11.5. **B.** Staining of CD8⁺ T cell clone IE6 with either an irrelevant or PPI15-24/HLA A2 tetramer ± pre-treatment with 50 nM dasatinib for 30 minutes at 37°C. **C.** Representative stainings with PPI/HLA A2 tetramer ± pre-treatment with 50 nM dasatinib for 30 minutes at 37°C. Left panels: control subject PBMC; middle panels: type I diabetic patient PBMC; right panels: a short-term line expanded by one round of peptide stimulation from a type 1 diabetic patient.(Data kindly provided by A.S kowera)

The beneficial effects of dasatinib on pMHCI tetramer staining were observed within seconds of dasatinib treatment (Figure 5.3 D), whereas significant increases in TCR and CD8 levels were not observed until >30 minutes (Figure 5.9). Therefore, this time-dependent accumulation of TCR and CD8 at the cell surface cannot explain the effects of dasatinib on tetramer binding. I next investigated whether the mechanism of PKI action operates through TCR- or CD8-mediated effects. Dasatinib treatment enhanced pMHCI tetramer staining of the HLA A2-restricted ELAGIGILTV-specific Melc5 $CD8^+$ T cell clone and a $CD8^+$ T cell line raised against the Melan-A/MART-1_{26-35} epitope (ELAGIGILTV) with both wildtype and CD8 null (DT227/8KA) tetramers (Figure 5.10), thereby demonstrating that PKIs can exert their effects in the absence of a pMHCI/CD8 interaction. Thus, consistent with effects on pMHCII tetramer binding (Figure 5.3), dasatinib does not enhance pMHCI tetramer binding via CD8-mediated effects.

I therefore decided to focus on what happens to the TCR on treatment with a PKI such as dasatinib. TCR expression levels are not static and TCRs are constantly being down-regulated from the cell surface (Krangel 1987). TCR internalisation is thought to be mediated by three different mechanisms: i) constitutive recycling of the TCR between intracellular compartments and the plasma membrane in resting cells by an unknown mechanism (Dietrich et al. 2002); ii) protein kinase C activation (Minami et al. 1987; Dietrich et al. 2002); and, iii) Lck-mediated tyrosine phosphorylation following TCR ligation by specific pMHC ligand. Dasatinib has been shown to target Lck and therefore has the potential to inhibit the latter pathway of TCR downregulation (Carter et al. 2005; Weichsel et al. 2008). Indeed, dasatinib treatment was found to block antigen-induced TCR downregulation from the $CD8^+$ T cell surface (Figure 5.11 A). pMHC tetramers are rapidly internalised under normal staining conditions (Whelan et al. 1999), and therefore I hypothesised that dasatinib might exert its beneficial effects by blocking this process. To this end, I performed fluorescence microscopy in the presence and absence of dasatinib (Figure 5.11 B). ILA/HLA A2 Alexa488-conjugated tetramer capping and internalisation was blocked in the presence of dasatinib and remained on the cell surface, where it formed a ring that was visibly brighter than tetramer that had been internalized (Figure 5.11 B). Thus, by preventing TCR downregulation, PK inhibition acts to drive the system towards

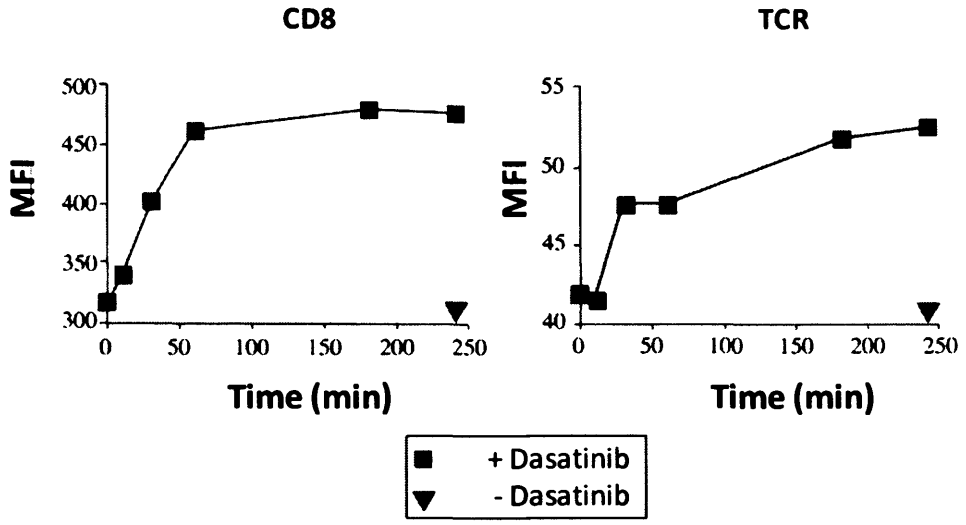

Figure 5.9 Dasatinib results in a time dependent increase in TCR and CD8 expression levels at the CD8⁺ T cell surface. The ILA1 CD8⁺ T cell clone was treated with PBS ± 50 nM dasatinib at 37°C and 10^5 CD8⁺ T cells were removed from the medium at 0, 10, 30, 60,180 and 250 minutes. ILA1 CD8⁺ T cells were subsequently stained with anti-CD8 FITC or anti-TCR FITC for 30 minutes on ice, washed twice and resuspended in PBS. Data were acquired on a FACS Calibur flow cytometer (BD) and analyzed using FlowJo software. Representative data of 3 separates experiments shown.

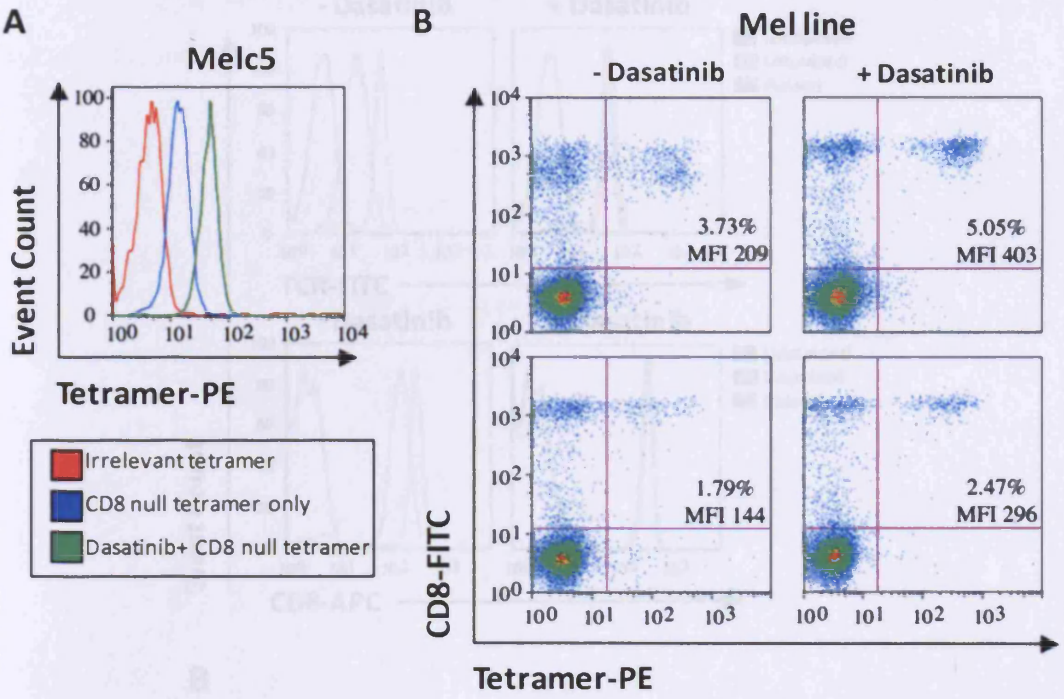

Figure 5.10: Beneficial effects of dasatinib are not CD8-mediated. A. Melc5 $CD8^+$ T cells were pre-treated with PBS ± 50nM dasatinib for 30 minutes at 37°C, then stained with HLA A2 DT227/8KA cognate tetramer for 20 minutes at 37°C. After washing twice, data were acquired on a FACSCalibur flow cytometer (BD) and analyzed using FlowJo software. **B.** Staining of HLA A2-restricted $CD8^+$ T cell lines expanded from PBMC by one round of stimulation with the Melan-A/MART-1_{26-35} peptide (ELAGIGILTV). Lines were stained with either wildtype or CD8 null cognate tetramer ± pre-treatment with 50 nM dasatinib for 30 minutes at 37°C.(D ata kindly provided by M. Clement).

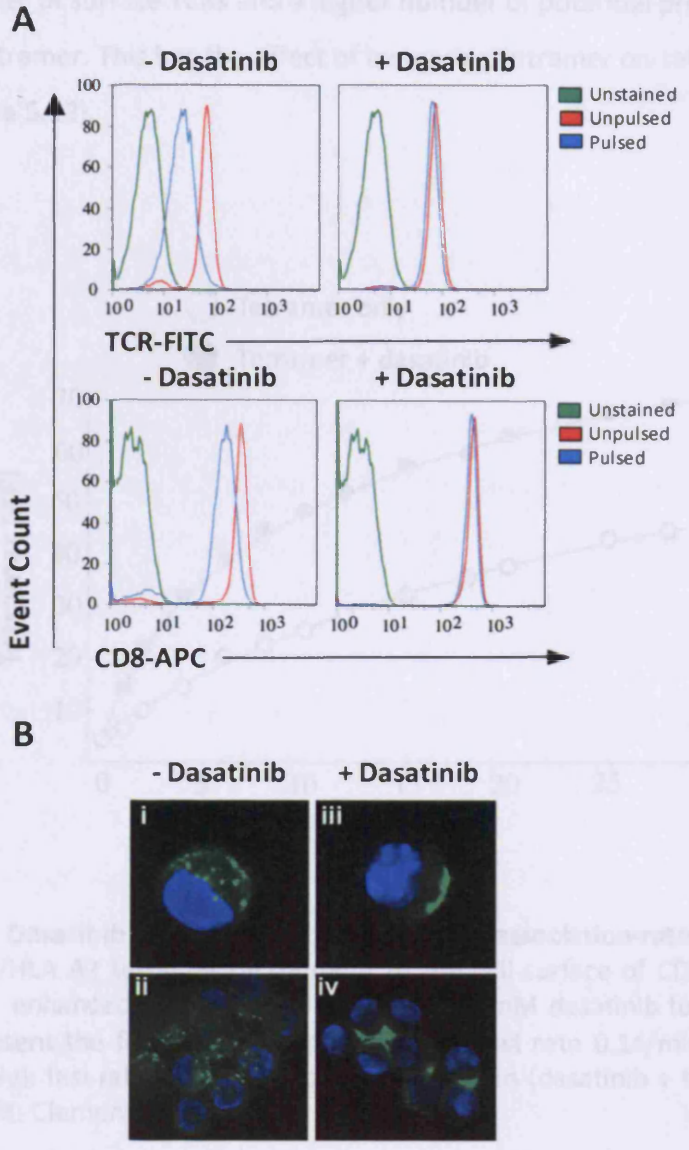

Figure 5.11: Dasatinib blocks antigen-induced TCR downregulation and tetramer internalization from the cell surface. A. Mel13 $CD8^+$ T cell clone was pre-treated with PBS ± 50 nM dasatinib and exposed to C1R-A2 B cells previously pulsed with 10^{-6} M ELAGIGILTV peptide or medium alone for 4 hours at 37°C. Cells were subsequently stained with anti-TCR-FITC and anti-CD8-APC antibodies for 30 minutes on ice, washed twice and resuspended in PBS. Data were acquired on a FACSCalibur flow cytometer (BD) and analyzed using FlowJo software. **B.** 10^5 ILA1 $CD8^+$ T cells were pre-treated with PBS (i & ii) or PBS+ 50 nM dasatinib (iii & iv) for 30 minutes at 37°C, then stained with 20 µg/ml ILAKFLHWL/HLA A2-Alexa488 tetramer for 15 minutes at 37°C. Representative data of 2 replicates (for A) and >3 replicates (for B) shown. Fluorescence microscopy was performed as described in the Materials and Methods.A lthough the pattern observed in B (i & ii) using fluorescence microscopy does not guarantee the presence of tetramer inside cells, evidence for internalisation of tetramer into early-endocytic vesicles at 37°C has previously been documented by Whelan *et al.*1 999 using confocal microscopy .

a higher number of surface TCRs and a higher number of potential productive engagements with pMHC tetramer. This has the effect of increasing tetramer on-rate, at least in pMHCI systems (Figure 5.12).

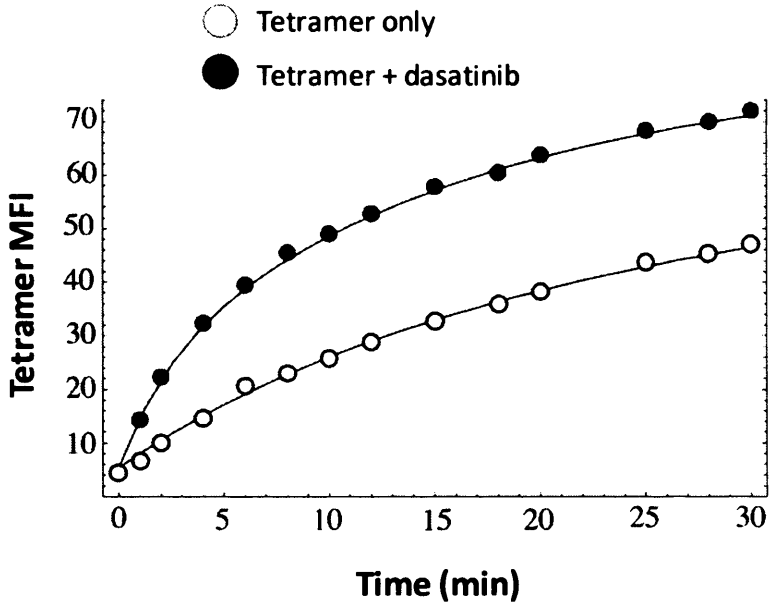

Figure 5.12: Dasatinib enhances pMHCI tetramer association-rate. Rate of $hTERT_{540-548}$ (ILAKFLHWL)/HLA A2 tetramer recruitment to the cell surface of $CD8^+$ T cell clone ILA1 is substantially enhanced following treatment with 50 nM dasatinib for 30 minutes at 37°C. Curves represent the following on-rate estimates: fast rate 0.14/min, slow rate 0.04/min (tetramer only); fast rate 0.42/min, slow rate 0.06/min (dasatinib + tetramer). (Data kindly provided by M. Clement).

5.3 Discussion

pMHC tetramer technology has revolutionised the study of antigen-specific T cells. However, one major limitation of this technique is that pMHC multimer staining is dependent on a distinct TCR affinity threshold that lies well above that required for T cell activation (Laugel et al. 2007). Consequently, pMHC tetramers fail to identify functional T cells that express TCRs with low affinity for cognate antigen. Such low affinity interactions characterise TCR/pMHCI binding in tumour-specific and autoreactive $CD8^+$ T cells (Cole et al. 2007). In this chapter I demonstrate that a short incubation with a reversible PKI such as dasatinib results in three major benefits in terms of pMHC tetramer staining. Firstly, substantial improvements in pMHC tetramer staining intensity are observed. This effect applies to both $CD4^+$ and $CD8^+$ T cells (Figure 5.3). Indeed, the beneficial effects are so striking even at low pMHC tetramer concentrations that dasatinib treatment could be used to conserve reagent. Secondly, dasatinib treatment reduces tetramer-induced cell death that has been previously reported to be an issue with pMHC multimer staining protocols (Purbhoo et al. 2001; Guillaume et al. 2003; Cebecauer et al. 2005). Thirdly, the benefits of dasatinib treatment are greater for TCR/pMHCI interactions of low affinity. This effect is particularly important in the setting of tumour-specific and autoreactive $CD8^+$ T cell populations. Such effects are also likely to apply to $CD4^+$ T cells, which typically bind cognate pMHCII antigens with affinities lower than those reported for pMHCI systems (Cole et al. 2007). Importantly, no increase in background staining was seen in any of the systems tested here (Figures 5.2 F, 5.3 B, 5.3 H, 5.9 B and 5.9 C). Similarly, positive staining of PBMC in the presence of dasatinib only ever coincided with a positive ELISpot result to the relevant peptide and never accompanied by an increase in background staining. Dasatinib proved to be a particularly powerful tool in the detection of autoreactive $CD8^+$ T cells from type I diabetic patients. No increase in the PPI tetramer positive population was observed in healthy donors and staining was only ever seen if a functional response to the preproinsulin peptide was evident.

I next examined the mechanism by which dasatinib enhances staining with cognate pMHC tetramers. Experiments with CD8-null tetramers (Figure 5.10) supported data

demonstrating that treatment enhanced pMHC staining of $CD4^+$ T cells (Figure 5.3 H), ruling out the possibility that staining enhancement was dominated by a CD8-dependent mechanism. Further experiments showed that the positive effects of dasatinib treatment were almost immediately evident (Figure 5.3 D) and were not reliant on the increased expression levels of TCR (and CD8) that are seen over a much longer timeframe (Figure 5.9). Dasatinib treatment also induced a substantially faster pMHC tetramer on-rate (Figure 5.12). Microscopic analysis of pMHC tetramer staining confirmed that staining was considerably brighter in the presence of dasatinib and that the tetramer was not internalised by dasatinib treated cells. The above data caused us to conclude that the enhanced staining observed was a direct result of preventing TCR downregulation.

When an individual pMHC molecule in a pMHC tetramer engages a cell surface TCR, this engagement can be described as either 'productive' or 'non-productive' in terms of whether it finally results in the capture of the tetramer from solution (Figure 5.13). A productive engagement requires a second pMHC in the tetramer to bind a second TCR before the first pMHC dissociates. As a result, the main factor that determines whether a pMHCI tetramer exhibits stable binding is likely to be the duration of the primary monomeric TCR/pMHC interaction. 'Non-productive' engagements are more likely to occur for low affinity, rapidly dissociating ligands. We hypothesise that dasatinib acts to prevent TCR downregulation after 'non-productive' engagement thereby maintaining TCRs at the cell surface where they are available for future interactions with pMHC. In simple terms, regular pMHC tetramer staining affords each initiating TCR/pMHC engagement just a single attempt to capture a tetramer from solution before it dissociated and the TCR is downregulated. The presence of dasatinib prevents this downregulation and in doing so allows the TCR further serial attempts at tetramer capture. Dasatinib treatment may also have a secondary effect as it is likely to block the internalisation of non-triggered TCRs that has been shown to occur at the same time as the internalisation of pMHC-engaged TCRs (Niedergang et al. 1997; San Jose et al. 2000). Dasatinib and other effective PKIs prevent TCR downregulation, acting to maintain surface TCRs and enabling a higher number of potential productive engagements with pMHC tetramer as indicated by the red arrows in Figure 5.13. Increased TCR availability at

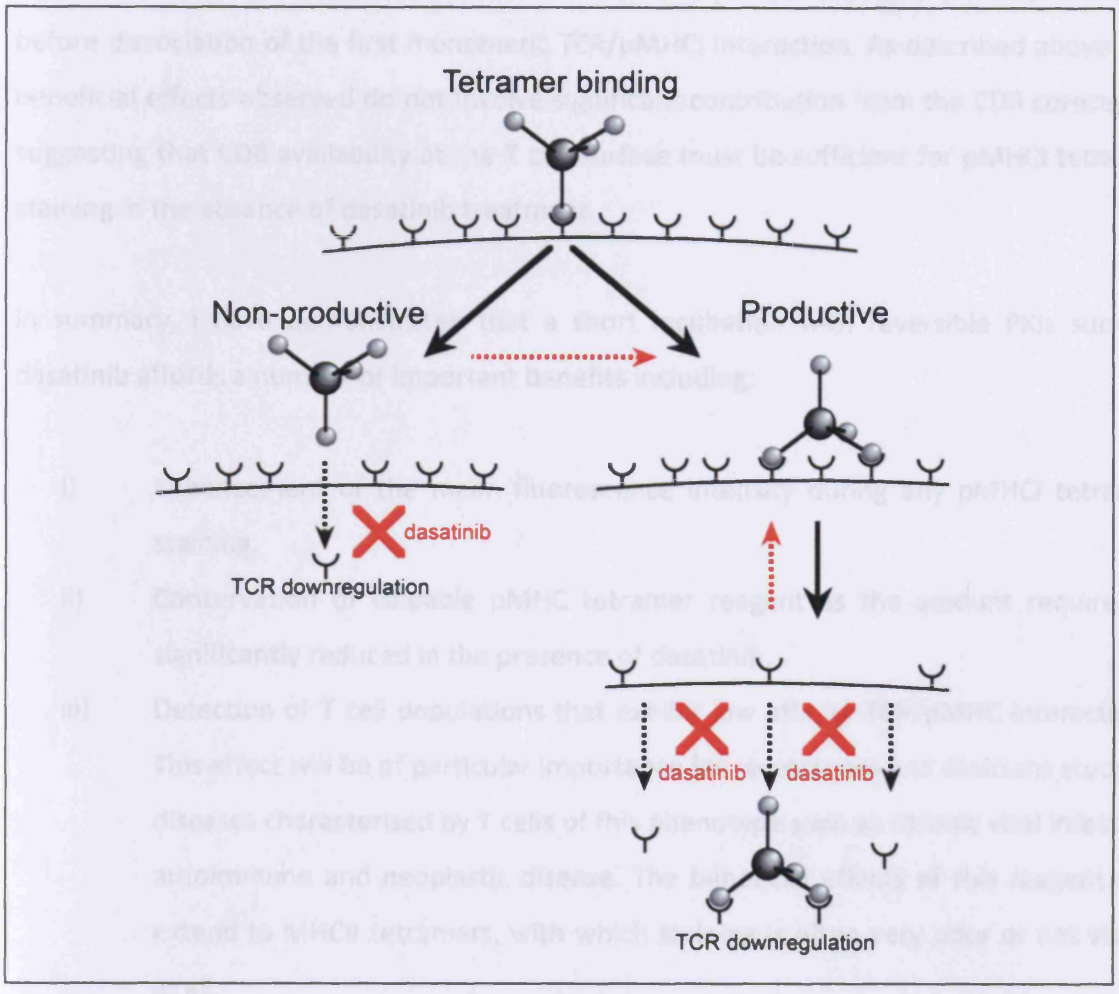

Figure 5.13: Dasatinib prevents downregulation of 'empty' TCRs. Proposed model for the mechanism by which dasatinib enhances cognate tetramer staining. Dasatinib treatment prevents TCR and coreceptor downregulation and maintains these receptors at the cell surface, thereby increasing molecular availability for further capture of pMHC tetramer from solution.

the T cell surface would increase the likelihood of a 'productive engagement' for low affinity ligands. This effect would be less obvious for higher affinity ligands, where slow TCR/pMHCI off-rates already increase the likelihood that a second pMHCI 'arm' in a tetramer can bind before dissociation of the first monomeric TCR/pMHCI interaction. As described above, the beneficial effects observed do not involve significant contribution from the CD8 coreceptor suggesting that CD8 availability at the T cell surface must be sufficient for pMHCI tetramer staining in the absence of dasatinib treatment.

In summary, I have demonstrated that a short incubation with reversible PKIs such as dasatinib affords a number of important benefits including:

i) Enhancement of the mean fluorescence intensity during any pMHCI tetramer staining.

ii) Conservation of valuable pMHC tetramer reagent as the amount required is significantly reduced in the presence of dasatinib.

iii) Detection of T cell populations that exhibit low affinity TCR/pMHC interactions. This effect will be of particular importance for researchers and clinicians studying diseases characterised by T cells of this phenotype such as chronic viral infection, autoimmune and neoplastic disease. The beneficial effects of this reagent also extend to MHCII tetramers, with which staining is often very poor or not visible at all.

iv) Inhibition of activation-induced cell death during staining. This affect results in a greater number of tetramer positive cells and is likely to be extremely useful when using pMHC tetramers to sort-clone antigen-specific T cells.

Importantly, these benefits are restricted to cognate T cells and are not accompanied by concomitant increases in background staining. More recent results obtained in collaboration with the Peakman group at Kings College have extended our findings that dasatinib treatment can expose concealed antigen-specific T cells that bear low affinity TCRs within a large cohort of Type 1 diabetics. Similar increases in staining were not observed in a group of healthy controls (manuscript in preparation).

I conclude that the use of PKIs such as dasatinib during pMHC multimer staining is a cheap, easy and effective way to improve results that can be applied to pMHCI and pMHCII reagents in both human and murine systems. My supervisor has recently heard that the benefits of pMHC multimer staining in the presence of dasatinib also extend to Macaque systems. The conservation of Src kinases (Yadav et al. 2008) makes it likely that the immense benefits of dasatinib during pMHC staining listed above will extend to any mammalian system. I therefore recommend a PKI such as dasatinib should be included when conducting any pMHC multimer staining.

Chapter 6

6

THE DEVELOPMENT AND OPTIMISATION OF TCR GENE TRANSFER PROTOCOLS

Chapter 6

6.1 Introduction

At the start of my project, the T cell modulation group was particularly interested in exploring whether modified TCRs could be useful in the clinic. Specifically, our interest was in TCRs with enhanced affinity for cognate antigen and TCRs with altered glycosylation (Chapter 7). Obviously, these approaches cannot be readily applied to natural endogenous TCRs. These studies therefore necessitated that we establish optimal TCR gene transfer protocols in Cardiff. I took the lead on these optimisation studies. As described in section 1.8.3 of the main Introduction, TCR gene transfer provides an efficient and relatively rapid way of generating large numbers patient-autologous T cells of required specificity that can be used for subsequent adoptive transfer. As described below, I considered several different strategies for the transfer of TCR genes to recipient primary T cells before I finally settled on a lentiviral system. We currently regularly achieve 60-90% transduction of primary T cells using my methodology. I will begin by summarising the various methodologies that can be used to introduce and express 'foreign' genes in mammalian cells.

6.1.1 Gene transfer into mammalian cells

There are several different ways of delivering genes of interest (GOI) for expression inside mammalian cells. Before choosing a method for gene delivery into cells, or transfection, two other factors should be considered:

1) The source of genetic material: The source of genetic material can be either DNA or RNA. Since mRNA does not require nuclear localisation for expression, transfecting mRNA has several advantages over DNA transfection (Yamamoto et al. 2009). These advantages include no risk of integration into the host genome, cell cycle-independent transfection efficiency, and adjustable and rapid expression (Yamamoto et al. 2009). Because transfection of mRNAs bypasses the need for translocation into the nucleus and transcription, expression of GOIs can be achieved within minutes of delivery into host cells (Job et al. 2001; Yamamoto et al. 2009). In contrast, transfected DNA must carry a host cell-specific promoter to be transcribed into mRNA, and the period between transfection and expression is considerably longer. Furthermore, the expression level is determined by strength of this exogenous

promoter. Matured mRNA consists of five significant structures: i) the cap; ii) 5' untranslated region (5'UTR); iii) open reading frame (ORF); iv) 3' untranslated region (3'UTR); and, v) poly-A tail (Elango et al. 2005). The efficiency of mRNA translation depends on the integrity of these structures, which can be affected by exposure to RNA-enzymes (RNAses). As a result, the *in vitro* preparation of mRNA is a laborious process that demands more caution than the preparation of DNA constructs (Elango et al. 2005).

2) Stable or transient transfection: Mammalian cells can be transfected transiently or stably (Recillas-Targa 2006). For transient transfection, the delivered genes are only expressed for a limited period of time as they are not integrated into the genome and their expression is lost with cell division (Recillas-Targa 2006). In order to achieve stable transfection, the foreign genetic material is integrated into the host cell genome and the resultant transgene expression is sustained even after host cells replicate (Glover et al. 2005). Since transient and stable transfection offer different durations for GOI expression, the choice between the two techniques depends on the objective of the experiment.

Many transfection methods have been developed. These can be classed into one of three categories: i) biological; ii) chemical; and, iii) physical.

i) Biological transfection: Biological transfection comprises virus-mediated transfection, also known as transduction. Viral transduction is highly efficient and represents the most commonly used method in clinical research (Pfeifer et al. 2001). Retroviruses such as the murine leukaemia virus (MLV) were used to make the earliest gene delivery vectors. More recently, retroviral vectors have been superseded by lentiviral vectors, which are largely based on the genome of the human immunodeficiency virus (HIV). Both retroviral and lentiviral vectors have been used to establish sustainable transgene expression in humans (Hacein-Bey-Abina et al. 2002; Woods et al. 2003). Once the virus gains access to a cell, its DNA is integrated into the host genome, so that as the host cell replicates the viral DNA segregates into each daughter cell. The advantages of viral-mediated transfection include: ease and high efficiency of transfection, sustained stable transfection, and transgene expression *in vivo*. The major drawbacks are immunogenicity, cytotoxicity, insertional

mutagenesis due to the random mature of viral genome integration, and a limit on the size of the foreign gene that can be inserted into the vector whilst preserving infectivity (Hacein-Bey-Abina et al. 2003; Woods et al. 2003).

ii) Chemical transfection: Chemical transfection represents the first method to be used to introduce foreign genes into mammalian cells. Chemical methods commonly use cationic polymer (one of the oldest chemicals used), calcium phosphate, cationic lipid (the most popular method) and cationic amino acid (Schenborn et al. 2000a; Schenborn et al. 2000b; Schenborn et al. 2000c). The underlying principles of gene delivery are similar for all types of chemical transfection. Essentially, a positively charged chemical adheres to intrinsically negatively-charged nucleic acids and masks their negative charge. The resultant positively-charged nucleic acid/chemical complexes bind to the negatively charged cell membrane of the host cell, and are believed to be internalised by endocytosis or phagocytosis. The advantages of chemical transfection methods are relatively low cytotoxicity, no mutagenesis, no extra-carrying DNA and no size limitation on the packaged nucleic acid. The major drawback however is that the techniques achieve low transfection efficiency, and are generally not applicable *in vivo*.

iii) Physical transfection: Physical transfection is the most contemporary group of transfection methods, which rely on the use diverse physical tools to deliver exogenous genetic material into mammalian cells. Physical transfection methods include electroporation, direct microinjection, biolistic particle delivery, laser-based transfection, sonoporation and the use of magnetic nanoparticles (Mehier-Humbert et al. 2005). Electroporation is the most widely used physical method (Mehier-Humbert et al. 2005; Kim et al. 2010). Although the exact mechanism of electroporation is not fully understood, it is presumed that a short electrical pulse causes perforations in the cell membrane through which nucleic acids can enter (Inoue et al. 2001; Mehier-Humbert et al. 2005; Kim et al. 2010). The advantages of physical transfection include their ease, the ability to transfect a large number of cells in a short time, and the ability to transfect a wide range of cell types. The disadvantages are the requirement for expensive instruments, and cell cytotoxicity due to the invasive nature of the techniques.

To summarise, although a wide range of transfection methodologies are available, each one has its own advantages and disadvantages. Therefore the selection of the best method depends upon the experimenter's objectives.

6.1.2 Methods for transferring more than one gene to cells

Many gene transfer applications require vectors that express more than one protein. Introduction of multiple genes into the same host cell and equimolar expression of these genes cannot be efficiently achieved by co-transduction with multiple vectors each carrying a single GOI. In such circumstances, a gene co-expression system is required. The co-expression of more than one gene from a single plasmid can be performed using a number of mechanisms: splicing, internal promoters, fusion proteins, internal ribosome entry sites (IRES), and ribosome skipping mechanisms (de Felipe et al. 1999; Yang et al. 2008). One of the challenges facing viral-assisted TCR transfer is that the TCR is composed of 2 chains that must be expressed in equal amounts for assembly. The most commonly used strategy in the construction of vectors for TCR expression is the insertion of an internal ribosome entry site (IRES) between the TCR alpha and beta chains (Ngoi et al. 2004). Thus, while translation of one chain (typically alpha) is initiated at the promoter, translation of the second chain (typically beta) is initiated through the IRES sequence. In such vectors however, the expression efficiency of the second chain is somewhat lower, resulting in inefficient cell surface TCR expression (Yang et al. 2005). This problem can be overcome by borrowing technology that is employed naturally by picornaviruses for the production of polyproteins from a single open reading frame (ORF) (Palmenberg 1990). This is orchestrated by a relatively short (17-20 amino acids long, depending on the virus) 2A peptide sequence, which causes the ribosome to skip a peptide bond between the last and second last amino acid of the 2A peptide sequence (Yang et al. 2008). Insertion of the 2A peptide between TCRα- and TCRβ-encoded sequences allows translation of the alpha chain without causing an arrest in beta chain synthesis. As a result, near equimolar amounts of both TCR chains are produced from a single open reading frame (Szymczak et al. 2004). Since the peptide-bond skipping event occurs after a portion of the 2A sequence has undergone translation, the first section of the peptide remains attached to the C-terminus of the TCR alpha chain, while the N-

terminus of the TCR beta chain gains a proline residue. The presence of these additional viral residues does not seem to affect the function or assembly of the TCR chains (Ryan et al. 1994; de Felipe et al. 1999; Donnelly et al. 2001; Yang et al. 2008). The expression of both genes from the same small construct offers several advantages and ensures that TCR cassettes are small enough to be carried efficiently by retroviral and lentiviral constructs.

6.1.3 The retroviral genome, virion structure and replication cycle

Retroviruses are single stranded RNA viruses that replicate via a double-stranded DNA intermediate (Temin et al. 1970). The retroviral RNA encodes the *gag* and *pol* genes that are expressed from an unspliced transcript, the *env* gene that is expressed from a spliced version of the genome, in addition to the u5, u3 and r regions located on either end of the genome (Figure 6.1). Retroviruses replicate by reverse-transcribing this RNA construct into a DNA form of the genome that is able to integrate into the chromosomal DNA of the host cell, where it is thereafter referred to as a provirus. On reverse transcription the ends of the genome undergo structural changes leading to the formation of 5' and 3' long terminal repeats (LTRs). This change permits appropriate expression of the viral genes *gag, pol* and *env*. The *gag* gene encodes structural proteins that make up the viral core: matrix, capsid and nucleocapsid. The *pol* gene encodes viral replication enzymes: protease, reverse transcriptase and integrase. Then *env* gene encodes the envelope glycoprotein (Env), which is processed into transmembrane (TM) and surface (SU) subunits. The TM and SU fragments assemble together with components of the lipid bilayer derived from the host cell to form the viral envelope around the core (Buchschacher 2001).

The infection of a cell by a retrovirus begins with recognition of a specific cellular receptor by the viral envelope glycoprotein and the fusion of viral and cellular membranes to permit the release of the viral core into the cytoplasm of the cell. Once inside, the RNA strands of the viral genome are uncoated and reverse transcribed into DNA using viral reverse transcriptase and the cellular tRNA molecule as a primer that recognises a sequence on the 5'LTR on the viral RNA. The viral DNA gains entry to the nucleus after nuclear envelope breakdown that occurs during cell division, and integrates itself into the chromosomal DNA. The resultant provirus simply hijacks the cellular transcription machinery to replicate its genome and form

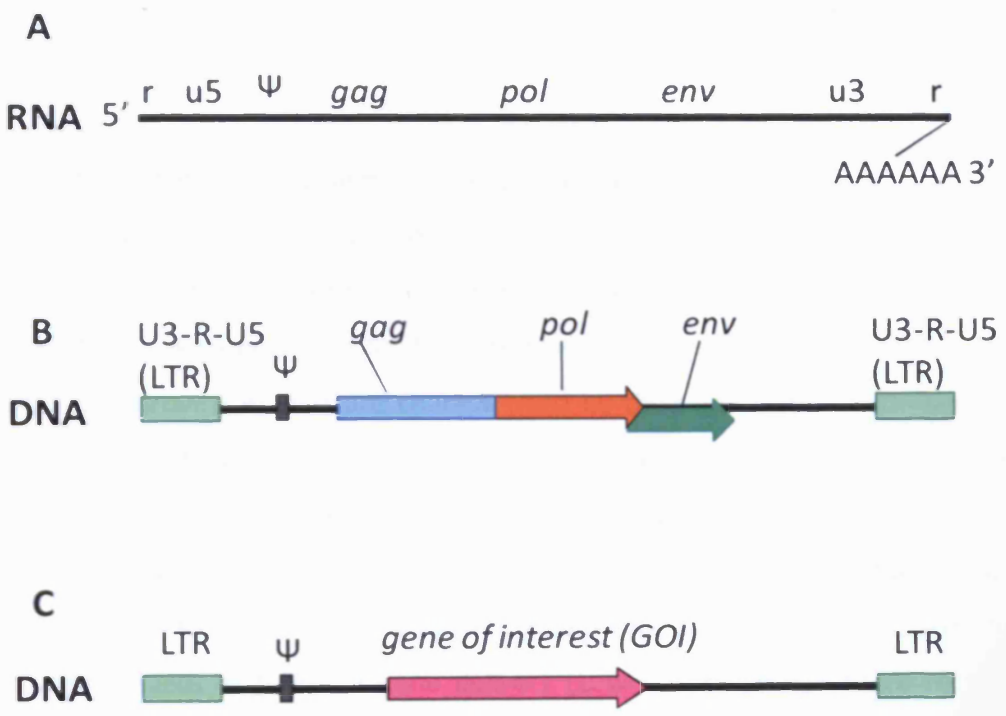

Figure 6.1: Structure of the retroviral genome and retroviral vector. The viral RNA is represented by the black line at the top of the figure (**A**), with the locations of the open reading frames (ORFs) *gag*, *pol* and *env* strung out along it. The genomic RNA (**B**)b egins with r (repeat) and u5 (unique 5' region) segments, and terminates with the u3 (unique 3' region) an r (repeat) region, and a poly-A tail. Reverse transcription of the RNA initiates a set of structural rearrangements of the genome termini, resulting in formation of long terminal repeat (LTR) structures. A retroviral vector (**C**) is constructed by replacing the retroviral *gag*, *pol* and *env* genes by a foreign gene of interest (GOI), and supplying the genes essential for formation of virions on separate plasmids. Full length retroviral transcripts and the retroviral vector also encode a packaging signal (Ψ) upstream of *gag/GOI* start codon, enabling full length transcripts to be encapsidated into newly formed viral particles.

the proteins that together assemble into new viral progeny, which can bud out of the cell. The events of the retroviral replication cycle are summarised in Figure 6.2 (Scherer et al. 2007).

6.1.5 General concepts of retro/lentiviral vector design

The unique property of retroviruses to deliver and integrate their genomes into a cell has been exploited for the delivery of GOIs to cellular targets by engineering retroviral vectors; derivatives of viruses capable of specific gene transfer (Demaison et al. 2002). Lentiviruses are a genus of retroviruses that are characterised by their association with 'slow' diseases that have long latent periods. The most well known example of a lentivirus is the human immunodeficiency virus (HIV). Although all retroviruses are capable of acting as vectors to deliver genetic information to the nucleus of a cell, lentiviruses have the unique ability among retroviruses to replicate in non-dividing cells and have therefore superseded other classes of retroviruses as tools for gene delivery (Lewis et al. 1994). More recent studies however, have highlighted the importance of cytokine-induced activation (but not necessarily division) of human T cells as a prerequisite for efficient infection with lentiviruses. Without cellular activation, the infection appears to be blocked at a pre-integration state by an incompletely understood mechanism (Unutmaz et al. 1999; Schumacher 2002).

The basic backbone of the vector (outlined in Figure 6.1) is constructed by removing the viral genes *gag*, *pol*, and *env* from the viral genome, freeing up space for insertion of a GOI and a number of elements which function to increase or regulate the expression of that gene. For instance, the viral LTRs flanking the GOI are often unsuitable for efficient expression, and are replaced by a stronger promoter from another virus such as CMV or SV40. Other design features include: i) a cassette of enzymatic restriction sites to facilitate insertion of several genetic elements into a single vector; ii) enhancers for optimal expression; iii) internal ribosome entry sites (IRES) for expression of more than one GOI; and, iv) post-transcriptional regulatory elements for regulation of protein production (Adam et al. 1991; Zufferey et al. 1998; Demaison et al. 2002). More recently, a range of self-inactivating (SIN) vectors, in which the U3 region of the 3'LTR has been truncated or deleted, have been developed. When

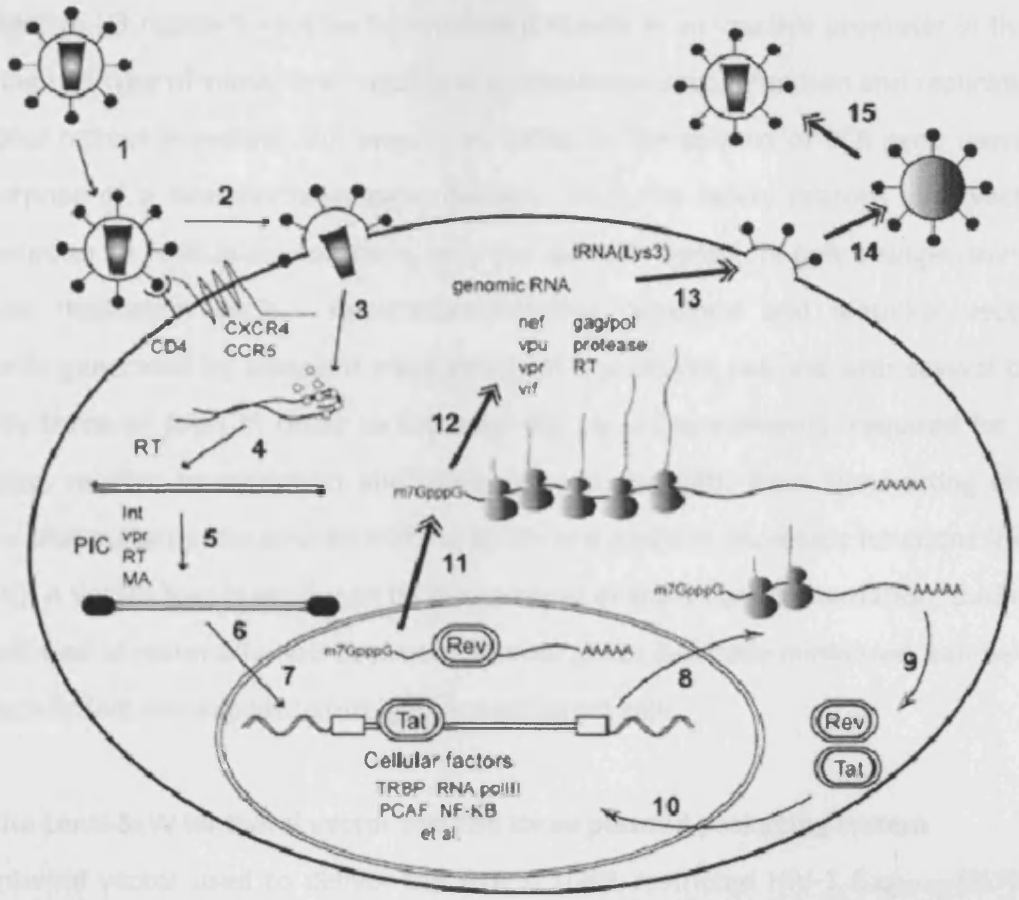

Figure 6.2: The retroviral replication cycle. 1. Binding of viral envelope glycoproteins to cell surface receptors (CD4, and CXCR4 or CCR5 in the case of HIV-1). **2.** Fusion. **3.** Unraveling of the viral RNA genome. **4.** Reverse transcription of the RNA into DNA by the reverse transcriptase enzyme (RT). **5.** Formation of pre-integration complex (PIC). **6.** Nuclear import of PIC. **7.** Integration of viral DNA into host genome to form a provirus. **8.** Transcription of multiply spliced mRNAs. **9.** Translation of Tat and Rev, the early regulatory proteins. **10.** Nuclear import of Tat and Rev. **11.** Export of singly spliced and unspliced mRNAs from the nucleus, mediated by Rev. **12.** Translation of viral structural proteins occurs in the cytosol. **13.** Assembly of viral RNA genome, proteins, and cellular factors including the cellular primer tRNA (essential for reverse transcription) into a virion occurs at the cell membrane. **14.** Budding. **15.** Viral maturation. (Figure taken from Scherer et al. 2007).

the defective U3 region is reverse transcribed it results in an inactive promoter in the 5'LTR, rendering this type of vector less capable of spontaneous recombination and replication than traditional retroviral vectors (Zufferey et al. 1998). In the context of TCR gene transfer, the sole purpose of a viral vector is gene delivery. Thus, for safety reasons viral vectors are engineered to be replication-defective, with the ability to complete only a single round of the retroviral replication cycle. Replication-defective retroviral and lentiviral vectors are commonly generated by transient transfection of a producer cell line with several plasmids (typically three or four) in order to separate the *cis*-acting elements; required for optimal packaging, reverse transcription and integration of the GOI, from *trans*-acting elements; proteins that make up the structure of the virion and perform enzymatic functions (Naldini et al. 1996). A vector that is produced by this method of *trans*-complementation, during which the likelihood of recombination between the viral genes is greatly minimised, can be used to transduce (infect and express a foreign gene in) target cells.

6.1.6 The Lenti-SxW lentiviral vector and the three plasmid packaging system

The lentiviral vector used to deliver the HLA A*0201 restricted HIV-1 $Gag_{77\text{-}85}$ (SLYNTVATL) specific TCR (868 TCR) genes to target cells for the purpose of this study was based ironically on the very virus the TCR was engineered to recognise, HIV-1. This lenti-SxW vector (also called pHR'SINcPPT-SFFV-x-WPRE) was developed and kindly donated by Qasim Waseem and others at the Molecular Immunology Unit, University College London. The design and development of the lenti-SxW vector is fully documented in (Demaison et al. 2002), and its various components are depicted in Figure 6.3. Since the vector was originally designed for gene delivery into non-dividing hematopoetic cells, which are notoriously problematic to transduce, it incorporates several additional elements geared towards enhancing gene expression: LTR sequences from the spleen focus forming virus (SFFV), post-transcriptional elements from the Woodchuck hepatitis virus (WPRE), and the central polypurine tract (cPPT) sequence of HIV-1. The authors found that the incorporation of these elements into the vector backbone resulted in between 20- and 73-fold increase in transgene expression in engrafted cell lineages compared to basic lentiviral vectors containing the CMV promoter (Demaison et al. 2002). Lenti-SxW is a self-inactivating vector, as the U3 region of its HIV-3'LTR has been deleted for additional safety.

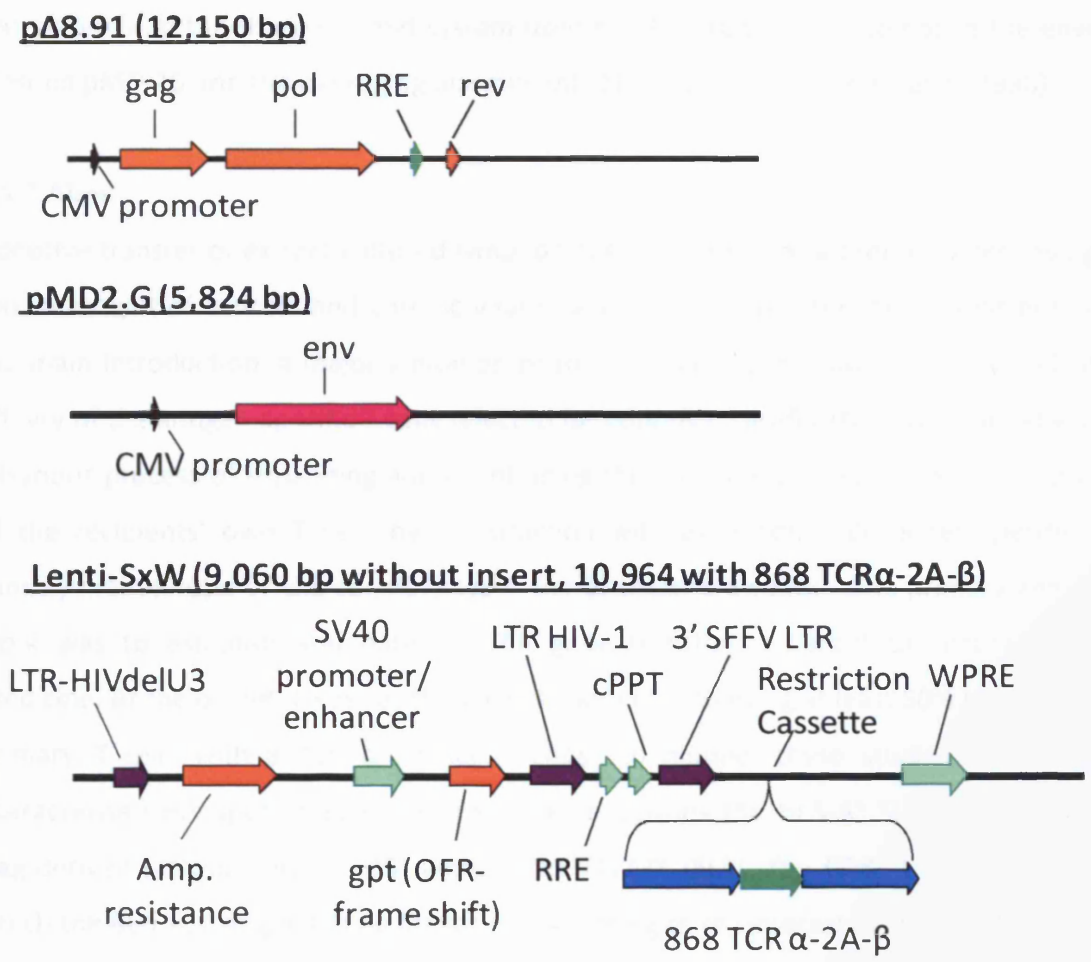

Figure 6.3: The lentivirus is assembled from three plasmids: pΔ8.91, pMD2.G, and lenti-SxW. The lentiviral vector used in this study, Lenti-SxW encodes the genes of interest (the 868 TCR alpha and beta chains, separated by 2A peptide), and several transduction-enhancing elements. The packaging plasmids pΔ8.91 (coding for matrix and transcription proteins) and pMD2.G (coding for envelope proteins) supply the other proteins required for viral assembly in *trans*.

As previously mentioned, replication-defective vectors are generated by co-transfection of a producer cell line with a number of additional plasmids carrying the *trans*-acting components. In the three-plasmid system used for this study, these comprise the envelope plasmid pMD.2G and the packaging plasmid pΔ8.91 (Figure 6.3) (Zufferey et al. 1998).

6.1.7 Aims

Adoptive transfer of *ex-vivo* cultured lymphocytes is emerging as a promising technology for the treatment of cancers and chronic viral infections. However, for the reasons outlined in the main Introduction, a major limitation of this approach is the low frequency and/or TCR affinity of the antigen-specific T cells selected for adoptive transfer therapy, coupled with the laborious process of expanding and maintaining the T cells in culture. Genetic manipulation of the recipients' own T cells by transduction with exogenous TCR genes specific for a cancer/viral epitope of choice alleviates many of these drawbacks. The primary aim of this work was to establish and optimise TCR gene transfer at Cardiff University School of Medicine. At the outset, I was set the goal of routinely achieving at least 50% transduction of primary T cells with a TCR of choice. I chose to pioneer these studies with the well-characterised HIV-specific 868 TCR. This TCR recognises the HLA-A*02-restricted, HIV p17 Gag-derived (amino acids 77–85) antigen SLYNTVATL (SL9). The $CD8^+$ T cell line 868 from which the 868 TCR originated no longer exists, adding to my interest in investigating whether the transduction of primary polyclonal T cells with the 868 TCR would generate T cells with similar properties to the 868 line (Sewell et al. 1997; Wilson et al. 1998). The ultimate aims of this chapter were thus to select the best system for the delivery of 868 TCR genes into primary $CD8^+$ T cells, optimise this process, and assess the ability of recipient $CD8^+$ T cells to respond to the SL9 antigen (both artificially pulsed on, and presented naturally by HIV-infected cells). As previously mentioned, one of the potential problems of introducing T cell receptors into cells that already have an endogenous TCR is the formation of mispaired TCR αβ dimers. For this reason, an additional goal was to assess whether TCR chain mispairing was an issue for the 868 TCR system.

6.2 Results

6.2.1 Efficiency of gene delivery by transient transfection techniques of DNA and mRNA electroporation is very poor

Electroporation involves the introduction of genes into cells using one of two sources of genetic material: a recombinant bacterial plasmid or *in vitro* transcribed (IVT) messenger RNA (mRNA) molecules, and a pulse of electricity. The pDNA or IVT mRNA can gain access to the cytoplasm of the cell by entering through pores in the cell membrane, generated by the electric pulse (Weaver 1993; Zhao et al. 2006). In the earliest days of this investigation, I experimented with these transient transfection techniques by using either a pUC plasmid containing a green fluorescent protein (GFP) construct or *in-vitro* transcribed GFP mRNA (prepared as described in section 2.5.2a) as markers of transfection efficiency, and a $CD4^+$ Jurkat T cell line as targets for transfection (Figure 6.4). $3x10^6$ Jurkat cells were electroporated in the presence of 10 μg GFP pDNA, 2 μg GFP mRNA, or R10 media (as a negative control), and analysed for expression of the GFP transgene 19 hours post transfection. The efficiency of transfection with GFP-mRNA (39%) was substantially higher compared to that with the GFP-encoding plasmid (11%). Despite this initial success, IVT RNA-transfection had many drawbacks: the laborious and expensive process of mRNA preparation, low RNA yield (typically only 20-30 μg of mRNA per reaction), and a low theoretical probability of cells being transfected with both TCR α and β chains in the eventual TCR transfection experiments. In addition, the process of electroporation, and bacterial lipopolysaccharide (LPS) contaminants in plasmid preparations resulted in extensive cell death, with a 50-70% reduction in live cells. The extent of cell death is predicted to be even greater for the less robust primary T cells (Beebe et al. 2003), which are the ultimate target for transfection with the 868 TCR. Finally, the transient nature of transgene expression imposes a strict time window on any functional assays that are to be carried out with transfected cells, and thus the information that can be gathered from such experiments. For all the above reasons, I decided to explore an alternative method for delivery of the 868 TCR into cells.

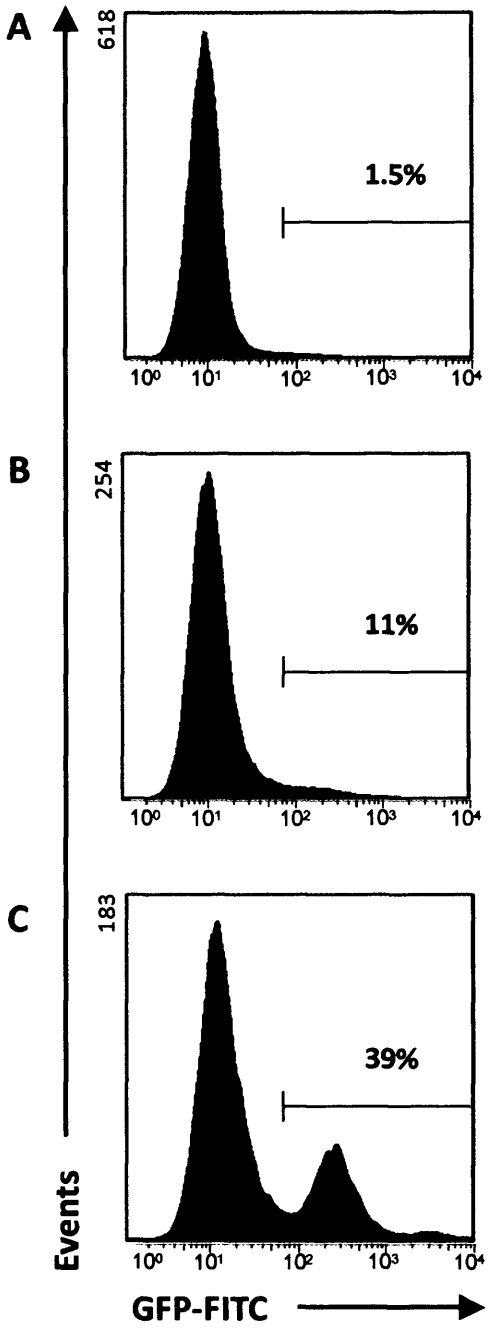

Figure 6.4: Transient transfection of Jurkat cells with plasmid GFP DNA versus *in vitro* transcribed (IVT) GFP mRNA under similar electroporation conditions. 3x10^6 Jurkat cells were either left untransfected (**A**), transfected with 10 µg plasmid GFP DNA (**B**),o r transfected with 2 µg GFP mRNA (**C**). The samples were analysed by flow cytometry 19 hours post transfection. The total number of cells recorded was kept constant for all samples. Figure shows representative data of 2 separate experiments.

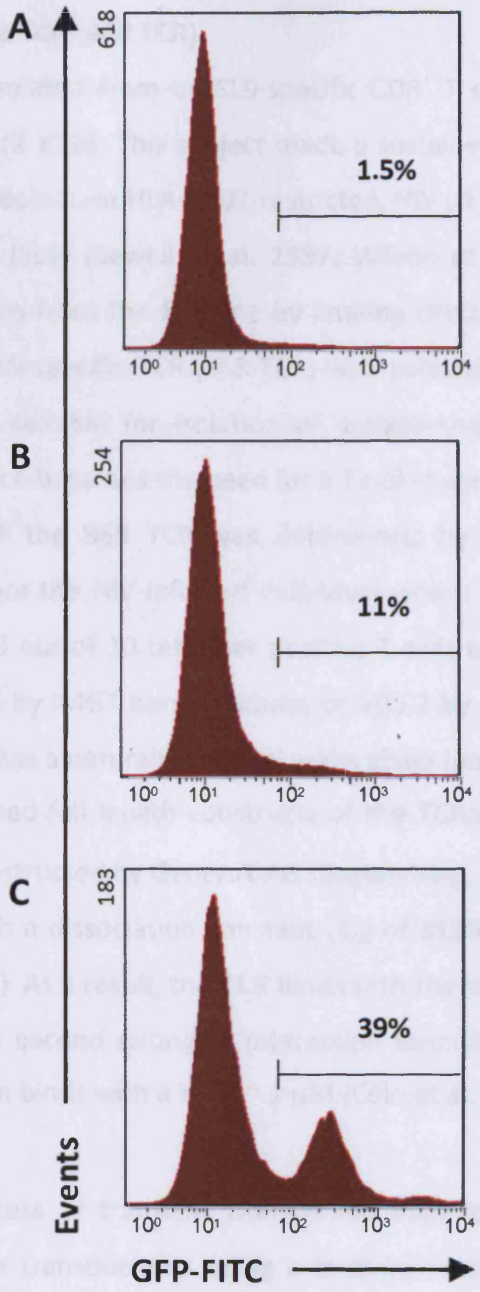

Figure 6.4: Transient transfection of Jurkat cells with plasmid GFP DNA versus *in vitro* transcribed (IVT) GFP mRNA under similar electroporation conditions. $3x10^6$ Jurkat cells were either left untransfected (**A**), transfected with 10 µg plasmid GFP DNA (**B**),o r transfected with 2 µg GFP mRNA (**C**). The samples were analysed by flow cytometry 19 hours post transfection. The total number of cells recorded was kept constant for all samples. Figure shows representative data of 2 separate experiments.

6.2.2 Construction of a lentivirus vector to deliver a HLA A*0201 restricted HIV-1 Gag_{77-85} (SLYNTVATL) specific TCR (868 TCR)

The 868 TCR was isolated from an SL9-specific $CD8^+$ T cell line, grown from HIV-infected individual 868 in April 1996. This subject made a sustained and robust $CD8^+$ T cell response against the immunodominant HLA-A*02-restricted, HIV p17 Gag-derived (amino acids 77–85) epitope SLYNTVATL (SL9) (Sewell et al. 1997; Wilson et al. 1998). Repeated attempts to generate T cell clones from the 868 line by limiting dilution were unsuccessful. Instead, an immunodominant SL9-specific TCR (868 TCR) was isolated from the line by phage display, a technique which is suitable for isolation of antigen-specific TCRs from polyclonal T cell populations and which bypasses the need for a T cell clone {Varela-Rohena, 2008a #882}. The dominant nature of the 868 TCR was determined by SL9/HLA A2 tetramer sorting of peripheral blood from the HIV-infected individual whom the $CD8^+$ T cell line was originally derived from, with 8 out of 10 tetramer positive T cells expressing a TCR with the 868 TCR beta chain (TRBV5-6 by IMGT nomenclature, or Vβ5.2 by Arden classification) (Wilson et al. 1998). The 868 TCR has a naturally unusual alpha chain (part TRAV12-2*01 part TRAV12-1, or Vα2). Codon-optimised full length constructs of the TCRα and TCRβ chains for mammalian expression were constructed by GeneArt AG (Regensburg, Germany). The 868 TCR binds to is cognate antigen with a dissociation constant (K_D) of ≤150 nM as measured by SPR {Varela-Rohena, 2008a #882}. As a result, this TCR binds with the highest affinity ever seen to date by some margin as the second strongest interaction described to date is that of the HTLV-I-specific TCR A6 which binds with a K_D of ~ 1 μM (Cole et al. 2007).

After the poor success of transient transfection techniques, I diverted my focus to the generation of stable transductants using a lentiviral vector system. Modified lentiviruses have shown great promise in the delivery of T cell receptor and other genes into various cell types. As previously discussed, the success of lentiviral transduction is determined by many factors, including the promoter and enhancer elements, and the nature of the envelope which coats the virus. The key feature of the HIV-based self-inactivating lenti-SxW vector used in this study, are outlined in section 6.1.6.

Prior to insertion into the lentiviral vector, the components of the 868 TCR construct were assembled in a pUC19 shuttle vector (Figure 6.5). The pUC plasmid was especially adapted for cloning of TCR alpha and beta genes by incorporating a cassette with additional restriction enzyme cleavage sites and the SGSG-2A region separating the TCR alpha and beta insertion sites. The 2A peptide used in this study is an 18-amino acid long fragment derived from the Thosea asigna virus ((Yang et al. 2008) and Appendix 1C). For the ribosome-skipping mechanism of 2A to function, the TCR alpha and beta chains must be part of the same open reading frame (ORF). It is thus essential that the stop codon on the C-terminus of the alpha chain is removed, to allow translation to proceed through the entire ORF. *In vitro* studies have estimated a cleavage of ~85% when 2A is used on its own, or ~95% if preceded by the amino-acid spacer sequence SGSG, which was incorporated into the 868 TCR α-2A-β construct (Yang et al. 2008).

The 868 TCR alpha chain was inserted into the modified pUC vector using XbaI and XhoI restriction sites, while the beta chain was cloned in using KpnI and Not I (Figure 6.5). The fully assembled 868 TCR α-SGSG-2A-β construct was subsequently excised from the pUC vector with a single BamHI digestion for transfer into the lenti-SxW vector (Figure 6.6), which was treated with the same enzyme. Following ligation of vector and insert, the construct was checked for presence of the 868 TCR insert by a further BamHI restriction digest (Figure 6.7) and sequenced in the region of the TCR insert to check for directionality (Appendix 4).

6.2.3 Successful transduction of $CD4^+$ Jurkat T cell line and primary $CD8^+$ T lymphocytes with the 868 TCR using a lentiviral vector system

To investigate the transduction efficiency of the lenti-SxW lentiviral vector, Jurkat cells were initially transduced with a version of the vector encoding GFP, which was kindly provided together with the lentiviral vector by Qasim Waseem *et al.* at the Molecular Immunology Unit, University College London. The GFP-encoding gene insert was chosen for optimisation of transduction because of its small size and ease of detection of its emission band (511nm) in transduced cells by fluorescence microscopy and flow cytometry. The GFP-expressing virus was initially generated by calcium phosphate transfection of the 293T packaging cell line,

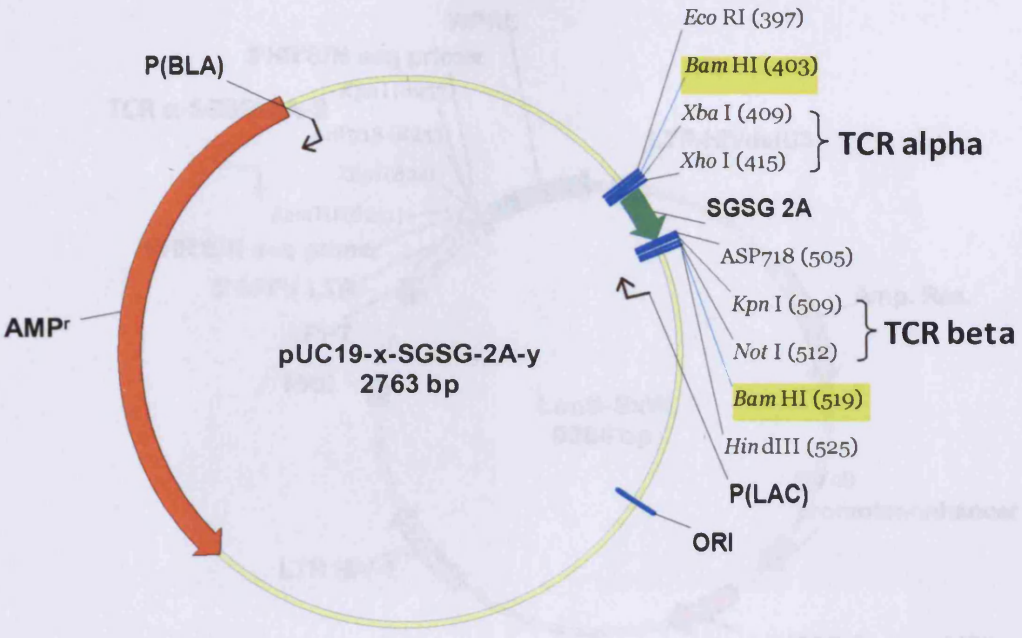

Figure 6.5: Schematic of the pUC19-x-SGSG-2A-y shuttle vector. The 2A peptide sequence and spacer sequence SGSG were cloned into the vector using the EcoRI and HindIII restriction sites. The 868 TCR alpha was cloned into the pUC19-x-SGSG-2A-y vector in position of 'x', using the XbaI and XhoI restriction enzymes. The 868 TCR beta chain was inserted into the same vector in position of 'y' using the KpnI and NotI restriction enzymes. The assembled 868 TCR alpha-SGSG-2A-beta construct was excised from the pUC vector using a single BamHI digestion (positions of BamHI restriction sites are highlighted in yellow), for transfer into the lentiviral vector (Figure 6.6).

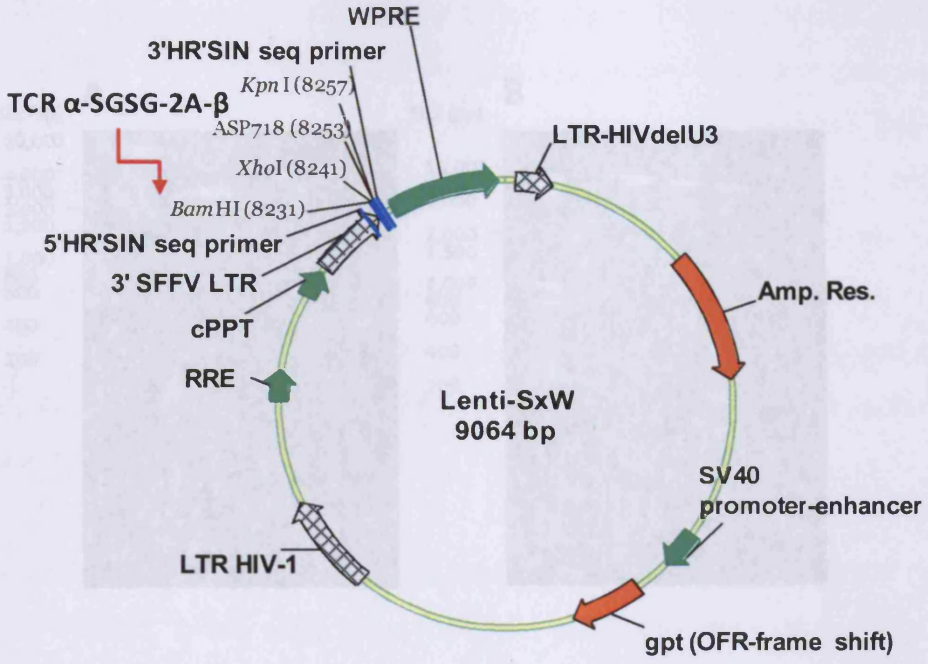

Figure 6.6: Schematic of the lentiviral Lenti-SxW vector. In the Lenti-SxW abbreviation, S refers to the SV40 promoter, x stands for any gene of interest, and W refers to the woodchuck hepatitis virus post-transcriptional element (WPRE). The SV40 promoter-enhancer, LTR sequences from the spleen focus forming virus (SFFV), the WPRE and the central polypurine tract (cPPT) sequence of HIV-1 act as enhancers of transduction efficiency.T he 868 TCR alpha-SGSG-2A-beta construct was excised from the pUC bacterial vector (Figure 6.5), and inserted into the Lenti-SxW vector in place of 'x' (red arrow) via the BamHI restriction site.

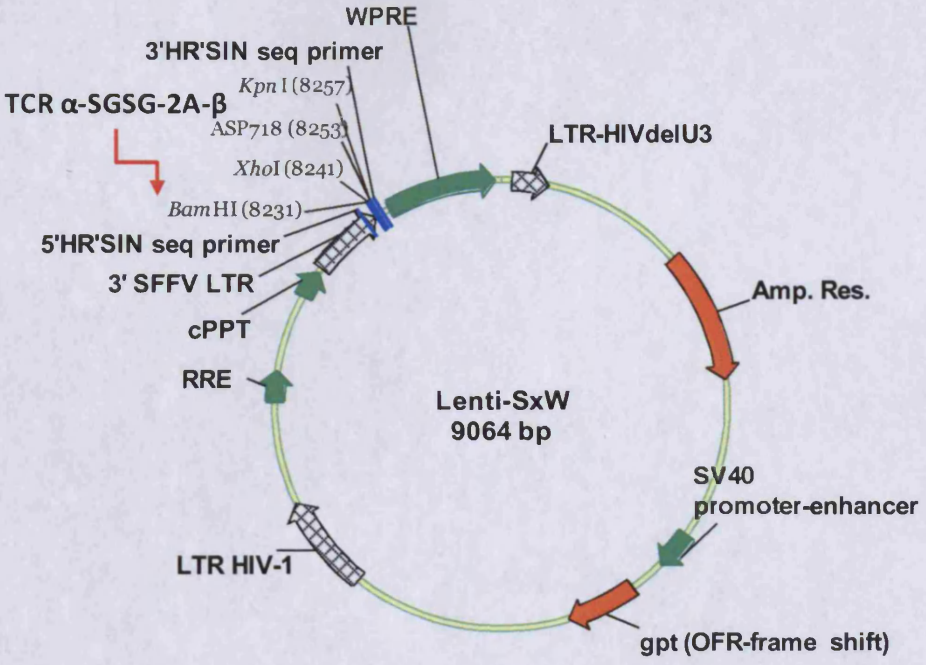

Figure 6.6: Schematic of the lentiviral Lenti-SxW vector. In the Lenti-SxW abbreviation, S refers to the SV40 promoter, x stands for any gene of interest, and W refers to the woodchuck hepatitis virus post-transcriptional element (WPRE). The SV40 promoter-enhancer, LTR sequences from the spleen focus forming virus (SFFV), the WPRE and the central polypurine tract (cPPT) sequence of HIV-1 act as enhancers of transduction efficiency.T he 868 TCR alpha-SGSG-2A-beta construct was excised from the pUC bacterial vector (Figure 6.5), and inserted into the Lenti-SxW vector in place of 'x' (red arrow) via the BamHI restriction site.

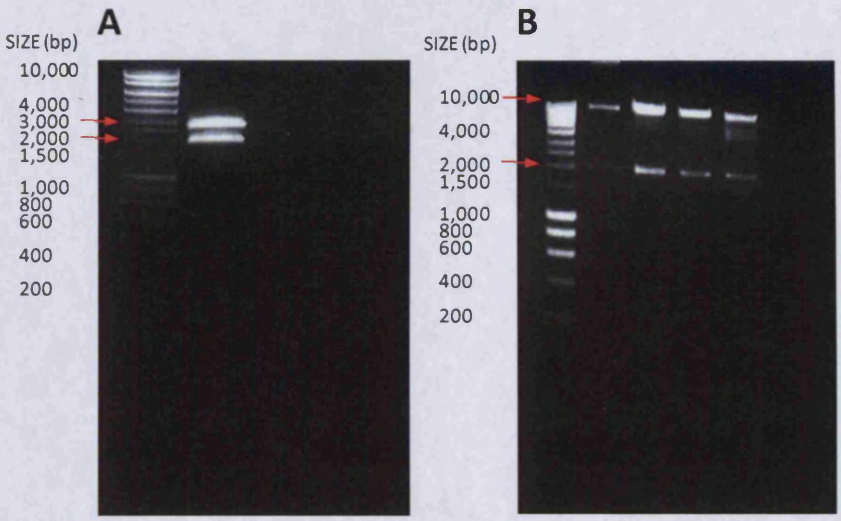

Figure 6.7: Cloning of the 868 TCR into the lentiviral vector, Lenti-SxW. A. A BamHI restriction digest of the pUC-868 TCR construct showing the pUC vector (larger band) and 868 TCRα-SGSG-2A-β insert (smaller band). **B.** BamHI restriction digest of Lenti-868 TCR construct after ligation of the product from A and BamHI-cleaved Lenti-SxW vector, showing that the ligation was successful.

using the 3-plasmid system of expression, comprising lenti-SeW, pMD2G, and pΔ8.91. Following a 24-48 hour incubation period, the viral supernatant was harvested, depleted of cell debris by centrifugation and applied to Jurkat cells in increasing amounts. The extent of GFP expression was determined by flow cytometry. Figure 6.8 illustrates the steady increase in GFP expression with increasing addition of GFP viral supernatant to a constant number of Jurkat cells. The multiplicity of infection (MOI), which is a measure of the number of infectious viral particles per cell for a particular batch of viral supernatant, was estimated from values on the linear range of the curve. For calculation of MOIs refer to section 2.6.4 of Materials and Methods.

Although application of ≥ 30 µl of crude viral supernatant (MOI 3-10) caused GFP expression in 55-90% of 2-10x10^5 Jurkat cells, application of 1 ml of the same virus to MACS-sorted primary $CD8^+$ T cells delivered a mere 0.5-1% GFP expression (Figure 6.9). At this point, several reasons for the low transduction efficiency of primary T cells were proposed: the low concentration of viral particles in the crude supernatant preparations applied to the cells, the toxicity of calcium phosphate contaminants, and the need for primary cells to be activated prior to infection. The first condition to be manipulated was the concentration of viral particles, which was increased by ultracentrifugation of the crude viral supernatant for several hours. Infection of primary $CD8^+$ T cells with 30 µl concentrated GFP-expressing virus resulted in 10-15% of the cells expressing GFP (figure 6.10 A). The efficiency of transduction of primary $CD8^+$ T cells with 868 TCR-virus (generated by the same method as the GFP virus) correlated directly with that for the GFP-virus, with 10-15% of cells exhibiting surface expression of the 868 TCR as determined by an HLA A2 tetramer refolded around the SL9 peptide (Figure 6.10 B). The modified TCR-negative Jurkat cell line (J.RT3.T3.5; (Weiss et al. 1984)) was used for subsequent 868 TCR-transduction experiments, as TCR expression can be assessed by analysis of rescued CD3 surface expression in addition to specific SL9/HLA A2 tetramer staining. The unusually high affinity of the 868 TCR for its cognate SL9/HLA A2 antigen (K_D ≤150 nM) ensured that cells expressing this TCR stained well in the absence of CD8 expression. The TCR negative Jurkat cells used to test the lentiviral expression system did not express CD8. This knowledge was factored in when I made the decision on which TCR to use for developing TCR gene transfer.

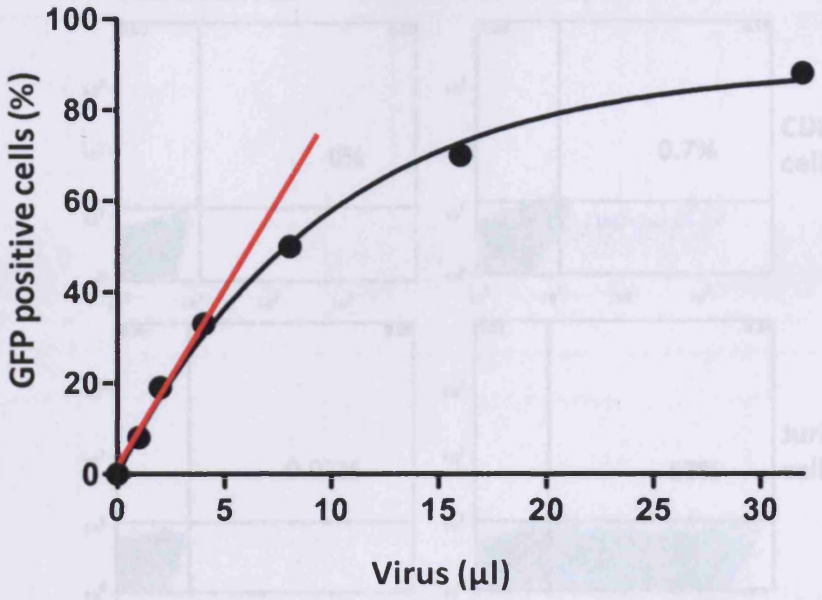

Figure 6.8: Determining the multiplicity of infection (MOI) of the concentrated lentiviral supernatant carrying the GFP construct, on the Jurkat cell line. Assuming that each viral particle infects a single cell and a constant number of cells is used for each transduction, it is possible to calculate the number of infectious particles/µl of supernatant.A n average of the values in linear part of the curve (ie. 1 µl,2 µl ,a nd 4 µl virus added) is taken.F rom the average number of cells infected it is possible to calculate the number of particles of virus per µl viral supernatant, assuming that 1 particle infects 1 cell.

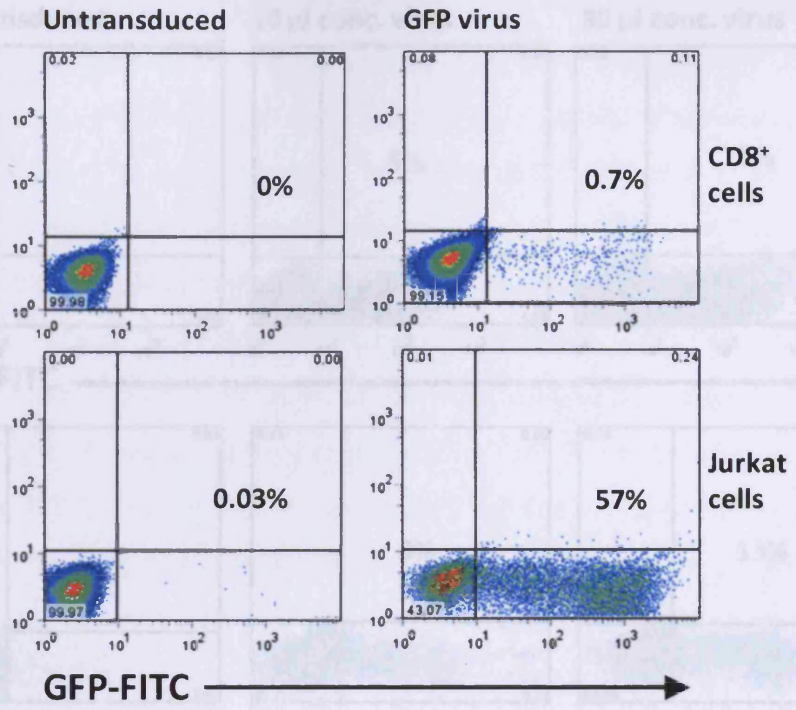

Figure 6.9: Transduction of CD4⁺ Jurkat T cell line and primary CD8⁺ T cells with a GFP-encoding lentiviral construct. 10^6 Jurkat cells (bottom panel) and 10^6 MACS-sorted CD8⁺ lymphocytes (top panel) were treated with 1 ml crude viral supernatant encoding the GFP construct. Following a 48 hour incubation with the virus, the cells were tested for GFP expression by flow cytometry. The numbers in the upper-right quadrants refer to the percentages of GFP⁺ transduced cells.

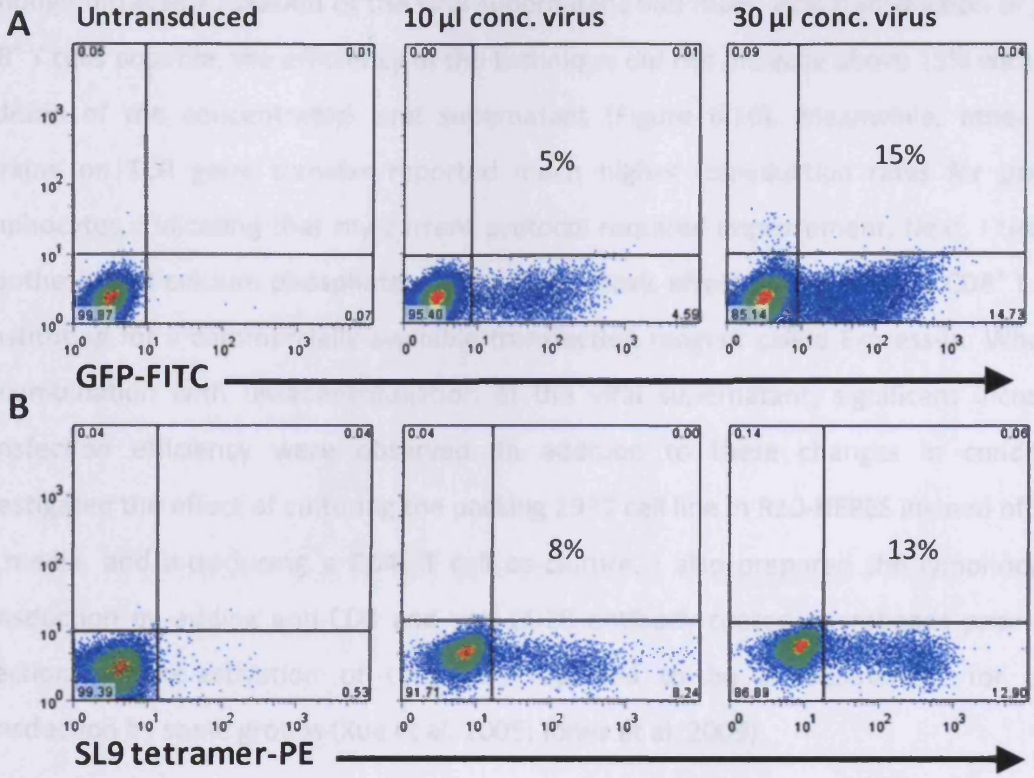

Figure 6.10: Transduction of primary CD8⁺ primary T cells using concentrated lentivirus. The transduction efficiency with a lentiviral vector carrying the GFP construct (**A**)a nd that of the lentiviral vector with the 868 TCRα-2A-β insert (**B**) using two different concentrations of lentivirus. In each case, the virus was concentrated by ultracentrifugation. The percentages indicate the proportions of cell expressing the gene interest for each transduction.

Although ultracentrifugation of the viral supernatant had made viral transduction of primary $CD8^+$ T cells possible, the efficiency of the technique did not increase above 15% with further addition of the concentrated viral supernatant (Figure 6.10). Meanwhile, other groups working on TCR gene transfer reported much higher transduction rates for primary T lymphocytes, indicating that my current protocol required improvement. Next, I tested the hypothesis that calcium phosphate was exerting a toxic effect on the primary $CD8^+$ T cells by substituting for a commercially available transfection reagent called Express-In. When used in combination with ultracentrifugation of the viral supernatant, significant increases in transfection efficiency were observed. In addition to these changes in conditions, I investigated the effect of culturing the packing 293T cell line in R10-HEPES instead of DMEM-10 media, and introducing a $CD4^+$ T cell co-culture. I also prepared the lymphocytes for transduction by adding anti-CD3 and anti-CD28 antibody-coated microbeads prior to viral infection, as pre-activation of cells was reported to be a requirement for efficient transduction by some groups (Xue et al. 2005; Jones et al. 2009).

As illustrated in Figure 6.11, the protocol achieved 70-99% transduction efficiency of primary $CD8^+$ T cells with GFP-virus. This high level of transgene expression was replicated using the 868 TCR-expressing virus (Figure 6.12), alleviating the need for any cell-sorting of the tetramer-specific population following subsequent transductions with the 868 TCR. The efficiency of transduction was significantly reduced when the 293T cells were cultured in the recommended R10-HEPES media compared to DMEM-10 (Figure 6.11), meaning all further transductions were carried out using DMEM-10 media. Co-culturing $CD8^+$ T cells with $CD4^+$ T lymphocytes produced a slight increase in the level of transduction, but this was not significant enough for the effort taken up by additional MACS separations, and this requirement of the protocol was deemed unnecessary for future transductions.

6.2.4 Primary $CD8^+$ T cells transduced with a lentiviral vector encoding the 868 TCR maintain a stable level of exogenous TCR expression in culture, and acquire specificity for the SL9 epitope

After transduction with the 868 TCR-lentivirus, primary $CD8^+$ T cells were expanded and maintained in culture for up to two months. During this time, the percentage of cells

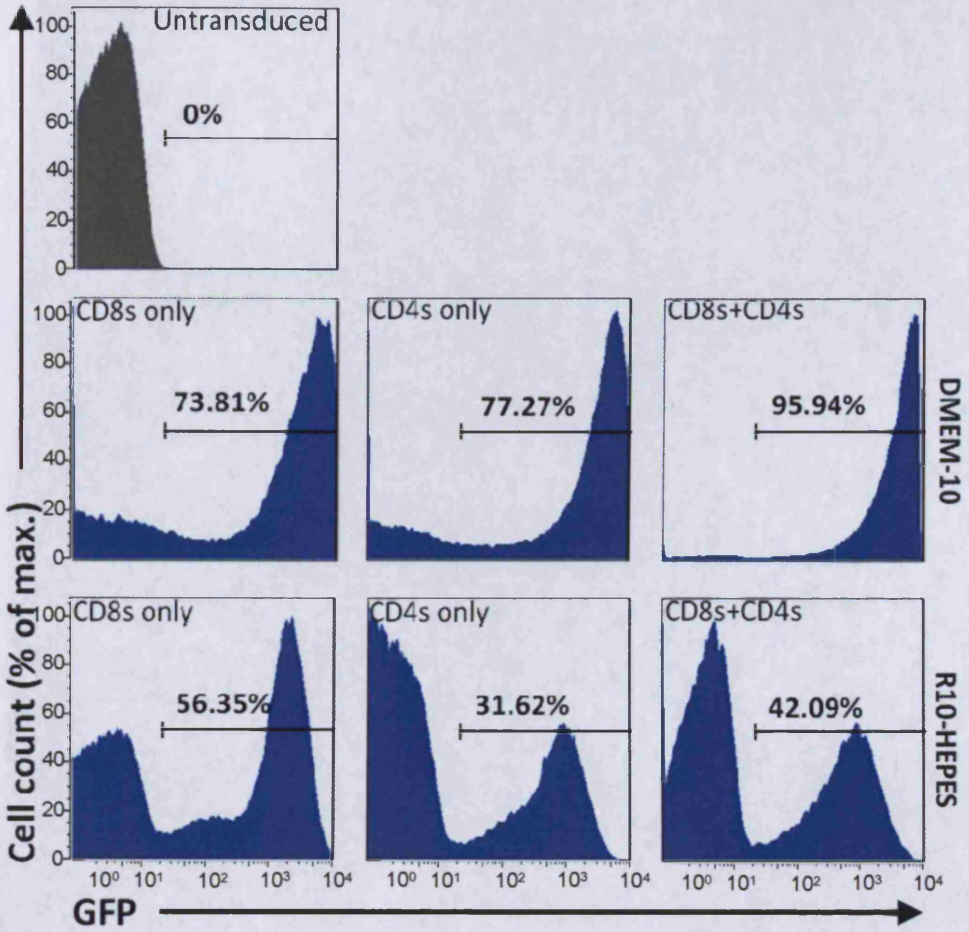

Figure 6.11: Optimisation of the lentiviral transduction protocol; Differences in transduction of CD8⁺ T cells with GFP-lentivirus using the recommended R10-HEPES and DMEM-10 media, and combinations of CD8⁺ and CD4⁺ T cells. 10^6 of either MACs-selected CD8⁺ cells, CD4⁺ cells, or 10^6 each of CD8⁺ and CD4⁺ were pre-activated with anti-CD3 and anti-CD28 antibody-coated microbeads prior to addition of 1 ml concentrated GFP-encoding lentivirus, manufactured using the 293T packaging cell line cultured in either DMEM-10 (top panel), or R10-HEPES (bottom panel), as recommended in the revised protocol. The uppermost plot (grey) shows CD8⁺ and CD4⁺ T lymphocytes that have not been infected with GFP-virus.

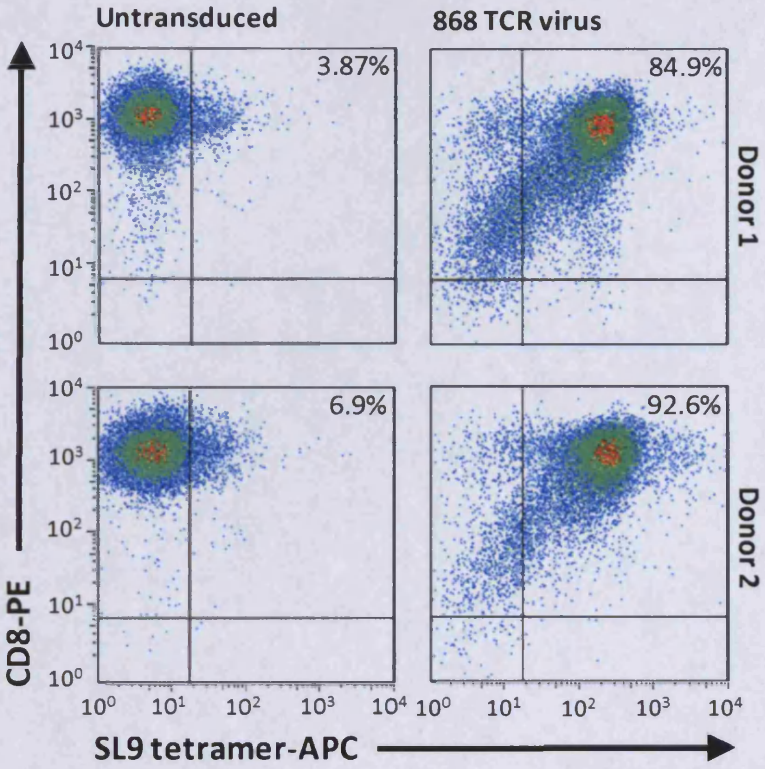

Figure 6.12: Transduction of primary CD8⁺ T lymphocytes with a lentiviral vector expressing the 868 TCR, using the revised and optimised TCR transduction protocol. 10^6 MACS-sorted CD8⁺ T cells isolated from two donors, were pre-activated with anti-CD3 and anti-CD28 antibody-coated microbeads prior to addition of 1 ml concentrated lentivirus encoding the 868 TCR.T he lentivirus was generated using 293T packaging cell line cultured in DMEM-10 media. Surface expression of the 868 TCR was determined 72 hours post infection with the lentivirus by SL9/HLA A2 tetramer staining.

expressing the 868 TCR, and the level of TCR expression determined by SL9/HLA A2 tetramer staining did not change. The cells were used in activation and killing assays to test their functionality. The 868 TCR-transduced $CD8^+$ T cells exhibited specific activation and killing in response to target cells presenting SL9 peptide in a concentration-dependent manner (Figure 6.13). Untransduced $CD8^+$ T cells, isolated from the same donor, did not produce significant levels of MIP-1β or induce target lysis in response to SL9-pulsed targets.

The 868 TCR-transduced $CD8^+$ T cells were also subjected to a combinatorial peptide library screen to determine the amino acid preference exhibited by the 868 TCR-transduced $CD8^+$ T cells at each position of the peptide (Figure 6.14). A 9mer peptide library was chosen for the screening, based on the length of the index SL9 (SLYNTVATL) peptide. Figure 6.15 summarises the extent of MIP-1β release by 868 TCR-transduced cells in response to a fixed amino acid at each of the nine positions. Despite some background activation, the transduced cells collectively responded to the index SL9 peptide, with the highest responses to index amino acids at positions 1, 3, 4, and 6. All of the residues located in the index peptide elicited a detectable response. However, on replicating the assay numerous times, a clear preference was seen for a proline at position 7.

5.2.5 Primary $CD8^+$ T cells transduced with a lentiviral vector encoding the 868 TCR are polyfunctional and are capable of killing HIV-infected cells.

Polyfunctionality, or the ability to produce high levels of several soluble factors simultaneously, has been shown to be a key feature of a successful immune response in both human and murine systems (Almeida et al. 2007; Darrah et al. 2007; Precopio et al. 2007). In a study, focusing on the factors associated with successful targeting of HIV-1 infected cells by $CD8^+$ T cells, Almeida *et al.* demonstrated that $CD8^+$ T cells that achieve optimal control of HIV-1 replication also display polyfunctionality. In keeping with this work, if TCR-transduced $CD8^+$ T cells are to be successful in the clinic, they would need to make a polyfunctional response to their target antigen. I investigated whether $CD8^+$ T cells transduced with the 868 TCR possessed this desired quality by measuring five effector functions of these cells in response to activation by target cells presenting cognate SL9 peptide. Figure 6.16 shows

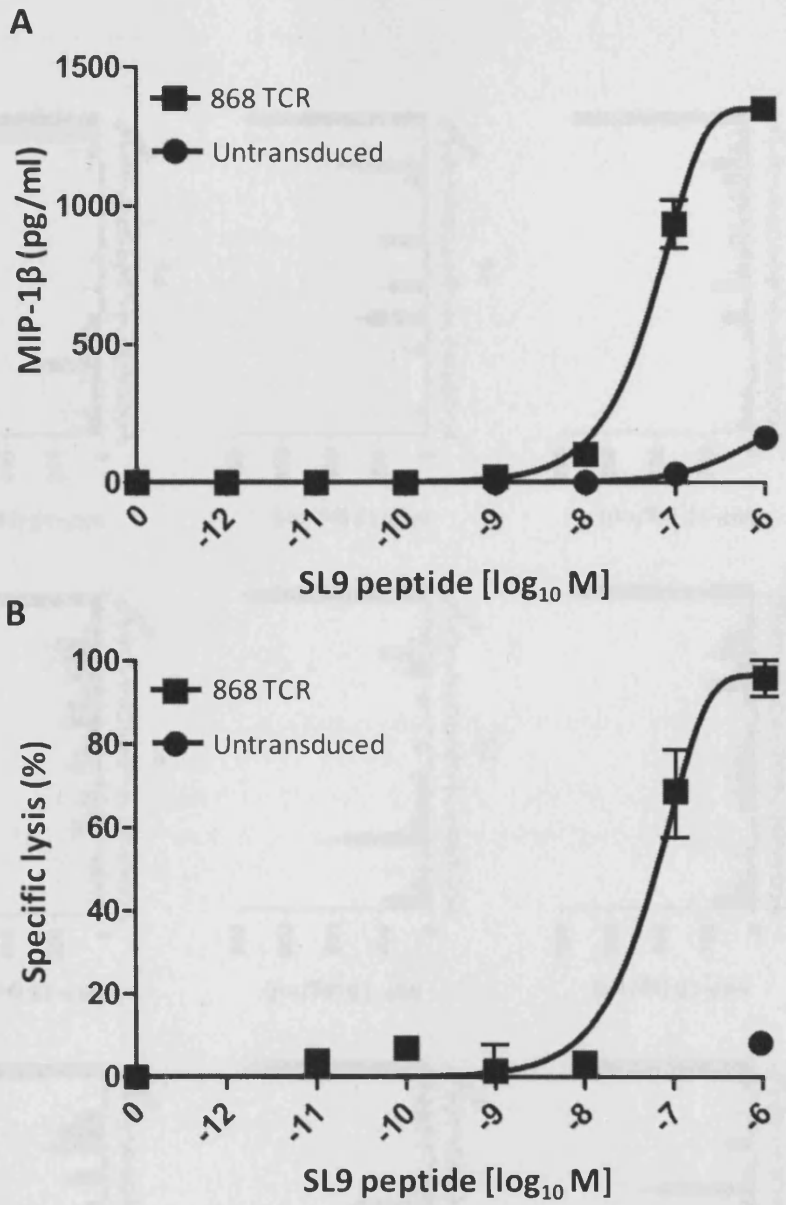

Figure 6.13: Primary CD8⁺ T cells transduced with the 868 TCR are capable of specific activation and killing in response to SL9 peptide-pulsed targets. A. A MIP-1β ELISA conducted with 95% SL9/HLA A2 tetramer positive CD8⁺ T cell line and C1R HLA A2-expressing target cells pulsed with different concentrations of SL9 peptide. **B.** A FATAL killing assay conducted with the same 868 TCR-transduced cells, SL9 peptide-pulsed HLA A2 positive T0 cell as targets, and unpulsed T0 cells as controls. Untransduced CD8⁺ T cells from the same donor were used as negative controls for both assays. Error bars represent s.d. from the mean of two replicates. Data in is representative of >2 separate experiments.

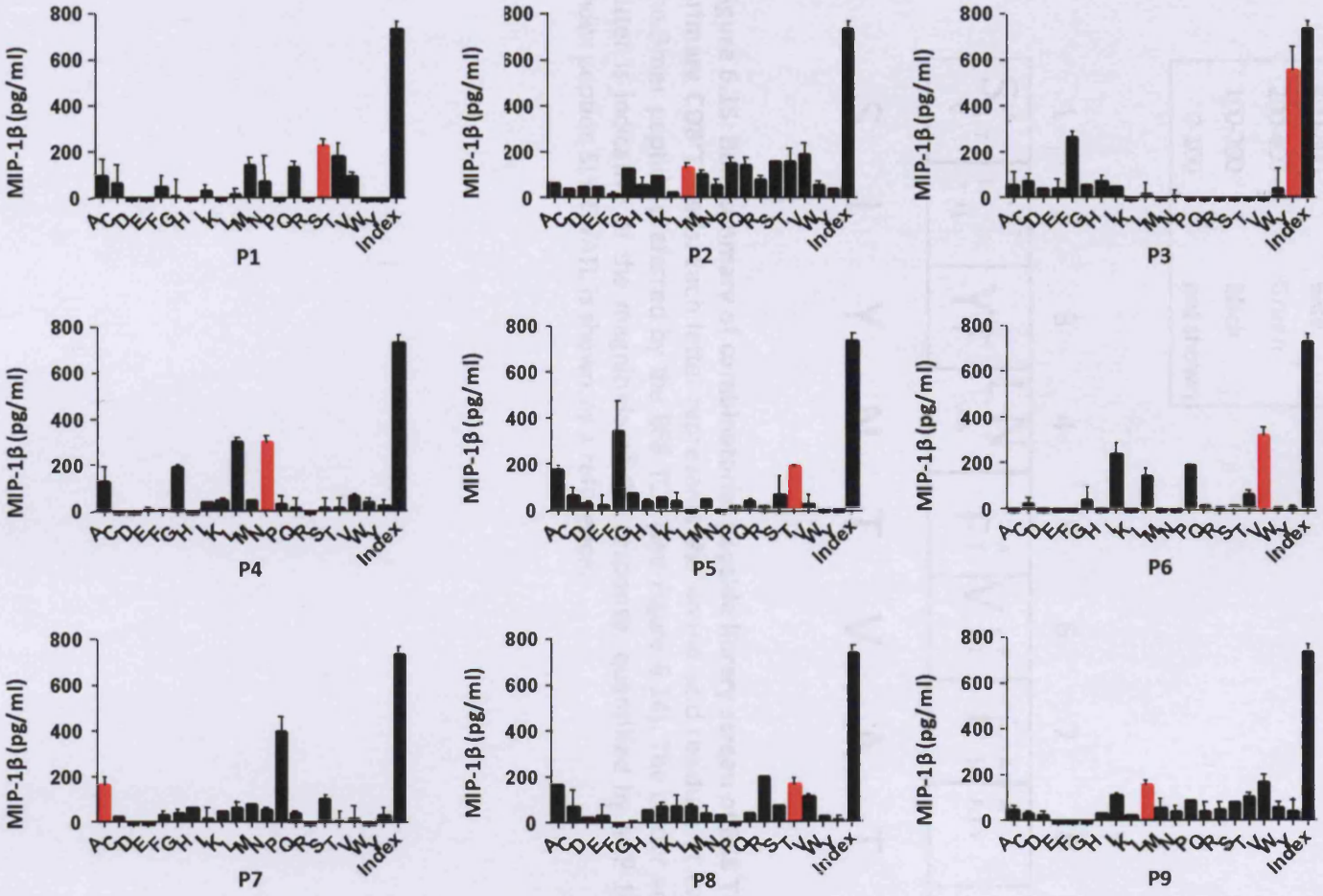

Figure 6.14: A 9-mer combinatorial peptide library screen of CD8⁺ T cells transduced with the 868 TCR. The CD8⁺ T cells screened in this assay were 95% positive for 868 TCR expression, determined by cognate SL9-tetramer staining. The P1-P9 refer to the positions of each of the 20 amino acid residues in the 9mer peptide. Responses to amino acids which are present in the index SL9 peptide are highlighted in red. 10^{-6} M index SL9 peptide was used as a positive control. Error bars represent s.d. from the mean of 2 replicates. Data is representative of 2 separate experiments.

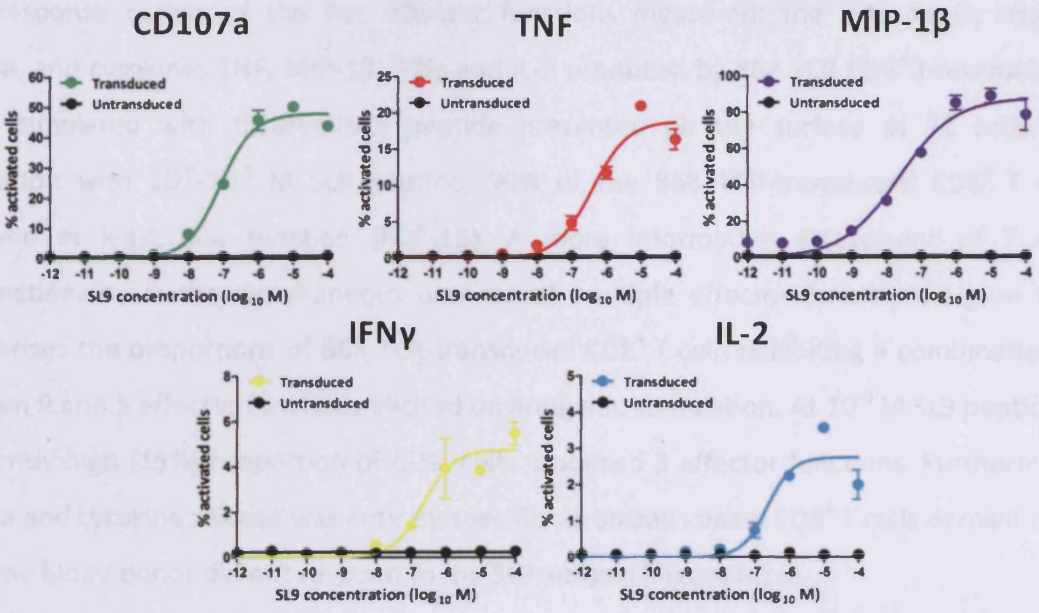

Figure 6.16: 868 TCR-transduced CD8⁺ T cells display specific activation to express multiple effector functions in response to target cells presenting cognate antigen. Target T2 cells pulsed with a range of SL9 peptide (SLYNTVATL) concentrations or mock-pulsed with medium alone were incubated with 868 TCR-transduced (~95% SL9/HLA A2 tetramer positive) CD8⁺ T cells or untransduced CD8⁺ T cells from the same donor for 12 hours at 37°C, in the presence of a directly conjugated αCD107a mAb and secretion inhibitors as described in section 2.11.5 of Materials and Methods. After incubation, cells were initially stained with the amine viability dye Aqua, and then with directly conjugated mAbs specific for the surface markers CD3 and CD8. After subsequent fixation and permeabilisation, intracellular staining for specific cytokines was performed. Surface mobilisation of CD107a (green), and intracellular production of the cytokines TNF (red), MIP-1β (purple), IFNγ (yellow), and IL-2 (turquoise) are shown. The line plots depict dose-response relationships between the SL9 peptide concentration and the percentage of CD8⁺ T cells activated to express each individual function. Error bars represent s.d. from the mean of 2 replicates.

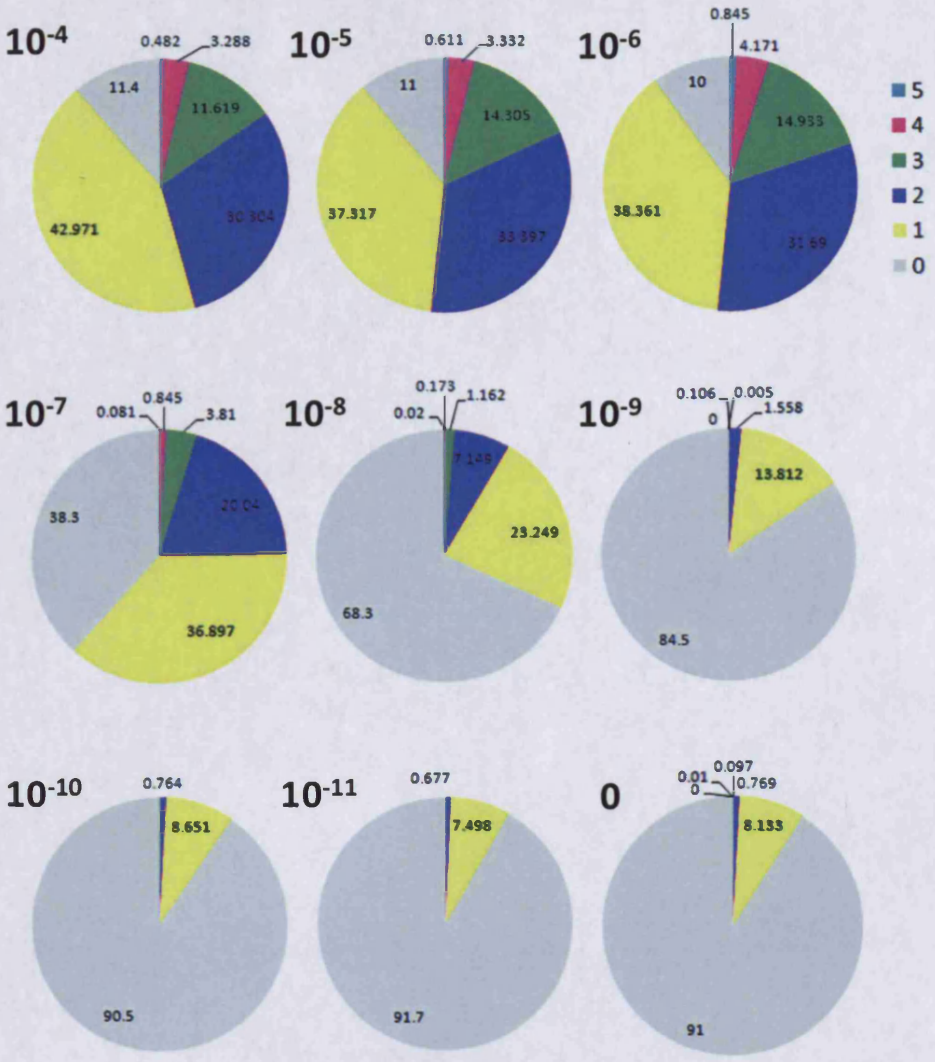

Figure 6.17: 868 TCR-transduced CD8⁺ T cells are highly polyfunctional. Pie chart representations of ICS data (from the same experiment as in Figure 6.16) depicts the percentages of 868 TCR-transduced CD8⁺ T cells exhibiting 0-5 of each of the five effector functions: CD107a, TNF, MIP-1β, IFNγ, and IL-2. The labels on the upper-left side of each pie chart correspond to the concentrations of SL9 peptide presented on target cells. Experimental details are outlined in Figure legend 6.16,a nd section 2.11.5 of Materials and Methods.

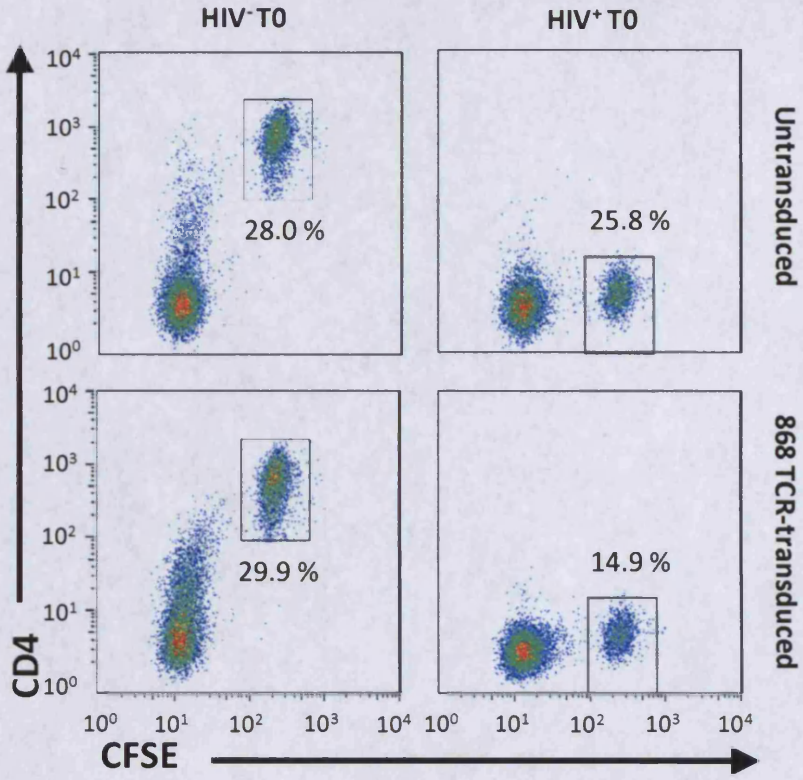

Figure 6.18: 868 TCR-transduced CD8⁺ T cells are capable of killing target cells infected with HIV-1. A FATAL killing assay conducted with 868 TCR-transduced CD8⁺ T cells and either HIV-1 infected (right panels) or uninfected (left panels) T0 cells as targets. The HIV⁺ T0 population was shown to be ~100% infected with HIV-1 by means of a p24 intracellular FACS stain prior to the experimental setup. Both HIV⁺ and HIV⁻ T0 populations were stained with the cellular dye CFSE to distinguish them from the CD8⁺ effector population, as infection with HIV-1 causes downregulation of the CD4 coreceptor (right panels). The assay was also conducted with untransduced CD8⁺ T cells from the same donor to assess the level of background lysis. Data is representative of >2 separate experiments.

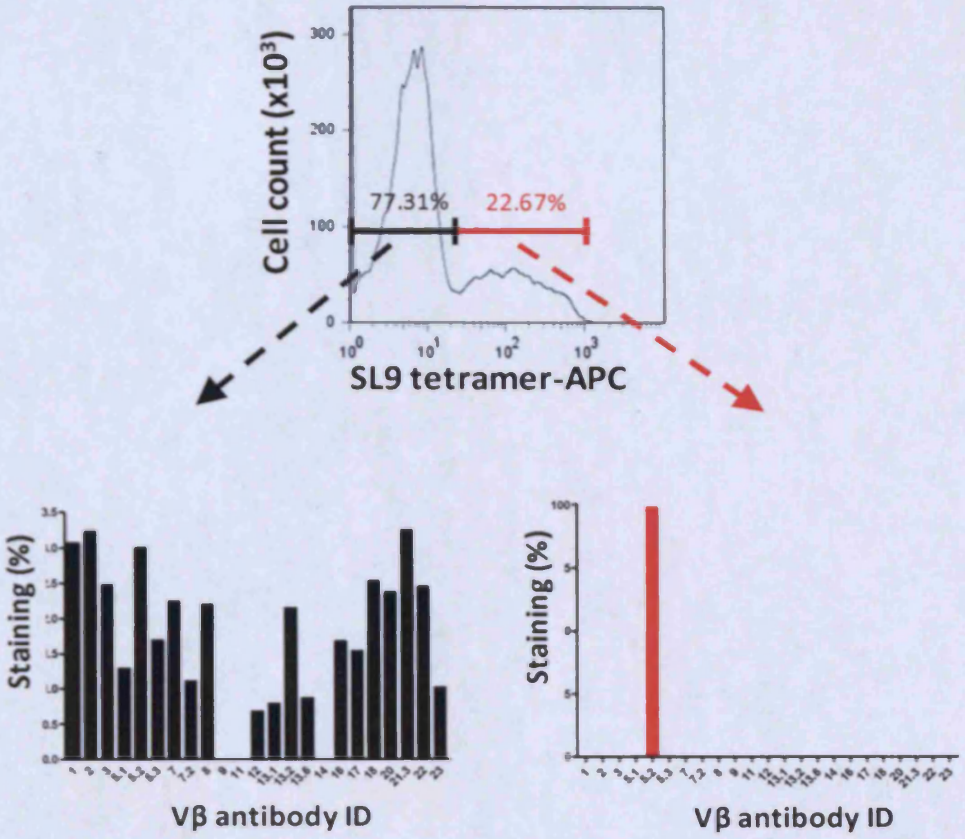

Figure 6.19: TCR Vβ antibody screen of 868 TCR-transduced and untransduced primary CD8⁺ T cells, distinguished by SL9 tetramer staining. 10^6 MACS-sorted CD8⁺ cells were transduced with 300 µl of concentrated 868 TCR-lentiviral supernatant and stained with a combination of SL9/HLA A2 tetramer-APC and a panel of TCR Vβ antibodies, before analysis by flow cytometry.

very positive initial result highlighted a possibility that mispairing of TCR chains abrogated tetramer binding, and thus SL9 tetramer staining did not provide an accurate representation of the TCR-transduced cell population. In further experiments, the transduced and untransduced populations were instead differentiated by staining with the TCR Vα2 antibody, specific for the 868 TCR alpha chain. Since a proportion of primary $CD8^+$ T cells naturally express a TCR α2 chain, any cells staining with the Vα2 antibody were MACS-depleted prior to transduction. Figure 6.20 shows the pattern of Vβ antibody staining for 868 TCR-transduced cells using PBMC taken from 3 donors. The transduced cells were identified by $Vα2^+$ staining. Although each donor showed a different pattern of Vβ antibody staining of untransduced cells, their 868 TCR-transduced cells all stained predominantly with the Vβ5.2 antibody (>90% frequency). Unlike in the previous example (Figure 6.19), identifying the transduced population with the Vα2 antibody instead of tetramer exposes a small number of cells staining with TCR Vβ antibodies other than Vβ 5.2. Since the tests for TCR mispairing were carried out on SL9 TCR-transduced cell lines (and not clones), it is possible that some of these Vβ responses are due to background staining of untransduced cells, and may not necessarily signify TCR chain mispairing.

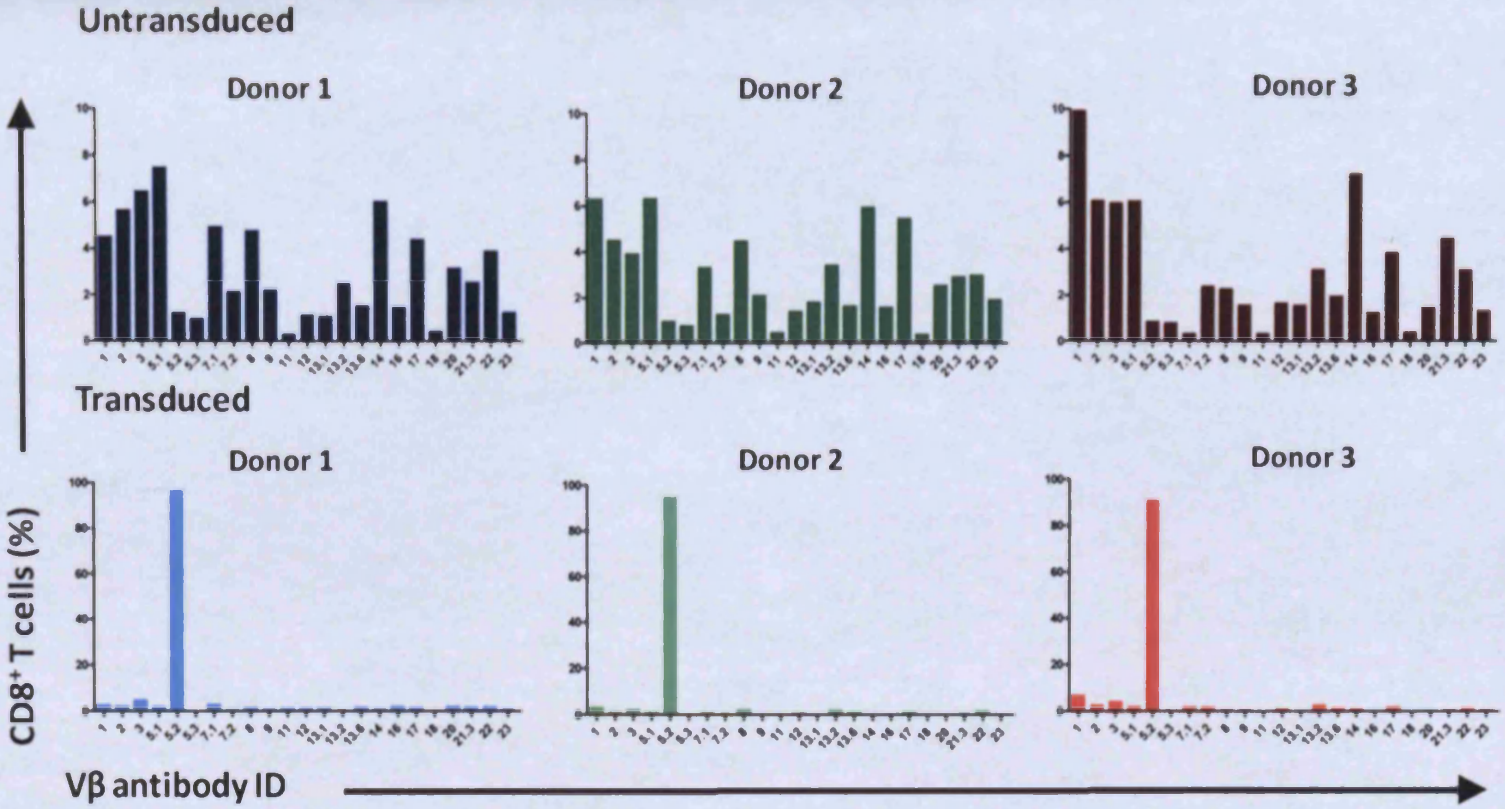

Figure 6.20: TCR Vβ antibody screen of 868 TCR-transduced and untransduced primary CD8⁺ T cells in three donors, distinguished by TCR Vα2 staining. 10^6 MACS-sorted $CD8^+$ T cells isolated from 3 different donors were each either transduced with 1 ml of concentrated 868 TCR-lentiviral supernatant (~95% transduction efficiency) or remained untransduced. Both sets were stained with a combination of TCR Vα2 antibody and a panel of TCR Vβ antibodies, before analysis by flow cytometry. The transduced graph shows results from the TCR $V\alpha2^+$ gate, while the untransduced graph shows Vβ staining patterns for the $V\alpha2^-$ population.

6.3 Discussion

Adoptive transfer therapy uses T cells isolated and cultured from patients to treat cancers and chronic viral infections. Although the technique has shown some initial success, it has a number of limitations, the most significant being the low frequency of antigen-specific T cells and the labour-intensive cell expansion process {Xue, 2005 #889;Kessels, 2002 #833;Varela-Rohena, 2008a #881;Schumacher, 2002 #869;Mansoor, 2005 #842;Heemskerk, 2006 #822}. Altering the specificity of a T cell by transfer of TCR genes bypasses some of these requirements, equipping T cells of varied specificities with the ability to target a desired antigen.

In this chapter I have evaluated and compared several methods available for the introduction of genes into T cells; pDNA and mRNA electroporation techniques to achieve transient transfection and a lentiviral vector for stable transduction. Electroporation of a Jurkat cell line with a GFP-encoding bacterial pUC plasmid resulted in GFP expression in 11% of the cells (Figure 6.4). Substituting the plasmid DNA for *in vitro*-transcribed (IVT) GFP mRNA raised the transfection efficiency to 39%. Although the IVT mRNA transfection technique was deemed successful, the cells expressing the foreign gene would have to be physically sorted in order to obtain a pure GFP-positive population for use in functional assays. Unfortunately, the transient nature of the technique results in the dilution of transgene expression with each cell division, meaning that any transfected cells have to be assayed immediately. Such a limited time frame would not allow for incorporation of a cell sorting step into the protocol. In addition, both DNA and mRNA electroporation techniques resulted in a considerable amount of cell death. With only ~30% of Jurkat cells remaining viable after the electroporation process, very large quantities of cells and mRNA would be consumed by this process. Typically only 20-30 μg of mRNA are generated by each IVT reaction, rendering this technique very expensive and time-consuming. Furthermore, it is predicted that the extent of cell death following the electroporation procedure would be even greater when using primary $CD8^+$ cells as targets, as these are reputedly less robust than Jurkat cell lines (Beebe et al. 2003). My results using mRNA electroporation contrasted with those obtained by Hofmann *et al.* (Hofmann et al. 2008). The problems I encountered with mRNA

electroporation and the success of lentiviral vectors reported by other groups meant that I did not pursue further optimisation of this technique.

The use of lentiviral vectors for the genetic modification of primary lymphocytes has improved enormously in recent years {Zhao, 2005 #1128;Morgan, 2006 #845;Varela-Rohena, 2008a #882;Schaft, 2003 #865}. The gene transduction experiments carried out in this chapter were performed using the pHR'SINcPPT-SFFV-x-WPRE (lenti-SxW) lentiviral vector, specifically designed for the transduction of non-dividing hematopoetic cells, which are notoriously difficult to transduce (Demaison et al. 2002). I began experimenting with the lentiviral system using a version of the lenti-SxW vector housing a gene encoding GFP (lenti-SeW). Infection of a TCR-negative Jurkat cell line with >30 µl crude lentiviral supernatant generated using the lenti-SeW construct, resulted in GFP expression in up to 98% of cells (Figures 6.8, 6.9). Applying viral supernatant with the same MOI to primary $CD8^+$ human T lymphocytes resulted in a much lower frequency (0.5-1.0%) of GFP positive cells (Figure 6.9). Although this confirmed other groups' findings that primary $CD8^+$ T cells require substantially higher MOIs than Jurkat cells for transduction (Toscano et al. 2004), the efficiency of transduction was much too low even at MOIs as high as 100.

A revised and optimised protocol for transduction finally produced the desired levels of transgene expression (70-99%) in primary $CD8^+$ T cells treated with anti-CD3/anti-CD28 antibody-coated microbeads and concentrated GFP-encoding lentivirus (Figure 6.11). Interestingly, although the infection of non-dividing cells is deemed to be a feature of lentiviruses, activation of primary lymphocytes was required for efficient infection. It appears lentiviruses are inefficient at infecting quiescent cells, whilst lentiviral vectors are even less so. Several groups have investigated the factors that permit lentiviruses but not lentiviral vectors to integrate into non-dividing cells. Agosto *et al.* have attributed the inefficient integration of conventional HIV-based lentiviral vectors to the presence of the VSV-G envelope (Agosto et al. 2009). Replacing the VSV-G envelope in the lentiviral vector construct with the natural CXCR4-tropic HIV *env* gene element increased the efficiency of transgene delivery to resting $CD4^+$ T cells (Agosto et al. 2009). Yamashita and colleagues undertook a different approach by mutating all the HIV proteins known to be involved in nuclear envelope

entry (including Vpr) both individually and together, but found that this did not prevent HIV infection of non-dividing cells (Yamashita and Emerman 2006). Based on their data Yamashita *et al.* hypothesised that the efficiency of lentiviral integration is somehow related to the action of the capsid protein, which facilitates uncoating of the virion (Yamashita et al. 2006). It is possible that the uncoating of the capsid represents a rate-limiting step in the infection process. Interestingly, while lentiviruses like HIV exhibit inefficient infectivity of quiescent cells *in vitro* this is not the case *in vivo* (Ravot et al. 2002; Yamashita et al. 2006). However, the complexity of the *in vivo* setting may continue to obstruct our understanding of the true mechanism of HIV infection of quiescent cells for years to come.

The transduction efficiency of primary $CD8^+$ T cells with a lentiviral vector encoding the HLA A2-restricted HIV gag-specific 868 TCR correlated directly with the transduction efficiency using the GFP-encoding virus (Figures 6.10 and 6.12). This was very encouraging as the efficiency of expressing two TCR chains that have to refold, pair, and be exported to the T cell surface was expected to be lower than a simple cytosolic GFP molecule. The high level of transduction achieved can be at least partially attributed to the design of the lentiviral vector itself. As described in Demaison *et al*, the incorporation of a strong SV40 promoter, SFFV and WPRE enhancer elements, and an amphotropic VSV-G envelope, all contribute to the success of this expression system (Demaison et al. 2002). In addition, the presence of the all-important 2A peptide and the SGSG spacer sequence function to express high quantities of each TCR chain, enabling efficient assembly of the chains into a functional TCR.

To test whether 868 TCR-transduced $CD8^+$ T cells could be functionally re-programmed with the specificity for the SL9 epitope SLYNTVATL, the TCR-transduced or untransduced cells were stimulated with T0 target cells loaded with various concentrations of SL9 peptide. The 868 TCR-expressing cells were capable of SL9 peptide specific activation demonstrated by MIP-1β release, and specific cytotoxic activity in a FATAL assay (Figure 6.13). The 868 TCR-transduced cells also displayed polyfunctionality (Figures 6.16 and 6.17). In addition to recognising the index SL9 peptide, the 868 TCR-transduced cells showed a high level of specificity in a combinatorial library peptide screen. The transduced cells responded to residues present at each position in the index peptide amongst mixtures of peptides

composed of thousands of different amino acid combinations (Figures 6.14 and 6.15). Most importantly, the 868 TCR-transduced $CD8^+$ T cells achieved their ultimate functional goal of lysing target cells infected with HIV-1 (Figure 6.18). Finally, the TCR-transduced cells retained their TCR expression and functionality throughout the period for which they were maintained in culture (typically 2 months).

Despite maintaining a high level of TCR expression, the activation and lytic threshold of the transgenic 868 TCR-expressing cells was higher than for the parental 868 line from which the 868 TCR originated (Sewell et al. 1997). A similar decrease in antigen sensitivity was observed in other TCR transduction studies (Schaft et al. 2003; Hofmann et al. 2008). There are a number of possible explanations for this phenomenon. It has been observed that the highly differentiated nature of a $CD8^+$ T cell clone or line means only a low concentration of target-peptide is sufficient to trigger their effector functions (Kimachi et al. 2003). In contrast, the MACS-sorted $CD8^+$ cells transduced for these experiments harbour a whole range of phenotypes, amongst some of which are naïve cells with high stimulation thresholds. However, since the cells are activated with anti-CD3/anti-CD28 coated beads prior to transduction, the percentage of cells that have not acquired the effector phenotype should be very low. A more plausible explanation is that the introduction of an exogenous TCR into a T cell population already expressing a range of endogenous receptors may lead to mispairing between the various native and introduced TCR α and β chains.

The inefficient expression of introduced TCR α and β chains in T lymphocytes can be one of the rate-limiting steps for TCR gene therapy. Once the lentiviral vector has integrated the TCR genes into the chromosomal DNA, the TCR α and β chains must be expressed in equimolar ratios, refolded, and assembled together with the CD3 γ, δ, ε, and ζ subunits on the cell surface. TCR chain mispairing and competition between the exogenous and endogenous TCRs for the CD3 complex may dilute the expression of relevant TCR $\alpha\beta$ heterodimers on the surface of TCR-transduced cells. As mentioned in the introduction to this chapter, several strategies have been employed to limit the mispairing of TCR chains, and enhance the preference of exogenous TCR chains for each other and the CD3 molecules (Boulter et al. 2003; Cohen et al. 2006; Cohen et al. 2007; Kuball et al. 2007; Sebestyen et al. 2008;

Okamoto et al. 2009). Although the 868 TCR used in this study was not subject to any such dramatic modifications, primary $CD8^+$ T cells transduced with the receptor did not display a significant amount of TCR chain mispairing (Figures 6.19 and 6.20). There can be a number of explanations for why we did not observe mispairing of the 868 TCR chains with the endogenous TCR chains. First, our system is likely to express the transduced TCR chains at much higher levels than the endogenous chains as the 868 TCR chains were codon optimised for mammalian expression and expressed under a very strong promoter. A number of groups have demonstrated that codon modification of TCR genes leads to enhanced functional expression of the TCR in transduced T cells (Heemskerk 2006; Scholten et al. 2006; Thomas et al. 2007; Bendle et al. 2009). In addition, an elegant theory proposed by Heemskerk *et al.* suggests there may exist a hierarchy of TCR chain-pairing events, with each chain exhibiting 'strong' or 'weak' TCR chain properties. The theory implies that 'strong' TCR chains will preferentially pair with each other and out-compete any endogenous TCRs for CD3-association, if these happen to display 'weaker' properties.

The T cell modulation group has attempted to manufacture over 70 different TCRs by refolding bacterially-expressed extracellular domains of the TCRα and β chains using dilution of denaturing conditions (Boulter et al. 2003). The efficiency of refolding varies widely. Some TCRs refold extremely well, while about 30% fail to refold at all. All the TCRs that we work with regularly, including the 868 TCR, fall at the high end of the refolding spectrum. We hypothesise that this is because they comprise TCRα and β chains that preferentially pair with each other. Indeed, our collection of HLA A2-restricted TCRs that fold well included a very limited number of $\alpha\beta$ TCR chain pairings. We therefore speculate that TCR chain pairings that refold very well *in vitro* will act as 'strong' TCRs whereas 'weak' TCRs will neither refold well nor compete well for cell surface expression. Marleen van Loenen of Leiden University in the Netherlands has recently been awarded a travelling fellowship and will come to Cardiff to test this hypothesis during 2011 using a spectrum of strong and weak TCRs that recognise the same HLA A2-restricted CMV-derived antigen. For the time being this idea remains conjecture. The discovery of means to predict whether a particular TCR will have a 'strong' or 'weak' phenotype with respect to competition with an endogenous TCR could aid TCR gene transfer strategies.

Chapter 7

7

THE INFLUENCE OF TCR GLYCOSYLATION ON T CELL RECOGNITION OF PEPTIDE-MHC LIGANDS

7.1 Introduction

As discussed in the previous chapter, the transfer of defined TCR genes into human T cells appears to be a promising new strategy for redirecting T cells against a number of antigens implicated in disease. However, many TCRs recognising antigens associated with cancer, autoimmunity, or rapidly evolving persistent pathogens are characterised by low affinities, making them ineffective candidates for TCR gene transfer therapy. Chapter 8 of this thesis deals with this issue, by addressing how the affinity of TCRs can be enhanced significantly by performing directed molecular evolution of soluble TCRs, by phage display. However, in addition to using laborious (albeit effective) surface display techniques (Holler et al. 2000; Li et al. 2005; Zhao et al. 2007), other strategies for increasing TCR affinity (Cohen et al. 2006; Kuball et al. 2007) should be explored. Glycosylation affects the flexibility, movement, and interactions of surface molecules, and is known to naturally regulate antigen sensitivity during T cell development (Demetriou et al. 2001; Baum 2002; Pappu et al. 2004). It is thus entirely plausible that manipulating the glycosylation status of a T cell may improve antigen recognition. In this chapter, I investigate whether reducing the level of T cell, and more specifically TCR glycosylation could provide an alternative strategy for enhancing TCR affinity and/or T cell sensitivity to cognate antigen. I assess the impact of: i) removing terminal sialic acid residues from the T cell surface; and, ii) individually silencing conserved N-glycosylation sites in the constant regions of TCR α or β chains; on the antigen sensitivity of T cells. I will begin by introducing how proteins become glycosylated in the first place, and what roles glycosylation plays in the T cell-mediated immune response.

7.1.1 Synthesis and function of N- and O- linked glycans on cell surface proteins

Nearly all mammalian cell surface proteins are terminally modified by glycosylation. The process of glycosylation is initiated in the cytosol and progresses through the lumen of the ER and the Golgi apparatus, where nucleoside-diphosphate-activated sugars are sequentially connected to branched polysaccharide chains by a complex set of enzyme-mediated reactions. The attachment of glycans to proteins can occur in a number of ways, but the initial step typically involves a glycosidic link to the amide nitrogen of asparagine

residues located within N-glycosylation motifs [N-X-S/T] (asparagine, followed by any amino acid other than proline, followed by serine or threonine) to form N-linked glycans. The resulting N-glycosylated proteins traverse the ER and Golgi apparatus, undergoing a further level of modification termed 'trimming' (Varki 2009); a process whereby glucose and mannose residues are cleaved off and replaced by N-acetylglucosamine, galactose, fucose, and sialic acid derivatives. O-linked glycosylation occurs at a later stage during protein processing, in the Golgi apparatus. This involves the addition of N-acetyl-galactosamine to serine or threonine residues, followed by other carbohydrates such as galactose and sialic acid (Varki 2009). Figure 7.1 illustrates the typical sugar composition and spatial distributions of N- and O-glycans.

The majority of proteoglycans are terminally decorated by sialic acids, a group of monosaccharides derived from neuraminic acid. These sugar molecules carry a carboxylate group at the 1-carbon position, which is normally ionized at physiological pH, giving it a characteristic negative charge (Varki 2009). The presence or absence of this negatively charged and highly hydrated glycan on cell surface proteins greatly influences the interaction of these proteins with each other and their environment (Varki 2009). Sialic acids are now known to have important roles in cell proliferation, protection of glycoproteins from the actions of proteases, and shielding of epithelial surfaces from infection, mechanical and enzymatic damage (Corfield et al. 1992; Rutledge et al. 1996; Fujita et al. 2000).

7.1.2 Removal of sialic acid from cell surface glycoproteins on T cells results in increased sensitivity to antigen

Sialic acid is a key molecule in cell-cell interactions and is involved in regulating: i) lateral mobility of proteins in the plasma membrane; ii) protein interactions with each other and their environment; and, iii) the organization of proteins into ordered domains (Kelm et al. 1997; Rudd et al. 1999; Sacchettini et al. 2001). However, sialyl-glycans only became of interest to immunologists, when it was shown that the high sialylation status of a T cell correlated with reduced sensitivity to antigen (Demetriou et al. 2001; Baum 2002). Around

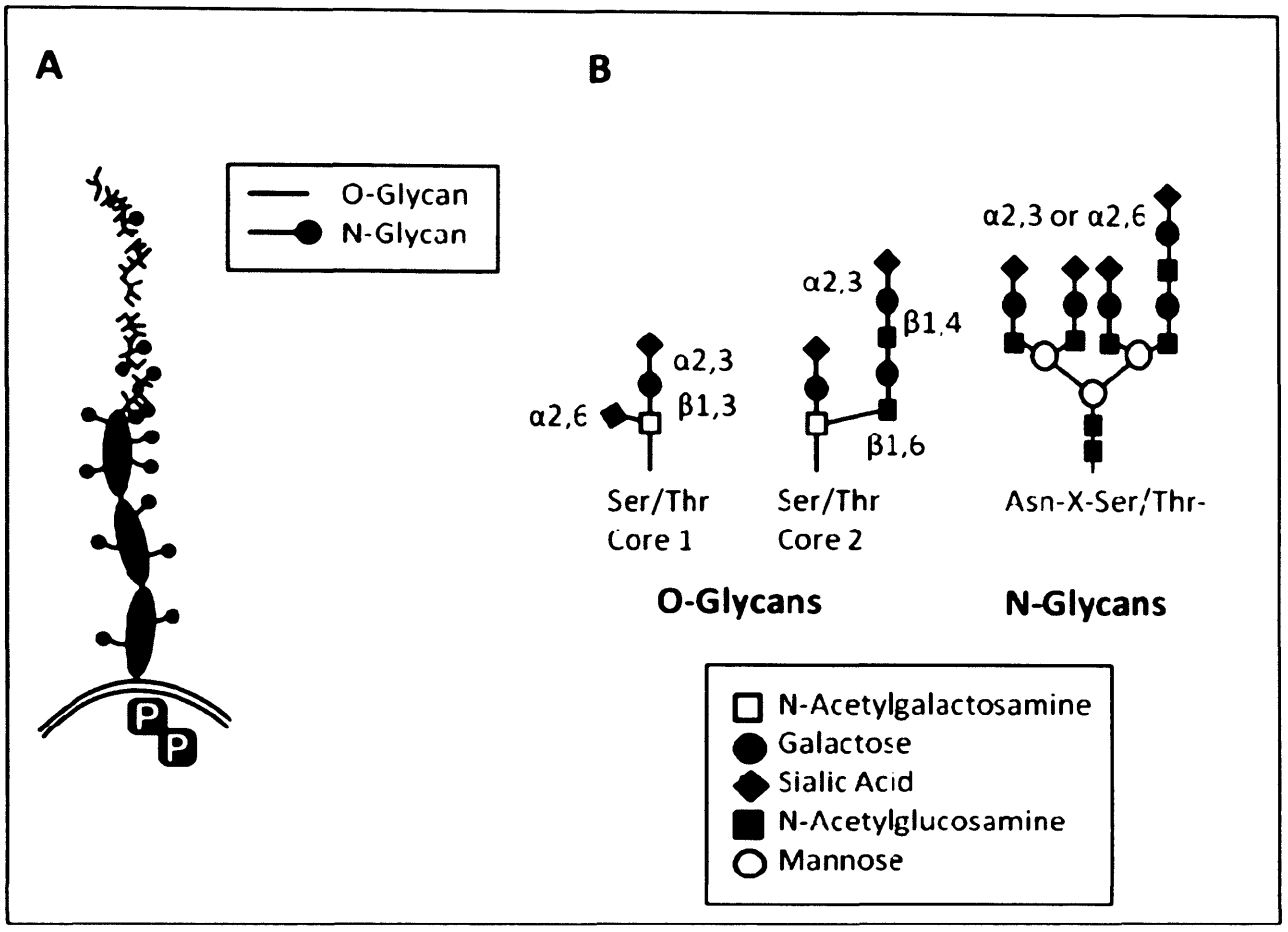

Figure 7.1: A schematic highlighting the differences between N -and O-linked glycosylation. A. The distribution of N- and O-linked glycans on a cell surface glycoprotein, in this case the protein tyrosine phosphatase CD45. The membrane proximal region contains multiple N-glycans, while the membrane distal region contains some N-glycans and abundant O-glycans. **B.** Examples of N- and O-glycan structures, both of which are typically terminated by addition of the negatively charged sialic acid (diamond symbols). Core 1 O-glycans can be modified by both α2,3 and α2,6 sialic acid, while core 2 O-glycans can be modified by α2,3 sialic acid at the termini of both branches. The termini of N-glycans can be modified by either α2,3 or α2,6 sialic acid. Figure reproduced from (Hernandez et al. 2007).

the same time, several groups reported that the formation of the immunological synapse was to some extent regulated by the glycosylation state of the proteoglycan agrin (Khan et al. 2001), and by the addition of branched N-glycans to cell surface glycoproteins such as CD8, CD45, CD43, and the TCR (Demetriou et al. 2001; Lowe 2001; Baum 2002). Furthermore, work by Pappu and Shrikant demonstrated that removal of sialic acid residues from naïve T cells enhanced early activation events and reduced the duration of antigen-TCR engagement required to initiate proliferation and differentiation of these T cells (Pappu et al. 2004). They expanded on their initial findings by showing that desialylation of naïve T cells augmented the cytotoxic response to tumour-associated antigens (TAAs). This represented an important achievement, considering that due to their low surface pMHCI expression and lack of costimulatory molecules, tumours are notoriously poor stimulators of naïve T cells (Pappu et al. 2004).

7.1.3 The key glycoproteins involved in T cell-antigen recognition

T cell recognition of antigen-presenting cells (APCs) comprises several stages: i) TCR engagement of pMHC antigen; ii) formation of a junction between the two cells known as the immunological synapse; and, iii) signal transduction by the TCR-associated machinery (Grakoui et al. 1999; van der Merwe 2000). Since most of the proteins implicated in this complex set of events are modified by glycosylation, individual glycans are likely to play important roles. For instance, it is not a mere coincidence that oligosaccharides found on proteins involved in the formation of supramolecular activation clusters (SMACs), the hallmark of immunological synapses established by T cells, are conserved across species {Dustin, 1997a #2369}. These glycans are likely to function by positioning cell surface receptors and coreceptors, thus dictating the alignment of T cell and target cell surfaces {Dustin, 1997a #2369}. As mentioned in the previous section, both desialylation and deglycosylation (removal of entire N-linked glycans) can enhance T cells sensitivity to antigen (Demetriou et al. 2001; Baum 2002; Pappu et al. 2004). However, T cell SMACs are complex molecular lattices comprising a multitude of receptors, coreceptors, and regulatory molecules (Grakoui et al. 1999). Pin pointing the key players, changes in whose glycosylation status can bring about these effects, becomes a veritable challenge. To date, the list of

suspects has been narrowed down to four: CD8, CD43, CD45, and the TCR. I will briefly summarise the evidence to support the involvement of varying glycosylation states of each of these molecules in controlling antigen recognition:

i) CD8 coreceptor glycosylation and T cell activation

Of the four main candidate molecules suggested to play a role in controlling the effects of T cell glycosylation status on antigen sensitivity, CD8 has been by far the best studied. Two independent studies by Moody *et al.* and Daniels *et al.* simultaneously published observations that immature $CD8^+$ $CD4^+$ double positive (DP) thymocytes were able to bind MHCI tetramer loaded with non-cognate peptides. Binding of non-cognate pMHC required the CD8 coreceptor (Daniels et al. 2001; Moody et al. 2001). The reason non-cognate MHCI tetramer binding was observed with DP and not single-positive (SP) mature $CD8^+$ thymocytes was attributed to the presence of sialic acid on the terminal glycans of mature but not immature thymocytes. The standard method for differentiating sialylated and unsialylated glycans is by exploiting their differential abilities to bind a plant lectin called peanut agglutinin (PNA). PNA recognizes all carbohydrates containing terminal galactose residues, but it binds with highest affinity to the disaccharide sequence Galβ1,3GalNAc ((Lotan et al. 1975; Wu et al. 1996) and Figure 7.1 B), which forms part of a common O-linked oligosaccharide structure present on several glycoproteins including CD8, CD45 and CD43 (Gillespie et al. 1993; Wu et al. 1996). PNA preferentially binds 'naked' unsialylated O-linked glycans, so on addition of sialic acid by the sialyltransferase enzyme its binding sites are obscured, resulting in a loss of PNA binding (Gillespie et al. 1993; Priatel et al. 2000). Importantly, the sialyltransferase enzyme is expressed by mature but not immature thymocytes (Gillespie et al. 1993; Priatel et al. 2000). It follows, that treatment of mature thymocytes with a bacterial neuraminidase to remove the sialic acid residues restores tetramer binding to the levels observed with immature thymocytes, implying that sialic acid somehow interferes with the pMHCI/CD8 interaction (Daniels et al. 2001; Moody et al. 2001). Although no detailed investigation into the mode of action of this small negatively charged glycan was conducted, the group proposed a number of theories for the enhanced pMHCI tetramer binding seen in the absence of sialic acid moieties. Sialic acid may

somehow affect the rigidity of the CD8 stalk, or the lateral mobility of CD8 within the lipid bilayer. Perhaps more plausibly, electrostatic repulsion between sialic acid moieties could affect the accessibility of CD8 to MHCI (Moody et al 2001, Daniels et al 2001). Since the CD8 coreceptor is involved in stabilising the TCR/pMHCI interaction (Wooldridge et al. 2005), increasing the affinity of pMHC/CD8 binding through removal of sialic acid would in turn results in enhancing the stability of the TCR/pMHCI complex. Although these publications by Moody *et al.* and Daniels *et al.* have been critical in exploring the question of how changes in glycosylation affect antigen recognition, their focus on CD8 alone failed to explain some key observations, such as the enhanced antigen recognition by T cells with aberrant pMHCI/CD8 interactions or those lacking the CD8 coreceptor altogether.

ii) CD45 and CD43 glycosylation and T cell activation

PNA also binds the protein tyrosine phosphatase CD45, and the heavily sialylated anti-adhesion molecule, CD43 on immature but not mature thymocytes. These molecules regulate T cell activation leading some groups to speculate that these molecules may be the most likely to mediate the enhanced sensitivity of T cells to antigen after removal of sialic acid (Wu et al. 1996; Hernandez et al. 2007). It has been reported that sialylation regulates the dimerisation and activity of CD45 (Xu et al. 2002). Dimerisation of CD45 is believed to interfere with its cytoplasmic associated phosphatase domains so that the dimer exhibits vastly reduced activity compared to the two monomers (Bilwes et al. 1996). Thus, desialylation of CD45 may reduce its negative effect on T cell signalling and increase T cell sensitivity to antigen.

iii) TCR glycosylation and T cell activation

More recently, the focus of investigation has shifted towards the molecule central to T cell antigen recognition, and common to all T cells, the TCR. Major evidence for how changes in the glycosylation status of the TCR impact on T cell-antigen recognition has come from an elegant study by Demetriou *et al*, who demonstrated that genetic disruption of the normal N-glycosylation pathway, more specifically a deficiency in the enzyme 1,6β N-acetylglucosaminyltransferase V (Mgat5) in mice resulted in enhanced antigen recognition

(Demetriou et al. 2001). The enhancement in T cell antigen recognition was attributed to improved TCR engagement (of pMHC), clustering and downregulation. In fact, the increase in TCR affinity was so dramatic that the mice developed autoimmunity (Demetriou et al. 2001). The fact that Mgat5 directly reduces the mobility of TCRs displaying Mgat5-modified glycans means that any disruption to its function would increase TCR mobility and subsequent clustering. As a result, the need for CD28-mediated costimulation is bypassed, with a subsequent reduction in the activation threshold for all T cells, irrespective of their specificities. Enhanced antigen recognition and loss of immune tolerance was therefore explained by enhanced TCR clustering at the site of antigen presentation and a reduced need for costimulation by CD28 (Demetriou et al. 2001).

7.1.4 T cell glycosylation and crossreactivity

The observations of Daniels *et al.* 2001 and Moody *et al.* 2001 showed that immature thymocytes can recognize non-cognate pMHC molecules (Daniels et al. 2001; Moody et al. 2001). This broader recognition profile of immature thymocytes is believed to be regulated by CD8 glycosylation and may represent a critical mechanism that allows immature thymocytes to gain a positive selection signal from self pMHCI molecules. My laboratory have recently shown that the strength of the pMHCI/CD8 interaction can control T cell crossreactivity in mature $CD8^+$ T cells (Wooldridge et al. 2010). The binding affinity and/or half-life of TCR/pMHC engagement is believed to be the critical parameter that determines whether or not a T cell responds to a given pMHC antigen. As described above, there is some evidence to indicate that TCR glycosylation can alter pMHC binding. Given the suggested role for TCR and CD8 glycosylation in T cell activation in response to cognate and non-cognate peptide ligands, I decided that it would be interesting to examine whether the T cell glycosylation status could alter T cell crossreactivity. I will begin by introducing this subject.

The rearrangement and recombination of genetic elements encoding a functional TCR achieves an astounding level of diversity and can theoretically produce over 10^{18} different human αβ TCRs (Davis et al. 1988; Venturi et al. 2008). Such a vast number of combinations

would in theory support a one TCR to one peptide specificity hypothesis, until we are reminded that there are only $5x10^{13}$ cells of human origin in the average human body. To put this into perspective, if 10^9 cells approximates to a gram of human tissue, then 10^{18} T cells would weigh a colossal 10^6 Kg or 1000 tons (Mason 1998). Thus, in order for T cell immunity to work as it does, theoretical considerations dictate that each individual T cell must be capable of recognising over a million different peptides (Mason 1998). More recent estimates suggest that there are only 2.5×10^7 TCRs in the human naïve T cell pool (Arstila et al. 1999), a number that is dwarfed by the potential magnitude of foreign peptide-MHC complexes that could be encountered and which it appears the body can mount a successful immune response to (Mason 1998). Thus, in theory at least, an extremely high level of T cell crossreactivity, sometimes referred to as polyspecificity, is an essential feature of T cell recognition. As described above, the questions of how T cells achieve crossreactivity, and how this property can be regulated (for instance by the CD8 coreceptor) form a major interest for members of my group. Their findings confirm that a high level of TCR crossreactivity is essential for effective T cell immunity (Mason 1998; Wooldridge et al. 2010). Given that the strength of the TCR/pMHC interaction is correlated with TCR crossreactivity, it will be extremely interesting to see if the glycosylation status of a T cell, and in particular its TCR, can influence T cell crossreactivity by affecting the stability of the TCR/pMHC antigen interaction.

7.1.5 Aims

Several groups have demonstrated the impact of differential sialylation of CD8 on modulation of TCR affinity during thymocyte selection (Daniels et al. 2001; Moody et al. 2001), while others have attributed the increase in antigen sensitivity, observed on desialylation, to changes in oligomerisation state and activity of costimulatory molecules CD45, and CD43 (Wu et al. 1996; Hernandez et al. 2007). Thus, the major question as to which glycoconjugates are responsible for the observed increase in antigen sensitivity which results from T cell deglycosylation, remains unanswered. As part of my study into optimisation of TCR-antigen interactions I aim to investigate how the sialylation state of a T cell and the N-glycosylation state of a TCR impacts on antigen recognition. Since glycosylation influences the structure of proteins and their interactions with each other and the environment, removal of sialic acid and/or glycosylation residues from the TCR may increase its antigen recognition capacity. In addition to carrying out global T cell desialylation I aim to investigate how the mutation of individual N-glycosylation sites on a specific TCR impacts on the antigen sensitivity and crossreactivity of the host $CD8^+$ T cells. The specific aims for this chapter were to:

i) Assess whether a functional pMHCI/CD8 interaction is a prerequisite for increasing $CD8^+$ T cell-mediated antigen recognition on desialylation.

ii) Determine whether the increase in antigen sensitivity on removal of cell surface sialic acid by the neuraminidase enzyme is experienced by T cell subsets other than $CD8^+$ T cells.

iii) Subject sialylated and desialylated $CD8^+$ T cells of known specificity to a combinatorial peptide library screen, to assess the impact of glycosylation on TCR crossreactivity.

iv) Investigate the role of TCR surface glycosylation in antigen recognition by performing site directed mutagenesis (SDM) of individual glycosylation sites and evaluating the functionality of T cells transduced with these TCR glycosylation mutants.

7.2 Results

7.2.1 Desialylation increases antigen sensitivity of three T cell subsets irrespective of CD8 coreceptor involvement

The standard method for differentiating sialylated and unsialylated O-linked glycans is by exploiting their differential abilities to bind peanut agglutinin (PNA). As mentioned in section 7.1.3 i), the sialylation status of a T cell can be verified by cell staining with PNA molecules that are conjugated to a fluorescent dye and analysed by flow cytometry (Gillespie et al. 1993; Priatel et al. 2000). In order to remove the sialic acid, T cells were subjected to treatment with neuraminidase (section 2.9.2 of Materials and Methods), a promiscuous enzyme derived from *vibrio cholerae*. As an example, the sialylation status of neuraminidase-treated and untreated tumour antigen-specific ILA1 $CD8^+$ T cell clone, which recognises the HLA A2-restricted ILA peptide ($hTERT_{540-548}$; ILAKFLHWL), was examined by its ability to bind PNA as a test to verify the success of the enzymatic reaction (Figure 7.2).

Removal of terminal sialic acid moieties from another tumour-reactive Melan-A-derived HLA A2-restricted Melan-A_{26-35}; ELAGIGILTV (ELA) peptide-specific Mel13 $CD8^+$ T cell clone enhanced its sensitivity to peptide antigen when presented on C1R cells (Figure 7.3). The Mel13 clone was either treated with neuraminidase or left untreated, and the success of the enzymatic reaction was verified by PNA-FITC staining. The PNA^+ and PNA^- fractions were subsequently used as effectors in a cytometric bead array (CBA) to measure their levels of activation in response to titrated cognate ELA peptide presented on C1R target cells expressing three types of surface HLA A2 molecule: 227/8 K/A (Purbhoo et al. 2001; Laugel et al. 2007), wildtype (WT), and Q115E (Wooldridge et al. 2005; Wooldridge et al. 2007). The HLA A2 molecules differ in the strength of their interactions with the CD8 coreceptor: i) 227/8 K/A mutant shows abrogated CD8 binding (CD8-null); ii) WT displays a normal physiological interaction with CD8; and, iii) Q115E binds CD8 with ~1.5 fold higher affinity than wildtype (CD8-enhanced). With all three targets, cytokine release from desialylated cells was observed at peptide concentrations a factor of 10 and even 100 fold

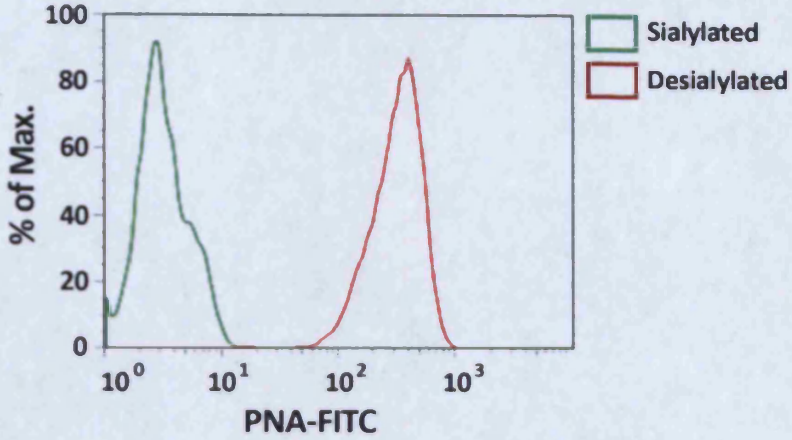

Figure 7.2: Desialylated T cells bind PNA. ILA1 $CD8^+$ T cell clone was treated with 0.011U of neuraminidase enzyme (from *vibrio cholerae*) as described in section 2.9.2 of Materials and Methods. The FACS histogram shows neuraminidase treated (red peak) and untreated (green peak) ILA1 cells incubated with FITC-conjugated peanut agglutinin (PNA), which binds desialylated but not sialylated glycans.

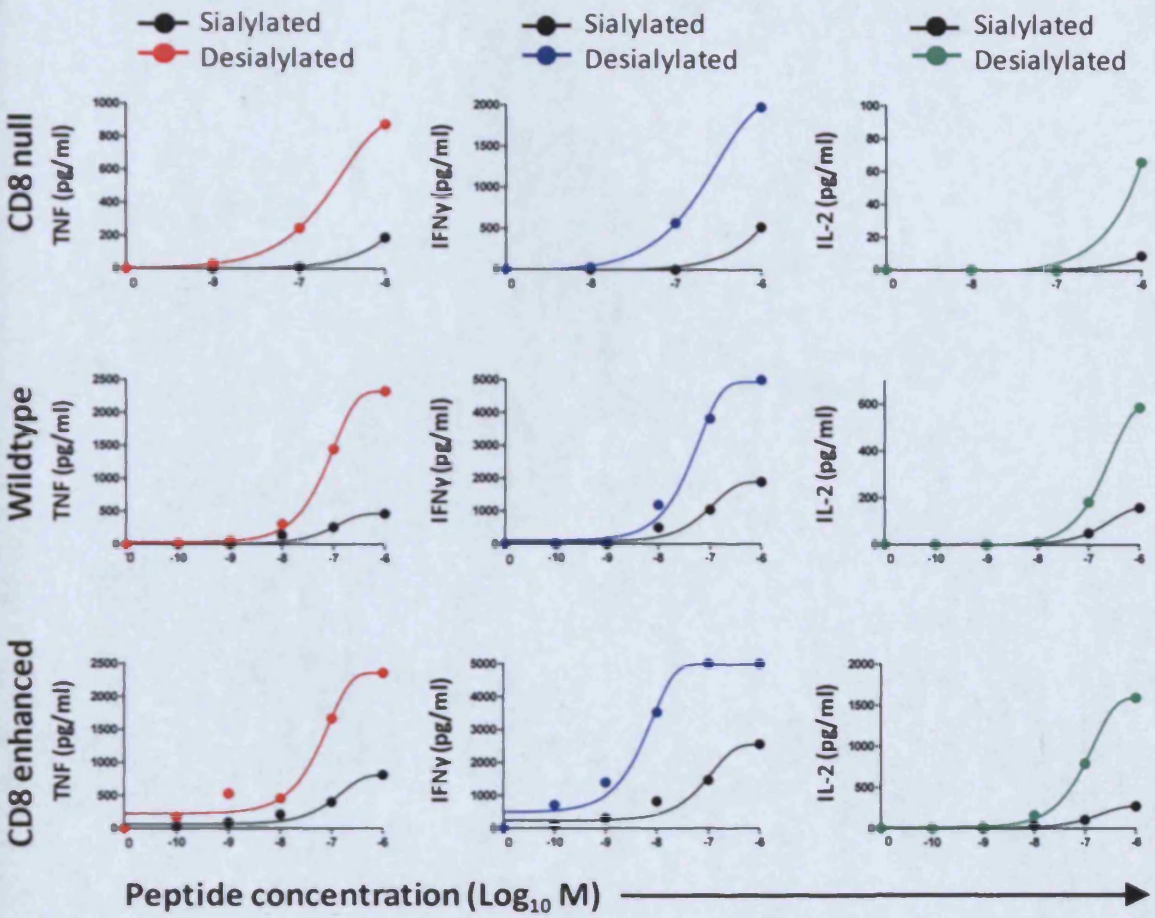

Figure 7.3: Neuraminidase treatment enhances antigen sensitivity of CD8⁺ T cells irrespective of CD8 involvement. Mel13 CD8⁺ T cell clone was incubated with titrated cognate Melan-A_{26-35} (ELAGIGILTV; ELA) peptide-pulsed C1R cells bearing surface HLA A*0201 molecules of three forms: CD8-null 227/8 K/A mutants (top panel), CD8 wildtype/normal (middle panel), or CD8-enhanced Q115E mutants (bottom panel). The Mel13 clone and C1R cells were incubated together for 4 hours at 37°C and the extent of TNF, IFNγ, and IL-2r elease was determined using a cytometric bead array (CBA) kit, recorded by flow cytometry on a FACSCalibur, analysed using FlowJo software and plotted using Prism graphpad software. The coloured data points indicate cytokine release by Mel13 cells that were pre-treated with neuraminidase, while the black data points show cytokine release by untreated cells. Representative data of 2 replicates shown.

lower than from untreated cells, and the strength of the readout signal was enhanced by as much as seven fold for some concentrations of peptide (Figure 7.3). In addition to investigating the effect of desialylation on $CD8^+$ T cell activation with target cells presenting cognate peptide, I examined how neuraminidase treatment influences pMHCI tetramer staining. For this role I decided to use the well characterised ILA system encountered in Chapters 3, 4, and 5. Neuraminidase treated and untreated ILA1 $CD8^+$ T cell clone was stained with HLA A2 tetramers refolded around three cognate ligands displaying a range of affinities for the ILA1 TCR, and a non-cognate ligand to evaluate any concomitant increases in background staining (Figure 7.4). Desialylation of ILA1 $CD8^+$ T cells had the most profound effect on staining with HLA A2 tetramers, presenting the low affinity 5Y ligand, with a two fold increase in MFI. Desialylation also increased the staining of ILA1 $CD8^+$ T cells with ILA index/HLA A2 tetramers. However, no difference in tetramer staining with the high affinity 3G/HLA A2 tetramers was observed between desialylated and sialylated ILA1 $CD8^+$ T cells.

The increase in antigen sensitivity observed on removal of sialic acid in the experiment with Mel13 $CD8^+$ T cells (Figure 7.3) was not affected by differences in CD8 binding. In fact, a substantial increase in antigen sensitivity was still observed even in the absence of a pMHCI/CD8 interaction (227/8 K/A targets). Based on the published data (Daniels et al. 2001; Moody et al. 2001), this finding was unexpected. If the effect of desialylation is observed in the absence of a pMHCI/CD8 interaction I reasoned that this might be apparent with CD8-negative T cells. I therefore decided to examine whether other T cell types, that do not rely on CD8 for antigen recognition, experienced increases in antigen sensitivity on desialylation. A $CD4^+$ T cell line (JF-HA) and clone (Flu2-5) were rendered more sensitive to their cognate antigen, an HLA DR*0101 (HLA DR1 from hereon)-restricted epitope of influenza hemagglutinin $(HA)_{307-319}$; PKYVKQNTLKLAT (PKY), on treatment with neuraminidase (Figure 7.5). Staining of the $CD4^+$ JF-HA T cell line with the PKY/HLA DR1 tetramer (Figure 7.5A) demonstrated how a population of low avidity cells, that is normally undetected by conventional pMHCII tetramer staining methods, becomes 'visible' on desialylation. An improvement in cognate PKY/HLA DR1 tetramer binding by the $CD4^+$ Flu2-5

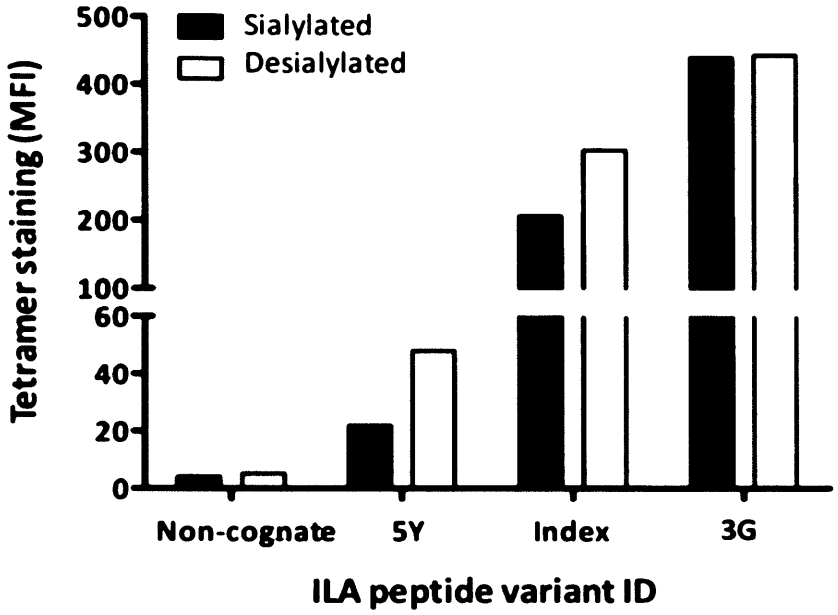

Figure 7.4: Neuraminidase treatment preferentially enhances staining of CD8⁺ T cells with pMHCI tetramers presenting low affinity cognate ligands. 10^5 ILA1 CD8⁺ T cells , either treated with neuraminidase (unfilled bars) or untreated (filled bars), were stained with 10 μg/ml PE-conjugated HLA A2 tetramers refolded around the index ILA peptide (K_D ~ 37 μM), the low affinity ILA altered peptide ligand (APL) 5Y (K_D ~ 242 μM), the high affinity ILA APL 3G (K_D ~ 3.7 μM), and a non-cognate peptide ligand (negative control), for 20 minutes at 37 °C. Data were acquired with a FACSCalibur flow cytometer (BD) and analysed using FlowJo software. The MFI of tetramer staining for each APL was presented in graphical form for ease of comparison. Data are representative of 2 replicates.

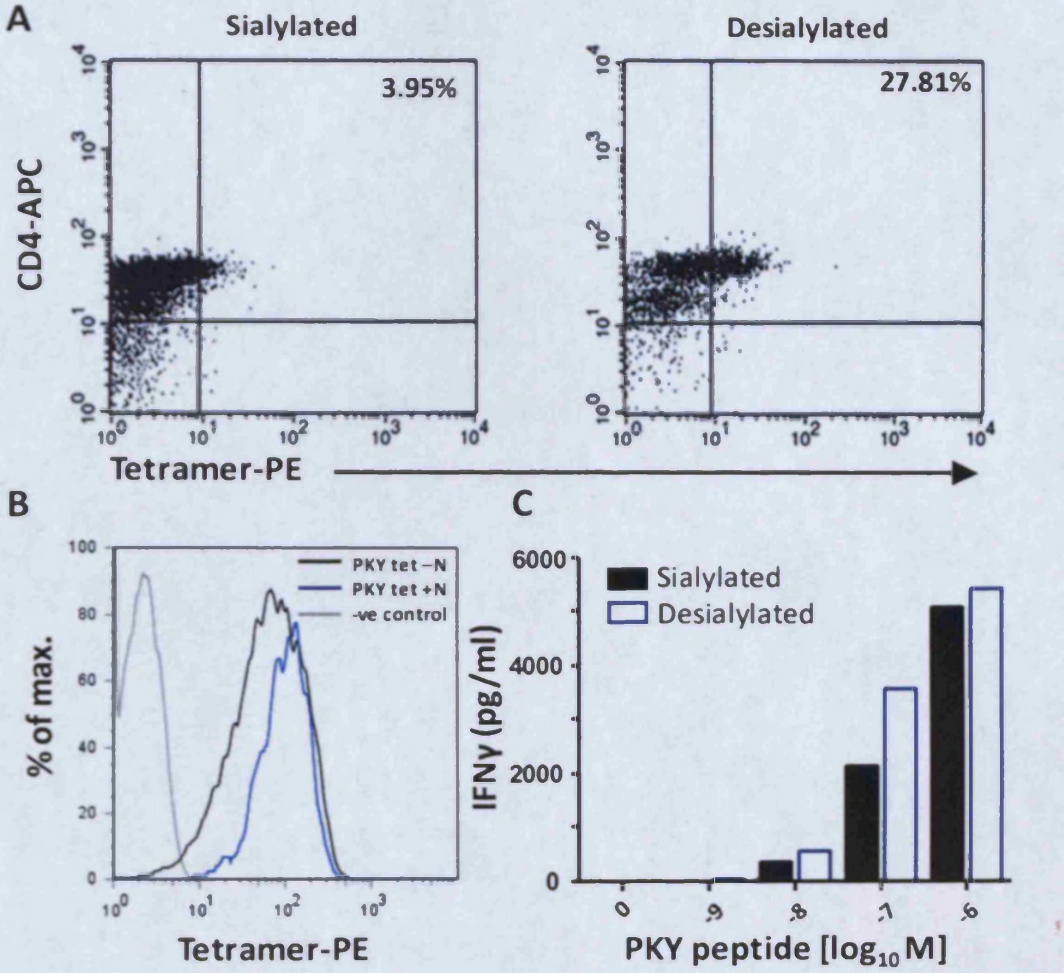

Figure 7.5: CD4⁺ T cells become more sensitive to antigen on desialylation. A. Cognate PKY/HLA DR*0101 tetramer staining of a CD4⁺ T cell line, JF-HA, specific for the influenza hemagglutinin $(HA)_{307-319}$; PKYVKQNTLKLAT (PKY) peptide, after incubation with neuraminidase (right panel) and untreated (left panel). The numbers in upper right quadrants refer to the percentage of tetramer positive T cells. **B.** A cognate PKY/HLA DR*0101 tetramer staining profile of a CD4⁺ T cell clone, Flu2-5, specific for the same peptide as the CD4⁺ T cell JF-HA line (A), in the presence (blue) and absence (black) of neuraminidase (N). **C.** CBA measurement of IFNγ release by the Flu2-5 CD4⁺ T cell clone either treated with neuraminidase (blue unfilled bars) or untreated (black filled bars) on activation with titrated PKY peptide, presented on HLA DR*0101 positive target cells. Data in B and C are representative of 2 separate experiments.

T cell clone was also observed on removal of terminal sialic acid moieties by neuraminidase (Figure 7.5B). This result was important for two reasons. Firstly, it demonstrates that desialylation can improve antigen engagement in the absence of the CD8 coreceptor; and, secondly it restricts the increase in antigen sensitivity to antigen engagement. Neither CD45 nor CD43 are thought to engage antigen. Collectively these statements suggest that the improvement in antigen engagement by desialylated T cells may be due to the direct effects of the TCR.

In accordance with the $CD8^+$ T cell results in Figure 7.3, desialylation of $CD4^+$ T cells also resulted in increased cytokine release (Figure 7.5C). Neuraminidase-treated Flu2-5 $CD4^+$ T cells secreted almost twice as much IFNγ in response to HLA DR1 positive targets cells presenting 10^{-7}M PKY peptide, compared to untreated cells. However, the effect was not as pronounced as for $CD8^+$ T cells, suggesting that the glycosylation of CD8 may still play some role in regulating antigen sensitivity. Neuraminidase treatment also enhanced the recognition of isopentenyl pyrophosphate (IPP) antigen by γδ T cells (Figure 7.6). A γδ T cell line (AJH), and a γδ T cell clone (Bob) showed increased TNF production in response to IPP. We have previously reported that recognition of aminobisphosphonates (nBPs) and IPP by human γδ T cells requires contact with cells of human origin (Green et al. 2004). The activation assays were therefore performed in the presence of C1R cells. The increase in antigen sensitivity was strongest for the AJH γδ line, which showed a two fold increase in cytokine production at 10^{-4}M IPP on desialylation.

In addition to documenting the effect of neuraminidase treatment on T cells by cytometric bead array activation assays and tetramer staining, I looked at how the sialylation status of a T cell impacts on pMHC tetramer association and dissociation rates. Figure 7.7A shows that a neuraminidase-treated Jurkat cell line transduced with the HLA A2-restricted, HIV p17 Gag-derived (amino acids 77–85) antigen SLYNTVATL (SL9)-reactive 868 TCR (introduced in Chapter 6) is able to capture cognate SL9/HLA A2 tetramer from solution at a faster rate than untreated 868 TCR Jurkat transductants. The SL9/HLA A2 tetramer dissociation curves in Figure 7.7B illustrate that desialylated 868 TCR^+ Jurkat cells display a slightly slower

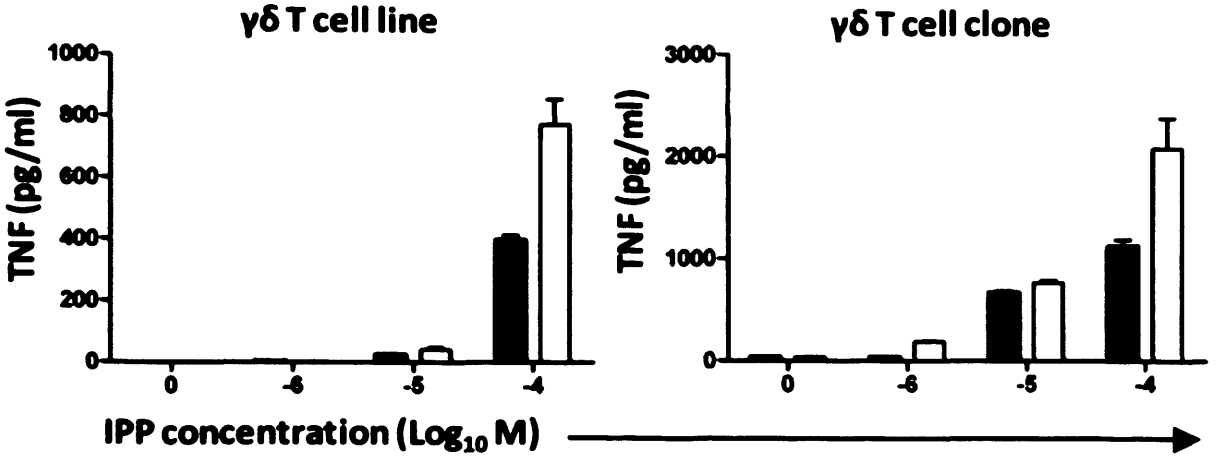

Figure 7.6: Desialylation of γδ T cells enhances their recognition of isopentenyl pyrophosphate (IPP) antigen. Cytometric bead array (CBA) measurement of TNF release by a γδ T cell line, AJH (left panel) and a γδ T cell clone (right panel), in response to titrated IPP antigen and in the presence of C1R cells. Unfilled bars represent γδ T cells treated with the enzyme neuraminidase before assaying. Filled bars refer to untreated γδ T cells. Error bars show s.d. from the mean of two replicates. Data are representative of 2 separate experiments.

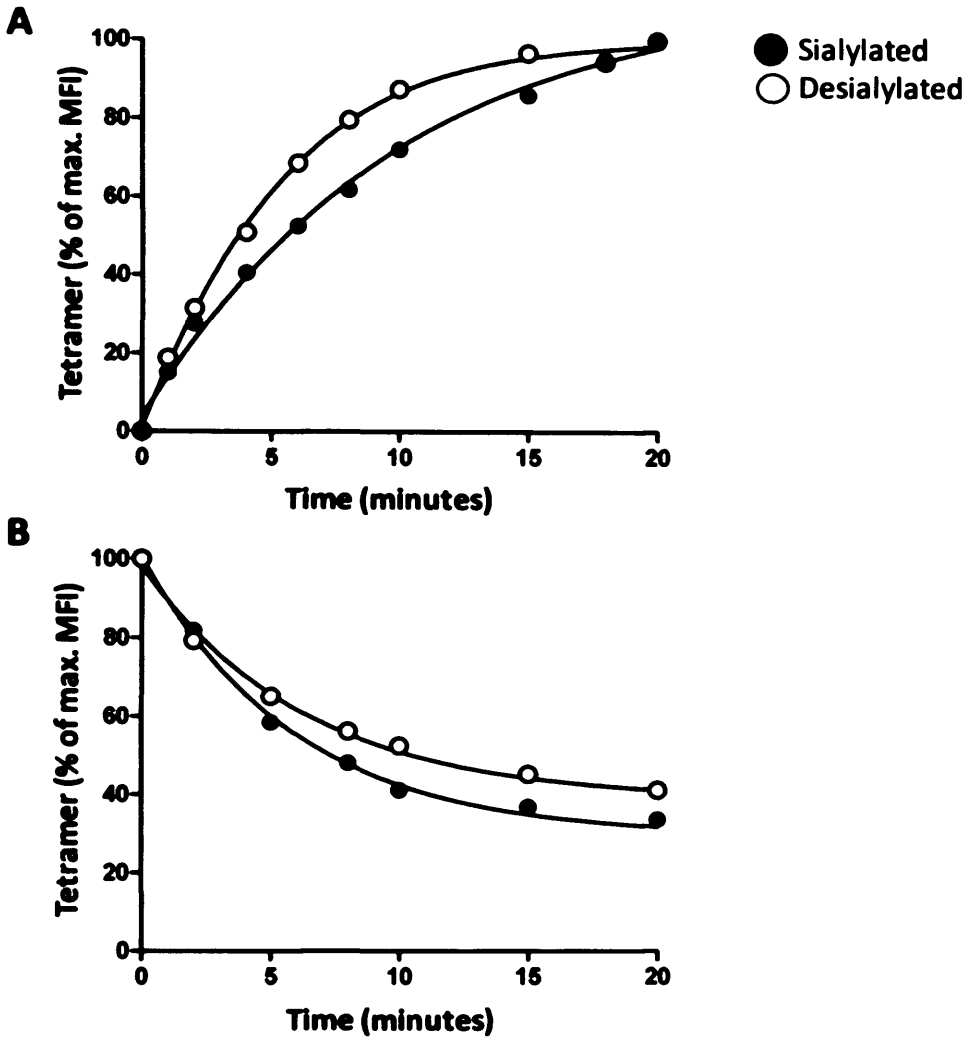

Figure 7.7: Desialylation of 868 TCR-transduced Jurkat cells enhances cognate SL9/HLA A2 tetramer association and dissociation rates. A. Tetramer association curves recorded over a 20 minute period for neuraminidase-treated (white squares) and untreated (black squares) 868 TCR-transduced Jurkat cells, stained with 10 μg/ml SL9/HLA A2 tetramer. **B.** Dissociation curves of SL9/HLA A2 tetramer (10 μg/ml) from sialylated/desialylated 868 TCR-transduced Jurkat cells over a 30 minute time period, in the presence of a competing anti-HLA A2 antibody. Representative data from 2 experiments shown. Assay details can be found in sections 2.8.2 and 2.8.3 of Materials and Methods.

tetramer off-rate than their sialylated counterparts. The difference in tetramer off-rates for the sialylated and desialylated 868 TCR-transduced Jurkat cell subsets appears to be less pronounced than the difference in on-rates.

7.2.2 Desialylation of $CD8^+$ T cells enhances the crossreactivity of their TCRs

The fact that desialylation of T cells enhances their sensitivity to antigen implies that glycosylation may control the ability of T cells to recognize many different antigens, in other words their crossreactivity. To test this hypothesis, ILA1 $CD8^+$ T cells were treated with neuraminidase to remove any surface sialic acid residues and subjected to a 9mer combinatorial peptide library screen. The screen was also performed in parallel with un-manipulated ILA1 cells, which had not undergone neuraminidase treatment. The organisation of the 9mer combinatorial peptide library and the details of the assay are described in section 2.11.2b of Materials and Methods. A comparison of MIP-1β release profiles for both neuraminidase-treated and untreated cell subsets in response to the 9mer peptide mixtures is summarised in Figure 7.8. Although the strongest responses made by desialylated cells (red bars) were observed at the same residue positions as for the sialylated cells (black bars), the magnitude of these responses was higher for the cells that had undergone neuraminidase treatment. In addition, the number of peptide sequences that induced MIP-1β release was greater for desialylated ILA1 cells. The differences in combinatorial library results for the sialylated and desialylated subsets are more clearly illustrated by Figure 7.9. The box summary representation highlights the residues that are preferred by the ILA1 TCR at each position of a 9mer peptide. Each box represents one of the 9 positions in the 9mer peptide, and the letters correspond to the residues that induce a MIP-1β response at each of these positions. Both sialylated (top panel) and desialylated (bottom panel) ILA1 cells show strong preference for amino acids leucine and glycine at positions 1 and 3, as well as the conserved FLH motif present in the index ILA (ILAKFLHWL) peptide at positions 5, 6, and 7, respectively. However, the number of amino acid residues recognised at each position of the screen, and subsequently the overall number of peptides that were recognised by the ILA1 clone was significantly higher for desialylated cells than sialylated cells.

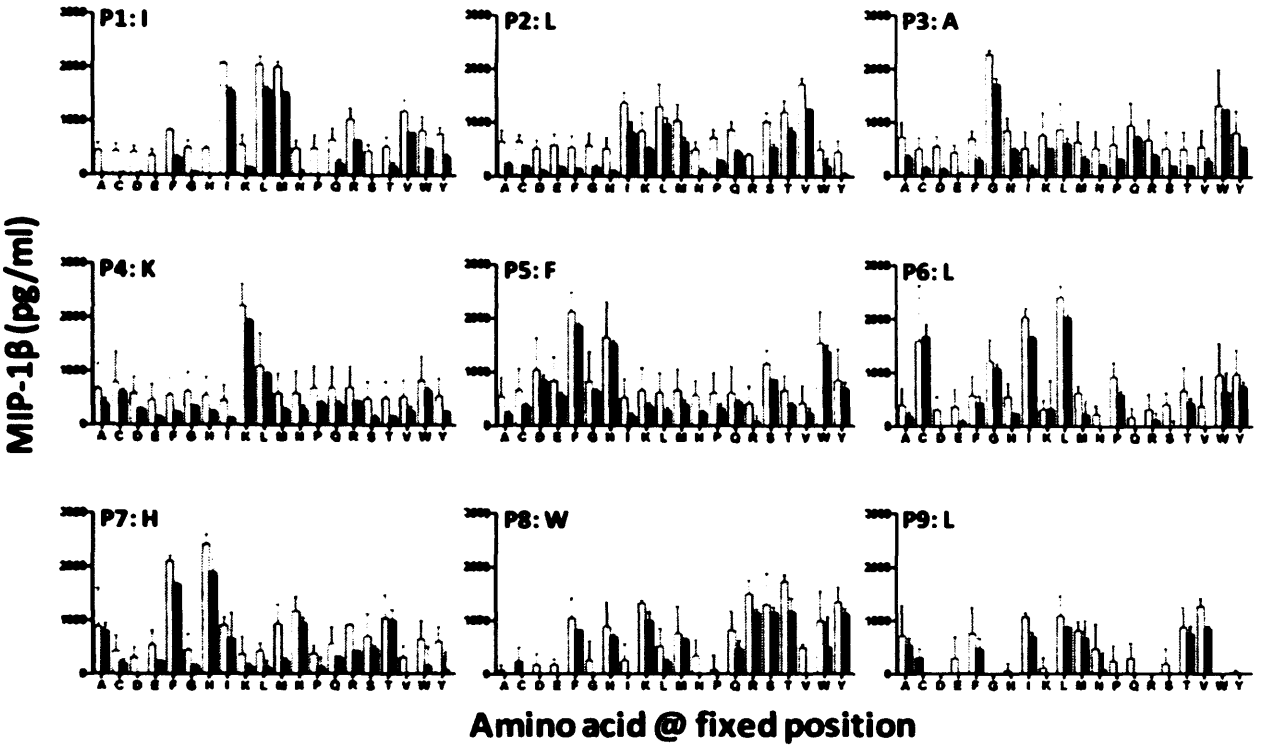

Figure 6: Desialylation of the ILA1 CD8⁺ T cell clone increases the magnitude of responses in a combinatorial peptide library screen. A. The ILA1 clone, either treated (white bars) or untreated (black bars) with neuraminidase enzyme was used to screen a nonamer combinatorial peptide library (CPL). Each graph in the figure represents a scan on a single amino acid position to determine the preference of the ILA1 TCR for a particular amino acid residue at that position. The responses were quantified by measuring the level of MIP-1β release by the ILA1 clone. The position index on the x-axis refers to the single letter amino acid code for the amino acid residue found in the fixed position of each peptide in the mixture. Error bars show s.d. from the mean of two replicates. Representative data from 2 separate experiments shown.

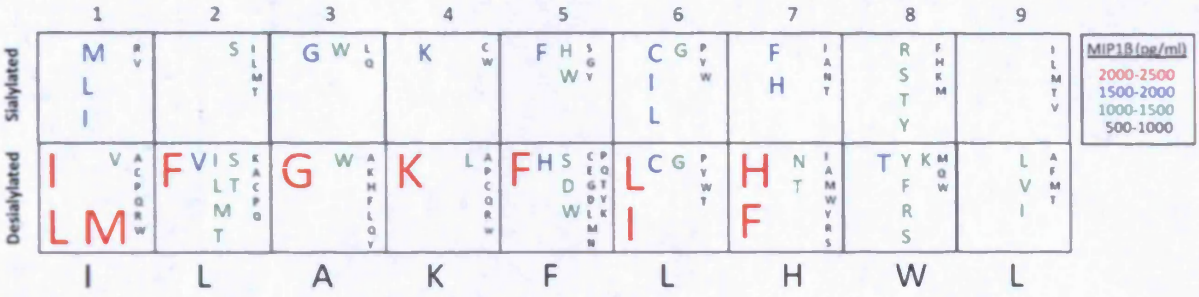

Figure 7.9: Box summary representation of the ILA1 CD8⁺ T cell clone 9mer peptide library screen data (shown in Figure 7.8). The hierarchy of the responses to various residues at each position in the nonamer screen was constructed by categorizing the level of MIP-1β production by the ILA1 clone into 5 distinct bands. MIP-1β responses below 500 pg/ml were excluded from this summary. Each box represents an amino acid position of a nonamer peptide, while the size and colour of the letters within each box indicate the amino acid residues preferred by the ILA1 TCR at that position. The letters underneath the box summaries refer to the residues found in the index peptide (ILAKFLHWL) at that position in the nonamer.

The combinatorial libraries are manufactured in such a way as to ensure that each peptide is present at the same concentration in every mixture. When the peptide mixtures are assayed at 100 μg/ml, the concentration of an individual peptide is $5.3x10^{-14}$M. In order to investigate how the removal of sialic acid from the surface a T cell impacts on recognition of a peptide antigen over a range of concentrations, I used 17 randomly generated peptides of the format XLXKFLXXL (where X refers to an amino acid residue apart from cysteine randomly selected from the 20 available). The leucine anchor residues at positions 2 and 9 were fixed, ensuring that no discrimination between peptides would occur at the level of peptide-MHCI binding. Figure 7.10 illustrates MIP-1β release by sialylated (panel A) and desialylated (panel B) ILA1 cells in response to C1R cells presenting each of the 17 'KFL-fixed' peptides over a range of concentrations. In accordance with the combinatorial peptide library screen results (Figure 7.8), desialylated ILA1 cells were able to recognize a greater number of peptides then sialylated cells.

7.2.3 Silencing of individual conserved N-glycosylation sites present on the 868 TCR does not increase its sensitivity to antigen

In Chapter 6, I described the process of engineering T cells specific for the HLA A2-restricted SL9 antigen derived from HIV-1 (HIV p17 Gag_{77-85}, SLYNTVATL), by transducing Jurkat and primary $CD8^+$ T cells with the 868 TCR. Due to the success of the 868 TCR transduction, I decided to use this system to test the hypothesis that the removal of certain N-glycosylation sites located in the TCR constant region increases its sensitivity to antigen. The N-glycosylation sites in the 868 TCR were located by scanning 868 TCR α and β chain amino acid sequences (Appendix 2 A and B) for N-X-[S/T]-Y (where N denotes an asparagine, S/T denote serine/threonine, and X and Y represent any amino acid other than proline) motifs using the ExPASy (Prosite) software. The scan retrieved seven N-glycosylation motifs; two in the 868 TCR β chain, and five in the α chain (Appendix 2). Figure 7.11 highlights the positions of these glycosylation motifs on a human αβ TCR. To abrogate glycan attachment at these sites, I designed a set of primers to mutate the asparagine (N) residues in the N-X-[S/T]-Y N-glycosylation sequence to glutamine (Q) (Appendix 3).

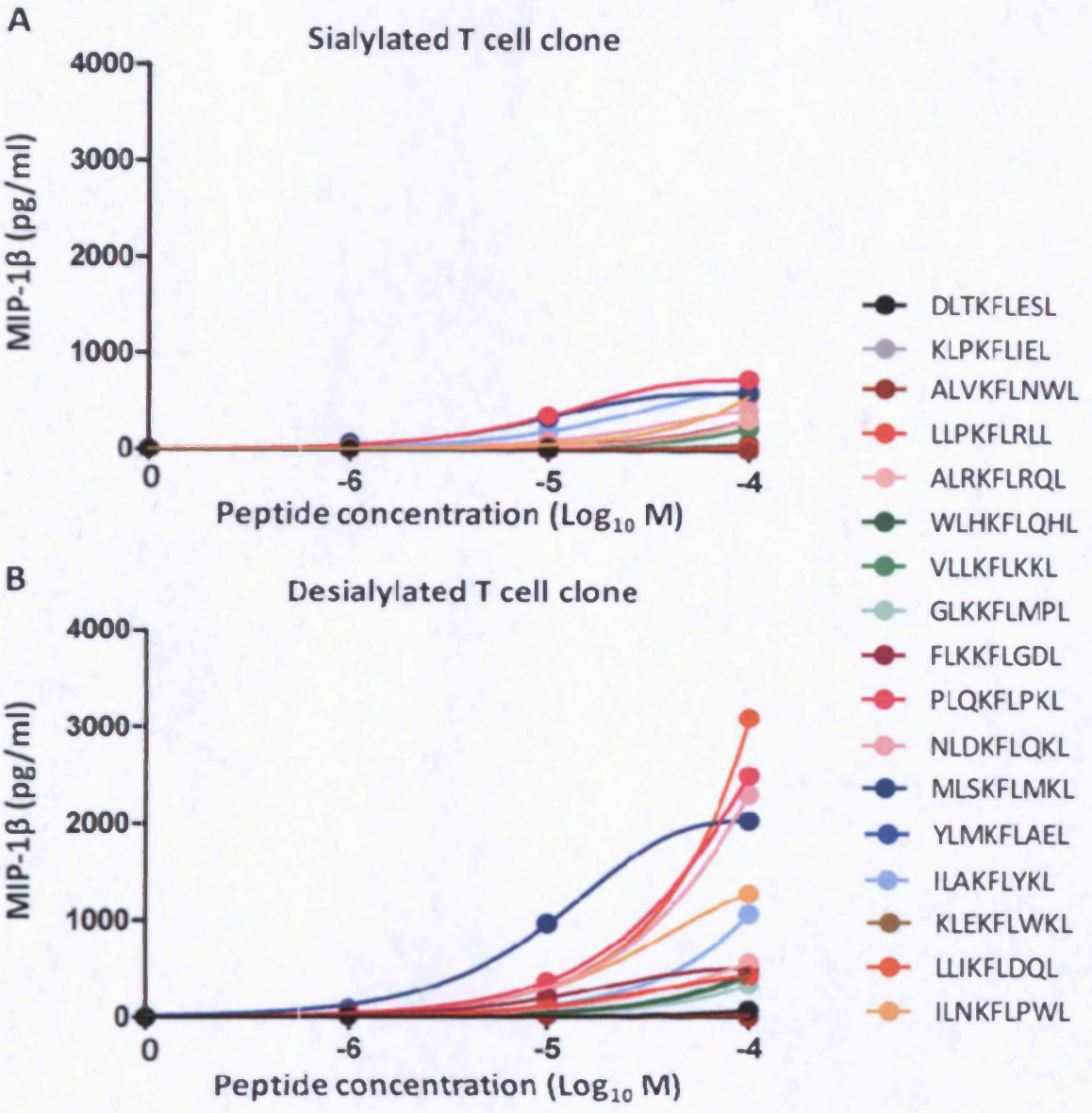

Figure 7.10: Titration profiles for 17 randomly generated ILA1 TCR-specific XLXKFLXXL peptides conducted with sialylated and desialylated ILA1 CD8⁺ T cell clone. A shows MIP-1β production by sialylated (neuraminidase untreated) ILA1 CD8⁺ T cell clone. B shows MIP-1β production by desialylated (neuramini-dase treated) ILA1 CD8⁺ T cell clone. The peptides assayed here were randomly selected from all the possible combinations of amino acids found in the 9mer peptide library. The leucine anchor residues at positions 2 and 9, and central conserved KFL motif were fixed. All other positions (shown as X) were varied. For cell numbers and assay details refer to section 2.11.2b of Materials and Methods.

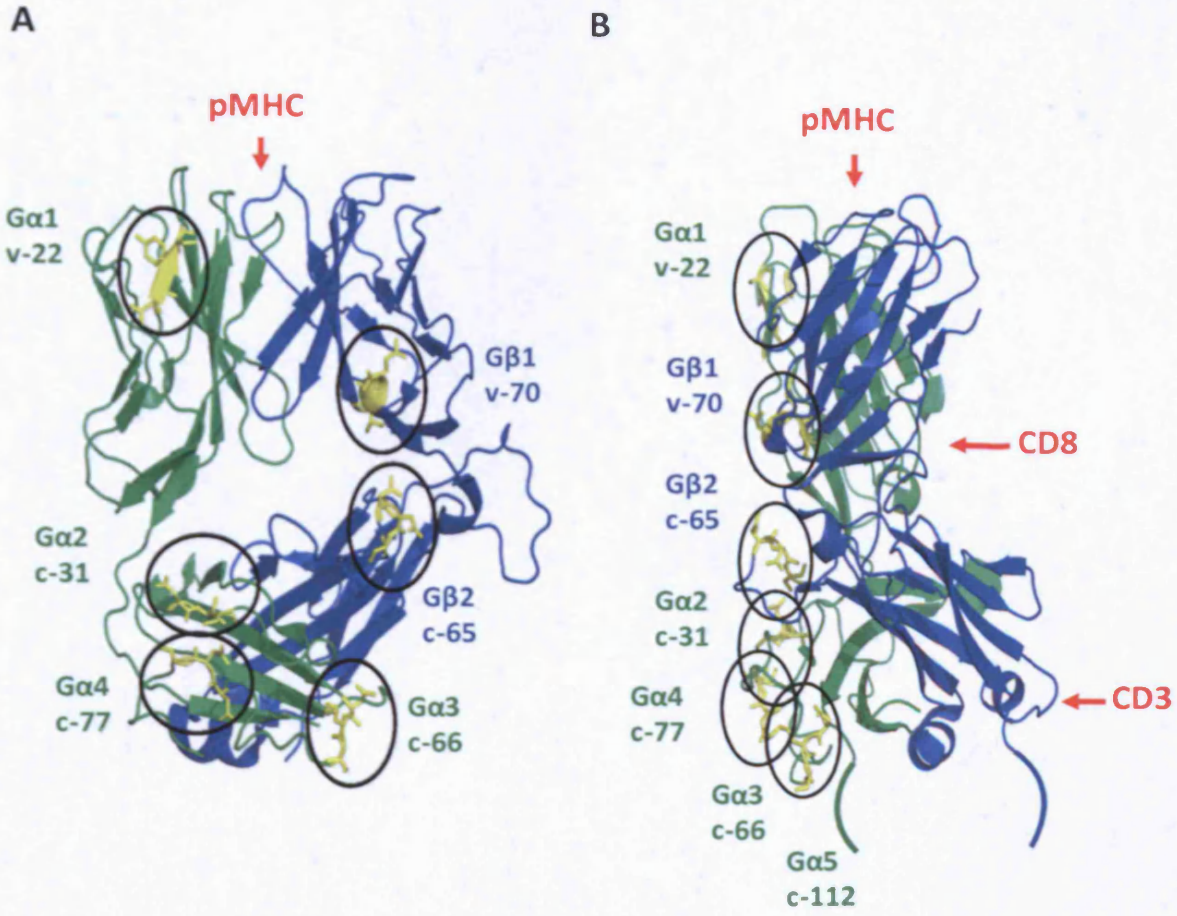

Figure 7.11: The front (A) and side (B) views of a human αβ TCR with highlighted N-glycosylation motifs. A total of seven sites of glycan attachment are highlighted (yellow and circled): two in the beta chain (blue), and five in the alpha chain (green). The labels next to each glycosylation motif denote the glycosylation mutant ID, the residue number of the asparagine that was mutated to silence the glycosylation site, and whether this residue is located in the variable (v) or constant domain (c) of the TCR (see Appendix 3). The α5 glycosylation site is not shown here as it is located in the stalk region of the TCR alpha chain, and is thus absent from the crystal structure. The approximate contract regions for the pMHC, CD8 and CD3 are indicated by the red arrows.

Glutamine was selected for the substitutions because its physico-chemical properties closely resemble those of asparagine, ensuring that the structure of the TCR was not altered by the amino acid substitutions themselves. The conditions for the N/Q site directed mutagenesis (SDM) of the glycosylation sites is described in section 2.5.1f of Materials and Methods. The SDM for each of the seven glycosylation TCR mutants was performed in the pUC (See Figure 6.5 of Chapter 6) vector background, since the sheer size (~9000 basepairs, without the insert) and looped secondary structure of the lentiviral vector made it unsuitable for this technique. The success of SDM was verified by automated sequencing of each of the SL9-specific glycosylation mutant TCR α and β chains, and aligning these with the 868 TCR wild type sequence (Appendix 4).

Once I was satisfied that the SDM of each glycosylation site had worked, the α or β TCR chains that contained a mutation were excised from the pUC vector and slotted into the Lenti-SxW lentiviral vector (Figure 6.6 of Chapter 6) in place of the existing wildtype α or β TCR chain.

Experiments with Jurkat transductants:

The resultant lentiviral constructs were used to make lentiviral supernatants with the methodology developed in Chapter 6 and described in section 2.6 of Materials and Methods. The multiplicity of infection (MOI) of each lentiviral preparation was determined by titering the viral supernatants on TCR negative Jurkat cells and monitoring the surface levels of CD3 expression with addition of virus using an anti-CD3 antibody (Figure 7.12 A). From the MOIs determined using these viral titration curves, volumes of viral supernatant containing the same number of infectious particles were calculated for each 868 TCR mutant. This ensured that the levels of surface TCR expression on transduced cells did not vary with each viral preparation, enabling a direct comparison between the antigen binding properties of the 868 TCR glycosylation mutants. Figure 7.12 B shows the differences in cognate SL9/HLA A2 tetramer staining levels of Jurkat cells transduced with lentiviruses (of equal MOIs) encoding the wildtype 868 TCR and seven 868 TCR glycosylation mutants. Lentiviral supernatants encoding glycosylation mutants Gβ2 and Gα5 did not lead to surface

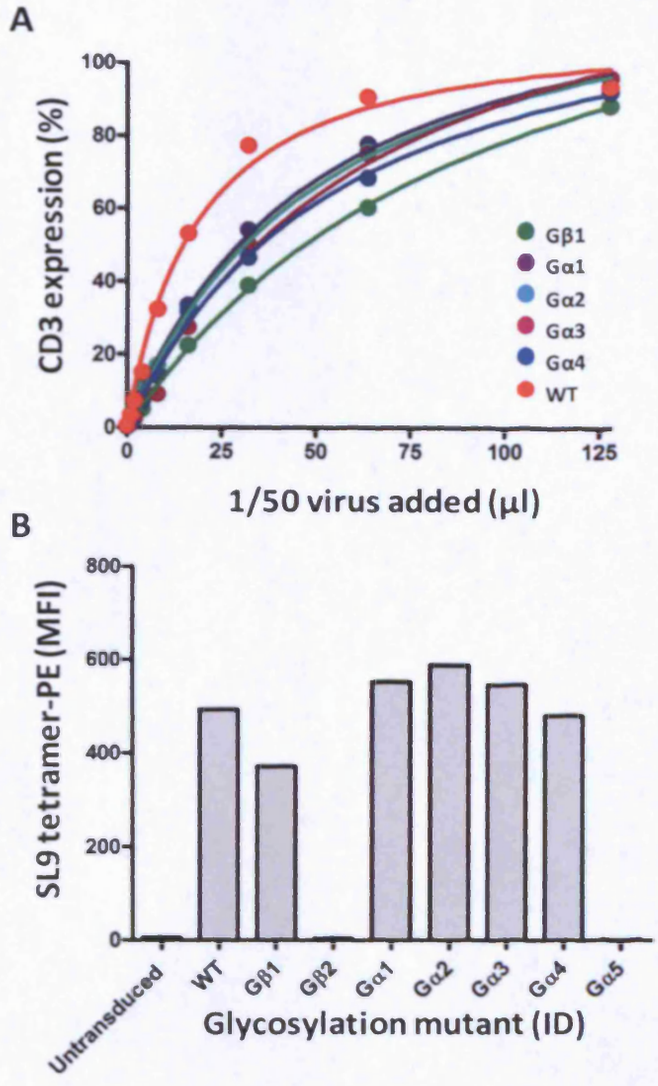

Figure 7.12: Testing transduction of Jurkat TCR-negative T cell line with 868 TCR glycosylation mutants. A. Titering of concentrated (but 1/50 diluted) lentiviral supernatant encoding each of the 868 wildtype (WT) TCR and the 868 TCR glycosylation mutants (Gβ1, Gβ2, Gα1, Gα2, Gα3, Gα4, and Gα5) on $2x10^5$ TCR negative Jurkat cells. Surface TCR expression with each addition of virus was determined by flow cytometry, with anti-CD3 antibody staining 72 hours post infection. **B.** SL9/HLA A2 tetramer staining of Jurkat cells transduced with lentivirus preparations of equal multiplicities of infection (MOIs, see section 2.6.4 of Materials and Methods), expressing the full panel of 868 TCR glycosylation mutants. No anti-CD3 or SL9 tetramer staining was detected for Jurkat cells transduced with Gβ2 and Gα5 glycosylation mutants. Representative data of >2 separate experiments shown.

TCR expression. To rule out the possibility that this was a result of faulty viral production, the procedure was repeated several times, each time with the same conclusion. It is therefore highly likely that eliminating the glycosylation motifs at these sites interferes with the stable cell surface expression of the TCR. In view of this, Gβ2 and Gα5 mutants were dropped from further investigation. The differences in SL9 tetramer staining for Jurkat cells transduced with the other 868 TCR glycosylation mutants were not immense. I therefore decided to study the TCR/pMHCI binding kinetics for each 868 TCR transductant in more detail by performing tetramer association and dissociation assays. Measuring tetramer on- and off-rates can reveal differences in TCR affinity that may not be apparent by simply examining steady-state mean fluorescence intensity after a typical 30 minute stain at physiological temperatures. Figure 7.13 depicts SL9 tetramer association and dissociation curves conducted with Jurkat cells transduced with the 868 TCR glycosylation variants. Unfortunately, the Gα4 variant was omitted from this experiment due to poor growth of the transduced cells. Although there was some increase in tetramer association rates for all the glycosylation mutants compared to WT, Gα2 and Gα3 displayed the highest rates. Their tetramer dissociation rates were not substantially dissimilar to that of WT 868 TCR-transduced Jurkat cells. The increase in tetramer on-rates observed with Gα2 and Gα3 glycosylation mutants, however, gave hope that this increase in antigen sensitivity might correlate with increased functional activity, as reported in the next section. I therefore proceeded to examine TCR-induced functional responses.

Experiments with primary CD8⁺ T cell transductants:

As mentioned in the previous paragraph, no substantial increase in SL9 tetramer staining (above MFI of wildtype 868 TCR transductant) level was observed for any of the glycosylation mutants. A possible reason is that Jurkat cells do not express the CD8 coreceptor, which is a key molecule implicated in TCR-antigen recognition. Amongst its various roles, CD8 stabilises the TCR/pMHCI interaction by approximately ~2 fold (Wooldridge et al. 2005). It is therefore possible that the differences in pMHCI tetramer staining between the wildtype 868 TCR and the glycosylation mutants would become more apparent if these TCRs were to be expressed on $CD8^+$ T cells. A further reason for using

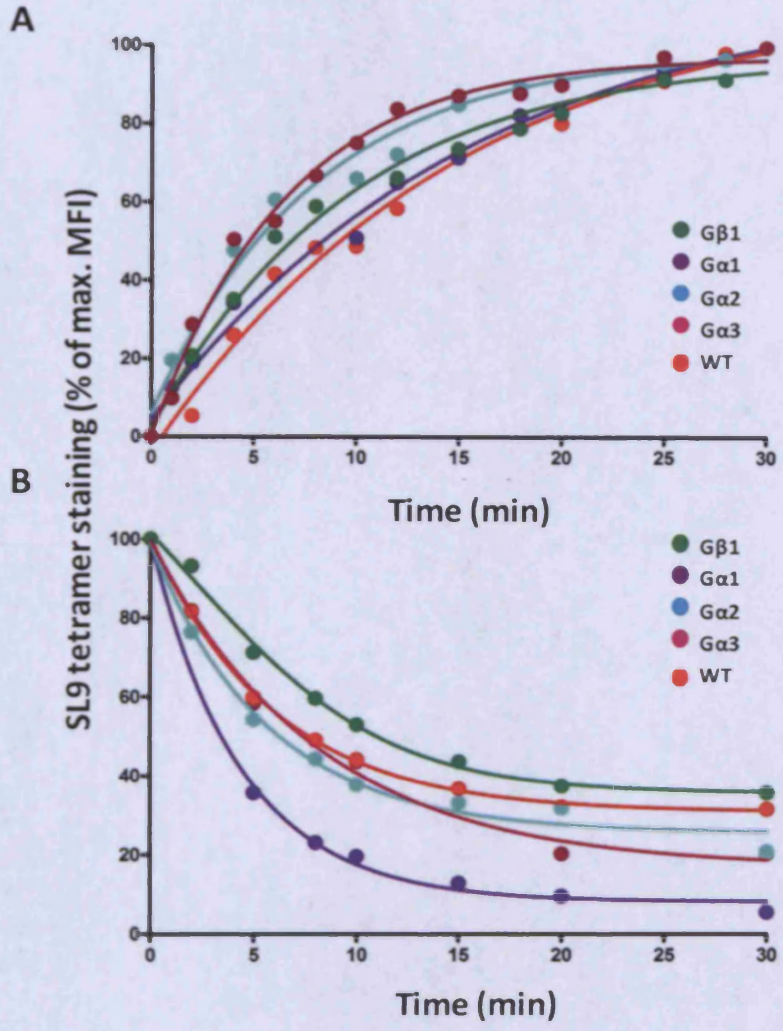

Figure 7.13: SL9/HLA A2 tetramer association and dissociation rates for Jurkat T cells transduced with the 868 TCR and 868 TCR glycosylation mutants. A shows % maximal binding over 30 min for the various 868 TCR-transduced Jurkat T cells stained with 10 μg/ml SLYNTVATL index MHC tetramer. **B.** Dissociation curves performed with same concentration of SL9/HLA A2 tetramer as in A, from 868 TCR $CD8^+$ T cell transductants over 30 min, in the presence of a competing anti-HLA A2 antibody. The assays were performed with 95-100% pure 868 TCR-transductants, and representative data are shown here. The protocols for pMHC tetramer association and dissociation assays can be found in sections 2.8.2 and 2.8.3 of Materials and Methods. Representative data of 2 separate experiments shown.

primary $CD8^+$ T cells as targets for lentiviral transduction is that, unlike Jurkat cells, these T cells are capable of eliciting a plethora of effector functions and cytotoxicity on stimulation with cognate antigen. Lentiviral transduction of polyclonal primary $CD8^+$ T cells (MACS-sorted from fresh PBMC) was previously described in Chapter 6 and further details can be found in section 2.6.3 of Materials and Methods. A high degree of transduction efficiency (~90%) was generally achieved when each of the 868 TCR-encoding lentiviruses was used to infect primary $CD8^+$ T cells (Figure 7.14). SL9/HLA A2 tetramer staining of these cells (Figure 7.15) revealed a similar pattern of MFIs as observed with transduced Jurkat cells (Figure 7.12 B). Again, although the Gα2 mutant displayed the highest level of SL9 tetramer staining, this was not substantially greater than the MFI for the wildtype 868 TCR-transduced cells. As demonstrated by the exceptionally high tetramer staining MFIs in Figure 7.15, the interaction between the 868 TCR and its cognate SL9/HLA A2 tetramer (in the presence of CD8) is already of very high affinity. As a consequence, any increase in TCR affinity, which may be afforded by removal of a particular glycosylation site may not manifest itself by means of tetramer staining. In view of this, I decided to look for any apparent functional differences between the transductants. After all, even if removal of certain glycosylation sites translated into increased pMHCI tetramer binding, proof that these cells performed better in target cell recognition and elimination than wildtype transductants would be required to justify their use in adoptive transfer therapy. To this end, I examined the functionality of the $CD8^+$ T cells transduced with the variant 868 TCRs in activation assays by using two readouts: i) release of MIP-1β cytokine in response to target cells presenting the SL9 peptide, detected using a MIP-1β ELISA (Figure 7.16A); and, ii) killing of SL9 peptide-pulsed target cells, measured using the FATAL assay (Figure 7.16B). Although, all 868 TCR transductants exhibited highly specific MIP-1β release and cytotoxicity in response to target cells presenting the cognate SL9 peptide, none of the glycosylation mutants performed substantially better than the wildtype 868 TCR.

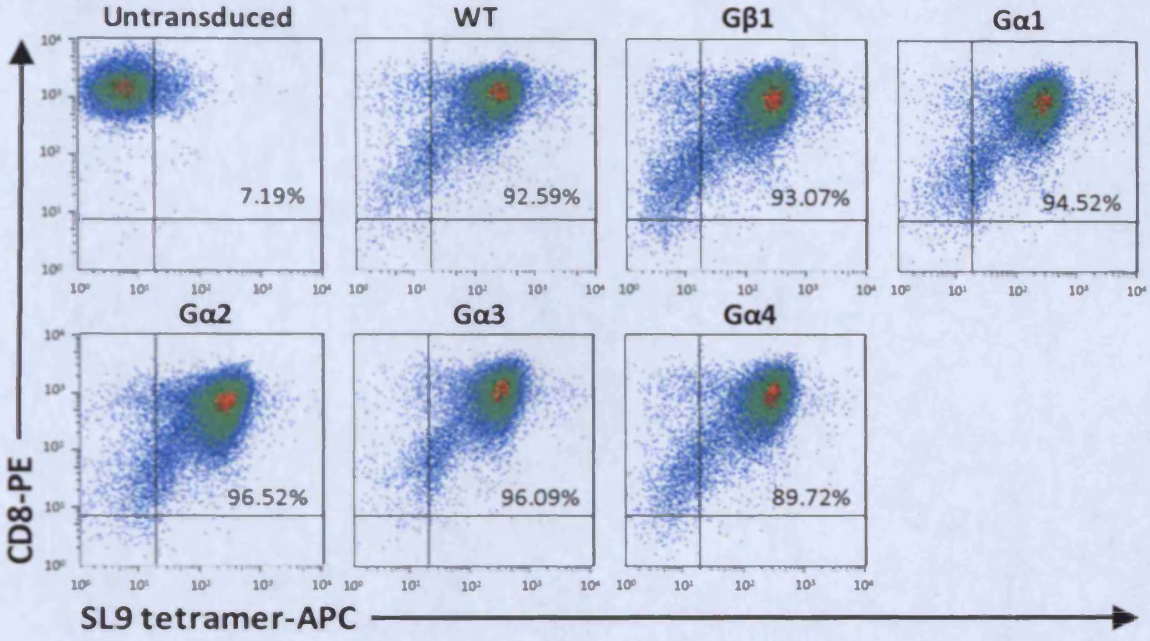

Figure 7.14: Transduction of polyclonal CD8⁺ T cells with the 868 TCR and 868 glycosylation mutant TCRs. 10^6 MACS-sorted polyclonal CD8⁺ T cells were activated with anti-CD3 and anti-CD28 antibody-coated microbeads prior to infection with 1ml of concentrated lentiviral supernatant, encoding the wildtype (WT) 868 TCR and five 868 TCR glycosylation mutants. Untransduced cells, and CD8⁺ T cells transduced with the 868 TCR and the following glycosylation mutants Gβ1, Gα1, Gα2, Gα3, and Gα4 were stained with cognate SL9/HLA A2 tetramer 72 hours post infection. The efficiency of lentiviral transduction was determined by flow cytometry, and analysed using FlowJo software. The numbers in the upper left quadrants refer to the percentage of CD8⁺ SL9/HLA A2 tetramer⁺ cells.

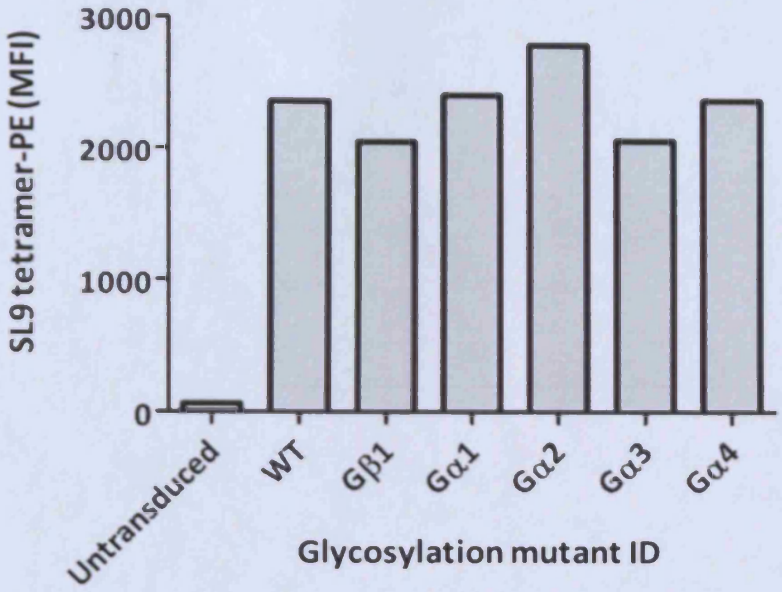

Figure 7.15: SL9/HLA A2 tetramer staining of primary CD8⁺ T cells transduced with lentiviral vectors encoding the 868 TCR and 868 TCR glycosylation mutants. Six lots of 10^6 MACs-sorted CD8⁺ T cells, isolated from the same blood donor were each transduced with 1ml concentrated lentiviral supernatant of similar MOI (determined by titration on Jurkat cells) encoding the 868 TCR and the 868 TCR glycosylation mutants (Gβ1, Gα1, Gα2, Gα3, and Gα4). The transductants were stained with 10 µg/ml SL9/HLA A2 tetramer 72 hours post infection. Untransduced CD8⁺ T cells isolated from the same donor were also stained with SL9 tetramer, as a negative control. Representative data of 2 separate experiments shown.

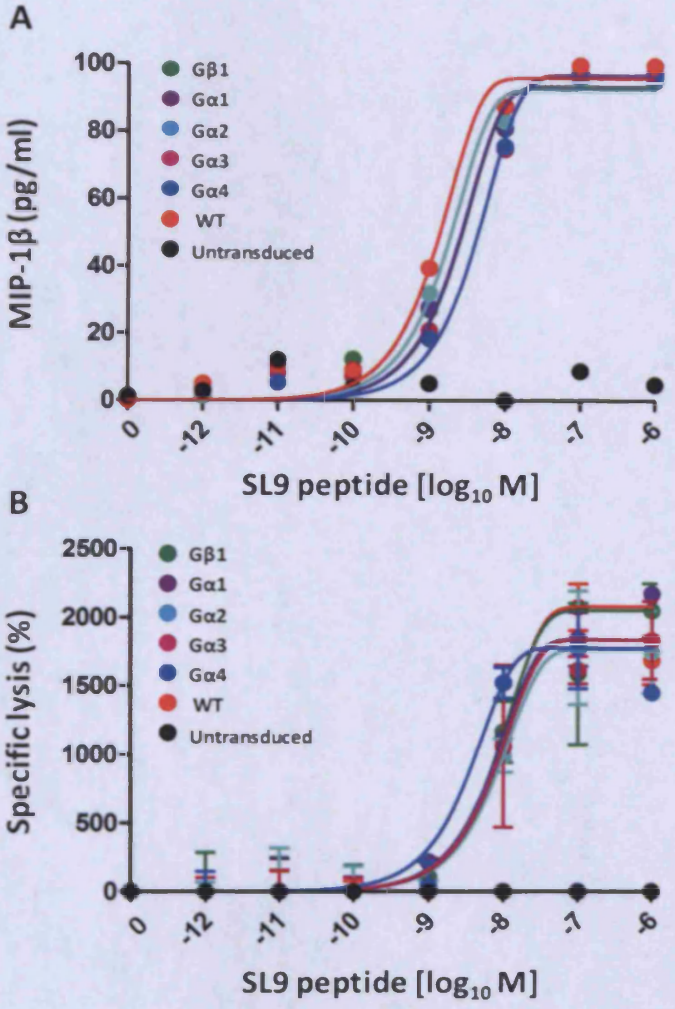

Figure 7.16: Primary CD8⁺ T cells transduced with the 868 TCR and 868 TCR glycosylation mutants are capable of specific activation and killing in response to SL9 peptide-pulsed targets. A. A MIP-1β ELISA conducted with 92-95% SL9/HLA A2 tetramer positive 868 TCR transductants and HLA A2-expressing C1R target cells pulsed with different concentrations of SL9 peptide. **B.** A FATAL killing assay conducted with the same glycosylation mutant 868 TCR transduced cells, SL9 peptide-pulsed HLA A2 positive T2 cell as targets, and unpulsed T2 cells as controls. Untransduced CD8⁺ T cells from the same donor were used as negative controls. Error bars depict s.d. from the mean of 2 replicates. Representative data from 2 separate experiments shown.

7.3 Discussion

Many TCRs implicated in targeting disease-associated antigens such tumour-derived epitopes, self-peptides and viral escape mutants, are weak. This low affinity for cognate antigen makes them suboptimal candidates in adoptive T cell therapy. Various methods to increase TCR affinity in the laboratory, mostly centring around yeast or phage display, have been developed (Li et al. 2005; Dunn et al. 2006; Zhao et al. 2007). However, despite being capable of achieving $>10^6$ fold increases in TCR affinity, these techniques are labour intensive (Li et al. 2005). Furthermore, they target the highly variable CDR loops, and must therefore be individualised for each TCR (Li et al. 2005; Dunn et al. 2006; Zhao et al. 2007). The glycosylation levels of a T cell have previously been reported to affect T cell function (Grigorian et al. 2007; Lau et al. 2007). Moreover, T cells in distinct differentiation states exhibit different levels of glycosylation (immature/mature and naïve/memory) which relate to their sensitivity to antigen (Moody et al. 2001; Pappu et al. 2004). In view of this, I decided to investigate the potential therapeutic benefit of glycosylation as a TCR affinity regulator, initially by studying the effect of desialylation on T cell antigen sensitivity, and later by silencing individual glycosylation sites on a TCR. Since only the invariable constant regions of the TCR are glycosylated, the prospect of increasing TCR affinity by abrogating key glycans could represent a universal method for enhancing T cell antigen sensitivity, irrespective of intrinsic TCR specificity. My key findings are:

i) Desialylated $CD8^+$ T cells are rendered substantially more sensitive to antigen than their sialylated counterparts (Figure 7.3). Importantly, removal of sialic acid from the T cell surface exerts the same effect on antigen recognition irrespective of the strength of the pMHCI/CD8 interaction, which suggests that the co-receptor is not responsible for the majority of this phenomenon.

ii) Desialylation of $CD8^+$ T cells enhances cognate pMHCI tetramer staining. The enhancement of pMHCI tetramer staining afforded by desialylation correlates with TCR/pMHCI affinity (Figure 7.4).

iii) Desialylation of other T cell subsets ($CD4^+$ T cells and γδ T cells) also increases sensitivity to antigen, both in terms of cytokine release and tetramer staining (for $CD4^+$ T cells only) (Figures 7.5 and 7.6).

iv) Removal of terminal sialic acid from the surface of 868 TCR-transduced $CD8^+$ T cells specific for the HLA A2-restricted, HIV-derived SL9 antigen increases cognate SL9/HLA A2 tetramer association, and decreases tetramer dissociation rates (Figure 7.7).

v) Desialylation of a $CD8^+$ T cell clone increases its TCR crossreactivity (Figures 7.8-7.10).

vi) Silencing of individual N-glycosylation sites present in the constant domains of the 868 TCR α and β chains does not correlate with increased antigen sensitivity (Figures 7.11-7.16).

As I was nearing completion of the second part of this study, investigating whether the glycosylation state of a TCR could be used as an affinity regulator, a paper was published by Kuball *et al.* in the *Journal of Experimental Medicine* (Kuball et al. 2009). The title of this publication: 'Increasing functional avidity of TCR-redirected T cells by removing defined N - glycosylation sites in the TCR constant domain' suggested that the authors had found results that were contrary to my own. The authors reported that silencing of one key glycosylation site in the constant domain of two murine and one human anti-tumour TCR resulted in increased sensitivity to cognate antigen, without concomitant increases in non-specific recognition (Kuball et al. 2009). The key mutations reported were: i) an N/Q substitution in the constant domain of the murine TCR alpha chain at position 90 (c-90 mutant); and, ii) an N/Q substitution in the constant domain of the human TCR alpha chain at position 36 (c-36 mutant). Since my own work was carried out on a human TCR, I will focus on how their findings with human WT-1 TCR relate to the 868 TCR. The constant domain of the human TCR alpha chain has three conserved glycosylation motifs: NVS, NKS, and NNS. The TCR affinity-enhancing mutation c-36 involves an N/Q substitution in the first NVS motif, thus silencing this glycosylation site. In the 868 TCR, the c-36 mutation corresponds to the N/Q substitution at position c-31 resulting in the Gα2 mutant (see Appendix 2). The Gα2 mutant did not exhibit a substantially increased sensitivity to antigen either in terms of cognate

tetramer staining (Figures 7.12 and 7.15), or in functional assays (Figure 7.16). Since the work with the c-36 mutant reported by Kuball *et al.* opposed my own claims, I speculated that perhaps our findings did not agree due to the different affinities of the TCRs we experimented on. The 868 TCR that I used in my study has the highest affinity of a natural TCR (K_D ~ 100 nM) ever described using the biophysical technique of choice for such weak protein-protein interactions, SPR {Varela-Rohena, 2008a #882}, whilst the TCRs used in the rival study are both lower affinity anti-tumour TCRs: i) two murine TCRs specific for epitopes of human p53 and MDM2 antigens; and, ii) a human TCR specific for a WT-1-derived epitope (Kuball et al. 2009). It was thus possible that an increase in TCR affinity afforded by deglycosylation of the 868 TCR only corresponded to a minute fraction of its overall affinity.

Meanwhile, in search for new technologies to increase TCR affinity, collaborators at Adaptimmune Ltd. decided to reproduce the affinity-enhancing c-36 mutation (in the conserved NVS glycosylation motif) reported by Kuball *et al*, in the 1G4 TCR, specific for a cancer testis antigen expressed in a wide range of cancers, NY-ESO-$1_{157\text{-}165}$ (SLLMWITQC/HLA A*0201). The 1G4 TCR binds to its cognate antigen with a K_D ~ 32 μM (Zhao et al. 2007). In accordance with my own studies, this mutation did not increase antigen sensitivity of recipient $CD8^+$ T cells after TCR transduction. Thus, the two attempts to repeat the data seen by Kuball *et al,* and reported in just one experiment using a human TCR (Kuball et al. 2009), have both failed to reproduce this promising result.

In summary, I demonstrate that the removal of cell-surface sialic acid increases T cell sensitivity to antigen (irrespective of the CD8 involvement). Further studies focusing on removing complete sugars by mutating conserved N-glycosylation sites on the TCR chains failed to demonstrate that T cells bearing any of these molecules were substantially more sensitive to antigen than those bearing the wildtype TCR. Overall, my studies confirm that the glycosylation of the T cell surface can play a substantial role in T cell sensitivity to cognate antigen. Unfortunately, my attempts to examine the role of individual N-linked glycans on the TCR in this phenomenon failed to reveal a hoped for 'global' solution that could be applied to any TCR being considered in TCR gene therapy and adoptive T cell

transfer therapy. Further studies will be required in order to understand how the glycosylation of T cell surface proteins regulates cellular antigen sensitivity.

Chapter 8

8

MONOCLONAL TCR-REDIRECTED TARGETING OF TUMOUR-TRANSFORMED AND HIV-INFECTED CELLS

8.1 Introduction

In Chapter 6, I described how the transfer of TCR genes, specific for an antigen of choice, into recipient host T cells offers a practical approach for redirecting T cell immunity. This was achieved by transduction of polyclonal $CD8^+$ T cells with a natural (albeit codon-optimised) HIV gag-specific 868 SL9 TCR. The 868 SL9 TCR binds to its cognate antigen with a dissociation constant (K_D) of ≤150 nM as measured by SPR {Varela-Rohena, 2008a #882}. As a result, this TCR binds its antigen with the highest affinity recorded to date for a natural TCR. However, using natural TCR genes is not always a viable option for TCR gene therapy. For instance, the vast majority of natural anti-tumour TCRs exhibit too weak an affinity for effective tumour eradication, whilst many natural anti-viral TCRs are inefficient at recognising viral escape mutants. The advancement of soluble TCR technologies (Molloy et al. 2005), to which my colleague Jonathan Boulter made a tremendous contribution (Boulter et al. 2003; Li et al. 2005), has revolutionised T cell immunotherapy. The transduction of T cells with affinity-enhanced TCRs generated by soluble TCR technologies has the potential to dramatically improve T cell-antigen recognition in a setting where naturally occurring TCRs would fail. In addition to using soluble TCR technology for advancing the success of TCR gene transfer therapy, soluble TCRs can themselves act as therapeutic agents, bypassing the need for laborious and costly cell culture systems. In this chapter, I evaluate the therapeutic potential of a novel class of soluble TCR reagents called Immune mobilising monoclonal TCRs Against Cancer/Virus (ImmTAC/Vs), targeting common cancer and HIV epitopes, respectively.

8.1.1 Soluble antibody- and TCR-based immunotherapies

The adaptive immune response is equipped with two main types of antigen-specific molecules: antibodies and TCRs. Antibodies recognise non-self aspects of circulating and cell-surface proteins, whereas αβTCRs monitor cells for the surface presentation of peptides complexed with MHC molecules (Chaplin 2010). Both of these immune receptors offer a unique potential for novel, highly specific, targeted therapeutics. Kohler and Miller were amongst the first to successfully harness the therapeutic potential of antibodies, and were

awarded a joint Nobel Prize in 1984 for their work. They developed a technique to generate monoclonal antibodies (mAbs) against any given antigen by fusing a line of myeloma cells, which exhibited impaired antibody production, with healthy antibody-producing B cells and successfully selected the fused hybridoma cells (Kohler et al. 1975). 35 years on, mAbs and their derivatives are the fastest growing class of therapeutic molecules, with more than 30 mAb products currently registered as approved drugs and hundreds being tested in clinical trials (Brekke et al. 2003; Casadevall et al. 2004; An 2010; Nelson et al. 2010). There are three categories of antibodies generated for use in therapeutics: i) 'naked' mAbs; ii) conjugated mAbs; and, iii) bi-specific mAbs.

i) 'Naked' mAbs:

'Naked' antibodies function as therapeutic agents by eliciting an antibody-dependent cell-mediated cytotoxicity (ADCC), whereby effector cells, primarily NK cells but also macrophages, lyse target cells that have been bound by specific mAbs by engaging the Fc portion of a mAb by their Fc receptors (most commonly CD16/FcγRIII) (Clynes et al. 2000).

ii) Conjugated mAbs:

In oncology, conjugated mAbs have been developed to deliver various 'payloads' to the target tumour cells *in vivo*, effectively acting like 'magic bullets'. The payloads are designed to enhance the ADCC process by inducing toxicity via agents such as cytotoxic drugs, prodrugs, or radioisotypes (Sievers et al. 2001; Wiseman et al. 2002; von Mehren et al. 2003). These antibody-drug conjugates (immuno-conjugates) are composed of a recombinant antibody covalently bound via a synthetic linker to a cytotoxic agent (Chari 2008). The main objective of immuno-conjugates is to combine the pharmacological potency of the cytotoxic drug and the high specificity of mAbs for tumour-associated antigen targets. The incorporation of anti-neoplastic drugs into mAb-based immunotherapy has demonstrated their ability to kill cancer cells (Bailly, 2009). However, the success of such immuno-conjugates as therapeutic molecules has been limited compared to 'naked' mAb therapies (Haeuw et al., 2009). To date, only one drug, namely gemtuzumab ozogamicin (Mylotarg; anti-CD33 mAb conjugated to calicheamycin, Pfizer/Wyeth) has been approved by the FDA in 2000 for the treatment of patients with acute myeloid leukaemia

(AML) (Polson et al. 2009). Shortly after being given the 'go ahead' by the FDA, gemtuzumab ozogamicin was voluntarily withdrawn from distribution. The reasons for the withdrawal included high levels of off-target toxicity due to protease-mediated degradation of the linker joining the mAb to the cytotoxic drug. Efforts are currently being made to improve both the antibody function (by enhancing the affinity and specificity of the Fv antibody portions) and limiting the off-target toxicity of the cytotoxic conjugates (for example by improving the stability of linkers so that their hydrolysis only occurs within the target cell cytoplasm) (Junutula et al. 2008; Beck et al. 2010).

iii) Bi-specific mAbs:

An alternative and increasingly powerful approach is to harness the high cytotoxic potential of T cells through the use of T cell-engaging bi-specific antibodies (Clynes et al. 2000; Cartron et al. 2002; Muller et al. 2007). Conventional antibodies lack the ability to recruit T cells because these cells are not equipped with Fcγ receptors. T cell-engaging bi-specific mAbs have been designed to target a desired antigen with one binding site and polyclonally activate T cells via the CD3 complex with the other binding site (Withoff et al. 2001; Wolf et al. 2005). Amongst this class of mAbs, the most successful therapeutic candidates are Bi-specific T cell Engaging (BiTE) antibodies (Wolf et al. 2005; Baeuerle et al. 2009). The BiTE construct blinatumomab (MT103), which has a dual specificity for CD19 and CD3 molecules, represents the most advanced bi-specific antibody to date (Loffler et al. 2000; Bargou et al. 2008). Blinatumomab has the ability to elicit lysis of tumour cells and has shown promising results in Phase I (non-Hodgkin's lymphoma) and Phase II (acute lymphoblastic leukaemia, ALL) clinical trials by instigating $CD3^+$ T cells to lyse $CD19^+$ lymphoma and leukaemia cells (Bargou et al. 2008; Baeuerle et al. 2009; Nagorsen et al. 2009). The enormous potency difference between BiTE antibody blinatumomab and a conventional antibody may be mainly due to two factors. Firstly, while a conventional mAb engages NK cells by binding myriads of Fc receptors, a BiTE antibody can activate cytotoxic $CD8^+$ T cells by engaging very few CD3 molecules. Secondly, cytotoxic T cells exhibit a higher lytic potential and serial mode of lysis (engaged by BiTE antibodies) than NK cells triggered by conventional mAbs (Bargou et al. 2008). Taking into consideration that normal B cells also express CD19, it is

encouraging that blinatumomab has thus far exhibited minimal side effects, at most resembling flu-like symptoms.

Despite showing great promise in certain situations, the success of therapeutic mAbs is limited by the nature of antigens that antibodies are designed to recognise. The majority of therapeutic antibodies target intact cell-surface proteins (Figure 8.1 and (Chaplin 2010)), the likes of which represent only a small fraction of the total antigen repertoire that distinguishes tumours and virally infected cells from normal cells. These tumour-associated and viral antigens are intracellular and are only displayed on the surface of cells after being processed into peptides and complexed with MHC molecules (Davis et al. 1998; Rudolph et al. 2006; Colf et al. 2007). Peptide antigens presented in the context of MHC class I (MHCI) are of particular interest for targeting applications because they are derived from the total pool of endogenously expressed proteins within a given cell. A number of attempts have been made to tap into this vast resource of disease-associated antigens by developing mAbs against various peptide-MHCI complexes. Wittman *et al.* succeeded in generating a murine IgG2a mAb called 3.2G1, capable of recognising the tumour-associated GVL peptide (GVLPALPQV) derived from human chorionic gonadotropin beta (CGB) presented in the context of HLA A2 (Wittman et al. 2006). The 3.2G1 mAb was able to recognise the endogenously-processed GVL/HLA A2 complex with TCR-like specificity. They designated this class of antibodies as TCR mimics (TCRm) to reflect this role (Wittman et al. 2006). Impressively, the 3.2G1 TCRm exhibited Ab-dependent cellular cytotoxicity of a human breast carcinoma line known to express the GVL antigen *in vitro*, and inhibited *in vivo* tumour implantation and growth in mice (Wittman et al. 2006). However, while this study elegantly demonstrates that generation of mAbs targeting peptide-MHC complexes is possible, it remains very difficult and to this day only a handful of TCRm Abs exist. In contrast to antibodies, TCRs are specifically designed to recognise endogenously processed peptides presented on the cell surface in the context of MHC (Figure 8.1 and (Davis et al. 1998; Rudolph et al. 2006; Colf et al. 2007)), making this type of antigen ideal for soluble TCR targeting. Like mAbs, soluble TCRs can now be engineered to deliver 'pay loads' such as radioisotopes, toxins or immunomodulatory molecules to their targets. In one of the earliest successful soluble TCR immunotherapy studies, Card *et al.* reported the production of a

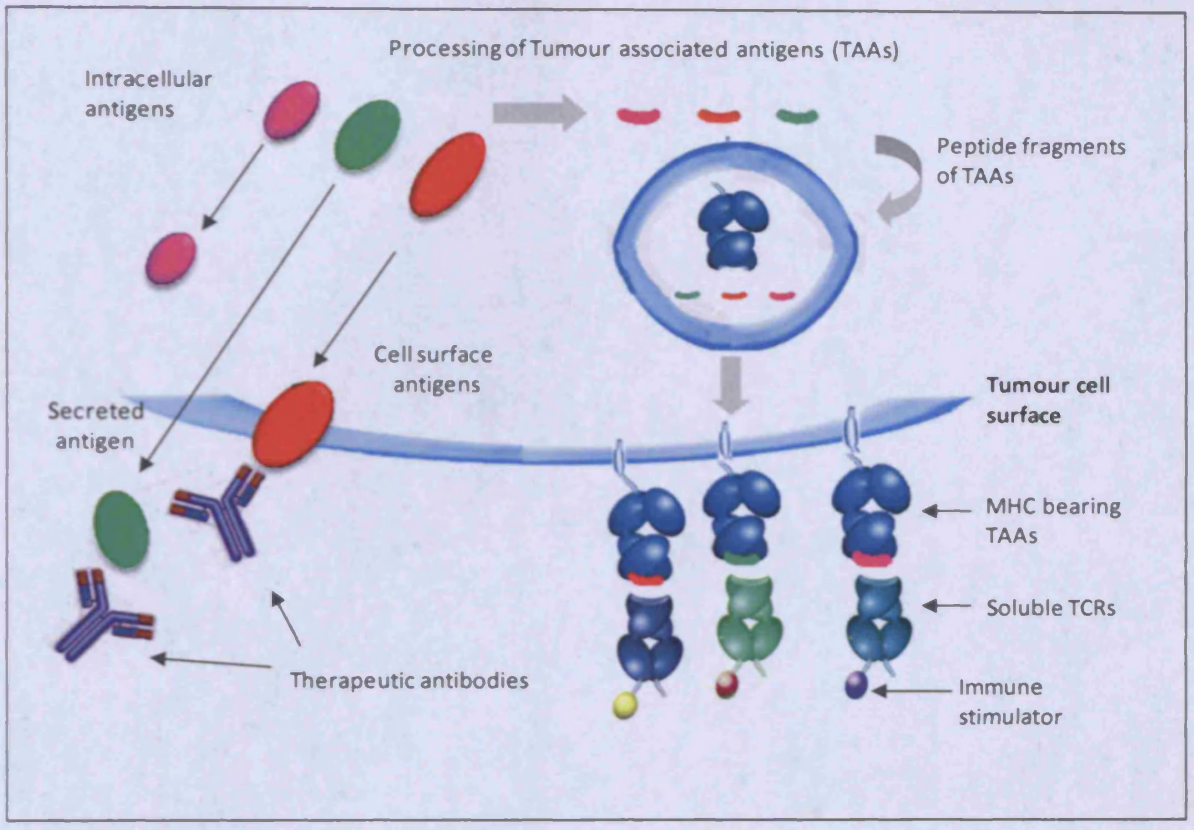

Figure 8.1: The differences in antigen recognition displayed by antibodies and TCRs. Cytoplasmic proteins, in this case tumour-associated antigens (TAAs) comprise intracellular proteins (pink), cell-surface-bound proteins (red), and secreted proteins (green). These proteins are degraded into short peptides by the proteasome. The peptide fragments are transported to the lumen of the endoplasmic reticulum where they can bind MHC class I, whereupon the complex cycles to the cell surface. The MHC molecules are shown on the surface of the cell with their intracellularly derived peptide fragments (red, pink and green). Whilst antibodies can only bind secreted or surface bound antigens typically in the form of whole proteins, TCRs have access to all antigens, regardless of cellular localisation, when these antigens are presented in complex with MHC on the surface of cells. Since the majority of TAAs and other pathogenic antigens are intracellular (i.e. not surface displayed, except in the context of HLA-peptide), soluble TCRs (when armed with cytotoxic agents or immune stimulators) are ideal candidates for immunotherapy (Figure taken from Molloy et al. 2005).

single-chain TCR–interleukin-2 (IL-2) fusion protein specific for an epitope of the p53 tumour suppressor protein (Card et al. 2004). This fusion protein, designated 264scTCR/IL-2, was capable of reducing lung metastases in an experimental HLA $A2^+$ mouse tumour model, and inhibited the growth of primary tumours derived from the A375 ($p53^+$/HLA $A2^+$) human melanoma cell line in these 'humanised' mice (Card et al. 2004; Belmont et al. 2006). Other immunomodulatory molecules that have shown great promise when fused to mAbs, can also be fitted to TCRs. These candidates include the cytokines interleukin-12 (IL-12) and tumour necrosis factor (TNF) (Halin et al. 2003; Dela Cruz et al. 2004), MHC class I (Lev et al. 2004), or a CD3 antibody (Davol et al. 2004; Gao et al. 2004). Collectively, these molecules share the function of redirecting T cells to target tumours or virally infected cells, and thus make ideal fusion partners for soluble TCRs.

The success of mAbs in soluble immunotherapy stems from the fact that antibodies: i) are naturally secreted by B cells and thus already exist as soluble molecules; and, ii) display naturally high affinities for antigen (0.1-10 nM K_D) (An 2009). On the contrary, naturally occurring TCRs: i) are exclusively expressed on the surface of T cells, where they are tethered to the cell surface via their insoluble transmembrane regions; and, ii) have low affinities for antigen (1–100 μM K_D) (van der Merwe et al. 2003) imposed by the processes of positive and negative selection in the thymus. The narrow range of affinities displayed by natural TCRs translates into antigen binding half-lives of 1-10 seconds (van der Merwe et al. 2003) at 25°C and considerably shorter at physiological temperatures (Willcox et al. 1999a). The short binding half-lives of natural TCRs are simply too low to enable soluble TCRs to localise to their target antigens and deliver a payload. Monoclonal antibodies on the other hand display much longer binding half-lives in the range of minutes to hours (Einhauer et al. 2001; Gerstner et al. 2002). If soluble TCRs are to rival mAbs as therapeutic agents, they must undergo a significant increase in affinity. This can be achieved by *in vitro* evolution techniques such as phage display, which require that the TCR is expressed in a suitable recombinant format. However, whilst 'affinity maturation' of mAb had become routine practice (Boder et al. 2000; Hanes et al. 2000), the poor stability of the TCRs meant that initial efforts to generate soluble high affinity TCRs for use as therapeutic agents were unsuccessful. The next section of this chapter describes how significant breakthroughs in

the manufacture of soluble TCRs has enabled the generation of TCRs with antibody-like binding properties, broadening our understanding of TCR-antigen interactions and making the development TCR-based therapeutic targeting agents a feasible goal.

8.1.2 Production of soluble monoclonal TCRs with enhanced affinities

Unlike antibodies, TCRs are not naturally expressed as soluble proteins but instead reside on the T cell surface. The extracellular domains of the TCR α and β chains are held together via a single membrane-proximal disulphide bond, the presence of which is required for TCR stability. Attempts to generate soluble TCRs containing this natural disulphide bond have been unsuccessful (Garboczi et al. 1996). In view of this failure, different means of stabilising TCR α-β heterodimeric pairing were attempted. The success of 'single-chain' TCR constructs, analogous to antibody scFv fragments (Vα-linker-VβCβ, where V=variable domain, C=constant domain), was limited and unpredictable (Plaksin et al. 1997). A more fruitful approach involved stabilising the extracellular TCR subunits by fusion to jun-fos leucine zippers (Willcox et al. 1999b). Although this innovation successfully yielded functional soluble TCRs, these TCRs had two significant drawbacks. Firstly, the flexibility of the leucine zippers interfered with the crystallisation process, and, secondly, the 'foreign' nature of the required linkers carried with it the potential for immunogenicity if the reagents were to be used in the clinic (Willcox et al. 1999b; Boulter et al. 2003). In 2003, my colleague Jonathan Boulter reported an alternative method for designing stable, soluble TCR constructs with a high degree of specificity and minimum sequence deviation from wildtype (Boulter et al. 2003). This involved the insertion of a non-native disulphide bond into the interface between the TCR constant domains, at a region distinct from where the native disulphide bond is naturally located. The approximate location of the new disulphide bond was predicted by molecular modelling of a known TCR crystal structure (Ding et al. 1998). Amongst several residues proposed for mutation to cysteines, threonine-48 in the TCR α constant domain (TRAC T48) and serine-57 in the TCR β constant domain (TRBC S57) were selected due to their orientation towards each other and close proximity (Boulter et al. 2003). With both of these residues mutated to cysteines, and the insoluble transmembrane regions truncated immediately N-terminal of the natural membrane proximal cysteines, the resultant disulphide-linked soluble (dsTCRs) (later designated

monoclonal TCRs, mTCRs) refolded well and showed a high degree of stability (Boulter et al. 2003). Importantly, the technique preserves the specificity and three-dimensional structure of the wildtype TCR, and yields soluble TCRs that are amenable to crystallisation (Boulter et al. 2003; Chen et al. 2005). Finally, because the disulphide bond is buried deep in the globular TCR αβ interface it presents a minimal risk of antigenicity and is thus suitable for therapeutic application (Boulter et al. 2003).

With the novel soluble mTCR manufacture system in place, Boulter *et al.* proceeded to increase the affinity of a number of monoclonal TCRs by displaying them on the surface of bacteriophage (Smith 1985; Li et al. 2005). Prior to the generation of stable mTCRs, 'phage display' to increase TCR affinity was not an option, as the TCR constructs were too unstable for presentation on the surface of phage. As an alternative, multimerization of TCRs (typically as TCR tetramers) was performed to take advantage of the 'avidity effect', the same effect that also allows pMHC tetramers to bind their target TCRs ((Subbramanian et al. 2004; Laugel et al. 2005), and section 1.6 of the main Introduction). However, at the molecular level, this approach relies on a high probability of TCR-antigen encounter enabling more than once TCR in a TCR tetramer to bind cognate pMHC. In reality, the number of cognate pMHC molecules naturally presented equates to only ≤50 per cell explaining why this technology was only partially successful at staining target cells expressing natural levels of antigen (Subbramanian et al. 2004; Laugel et al. 2005).

The unique stability of dsTCRs made them highly suitable for phage display, a technique that is used for the high-throughput screening of protein interactions (Li et al. 2005). Holler *et al.* had already demonstrated the success of a similar yeast display approach by showing that generating mutations within the TCR α-chain complementarity determining region (CDR)3 loop of the murine 2C TCR (expressed as a single-chain construct) increased its affinity by >100 to 9 nM K_D, without incurring a loss in specificity in *in vitro* binding assays (Holler et al. 2000). Display techniques such as yeast and phage display enable the study of protein-protein interactions (in this case the TCR and pMHCI antigen) by providing a connection between the genotype and phenotype of the proteins of interest. Production of high affinity dsTCRs that fall outside of normal *in vivo* constraints by phage display is a laborious process

that involves: i) random mutagenesis of specific CDR loops within the individual TCR α and β chains; ii) cloning of mTCR α and β genes into phagemid vectors; iii) fusion of the TCR β gene construct to gene III of M13 bacteriophage (downstream of the TCR αβ sequence), the product of which will be eventually displayed on the phagemid surface as a bi-cistronic protein; iv) screening the mTCR-expressing phage by a phage ELISA using streptavidin-immobilised, biotin-tagged, pMHCI complexes as targets and detecting bound phage using anti-gene III protein antibodies (Smith 1985; Li et al. 2005); and, v) sequencing of the genomes of phage clones which produce a signal in the ELISA, and recording the TCR affinity-enhancing mutations in the CDR loops. The probability that a randomly introduced mutation enhances the affinity of a given TCR is very low. The success of phage display depends on millions of mTCR clones being generated. These are organised into phagemid libraries (comprising up to 10^{10} clones, Liddy et al. submitted). The phage libraries undergo several rounds of screening of decreasing concentrations of immobilised pMHCI in a process called 'molecular evolution'. The end product of molecular evolution is a handful of phage, expressing mTCRs displaying the strongest affinity for cognate pMHCI. To increase TCR affinity further still, second-generation libraries are constructed by combining several CDR loop mutations (discovered using first-generation phage display libraries) in a single TCR (Li et al. 2005; Dunn et al. 2006). Using directed molecular evolution, Li *et al.* demonstrated that the affinity of TCRs can be increased dramatically, by at least 10^6-fold (Li et al. 2005). For instance, the affinity of a TCR (1G4) specific for the HLA A2-restricted tumour associated antigen NY-ESO-$1_{157\text{-}165}$ (SLLMWITQC), which is expressed in a large variety of cancers, was increased from 11 μM to 26 pM. This increase in affinity translates into a shift in TCR/pMHCI binding half-life from 7 seconds to >15 hours at 25°C (Li et al. 2005). Importantly, the 1G4 and other high affinity monoclonal dsTCRs (mTCRs) generated by phage display, bound cognate cell surface pMHCI even at very low levels of peptide and exhibited no crossreactivity to endogenously derived non-specific peptides (Li et al. 2005). The next section introduces a novel type of soluble TCR targeting reagents, generated using the advances just described.

8.1.3 ImmTAC/Vs

The combination of advances in soluble TCR technology and molecular affinity evolution systems, have enabled the production of 'Immune-mobilising monoclonal TCRs Against Cancer/Viruses (ImmTAC/Vs) (Liddy et al. submitted). ImmTAC/Vs are TCR-based bi-specific immunotherapeutic molecules designed to redirect the lysis of target cells presenting a specific pMHCI antigen by engaging and recruiting polyclonal $CD8^+$ T cells. While the soluble high-affinity TCR portion of the ImmTAC/V molecule targets a desired antigen, the anti-CD3 single-chain (sc)Fv antibody fragment polyclonally activates T cells via the CD3 complex, effectively redirecting T cells to kill its target be it a tumour or a virally infected cell. ImmTACs, designed to target tumour associated antigens (TAAs), represent the more advanced of the two types of reagent to date, although a number of ImmTAVs recognising viral antigens are currently being optimised (one of which is described in Section 8.2.5). Figure 8.2 illustrates the ImmTAC mode of action when applied to the targeting of tumours. The four ImmTACs studied in this chapter were generated by firstly producing soluble monoclonal mTCRs from $CD8^+$ T cell clones (Boulter et al. 2003) with specificities for the following TAAs: i) $gp100_{280\text{-}288}$ (YLEPGPVTA/HLA A*0201); ii) $MAGE\text{-}A3_{168\text{-}176}$ (EVDPIGHLY/HLA A*0101); iii) $Melan\text{-}A/MART\text{-}1_{26\text{-}35}$ (EAAGIGILTV/HLA A*0201); and, iv) a cancer testis antigen expressed in a wide range of cancers, $NY\text{-}ESO\text{-}1_{157\text{-}165}$ (SLLMWITQC/HLA A*0201) (see Table 1.2 of the main Introduction). The nomenclature for the four ImmTACs was devised according to the antigens the mTCR components were designed to recognise: ImmTAC-gp100, ImmTAC-MAGE, ImmTAC-MEL and ImmTAC-NYE. Surface plasmon resonance (SPR) established that the wildtype mTCRs bound their respective antigens with K_D values of ~30 μM, ~248 μM, ~18 μM, and ~11 μM (Liddy et al. submitted). High affinity versions of the wild type mTCRs were subsequently generated by subjecting the TCR sequences to directed molecular evolution and phage display selection, as described in section 8.1.2 of this chapter ((Li et al. 2005; Dunn et al. 2006), and Liddy et al. submitted). The bi-specific ImmTAC molecules were then engineered by fusing a humanised anti-CD3 scFv to the high affinity mTCR β chain via a flexible linker (Liddy et al. submitted). The ImmTAC α and β chain were expressed separately in *E. coli* as inclusion bodies, and refolded *in vitro* (Boulter et al. 2003). The TCR/pMHCI antigen binding

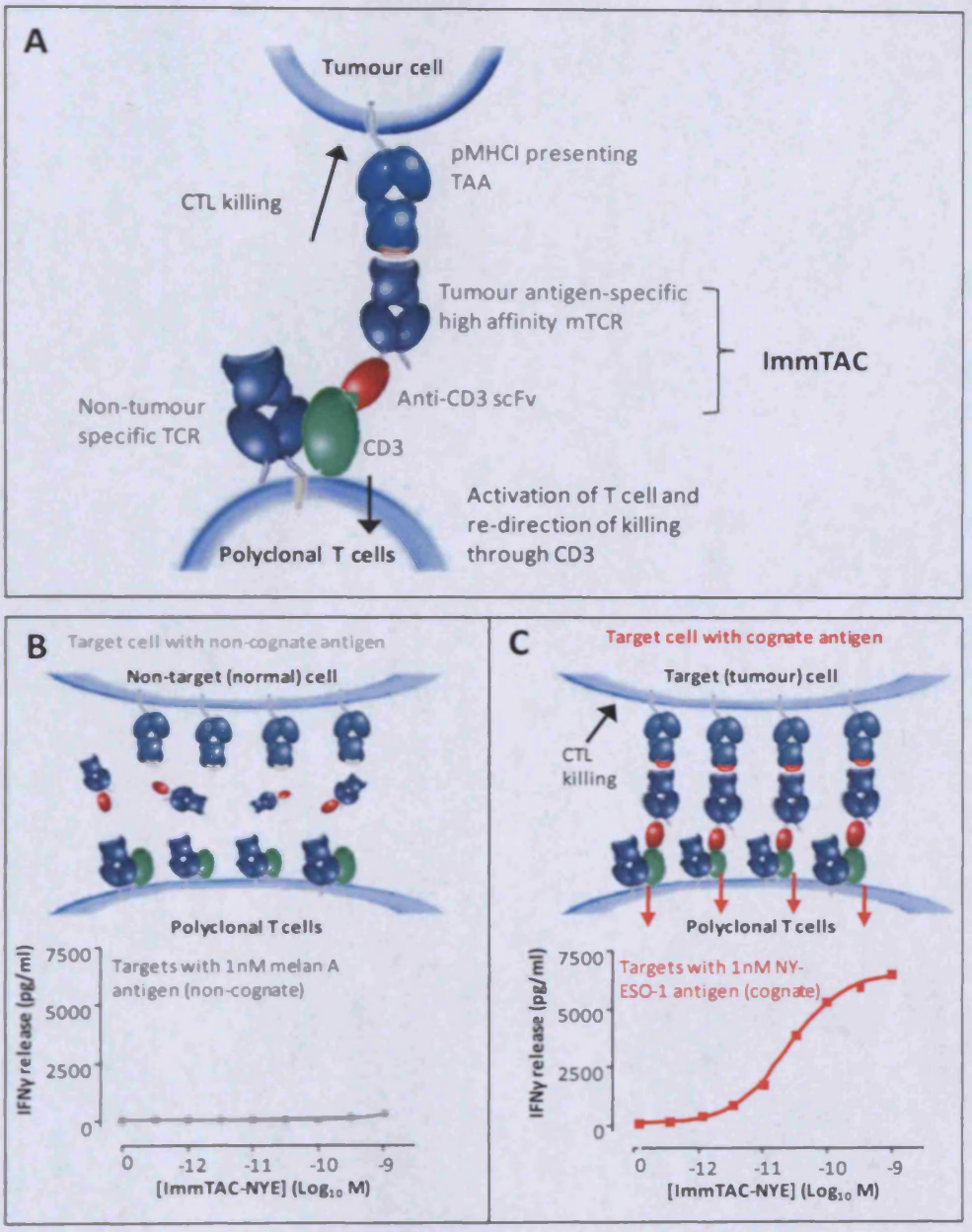

Figure 8.2: Re-directing T cell responses to kill tumour cells. A. The high affinity monoclonal TCR portion of the ImmTAC molecule binds a unique antigen on the tumour cell surface, while the anti-CD3 single-chain (sc)Fv antibody portion recruits T cells of all specificities to kill the tumour cell. **B.** Normal cells presenting a non-cognate melan A antigen do not bind the ImmTAC-NYE reagent specific for the NY-ESO-1 tumour antigen. **C.** Tumour cells presenting the cognate NY-ESO-1 antigen are decorated by ImmTAC-NYE molecules, which elicit activation of a polyclonal population of T cells, culminating in killing of the target cells. The action of the ImmTAC reagent can be quantified by monitoring cytokine production (panels B and C) or cell lysis.

kinetics for the high affinity mTCRs and the corresponding ImmTAC molecules were determined by SPR, and are summarised in Table 8.1. As indicated, the biophysical parameters for the CD3 scFv-fused and unfused mTCRs were very similar, implying that the structure integrity of each mTCR was not altered by the fusion process.

A

ImmTAC	Target Protein/Peptide	HLA	TCR binding to peptide/HLA complex			
			K_{on} ($M^{-1}s^{-1}$)	K_{off} (s^{-1})	T½ (h)	K_D (pM)
ImmTAC-NYE	NY-ESO-$1_{157-165}$ SLLMWITQC	HLA*0201	$5.70x10^5$	$2.72x10^{-5}$	12	26
ImmTAC-gp100	$Gp100_{280-288}$ YLEPGPVTA	HLA*0201	$5.25x10^5$	$5.79x10^{-6}$	33.1	11
ImmTAC-MAGE	Mage-$A3_{168-176}$ EVDPIGHLY	HLA*0101	$3.17x10^5$	$1.81x10^{-5}$	10.5	57
ImmTAC-MEL	Melan A_{26-35} EAAGIGILTV	HLA*0201	$1.97x10^5$	$3.62x10^{-6}$	53	18

B

ImmTAC	Target Protein/Peptide	HLA	TCR binding to peptide/HLA complex			
			K_{on} ($M^{-1}s^{-1}$)	K_{off} (s^{-1})	T½ (h)	K_D (pM)
ImmTAC-NYE	NY-ESO-$1_{157-165}$ SLLMWITQC	HLA*0201	$6.25x10^5$	$1.13x10^{-5}$	17	18
ImmTAC-gp100	$Gp100_{280-288}$ YLEPGPVTA	HLA*0201	$3.67x10^5$	$1.80x10^{-5}$	15	33
ImmTAC-MAGE	Mage-$A3_{168-176}$ EVDPIGHLY	HLA*0101	$4.54x10^5$	$1.92x10^{-5}$	12	44
ImmTAC-MEL	Melan A_{26-35} EAAGIGILTV	HLA*0201	$1.33x10^5$	$5.20x10^{-6}$	37	39

Table 8.1: Biophysical characteristics of 'free' soluble TCRs and TCR portions of ImmTAC molecules with four different specificities. Kinetics and equilibrium binding properties of 'free' TCRs (**A**) and the same TCRs incorporated into ImmTAC molecules (**B**) determined by SPR. Measurements were conducted by flowing soluble TCRs or ImmTACs over cognate peptide/MHC class I molecules immobilised via a biotin tag on the surface of streptavidin-coated CM-5 chips. In most cases, the heteroclitic peptide was used for SPR due to increased stability when complexed to relevant MHCI as a soluble molecule. (SPR measurements kindly provided by Immunocore Ltd.).

8.1.4 Aims

A major breakthrough in the production of soluble mTCRs, and advances in directed molecular evolution by phage display represent two critical events which enabled the generation of high affinity TCRs suitable for use as immunomodulatory therapeutic reagents (Boulter et al. 2003; Li et al. 2005). In this chapter I present data obtained with a novel class of mTCR-based therapeutic agents called 'Immune-mobilising monoclonal TCRs Against Cancer/Viruses' (ImmTAC/Vs) as part of a collaboration with Immunocore Ltd (Oxford). Immuncore are experts in the production and molecular engineering of soluble versions of lymphocyte cell surface proteins such and pMHC and TCRs. The company has less expertise in T cell assays. I was delighted to be given the opportunity to help them test the effects of their reagents in a range of *in vitro* and *ex vivo* assays. The aims for this work were to:

i) Test the ability of ImmTAC reagents, targeting four common TAAs (gp100, MAGE-3, Melan-A and NY-ESO-1), to specifically activate polyclonal $CD8^+$ T cells.

ii) Evaluate the ability of ImmTACs to incite a specific polyfunctional $CD8^+$ T cell response, and determine which $CD8^+$ T cell phenotypes are responding.

iii) Assess the ability of ImmTACs to redirect $CD8^+$ T cells to lyse peptide-pulsed targets and tumour cell lines presenting the relevant TAAs.

iv) Preliminarily assess whether the presence of regulatory T cells (Tregs) affects ImmTAC function.

v) Determine whether ImmTACs are capable of inhibiting tumour growth *in vivo*.

vi) Explore whether an ImmTAV designed to target a common epitope derived from HIV-1, can redirect polyclonal $CD8^+$ T cells to respond to this antigen.

8.2 Results

8.2.1 ImmTACs specifically target tumour cells and activate CD8$^+$ T cells

Initially, the *in vitro* biological activity of ImmTACs was assessed by measuring the activation of a polyclonal population of CD8$^+$ T cells in the presence of tumour cell lines presenting the relevant antigen: i) NY-ESO-1 on IM9 EBV-transformed B-lymphoblastoid cells; ii) gp100 on Mel526 melanoma cells; iii) MAGE-3 on A375 melanoma cells; and, iv) Melan-A on Mel624 melanoma cells. The CD8$^+$ T cells were obtained by positive MACS selection using PBMC prepared from healthy donors, and kept in a cytokine-free environment for several days prior to assaying in order to minimise background activation. IFNγ cytokine production (measured by IFNγ ELISpot) was chosen as the readout for CD8$^+$ T activation in the presence of tumour lines and titrated levels of ImmTAC. The number of IFNγ-spot forming cells (SFC) per 10^6 CD8$^+$ T cells was recorded at each concentration of ImmTAC. Representative data are shown in Figure 8.3 A-D. In all cases, CD8$^+$ T cells were only activated in the presence of tumour cells and the ImmTAC reagent. The number of activated IFNγ-producing CD8$^+$ T cells correlated with the concentration of ImmTAC used. Furthermore, all four ImmTACs produced EC_{50} values within the same range as the K_D values for the corresponding ImmTAC/pMHCI interactions determined by SPR (Figure 8.3 and Table 8.1). Tumour cells are renowned for expressing extremely low levels of surface pMHCI antigen. Epitope counting studies performed by Immunocore Ltd. using PE-labelled high-affinity TCRs show that there are ~10-50 copies of popular HLA A2-restricted TAA-derived peptides on the surface of an average tumour cell (unpublished and (Purbhoo et al. 2006)). In contrast, peptide-pulsed cells can present ~100-1000 peptide copies (unpublished and (Purbhoo et al. 2006)). Therefore, the fact that ImmTACs were able to redirect CD8$^+$ T cells to recognise these tumour lines efficiently represents a remarkable degree of antigen sensitivity.

8.2.2 ImmTACs elicit polyfunctional responses in memory CD8$^+$ T cells directly *ex vivo*

Clearly, if ImmTACs are to eventually fulfil their roles as therapeutic reagents, their actions would have to be assessed under more physiological conditions than used in the experiments described so far. The closest system to the use of ImmTACs *in vivo* is to

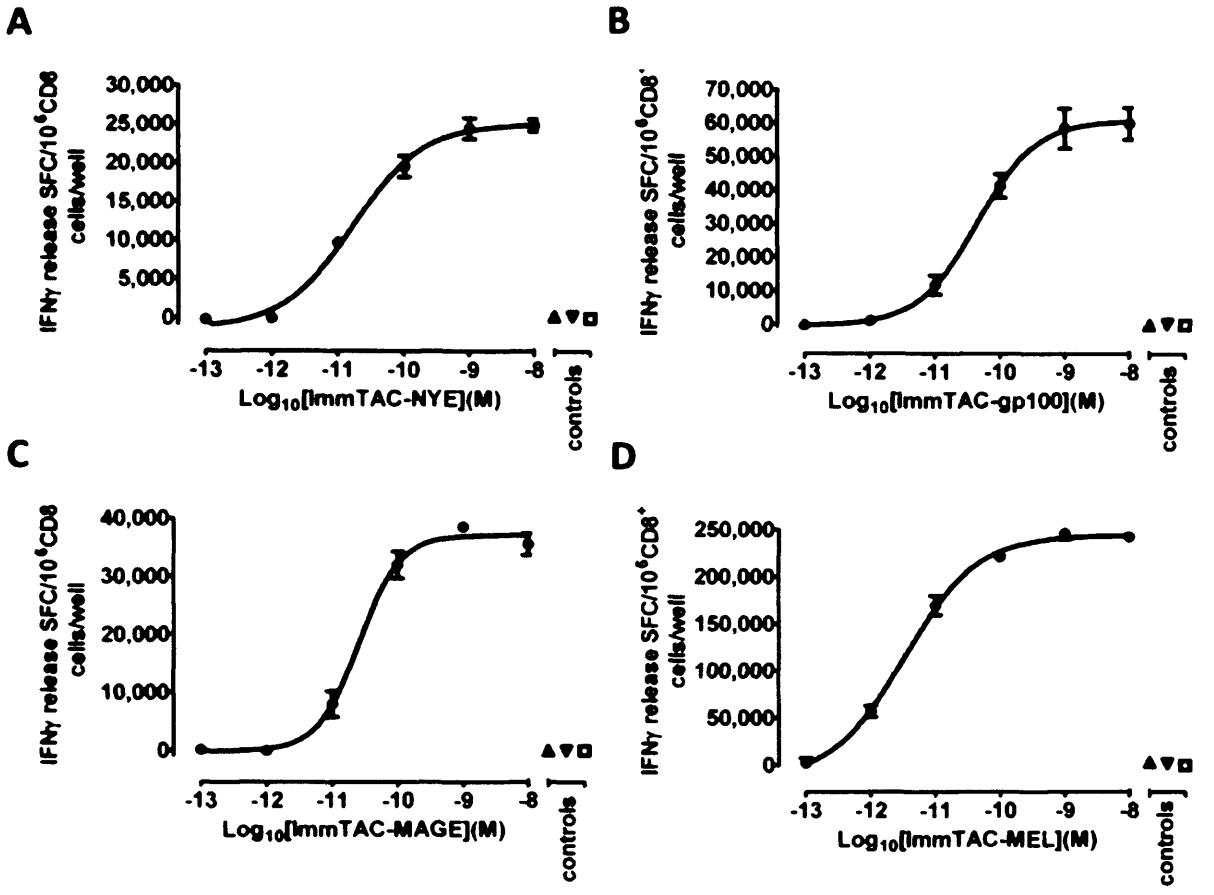

Figure 8.3: Biological activity of ImmTAC molecules with different specificities. (A-D) IFNγ ELISpot assays showing activation of purified $CD8^+$ T cells mediated by titrated concentrations of ImmTAC molecules in the presence of tumour cells expressing endogenous levels of antigen. E=effector; T=target. ImmTAC molecules+ E + T (circle); E + T alone (triangle); E + ImmTAC alone (inverted triangle); T + ImmTAC alone (square). The numbers on the y-axis represent the number of spot forming cells (SFC) per 10^6 $CD8^+$ T cells assayed. Error bars depict mean values ± s.e.m. **A.** ImmTAC-NYE and IM9 EBV-transformed B-lymphoblastoid cells; **B.** ImmTAC-gp100 and Mel526 melanoma cells; **C.** ImmTAC-MAGE and A375 melanoma cells; and, **D.** ImmTAC-MEL and Mel624 melanoma cells. (Figure kindly provided by Immunocore Ltd.).

examine their behaviour using fresh *ex vivo*-derived PBMC instead of purified populations of $CD8^+$ T cells. To this effect, I set up *in vitro* activation assay comprising PBMC isolated from an HLA $A2^+$ healthy donor. In this experiment, the PBMC were either pulsed with 10^{-6} M NY-ESO-$1_{157-165}$ peptide or were incubated with media alone, in the presence of a titrated ImmTAC-NYE and unpulsed PBMC from the same donor acting as effectors. The cells and ImmTAC-NYE were incubated with a directly conjugated αCD107a mAb and secretion inhibitors as described in the Materials and Methods section 2.11.5. After incubation, the cells were initially stained with the amine viability dye ViViD, and then with directly conjugated mAbs specific for the surface markers CD3, CD4, CD8, CD27, CD45RO and CD57 to enable phenotypic analysis of the $CD8^+$ and $CD4^+$ T cells in the assay. Intracellular staining for specific cytokines (IFNγ, TNF, and IL-2) was then performed, following fixation and permeabilisation. Details of the typical gating strategy adopted for phenotyping PBMC can be found in section 2.10.3 of Materials and Methods. The extent of ImmTAC-mediated activation was determined for $CD8^+$, $CD4^+$ and γδ T cell subsets present within the PBMC sample. Although γδ T cells also express surface CD3, the level of ImmTAC-specific activation for these lymphocytes was negligible (data not shown). Figure 8.4 A shows the activation profiles of $CD8^+$ and $CD4^+$ T cells in the presence of titrated ImmTAC-NYE. Based on the extent of degranulation (surface CD107a mobilisation) and production of cytokines (IFNγ, TNF, and IL-2), $CD8^+$ T cells appeared to be substantially more sensitive to ImmTAC-mediated activation than $CD4^+$ T cells (Figure 8.4 A). These findings were important for two reasons. They demonstrated that ImmTACs: i) preferentially engaged $CD8^+$ T cells; and, ii) elicited a polyfunctional $CD8^+$ T cell response.

I was also interested in dissecting the ImmTAC-T cell response further to determine which phenotypes within the $CD8^+$ and $CD4^+$ T cell populations were being activated. The potential of the CD3 scFv portion of an ImmTAC to activate a naive T cell subset in the absence of a TCR signal could carry the risk of 'awakening' potentially autoreactive T cells. Phenotypic characterisation of activated $CD8^+$ T cells was performed by staining with antibodies directed against CD27 and CD45RO T cell differentiation markers. Superimposition of phenotypic profiles of activated $CD8^+$ T cells and the overall $CD8^+$ T cell population revealed

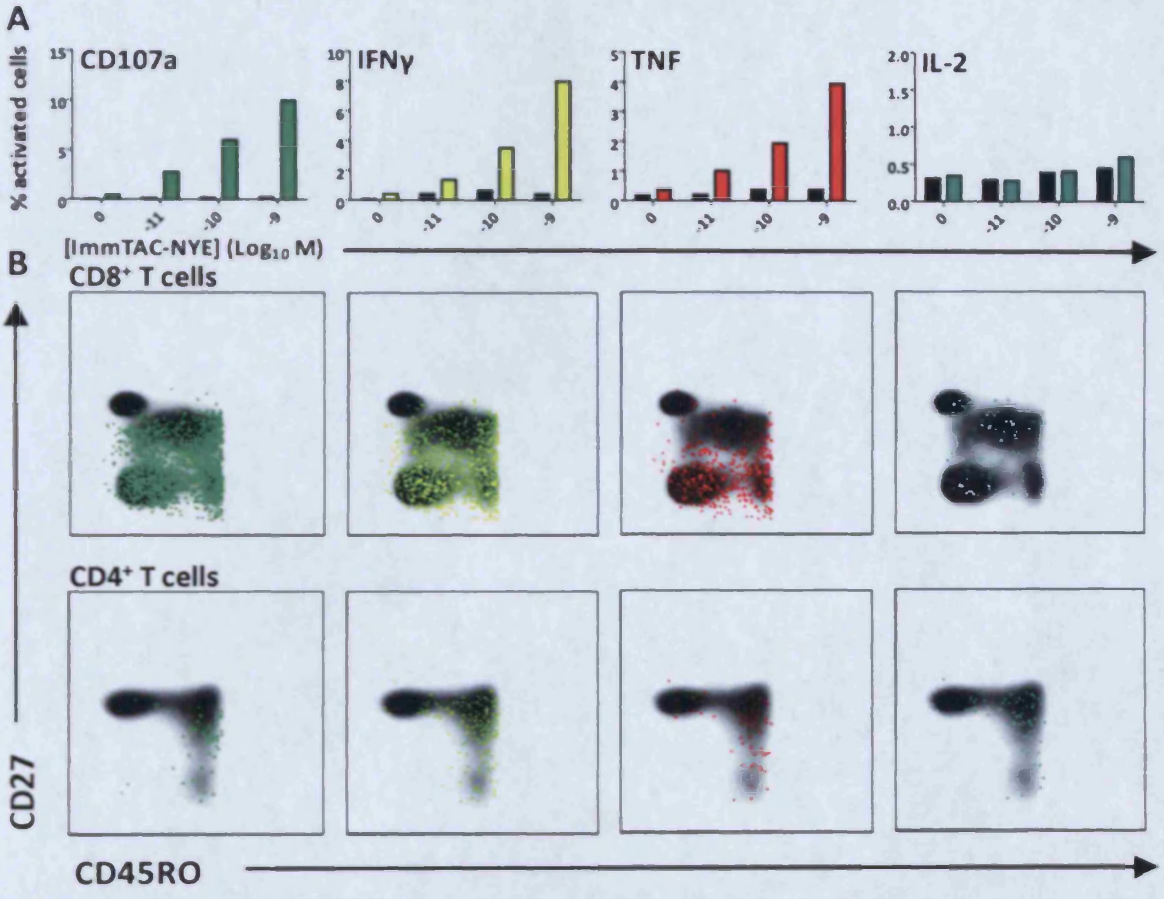

Figure 8.4:I mmTACs target primarily CD8⁺ T cells. Flow cytometry was used to measure extent of activation (determined by surface CD107a expression and intracellular cytokine release) of CD8⁺ and CD4⁺ T cell subsets in a sample of *ex vivo*-derived human PBMC, in the presence of titrated ImmTAC-NYE reagent. The numbers assigned to each FACS gate, correspond to the percentage of activated CD4⁺ or CD8⁺ T cells. **A** shows the dose-response relationship between ImmTAC-NYE concentration and the relative percentages of CD8⁺ (coloured bars) and CD4⁺ (black bars) T cells activated to express each of the four effector functions (CD107a, green;IF Nγ, yellow;T NF, red;an d, IL-2, turquoise) in the presence of a sample of PBMC target cells pre-pulsed with cognate NY-ESO-1 peptide. **B.** Phenotypic profile of CD8⁺ (upper panels) and CD4⁺ (lower panels) T cells activated with 10^{-11} M ImmTAC-NYE in the presence of NY-ESO-1 peptide-pulsed PBMC. Coloured dots depict individual cells that elicit a distinct function, as indicated in A, superimposed on cloud plots showing the phenotypic profile of the overall CD8⁺ and CD4⁺T cell population;t he upper panels show events from the corresponding panels in A and are colour-coded to match. Representative data of >2 separate experiments shown.

that the vast majority of responding $CD8^+$ and $CD4^+$ T cells belonged to the effector ($CD27^-$ $CD45RO^-$/effector memory ($CD27^-$ $CD45RO^+$) subsets (Figure 8.4 B).

Based on the fact that ImmTACs preferentially activated $CD8^+$ T cells, ImmTAC/V-mediated $CD4^+$ T cell engagement was not investigated further. Figure 8.5 shows *ex vivo*-derived PBMC activation results obtained with ImmTAC-gp100, focusing on $CD8^+$ T cells. Target PBMC pulsed with 10^{-6} M $gp100_{280-288}$ heteroclitic peptide YLEPGPVTV (or unpulsed), or Mel526 melanoma cells, were incubated for 12 hours with fresh autologous (unpulsed) PBMC in the presence or absence of ImmTAC-gp100 at the indicated concentrations, a directly conjugated αCD107a mAb and secretion inhibitors as described in the previous paragraphs and in the Materials and Methods section 2.11.5. In the peptide-pulsed PBMC samples containing ImmTAC-gp100, substantial numbers of $CD8^+$ T cells were activated in a sensitive and dose-dependent manner to elicit multiple effector functions (Figure 8.5 A). In agreement with ImmTAC-NYE data presented in Figure 8.4 B, the vast majority of ImmTAC-gp100-responding $CD8^+$ T cells belonged to the effector memory ($CD27^-$ $CD45RO^+$) subset (Figure 8.4 B). These effector memory $CD8^+$ T cells also exhibited a terminally differentiated phenotype characterised by expression of the senescence marker CD57. T cells expressing this marker are associated with maximal lytic capacity (Chattopadhyay et al. 2009), a desirable feature for an immunotherapeutic agent designed to target tumour cells. Encouragingly, ImmTAC-gp100 was equally capable of eliciting a polyfunctional $CD8^+$ T cell response with a similar phenotypic distribution when using the Mel 526 melanoma cell line, a natural tumour cell line that expresses very low levels of gp100 antigen, as targets (Figure 8.5 B bottom panels), as when using peptide-pulsed PBMC (Figure 8.5 B top panels).

8.2.3 ImmTACs redirect T cells without tumour specificity to lyse tumour-transformed cells

In order to be effective therapeutic agents, ImmTAC/Vs must not only activate $CD8^+$ T cells in a polyfunctional manner, but also re-direct these effector cells to lyse the tumour/infected target cells. To investigate whether polyclonal $CD8^+$ T cells were able to respond to ImmTACs in this way, I set out to optimise a flow cytometric cytotoxicity assay

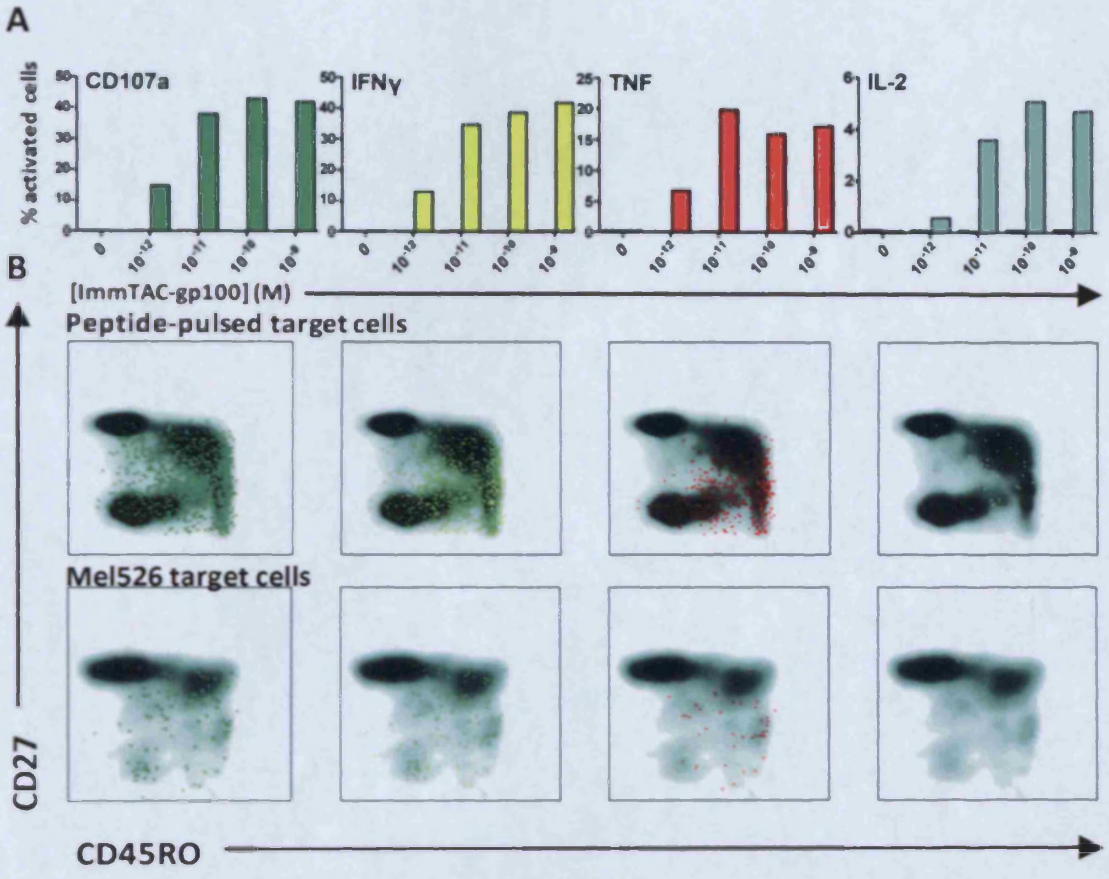

Figure 8.5: Efficient activation of multiple CD8⁺ T cell effector functions by ImmTAC-gp100. A. Dose-response relationship between the concentration of ImmTAC-gp100 and the percentage of CD8⁺ T cells activated to express each individual function in the presence of cognate gp-100 peptide-pulsed PBMC. Surface expression of CD107a (green), and intracellular production of the cytokines IFNγ (yellow), TNF (red) and IL-2 (turquoise), are shown. Coloured bars represent activation in response to peptide-pulsed targets; black bars represent activation in response to unpulsed targets. **B.** Phenotypic profile of CD8⁺ T cells activated with ImmTAC-gp100 at a concentration of 10^{-11} M in the presence of peptide-pulsed PBMC (upper panels) or Mel526 cells (lower panels). Coloured dots depict individual cells that elicit a distinct function, as indicated in A, superimposed on cloud plots showing the phenotypic profile of the overall CD8⁺ T cell population; the upper panels show events from the corresponding panels in A and are colour-coded to match. Representative data of 2 experiments shown.

otherwise known as a FATAL assay (Materials and Methods section 2.11.7). I experimented with two parameters: i) effector to target ratio (E:T) (Figure 8.6 A); and, ii) donor dependence (ie. whether $CD8^+$ T cells isolated from different blood donors influenced the efficiency of ImmTAC function (Figure 8.6 B)). These optimisation assays were conducted with 1 nM ImmTAC-NYE, using $CD8^+$ T cells, derived from PBMC by magnetic cell sorting, as effectors and NY-ESO-$1_{157\text{-}165}$-peptide pulsed T2 cells as targets. Firstly, increasing the E:T ratio > 5:1 did not correspond with higher levels of peptide-pulsed target cell lysis, indicating that the efficacy of ImmTACs was not limited by the number of responding $CD8^+$ T cells. This observation implies that over the course of the assay, a single $CD8^+$ T cell activated by a specific ImmTAC is capable of serially killing several targets. The speculation that ImmTACs are capable of causing individual $CD8^+$ T cells to serially kill their targets was confirmed using time lapse video microscopy footage of a single $CD8^+$ T cell (of the EBV-specific clone 176.c4.1) lysing three Mel624 (gp$100_{280\text{-}288}$ peptide-expressing melanoma cell line) target cells. Three screen capture images taken at 0, 1.5, and 5.5 hours illustrate the serial killing process (Figure 8.7). The fact that ImmTACs can elicit $CD8^+$ T cells to serially kill their targets is likely to contribute to their anti-tumour potency. In the second set of FATAL optimisation experiments (Figure 8.6 B), the source of $CD8^+$ T cells did not significantly alter the efficiency of target cell lysis. This was welcome news, as it meant that further data generated using ImmTACs was not skewed by donor-dependent differences in $CD8^+$ T cells. It also implied that ImmTACs were likely to function in most individuals, provided these individuals presented the target peptide in the context of an HLA allele to which the ImmTAC mTCR was restricted.

Since higher E:T afforded no advantage in terms of ImmTAC-mediated target cell lysis, further killing assays using pure $CD8^+$ T cell populations as effectors adhered to a ratio of 5:1 to conserve cells. Clearly, in experiments where PBMC were used as both targets and effectors, the E:T ratio was difficult to determine. Assuming that $CD8^+$ T cells constitute ~15% of total PBMC, 10^6 PBMC were typically used per assay condition. This corresponds to roughly the same number (~$1.5x10^5$) of effectors used in a FATAL killing assay conducted with pure $CD8^+$ T cells. In experiments performed with PBMC isolated directly *ex vivo*, ImmTAC reagents induced specific lysis in a dose-dependent manner (Figure 8.8 A and B).

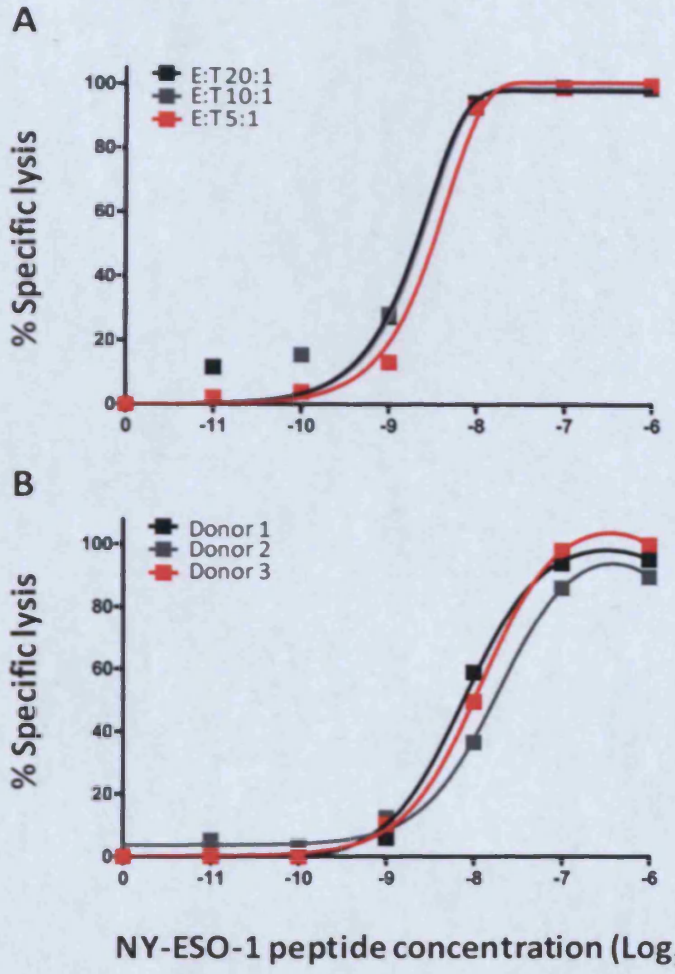

Figure 8.6: Optimisation of the FATAL assay for measuring ImmTAC-mediated cytotoxicity. **A.** $3x10^4$ T2 cells pulsed with titrated concentrations of NY-ESO-$1_{157-165}$ peptide were combined in a cytometric cytotoxicity FATAL assay with 1 nM ImmTAC-NYE and three different quantities of effector PBMC -derived $CD8^+$ T cells according to effector to target ratios (E:T) of 5:1, 10:1, and 20:1. Representative data of 2 experiments shown. **B.** $3x10^4$ NY-ESO-$1_{157-165}$ peptide pulsed T0 cells were assayed with 1n M ImmTAC-NYE reagent combined with $CD8^+$ T cells isolated from the PBMC of three different donors in an E:T ratio of 5:1. In each case the assays were performed over a 16 hour incubation period, and the target cell lysis was determined by flow cytometric quantification of labelled target cell elimination relative to an internal control.

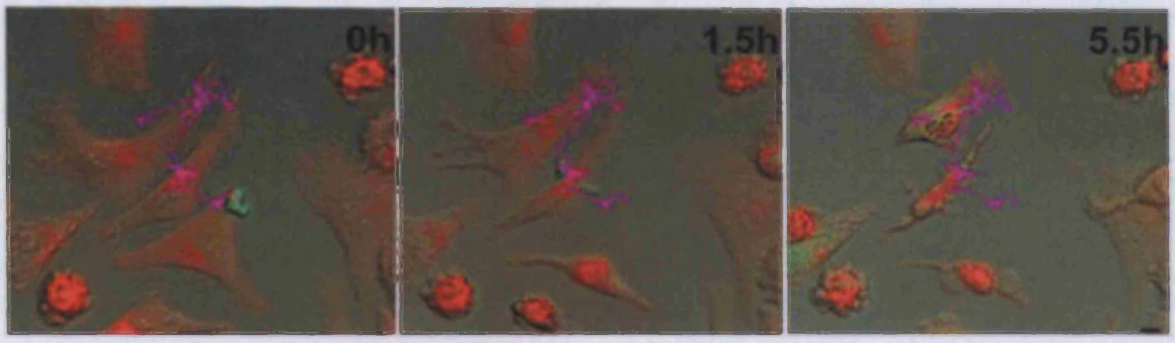

Figure 8.7: Visualisation of redirected lysis of Mel642 melanoma CD8⁺ T cells in the presence of ImmTAC-gp100. Time lapse video microscopy showing serial killing of three Mel624 melanoma cells (orange) by a single CD8⁺ T cell (EBV-specific clone 176.c4.1) without tumour specificity (green) in the presence of 10^{-10} M ImmTAC-gp100. The pink line tracks the path of the single CD8⁺ T cell over a period of 5.5 hours. Melanoma cells were plated at 3 x 10^4 cell/well and the T cell clone was plated at 8 x 10^3 cell/well. (Figure kindly provided by Immunocore Ltd.)

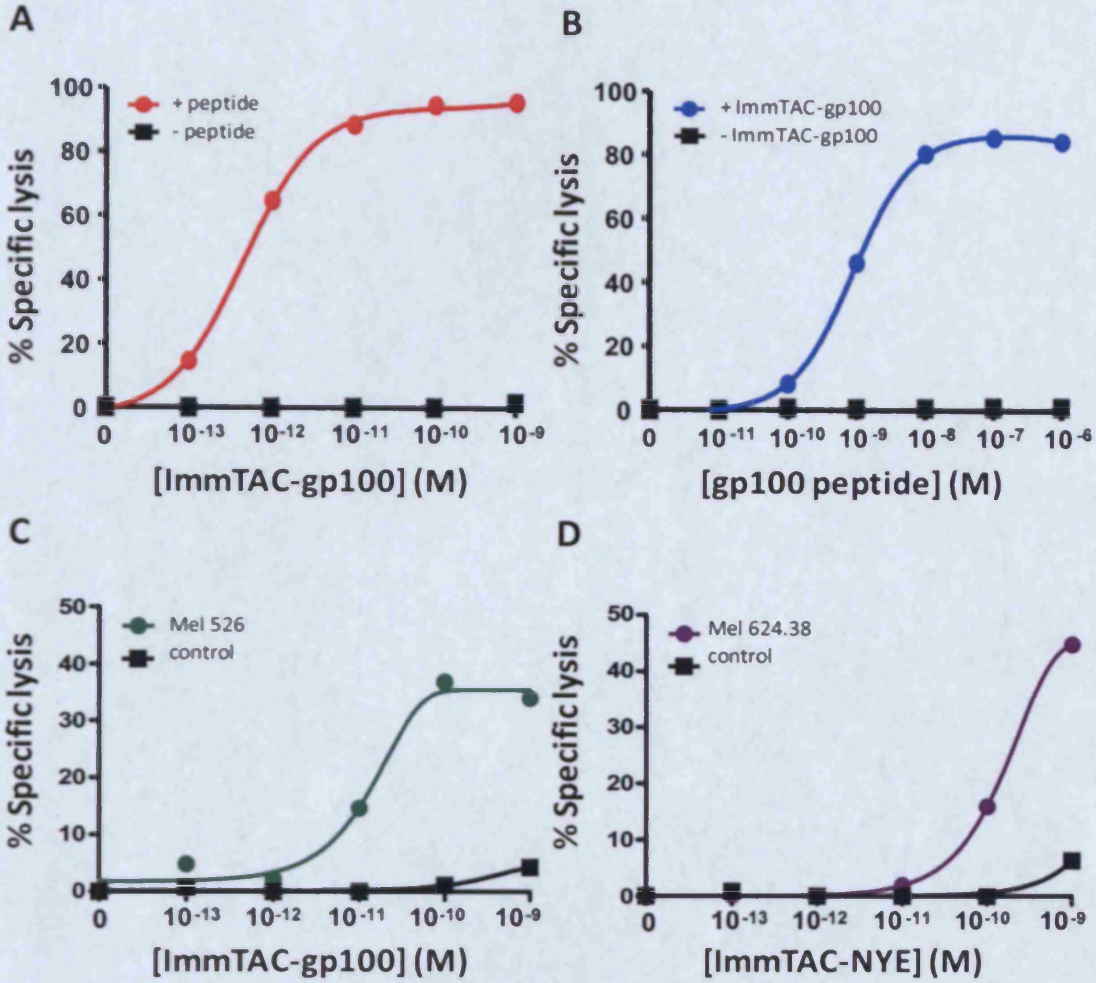

Figure 8.8: Redirected lysis of tumour cells and peptide-pulsed targets by PBMC in the presence of ImmTAC molecules. A. Redirected lysis over 16 hours of PBMC pulsed with (red circles) or without (black squares) $gp100_{280-288}$ heteroclitic peptide YLEPGPVTV at a concentration of 10^{-6} M in the presence of titrated doses of ImmTAC-gp100 and autologous PBMC.**B .** Redirected lysis over 16 hours of PBMC pulsed with various concentrations of the $gp100_{280-288}$ heteroclitic peptide YLEPGPVTV in the presence (blue circles) or absence (black squares) of 10^{-9} M ImmTAC-gp100 and autologous PBMC. **C.** Redirected lysis over 16 hours of Mel526 cells (green circles) or control (T0) cells (black squares) in the presence of titrated doses of ImmTAC-gp100 and PBMC. **D.** Redirected lysis over 16 hours of Mel624 cells (mauve circles) or control (T0) cells (black squares) in the presence of titrated doses of ImmTAC-NYE and PBMC.L ysis was determined by flow cytometric quantification of labelled target cell elimination (FATAL assay). Representative data of >2 replicates shown.

Furthermore, $CD8^+$ T cells present within these PBMC were effectively redirected to lyse tumour cells in dose titrations of ImmTAC-gp100 and ImmTAC-NYE (Figure 8.8 C and D).

8.2.4 ImmTAC function is not reduced in the presence of $CD4^+CD25^-CD127^{Lo}$ regulatory T cells (Tregs)

A small subset of αβ T cells called regulatory T cells (Tregs) is regarded as a major concern by tumour immunologists. The role of Tregs as their name suggests is to regulate the activities of other T cells such as $CD8^+$ T cells, typically in an inhibitory capacity. There is increasing evidence to suggest that the recruitment of these inhibitory Tregs into the tumour environment constitutes one of the many mechanisms that tumours have developed to evade the cytotoxic immune response ((Turk et al. 2004; Wang et al. 2007), and section 1.7.2 of the main Introduction). For example, a recent study has confirmed that enrichment of Tregs in the tumour mass correlates with impaired $CD8^+$ T cell function and poor prognosis of breast cancer (Xu et al. 2010). Most Treg subsets are characterised by a $CD4^+CD25^{Hi}$profile, and constitutive expression of the transcription factor Forkhead box protein 3 (Foxp3). Tregs are capable of effectively suppressing the proliferation and activity of both $CD4^+CD25^-$ and $CD8^+$ T cells in a contact-dependent manner by inhibiting the production of immunostimulatory cytokine interleuking-2 (IL-2) (Annunziato et al. 2002; Curiel et al. 2004). Since Tregs also express surface CD3, activation of these cells by ImmTACs could result in a counterproductive inhibition of $CD8^+$ T cell-mediated cytotoxicity. To investigate whether regulatory T cells did indeed have an inhibitory effect on ImmTAC-mediated cytotoxic activity, I conducted a killing assay in which autologous $CD8^+$ T cells (present within the PBMC) were redirected to lyse PBMC pulsed with NY-ESO-1 peptide by ImmTAC-NYE, under three conditions: i) no Tregs (PBMC depleted of Tregs); ii) normal levels of Tregs (unmanipulated PBMC); and, iii) high numbers of Tregs (PBMC supplemented with Tregs in an effector to Treg ratio of 1:10). Although, there was a large difference in Treg numbers between the Treg-enriched PBMC and the unmanipulated/Treg-depleted PBMC samples, no significant difference in specific ImmTAC-redirected cytotoxicity was apparent (Figure 8.9 A, and Figure 8.10). To rule out the possibility that the Treg isolation process (performed using a human Treg isolation kit, Invitrogen) had somehow impaired Treg function, I analysed the supernatant from the killing assay depicted in Figure 8.8 A for

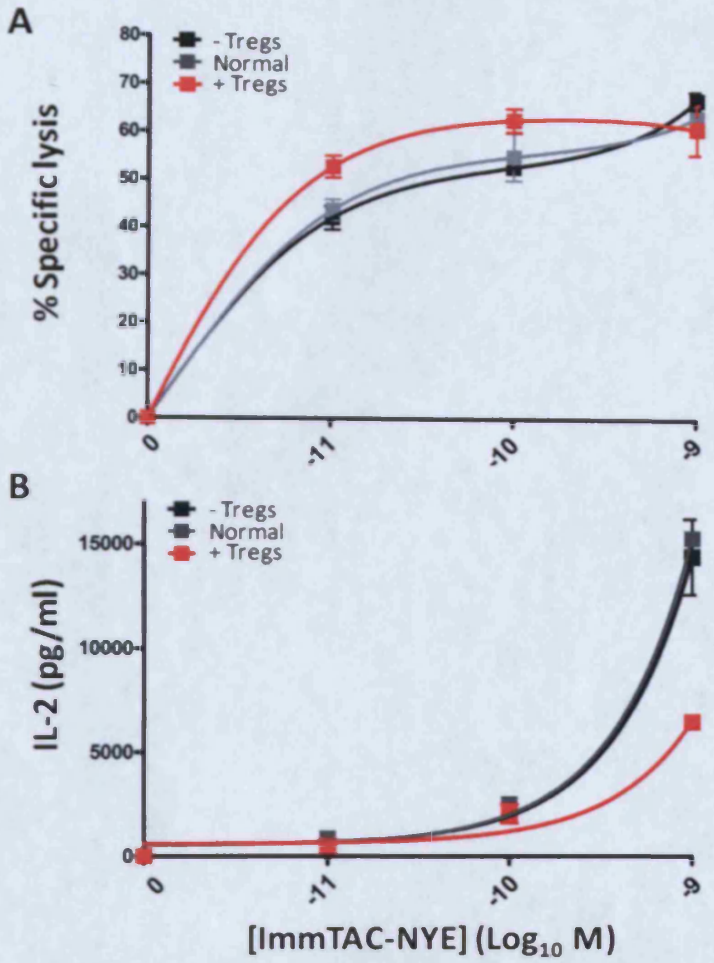

Figure 8.9: Assessing the effect of regulatory T cells on ImmTAC-NYE redirected lysis. A. The ability of ImmTAC-NYE to specifically redirect lysis of NY-ESO-$1_{157-168}$ peptide-pulsed PBMC (derived from an HLA $A2^+$ donor) by autologous $CD8^+$ T cells (within the PBMC) was recorded in a FATAL assay under conditions where regulatory T cells (Tregs) were either depleted (black squares), supplemented (red squares), or left unmanipulated (grey squares).**B .** The supernatant taken from A was analysed for the release of IL-2 after the 16 hour incubation period using a cytometric bead array (CBA). Tregs were isolated using a human Treg isolation kit (Invitrogen), and were tested for purity by FACS staining of T cells with the following staining profile $CD4^+CD25^+CD127^{Lo}$. Error bars depict s.d.fro m the mean of 2 replicates.

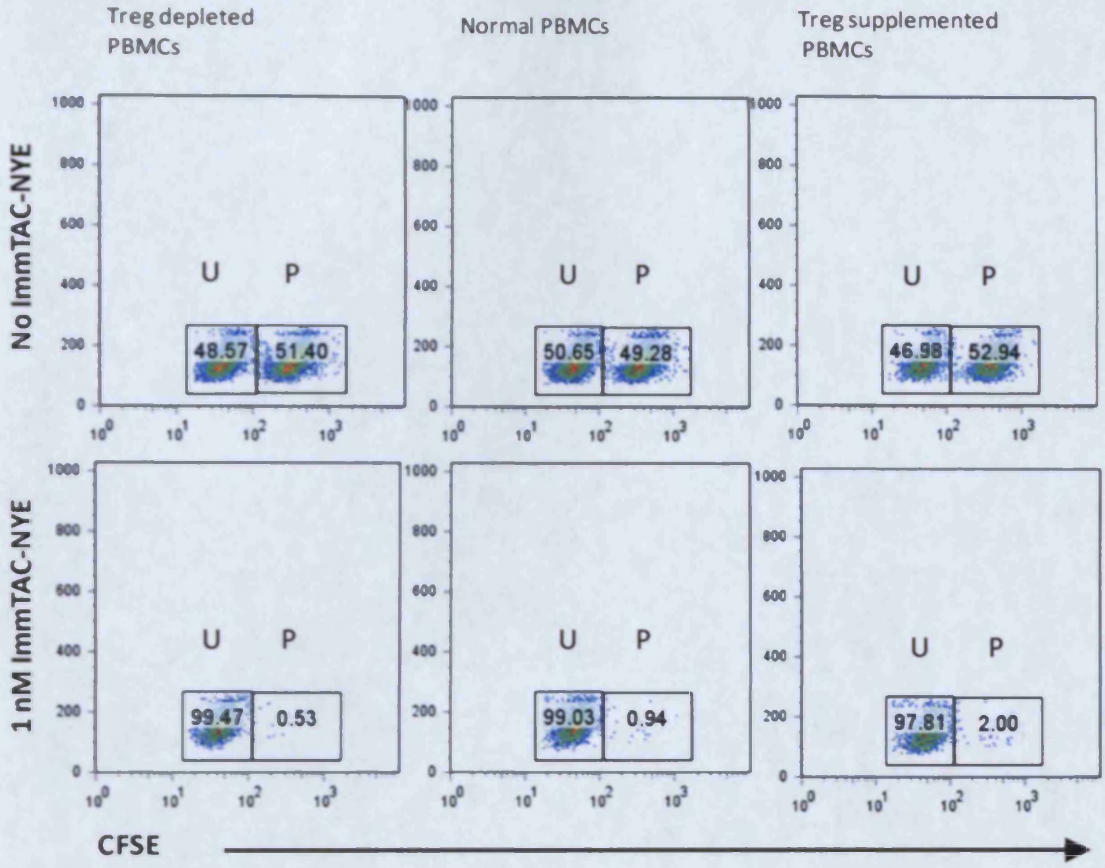

Figure 8.10: Assessing the effect of regulatory T cells on ImmTAC-NYE redirected lysis. FACS plots depicting the lysis of target (P=PBMC pulsed with NY-ESO-$1_{157\text{-}168}$ peptide) versus control (U=unpulsed PBMC) cell populations in a FATAL killing assay performed with autologous $CD8^+$ T cells (within the PBMC) in the presence (of 1 nM, bottom panel) or absence (top panel) of ImmTAC-NYE reagent, under conditions where regulatory T cells (Tregs) were either depleted (left plots), supplemented (middle plots), or left unmanipulated (right plots). The numbers within each gate correspond to the percentage of cells present within each U or P population relative to each other. The U and P populations were distinguished by staining with two different concentrations of CFSE dye.

various cytokines including IFNγ, TNF and IL-2. Although the levels of IFNγ and TNF were unperturbed for all three Treg conditions (data not shown), the level of IL-2 was significantly reduced in the Treg-enriched sample (Figure 8.8 B). This finding is consistent with the role of Tregs as 'IL-2 sinks', and confirms that the Tregs used in the killing assay (Figure 8.9 A and Figure 8.10) were functional in this respect. Although a more extensive study on the effect of Tregs on ImmTAC function may need to be performed, these initial data, implying that ImmTACs are effective even in the presence of large numbers of these inhibitory cells, are very encouraging and suggest that the presence of Tregs in tumours may not represent a major problem for ImmTAC-based therapies.

8.2.5 ImmTACs control tumour growth *in vivo*

To determine if ImmTAC reagents could affect tumour growth *in vivo*, a xenograft model was used. Immunocompromised NOD/SCID or Beige/SCID mice were engrafted with tumour cell lines (Mel526 or A375) and unstimulated PBMC on day 0, and the ImmTACs were administered intravenously (iv) an hour later and then every 24 hours for four-nine days. The size of the tumours was then measured by taking calliper readings in two perpendicular dimensions, and calculating the tumour volume using the formula: volume (mm^3) = (length x $width^2$)/2. Tumour volumes were recorded in this way three times per week, and plotted against the number of days post tumour engraftment to generate tumour growth curves (Figure 8.11). Figure 8.11 A presents data generated from mice that were engrafted with the Mel526 tumour cell line and treated intravenously with ImmTAC-gp100. In this experiment, mice received the following doses of ImmTAC-gp100: 0.1, 0.04, 0.01 and 0.004 mg/kg, post tumour engraftment. Dosing regimens were based on data derived from *in vitro* experiments (for example, 0.1-1 nM for ImmTAC-gp100, Figure 8.8 C). All four doses of ImmTAC-gp100 in this schedule inhibited tumour growth over the study period of 32 days, with the highest doses (0.1, 0.04 and 0.01 mg/kg) exhibiting substantial tumour inhibition. No reduction in tumour growth was observed in mice receiving either no ImmTAC or no PBMC, indicating that the inhibition in tumour growth was dependent on the interaction between ImmTACs and presumably $CD8^+$ T cells and possibly $CD4^+$ T cells in the PBMC sample. In Figure 8.11 B, a similar assay set-up (to the ImmTAC-gp100 experiment) was used to test the effect of ImmTAC-MAGE on the growth of the engrafted A375 tumour cell

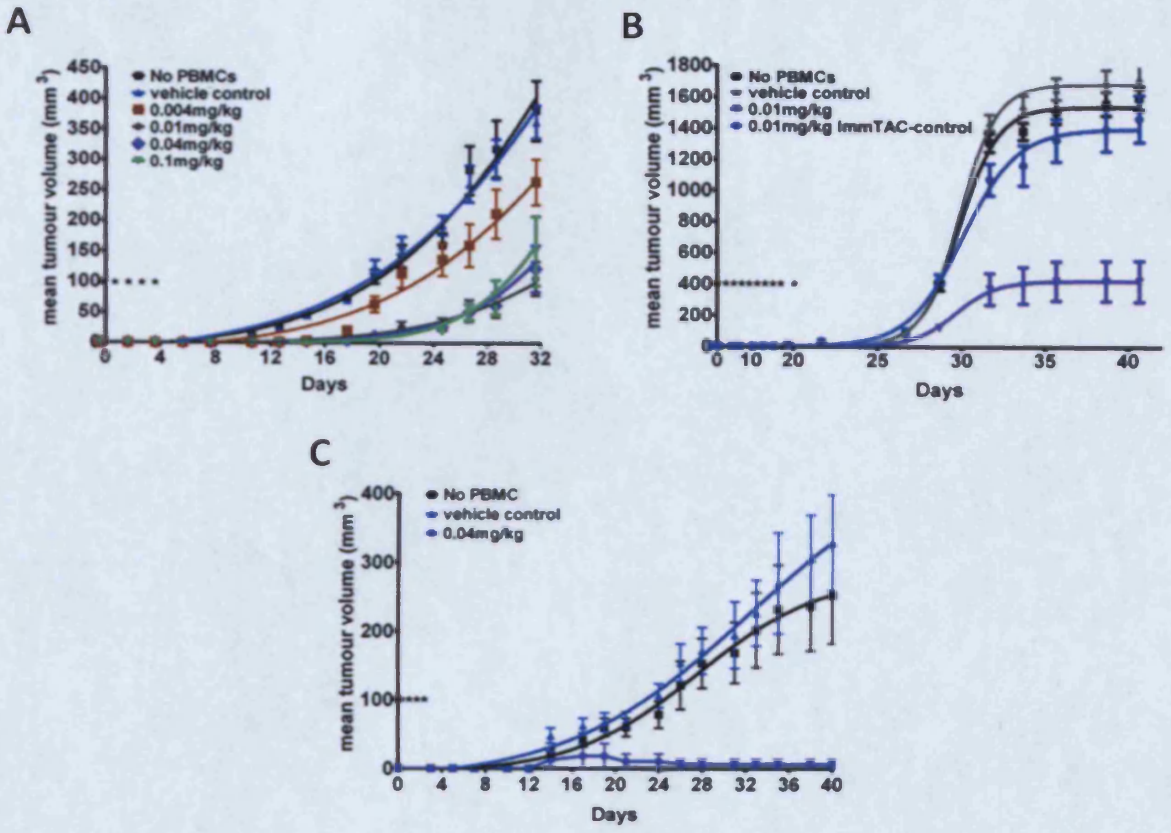

Figure 8.11: In vivo efficacy of ImmTAC molecules in NOD/SCID and Beige/SCID xenograft models. A. Dose titration of ImmTAC-gp100 in a Beige/SCID xenograft model (n=8 mice). Mel526 melanoma cells (2 x 10^6) and PBMC (5 x 10^6) were engrafted subcutaneously (sc) at day 0. Treatment with ImmTAC-gp100 commenced one hour post-engraftment and was then administered every 24 hours from days 1-4 (indicated by *) at intravenous (iv) doses of 0.1 (green inverted triangles), 0.04 (purple diamonds), 0.01 (grey circles) and 0.004 (brown squares) mg/kg. As controls, Mel526 cells were engrafted without (black squares) or with (blue triangles) PBMC and dosed with vehicle (PBS). **B.** A375 melanoma cells (2.5x10^6) were engrafted sc at day 0 with PBMC (2.5x10^6) in a NOD/SCID xenograft model (n=12 mice). ImmTAC-MAGE at 0.01 mg/kg (purple inverted triangles) or control ImmTAC at 0.01 mg/kg (blue circles) was administered iv one hour post-engraftment and every other day for an additional nine doses (indicated by *). As controls, A375 cells were engrafted without (black squares) or with (grey triangles) PBMC and dosed with vehicle (PBS). **C.** Mel526 melanoma cells (10^6) were engrafted with PBMC (10^6) at day 0 in a NOD/SCID xenograft model (n=6 mice) and dosed iv at 0.04 mg/kg with ImmTAC-MEL (purple circles) one hour post-engraftment and then every day from days 1-4 (indicated by *). As controls, Mel526 cells were engrafted without (black squares) or with (blue triangles) PBMC and dosed with vehicle (PBS). Error bars depict mean values ± s.e.m. (Figure kindly provided by Immunocore Ltd.)

line. In this trial however, a MAGE antigen-specific ImmTAC was tested alongside a non-specific control ImmTAC, both dosed at 0.01 mg/kg, and administered iv one hour post engraftment and every other day for a further nine doses. Over the 42 day data collection period, ImmTAC-MAGE substantially inhibited tumour growth, while administration of irrelevant ImmTAC did not coincide with a significant tumour grown reduction. Importantly, this investigation highlighted the fact that the scFv CD3 portion alone (albeit administered as part of an irrelevant ImmTAC) was not responsible for exerting the anti-tumour effects. The finding demonstrates that ImmTAC reagents need to bind both effector and target cells together in order to exhibit efficacy. Figure 8.11 C, summarises the results obtained with the third murine study, conducted with ImmTAC-MEL. Over a period of 40 days, a 0.04 mg/dose of ImmTAC-MEL completely inhibited tumour growth. This represented the strongest inhibitory response out of the three ImmTACs tested.

8.2.6 ImmTAVs for the eradication of HIV-infected cells

In addition to designing new therapeutic tools aimed at cancer eradication, immunologists are preoccupied with harnessing the power of the adaptive immune response to combat persistent viral infections. In particular, HIV-1 infection presents a tremendous challenge. Due to its many clever defences (see section 1.7.1 of the main Introduction), HIV-1 can evade the immune response to give it sufficient time to infect its target $CD4^+$ T cells and severely immunocompromise its host, resulting in a fatal condition called Acquired Immunodeficiency Syndrome (AIDS). One of HIV's main evasion mechanisms is the rapid generation of 'escape mutants'; epitopes derived from the virus, which are not well presented to, or recognised by the majority of naturally occurring $CD8^+$ T cells. As a result, the virus simply outpaces the $CD8^+$ T cell response and leaves these cells 'exhausted' and unable to perform their immune functions {Barnes, 2004 #2312;Oxenius, 2002b #2313}. However, a recent study involving members of my research team, reported the control of HIV-1 immune escape by $CD8^+$ T cells expressing an enhanced HIV-specific TCR {Varela-Rohena, 2008a #882}. The high affinity TCR described in this study was capable of recognising all the HIV-1 escape mutants commonly generated by the virus. As a direct result of these findings and the ImmTAC data presented in this chapter, Immunocore generated a series of ImmTAV molecules designed to redirect $CD8^+$ T cells to target common

epitopes derived from HIV-1. Although these ImmTAV-HIV molecules are still at a relatively early stage of development, some preliminary data is presented in Figures 8.12 and 8.13. In the same way that ImmTACs mediate the lysis of target cells expressing tumour antigens, ImmTAV-HIV is able to redirect polyclonal $CD8^+$ T cells to kill target cells presenting the cognate SL9 peptide (derived from p17 HIV gag) in the context of HLA A2 (Figure 8.12 A and B). More importantly, ImmTAV-HIV can elicit $CD8^+$ T cell driven lysis of HIV-infected $CD4^+$ T cells, presenting naturally low levels of endogenously processed antigen (Figure 8.12 C and Figure 8.13). Although the body of data generated with HIV-specific ImmTAVs is nowhere near as extensive as that obtained with ImmTACs, these preliminary results are certainly encouraging.

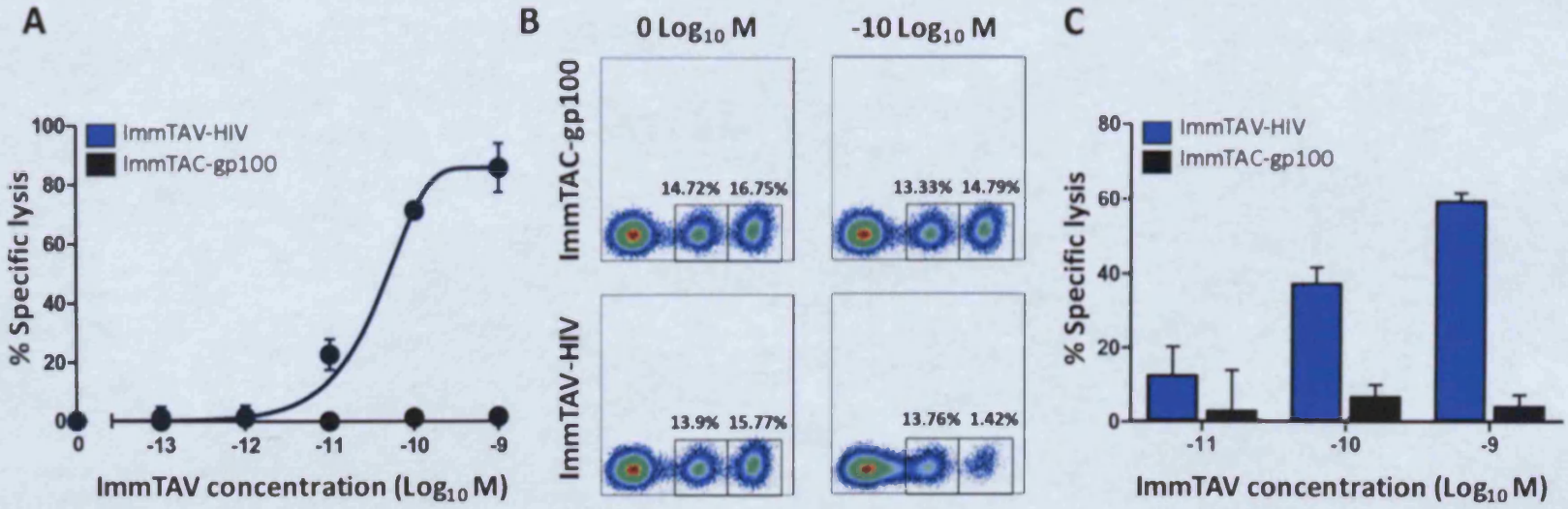

Figure 8.12: Redirected lysis of HIV-infected and SL9 peptide-pulsed target cells by primary CD8+ T cells in the presence of ImmTAV-HIV. A. Specific redirected lysis over 16 hours of T2 cells pulsed with 1 nM HIV01 $gag_{77\text{-}85}$, SL9 (SLYNTVATL) peptide in the presence of titrated doses of ImmTAV-HIV (blue circles) or ImmTAC-gp100 (black circles) negative control, and primary $CD8^+$ T cells (isolated from PBMC by MACS separation). **B.** A flow cytometric plot depicting the relative percentages of target (T2 cells pulsed with 1 nM SL9 peptide, right $CFSE^{Hi}$ population) and control (unpulsed T2 cells, left $CFSE^{Lo}$ population) in the presence of two concentrations of ImmTAV-HIV (bottom panels) or ImmTAC-gp100 (top panels), and primary $CD8^+$ T cells. **C.** Specific redirected lysis over 16 hours of HIV-infected T0 cells in the presence of titrated doses of ImmTAV-HIV (blue bars) or control ImmTAC-gp100 (black bars), and primary $CD8^+$ T cells. Lysis of HIV- infected T0 cells was compared to lysis of an internal control (uninfected HLA $A2^+$ C1R cells). Error bars depict means ± s.e.m. Representative data from 2 separate experiments shown.

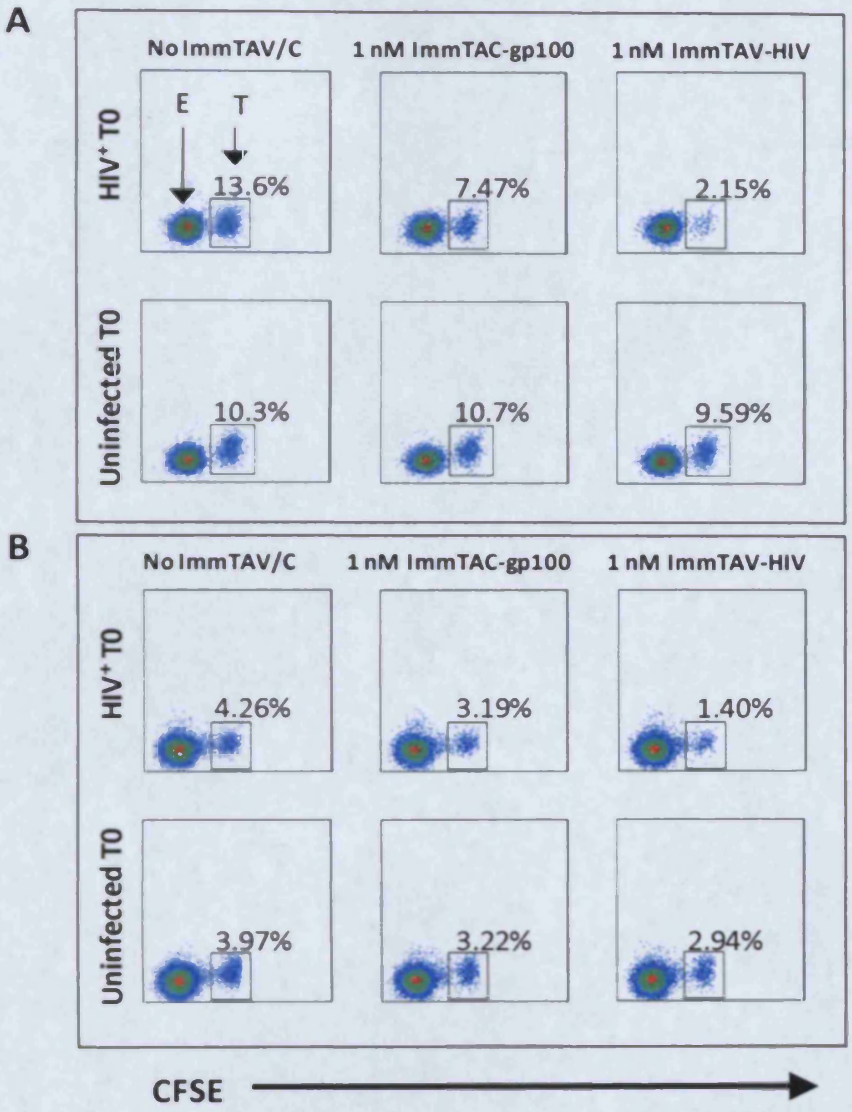

Figure 8.13: ImmTAV-HIV redirects polyclonal CD8⁺ T cells and PBMC to specifically kill HIV infected T0 cells. Flow cytometric plots summarise data from a FATAL assay performed over 12 hours, using $3x10^4$ of either HIV-1 infected (90-100% p24⁺)o r uninfected T0 cells as targets labelled with CFSE in the presence of 1n M ImmTAV-HIV, ImmTAC-gp100 (negative control) or no ImmTAV/C and an effector population. In **A**, the effectors consisted of a pure population of $15x10^4$ MACS-sorted polyclonal CD8⁺ T cells. In **B**, 10^6 unsorted PBMC were used as effectors giving a final E:T in the assay of approximately 5:1.(as in A). The numbers within each FACS plot correspond to the percentages of CFSE-labelled target (T) T0 cells relative to the CFSE-unlabelled effector (E) population.

8.3 Discussion

Harnessing the power of the adaptive immune response to combat cancer and persistent viral infections has been a long-term goal for immunotherapy. Since it is now widely recognised that the T cell response is required for the efficient *in vivo* elimination of tumour-transformed and virally-infected cells, inciting T cells to target known disease-specific antigens is of utmost clinical importance (Alexander-Miller et al. 1996; Zeh et al. 1999). Initial research, focusing on the use of bi-specific monoclonal antibodies (mAbs), has shown that redirecting the cytotoxic T cell response can achieve tumour clearance *in vivo* (Bargou et al. 2008; Baeuerle et al. 2009; Nagorsen et al. 2009). However, the success of mAbs is limited by the nature of antigens they are designed to recognise ((Chaplin 2010) and Figure 8.1).

In contrast to antibodies, TCRs can recognise any endogenously processed antigen in the form of pMHC class I molecules presented on the surface of all nucleated cells. Until recently, two issues have hindered the development of soluble TCR-directed therapy: the lack of soluble TCR production systems and the low affinities of TCRs for their antigen. A major advance in the production of soluble monoclonal TCRs (mTCRs) led by my colleague Jonathan Boulter, has yielded mTCRs which are sufficiently stable for expression on the surface of bacteriophage, and hence could be subjected to affinity maturation by phage display (Boulter et al. 2003; Li et al. 2005). Using this technique, directed molecular evolution of a number of mTCRs specific for common tumour associated antigens (TAAs) was performed, increasing the affinity of some of these wild type TCRs $>10^6$ fold to pM K_Ds ((Li et al. 2005) and Liddy et al. submitted). The fusion of these high affinity mTCRs to humanised anti-CD3 single chain (sc) Fv antibody fragments, gave rise to a novel set of reagents called Immune mobilising monoclonal TCRs Against Cancer (ImmTACs) (Figure 8.2). The work presented in this chapter demonstrates that these ImmTACs can overcome the limitations of natural TCR-mediated recognition and redirect the full might of T cell effector functions to kill tumours expressing natural epitope numbers on the cell surface (as low as 2-10 copies per cells, Liddy et al. submitted). The key features of ImmTAC design include: i) an anti-CD3 scFv moiety that activates T cells regardless of their TCR specificity; ii) a high

affinity mTCR, which binds to its cognate pMHCI with an affinity and half-life several orders of magnitude higher than the anti-CD3 scFv/CD3 interaction; and, iii) the observation that mTCRs are not internalised on binding. It is likely that these features have collectively contributed to the success of ImmTAC molecules in the eradication of tumour cells, by effectively marking these cells for execution by bystander $CD8^+$ T cells of any specificity.

The majority of the work presented in this chapter concerns the study of four ImmTACs (Table 8.1). I demonstrated that the ImmTACs used in this study are united by the following pertinent features:

i) The majority of lymphocytes activated by ImmTACs are $CD8^+$ T cells (Figure 8.4).

ii) ImmTACs activate $CD8^+$ T cells in a dose-dependent manner at cellular EC_{50} values in the low picomolar range, consistent with the K_D of the corresponding monomeric mTCR/pMHCI interactions (Table 8.1 and Figure 8.3).

iii) Polyclonal $CD8^+$ T cell activation triggered by ImmTACs elicits a polyfunctional response that includes cytokine production and lytic activity (Figures 8.4 and 8.5).

iv) The majority of $CD8^+$ T cells responding to ImmTAC stimulation display the effector memory phenotype (Figure 8.5).

v) ImmTAC-mediated effector cell activation and target cell lysis is specific and limited to cells that express cognate pMHCI molecules (Figures 8.3-8.10).

vi) The potency of ImmTACs is associated with their ability to elicit serial killing by $CD8^+$ T cells (Figures 8.6 and 8.7).

vii) ImmTAC-driven target cell lysis is not inhibited by potential activation of bystander regulatory T cells (Tregs) (Figures 8.8 and 8.9).

viii) ImmTACs exhibit *in vivo* efficacy by significantly inhibiting tumour growth in xenograft tumour NOD/SCID and Beige/SCID mouse models (Figure 8.10).

Investigating the behaviour of these novel reagents both *in vitro* and *in vivo* lead us to speculate about their mode of action in the context of the adaptive immune response as a whole. For instance, the high levels of tumour growth inhibition observed with only 5 doses of ImmTAC in two out of three mouse models (Figure 8.10 A and C) could not be entirely enacted through redirected $CD8^+$ T cells within the engrafted PBMC sample alone (Figure

8.10 A and C). Further observations that ImmTACs possess the power to induce polyfunctional $CD8^+$ T cell responses (comprising both lytic activity and the production of soluble factors) (Figure 8.5) and cause these effector cells to serially kill their targets (Figure 8.7), support a scenario in which the initial redirection of $CD8^+$ T cells acts as a catalyst that drives the recruitment of additional immune effectors to the tumour (Price et al. 1999). In simple terms, by targeting tumour antigens, ImmTACs serve to expose the tumour's identity, drawing in T cells that are naturally 'blind' to its whereabouts. The unmasking of the tumour thus represents the critical step, after which the interplay between activated redirected $CD8^+$ T cells and other mediators of the adaptive immune response guides the remainder of the tumour eradication process. It is therefore entirely possible that the initial minimal dose of ImmTAC reagent is all that is needed to instigate an amplification of the primary $CD8^+$ T cell response (potentially through epitope spreading), which could then serve to generate a self-sustaining tumour-specific immune reactivity. Further extensive work will be required to demonstrate that ImmTACs can induce a wider immune response via epitope-spreading.

In the final part of this chapter, I introduced a relative of ImmTACs, designed to target cells presenting viral antigens indicative of persistent viral infections. These molecules are called Immune mobilising monoclonal TCRs Against Viruses (ImmTAVs) to reflect this role. In particular, my studies focused on assessing the function of ImmTAV-HIV, a bi-specific immunomodulatory reagent comprising a high affinity mTCR specific for a common epitope of HIV-1. Although the optimisation of ImmTAV-HIV has not reached the same advanced stage as ImmTAC development, its ability to redirect polyclonal $CD8^+$ T cells to kill target cells pulsed with the relevant peptide and later those infected with HIV-1 is very promising (Figures 8.11 and 8.12). Further ImmTAV-HIV experiments are underway. The lack of pathogen containment facilities at Immunocore Ltd. means that the experiments will be conducted at the Cardiff University School of Medicine.

To conclude, ImmTACs and ImmTAVs collectively represent an exciting new class of soluble mTCR-based immunotherapeutic reagents. These bi-specific molecules manifest their immunomodulatory effects by: i) utilising their high affinity mTCR components to target

pMHCI molecules implicated in disease; and, ii) bringing them to the attention of polyclonal $CD8^+$ T cells by anti-CD3 scFv-mediated targeting of CD3 molecules on these immune cells. The fact that ImmTAC/Vs can redirect $CD8^+$ T cells to target any antigen, regardless of their intrinsic specificity, gives this strategy a considerable advantage over cell-based therapies (ACT and TCR gene transfer therapy, described in sections 1.8.2 and 1.8.3 of the general Introduction, and Chapter 6) that require extensive *ex vivo* lymphocyte manipulations on an individualised basis. Instead, ImmTAC/Vs can be formulated as "off-the-shelf" drugs for administration in defined dosing schedules to any patient with the relevant HLA allele and an antigen-positive tumour. These features all favour the advancement of ImmTACs into the clinic.

Chapter 9

9

GENERAL DISCUSSION

The work outlined in my thesis is linked by the common theme of optimising interactions between peptide-MHC molecules and the receptors that engages these ligands at the T cell surface (TCR and CD8/CD4 coreceptors). I have explored several translational aspects of this topic. The principal aims of this thesis were to develop strategies for enhancing the affinity of T cell/antigen interaction to:

i) Enable detection of T cells displaying low affinities for antigen with pMHC multimers;

ii) Explore means of increasing TCR affinity for antigen at the T cell surface; and,

iii) Investigate the use of soluble high affinity TCRs as therapeutic agents.

9.1 Enhancing TCR/pMHC affinity to improve T cell detection with pMHC multimers

pMHC multimer technology has transformed the study of antigen-specific T cell responses by enabling visualisation, enumeration, phenotypic characterisation and isolation of antigen specific T cells in direct *ex vivo* samples by flow cytometry. The technique has some specific advantages over other detection methods as it can identify antigen-specific cells without the need to activate them and alter their phenotype. pMHC multimers can also detect cells regardless of what effector function they possess. The extraordinary utility of such reagents is demonstrated by their use in over 7000 published studies in the last 15 years. A major obstacle standing in the way of efficient flow cytometric detection of T cells is the fact that pMHC multimer staining is dependent on a distinct TCR/pMHC affinity threshold that lies above that required for T cell activation (Laugel et al. 2007). As a consequence, conventional pMHC multimer staining procedures fail to identify functional T cells expressing low affinity TCRs that are characteristic of the majority of tumour-specific and autoreactive $CD8^+$ T cells and the nearly all $CD4^+$ T cells (Cole et al. 2007). This problem had been identified as an urgent, unmet need when I started my studies and I was tasked with testing various strategies to reduce the TCR/pMHC binding threshold required for pMHC multimer staining

and thereby open up these technologies to tumour-specific, autoimmune and MHC class II T cells.

Chapters 3, 4, and 5, comprising the first half of my thesis are united by the common theme of improving the detection of low affinity T cells using fluorochrome-conjugated pMHC multimers. Laugel *et al.* established that a K_D of ≤ 40 μM is required to observe a level of staining that allows clearly distinct tetramer positive populations of polyclonal T cells stained with conventional pMHCI reagents and 'standard' staining conditions (10 μg/ml pMHCI tetramer, for 30 minutes at 37°C) (Laugel et al. 2007). In the first part of my PhD, I aimed to reduce the TCR/pMHC affinity threshold that governs the detection of T cells with pMHC multimers. I began by investigating the properties of tetrameric pHLA A*0201 complexes containing the Q115E mutation in the α2 domain of the heavy chain (Chapter 3). By adding one further hydrogen bond to the pMHCI/CD8 interface, the Q115E substitution enhances CD8 binding by ~50% (Wooldridge et al. 2005; Wooldridge et al. 2007). MHCI molecules containing the Q115E mutation are able to engage the CD8 coreceptor with enhanced affinity without affecting the integrity of the TCR/pMHCI interaction (Wooldridge et al. 2007). Using a well characterised HLA A2-restricted, telomerase-specific system with a wide range of biophysically characterised ligands as a model, I have quantified the ability of these CD8-enhanced pMHCI tetramers to detect T cells bearing substantially weaker TCR/pMHCI interactions (approximate K_D ≥ 250 μM) than wildtype reagents (approximate K_D ≥ 80 μM). I demonstrated that the effect is achieved through a disproportionate increase in the TCR/pMHCI association rate. I went on to demonstrate that the CD8-enhanced tetramers can stain functional derived $CD8^+$ T cells in direct *ex vivo* samples that remain undetected with wildtype pMHCI tetramers.

I then went on to investigate the importance of increasing pMHC and fluorochrome valency by using an alternative multimerization scaffold called a dextramer (Chapter 4). Whilst pMHC tetramers are assembled from four pMHC molecules, dextramers are higher valency structures comprising as many as ~40 monomeric pMHCs. Dextramers offer a considerable advantage over tetramers in the detection of both $CD8^+$ and $CD4^+$ T cell populations and allow the staining of T cells bearing lower affinity TCRs than cannot be visualised by regular

pMHC tetramer staining using identical pMHC monomer. My attempts to provide a mechanistic explanation for the staining advantage afforded by dextramers over conventional tetramers were not entirely successful. Assessment of dextramer versus tetramer association rates showed that increased valency did not translate into higher rates of TCR/pMHC association. In contrast, dextramer on-rates were substantially slower than the rapid association kinetics displayed by pMHC tetramers. Microscopic imaging of T cells stained with dextramers or tetramers at physiological temperatures showed that both reagents were internalised into endocytic vesicles. Higher order pMHC multimers (pentamers, octamers, dextramers and polymers) are predicted to have generally longer interaction half-lives at the cell surface than pMHC tetramers. However, at physiological temperatures, the potential advantage of longer multimer dwell times afforded by the higher valency of dextramers is rendered largely irrelevant due to rapid internalisation kinetics (Whelan et al. 1999). Eliminating the above possible explanations for the increased success with pMHC dextramers led us to speculate that that the answer might lie in the nature of the multimerization scaffold. Unlike pMHC tetramers, which are assembled around a single streptavidin molecule, the dextran scaffold of dextramers is a polymer of glucose. The large dextran scaffold can accommodate high valencies of streptavidin, pMHC, and fluorochrome moieties, analogous to beads on a string (Figure 4.1). Furthermore, the flexibility of the dextran polymer is likely to greatly affect the conformational freedom of the attached pMHC monomers. In view of these structural differences between tetramers and dextramers, we speculate that dextramers hold an advantage over tetramers in staining low affinity T cells by engaging TCRs which are located much further apart than the pMHC 'arms' of the tetramer can extend to (pMHC multimer 'arm-span'). Therefore, while pMHC tetramer (short 'arm-span') binding relies on the close proximity of cognate TCRs (a high TCR concentration), dextramers (long 'arm-span') are able to stain cells displaying much lower TCR densities (Figure 9.1). During the course of pMHC multimer staining, the internalisation of pMHC-triggered TCRs from the T cell surface reduces the concentration of TCRs further. Since TCR density is a critical parameter in determining the efficiency of pMHC multimer staining, the 'arm-span effect' could explain why dextramers outperform tetramers in cell staining. Dextramers might be capable of continuing to bind to the cell surface long after the TCR cell surface density has gone below the threshold to allow

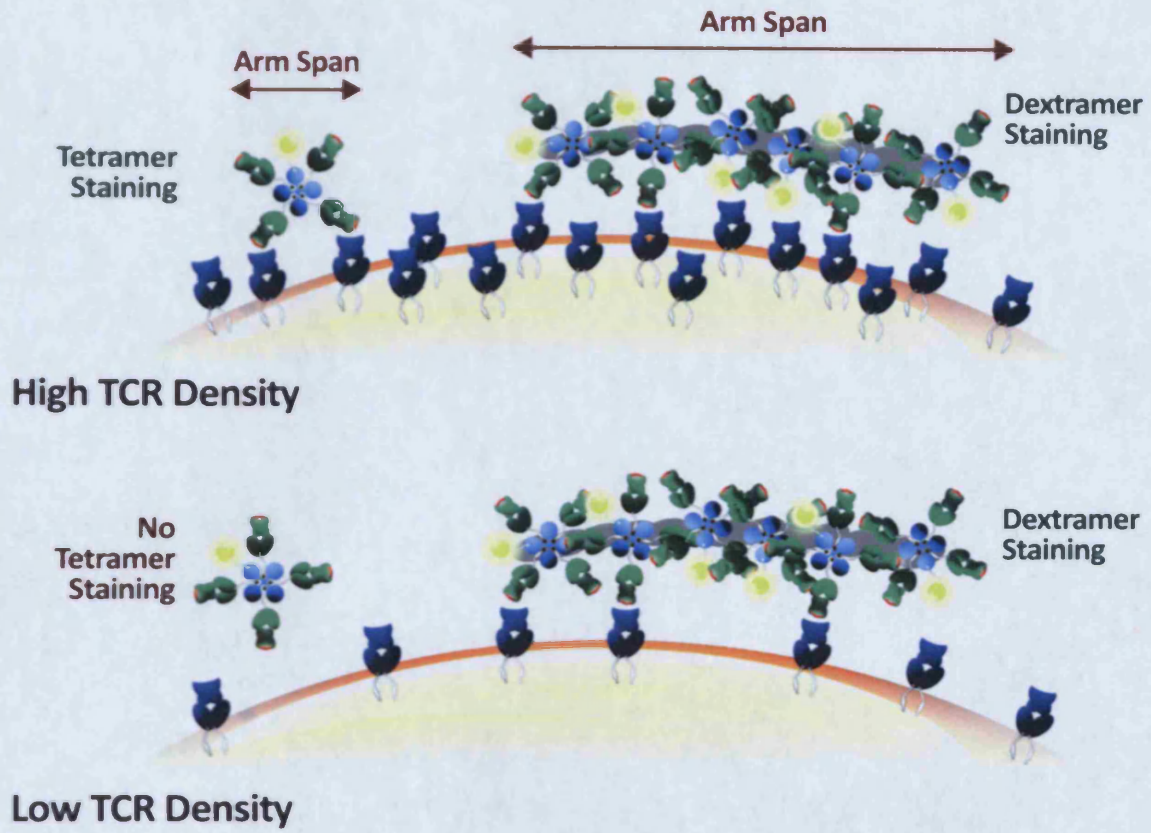

Figure 9.1: Dextramer versus tetramer staining. Successful pMHC multimer staining of T cells requires the formation of two or more productive TCR/pMHC interactions. The figure illustrates how the 'arm span' effect permits pMHC dextramers (with a long arm span) to stain T cells displaying low surface TCR densities by productively engaging TCRs located far apart. Meanwhile, pMHC tetramers (with a short arm span) require a high TCR concentration to engage two or more TCRs, and fail to stain T cells with low TCR densities. In addition, the fluorescence signal resulting from dextramer staining is substantially brighter (than tetramer staining) due to the high valency of fluorochrome molecules present on the dextran backbone. Refer to Figure 4.1 for key.

continued tetramer staining. In addition, compared to a single fluorochrome molecule conjugated to a pMHCI tetramer streptavidin scaffold, the dextran backbone is decorated by large numbers of fluorochrome molecules. Undoubtedly, the difference in fluorochrome valency between tetramers and dextramers accounts for a large part of the difference in the staining brightness that can be achieved with each reagent (Figure 9.1).

In Chapter 5, I demonstrate the importance of TCR (and CD8, where applicable) concentration in the pMHC-mediated staining of T cells. I show that the reversible protein kinase inhibitor (PKI) dasatinib improves the staining intensity of human ($CD8^+$ and $CD4^+$) and murine T cells without concomitant increases in background staining. Dasatinib enhances the capture of cognate pMHC tetramers from solution, produces higher intensity staining at lower pMHC concentrations, and substantially lowers the TCR/pMHC interaction affinity threshold required for cell staining. Accordingly, dasatinib permits the identification of T cells with very low affinity TCR/pMHC interactions, such as those indicative of tumour-specific responses and autoimmune conditions, which are not susceptible to detection by ordinary pMHC tetramer technology. Dasatinib has the additional benefit of reducing tetramer-induced cell death of the targeted cells. Although preliminary, my own experience of including dasatinib treatment in a sort-cloning protocol resulted in the growth of three $CD8^+$ T cell clones. In contrast, no T cell clones were generated following single-cell sorting of the same sample in the absence of the PKI. Dasatinib is now included in the majority of cell-sorting protocols performed in my laboratory to validate these findings.

Collectively, the findings summarised above represent novel 'tricks' aimed at increasing the detection of T cells displaying sub-optimal affinities for antigen. Whilst these 'tricks' share the goal of increasing the affinity of the TCR/pMHC interaction, they achieve this in different ways: i) CD8-enhanced pMHCI tetramers rely on the subtle increase in pMHCI/CD8 binding afforded by the Q115E substitution in the α2 domain of HLA A2; ii) dextramers owe their T cell staining efficiency to increased pMHC and fluorochrome valency, and a large, flexible multimerization scaffold; and, iii) the PKI dasatinib represents a universal way of enhancing the staining potential of $CD8^+$ and $CD4^+$ T cell subsets by increasing the TCR (and coreceptor) concentration on the T cell surface by preventing downregulation of triggered receptors.

Combining the advantages of these 'tricks' can lower the TCR/pMHC threshold of detection even further. Therefore a combination of CD8-enhanced tetramers (or dextramers) at high concentration, high staining temperature (37°C) and in the presence of dasatinib would guarantee to stain the majority of antigen-specific T cells within the T cell repertoire. However, other factors in addition to TCR/pMHC affinity are likely to control the sensitivity of T cells to pMHC antigen on the target cell surface. Factors such as TCR expression, TCR valency, CD8 expression and TCR-coreceptor adduct levels are likely to affect both the sensitivity to antigen and pMHC tetramer staining in a similar direction. Other factors such as altered expression of costimulatory molecules or inhibitory phosphatases might be expected to alter the sensitivity of T cells without necessarily affecting their avidity for multimeric cognate antigen.

In addition to enabling the characterisation of T cell responses, pMHC multimers have the potential for use as therapeutic agents. pMHC multimers can be used to manipulate a specific T cell-mediated immune response both *ex vivo* and *in vivo*, be it either to boost desirable or suppress unwanted T cell responses. Several groups have demonstrated the use of pMHC multimers in the *ex vivo* depletion of undesired (e.g. graft-versus-host disease [GvHD]-associated) T cells from transplant material before transfer to the recipient (Yuan et al. 2004; Bakker et al. 2005) and in the *in vivo* inactivation of undesired (e.g. autoreactive) T cells for the prevention or treatment of autoimmune diseases such as type I diabetes (Casares et al. 2002; Masteller et al. 2003) and rheumatoid arthritis (Zuo et al. 2002). In addition to conventional pMHC tetramers, which rely on TCR engagement to elicit activation-induced cell death (AICD) of undesired T cell populations, a class of 'suicide tetramers' promises to deliver higher levels of cytotoxicity. Currently these reagents mediate their cytotoxic effects through incorporation of radioactive isotopes such as ^{225}Ac (McDevitt et al. 2001; Yuan et al. 2004). However, the *in vivo* efficacy and off-target toxicity of 'suicide tetramers' remains to be confirmed.

Another important use of pMHC multimers is in the *ex vivo* detection and isolation of specific populations of T cells for use in adoptive therapy (Oelke et al. 2003; Barnes et al. 2004; Casalegno-Garduno et al. 2010). The rationale behind adoptive therapy is the

expansion and re-infusion of T cells with desired specificities into a patient (adoptive transfer) to enhance reactivity against defined tumour- or virus-associated antigens. Adoptive therapy has shown considerable promise in the treatment of infectious diseases (Haque et al. 2002; Heslop et al. 2010) and malignant tumours {Rosenberg, 2004a #382}. However, the viability and occasionally functional activity of pMHC multimer-enriched T cells is hampered by the persistence of TCR/pMHC interactions, subsequent signalling events, and ultimately TCR/pMHC complex internalisation (Whelan et al. 1999; Maile et al. 2001; Xu et al. 2001). Knabel and colleagues have provided a clever solution to this problem by engineering 'reversible' pMHC tetramers (also called streptamers). Streptamers dissociate into their pMHC monomeric components in the presence of a competitor such as free biotin, resulting in rapid loss of T cell staining (Knabel et al. 2002; Neudorfer et al. 2007). My study with the reversible PKI dasatinib has not only demonstrated its ability to enhance the staining of low avidity T cells, but has shown promise in reducing pMHC tetramer-induced cell death. Work is currently ongoing to confirm these preliminary findings. If successful, I envisage that dasatinib will form a crucial aspect of pMHC multimer-mediated *ex vivo* T cell purification protocols.

9.2 Enhancing TCR/pMHC affinity to increase T cell sensitivity to antigen

Adoptive transfer of *ex vivo*-derived and *in vitro*-expanded specific T cell populations is becoming an increasingly desirable strategy for the treatment of patients with cancer or infectious diseases. Numerous studies have demonstrated that T cells with an inherent ability to recognise very low antigen densities are the most effective at eliminating tumours and viruses *in vivo* (Alexander-Miller et al. 1996; Yee et al. 1999; Zeh et al. 1999; Dutoit et al. 2002). In view of this, it is becoming increasingly accepted that the quality of a T cell response may be just as important as its quantity. Studies of more than 30 TCR/pMHC interactions by members of my group have confirmed that the most sensitive T cells bear the highest affinity receptors and are also the most independent of CD8 engagement for T cell activation and pMHCI tetramer staining (unpublished and (Cole et al. 2007)). In compliance with these data, low TCR/pMHC affinity is often associated with poor clinical outcome, and strategies for increasing TCR affinity are urgently needed to improve the efficacy of adoptive T cell transfer therapies.

T cells displaying low affinities for antigen are especially prevalent within T cell subsets targeting tumour-associated or self-antigens. Isolation of these cells can be achieved using pMHC multimers and the various 'tricks' outlined in the previous section of this discussion. The *ex vivo* purified T cells can be subsequently expanded for use in adoptive therapy. Alternatively, their TCR genes can be extracted and delivered to autologous primary T lymphocytes. Optimisation of TCR gene delivery using a replication-deficient lentiviral vector (described in Chapter 6) was a prerequisite for my investigation of modulation of TCR affinity. At the outset of my PhD I had hoped to use TCR gene transfer to study how altered glycosylation affected TCR expression and function (Chapter 7) and to examine the effects of enhanced TCR affinity for cognate antigen. I abandoned plans to investigate the effects of enhanced affinity TCRs as this study was overtaken by the work of our collaborators at the University of Pennsylvania {Varela-Rohena, 2008a #882}. My interest in investigating the impact of altered surface glycosylation on T cell antigen recognition stemmed from observations that the desialylation of T cells enhanced their sensitivity to antigen (Moody et al. 2001; Daniels et al. 2002; Starr et al. 2003; Pappu et al. 2004; Brennan et al. 2006). My own studies repeated and extended these observations. Various studies have attributed the affects of desialylation to four T cell surface molecules: TCR, CD8, CD43 and CD45. My initial experiments showed that pMHCI tetramer staining increased when T cells were desialylated. It is difficult to envisage how this effect could be attributed to CD43 or CD45 when these molecules do not bind to pMHCI antigen. I next ruled out the involvement of the CD8 molecule in increased antigen engagement by showing that CD8-null tetramer staining was also enhanced by desialylation. I also showed that desialylation enhanced antigen engagement in the complete absence of the CD8 molecule using pMHCII and $CD4^+$ T cells. Desialylation was also shown to enhance antigen recognition by both $CD4^+$ T cells and γδ T cells. Collectively, these experiments strongly suggest that enhanced antigen binding and antigen recognition of desialylated T cells functions directly through events on the TCR/CD3 complex. This conclusion suggested that manipulation of TCR glycosylation might provide a universal means to enhance the antigen binding and antigen sensitivity of TCR-transduced T cells.

I proceeded to silence the N-glycosylation sites within an HIV-specific 868 TCR by site directed mutagenesis. Expression of the resultant de-glycosylated 868 TCR mutants was achieved by transduction of T cells using the optimised transduction protocol described in Chapter 6. While I was undertaking these studies, a paper was published claiming that the silencing of a single glycosylation site in a transduced TCR could be used to enhance antigen sensitivity (Kuball et al. 2009). My own studies failed to repeat the findings of Kuball *et al.* (Kuball et al. 2009). Silencing of individual N-glycosylation sites, including the conserved Gα2 N-glycosylation site analogous to the 'affinity-enhancing' c-36 site, did not result in increased antigen sensitivity. My negative findings were echoed by collaborators at Adaptimmune Ltd, who reproduced the c-36 mutation in another tumour-reactive TCR, specific for the NY-ESO-$1_{157\text{-}165}$ (SLLMWITQC) peptide antigen. Thus, whilst I have demonstrated that the removal of surface sialic acid increases antigen sensitivity of T cells, and that the effect observed is not CD8-dependent, abrogation of TCR glycosylation failed to increase the functional sensitivity of the recipient T cells. In view of this, I do not believe that the manipulation of individual TCR-specific N-glycosylation sites represents a universal way to increase TCR affinity and the antigen-sensitivity of T cells used in TCR gene transfer and adoptive T cell therapy.

TCR crystal structures such as shown in Figure 7.10 B reveal that the glycosylation motifs are strictly aligned, and are restricted to one face of the TCR. It is improbable that such ordering of glycans exists by chance. The presence of large sugar residues along one face of the TCR/pMHC complex is bound to affect how TCRs can come together. Further work will be required in order to establish how the TCR α and β chains interact with the CD3 and ζ components of the TCR before we can gain a picture of how TCRs might aggregate. I predict that glycosylation regulates T cell antigen recognition by limiting molecular interactions compared to the 'naked' glycan-free face of the TCR and by separating adjacent TCRs and components of the CD3 complex, both physically and electrostatically. Since the extent of TCR/TCR and TCR/CD3 cluster formation is an important parameter affecting T cell antigen recognition, glycosylation may regulate T cell antigen sensitivity by limiting the formation of these activation clusters. It is well documented that the TCR-TCR distance is a critical parameter in TCR-mediated signalling. TCRs fail to signal when they bind antigen but

are held >80 Å apart and exhibit progressively stronger signalling as this distance is shortened (Cebecauer et al. 2005). The increase in antigen sensitivity observed on removal of negatively charged terminal sialic acid moieties from the surface of a T cell could be explained by increased TCR clustering due to reduced electrostatic repulsion between individual TCRs.

Sialic acid forms a small component of the much bulkier glycan structures (Figure 7.1 B). We envisaged that silencing of entire N-linked glycosylation sites on a TCR would have a more dramatic effect on antigen recognition than sialylation, by allowing TCRs to come into even closer contact with each other. Although silencing of individual TCR N-glycosylation sites did not result in a substantial increase in antigen sensitivity, it is possible that the collective removal of glycans from the glycosylated face of the TCR would have a more favourable outcome. However, glycans have many important roles other than regulating T cell antigen sensitivity. My own experience has taught me that glycans at particular sites are essential for stable surface TCR expression. Furthermore, surface expression of a 'naked' TCR lacking glycosylation would leave it vulnerable to protease-mediated degradation. These obstacles are likely to impede further N-glycosylation knockout studies of the role of glycosylation in TCR-antigen recognition and rule this approach out as a way of universally increasing the efficacy of transduced TCRs. Further studies will be required in order to determine whether mechanisms that specifically target TCR sialylation could be useful in the setting of TCR gene transfer therapy.

9.3 High affinity TCRs as therapeutic agents

Soluble TCR-directed therapy has been made possible by the development of efficient soluble TCR production systems and TCR affinity maturation techniques. In Chapter 8 I evaluate the potential of soluble high affinity TCRs conjugated to immunomodulatory anti-CD3 scFv fragments to act as therapeutic molecules. These novel reagents called Immune mobilising monoclonal TCRs Against Cancer or Viruses (ImmTAC/Vs) overcome the limitations of natural TCR-mediated recognition by redirecting the polyclonal T cell immune response towards cells expressing various tumour-associated antigens and an immunodominant epitope of HIV-1. ImmTAC/Vs are designed according to the same

principles as the Bi-specific T cell Engaging (BiTE) antibodies introduced in Chapter 8. Both therapeutic molecules employ lymphocyte receptors (ImmTAC/Vs: soluble TCRs; BiTE antibodies: soluble BCRs/mAbs) for antigen recognition, and an immunomodulatory antibody to redirect the polyclonal T cell response. ImmTAC/Vs and BiTE antibodies represent an alternative to TCR gene transfer therapy for the eradication of tumours, and virally-infected cells. The advantages and disadvantages of each therapeutic approach are summarised in Table 9.1. While ImmTAV development is still at a relatively early stage, ImmTACs have demonstrated very promising *in vivo* efficacy by inhibiting tumour growth in xenograft tumour mouse models. If the protein levels that have been used in mice were scaled up to human systems it might be possible to successfully treat a patient with just milligram quantities of ImmTAC. This extends the boundaries of protein therapeutics by several orders of magnitude (Liddy et al. submitted), in addition to making ImmTAC-based therapies potentially both cheap and easy when compared to adoptive T cell therapy approaches. Preliminary results have demonstrated that the encouraging *in vivo* tumour growth results extend to murine tumour regression models (Liddy et al. submitted). These exciting data have resulted in the initiation of human clinical trials of ImmTACs in the UK and USA this year; the outcome of these trials is eagerly anticipated by all involved. To conclude, ImmTACs and ImmTAVs represent a novel class of soluble TCR-based immunotherapeutic reagents. These therapeutic molecules are a testament to rational drug design and demonstrate just how much our understanding of the TCR/pMHC interaction has increased over the past decade.

9.4 Summary

During my PhD, I have contributed to development of several strategies aimed to enhance the TCR/pMHC interaction to improve the detection and characterisation of T cells displaying low antigen sensitivity using pMHC multimers, and enhance T cell sensitivity to cognate antigen. I am hopeful that as our knowledge of the TCR/pMHC interaction central to T cell immunology develops further, its manipulation will give rise to increasingly more sophisticated therapies for cancer and infectious diseases.

Immunotherapy	Advantages	Disadvantages
TCR gene transfer	• Increases the frequency of T cells in the periphery specific for a desired disease-associated pMHC antigen. • T cells for transduction can be selected based on advantageous qualities such as polyfunctionality, cytotoxicity and persistence *in vivo*. • Transduction of different T cell subsets (eg. $CD8^+$ T cells, $CD4^+$ T cells, Tregs) to suit desired function. • Long-term persistence of antigen-specific memory T cells.	• Requirement for expensive, sterile T cell culture systems. • TCR gene therapy requires host conditioning by lymphodepletion, with toxic side effects. •Transduced T cells often less effective then parent T cells (source of TCR used for transduction). • Possible risks of TCR autoimmunity: TCR chain mispairing and reactivity against host MHC haplotypes.
Bi-specific T cell Engaging (BiTE) antibody	• mAbs are naturally soluble and are easy to manufacture. • mAbs are naturally high affinity. • BiTEs can engage T cells unlike conventional mAbs. • Can be administered as 'off the shelf' drugs. • No need for host conditioning.	• Difficulty in generating mAbs against pMHC antigen. • Possible risk of immunpathology: host against BiTE, and BiTE against host (eg. mismatched MHC haplotypes).
Immune mobilising monoclonal TCR Against Cancer/ Virus (ImmTAC/V)	• Soluble TCRs produced in bacterial cell culture systems (easy and inexpensive). • Higher affinity than BiTEs. • Engage cytotoxic $CD8^+$ T cells preferentially. • Low off-target cytotoxicity. • Can be administered as 'off the shelf' drugs. • No need for host conditioning.	• Possible risk of immunopathology: host against ImmTAC/V, and ImmTAC/V against host (eg. mismatched MHC haplotypes).

Table 9.1: Comparison of three immunotherapies.

9.5 Future Directions

Protein Kinase Inhibitors

The use of PKIs like dasatinib in improving pMHC tetramer staining has been published (Lissina et al. 2009). It would be interesting, and potentially very useful, to further formally investigate the additional benefit of this PKI in reducing pMHC multimer-mediated AICD of the targeted cells. AICD is a metabolic phenomenon that arises due to the prolonged TCR triggering which accompanies pMHC-multimer staining. AICD is therefore a major problem affecting conventional flow cytometric cell sorting protocols. By blocking early T cell signalling events downstream of TCR/pMHC engagement, dasatinib is predicted to prevent AICD and improve the efficiency of flow cytometric cell sorting. Although this property also results in the inhibition of T cell effector functions including proliferation, activation, cytokine production and degranulation, the effects of dasatinib are said to be reversible (Weichsel et al. 2008). Indeed, members of my laboratory have shown that T cells can still respond to antigen after being incubated in 50 nM dasatinib for 24h and then washed. It would therefore be interesting to determine if there are additional benefits to including dasatinib in cell sorting protocols, and compare the functionality of T cells sorted in the presence and absence of the PKI. I have obtained some preliminary data showing that sort-cloning of T cells post-dasatinib treatment rescued cells from AICD, and that the proliferation capacity of the sorted cells was not impaired. In contrast, T cells sorted from the same sample in the absence of dasatinib perished. I would like to expand on these initial findings to determine whether the effect seen with dasatinib in tetramer sort-cloning is real and reproducible. Any means to prevent pMHC multimer-mediated AICD would be a huge benefit to the T cell research community and the pursuit of this aim is extremely worthwhile.

ImmTAC/Vs

Since my involvement in the project, ImmTAC development has progressed to the exciting stage of human clinical trials. Soluble TCR-based ImmTACs hold several advantages over adoptive T cell (ACT) therapeutic approaches (see Table 9.1). One of these advantages is the low cost of ImmTAC manufacture and treatment. The projected costs of 'off the shelf' ImmTAC therapy (estimated at ~£5000/patient) are many times lower than those for ACT

(estimated at ~£100,000/patient). Thus, ImmTACs might form a new weapon in the anti-cancer armoury that will supersede current ACT efforts. However, there are areas where adoptive T therapy using TCR gene-transduced cells may have an advantage over ImmTAC/Vs. Introduction of specific TCR genes into a precisely defined cell permits the selection of cells with desired antigen specificity and required effector function (eg. improved cytotoxicity, cytokine production and persistence *in vivo*). For instance, the administration of IL-2, a cytokine produced by certain subsets of $CD4^+$ T helper cells has been shown to improve the efficacy of effector $CD8^+$ T cells transferred to patients undergoing ACT (Yee et al. 2000). In light of this, co-infusion of TAA-reactive TCR-transduced $CD8^+$ and $CD4^+$ T cells is predicted to result in a more effective anti-tumour response than infusion of each T cell subset alone. The limited number of characterised MHCII-associated TAAs has impeded the generation of pMHCII-restricted $CD4^+$ T cells for use in adoptive therapy. However, Morris *et al.* have successfully demonstrated the use of IL-2-producing $CD4^+$ T cells transduced with a high affinity pMHCI-restricted TCR to improve the *in vivo* clearance of melanoma in a murine xenograft tumour model (Morris et al. 2005). Since infusion of IFN-γ-producing $CD4^+$ T cells transduced with the same TAA-specific TCR failed to improve tumour clearance, the effective anti-tumour response was attributed to the ability of the previous subset of $CD4^+$ T cells to produce IL-2, thus providing help for $CD8^+$ T cell-mediated anti-tumour cytotoxicity. Interestingly, although $CD4^+$ T cells are not normally associated with high cytotoxicity themselves, adoptive transfer of $CD4^+$ T cells transduced with a high affinity MHCI-restricted NY-ESO-1 antigen-specific TCR were recently shown to elicit tumour lysis and clinical remission of cancer in melanoma patients (Hunder et al. 2008). In addition to transduction of T cells to achieve cytotoxicity of target cells, several groups have investigated the use of Tregs as TCR recipients (Tsang et al. 2008; Hombach et al. 2009; Brusko et al. 2010). In this scenario, Tregs transduced with a TCR specific for a targeted self-epitope would act as antigen-specific suppressor cells. A recent study has demonstrated the effective use of Tregs transduced with TCRs specific for MHCII molecules in promoting transplantation tolerance in a mouse model (Tsang et al. 2008). Such redirected Tregs might be useful in clinical applications in the context of autoimmunity and transplantation.

Another important attribute of ACT is that the infused T cells (unlike ImmTAC/Vs and other drugs) are retained within the host and can offer immune protection in cases of disease relapse. This is elegantly demonstrated by a long-term follow-up study on patients who received donor-derived EBV-specific $CD8^+$ T cells (Heslop et al. 2010). The transferred T cells were detected in the patients beyond a 9 year period, implying that they had entered the memory pool even though the infused cell lines were predominantly of the effector memory phenotype (Heslop et al. 2010). Taking the above points into consideration, it remains to be seen whether ImmTAC/Vs offer an overall therapeutic advantage over adoptive T cell therapy in the long term.

REFERENCES

Abraham, N. and A. Veillette (1990). Activation of p56lck through mutation of a regulatory carboxy-terminal tyrosine residue requires intact sites of autophosphorylation and myristylation. *Mol Cell Biol* 10 (10): 5197-5206.

Adam, M. A., N. Ramesh, A. D. Miller and W. R. Osborne (1991). Internal initiation of translation in retroviral vectors carrying picornavirus 5' nontranslated regions. *J Virol* 65 (9): 4985-4990.

Adema, G. J., A. J. de Boer, R. van 't Hullenaar, M. Denijn, D. J. Ruiter, A. M. Vogel and C. G. Figdor (1993). Melanocyte lineage-specific antigens recognized by monoclonal antibodies NKI-beteb, HMB-50, and HMB-45 are encoded by a single cDNA. *Am J Pathol* 143 (6): 1579-1585.

Agosto, L. M., J. J. Yu, M. K. Liszewski, C. Baytop, N. Korokhov, L. M. Humeau and U. O'Doherty (2009). The CXCR4-tropic human immunodeficiency virus envelope promotes more-efficient gene delivery to resting CD4+ T cells than the vesicular stomatitis virus glycoprotein G envelope. *J Virol* 83 (16): 8153-8162.

Alexander-Miller, M. A. (2000). Differential expansion and survival of high and low avidity cytotoxic T cell populations during the immune response to a viral infection. *Cell Immunol* 201 (1): 58-62.

Alexander-Miller, M. A., G. R. Leggatt and J. A. Berzofsky (1996). Selective expansion of high- or low-avidity cytotoxic T lymphocytes and efficacy for adoptive immunotherapy. *Proc Natl Acad Sci U S A* 93 (9): 4102-4107.

Almeida, J. R., D. A. Price, L. Papagno, Z. A. Arkoub, D. Sauce, E. Bornstein, T. E. Asher, A. Samri, A. Schnuriger, I. Theodorou, D. Costagliola, C. Rouzioux, H. Agut, A. G. Marcelin, D. Douek, B. Autran and V. Appay (2007). Superior control of HIV-1 replication by CD8+ T cells is reflected by their avidity, polyfunctionality, and clonal turnover. *J Exp Med* 204 (10): 2473-2485.

Altman, J. D., P. A. Moss, P. J. Goulder, D. H. Barouch, M. G. McHeyzer-Williams, J. I. Bell, A. J. McMichael and M. M. Davis (1996). Phenotypic analysis of antigen-specific T lymphocytes. *Science* 274 (5284): 94-96.

An, Z. (2009). Therapeutic Monoclonal Antibodies: From Bench to Clinic. Wiley.

An, Z. (2010). Monoclonal antibodies - a proven and rapidly expanding therapeutic modality for human diseases. *Protein Cell* 1 (4): 319-330.

Annunziato, F., L. Cosmi, F. Liotta, E. Lazzeri, R. Manetti, V. Vanini, P. Romagnani, E. Maggi and S. Romagnani (2002). Phenotype, localization, and mechanism of suppression of CD4(+)CD25(+) human thymocytes. *J Exp Med* 196 (3): 379-387.

Anson, D. S. and M. Fuller (2003). Rational development of a HIV-1 gene therapy vector. *J Gene Med* 5 (10): 829-838.

Arcaro, A., C. Gregoire, T. R. Bakker, L. Baldi, M. Jordan, L. Goffin, N. Boucheron, F. Wurm, P. A. van der Merwe, B. Malissen and I. F. Luescher (2001). CD8beta endows CD8 with efficient coreceptor function by coupling T cell receptor/CD3 to raft-associated CD8/p56(lck) complexes. *J Exp Med* 194 (10): 1485-1495.

Arcaro, A., C. Gregoire, N. Boucheron, S. Stotz, E. Palmer, B. Malissen and I. F. Luescher (2000). Essential role of CD8 palmitoylation in CD8 coreceptor function. *J Immunol* 165 (4): 2068-2076.

Arstila, T. P., A. Casrouge, V. Baron, J. Even, J. Kanellopoulos and P. Kourilsky (1999). A direct estimate of the human alphabeta T cell receptor diversity. *Science* 286 (5441): 958-961.

Ashton-Rickardt, P. G., A. Bandeira, J. R. Delaney, L. Van Kaer, H. P. Pircher, R. M. Zinkernagel and S. Tonegawa (1994). Evidence for a differential avidity model of T cell selection in the thymus. *Cell* 76 (4): 651-663.

Baeuerle, P. A., P. Kufer and R. Bargou (2009). BiTE: Teaching antibodies to engage T-cells for cancer therapy. *Curr Opin Mol Ther* 11 (1): 22-30.

Baird, P. N. and P. J. Simmons (1997). Expression of the Wilms' tumor gene (WT1) in normal hemopoiesis. *Exp Hematol* 25 (4): 312-320.

Bakker, A. H. and T. N. Schumacher (2005). MHC multimer technology: current status and future prospects. *Curr Opin Immunol* 17 (4): 428-433.

Barber, E. K., J. D. Dasgupta, S. F. Schlossman, J. M. Trevillyan and C. E. Rudd (1989). The CD4 and CD8 antigens are coupled to a protein-tyrosine kinase (p56lck) that phosphorylates the CD3 complex. *Proc Natl Acad Sci U S A* 86 (9): 3277-3281.

Bargou, R., E. Leo, G. Zugmaier, M. Klinger, M. Goebeler, S. Knop, R. Noppeney, A. Viardot, G. Hess, M. Schuler, H. Einsele, C. Brandl, A. Wolf, P. Kirchinger, P. Klappers, M. Schmidt, G. Riethmuller, C. Reinhardt, P. A. Baeuerle and P. Kufer (2008). Tumor regression in cancer patients by very low doses of a T cell-engaging antibody. *Science* 321 (5891): 974-977.

Barnes, E., S. M. Ward, V. O. Kasprowicz, G. Dusheiko, P. Klenerman and M. Lucas (2004). Ultra-sensitive class I tetramer analysis reveals previously undetectable populations of antiviral CD8+ T cells. *Eur J Immunol* 34 (6): 1570-1577.

Batard, P., D. A. Peterson, E. Devevre, P. Guillaume, J. C. Cerottini, D. Rimoldi, D. E. Speiser, L. Winther and P. Romero (2006). Dextramers: new generation of fluorescent MHC class I/peptide multimers for visualization of antigen-specific CD8+ T cells. *J Immunol Methods* 310 (1-2): 136-148.

Baum, L. G. (2002). Developing a taste for sweets. *Immunity* 16 (1): 5-8.

Baum, L. G., K. Derbin, N. L. Perillo, T. Wu, M. Pang and C. Uittenbogaart (1996). Characterization of terminal sialic acid linkages on human thymocytes. Correlation

between lectin-binding phenotype and sialyltransferase expression. *J Biol Chem* 271 (18): 10793-10799.

Beck, A., T. Wurch, C. Bailly and N. Corvaia (2010). Strategies and challenges for the next generation of therapeutic antibodies. *Nat Rev Immunol* 10 (5): 345-352.

Beebe, S. J., P. M. Fox, L. J. Rec, E. L. Willis and K. H. Schoenbach (2003). Nanosecond, high-intensity pulsed electric fields induce apoptosis in human cells. *FASEB J* 17 (11): 1493-1495.

Belmont, H. J., S. Price-Schiavi, B. Liu, K. F. Card, H. I. Lee, K. P. Han, J. Wen, S. Tang, X. Zhu, J. Merrill, P. A. Chavillaz, J. L. Wong, P. R. Rhode and H. C. Wong (2006). Potent antitumor activity of a tumor-specific soluble TCR/IL-2 fusion protein. *Clin Immunol* 121 (1): 29-39.

Bendle, G. M., J. B. Haanen and T. N. Schumacher (2009). Preclinical development of T cell receptor gene therapy. *Curr Opin Immunol* 21 (2): 209-214.

Bendle, G. M., C. Linnemann, A. I. Hooijkaas, L. Bies, M. A. de Witte, A. Jorritsma, A. D. Kaiser, N. Pouw, R. Debets, E. Kieback, W. Uckert, J. Y. Song, J. B. Haanen and T. N. Schumacher (2010). Lethal graft-versus-host disease in mouse models of T cell receptor gene therapy. *Nat Med* 16 (5): 565-570, 561p following 570.

Bennett, S. R., F. R. Carbone, F. Karamalis, R. A. Flavell, J. F. Miller and W. R. Heath (1998). Help for cytotoxic-T-cell responses is mediated by CD40 signalling. *Nature* 393 (6684): 478-480.

Biglari, A., T. D. Southgate, L. J. Fairbairn and D. E. Gilham (2006). Human monocytes expressing a CEA-specific chimeric CD64 receptor specifically target CEA-expressing tumour cells in vitro and in vivo. *Gene Ther* 13 (7): 602-610.

Bilwes, A. M., J. den Hertog, T. Hunter and J. P. Noel (1996). Structural basis for inhibition of receptor protein-tyrosine phosphatase-alpha by dimerization. *Nature* 382 (6591): 555-559.

Bjorkman, P. J. (1997). MHC restriction in three dimensions: a view of T cell receptor/ligand interactions. *Cell* 89 (2): 167-170.

Boder, E. T., K. S. Midelfort and K. D. Wittrup (2000). Directed evolution of antibody fragments with monovalent femtomolar antigen-binding affinity. *Proc Natl Acad Sci U S A* 97 (20): 10701-10705.

Boniface, J. J., J. D. Rabinowitz, C. Wulfing, J. Hampl, Z. Reich, J. D. Altman, R. M. Kantor, C. Beeson, H. M. McConnell and M. M. Davis (1998). Initiation of signal transduction through the T cell receptor requires the multivalent engagement of peptide/MHC ligands [corrected]. *Immunity* 9 (4): 459-466.

Bonilla, F. A. and H. C. Oettgen (2010). Adaptive immunity. *J Allergy Clin Immunol* 125 (2 Suppl 2): S33-40.

Boulter, J. M., M. Glick, P. T. Todorov, E. Baston, M. Sami, P. Rizkallah and B. K. Jakobsen (2003). Stable, soluble T-cell receptor molecules for crystallization and therapeutics. *Protein Eng* 16 (9): 707-711.

Bradel-Tretheway, B. G., Z. Zhen and S. Dewhurst (2003). Effects of codon-optimization on protein expression by the human herpesvirus 6 and 7 U51 open reading frame. *J Virol Methods* 111 (2): 145-156.

Brady, R. L. and A. N. Barclay (1996). The structure of CD4. *Curr Top Microbiol Immunol* 205: 1-18.

Brekke, O. H. and I. Sandlie (2003). Therapeutic antibodies for human diseases at the dawn of the twenty-first century. *Nat Rev Drug Discov* 2 (1): 52-62.

Brennan, P. J., S. J. Saouaf, S. Van Dyken, J. D. Marth, B. Li, A. Bhandoola and M. I. Greene (2006). Sialylation regulates peripheral tolerance in CD4+ T cells. *Int Immunol* 18 (5): 627-635.

Brusko, T. M., R. C. Koya, S. Zhu, M. R. Lee, A. L. Putnam, S. A. McClymont, M. I. Nishimura, S. Han, L. J. Chang, M. A. Atkinson, A. Ribas and J. A. Bluestone (2010). Human antigen-specific regulatory T cells generated by T cell receptor gene transfer. *PLoS One* 5 (7): e11726.

Buchschacher, G. L., Jr. (2001). Introduction to retroviruses and retroviral vectors. *Somat Cell Mol Genet* 26 (1-6): 1-11.

Buslepp, J., R. Zhao, D. Donnini, D. Loftus, M. Saad, E. Appella and E. J. Collins (2001). T cell activity correlates with oligomeric peptide-major histocompatibility complex binding on T cell surface. *J Biol Chem* 276 (50): 47320-47328.

Card, K. F., S. A. Price-Schiavi, B. Liu, E. Thomson, E. Nieves, H. Belmont, J. Builes, J. A. Jiao, J. Hernandez, J. Weidanz, L. Sherman, J. L. Francis, A. Amirkhosravi and H. C. Wong (2004). A soluble single-chain T-cell receptor IL-2 fusion protein retains MHC-restricted peptide specificity and IL-2 bioactivity. *Cancer Immunol Immunother* 53 (4): 345-357.

Carter, T. A., L. M. Wodicka, N. P. Shah, A. M. Velasco, M. A. Fabian, D. K. Treiber, Z. V. Milanov, C. E. Atteridge, W. H. Biggs, 3rd, P. T. Edeen, M. Floyd, J. M. Ford, R. M. Grotzfeld, S. Herrgard, D. E. Insko, S. A. Mehta, H. K. Patel, W. Pao, C. L. Sawyers, H. Varmus, P. P. Zarrinkar and D. J. Lockhart (2005). Inhibition of drug-resistant mutants of ABL, KIT, and EGF receptor kinases. *Proc Natl Acad Sci U S A* 102 (31): 11011-11016.

Cartron, G., L. Dacheux, G. Salles, P. Solal-Celigny, P. Bardos, P. Colombat and H. Watier (2002). Therapeutic activity of humanized anti-CD20 monoclonal antibody and polymorphism in IgG Fc receptor FcgammaRIIIa gene. *Blood* 99 (3): 754-758.

Casadevall, A., E. Dadachova and L. A. Pirofski (2004). Passive antibody therapy for infectious diseases. *Nat Rev Microbiol* 2 (9): 695-703.

Casalegno-Garduno, R., A. Schmitt, J. Yao, X. Wang, X. Xu, M. Freund and M. Schmitt (2010). Multimer technologies for detection and adoptive transfer of antigen-specific T cells. *Cancer Immunol Immunother* 59 (2): 195-202.

Casares, S., A. Hurtado, R. C. McEvoy, A. Sarukhan, H. von Boehmer and T. D. Brumeanu (2002). Down-regulation of diabetogenic CD4+ T cells by a soluble dimeric peptide-MHC class II chimera. *Nat Immunol* 3 (4): 383-391.

Cebecauer, M., P. Guillaume, P. Hozak, S. Mark, H. Everett, P. Schneider and I. F. Luescher (2005). Soluble MHC-peptide complexes induce rapid death of CD8+ CTL. *J Immunol* 174 (11): 6809-6819.

Cebecauer, M., P. Guillaume, P. Hozak, S. Mark, H. Everett, P. Schneider and I. F. Luescher (2005a). Soluble MHC-peptide complexes induce rapid death of CD8+ CTL. *J Immunol* 174 (11): 6809-6819.

Celis, E., V. Tsai, C. Crimi, R. DeMars, P. A. Wentworth, R. W. Chesnut, H. M. Grey, A. Sette and H. M. Serra (1994). Induction of anti-tumor cytotoxic T lymphocytes in normal humans using primary cultures and synthetic peptide epitopes. *Proc Natl Acad Sci U S A* 91 (6): 2105-2109.

Chae, W. J., H. K. Lee, J. H. Han, S. W. Kim, A. L. Bothwell, T. Morio and S. K. Lee (2004). Qualitatively differential regulation of T cell activation and apoptosis by T cell receptor zeta chain ITAMs and their tyrosine residues. *Int Immunol* 16 (9): 1225-1236.

Chan, A. C., M. Dalton, R. Johnson, G. H. Kong, T. Wang, R. Thoma and T. Kurosaki (1995). Activation of ZAP-70 kinase activity by phosphorylation of tyrosine 493 is required for lymphocyte antigen receptor function. *EMBO J* 14 (11): 2499-2508.

Chan, A. C., D. M. Desai and A. Weiss (1994). The role of protein tyrosine kinases and protein tyrosine phosphatases in T cell antigen receptor signal transduction. *Annu Rev Immunol* 12: 555-592.

Chaplin, D. D. (2010). Overview of the immune response. *J Allergy Clin Immunol* 125 (2 Suppl 2): S3-23.

Chattopadhyay, P. K., M. R. Betts, D. A. Price, E. Gostick, H. Horton, M. Roederer and S. C. De Rosa (2009). The cytolytic enzymes granyzme A, granzyme B, and perforin: expression patterns, cell distribution, and their relationship to cell maturity and bright CD57 expression. *J Leukoc Biol* 85 (1): 88-97.

Cheadle, E. J., R. E. Hawkins, H. Batha, D. G. Rothwell, G. Ashton and D. E. Gilham (2009). Eradication of established B-cell lymphoma by CD19-specific murine T cells is dependent on host lymphopenic environment and can be mediated by CD4+ and CD8+ T cells. *J Immunother* 32 (3): 207-218.

Chen, J. L., G. Stewart-Jones, G. Bossi, N. M. Lissin, L. Wooldridge, E. M. Choi, G. Held, P. R. Dunbar, R. M. Esnouf, M. Sami, J. M. Boulter, P. Rizkallah, C. Renner, A. Sewell, P. A. van der Merwe, B. K. Jakobsen, G. Griffiths, E. Y. Jones and V. Cerundolo (2005). Structural

and kinetic basis for heightened immunogenicity of T cell vaccines. *J Exp Med* 201 (8): 1243-1255.

Chen, Y. T., M. J. Scanlan, U. Sahin, O. Tureci, A. O. Gure, S. Tsang, B. Williamson, E. Stockert, M. Pfreundschuh and L. J. Old (1997). A testicular antigen aberrantly expressed in human cancers detected by autologous antibody screening. *Proc Natl Acad Sci U S A* 94 (5): 1914-1918.

Chesla, S. E., P. Selvaraj and C. Zhu (1998). Measuring two-dimensional receptor-ligand binding kinetics by micropipette. *Biophys J* 75 (3): 1553-1572.

Chicz, R. M., R. G. Urban, W. S. Lane, J. C. Gorga, L. J. Stern, D. A. Vignali and J. L. Strominger (1992). Predominant naturally processed peptides bound to HLA-DR1 are derived from MHC-related molecules and are heterogeneous in size. *Nature* 358 (6389): 764-768.

Choi, E. M., J. L. Chen, L. Wooldridge, M. Salio, A. Lissina, N. Lissin, I. F. Hermans, J. D. Silk, F. Mirza, M. J. Palmowski, P. R. Dunbar, B. K. Jakobsen, A. K. Sewell and V. Cerundolo (2003). High avidity antigen-specific CTL identified by CD8-independent tetramer staining. *J Immunol* 171 (10): 5116-5123.

Chouaib, S., C. Asselin-Paturel, F. Mami-Chouaib, A. Caignard and J. Y. Blay (1997). The host-tumor immune conflict: from immunosuppression to resistance and destruction. *Immunol Today* 18 (10): 493-497.

Choudhuri, K. and P. A. van der Merwe (2007). Molecular mechanisms involved in T cell receptor triggering. *Semin Immunol* 19 (4): 255-261.

Choudhuri, K., D. Wiseman, M. H. Brown, K. Gould and P. A. van der Merwe (2005). T-cell receptor triggering is critically dependent on the dimensions of its peptide-MHC ligand. *Nature* 436 (7050): 578-582.

Chow, L. M. and A. Veillette (1995). The Src and Csk families of tyrosine protein kinases in hemopoietic cells. *Semin Immunol* 7 (4): 207-226.

Clynes, R. A., T. L. Towers, L. G. Presta and J. V. Ravetch (2000). Inhibitory Fc receptors modulate in vivo cytoxicity against tumor targets. *Nat Med* 6 (4): 443-446.

Cohen, C. J., Y. F. Li, M. El-Gamil, P. F. Robbins, S. A. Rosenberg and R. A. Morgan (2007). Enhanced antitumor activity of T cells engineered to express T-cell receptors with a second disulfide bond. *Cancer Res* 67 (8): 3898-3903.

Cohen, C. J., Y. Zhao, Z. Zheng, S. A. Rosenberg and R. A. Morgan (2006). Enhanced antitumor activity of murine-human hybrid T-cell receptor (TCR) in human lymphocytes is associated with improved pairing and TCR/CD3 stability. *Cancer Res* 66 (17): 8878-8886.

Cole, D. K., N. J. Pumphrey, J. M. Boulter, M. Sami, J. I. Bell, E. Gostick, D. A. Price, G. F. Gao, A. K. Sewell and B. K. Jakobsen (2007). Human TCR-binding affinity is governed by MHC class restriction. *J Immunol* 178 (9): 5727-5734.

Colf, L. A., A. J. Bankovich, N. A. Hanick, N. A. Bowerman, L. L. Jones, D. M. Kranz and K. C. Garcia (2007). How a single T cell receptor recognizes both self and foreign MHC. *Cell* 129 (1): 135-146.

Corfield, A. P., S. A. Wagner, C. Paraskeva, J. R. Clamp, P. Durdey, G. Reuter and R. Schauer (1992). Loss of sialic acid O-acetylation in human colorectal cancer cells. *Biochem Soc Trans* 20 (2): 94S.

Coulie, P. G., V. Brichard, A. Van Pel, T. Wolfel, J. Schneider, C. Traversari, S. Mattei, E. De Plaen, C. Lurquin, J. P. Szikora, J. C. Renauld and T. Boon (1994). A new gene coding for a differentiation antigen recognized by autologous cytolytic T lymphocytes on HLA-A2 melanomas. *J Exp Med* 180 (1): 35-42.

Cox, A. L., J. Skipper, Y. Chen, R. A. Henderson, T. L. Darrow, J. Shabanowitz, V. H. Engelhard, D. F. Hunt and C. L. Slingluff, Jr. (1994). Identification of a peptide recognized by five melanoma-specific human cytotoxic T cell lines. *Science* 264 (5159): 716-719.

Crawford, F., H. Kozono, J. White, P. Marrack and J. Kappler (1998). Detection of antigen-specific T cells with multivalent soluble class II MHC covalent peptide complexes. *Immunity* 8 (6): 675-682.

Crawford, H., J. G. Prado, A. Leslie, S. Hue, I. Honeyborne, S. Reddy, M. van der Stok, Z. Mncube, C. Brander, C. Rousseau, J. I. Mullins, R. Kaslow, P. Goepfert, S. Allen, E. Hunter, J. Mulenga, P. Kiepiela, B. D. Walker and P. J. Goulder (2007). Compensatory mutation partially restores fitness and delays reversion of escape mutation within the immunodominant HLA-B*5703-restricted Gag epitope in chronic human immunodeficiency virus type 1 infection. *J Virol* 81 (15): 8346-8351.

Crise, B. and J. K. Rose (1992). Identification of palmitoylation sites on CD4, the human immunodeficiency virus receptor. *J Biol Chem* 267 (19): 13593-13597.

Curiel, T. J., G. Coukos, L. Zou, X. Alvarez, P. Cheng, P. Mottram, M. Evdemon-Hogan, J. R. Conejo-Garcia, L. Zhang, M. Burow, Y. Zhu, S. Wei, I. Kryczek, B. Daniel, A. Gordon, L. Myers, A. Lackner, M. L. Disis, K. L. Knutson, L. Chen and W. Zou (2004). Specific recruitment of regulatory T cells in ovarian carcinoma fosters immune privilege and predicts reduced survival. *Nat Med* 10 (9): 942-949.

D'Oro, U., M. S. Vacchio, A. M. Weissman and J. D. Ashwell (1997). Activation of the Lck tyrosine kinase targets cell surface T cell antigen receptors for lysosomal degradation. *Immunity* 7 (5): 619-628.

Daniels, M. A., L. Devine, J. D. Miller, J. M. Moser, A. E. Lukacher, J. D. Altman, P. Kavathas, K. A. Hogquist and S. C. Jameson (2001). CD8 binding to MHC class I molecules is influenced by T cell maturation and glycosylation. *Immunity* 15 (6): 1051-1061.

Daniels, M. A., K. A. Hogquist and S. C. Jameson (2002). Sweet 'n' sour: the impact of differential glycosylation on T cell responses. *Nat Immunol* 3 (10): 903-910.

Darrah, P. A., D. T. Patel, P. M. De Luca, R. W. Lindsay, D. F. Davey, B. J. Flynn, S. T. Hoff, P. Andersen, S. G. Reed, S. L. Morris, M. Roederer and R. A. Seder (2007). Multifunctional

TH1 cells define a correlate of vaccine-mediated protection against Leishmania major. *Nat Med* 13 (7): 843-850.

Davis, M. M. and P. J. Bjorkman (1988). T-cell antigen receptor genes and T-cell recognition. *Nature* 334 (6181): 395-402.

Davis, M. M., J. J. Boniface, Z. Reich, D. Lyons, J. Hampl, B. Arden and Y. Chien (1998). Ligand recognition by alpha beta T cell receptors. *Annu Rev Immunol* 16: 523-544.

Davis, S. J. and P. A. van der Merwe (1996). The structure and ligand interactions of CD2: implications for T-cell function. *Immunol Today* 17 (4): 177-187.

Davol, P. A., J. A. Smith, N. Kouttab, G. J. Elfenbein and L. G. Lum (2004). Anti-CD3 x anti-HER2 bispecific antibody effectively redirects armed T cells to inhibit tumor development and growth in hormone-refractory prostate cancer-bearing severe combined immunodeficient beige mice. *Clin Prostate Cancer* 3 (2): 112-121.

de Felipe, P., V. Martin, M. L. Cortes, M. Ryan and M. Izquierdo (1999). Use of the 2A sequence from foot-and-mouth disease virus in the generation of retroviral vectors for gene therapy. *Gene Ther* 6 (2): 198-208.

Dela Cruz, J. S., T. H. Huang, M. L. Penichet and S. L. Morrison (2004). Antibody-cytokine fusion proteins: innovative weapons in the war against cancer. *Clin Exp Med* 4 (2): 57-64.

Delves, P. J. and I. M. Roitt (2000a). The immune system. First of two parts. *N Engl J Med* 343 (1): 37-49.

Delves, P. J. and I. M. Roitt (2000b). The immune system. Second of two parts. *N Engl J Med* 343 (2): 108-117.

Demaison, C., K. Parsley, G. Brouns, M. Scherr, K. Battmer, C. Kinnon, M. Grez and A. J. Thrasher (2002). High-level transduction and gene expression in hematopoietic repopulating cells using a human immunodeficiency [correction of imunodeficiency] virus type 1-based lentiviral vector containing an internal spleen focus forming virus promoter. *Hum Gene Ther* 13 (7): 803-813.

Dembic, Z., W. Haas, S. Weiss, J. McCubrey, H. Kiefer, H. von Boehmer and M. Steinmetz (1986). Transfer of specificity by murine alpha and beta T-cell receptor genes. *Nature* 320 (6059): 232-238.

Demetriou, M., M. Granovsky, S. Quaggin and J. W. Dennis (2001). Negative regulation of T-cell activation and autoimmunity by Mgat5 N-glycosylation. *Nature* 409 (6821): 733-739.

Despont, J. P., C. A. Abel and H. M. Grey (1975). Sialic acids and sialyltransferases in murine lymphoid cells: indicators of T cell maturation. *Cell Immunol* 17 (2): 487-494.

Dietrich, J., C. Menne, J. P. Lauritsen, M. von Essen, A. B. Rasmussen, N. Odum and C. Geisler (2002). Ligand-induced TCR down-regulation is not dependent on constitutive TCR cycling. *J Immunol* 168 (11): 5434-5440.

Ding, Y. H., K. J. Smith, D. N. Garboczi, U. Utz, W. E. Biddison and D. C. Wiley (1998). Two human T cell receptors bind in a similar diagonal mode to the HLA-A2/Tax peptide complex using different TCR amino acids. *Immunity* 8 (4): 403-411.

Donnelly, M. L., G. Luke, A. Mehrotra, X. Li, L. E. Hughes, D. Gani and M. D. Ryan (2001). Analysis of the aphthovirus 2A/2B polyprotein 'cleavage' mechanism indicates not a proteolytic reaction, but a novel translational effect: a putative ribosomal 'skip'. *J Gen Virol* 82 (Pt 5): 1013-1025.

Doucey, M. A., L. Goffin, D. Naeher, O. Michielin, P. Baumgartner, P. Guillaume, E. Palmer and I. F. Luescher (2003). CD3 delta establishes a functional link between the T cell receptor and CD8. *J Biol Chem* 278 (5): 3257-3264.

Drake, D. R., 3rd, R. M. Ream, C. W. Lawrence and T. J. Braciale (2005). Transient loss of MHC class I tetramer binding after CD8+ T cell activation reflects altered T cell effector function. *J Immunol* 175 (3): 1507-1515.

Dudley, M. E., J. R. Wunderlich, P. F. Robbins, J. C. Yang, P. Hwu, D. J. Schwartzentruber, S. L. Topalian, R. Sherry, N. P. Restifo, A. M. Hubicki, M. R. Robinson, M. Raffeld, P. Duray, C. A. Seipp, L. Rogers-Freezer, K. E. Morton, S. A. Mavroukakis, D. E. White and S. A. Rosenberg (2002). Cancer regression and autoimmunity in patients after clonal repopulation with antitumor lymphocytes. *Science* 298 (5594): 850-854.

Dunn, S. M., P. J. Rizkallah, E. Baston, T. Mahon, B. Cameron, R. Moysey, F. Gao, M. Sami, J. Boulter, Y. Li and B. K. Jakobsen (2006). Directed evolution of human T cell receptor CDR2 residues by phage display dramatically enhances affinity for cognate peptide-MHC without increasing apparent cross-reactivity. *Protein Sci* 15 (4): 710-721.

Dustin, M. L., S. K. Bromley, M. M. Davis and C. Zhu (2001). Identification of self through two-dimensional chemistry and synapses. *Annu Rev Cell Dev Biol* 17: 133-157.

Dustin, M. L., S. K. Bromley, Z. Kan, D. A. Peterson and E. R. Unanue (1997a). Antigen receptor engagement delivers a stop signal to migrating T lymphocytes. *Proc Natl Acad Sci U S A* 94 (8): 3909-3913.

Dustin, M. L., L. M. Ferguson, P. Y. Chan, T. A. Springer and D. E. Golan (1996). Visualization of CD2 interaction with LFA-3 and determination of the two-dimensional dissociation constant for adhesion receptors in a contact area. *J Cell Biol* 132 (3): 465-474.

Dustin, M. L., D. E. Golan, D. M. Zhu, J. M. Miller, W. Meier, E. A. Davies and P. A. van der Merwe (1997b). Low affinity interaction of human or rat T cell adhesion molecule CD2 with its ligand aligns adhering membranes to achieve high physiological affinity. *J Biol Chem* 272 (49): 30889-30898.

Dutoit, V., V. Rubio-Godoy, P. Y. Dietrich, A. L. Quiqueres, V. Schnuriger, D. Rimoldi, D. Lienard, D. Speiser, P. Guillaume, P. Batard, J. C. Cerottini, P. Romero and D. Valmori (2001). Heterogeneous T-cell response to MAGE-A10(254-262): high avidity-specific cytolytic T lymphocytes show superior antitumor activity. *Cancer Res* 61 (15): 5850-5856.

Dutoit, V., V. Rubio-Godoy, M. A. Doucey, P. Batard, D. Lienard, D. Rimoldi, D. Speiser, P. Guillaume, J. C. Cerottini, P. Romero and D. Valmori (2002). Functional avidity of tumor antigen-specific CTL recognition directly correlates with the stability of MHC/peptide multimer binding to TCR. *J Immunol* 168 (3): 1167-1171.

Einhauer, A. and A. Jungbauer (2001). Affinity of the monoclonal antibody M1 directed against the FLAG peptide. *J Chromatogr A* 921 (1): 25-30.

Elango, N., S. Elango, P. Shivshankar and M. S. Katz (2005). Optimized transfection of mRNA transcribed from a d(A/T)100 tail-containing vector. *Biochem Biophys Res Commun* 330 (3): 958-966.

Eshhar, Z., T. Waks, G. Gross and D. G. Schindler (1993). Specific activation and targeting of cytotoxic lymphocytes through chimeric single chains consisting of antibody-binding domains and the gamma or zeta subunits of the immunoglobulin and T-cell receptors. *Proc Natl Acad Sci U S A* 90 (2): 720-724.

Fantl, W. J., J. A. Escobedo, G. A. Martin, C. W. Turck, M. del Rosario, F. McCormick and L. T. Williams (1992). Distinct phosphotyrosines on a growth factor receptor bind to specific molecules that mediate different signaling pathways. *Cell* 69 (3): 413-423.

Fitzer-Attas, C. J., D. G. Schindler, T. Waks and Z. Eshhar (1998). Harnessing Syk family tyrosine kinases as signaling domains for chimeric single chain of the variable domain receptors: optimal design for T cell activation. *J Immunol* 160 (1): 145-154.

Fraser, I. P., H. Koziel and R. A. Ezekowitz (1998). The serum mannose-binding protein and the macrophage mannose receptor are pattern recognition molecules that link innate and adaptive immunity. *Semin Immunol* 10 (5): 363-372.

Frazer, I. H., G. R. Leggatt and S. R. Mattarollo (2010). Prevention and Treatment of Papillomavirus-Related Cancers Through Immunization. *Annu Rev Immunol*

Friedrich, T. C., E. J. Dodds, L. J. Yant, L. Vojnov, R. Rudersdorf, C. Cullen, D. T. Evans, R. C. Desrosiers, B. R. Mothe, J. Sidney, A. Sette, K. Kunstman, S. Wolinsky, M. Piatak, J. Lifson, A. L. Hughes, N. Wilson, D. H. O'Connor and D. I. Watkins (2004). Reversion of CTL escape-variant immunodeficiency viruses in vivo. *Nat Med* 10 (3): 275-281.

Fujita, T., S. Ohara, T. Sugaya, K. Saigenji and K. Hotta (2000). Effects of rabbit gastrointestinal mucins and dextran on hydrochloride diffusion in vitro. *Comp Biochem Physiol B Biochem Mol Biol* 126 (3): 353-359.

Fung-Leung, W. P., M. W. Schilham, A. Rahemtulla, T. M. Kundig, M. Vollenweider, J. Potter, W. van Ewijk and T. W. Mak (1991). CD8 is needed for development of cytotoxic T cells but not helper T cells. *Cell* 65 (3): 443-449.

Gakamsky, D. M., I. F. Luescher, A. Pramanik, R. B. Kopito, F. Lemonnier, H. Vogel, R. Rigler and I. Pecht (2005). CD8 kinetically promotes ligand binding to the T-cell antigen receptor. *Biophys J* 89 (3): 2121-2133.

Galvan, M., K. Murali-Krishna, L. L. Ming, L. Baum and R. Ahmed (1998). Alterations in cell surface carbohydrates on T cells from virally infected mice can distinguish effector/memory CD8+ T cells from naive cells. *J Immunol* 161 (2): 641-648.

Gangadharan, D. and H. Cheroutre (2004). The CD8 isoform CD8alphaalpha is not a functional homologue of the TCR co-receptor CD8alphabeta. *Curr Opin Immunol* 16 (3): 264-270.

Gao, G. F., J. Tormo, U. C. Gerth, J. R. Wyer, A. J. McMichael, D. I. Stuart, J. I. Bell, E. Y. Jones and B. K. Jakobsen (1997). Crystal structure of the complex between human CD8alpha(alpha) and HLA-A2. *Nature* 387 (6633): 630-634.

Gao, G. F., B. E. Willcox, J. R. Wyer, J. M. Boulter, C. A. O'Callaghan, K. Maenaka, D. I. Stuart, E. Y. Jones, P. A. Van Der Merwe, J. I. Bell and B. K. Jakobsen (2000). Classical and nonclassical class I major histocompatibility complex molecules exhibit subtle conformational differences that affect binding to CD8alphaalpha. *J Biol Chem* 275 (20): 15232-15238.

Gao, Y., D. Xiong, M. Yang, H. Liu, H. Peng, X. Shao, Y. Xu, C. Xu, D. Fan, L. Qin, C. Yang and Z. Zhu (2004). Efficient inhibition of multidrug-resistant human tumors with a recombinant bispecific anti-P-glycoprotein x anti-CD3 diabody. *Leukemia* 18 (3): 513-520.

Garboczi, D. N., P. Ghosh, U. Utz, Q. R. Fan, W. E. Biddison and D. C. Wiley (1996). Structure of the complex between human T-cell receptor, viral peptide and HLA-A2. *Nature* 384 (6605): 134-141.

Garcia, G. G., S. B. Berger, A. A. Sadighi Akha and R. A. Miller (2005). Age-associated changes in glycosylation of CD43 and CD45 on mouse CD4 T cells. *Eur J Immunol* 35 (2): 622-631.

Garcia, G. G. and R. A. Miller (2003). Age-related defects in CD4+ T cell activation reversed by glycoprotein endopeptidase. *Eur J Immunol* 33 (12): 3464-3472.

Garcia, K. C., C. A. Scott, A. Brunmark, F. R. Carbone, P. A. Peterson, I. A. Wilson and L. Teyton (1996). CD8 enhances formation of stable T-cell receptor/MHC class I molecule complexes. *Nature* 384 (6609): 577-581.

Gascoigne, N. R., T. Zal and S. M. Alam (2001). T-cell receptor binding kinetics in T-cell development and activation. *Expert Rev Mol Med* 2001: 1-17.

Gaugler, B., B. Van den Eynde, P. van der Bruggen, P. Romero, J. J. Gaforio, E. De Plaen, B. Lethe, F. Brasseur and T. Boon (1994). Human gene MAGE-3 codes for an antigen recognized on a melanoma by autologous cytolytic T lymphocytes. *J Exp Med* 179 (3): 921-930.

Geiger, T. L., P. Nguyen, D. Leitenberg and R. A. Flavell (2001). Integrated src kinase and costimulatory activity enhances signal transduction through single-chain chimeric receptors in T lymphocytes. *Blood* 98 (8): 2364-2371.

Germeau, C., W. Ma, F. Schiavetti, C. Lurquin, E. Henry, N. Vigneron, F. Brasseur, B. Lethe, E. De Plaen, T. Velu, T. Boon and P. G. Coulie (2005). High frequency of antitumor T cells in the blood of melanoma patients before and after vaccination with tumor antigens. *J Exp Med* 201 (2): 241-248.

Gerstner, R. B., P. Carter and H. B. Lowman (2002). Sequence plasticity in the antigen-binding site of a therapeutic anti-HER2 antibody. *J Mol Biol* 321 (5): 851-862.

Gil, D., W. W. Schamel, M. Montoya, F. Sanchez-Madrid and B. Alarcon (2002). Recruitment of Nck by CD3 epsilon reveals a ligand-induced conformational change essential for T cell receptor signaling and synapse formation. *Cell* 109 (7): 901-912.

Gilham, D. E., A. O'Neil, C. Hughes, R. D. Guest, N. Kirillova, M. Lehane and R. E. Hawkins (2002). Primary polyclonal human T lymphocytes targeted to carcino-embryonic antigens and neural cell adhesion molecule tumor antigens by CD3zeta-based chimeric immune receptors. *J Immunother* 25 (2): 139-151.

Gillespie, W., J. C. Paulson, S. Kelm, M. Pang and L. G. Baum (1993). Regulation of alpha 2,3-sialyltransferase expression correlates with conversion of peanut agglutinin (PNA)+ to PNA- phenotype in developing thymocytes. *J Biol Chem* 268 (6): 3801-3804.

Glebov, O. O. and B. J. Nichols (2004). Lipid raft proteins have a random distribution during localized activation of the T-cell receptor. *Nat Cell Biol* 6 (3): 238-243.

Glover, D. J., H. J. Lipps and D. A. Jans (2005). Towards safe, non-viral therapeutic gene expression in humans. *Nat Rev Genet* 6 (4): 299-310.

Godfrey, D. I., J. Kennedy, T. Suda and A. Zlotnik (1993). A developmental pathway involving four phenotypically and functionally distinct subsets of CD3-CD4-CD8- triple-negative adult mouse thymocytes defined by CD44 and CD25 expression. *J Immunol* 150 (10): 4244-4252.

Goedert, J. J. (2000). The epidemiology of acquired immunodeficiency syndrome malignancies. *Semin Oncol* 27 (4): 390-401.

Gotter, J., B. Brors, M. Hergenhahn and B. Kyewski (2004). Medullary epithelial cells of the human thymus express a highly diverse selection of tissue-specific genes colocalized in chromosomal clusters. *J Exp Med* 199 (2): 155-166.

Graham, F. L., J. Smiley, W. C. Russell and R. Nairn (1977). Characteristics of a human cell line transformed by DNA from human adenovirus type 5. *J Gen Virol* 36 (1): 59-74.

Grakoui, A., S. K. Bromley, C. Sumen, M. M. Davis, A. S. Shaw, P. M. Allen and M. L. Dustin (1999). The immunological synapse: a molecular machine controlling T cell activation. *Science* 285 (5425): 221-227.

Green, A. E., A. Lissina, S. L. Hutchinson, R. E. Hewitt, B. Temple, D. James, J. M. Boulter, D. A. Price and A. K. Sewell (2004). Recognition of nonpeptide antigens by human V gamma 9V delta 2 T cells requires contact with cells of human origin. *Clin Exp Immunol* 136 (3): 472-482.

Grigorian, A., S. U. Lee, W. Tian, I. J. Chen, G. Gao, R. Mendelsohn, J. W. Dennis and M. Demetriou (2007). Control of T Cell-mediated autoimmunity by metabolite flux to N-glycan biosynthesis. *J Biol Chem* 282 (27): 20027-20035.

Gross, G., T. Waks and Z. Eshhar (1989). Expression of immunoglobulin-T-cell receptor chimeric molecules as functional receptors with antibody-type specificity. *Proc Natl Acad Sci U S A* 86 (24): 10024-10028.

Guillaume, P., D. F. Legler, N. Boucheron, M. A. Doucey, J. C. Cerottini and I. F. Luescher (2003). Soluble major histocompatibility complex-peptide octamers with impaired CD8 binding selectively induce Fas-dependent apoptosis. *J Biol Chem* 278 (7): 4500-4509.

Guttinger, M., M. Gassmann, K. E. Amrein and P. Burn (1992). CD45 phosphotyrosine phosphatase and p56lck protein tyrosine kinase: a functional complex crucial in T cell signal transduction. *Int Immunol* 4 (11): 1325-1330.

Hacein-Bey-Abina, S., A. Garrigue, G. P. Wang, J. Soulier, A. Lim, E. Morillon, E. Clappier, L. Caccavelli, E. Delabesse, K. Beldjord, V. Asnafi, E. MacIntyre, L. Dal Cortivo, I. Radford, N. Brousse, F. Sigaux, D. Moshous, J. Hauer, A. Borkhardt, B. H. Belohradsky, U. Wintergerst, M. C. Velez, L. Leiva, R. Sorensen, N. Wulffraat, S. Blanche, F. D. Bushman, A. Fischer and M. Cavazzana-Calvo (2008). Insertional oncogenesis in 4 patients after retrovirus-mediated gene therapy of SCID-X1. *J Clin Invest* 118 (9): 3132-3142.

Hacein-Bey-Abina, S., F. Le Deist, F. Carlier, C. Bouneaud, C. Hue, J. P. De Villartay, A. J. Thrasher, N. Wulffraat, R. Sorensen, S. Dupuis-Girod, A. Fischer, E. G. Davies, W. Kuis, L. Leiva and M. Cavazzana-Calvo (2002). Sustained correction of X-linked severe combined immunodeficiency by ex vivo gene therapy. *N Engl J Med* 346 (16): 1185-1193.

Hacein-Bey-Abina, S., C. von Kalle, M. Schmidt, F. Le Deist, N. Wulffraat, E. McIntyre, I. Radford, J. L. Villeval, C. C. Fraser, M. Cavazzana-Calvo and A. Fischer (2003). A serious adverse event after successful gene therapy for X-linked severe combined immunodeficiency. *N Engl J Med* 348 (3): 255-256.

Halin, C., V. Gafner, M. E. Villani, L. Borsi, A. Berndt, H. Kosmehl, L. Zardi and D. Neri (2003). Synergistic therapeutic effects of a tumor targeting antibody fragment, fused to interleukin 12 and to tumor necrosis factor alpha. *Cancer Res* 63 (12): 3202-3210.

Hamad, A. R., S. M. O'Herrin, M. S. Lebowitz, A. Srikrishnan, J. Bieler, J. Schneck and D. Pardoll (1998). Potent T cell activation with dimeric peptide-major histocompatibility complex class II ligand: the role of CD4 coreceptor. *J Exp Med* 188 (9): 1633-1640.

Hamai, A., H. Benlalam, F. Meslin, M. Hasmim, T. Carre, I. Akalay, B. Janji, G. Berchem, M. Z. Noman and S. Chouaib (2010). Immune surveillance of human cancer: if the cytotoxic T-lymphocytes play the music, does the tumoral system call the tune? *Tissue Antigens* 75 (1): 1-8.

Hanahan, D. and R. A. Weinberg (2000). The hallmarks of cancer. *Cell* 100 (1): 57-70.

Hanes, J., C. Schaffitzel, A. Knappik and A. Pluckthun (2000). Picomolar affinity antibodies from a fully synthetic naive library selected and evolved by ribosome display. *Nat Biotechnol* 18 (12): 1287-1292.

Hansen, T. H. and M. Bouvier (2009). MHC class I antigen presentation: learning from viral evasion strategies. *Nat Rev Immunol* 9 (7): 503-513.

Haque, T., G. M. Wilkie, M. M. Jones, C. D. Higgins, G. Urquhart, P. Wingate, D. Burns, K. McAulay, M. Turner, C. Bellamy, P. L. Amlot, D. Kelly, A. MacGilchrist, M. K. Gandhi, A. J. Swerdlow and D. H. Crawford (2007). Allogeneic cytotoxic T-cell therapy for EBV-positive posttransplantation lymphoproliferative disease: results of a phase 2 multicenter clinical trial. *Blood* 110 (4): 1123-1131.

Haque, T., G. M. Wilkie, C. Taylor, P. L. Amlot, P. Murad, A. Iley, D. Dombagoda, K. M. Britton, A. J. Swerdlow and D. H. Crawford (2002). Treatment of Epstein-Barr-virus-positive post-transplantation lymphoproliferative disease with partly HLA-matched allogeneic cytotoxic T cells. *Lancet* 360 (9331): 436-442.

Harrington, L. E., M. Galvan, L. G. Baum, J. D. Altman and R. Ahmed (2000). Differentiating between memory and effector CD8 T cells by altered expression of cell surface O-glycans. *J Exp Med* 191 (7): 1241-1246.

Haynes, N. M., M. B. Snook, J. A. Trapani, L. Cerruti, S. M. Jane, M. J. Smyth and P. K. Darcy (2001). Redirecting mouse CTL against colon carcinoma: superior signaling efficacy of single-chain variable domain chimeras containing TCR-zeta vs Fc epsilon RI-gamma. *J Immunol* 166 (1): 182-187.

Heemskerk, M. H. (2006). Optimizing TCR gene transfer. *Clin Immunol* 119 (2): 121-122.

Hennecke, J. and D. C. Wiley (2001). T cell receptor-MHC interactions up close. *Cell* 104 (1): 1-4.

Hernandez, J. D., J. Klein, S. J. Van Dyken, J. D. Marth and L. G. Baum (2007). T-cell activation results in microheterogeneous changes in glycosylation of CD45. *Int Immunol* 19 (7): 847-856.

Heslop, H. E., K. S. Slobod, M. A. Pule, G. A. Hale, A. Rousseau, C. A. Smith, C. M. Bollard, H. Liu, M. F. Wu, R. J. Rochester, P. J. Amrolia, J. L. Hurwitz, M. K. Brenner and C. M. Rooney (2010). Long-term outcome of EBV-specific T-cell infusions to prevent or treat EBV-related lymphoproliferative disease in transplant recipients. *Blood* 115 (5): 925-935.

Hess, P. R., C. Barnes, M. D. Woolard, M. D. Johnson, J. M. Cullen, E. J. Collins and J. A. Frelinger (2007). Selective deletion of antigen-specific CD8+ T cells by MHC class I tetramers coupled to the type I ribosome-inactivating protein saporin. *Blood* 109 (8): 3300-3307.

Heuser, C., A. Hombach, C. Losch, K. Manista and H. Abken (2003). T-cell activation by recombinant immunoreceptors: impact of the intracellular signalling domain on the stability of receptor expression and antigen-specific activation of grafted T cells. *Gene Ther* 10 (17): 1408-1419.

Hofmann, C., T. Harrer, V. Kubesch, K. Maurer, K. J. Metzner, K. Eismann, S. Bergmann, M. Schmitt-Haendle, G. Schuler, J. Dorrie and N. Schaft (2008). Generation of HIV-1-specific T cells by electroporation of T-cell receptor RNA. *AIDS* 22 (13): 1577-1582.

Holler, P. D., P. O. Holman, E. V. Shusta, S. O'Herrin, K. D. Wittrup and D. M. Kranz (2000). In vitro evolution of a T cell receptor with high affinity for peptide/MHC. *Proc Natl Acad Sci U S A* 97 (10): 5387-5392.

Holler, P. D. and D. M. Kranz (2003). Quantitative analysis of the contribution of TCR/pepMHC affinity and CD8 to T cell activation. *Immunity* 18 (2): 255-264.

Hombach, A. A., D. Kofler, G. Rappl and H. Abken (2009). Redirecting human CD4+CD25+ regulatory T cells from the peripheral blood with pre-defined target specificity. *Gene Ther* 16 (9): 1088-1096.

Hombach, A. A., V. Schildgen, C. Heuser, R. Finnern, D. E. Gilham and H. Abken (2007). T cell activation by antibody-like immunoreceptors: the position of the binding epitope within the target molecule determines the efficiency of activation of redirected T cells. *J Immunol* 178 (7): 4650-4657.

Horejsi, V. (2005). Lipid rafts and their roles in T-cell activation. *Microbes Infect* 7 (2): 310-316.

Huang, J., V. I. Zarnitsyna, B. Liu, L. J. Edwards, N. Jiang, B. D. Evavold and C. Zhu (2010). The kinetics of two-dimensional TCR and pMHC interactions determine T-cell responsiveness. *Nature* 464 (7290): 932-936.

Hunder, N. N., H. Wallen, J. Cao, D. W. Hendricks, J. Z. Reilly, R. Rodmyre, A. Jungbluth, S. Gnjatic, J. A. Thompson and C. Yee (2008). Treatment of metastatic melanoma with autologous CD4+ T cells against NY-ESO-1. *N Engl J Med* 358 (25): 2698-2703.

Iezzi, G., K. Karjalainen and A. Lanzavecchia (1998). The duration of antigenic stimulation determines the fate of naive and effector T cells. *Immunity* 8 (1): 89-95.

Inoue, T. and R. Krumlauf (2001). An impulse to the brain--using in vivo electroporation. *Nat Neurosci* 4 Suppl: 1156-1158.

Irles, C., A. Symons, F. Michel, T. R. Bakker, P. A. van der Merwe and O. Acuto (2003). CD45 ectodomain controls interaction with GEMs and Lck activity for optimal TCR signaling. *Nat Immunol* 4 (2): 189-197.

Irvine, D. J., M. A. Purbhoo, M. Krogsgaard and M. M. Davis (2002). Direct observation of ligand recognition by T cells. *Nature* 419 (6909): 845-849.

Janeway, C. A., Jr. (1992). The T cell receptor as a multicomponent signalling machine: CD4/CD8 coreceptors and CD45 in T cell activation. *Annu Rev Immunol* 10: 645-674.

Janeway, C. A., Jr. (2001). How the immune system protects the host from infection. *Microbes Infect* 3 (13): 1167-1171.

Janeway, C. A., Jr. and R. Medzhitov (2002). Innate immune recognition. *Annu Rev Immunol* 20: 197-216.

Jenkins, M. K., P. S. Taylor, S. D. Norton and K. B. Urdahl (1991). CD28 delivers a costimulatory signal involved in antigen-specific IL-2 production by human T cells. *J Immunol* 147 (8): 2461-2466.

Job, C. and J. Eberwine (2001). Identification of sites for exponential translation in living dendrites. *Proc Natl Acad Sci U S A* 98 (23): 13037-13042.

Johnson, L. A., R. A. Morgan, M. E. Dudley, L. Cassard, J. C. Yang, M. S. Hughes, U. S. Kammula, R. E. Royal, R. M. Sherry, J. R. Wunderlich, C. C. Lee, N. P. Restifo, S. L. Schwarz, A. P. Cogdill, R. J. Bishop, H. Kim, C. C. Brewer, S. F. Rudy, C. VanWaes, J. L. Davis, A. Mathur, R. T. Ripley, D. A. Nathan, C. M. Laurencot and S. A. Rosenberg (2009). Gene therapy with human and mouse T-cell receptors mediates cancer regression and targets normal tissues expressing cognate antigen. *Blood* 114 (3): 535-546.

Jones, S., P. D. Peng, S. Yang, C. Hsu, C. J. Cohen, Y. Zhao, J. Abad, Z. Zheng, S. A. Rosenberg and R. A. Morgan (2009). Lentiviral vector design for optimal T cell receptor gene expression in the transduction of peripheral blood lymphocytes and tumor-infiltrating lymphocytes. *Hum Gene Ther* 20 (6): 630-640.

Junutula, J. R., H. Raab, S. Clark, S. Bhakta, D. D. Leipold, S. Weir, Y. Chen, M. Simpson, S. P. Tsai, M. S. Dennis, Y. Lu, Y. G. Meng, C. Ng, J. Yang, C. C. Lee, E. Duenas, J. Gorrell, V. Katta, A. Kim, K. McDorman, K. Flagella, R. Venook, S. Ross, S. D. Spencer, W. Lee Wong, H. B. Lowman, R. Vandlen, M. X. Sliwkowski, R. H. Scheller, P. Polakis and W. Mallet (2008). Site-specific conjugation of a cytotoxic drug to an antibody improves the therapeutic index. *Nat Biotechnol* 26 (8): 925-932.

Kabouridis, P. S., A. I. Magee and S. C. Ley (1997). S-acylation of LCK protein tyrosine kinase is essential for its signalling function in T lymphocytes. *EMBO J* 16 (16): 4983-4998.

Kagi, D., B. Ledermann, K. Burki, R. M. Zinkernagel and H. Hengartner (1996). Molecular mechanisms of lymphocyte-mediated cytotoxicity and their role in immunological protection and pathogenesis in vivo. *Annu Rev Immunol* 14: 207-232.

Kaplanski, G., C. Farnarier, O. Tissot, A. Pierres, A. M. Benoliel, M. C. Alessi, S. Kaplanski and P. Bongrand (1993). Granulocyte-endothelium initial adhesion. Analysis of transient binding events mediated by E-selectin in a laminar shear flow. *Biophys J* 64 (6): 1922-1933.

Kappel, B. J., J. Pinilla-Ibarz, A. A. Kochman, J. M. Eng, V. M. Hubbard, I. Leiner, E. G. Pamer, G. Heller, M. R. van den Brink and D. A. Scheinberg (2006). Remodeling specific immunity by use of MHC tetramers: demonstration in a graft-versus-host disease model. *Blood* 107 (5): 2045-2051.

Kawakami, Y., S. Eliyahu, C. H. Delgado, P. F. Robbins, L. Rivoltini, S. L. Topalian, T. Miki and S. A. Rosenberg (1994). Cloning of the gene coding for a shared human melanoma antigen recognized by autologous T cells infiltrating into tumor. *Proc Natl Acad Sci U S A* 91 (9): 3515-3519.

Kelm, S. and R. Schauer (1997). Sialic acids in molecular and cellular interactions. *Int Rev Cytol* 175: 137-240.

Kersh, E. N., A. S. Shaw and P. M. Allen (1998). Fidelity of T cell activation through multistep T cell receptor zeta phosphorylation. *Science* 281 (5376): 572-575.

Kershaw, M. H., J. A. Westwood, L. L. Parker, G. Wang, Z. Eshhar, S. A. Mavroukakis, D. E. White, J. R. Wunderlich, S. Canevari, L. Rogers-Freezer, C. C. Chen, J. C. Yang, S. A. Rosenberg and P. Hwu (2006). A phase I study on adoptive immunotherapy using gene-modified T cells for ovarian cancer. *Clin Cancer Res* 12 (20 Pt 1): 6106-6115.

Kessels, H. W., M. C. Wolkers and T. N. Schumacher (2002). Adoptive transfer of T-cell immunity. *Trends Immunol* 23 (5): 264-269.

Khan, A. A., C. Bose, L. S. Yam, M. J. Soloski and F. Rupp (2001). Physiological regulation of the immunological synapse by agrin. *Science* 292 (5522): 1681-1686.

Kim, T. K. and J. H. Eberwine (2010). Mammalian cell transfection: the present and the future. *Anal Bioanal Chem* 397 (8): 3173-3178.

Kimachi, K., K. Sugie and H. M. Grey (2003). Effector T cells have a lower ligand affinity threshold for activation than naive T cells. *Int Immunol* 15 (7): 885-892.

Kisielow, P., H. Bluthmann, U. D. Staerz, M. Steinmetz and H. von Boehmer (1988). Tolerance in T-cell-receptor transgenic mice involves deletion of nonmature CD4+8+ thymocytes. *Nature* 333 (6175): 742-746.

Knabel, M., T. J. Franz, M. Schiemann, A. Wulf, B. Villmow, B. Schmidt, H. Bernhard, H. Wagner and D. H. Busch (2002). Reversible MHC multimer staining for functional isolation of T-cell populations and effective adoptive transfer. *Nat Med* 8 (6): 631-637.

Konig, R., S. Fleury and R. N. Germain (1996). The structural basis of CD4-MHC class II interactions: coreceptor contributions to T cell receptor antigen recognition and oligomerization-dependent signal transduction. *Curr Top Microbiol Immunol* 205: 19-46.

Krangel, M. S. (1987). Endocytosis and recycling of the T3-T cell receptor complex. The role of T3 phosphorylation. *J Exp Med* 165 (4): 1141-1159.

Kruschinski, A., A. Moosmann, I. Poschke, H. Norell, M. Chmielewski, B. Seliger, R. Kiessling, T. Blankenstein, H. Abken and J. Charo (2008). Engineering antigen-specific primary human NK cells against HER-2 positive carcinomas. *Proc Natl Acad Sci U S A* 105 (45): 17481-17486.

Kuball, J., M. L. Dossett, M. Wolfl, W. Y. Ho, R. H. Voss, C. Fowler and P. D. Greenberg (2007). Facilitating matched pairing and expression of TCR chains introduced into human T cells. *Blood* 109 (6): 2331-2338.

Kuball, J., B. Hauptrock, V. Malina, E. Antunes, R. H. Voss, M. Wolfl, R. Strong, M. Theobald and P. D. Greenberg (2009). Increasing functional avidity of TCR-redirected T cells by removing defined N-glycosylation sites in the TCR constant domain. *J Exp Med* 206 (2): 463-475.

Kuo, C. T. and J. M. Leiden (1999). Transcriptional regulation of T lymphocyte development and function. *Annu Rev Immunol* 17: 149-187.

Lau, K. S., E. A. Partridge, A. Grigorian, C. I. Silvescu, V. N. Reinhold, M. Demetriou and J. W. Dennis (2007). Complex N-glycan number and degree of branching cooperate to regulate cell proliferation and differentiation. *Cell* 129 (1): 123-134.

Laugel, B., J. M. Boulter, N. Lissin, A. Vuidepot, Y. Li, E. Gostick, L. E. Crotty, D. C. Douek, J. Hemelaar, D. A. Price, B. K. Jakobsen and A. K. Sewell (2005). Design of soluble recombinant T cell receptors for antigen targeting and T cell inhibition. *J Biol Chem* 280 (3): 1882-1892.

Laugel, B., H. A. van den Berg, E. Gostick, D. K. Cole, L. Wooldridge, J. Boulter, A. Milicic, D. A. Price and A. K. Sewell (2007). Different T cell receptor affinity thresholds and CD8 coreceptor dependence govern cytotoxic T lymphocyte activation and tetramer binding properties. *J Biol Chem* 282 (33): 23799-23810.

Leroux-Roels, G., A. H. Batens, I. Desombere, B. Van Den Steen, C. Vander Stichele, G. Maertens and F. Hulstaert (2005). Immunogenicity and tolerability of intradermal administration of an HCV E1-based vaccine candidate in healthy volunteers and patients with resolved or ongoing chronic HCV infection. *Hum Vaccin* 1 (2): 61-65.

Leslie, A. J., K. J. Pfafferott, P. Chetty, R. Draenert, M. M. Addo, M. Feeney, Y. Tang, E. C. Holmes, T. Allen, J. G. Prado, M. Altfeld, C. Brander, C. Dixon, D. Ramduth, P. Jeena, S. A. Thomas, A. St John, T. A. Roach, B. Kupfer, G. Luzzi, A. Edwards, G. Taylor, H. Lyall, G. Tudor-Williams, V. Novelli, J. Martinez-Picado, P. Kiepiela, B. D. Walker and P. J. Goulder (2004). HIV evolution: CTL escape mutation and reversion after transmission. *Nat Med* 10 (3): 282-289.

Lev, A., R. Noy, K. Oved, H. Novak, D. Segal, P. Walden, D. Zehn and Y. Reiter (2004). Tumor-specific Ab-mediated targeting of MHC-peptide complexes induces regression of human tumor xenografts in vivo. *Proc Natl Acad Sci U S A* 101 (24): 9051-9056.

Lewis, P. F. and M. Emerman (1994). Passage through mitosis is required for oncoretroviruses but not for the human immunodeficiency virus. *J Virol* 68 (1): 510-516.

Li, L., L. N. Liu, S. Feller, C. Allen, R. Shivakumar, J. Fratantoni, L. A. Wolfraim, H. Fujisaki, D. Campana, N. Chopas, S. Dzekunov and M. Peshwa (2009). Expression of chimeric antigen receptors in natural killer cells with a regulatory-compliant non-viral method. *Cancer Gene Ther* 17 (3): 147-154.

Li, Y., R. Moysey, P. E. Molloy, A. L. Vuidepot, T. Mahon, E. Baston, S. Dunn, N. Liddy, J. Jacob, B. K. Jakobsen and J. M. Boulter (2005). Directed evolution of human T-cell receptors with picomolar affinities by phage display. *Nat Biotechnol* 23 (3): 349-354.

Lieberman, J. (2003). The ABCs of granule-mediated cytotoxicity: new weapons in the arsenal. *Nat Rev Immunol* 3 (5): 361-370.

Lin, J. and A. Weiss (2003). The tyrosine phosphatase CD148 is excluded from the immunologic synapse and down-regulates prolonged T cell signaling. *J Cell Biol* 162 (4): 673-682.

Lissina, A., K. Ladell, A. Skowera, M. Clement, E. Edwards, R. Seggewiss, H. A. van den Berg, E. Gostick, K. Gallagher, E. Jones, J. J. Melenhorst, A. J. Godkin, M. Peakman, D. A. Price, A. K. Sewell and L. Wooldridge (2009). Protein kinase inhibitors substantially improve the physical detection of T-cells with peptide-MHC tetramers. *J Immunol Methods* 340 (1): 11-24.

Liu, G. Y., P. J. Fairchild, R. M. Smith, J. R. Prowle, D. Kioussis and D. C. Wraith (1995). Low avidity recognition of self-antigen by T cells permits escape from central tolerance. *Immunity* 3 (4): 407-415.

Loffler, A., P. Kufer, R. Lutterbuse, F. Zettl, P. T. Daniel, J. M. Schwenkenbecher, G. Riethmuller, B. Dorken and R. C. Bargou (2000). A recombinant bispecific single-chain antibody, CD19 x CD3, induces rapid and high lymphoma-directed cytotoxicity by unstimulated T lymphocytes. *Blood* 95 (6): 2098-2103.

Lombardo, L. J., F. Y. Lee, P. Chen, D. Norris, J. C. Barrish, K. Behnia, S. Castaneda, L. A. Cornelius, J. Das, A. M. Doweyko, C. Fairchild, J. T. Hunt, I. Inigo, K. Johnston, A. Kamath, D. Kan, H. Klei, P. Marathe, S. Pang, R. Peterson, S. Pitt, G. L. Schieven, R. J. Schmidt, J. Tokarski, M. L. Wen, J. Wityak and R. M. Borzilleri (2004). Discovery of N-(2-chloro-6-methyl- phenyl)-2-(6-(4-(2-hydroxyethyl)- piperazin-1-yl)-2-methylpyrimidin-4-ylamino)thiazole-5-carboxamide (BMS-354825), a dual Src/Abl kinase inhibitor with potent antitumor activity in preclinical assays. *J Med Chem* 47 (27): 6658-6661.

Lotan, R., E. Skutelsky, D. Danon and N. Sharon (1975). The purification, composition, and specificity of the anti-T lectin from peanut (Arachis hypogaea). *J Biol Chem* 250 (21): 8518-8523.

Lowe, J. B. (2001). Glycosylation, immunity, and autoimmunity. *Cell* 104 (6): 809-812.

Luton, F., M. Buferne, J. Davoust, A. M. Schmitt-Verhulst and C. Boyer (1994). Evidence for protein tyrosine kinase involvement in ligand-induced TCR/CD3 internalization and surface redistribution. *J Immunol* 153 (1): 63-72.

Madakamutil, L. T., U. Christen, C. J. Lena, Y. Wang-Zhu, A. Attinger, M. Sundarrajan, W. Ellmeier, M. G. von Herrath, P. Jensen, D. R. Littman and H. Cheroutre (2004). CD8alphaalpha-mediated survival and differentiation of CD8 memory T cell precursors. *Science* 304 (5670): 590-593.

Magnusson, M. K., K. E. Meade, R. Nakamura, J. Barrett and C. E. Dunbar (2002). Activity of STI571 in chronic myelomonocytic leukemia with a platelet-derived growth factor beta receptor fusion oncogene. *Blood* 100 (3): 1088-1091.

Maile, R., B. Wang, W. Schooler, A. Meyer, E. J. Collins and J. A. Frelinger (2001). Antigen-specific modulation of an immune response by in vivo administration of soluble MHC class I tetramers. *J Immunol* 167 (7): 3708-3714.

Mansoor, W., D. E. Gilham, F. C. Thistlethwaite and R. E. Hawkins (2005). Engineering T cells for cancer therapy. *Br J Cancer* 93 (10): 1085-1091.

Marin, V., H. Kakuda, E. Dander, C. Imai, D. Campana, A. Biondi and G. D'Amico (2007). Enhancement of the anti-leukemic activity of cytokine induced killer cells with an anti-CD19 chimeric receptor delivering a 4-1BB-zeta activating signal. *Exp Hematol* 35 (9): 1388-1397.

Maroun, C. R. and M. Julius (1994). Distinct roles for CD4 and CD8 as co-receptors in T cell receptor signalling. *Eur J Immunol* 24 (4): 959-966.

Masiero, S., C. Del Vecchio, R. Gavioli, G. Mattiuzzo, M. G. Cusi, L. Micheli, F. Gennari, A. Siccardi, W. A. Marasco, G. Palu and C. Parolin (2005). T-cell engineering by a chimeric T-cell receptor with antibody-type specificity for the HIV-1 gp120. *Gene Ther* 12 (4): 299-310.

Mason, D. (1998). A very high level of crossreactivity is an essential feature of the T-cell receptor. *Immunol Today* 19 (9): 395-404.

Mason, D. W. and A. F. Williams (1980). The kinetics of antibody binding to membrane antigens in solution and at the cell surface. *Biochem J* 187 (1): 1-20.

Masteller, E. L., M. R. Warner, W. Ferlin, V. Judkowski, D. Wilson, N. Glaichenhaus and J. A. Bluestone (2003). Peptide-MHC class II dimers as therapeutics to modulate antigen-specific T cell responses in autoimmune diabetes. *J Immunol* 171 (10): 5587-5595.

Maugh, T. H. (1981). FDA approves hepatitis B vaccine. *Science* 214 (4525): 1113.

McDevitt, M. R., D. Ma, L. T. Lai, J. Simon, P. Borchardt, R. K. Frank, K. Wu, V. Pellegrini, M. J. Curcio, M. Miederer, N. H. Bander and D. A. Scheinberg (2001). Tumor therapy with targeted atomic nanogenerators. *Science* 294 (5546): 1537-1540.

McKeithan, T. W. (1995). Kinetic proofreading in T-cell receptor signal transduction. *Proc Natl Acad Sci U S A* 92 (11): 5042-5046.

McMichael, A. J. and C. A. O'Callaghan (1998). A new look at T cells. *J Exp Med* 187 (9): 1367-1371.

Mehier-Humbert, S. and R. H. Guy (2005). Physical methods for gene transfer: improving the kinetics of gene delivery into cells. *Adv Drug Deliv Rev* 57 (5): 733-753.

Melenhorst, J. J., P. Scheinberg, P. K. Chattopadhyay, A. Lissina, E. Gostick, D. K. Cole, L. Wooldridge, H. A. van den Berg, E. Bornstein, N. F. Hensel, D. C. Douek, M. Roederer, A. K. Sewell, A. J. Barrett and D. A. Price (2008). Detection of low avidity CD8(+) T cell populations with coreceptor-enhanced peptide-major histocompatibility complex class I tetramers. *J Immunol Methods* 338 (1-2): 31-39.

Messer, G., J. Zemmour, H. T. Orr, P. Parham, E. H. Weiss and J. Girdlestone (1992). HLA-J, a second inactivated class I HLA gene related to HLA-G and HLA-A. Implications for the evolution of the HLA-A-related genes. *J Immunol* 148 (12): 4043-4053.

Michel, M. L., S. Pol, C. Brechot and P. Tiollais (2001). Immunotherapy of chronic hepatitis B by anti HBV vaccine: from present to future. *Vaccine* 19 (17-19): 2395-2399.

Miller, M. J., O. Safrina, I. Parker and M. D. Cahalan (2004). Imaging the single cell dynamics of CD4+ T cell activation by dendritic cells in lymph nodes. *J Exp Med* 200 (7): 847-856.

Miller, M. J., S. H. Wei, I. Parker and M. D. Cahalan (2002). Two-photon imaging of lymphocyte motility and antigen response in intact lymph node. *Science* 296 (5574): 1869-1873.

Minami, Y., L. E. Samelson and R. D. Klausner (1987). Internalization and cycling of the T cell antigen receptor. Role of protein kinase C. *J Biol Chem* 262 (27): 13342-13347.

Minguet, S., M. Swamy, B. Alarcon, I. F. Luescher and W. W. Schamel (2007). Full activation of the T cell receptor requires both clustering and conformational changes at CD3. *Immunity* 26 (1): 43-54.

Mitsuyasu, R. T., P. A. Anton, S. G. Deeks, D. T. Scadden, E. Connick, M. T. Downs, A. Bakker, M. R. Roberts, C. H. June, S. Jalali, A. A. Lin, R. Pennathur-Das and K. M. Hege (2000). Prolonged survival and tissue trafficking following adoptive transfer of CD4zeta gene-modified autologous CD4(+) and CD8(+) T cells in human immunodeficiency virus-infected subjects. *Blood* 96 (3): 785-793.

Moebius, U., G. Kober, A. L. Griscelli, T. Hercend and S. C. Meuer (1991). Expression of different CD8 isoforms on distinct human lymphocyte subpopulations. *Eur J Immunol* 21 (8): 1793-1800.

Molldrem, J. J., P. P. Lee, S. Kant, E. Wieder, W. Jiang, S. Lu, C. Wang and M. M. Davis (2003). Chronic myelogenous leukemia shapes host immunity by selective deletion of high-avidity leukemia-specific T cells. *J Clin Invest* 111 (5): 639-647.

Molloy, P. E., A. K. Sewell and B. K. Jakobsen (2005). Soluble T cell receptors: novel immunotherapies. *Curr Opin Pharmacol* 5 (4): 438-443.

Monks, C. R., B. A. Freiberg, H. Kupfer, N. Sciaky and A. Kupfer (1998). Three-dimensional segregation of supramolecular activation clusters in T cells. *Nature* 395 (6697): 82-86.

Moody, A. M., D. Chui, P. A. Reche, J. J. Priatel, J. D. Marth and E. L. Reinherz (2001). Developmentally regulated glycosylation of the CD8alphabeta coreceptor stalk modulates ligand binding. *Cell* 107 (4): 501-512.

Morgan, R. A., M. E. Dudley, J. R. Wunderlich, M. S. Hughes, J. C. Yang, R. M. Sherry, R. E. Royal, S. L. Topalian, U. S. Kammula, N. P. Restifo, Z. Zheng, A. Nahvi, C. R. de Vries, L. J. Rogers-Freezer, S. A. Mavroukakis and S. A. Rosenberg (2006). Cancer regression in patients after transfer of genetically engineered lymphocytes. *Science* 314 (5796): 126-129.

Morris, E., D. Hart, L. Gao, A. Tsallios, S. A. Xue and H. Stauss (2006). Generation of tumor-specific T-cell therapies. *Blood Rev* 20 (2): 61-69.

Morris, E. C., A. Tsallios, G. M. Bendle, S. A. Xue and H. J. Stauss (2005). A critical role of T cell antigen receptor-transduced MHC class I-restricted helper T cells in tumor protection. *Proc Natl Acad Sci U S A* 102 (22): 7934-7939.

Muller, D. and R. E. Kontermann (2007). Recombinant bispecific antibodies for cellular cancer immunotherapy. *Curr Opin Mol Ther* 9 (4): 319-326.

Myung, P. S., N. J. Boerthe and G. A. Koretzky (2000). Adapter proteins in lymphocyte antigen-receptor signaling. *Curr Opin Immunol* 12 (3): 256-266.

Nagorsen, D., R. Bargou, D. Ruttinger, P. Kufer, P. A. Baeuerle and G. Zugmaier (2009). Immunotherapy of lymphoma and leukemia with T-cell engaging BiTE antibody blinatumomab. *Leuk Lymphoma* 50 (6): 886-891.

Naldini, L., U. Blomer, P. Gallay, D. Ory, R. Mulligan, F. H. Gage, I. M. Verma and D. Trono (1996). In vivo gene delivery and stable transduction of nondividing cells by a lentiviral vector. *Science* 272 (5259): 263-267.

Nel, A. E. (2002a). T-cell activation through the antigen receptor. Part 1: signaling components, signaling pathways, and signal integration at the T-cell antigen receptor synapse. *J Allergy Clin Immunol* 109 (5): 758-770.

Nel, A. E. and N. Slaughter (2002b). T-cell activation through the antigen receptor. Part 2: role of signaling cascades in T-cell differentiation, anergy, immune senescence, and development of immunotherapy. *J Allergy Clin Immunol* 109 (6): 901-915.

Nelson, A. L., E. Dhimolea and J. M. Reichert (2010). Development trends for human monoclonal antibody therapeutics. *Nat Rev Drug Discov* 9 (10): 767-774.

Neudorfer, J., B. Schmidt, K. M. Huster, F. Anderl, M. Schiemann, G. Holzapfel, T. Schmidt, L. Germeroth, H. Wagner, C. Peschel, D. H. Busch and H. Bernhard (2007). Reversible HLA multimers (Streptamers) for the isolation of human cytotoxic T lymphocytes functionally active against tumor- and virus-derived antigens. *J Immunol Methods* 320 (1-2): 119-131.

Ngoi, S. M., A. C. Chien and C. G. Lee (2004). Exploiting internal ribosome entry sites in gene therapy vector design. *Curr Gene Ther* 4 (1): 15-31.

Nguyen, H. H., M. Zemlin, Ivanov, II, J. Andrasi, C. Zemlin, H. L. Vu, R. Schelonka, H. W. Schroeder, Jr. and J. Mestecky (2007). Heterosubtypic immunity to influenza A virus infection requires a properly diversified antibody repertoire. *J Virol* 81 (17): 9331-9338.

Niedergang, F., A. Dautry-Varsat and A. Alcover (1997). Peptide antigen or superantigen-induced down-regulation of TCRs involves both stimulated and unstimulated receptors. *J Immunol* 159 (4): 1703-1710.

Niedermann, G. (2002). Immunological functions of the proteasome. *Curr Top Microbiol Immunol* 268: 91-136.

Nitta, T., S. Murata, T. Ueno, K. Tanaka and Y. Takahama (2008). Thymic microenvironments for T-cell repertoire formation. *Adv Immunol* 99: 59-94.

Nolan, K. F., C. O. Yun, Y. Akamatsu, J. C. Murphy, S. O. Leung, E. J. Beecham and R. P. Junghans (1999). Bypassing immunization: optimized design of "designer T cells" against carcinoembryonic antigen (CEA)-expressing tumors, and lack of suppression by soluble CEA. *Clin Cancer Res* 5 (12): 3928-3941.

Norment, A. M., R. D. Salter, P. Parham, V. H. Engelhard and D. R. Littman (1988). Cell-cell adhesion mediated by CD8 and MHC class I molecules. *Nature* 336 (6194): 79-81.

O'Callaghan C, A., M. F. Byford, J. R. Wyer, B. E. Willcox, B. K. Jakobsen, A. J. McMichael and J. I. Bell (1999). BirA enzyme: production and application in the study of membrane receptor-ligand interactions by site-specific biotinylation. *Anal Biochem* 266 (1): 9-15.

Obar, J. J. and L. Lefrancois (2010). Memory CD8+ T cell differentiation. *Ann N Y Acad Sci* 1183: 251-266.

Oehen, S. U., P. S. Ohashi, K. Burki, H. Hengartner, R. M. Zinkernagel and P. Aichele (1994). Escape of thymocytes and mature T cells from clonal deletion due to limiting tolerogen expression levels. *Cell Immunol* 158 (2): 342-352.

Oelke, M., M. V. Maus, D. Didiano, C. H. June, A. Mackensen and J. P. Schneck (2003). Ex vivo induction and expansion of antigen-specific cytotoxic T cells by HLA-Ig-coated artificial antigen-presenting cells. *Nat Med* 9 (5): 619-624.

Ogg, G. S., A. S. King, P. R. Dunbar and A. J. McMichael (1999). Isolation of HIV-1-specific cytotoxic T lymphocytes using human leukocyte antigen-coated beads. *AIDS* 13 (14): 1991-1993.

Oji, Y., H. Inohara, M. Nakazawa, Y. Nakano, S. Akahani, S. Nakatsuka, S. Koga, A. Ikeba, S. Abeno, Y. Honjo, Y. Yamamoto, S. Iwai, K. Yoshida, Y. Oka, H. Ogawa, J. Yoshida, K. Aozasa, T. Kubo and H. Sugiyama (2003a). Overexpression of the Wilms' tumor gene WT1 in head and neck squamous cell carcinoma. *Cancer Sci* 94 (6): 523-529.

Oji, Y., Y. Miyoshi, S. Koga, Y. Nakano, A. Ando, S. Nakatsuka, A. Ikeba, E. Takahashi, N. Sakaguchi, A. Yokota, N. Hosen, K. Ikegame, M. Kawakami, A. Tsuboi, Y. Oka, H. Ogawa, K. Aozasa, S. Noguchi and H. Sugiyama (2003b). Overexpression of the Wilms' tumor gene WT1 in primary thyroid cancer. *Cancer Sci* 94 (7): 606-611.

Oji, Y., H. Yamamoto, M. Nomura, Y. Nakano, A. Ikeba, S. Nakatsuka, S. Abeno, E. Kiyotoh, T. Jomgeow, M. Sekimoto, R. Nezu, Y. Yoshikawa, Y. Inoue, N. Hosen, M. Kawakami, A. Tsuboi, Y. Oka, H. Ogawa, S. Souda, K. Aozasa, M. Monden and H. Sugiyama (2003c). Overexpression of the Wilms' tumor gene WT1 in colorectal adenocarcinoma. *Cancer Sci* 94 (8): 712-717.

Okamoto, S., J. Mineno, H. Ikeda, H. Fujiwara, M. Yasukawa, H. Shiku and I. Kato (2009). Improved expression and reactivity of transduced tumor-specific TCRs in human lymphocytes by specific silencing of endogenous TCR. *Cancer Res* 69 (23): 9003-9011.

Ostergaard, H. L. and I. S. Trowbridge (1990). Coclustering CD45 with CD4 or CD8 alters the phosphorylation and kinase activity of p56lck. *J Exp Med* 172 (1): 347-350.

Oxenius, A., D. A. Price, H. F. Gunthard, S. J. Dawson, C. Fagard, L. Perrin, M. Fischer, R. Weber, M. Plana, F. Garcia, B. Hirschel, A. McLean and R. E. Phillips (2002a). Stimulation of HIV-specific cellular immunity by structured treatment interruption fails to enhance viral control in chronic HIV infection. *Proc Natl Acad Sci U S A* 99 (21): 13747-13752.

Oxenius, A., A. K. Sewell, S. J. Dawson, H. F. Gunthard, M. Fischer, G. M. Gillespie, S. L. Rowland-Jones, C. Fagard, B. Hirschel, R. E. Phillips and D. A. Price (2002b). Functional discrepancies in HIV-specific CD8+ T-lymphocyte populations are related to plasma virus load. *J Clin Immunol* 22 (6): 363-374.

Palmenberg, A. C. (1990). Proteolytic processing of picornaviral polyprotein. *Annu Rev Microbiol* 44: 603-623.

Pappu, B. P. and P. A. Shrikant (2004). Alteration of cell surface sialylation regulates antigen-induced naive CD8+ T cell responses. *J Immunol* 173 (1): 275-284.

Patel, S. D., M. Moskalenko, D. Smith, B. Maske, M. H. Finer and J. G. McArthur (1999). Impact of chimeric immune receptor extracellular protein domains on T cell function. *Gene Ther* 6 (3): 412-419.

Pfeifer, A. and I. M. Verma (2001). Gene therapy: promises and problems. *Annu Rev Genomics Hum Genet* 2: 177-211.

Pink, J. R. (1983). Changes in T-lymphocyte glycoprotein structures associated with differentiation. *Contemp Top Mol Immunol* 9: 89-113.

Piper, J. W., R. A. Swerlick and C. Zhu (1998). Determining force dependence of two-dimensional receptor-ligand binding affinity by centrifugation. *Biophys J* 74 (1): 492-513.

Pittet, M. J., V. Rubio-Godoy, G. Bioley, P. Guillaume, P. Batard, D. Speiser, I. Luescher, J. C. Cerottini, P. Romero and A. Zippelius (2003). Alpha 3 domain mutants of peptide/MHC class I multimers allow the selective isolation of high avidity tumor-reactive CD8 T cells. *J Immunol* 171 (4): 1844-1849.

Plaksin, D., K. Polakova, P. McPhie and D. H. Margulies (1997). A three-domain T cell receptor is biologically active and specifically stains cell surface MHC/peptide complexes. *J Immunol* 158 (5): 2218-2227.

Polson, A. G., J. Calemine-Fenaux, P. Chan, W. Chang, E. Christensen, S. Clark, F. J. de Sauvage, D. Eaton, K. Elkins, J. M. Elliott, G. Frantz, R. N. Fuji, A. Gray, K. Harden, G. S. Ingle, N. M. Kljavin, H. Koeppen, C. Nelson, S. Prabhu, H. Raab, S. Ross, D. S. Slaga, J. P. Stephan, S. J. Scales, S. D. Spencer, R. Vandlen, B. Wranik, S. F. Yu, B. Zheng and A. Ebens (2009). Antibody-drug conjugates for the treatment of non-Hodgkin's lymphoma: target and linker-drug selection. *Cancer Res* 69 (6): 2358-2364.

Precopio, M. L., M. R. Betts, J. Parrino, D. A. Price, E. Gostick, D. R. Ambrozak, T. E. Asher, D. C. Douek, A. Harari, G. Pantaleo, R. Bailer, B. S. Graham, M. Roederer and R. A. Koup (2007). Immunization with vaccinia virus induces polyfunctional and phenotypically distinctive CD8(+) T cell responses. *J Exp Med* 204 (6): 1405-1416.

Priatel, J. J., D. Chui, N. Hiraoka, C. J. Simmons, K. B. Richardson, D. M. Page, M. Fukuda, N. M. Varki and J. D. Marth (2000). The ST3Gal-I sialyltransferase controls CD8+ T lymphocyte homeostasis by modulating O-glycan biosynthesis. *Immunity* 12 (3): 273-283.

Price, D. A., P. Klenerman, B. L. Booth, R. E. Phillips and A. K. Sewell (1999). Cytotoxic T lymphocytes, chemokines and antiviral immunity. *Immunol Today* 20 (5): 212-216.

Purbhoo, M. A., J. M. Boulter, D. A. Price, A. L. Vuidepot, C. S. Hourigan, P. R. Dunbar, K. Olson, S. J. Dawson, R. E. Phillips, B. K. Jakobsen, J. I. Bell and A. K. Sewell (2001). The human CD8 coreceptor effects cytotoxic T cell activation and antigen sensitivity primarily by mediating complete phosphorylation of the T cell receptor zeta chain. *J Biol Chem* 276 (35): 32786-32792.

Purbhoo, M. A., D. J. Irvine, J. B. Huppa and M. M. Davis (2004). T cell killing does not require the formation of a stable mature immunological synapse. *Nat Immunol* 5 (5): 524-530.

Purbhoo, M. A., Y. Li, D. H. Sutton, J. E. Brewer, E. Gostick, G. Bossi, B. Laugel, R. Moysey, E. Baston, N. Liddy, B. Cameron, A. D. Bennett, R. Ashfield, A. Milicic, D. A. Price, B. J. Classon, A. K. Sewell and B. K. Jakobsen (2007). The HLA A*0201-restricted hTERT(540-548) peptide is not detected on tumor cells by a CTL clone or a high-affinity T-cell receptor. *Mol Cancer Ther* 6 (7): 2081-2091.

Purbhoo, M. A., D. H. Sutton, J. E. Brewer, R. E. Mullings, M. E. Hill, T. M. Mahon, J. Karbach, E. Jager, B. J. Cameron, N. Lissin, P. Vyas, J. L. Chen, V. Cerundolo and B. K. Jakobsen (2006). Quantifying and imaging NY-ESO-1/LAGE-1-derived epitopes on tumor cells using high affinity T cell receptors. *J Immunol* 176 (12): 7308-7316.

Qian, D. and A. Weiss (1997). T cell antigen receptor signal transduction. *Curr Opin Cell Biol* 9 (2): 205-212.

Rabinowitz, J. D., C. Beeson, D. S. Lyons, M. M. Davis and H. M. McConnell (1996). Kinetic discrimination in T-cell activation. *Proc Natl Acad Sci U S A* 93 (4): 1401-1405.

Rahemtulla, A., W. P. Fung-Leung, M. W. Schilham, T. M. Kundig, S. R. Sambhara, A. Narendran, A. Arabian, A. Wakeham, C. J. Paige, R. M. Zinkernagel and et al. (1991). Normal development and function of CD8+ cells but markedly decreased helper cell activity in mice lacking CD4. *Nature* 353 (6340): 180-184.

Ramsdell, F. and B. J. Fowlkes (1992). Maintenance of in vivo tolerance by persistence of antigen. *Science* 257 (5073): 1130-1134.

Rapoport, A. P., E. A. Stadtmauer, N. Aqui, A. Badros, J. Cotte, L. Chrisley, E. Veloso, Z. Zheng, S. Westphal, R. Mair, N. Chi, B. Ratterree, M. F. Pochran, S. Natt, J. Hinkle, C. Sickles, A. Sohal, K. Ruehle, C. Lynch, L. Zhang, D. L. Porter, S. Luger, C. Guo, H. B. Fang, W. Blackwelder, K. Hankey, D. Mann, R. Edelman, C. Frasch, B. L. Levine, A. Cross and C. H. June (2005). Restoration of immunity in lymphopenic individuals with cancer by vaccination and adoptive T-cell transfer. *Nat Med* 11 (11): 1230-1237.

Ravot, E., G. Comolli, F. Lori and J. Lisziewicz (2002). High efficiency lentiviral gene delivery in non-dividing cells by deoxynucleoside treatment. *J Gene Med* 4 (2): 161-169.

Recillas-Targa, F. (2006). Multiple strategies for gene transfer, expression, knockdown, and chromatin influence in mammalian cell lines and transgenic animals. *Mol Biotechnol* 34 (3): 337-354.

Reisner, Y., M. Linker-Israeli and N. Sharon (1976). Separation of mouse thymocytes into two subpopulations by the use of peanut agglutinin. *Cell Immunol* 25 (1): 129-134.

Resh, M. D. and H. P. Ling (1990). Identification of a 32K plasma membrane protein that binds to the myristylated amino-terminal sequence of p60v-src. *Nature* 346 (6279): 84-86.

Robbins, P. F., R. A. Morgan, S. A. Feldman, J. C. Yang, R. M. Sherry, M. E. Dudley, J. R. Wunderlich, A. V. Nahvi, L. J. Helman, C. L. Mackall, U. S. Kammula, M. S. Hughes, N. P. Restifo, M. Raffeld, C. C. Lee, C. L. Levy, Y. F. Li, M. El-Gamil, S. L. Schwarz, C. Laurencot and S. A. Rosenberg (2011). Tumor Regression in Patients With Metastatic Synovial Cell Sarcoma and Melanoma Using Genetically Engineered Lymphocytes Reactive With NY-ESO-1. *J Clin Oncol* 29 (7): 917-924.

Rocha, B. and H. von Boehmer (1991). Peripheral selection of the T cell repertoire. *Science* 251 (4998): 1225-1228.

Romieu, R., M. Baratin, M. Kayibanda, V. Lacabanne, M. Ziol, J. G. Guillet and M. Viguier (1998). Passive but not active CD8+ T cell-based immunotherapy interferes with liver tumor progression in a transgenic mouse model. *J Immunol* 161 (10): 5133-5137.

Rooney, C. M., C. A. Smith, C. Y. Ng, S. Loftin, C. Li, R. A. Krance, M. K. Brenner and H. E. Heslop (1995). Use of gene-modified virus-specific T lymphocytes to control Epstein-Barr-virus-related lymphoproliferation. *Lancet* 345 (8941): 9-13.

Rosenberg, S. A. (2001). Progress in human tumour immunology and immunotherapy. *Nature* 411 (6835): 380-384.

Rosenberg, S. A. and M. E. Dudley (2004a). Cancer regression in patients with metastatic melanoma after the transfer of autologous antitumor lymphocytes. *Proc Natl Acad Sci U S A* 101 Suppl 2: 14639-14645.

Rosenberg, S. A., M. T. Lotze, L. M. Muul, S. Leitman, A. E. Chang, S. E. Ettinghausen, Y. L. Matory, J. M. Skibber, E. Shiloni, J. T. Vetto and et al. (1985). Observations on the systemic administration of autologous lymphokine-activated killer cells and recombinant interleukin-2 to patients with metastatic cancer. *N Engl J Med* 313 (23): 1485-1492.

Rosenberg, S. A., J. C. Yang and N. P. Restifo (2004b). Cancer immunotherapy: moving beyond current vaccines. *Nat Med* 10 (9): 909-915.

Rosenberg, S. A., J. C. Yang, D. E. White and S. M. Steinberg (1998). Durability of complete responses in patients with metastatic cancer treated with high-dose interleukin-2: identification of the antigens mediating response. *Ann Surg* 228 (3): 307-319.

Rudd, P. M., M. R. Wormald, R. L. Stanfield, M. Huang, N. Mattsson, J. A. Speir, J. A. DiGennaro, J. S. Fetrow, R. A. Dwek and I. A. Wilson (1999). Roles for glycosylation of cell surface receptors involved in cellular immune recognition. *J Mol Biol* 293 (2): 351-366.

Rudolph, M. G., R. L. Stanfield and I. A. Wilson (2006). How TCRs bind MHCs, peptides, and coreceptors. *Annu Rev Immunol* 24: 419-466.

Rudolph, M. G. and I. A. Wilson (2002). The specificity of TCR/pMHC interaction. *Curr Opin Immunol* 14 (1): 52-65.

Rutledge, E. A. and C. A. Enns (1996). Cleavage of the transferrin receptor is influenced by the composition of the O-linked carbohydrate at position 104. *J Cell Physiol* 168 (2): 284-293.

Ryan, M. D. and J. Drew (1994). Foot-and-mouth disease virus 2A oligopeptide mediated cleavage of an artificial polyprotein. *EMBO J* 13 (4): 928-933.

Sacchettini, J. C., L. G. Baum and C. F. Brewer (2001). Multivalent protein-carbohydrate interactions. A new paradigm for supermolecular assembly and signal transduction. *Biochemistry* 40 (10): 3009-3015.

Sadegh-Nasseri, S., M. Chen, K. Narayan and M. Bouvier (2008). The convergent roles of tapasin and HLA-DM in antigen presentation. *Trends Immunol* 29 (3): 141-147.

Salmond, R. J., A. Filby, I. Qureshi, S. Caserta and R. Zamoyska (2009). T-cell receptor proximal signaling via the Src-family kinases, Lck and Fyn, influences T-cell activation, differentiation, and tolerance. *Immunol Rev* 228 (1): 9-22.

San Jose, E., A. Borroto, F. Niedergang, A. Alcover and B. Alarcon (2000). Triggering the TCR complex causes the downregulation of nonengaged receptors by a signal transduction-dependent mechanism. *Immunity* 12 (2): 161-170.

Savage, P. A. and M. M. Davis (2001). A kinetic window constricts the T cell receptor repertoire in the thymus. *Immunity* 14 (3): 243-252.

Schachter, H. and H. H. Freeze (2009). Glycosylation diseases: quo vadis? *Biochim Biophys Acta* 1792 (9): 925-930.

Schaft, N., R. A. Willemsen, J. de Vries, B. Lankiewicz, B. W. Essers, J. W. Gratama, C. G. Figdor, R. L. Bolhuis, R. Debets and G. J. Adema (2003). Peptide fine specificity of anti-glycoprotein 100 CTL is preserved following transfer of engineered TCR alpha beta genes into primary human T lymphocytes. *J Immunol* 170 (4): 2186-2194.

Schatz, D. G., M. A. Oettinger and M. S. Schlissel (1992). V(D)J recombination: molecular biology and regulation. *Annu Rev Immunol* 10: 359-383.

Schenborn, E. T. and V. Goiffon (2000a). DEAE-dextran transfection of mammalian cultured cells. *Methods Mol Biol* 130: 147-153.

Schenborn, E. T. and V. Goiffon (2000b). Calcium phosphate transfection of mammalian cultured cells. *Methods Mol Biol* 130: 135-145.

Schenborn, E. T. and J. Oler (2000c). Liposome-mediated transfection of mammalian cells. *Methods Mol Biol* 130: 155-164.

Scherer, L., J. J. Rossi and M. S. Weinberg (2007). Progress and prospects: RNA-based therapies for treatment of HIV infection. *Gene Ther* 14 (14): 1057-1064.

Schmid, D. A., M. B. Irving, V. Posevitz, M. Hebeisen, A. Posevitz-Fejfar, J. C. Sarria, R. Gomez-Eerland, M. Thome, T. N. Schumacher, P. Romero, D. E. Speiser, V. Zoete, O. Michielin and N. Rufer (2010). Evidence for a TCR affinity threshold delimiting maximal CD8 T cell function. *J Immunol* 184 (9): 4936-4946.

Scholten, K. B., D. Kramer, E. W. Kueter, M. Graf, T. Schoedl, C. J. Meijer, M. W. Schreurs and E. Hooijberg (2006). Codon modification of T cell receptors allows enhanced functional expression in transgenic human T cells. *Clin Immunol* 119 (2): 135-145.

Schumacher, T. N. (2002). T-cell-receptor gene therapy. *Nat Rev Immunol* 2 (7): 512-519.

Sebestyen, Z., E. Schooten, T. Sals, I. Zaldivar, E. San Jose, B. Alarcon, S. Bobisse, A. Rosato, J. Szollosi, J. W. Gratama, R. A. Willemsen and R. Debets (2008). Human TCR that incorporate CD3zeta induce highly preferred pairing between TCRalpha and beta chains following gene transfer. *J Immunol* 180 (11): 7736-7746.

Sebzda, E., S. Mariathasan, T. Ohteki, R. Jones, M. F. Bachmann and P. S. Ohashi (1999). Selection of the T cell repertoire. *Annu Rev Immunol* 17: 829-874.

Sebzda, E., V. A. Wallace, J. Mayer, R. S. Yeung, T. W. Mak and P. S. Ohashi (1994). Positive and negative thymocyte selection induced by different concentrations of a single peptide. *Science* 263 (5153): 1615-1618.

Sedlik, C., G. Dadaglio, M. F. Saron, E. Deriaud, M. Rojas, S. I. Casal and C. Leclerc (2000). In vivo induction of a high-avidity, high-frequency cytotoxic T-lymphocyte response is associated with antiviral protective immunity. *J Virol* 74 (13): 5769-5775.

Sercarz, E. E. and E. Maverakis (2003). Mhc-guided processing: binding of large antigen fragments. *Nat Rev Immunol* 3 (8): 621-629.

Sewell, A. K. (2002). Breaking the kinetic window of T-cell activation. *Trends Immunol* 23 (2): 67.

Sewell, A. K., G. C. Harcourt, P. J. Goulder, D. A. Price and R. E. Phillips (1997). Antagonism of cytotoxic T lymphocyte-mediated lysis by natural HIV-1 altered peptide ligands requires simultaneous presentation of agonist and antagonist peptides. *Eur J Immunol* 27 (9): 2323-2329.

Shah, N. P., C. Tran, F. Y. Lee, P. Chen, D. Norris and C. L. Sawyers (2004). Overriding imatinib resistance with a novel ABL kinase inhibitor. *Science* 305 (5682): 399-401.

Shankaran, V., H. Ikeda, A. T. Bruce, J. M. White, P. E. Swanson, L. J. Old and R. D. Schreiber (2001). IFNgamma and lymphocytes prevent primary tumour development and shape tumour immunogenicity. *Nature* 410 (6832): 1107-1111.

Shaw, A. S., J. Chalupny, J. A. Whitney, C. Hammond, K. E. Amrein, P. Kavathas, B. M. Sefton and J. K. Rose (1990). Short related sequences in the cytoplasmic domains of CD4 and CD8 mediate binding to the amino-terminal domain of the p56lck tyrosine protein kinase. *Mol Cell Biol* 10 (5): 1853-1862.

Sievers, E. L., R. A. Larson, E. A. Stadtmauer, E. Estey, B. Lowenberg, H. Dombret, C. Karanes, M. Theobald, J. M. Bennett, M. L. Sherman, M. S. Berger, C. B. Eten, M. R. Loken, J. J. van Dongen, I. D. Bernstein and F. R. Appelbaum (2001). Efficacy and safety of gemtuzumab ozogamicin in patients with CD33-positive acute myeloid leukemia in first relapse. *J Clin Oncol* 19 (13): 3244-3254.

Sigal, L. J., S. Crotty, R. Andino and K. L. Rock (1999). Cytotoxic T-cell immunity to virus-infected non-haematopoietic cells requires presentation of exogenous antigen. *Nature* 398 (6722): 77-80.

Smith, G. P. (1985). Filamentous fusion phage: novel expression vectors that display cloned antigens on the virion surface. *Science* 228 (4705): 1315-1317.

Smyth, M. J., D. I. Godfrey and J. A. Trapani (2001). A fresh look at tumor immunosurveillance and immunotherapy. *Nat Immunol* 2 (4): 293-299.

Southam, C. M., A. Brunschwig, A. G. Levin and Q. S. Dizon (1966). Effect of leukocytes on transplantability of human cancer. *Cancer* 19 (11): 1743-1753.

Stancovski, I., D. G. Schindler, T. Waks, Y. Yarden, M. Sela and Z. Eshhar (1993). Targeting of T lymphocytes to Neu/HER2-expressing cells using chimeric single chain Fv receptors. *J Immunol* 151 (11): 6577-6582.

Starr, T. K., M. A. Daniels, M. M. Lucido, S. C. Jameson and K. A. Hogquist (2003). Thymocyte sensitivity and supramolecular activation cluster formation are developmentally regulated: a partial role for sialylation. *J Immunol* 171 (9): 4512-4520.

Stone, J. D., A. S. Chervin and D. M. Kranz (2009). T-cell receptor binding affinities and kinetics: impact on T-cell activity and specificity. *Immunology* 126 (2): 165-176.

Storkus, W. J., J. Alexander, J. A. Payne, P. Cresswell and J. R. Dawson (1989). The alpha 1/alpha 2 domains of class I HLA molecules confer resistance to natural killing. *J Immunol* 143 (11): 3853-3857.

Subbramanian, R. A., C. Moriya, K. L. Martin, F. W. Peyerl, A. Hasegawa, A. Naoi, H. Chhay, P. Autissier, D. A. Gorgone, M. A. Lifton, K. Kuus-Reichel, J. E. Schmitz, N. L. Letvin and M. J. Kuroda (2004). Engineered T-cell receptor tetramers bind MHC-peptide complexes with high affinity. *Nat Biotechnol* 22 (11): 1429-1434.

Surh, C. D. and J. Sprent (1994). T-cell apoptosis detected in situ during positive and negative selection in the thymus. *Nature* 372 (6501): 100-103.

Swain, S. L. (1983). T cell subsets and the recognition of MHC class. *Immunol Rev* 74: 129-142.

Szymczak, A. L., C. J. Workman, Y. Wang, K. M. Vignali, S. Dilioglou, E. F. Vanin and D. A. Vignali (2004). Correction of multi-gene deficiency in vivo using a single 'self-cleaving' 2A peptide-based retroviral vector. *Nat Biotechnol* 22 (5): 589-594.

Temin, H. M. (1990). Safety considerations in somatic gene therapy of human disease with retrovirus vectors. *Hum Gene Ther* 1 (2): 111-123.

Temin, H. M. and S. Mizutani (1970). RNA-dependent DNA polymerase in virions of Rous sarcoma virus. *Nature* 226 (5252): 1211-1213.

Terry, L. A., J. P. DiSanto, T. N. Small and N. Flomenberg (1990). Differential expression and regulation of the human CD8 alpha and CD8 beta chains. *Tissue Antigens* 35 (2): 82-91.

Thomas, M. L. (1989). The leukocyte common antigen family. *Annu Rev Immunol* 7: 339-369.

Thomas, S., S. A. Xue, M. Cesco-Gaspere, E. San Jose, D. P. Hart, V. Wong, R. Debets, B. Alarcon, E. Morris and H. J. Stauss (2007). Targeting the Wilms tumor antigen 1 by TCR gene transfer: TCR variants improve tetramer binding but not the function of gene modified human T cells. *J Immunol* 179 (9): 5803-5810.

Toscano, M. G., C. Frecha, C. Ortega, M. Santamaria, F. Martin and I. J. Molina (2004). Efficient lentiviral transduction of Herpesvirus saimiri immortalized T cells as a model for gene therapy in primary immunodeficiencies. *Gene Ther* 11 (12): 956-961.

Tsang, J. Y., Y. Tanriver, S. Jiang, S. A. Xue, K. Ratnasothy, D. Chen, H. J. Stauss, R. P. Bucy, G. Lombardi and R. Lechler (2008). Conferring indirect allospecificity on CD4+CD25+ Tregs by TCR gene transfer favors transplantation tolerance in mice. *J Clin Invest* 118 (11): 3619-3628.

Turk, M. J., J. A. Guevara-Patino, G. A. Rizzuto, M. E. Engelhorn, S. Sakaguchi and A. N. Houghton (2004). Concomitant tumor immunity to a poorly immunogenic melanoma is prevented by regulatory T cells. *J Exp Med* 200 (6): 771-782.

Turley, S. J., K. Inaba, W. S. Garrett, M. Ebersold, J. Unternaehrer, R. M. Steinman and I. Mellman (2000). Transport of peptide-MHC class II complexes in developing dendritic cells. *Science* 288 (5465): 522-527.

Unutmaz, D., V. N. KewalRamani, S. Marmon and D. R. Littman (1999). Cytokine signals are sufficient for HIV-1 infection of resting human T lymphocytes. *J Exp Med* 189 (11): 1735-1746.

Vaccari, M., P. Poonam and G. Franchini (2010). Phase III HIV vaccine trial in Thailand: a step toward a protective vaccine for HIV. *Expert Rev Vaccines* 9 (9): 997-1005.

Valitutti, S. and A. Lanzavecchia (1997). Serial triggering of TCRs: a basis for the sensitivity and specificity of antigen recognition. *Immunol Today* 18 (6): 299-304.

Valitutti, S., S. Muller, M. Cella, E. Padovan and A. Lanzavecchia (1995). Serial triggering of many T-cell receptors by a few peptide-MHC complexes. *Nature* 375 (6527): 148-151.

van't Hof, W. and M. D. Resh (1999). Dual fatty acylation of p59(Fyn) is required for association with the T cell receptor zeta chain through phosphotyrosine-Src homology domain-2 interactions. *J Cell Biol* 145 (2): 377-389.

van der Merwe, P. A. (2000). Modeling costimulation. *Nat Immunol* 1 (3): 194-195.

van der Merwe, P. A. (2001). The TCR triggering puzzle. *Immunity* 14 (6): 665-668.

van der Merwe, P. A. and S. J. Davis (2003). Molecular interactions mediating T cell antigen recognition. *Annu Rev Immunol* 21: 659-684.

Van Laethem, F., S. D. Sarafova, J. H. Park, X. Tai, L. Pobezinsky, T. I. Guinter, S. Adoro, A. Adams, S. O. Sharrow, L. Feigenbaum and A. Singer (2007). Deletion of CD4 and CD8 coreceptors permits generation of alphabetaT cells that recognize antigens independently of the MHC. *Immunity* 27 (5): 735-750.

van Loenen, M. M., R. de Boer, A. L. Amir, R. S. Hagedoorn, G. L. Volbeda, R. Willemze, J. J. van Rood, J. H. Falkenburg and M. H. Heemskerk (2010). Mixed T cell receptor dimers harbor potentially harmful neoreactivity. *Proc Natl Acad Sci U S A* 107 (24): 10972-10977.

Varela-Rohena, A., C. Carpenito, E. E. Perez, M. Richardson, R. V. Parry, M. Milone, J. Scholler, X. Hao, A. Mexas, R. G. Carroll, C. H. June and J. L. Riley (2008a). Genetic engineering of T cells for adoptive immunotherapy. *Immunol Res* 42 (1-3): 166-181.

Varela-Rohena, A., P. E. Molloy, S. M. Dunn, Y. Li, M. M. Suhoski, R. G. Carroll, A. Milicic, T. Mahon, D. H. Sutton, B. Laugel, R. Moysey, B. J. Cameron, A. Vuidepot, M. A. Purbhoo, D. K. Cole, R. E. Phillips, C. H. June, B. K. Jakobsen, A. K. Sewell and J. L. Riley (2008). Control of HIV-1 immune escape by CD8 T cells expressing enhanced T-cell receptor. *Nat Med* 14 (12): 1390-1395.

Varela-Rohena, A., P. E. Molloy, S. M. Dunn, Y. Li, M. M. Suhoski, R. G. Carroll, A. Milicic, T. Mahon, D. H. Sutton, B. Laugel, R. Moysey, B. J. Cameron, A. Vuidepot, M. A. Purbhoo, D. K. Cole, R. E. Phillips, C. H. June, B. K. Jakobsen, A. K. Sewell and J. L. Riley (2008b). Control of HIV-1 immune escape by CD8 T cells expressing enhanced T-cell receptor. *Nat Med* 14 (12): 1390-1395.

Varki, A., Ed. (2009). The essentials of glycobiology. New York

Veillette, A., M. A. Bookman, E. M. Horak and J. B. Bolen (1988a). The CD4 and CD8 T cell surface antigens are associated with the internal membrane tyrosine-protein kinase p56lck. *Cell* 55 (2): 301-308.

Veillette, A., I. D. Horak, E. M. Horak, M. A. Bookman and J. B. Bolen (1988b). Alterations of the lymphocyte-specific protein tyrosine kinase (p56lck) during T-cell activation. *Mol Cell Biol* 8 (10): 4353-4361.

Venturi, V., K. Kedzierska, M. M. Tanaka, S. J. Turner, P. C. Doherty and M. P. Davenport (2008). Method for assessing the similarity between subsets of the T cell receptor repertoire. *J Immunol Methods* 329 (1-2): 67-80.

Viola, A. (2001). The amplification of TCR signaling by dynamic membrane microdomains. *Trends Immunol* 22 (6): 322-327.

Virchow, R. (1863). *Die Krankenhaften Geschwulste*. Berlin,

von Mehren, M., G. P. Adams and L. M. Weiner (2003). Monoclonal antibody therapy for cancer. *Annu Rev Med* 54: 343-369.

Walter, E. A., P. D. Greenberg, M. J. Gilbert, R. J. Finch, K. S. Watanabe, E. D. Thomas and S. R. Riddell (1995). Reconstitution of cellular immunity against cytomegalovirus in recipients of allogeneic bone marrow by transfer of T-cell clones from the donor. *N Engl J Med* 333 (16): 1038-1044.

Wang, H. Y. and R. F. Wang (2007). Regulatory T cells and cancer. *Curr Opin Immunol* 19 (2): 217-223.

Wang, J. H., R. Meijers, Y. Xiong, J. H. Liu, T. Sakihama, R. Zhang, A. Joachimiak and E. L. Reinherz (2001). Crystal structure of the human CD4 N-terminal two-domain fragment complexed to a class II MHC molecule. *Proc Natl Acad Sci U S A* 98 (19): 10799-10804.

Weaver, J. C. (1993). Electroporation: a general phenomenon for manipulating cells and tissues. *J Cell Biochem* 51 (4): 426-435.

Weichsel, R., C. Dix, L. Wooldridge, M. Clement, A. Fenton-May, A. K. Sewell, J. Zezula, E. Greiner, E. Gostick, D. A. Price, H. Einsele and R. Seggewiss (2008). Profound inhibition of antigen-specific T-cell effector functions by dasatinib. *Clin Cancer Res* 14 (8): 2484-2491.

Weiss, A. and D. R. Littman (1994). Signal transduction by lymphocyte antigen receptors. *Cell* 76 (2): 263-274.

Weiss, A. and J. D. Stobo (1984). Requirement for the coexpression of T3 and the T cell antigen receptor on a malignant human T cell line. *J Exp Med* 160 (5): 1284-1299.

Whelan, J. A., P. R. Dunbar, D. A. Price, M. A. Purbhoo, F. Lechner, G. S. Ogg, G. Griffiths, R. E. Phillips, V. Cerundolo and A. K. Sewell (1999). Specificity of CTL interactions with peptide-MHC class I tetrameric complexes is temperature dependent. *J Immunol* 163 (8): 4342-4348.

Willcox, B. E., G. F. Gao, J. R. Wyer, J. E. Ladbury, J. I. Bell, B. K. Jakobsen and P. A. van der Merwe (1999a). TCR binding to peptide-MHC stabilizes a flexible recognition interface. *Immunity* 10 (3): 357-365.

Willcox, B. E., G. F. Gao, J. R. Wyer, C. A. O'Callaghan, J. M. Boulter, E. Y. Jones, P. A. van der Merwe, J. I. Bell and B. K. Jakobsen (1999b). Production of soluble alphabeta T-cell receptor heterodimers suitable for biophysical analysis of ligand binding. *Protein Sci* 8 (11): 2418-2423.

Willimsky, G. and T. Blankenstein (2005). Sporadic immunogenic tumours avoid destruction by inducing T-cell tolerance. *Nature* 437 (7055): 141-146.

Wilson, J. D., G. S. Ogg, R. L. Allen, P. J. Goulder, A. Kelleher, A. K. Sewell, C. A. O'Callaghan, S. L. Rowland-Jones, M. F. Callan and A. J. McMichael (1998). Oligoclonal expansions of CD8(+) T cells in chronic HIV infection are antigen specific. *J Exp Med* 188 (4): 785-790.

Wing, K., Y. Onishi, P. Prieto-Martin, T. Yamaguchi, M. Miyara, Z. Fehervari, T. Nomura and S. Sakaguchi (2008). CTLA-4 control over Foxp3+ regulatory T cell function. *Science* 322 (5899): 271-275.

Wiseman, G. A., B. Leigh, W. D. Erwin, D. Lamonica, E. Kornmehl, S. M. Spies, D. H. Silverman, T. E. Witzig, R. B. Sparks and C. A. White (2002). Radiation dosimetry results for Zevalin radioimmunotherapy of rituximab-refractory non-Hodgkin lymphoma. *Cancer* 94 (4 Suppl): 1349-1357.

Withoff, S., W. Helfrich, L. F. de Leij and G. Molema (2001). Bi-specific antibody therapy for the treatment of cancer. *Curr Opin Mol Ther* 3 (1): 53-62.

Wittman, V. P., D. Woodburn, T. Nguyen, F. A. Neethling, S. Wright and J. A. Weidanz (2006). Antibody targeting to a class I MHC-peptide epitope promotes tumor cell death. *J Immunol* 177 (6): 4187-4195.

Wolf, E., R. Hofmeister, P. Kufer, B. Schlereth and P. A. Baeuerle (2005). BiTEs: bispecific antibody constructs with unique anti-tumor activity. *Drug Discov Today* 10 (18): 1237-1244.

Woods, N. B., A. Muessig, M. Schmidt, J. Flygare, K. Olsson, P. Salmon, D. Trono, C. von Kalle and S. Karlsson (2003). Lentiviral vector transduction of NOD/SCID repopulating cells results in multiple vector integrations per transduced cell: risk of insertional mutagenesis. *Blood* 101 (4): 1284-1289.

Wooldridge, L., S. L. Hutchinson, E. M. Choi, A. Lissina, E. Jones, F. Mirza, P. R. Dunbar, D. A. Price, V. Cerundolo and A. K. Sewell (2003). Anti-CD8 antibodies can inhibit or enhance peptide-MHC class I (pMHCI) multimer binding: this is paralleled by their effects on CTL activation and occurs in the absence of an interaction between pMHCI and CD8 on the cell surface. *J Immunol* 171 (12): 6650-6660.

Wooldridge, L., B. Laugel, J. Ekeruche, M. Clement, H. A. van den Berg, D. A. Price and A. K. Sewell (2010). CD8 controls T cell cross-reactivity. *J Immunol* 185 (8): 4625-4632.

Wooldridge, L., A. Lissina, D. K. Cole, H. A. van den Berg, D. A. Price and A. K. Sewell (2009). Tricks with tetramers: how to get the most from multimeric peptide-MHC. *Immunology* 126 (2): 147-164.

Wooldridge, L., A. Lissina, J. Vernazza, E. Gostick, B. Laugel, S. L. Hutchinson, F. Mirza, P. R. Dunbar, J. M. Boulter, M. Glick, V. Cerundolo, H. A. van den Berg, D. A. Price and A. K. Sewell (2007). Enhanced immunogenicity of CTL antigens through mutation of the CD8 binding MHC class I invariant region. *Eur J Immunol* 37 (5): 1323-1333.

Wooldridge, L., T. J. Scriba, A. Milicic, B. Laugel, E. Gostick, D. A. Price, R. E. Phillips and A. K. Sewell (2006). Anti-coreceptor antibodies profoundly affect staining with peptide-MHC class I and class II tetramers. *Eur J Immunol* 36 (7): 1847-1855.

Wooldridge, L., H. A. van den Berg, M. Glick, E. Gostick, B. Laugel, S. L. Hutchinson, A. Milicic, J. M. Brenchley, D. C. Douek, D. A. Price and A. K. Sewell (2005). Interaction between the CD8 coreceptor and major histocompatibility complex class I stabilizes T cell receptor-antigen complexes at the cell surface. *J Biol Chem* 280 (30): 27491-27501.

Wu, H., P. D. Kwong and W. A. Hendrickson (1997). Dimeric association and segmental variability in the structure of human CD4. *Nature* 387 (6632): 527-530.

Wu, W., P. H. Harley, J. A. Punt, S. O. Sharrow and K. P. Kearse (1996). Identification of CD8 as a peanut agglutinin (PNA) receptor molecule on immature thymocytes. *J Exp Med* 184 (2): 759-764.

Wyer, J. R., B. E. Willcox, G. F. Gao, U. C. Gerth, S. J. Davis, J. I. Bell, P. A. van der Merwe and B. K. Jakobsen (1999). T cell receptor and coreceptor CD8 alphaalpha bind peptide-MHC independently and with distinct kinetics. *Immunity* 10 (2): 219-225.

Wynn, R. F., P. D. Arkwright, T. Haque, M. I. Gharib, G. Wilkie, M. Morton-Jones and D. H. Crawford (2005). Treatment of Epstein-Barr-virus-associated primary CNS B cell lymphoma with allogeneic T-cell immunotherapy and stem-cell transplantation. *Lancet Oncol* 6 (5): 344-346.

Xiao, Z., M. F. Mescher and S. C. Jameson (2007). Detuning CD8 T cells: down-regulation of CD8 expression, tetramer binding, and response during CTL activation. *J Exp Med* 204 (11): 2667-2677.

Xiong, Y., P. Kern, H. Chang and E. Reinherz (2001). T Cell Receptor Binding to a pMHCII Ligand Is Kinetically Distinct from and Independent of CD4. *J Biol Chem* 276 (8): 5659-5667.

Xu, L., W. Xu, S. Qiu and S. Xiong (2010). Enrichment of CCR6+Foxp3+ regulatory T cells in the tumor mass correlates with impaired CD8+ T cell function and poor prognosis of breast cancer. *Clin Immunol* 135 (3): 466-475.

Xu, X. N., M. A. Purbhoo, N. Chen, J. Mongkolsapaya, J. H. Cox, U. C. Meier, S. Tafuro, P. R. Dunbar, A. K. Sewell, C. S. Hourigan, V. Appay, V. Cerundolo, S. R. Burrows, A. J. McMichael and G. R. Screaton (2001). A novel approach to antigen-specific deletion of CTL with minimal cellular activation using alpha3 domain mutants of MHC class I/peptide complex. *Immunity* 14 (5): 591-602.

Xu, Z. and A. Weiss (2002). Negative regulation of CD45 by differential homodimerization of the alternatively spliced isoforms. *Nat Immunol* 3 (8): 764-771.

Xue, S., R. Gillmore, A. Downs, A. Tsallios, A. Holler, L. Gao, V. Wong, E. Morris and H. J. Stauss (2005). Exploiting T cell receptor genes for cancer immunotherapy. *Clin Exp Immunol* 139 (2): 167-172.

Yadav, S. S. and W. T. Miller (2008). The evolutionarily conserved arrangement of domains in SRC family kinases is important for substrate recognition. *Biochemistry* 47 (41): 10871-10880.

Yamamoto, A., M. Kormann, J. Rosenecker and C. Rudolph (2009). Current prospects for mRNA gene delivery. *Eur J Pharm Biopharm* 71 (3): 484-489.

Yamashita, M. and M. Emerman (2006). Retroviral infection of non-dividing cells: old and new perspectives. *Virology* 344 (1): 88-93.

Yang, L. and D. Baltimore (2005). Long-term in vivo provision of antigen-specific T cell immunity by programming hematopoietic stem cells. *Proc Natl Acad Sci U S A* 102 (12): 4518-4523.

Yang, S., C. J. Cohen, P. D. Peng, Y. Zhao, L. Cassard, Z. Yu, Z. Zheng, S. Jones, N. P. Restifo, S. A. Rosenberg and R. A. Morgan (2008). Development of optimal bicistronic lentiviral vectors facilitates high-level TCR gene expression and robust tumor cell recognition. *Gene Ther* 15 (21): 1411-1423.

Yee, C., P. A. Savage, P. P. Lee, M. M. Davis and P. D. Greenberg (1999). Isolation of high avidity melanoma-reactive CTL from heterogeneous populations using peptide-MHC tetramers. *J Immunol* 162 (4): 2227-2234.

Yee, C., J. A. Thompson, P. Roche, D. R. Byrd, P. P. Lee, M. Piepkorn, K. Kenyon, M. M. Davis, S. R. Riddell and P. D. Greenberg (2000). Melanocyte destruction after antigen-specific immunotherapy of melanoma: direct evidence of t cell-mediated vitiligo. *J Exp Med* 192 (11): 1637-1644.

Yuan, R. R., P. Wong, M. R. McDevitt, E. Doubrovina, I. Leiner, W. Bornmann, R. O'Reilly, E. G. Pamer and D. A. Scheinberg (2004). Targeted deletion of T-cell clones using alpha-emitting suicide MHC tetramers. *Blood* 104 (8): 2397-2402.

Zamoyska, R. (1998). CD4 and CD8: modulators of T-cell receptor recognition of antigen and of immune responses? *Curr Opin Immunol* 10 (1): 82-87.

Zamoyska, R., A. Basson, A. Filby, G. Legname, M. Lovatt and B. Seddon (2003). The influence of the src-family kinases, Lck and Fyn, on T cell differentiation, survival and activation. *Immunol Rev* 191: 107-118.

Zeh, H. J., 3rd, D. Perry-Lalley, M. E. Dudley, S. A. Rosenberg and J. C. Yang (1999). High avidity CTLs for two self-antigens demonstrate superior in vitro and in vivo antitumor efficacy. *J Immunol* 162 (2): 989-994.

Zhang, W., J. Sloan-Lancaster, J. Kitchen, R. P. Trible and L. E. Samelson (1998a). LAT: the ZAP-70 tyrosine kinase substrate that links T cell receptor to cellular activation. *Cell* 92 (1): 83-92.

Zhang, W., R. P. Trible and L. E. Samelson (1998b). LAT palmitoylation: its essential role in membrane microdomain targeting and tyrosine phosphorylation during T cell activation. *Immunity* 9 (2): 239-246.

Zhao, Y., A. D. Bennett, Z. Zheng, Q. J. Wang, P. F. Robbins, L. Y. Yu, Y. Li, P. E. Molloy, S. M. Dunn, B. K. Jakobsen, S. A. Rosenberg and R. A. Morgan (2007). High-affinity TCRs generated by phage display provide CD4+ T cells with the ability to recognize and kill tumor cell lines. *J Immunol* 179 (9): 5845-5854.

Zhao, Y., Z. Zheng, C. J. Cohen, L. Gattinoni, D. C. Palmer, N. P. Restifo, S. A. Rosenberg and R. A. Morgan (2006). High-efficiency transfection of primary human and mouse T lymphocytes using RNA electroporation. *Mol Ther* 13 (1): 151-159.

Zhao, Y., Z. Zheng, P. F. Robbins, H. T. Khong, S. A. Rosenberg and R. A. Morgan (2005). Primary human lymphocytes transduced with NY-ESO-1 antigen-specific TCR genes recognize and kill diverse human tumor cell lines. *J Immunol* 174 (7): 4415-4423.

Zhu, M., S. Shen, Y. Liu, O. Granillo and W. Zhang (2005). Cutting Edge: Localization of linker for activation of T cells to lipid rafts is not essential in T cell activation and development. *J Immunol* 174 (1): 31-35.

Zinkernagel, R. M. and P. C. Doherty (1997). The discovery of MHC restriction. *Immunol Today* 18 (1): 14-17.

Zufferey, R., T. Dull, R. J. Mandel, A. Bukovsky, D. Quiroz, L. Naldini and D. Trono (1998). Self-inactivating lentivirus vector for safe and efficient in vivo gene delivery. *J Virol* 72 (12): 9873-9880.

Zuo, L., C. M. Cullen, M. L. DeLay, S. Thornton, L. K. Myers, E. F. Rosloniec, G. P. Boivin and R. Hirsch (2002). A single-chain class II MHC-IgG3 fusion protein inhibits autoimmune arthritis by induction of antigen-specific hyporesponsiveness. *J Immunol* 168 (5): 2554-2559.

APPENDICES

Appendix 1: Sequences of 868 TCR α and β chains and SGSG-2A peptide

A. 868 TCR α:

acgcgtgctagccgccaccatgatgaagagcctgagggtgctgctggtgatcctgtggctgcagctgtcctgggtgtggagccagcag
aaggaggtggagcagaatagcggccctctgagcgtgcccgagggcgccatcgccagcctgaactgtacctacagcgacagaggca
gccagagcttcttctggtacaggcagtacagcggcaagagccccgagctgattatgttcatctacagcaacggcgacaaggaggac
ggcagattcaccgcccagctgaacaaggccagccagtacatcagcctgctgatccgggatagcaagctgtccgacagcgccaccta
cctgtgtgccgtgagaaccaatagcggctacgccctgaatttcggcaagggcaccagcctgctggtgacccccccacatccagaatcct
gaccccgccgtgtaccagctgagagacagcaagagcagcgacaagagcgtgtgtctgttcaccgacttcgacagccagaccaacgt
gtcccagagcaaggacagcgacgtgtacatcaccgacaagaccgtgctggacatgaggagcatggacttcaagagcaacagcgcc
gtggcctggagcaacaagagcgacttcgcctgtgccaacgccttcaacaacagcatcatccccgaggacacctttttccccagccctg
agagcagctgtgacgtgaaactggtggagaagagcttcgagaccgacaccaacctgaacttccagaacctgagcgtgatcggcttc
agaatcctgctgctgaaggtggccggattcaacctgctgatgaccctgagactgtggagcagcctcgagagatct

B. 868 TCR β:

cctaggcccgggatgggacccggcctgctgtgctgggccctgctgtgcctgctgggagccggactggtggacgccggagtgacccag
agccccacccacctgattaagaccaggggccagcaggtgaccctgagatgtagccctaagagcggccacgataccgtgtcctggtat
cagcaggccctgggccagggaccccagttcatcttccagtactacgaggaggaggagaggcagagaggcaacttccccgacagatt
cagcggccaccagttccccaattacagcagcgagctgaacgtgaatgccctgctgctgggcgacagcgccctgtacctgtgtgccag
cagcgacacagtgagctacgagcagtacttcggccctggcaccagactgaccgtgaccgaggacctgaagaacgtgttccctcctga
ggtggccgtgttcgagcccagcgaggccgagatcagccacacccagaaggccaccctggtgtgtctggccaccggcttctaccccga
ccacgtggagctgtcctggtgggtgaacggcaaggaggtgcacagcggcgtgtccaccgacccccagcccctgaaggagcagcccg
ccctgaacgatagcaggtactgcctgagcagcaggctgagagtgagcgccaccttctggcagaaccccccggaaccacttcagatgcc
aggtgcagttctacggcctgagcgagaacgacgagtggacccaggatagagccaagcccgtgacccagatcgtgtccgccgaggcc
tggggcagagccgactgtggcttcaccagcgagagctaccagcagggcgtgctgtccgccaccatcctgtacgagatcctgctgggc
aaggccacactgtacgccgtgctggtgtccgccctggtgctgatggctatggtgaagcggaaggacagcaggggctgatagtcga

C. SGSG-2A sequence (T2A from the Thosea asigna virus):

agcggcagcgggcgcagcggcagcggcgaaggccgcggcagcctgctgacctgcggcgatgtggaagaaaaccctggcccg
(Translates to: SGSGRSGSGEGRGSLLTCGDVEENPGP)

Appendix 2: 868 TCR N-glycosylation sites

The 7 putative N-glycosylation sites found on the 868 TCR were located by subjecting the 868 TCR amino acid sequence to an ExPASy (Prosite) search for the N-X-[S/T]-Y N-linked glycosylation motif (where X and Y are any amino acid apart from proline). Variable (v) domains are shown in green, and constant (c) domains in blue, and glycosylation motifs in red. The numbers underneath the sequences refer to the amino acid positions of the corresponding glycosylation motif in the variable or constant region of the alpha or beta TCR chain.

A. 868 TCR α:

RVLAATMMKSLRVLLVILWLQLSWVWSQQKEVEQNSGPLSVPEGAIASLNCTYSDRGSQSFFWYRQYSG
KSPELIMFIYSNGDKEDGRFTAQLNKASQYISLLIRDSKLSDSATYLCAVRTNSGYALNFGKGTSLLVTPHIQ
NPDPAVYQLRDSKSSDKSVCLFTDFDSQTNVSQSKDSDVYITDKTVLDMRSMDFKSNSAVAWSNKSDFA
CANAFNNSIIPEDTFFPSPESSCDVKLVEKSFETDTNLNFQNLSVIGFRILLLKVAGFNLLMTLRLWSSLERS

v 22-24	NCT
c 31-33	NVS
c 66-68	NKS
c 77-79	NNS
c 112-114	NLS

B. 868 TCR β:

PRPGMGPGLLCWALLCLLGAGLVDAGVTQSPTHLIKTRGQQVTLRCSPKSGHDTVSWYQQALGQGPQF
IFQYYEEEERQRGNFPDRFSGHQFPNYSSELNVNALLLGDSALYLCASSDTVSYEQYFGPGTRLTVTEDLKN
VFPPEVAVFEPSEAEISHTQKATLVCLATGFYPDHVELSWWVNGKEVHSGVSTDPQPLKEQPALNDSRYC
LSSRLRVSATFWQNPRNHFRCQVQFYGLSENDEWTQDRAKPVTQIVSAEAWGRADCGFTSESYQQGVL
SATILYEILLGKATLYAVLVSALVLMAMVKRKDSRG**S

v 70-72	NYS
c 65-67	NDS

Appendix 3: List of primers for site directed mutagenesis of N-glycosylation sites located on the 868 TCR

The name of each primer is highlighted in red, while the glycosylation site being mutated and the amino acid position and substitution details are shown in blue. For example, the G1 forward 5' primer substitutes a glutamine (Q) for an asparagine (N) at position 94 in the beta chain of the 868 TCR.

G1 => 5'glyc1B_N94Q
ccagttcccccagtacagcagcgagc
G2 => 3'glyc1B_N94Q
gctcgctgctgtactgggggaactgg
G3 => 5'glyc2B_N205Q
gagcagcccgccctgcaagatagcaggtactgc
G4 => 3'glyc2B_N205Q
gcagtacctgctatcgttcagggcgggctgctc
G5 => 5'glyc1A_N50Q
catcgccagcctgcagtgtacctacagc
G6 => 3'glyc1A_N50Q
gctgtaggtacactgcaggctggcgatg
G7 => 5'glyc2A_N172Q
cgacagccagacccaggtgtcccagagc
G8 => 3'glyc2A_N172Q
gctctgggacacctgggtctggctgtcg
G9 => 5'glyc3A_N206Q
gtggcctggagccagaagagcgacttcg
G10 => 3'glyc3A_N206Q
cgaagtcgctcttctggctccaggccac
G11 => 5'glyc4A_N217/8Q
tgtgccaacgccttccagcagagcatcatccccg
G12 => 3'glyc4A_N217/8Q
cggggatgatgctctgctggaaggcgttggcaca
G13 => 5'glyc5A_N253Q
cctgaacttccagcagctgagcgtgatc
G14 => 3'glyc5A_N253Q
gatcacgctcagctgctggaagttcagg

Appendix 4: DNA sequence alignment of the 868 TCR and 868 TCR glycosylation mutants

A. Sequence alignment results for 868 TCR α chain with the five α chain glycosylation mutants (A1-A5).

The point mutations are highlighted in green. (A1=Gα1, A2= Gα2, A3= Gα3, A4= Gα4, A5= Gα5)

CLUSTAL 2.0.12 multiple sequence alignment

```
gag_alpha_WT       ---------------------------ACGCGTGCTAGCCGCCACC-ATGATGAAGAGCCT  33
gag_alpha_A4       -----------------------------------GCCGCCACAGAAGAAAAGGAGCCT  24
gag_alpha_A1       -----------------------------------GCCGCCATGATGGACGCAGAGCCT  24
gag_alpha_A3       -----------------------------------GCCGCCATA-TGGGCGCAGAGCCT  23
gag_alpha_A2       -----------------------------------GCCGCCATGATGGACGCAGAGCCT  24
gag_alpha_A5       AAGGTGGCCGGATTCAACCTGCTGATGACCCCTGGAGCCGCCATGATGGACGCAGAGCCT  60
                                                       *******     *     ******

gag_alpha_WT       GAGGGTGCTGCTGGTGATCCTGTGGCTGCAGCTGTCCTGGGTGTGGAGCCAGCAGAAGGA  93
gag_alpha_A4       GAGGGTGCTGCTGGTGATCCTGTGGCTGCAGCTGTCCTGGGTGTGGAGCCAGCAGAAGGA  84
gag_alpha_A1       GAGGGTGCTGCTGGTGATCCTGTGGCTGCAGCTGTCCTGGGTGTGGAGCCAGCAGAAGGA  84
gag_alpha_A3       GAGGGTGCTGCTGGTGATCCTGTGGCTGCAGCTGTCCTGGGTGTGGAGCCAGCAGAAGGA  83
gag_alpha_A2       GAGGGTGCTGCTGGTGATCCTGTGGCTGCAGCTGTCCTGGGTGTGGAGCCAGCAGAAGGA  84
gag_alpha_A5       GAGGGTGCTGCTGGTGATCCTGTGGCTGCAGCTGTCCTGGGTGTGGAGCCAGCAGAAGGA 120
                   ************************************************************

gag_alpha_WT       GGTGGAGCAGAATAGCGGCCCTCTGAGCGTGCCCGAGGGCGCCATCGCCAGCCTGAACTG 153
gag_alpha_A4       GGTGGAGCAGAATAGCGGCCCTCTGAGCGTGCCCGAGGGCGCCATCGCCAGCCTGAACTG 144
gag_alpha_A1       GGTGGAGCAGAATAGCGGCCCTCTGAGCGTGCCCGAGGGCGCCATCGCCAGCCTG[redacted]TG 144
gag_alpha_A3       GGTGGAGCAGAATAGCGGCCCTCTGAGCGTGCCCGAGGGCGCCATCGCCAGCCTGAACTG 143
gag_alpha_A2       GGTGGAGCAGAATAGCGGCCCTCTGAGCGTGCCCGAGGGCGCCATCGCCAGCCTGAACTG 144
gag_alpha_A5       GGTGGAGCAGAATAGCGGCCCTCTGAGCGTGCCCGAGGGCGCCATCGCCAGCCTGAACTG 180
                   ************************************************** * **

gag_alpha_WT       TACCTACAGCGACAGAGGCAGCCAGAGCTTCTTCTGGTACAGGCAGTACAGCGGCAAGAG 213
gag_alpha_A4       TACCTACAGCGACAGAGGCAGCCAGAGCTTCTTCTGGTACAGGCAGTACAGCGGCAAGAG 204
gag_alpha_A1       TACCTACAGCGACAGAGGCAGCCAGAGCTTCTTCTGGTACAGGCAGTACAGCGGCAAGAG 204
gag_alpha_A3       TACCTACAGCGACAGAGGCAGCCAGAGCTTCTTCTGGTACAGGCAGTACAGCGGCAAGAG 203
gag_alpha_A2       TACCTACAGCGACAGAGGCAGCCAGAGCTTCTTCTGGTACAGGCAGTACAGCGGCAAGAG 204
gag_alpha_A5       TACCTACAGCGACAGAGGCAGCCAGAGCTTCTTCTGGTACAGGCAGTACAGCGGCAAGAG 240
                   ************************************************************

gag_alpha_WT       CCCCGAGCTGATTATGTTCATCTACAGCAACGGCGACAAGGAGGACGGCAGATTCACCGC 273
gag_alpha_A4       CCCCGAGCTGATTATGTTCATCTACAGCAACGGCGACAAGGAGGACGGCAGATTCACCGC 264
gag_alpha_A1       CCCCGAGCTGATTATGTTCATCTACAGCAACGGCGACAAGGAGGACGGCAGATTCACCGC 264
gag_alpha_A3       CCCCGAGCTGATTATGTTCATCTACAGCAACGGCGACAAGGAGGACGGCAGATTCACCGC 263
gag_alpha_A2       CCCCGAGCTGATTATGTTCATCTACAGCAACGGCGACAAGGAGGACGGCAGATTCACCGC 264
gag_alpha_A5       CCCCGAGCTGATTATGTTCATCTACAGCAACGGCGACAAGGAGGACGGCAGATTCACCGC 300
                   ************************************************************

gag_alpha_WT       CCAGCTGAACAAGGCCAGCCAGTACATCAGCCTGCTGATCCGGGATAGCAAGCTGTCCGA 333
gag_alpha_A4       CCAGCTGAACAAGGCCAGCCAGTACATCAGCCTGCTGATCCGGGATAGCAAGCTGTCCGA 324
gag_alpha_A1       CCAGCTGAACAAGGCCAGCCAGTACATCAGCCTGCTGATCCGGGATAGCAAGCTGTCCGA 324
gag_alpha_A3       CCAGCTGAACAAGGCCAGCCAGTACATCAGCCTGCTGATCCGGGATAGCAAGCTGTCCGA 323
gag_alpha_A2       CCAGCTGAACAAGGCCAGCCAGTACATCAGCCTGCTGATCCGGGATAGCAAGCTGTCCGA 324
gag_alpha_A5       CCAGCTGAACAAGGCCAGCCAGTACATCAGCCTGCTGATCCGGGATAGCAAGCTGTCCGA 360
                   ************************************************************

gag_alpha_WT       CAGCGCCACCTACCTGTGTGCCGTGAGAACCAATAGCGGCTACGCCCTGAATTTCGGCAA 393
gag_alpha_A4       CAGCGCCACCTACCTGTGTGCCGTGAGAACCAATAGCGGCTACGCCCTGAATTTCGGCAA 384
gag_alpha_A1       CAGCGCCACCTACCTGTGTGCCGTGAGAACCAATAGCGGCTACGCCCTGAATTTCGGCAA 384
gag_alpha_A3       CAGCGCCACCTACCTGTGTGCCGTGAGAACCAATAGCGGCTACGCCCTGAATTTCGGCAA 383
```

```
gag_alpha_A2      CAGCGCCACCTACCTGTGTGCCGTGAGAACCAATAGCGGCTACGCCCTGAATTTCGGCAA 384
gag_alpha_A5      CAGCGCCACCTACCTGTGTGCCGTGAGAACCAATAGCGGCTACGCCCTGAATTTCGGCAA 420
                  ************************************************************

gag_alpha_WT      GGGCACCAGCCTGCTGGTGACCCCCCACATCCAGAATCCTGACCCCGCCGTGTACCAGCT 453
gag_alpha_A4      GGGCACCAGCCTGCTGGTGACCCCCCACATCCAGAATCCTGACCCCGCCGTGTACCAGCT 444
gag_alpha_A1      GGGCACCAGCCTGCTGGTGACCCCCCACATCCAGAATCCTGACCCCGCCGTGTACCAGCT 444
gag_alpha_A3      GGGCACCAGCCTGCTGGTGACCCCCCACATCCAGAATCCTGACCCCGCCGTGTACCAGCT 443
gag_alpha_A2      GGGCACCAGCCTGCTGGTGACCCCCCACATCCAGAATCCTGACCCCGCCGTGTACCAGCT 444
gag_alpha_A5      GGGCACCAGCCTGCTGGTGACCCCCCACATCCAGAATCCTGACCCCGCCGTGTACCAGCT 480
                  ************************************************************

gag_alpha_WT      GAGAGACAGCAAGAGCAGCGACAAGAGCGTGTGTCTGTTCACCGACTTCGACAGCCAGAC 513
gag_alpha_A4      GAGAGACAGCAAGAGCAGCGACAAGAGCGTGTGTCTGTTCACCGACTTCGACAGCCAGAC 504
gag_alpha_A1      GAGAGACAGCAAGAGCAGCGACAAGAGCGTGTGTCTGTTCACCGACTTCGACAGCCAGAC 504
gag_alpha_A3      GAGAGACAGCAAGAGCAGCGACAAGAGCGTGTGTCTGTTCACCGACTTCGACAGCCAGAC 503
gag_alpha_A2      GAGAGACAGCAAGAGCAGCGACAAGAGCGTGTGTCTGTTCACCGACTTCGACAGCCAGAC 504
gag_alpha_A5      GAGAGACAGCAAGAGCAGCGACAAGAGCGTGTGTCTGTTCACCGACTTCGACAGCCAGAC 540
                  ************************************************************

gag_alpha_WT      CAACGTGTCCCAGAGCAAGGACAGCGACGTGTACATCACCGACAAGACCGTGCTGGACAT 573
gag_alpha_A4      CAACGTGTCCCAGAGCAAGGACAGCGACGTGTACATCACCGACAAGACCGTGCTGGACAT 564
gag_alpha_A1      CAACGTGTCCCAGAGCAAGGACAGCGACGTGTACATCACCGACAAGACCGTGCTGGACAT 564
gag_alpha_A3      CAACGTGTCCCAGAGCAAGGACAGCGACGTGTACATCACCGACAAGACCGTGCTGGACAT 563
gag_alpha_A2      C[redacted]GTGTCCCAGAGCAAGGACAGCGACGTGTACATCACCGACAAGACCGTGCTGGACAT 564
gag_alpha_A5      CAACGTGTCCCAGAGCAAGGACAGCGACGTGTACATCACCGACAAGACCGTGCTGGACAT 600
                  * * ************************************************************

gag_alpha_WT      GAGGAGCATGGACTTCAAGAGCAACAGCGCCGTGGCCTGGAGCAACAAGAGCGACTTCGC 633
gag_alpha_A4      GAGGAGCATGGACTTCAAGAGCAACAGCGCCGTGGCCTGGAGCAACAAGAGCGACTTCGC 624
gag_alpha_A1      GAGGAGCATGGACTTCAAGAGCAACAGCGCCGTGGCCTGGAGCAACAAGAGCGACTTCGC 624
gag_alpha_A3      GAGGAGCATGGACTTCAAGAGCAACAGCGCCGTGGCCTGGAGC[redacted]AAGAGCGACTTCGC 623
gag_alpha_A2      GAGGAGCATGGACTTCAAGAGCAACAGCGCCGTGGCCTGGAGCAACAAGAGCGACTTCGC 624
gag_alpha_A5      GAGGAGCATGGACTTCAAGAGCAACAGCGCCGTGGCCTGGAGCAACAAGAGCGACTTCGC 660
                  ******************************************** * **************

gag_alpha_WT      CTGTGCCAACGCCTTCAACAACAGCATCATCCCCGAGGACACCTTTTTCCCCAGCCCTGA 693
gag_alpha_A4      CTGTGCCAACGCCTTC[redacted]AGCATCATCCCCGAGGACACCTTTTTCCCCAGCCCTGA 684
gag_alpha_A1      CTGTGCCAACGCCTTCAACAACAGCATCATCCCCGAGGACACCTTTTTCCCCAGCCCTGA 684
gag_alpha_A3      CTGTGCCAACGCCTTCAACAACAGCATCATCCCCGAGGACACCTTTTTCCCCAGCCCTGA 683
gag_alpha_A2      CTGTGCCAACGCCTTCAACAACAGCATCATCCCCGAGGACACCTTTTTCCCCAGCCCTGA 684
gag_alpha_A5      CTGTGCCAACGCCTTCAACAACAGCATCATCCCCGAGGACACCTTTTTCCCCAGCCCTGA 720
                  *************** *  * ************************************

gag_alpha_WT      GAGCAGCTGTGACGTGAAACTGGTGGAGAAGAGCTTCGAGACCGACACCAACCTGAACTT 753
gag_alpha_A4      GAGCAGCTGTGACGTGAAACTGGTGGAGAAGAGCTTCGAGACCGACACCAACCTGAACTT 744
gag_alpha_A1      GAGCAGCTGTGACGTGAAACTGGTGGAGAAGAGCTTCGAGACCGACACCAACCTGAACTT 744
gag_alpha_A3      GAGCAGCTGTGACGTGAAACTGGTGGAGAAGAGCTTCGAGACCGACACCAACCTGAACTT 743
gag_alpha_A2      GAGCAGCTGTGACGTGAAACTGGTGGAGAAGAGCTTCGAGACCGACACCAACCTGAACTT 744
gag_alpha_A5      GAGCAGCTGTGACGTGAAACTGGTGGAGAAGAGCTTCGAGACCGACACCAACCTGAACTT 780
                  ************************************************************

gag_alpha_WT      CC-AGAACCTGAGCGTGATCGG-CTTCAGAAT-CCTGCTGCTGAAGG-TGGCCGGATTCA 809
gag_alpha_A4      CC-AGAACCTGAGCGTGATCGG-CTTCAGAATTCCTGCTGCTGAAGGGTGGCCGGATTCA 802
gag_alpha_A1      CC-AGAACCTGAGCGTGATCGG-CTTCAGAAT-CCTGCTGCTGAAGG-TGGCCGGATTCA 800
gag_alpha_A3      CCCAGAACCTGAGCGTGATCGGGCTTCAGAAT-CCTGCTGCTGAAGG-TGGCCGGATTCA 801
gag_alpha_A2      CC-AGAACCTGAGCGTGATCGG-CTTCAGAAT-CCTGCTGCTG----------------- 784
gag_alpha_A5      CC-AG[redacted]CTGAGCGTGATCGG-CTTCAGAAT-CCTGCTGCTG----------------- 820
                  ** ** * ************** ********* **********

gag_alpha_WT      ACCTGCTGATGACCCTGAGACTGTGGAGCAGCCTCGAGAGATCT 853
gag_alpha_A4      AC---------------------------------------- 804
gag_alpha_A1      ACCTGCTGATGACCCCTGGA---------------------- 820
gag_alpha_A3      ACCTG------------------------------------- 806
gag_alpha_A2      ----------------------------------------
gag_alpha_A5      ----------------------------------------
```

B. Sequence alignment results for 868 TCR β chain with the two 868 TCR β chain glycosylation mutants (B1 and B2).

The point mutations are highlighted in green. (beta= β wild type, B1= Gβ1, B2= Gβ2)

CLUSTAL 2.0.12 multiple sequence alignment

```
beta            CCTAGGCCCGGGATGGGACCCGGCCTGCTGTGCTGGGCCCTGCTGTGCCTGCTGGGAGCC 60
gag_beta_B1     ------------------------------------------------------------
gag_beta_B2     ------------------------------------------------------------

beta            GGACTGGTGGACGCCGGAGTGACCCAGAGCCCCACCCACCTGATTAAGACCAGGGGCCAG 120
gag_beta_B1     ------------------------------------------------------------
gag_beta_B2     ------------------------------------------------------------

beta            CAGGTGACCCTGAGATGTAGCCCTAAGAGCGGGCACGATACCGTGTCCTGGTATCAGCAG 180
gag_beta_B1     ------------------------------------------------------------
gag_beta_B2     ------------------------GAGCGGGCCAGCGATACCGTGTCCTGGTATCAGCAG 36

beta            GCCCTGGGCCAGGGACCCCAGTTCATCTTCCAGTACTACGAGGAGGAGGAGAGGCAGAGA 240
gag_beta_B1     ------------GGACCCCAGTTCATCTTCCAGTACTACGAGGAGGAGGAGAGGCAGAGA 48
gag_beta_B2     GCCCTGGGCCAGGGACCCCAGTTCATCTTCCAGTACTACGAGGAGGAGGAGAGGCAGAGA 96
                            ************************************************

beta            GGCAACTTCCCCGACAGATTCAGCGGCCACCAGTTCCCCAATTACAGCAGCGAGCTGAAC 300
gag_beta_B1     GGCAACTTCCCCGACAGATTCAGCGGCCACCAGTTCCCC[redacted]TACAGCAGCGAGCTGAAC 108
gag_beta_B2     GGCAACTTCCCCGACAGATTCAGCGGCCACCAGTTCCCCAATTACAGCAGCGAGCTGAAC 156
                ************************************ * ********************

beta            GTGAATGCCCTGCTGCTGGGCGACAGCGCCCTGTACCTGTGTGCCAGCAGCGACACAGTG 360
gag_beta_B1     GTGAATGCCCTGCTGCTGGGCGACAGCGCCCTGTACCTGTGTGCCAGCAGCGACACAGTG 168
gag_beta_B2     GTGAATGCCCTGCTGCTGGGCGACAGCGCCCTGTACCTGTGTGCCAGCAGCGACACAGTG 216
                ************************************************************

beta            AGCTACGAGCAGTACTTCGGCCCTGGCACCAGACTGACCGTGACCGAGGACCTGAAGAAC 420
gag_beta_B1     AGCTACGAGCAGTACTTCGGCCCTGGCACCAGACTGACCGTGACCGAGGACCTGAAGAAC 228
gag_beta_B2     AGCTACGAGCAGTACTTCGGCCCTGGCACCAGACTGACCGTGACCGAGGACCTGAAGAAC 276
                ************************************************************

beta            GTGTTCCCTCCTGAGGTGGCCGTGTTCGAGCCCAGCGAGGCCGAGATCAGCCACACCCAG 480
gag_beta_B1     GTGTTCCCTCCTGAGGTGGCCGTGTTCGAGCCCAGCGAGGCCGAGATCAGCCACACCCAG 288
gag_beta_B2     GTGTTCCCTCCTGAGGTGGCCGTGTTCGAGCCCAGCGAGGCCGAGATCAGCCACACCCAG 336
                ************************************************************

beta            AAGGCCACCCTGGTGTGTCTGGCCACCGGCTTCTACCCCGACCACGTGGAGCTGTCCTGG 540
gag_beta_B1     AAGGCCACCCTGGTGTGTCTGGCCACCGGCTTCTACCCCGACCACGTGGAGCTGTCCTGG 348
gag_beta_B2     AAGGCCACCCTGGTGTGTCTGGCCACCGGCTTCTACCCCGACCACGTGGAGCTGTCCTGG 396
                ************************************************************

beta            TGGGTGAACGGCAAGGAGGTGCACAGCGGCGTGTCCACCGACCCCCAGCCCCTGAAGGAG 600
gag_beta_B1     TGGGTGAACGGCAAGGAGGTGCACAGCGGCGTGTCCACCGACCCCCAGCCCCTGAAGGAG 408
gag_beta_B2     TGGGTGAACGGCAAGGAGGTGCACAGCGGCGTGTCCACCGACCCCCAGCCCCTGAAGGAG 456
                ************************************************************

beta            CAGCCCGCCCCTGAACGATAGCAGGTACTGCCTGAGCAGCAGGCTGAGAGTGAGCGCCACC 660
gag_beta_B1     CAGCCCGCCCCTGAACGATAGCAGGTACTGCCTGAGCAGCAGGCTGAGAGTGAGCGCCACC 468
gag_beta_B2     CAG[redacted]GATAGCAGGTACTGCCTGAGCAGCAGGCTGAGAGTGAGCGCCACC 516
                *********** * ************************************************

beta            TTCTGGCAGAACCCCCGGAACCACTTCAGATGCCAGGTGCAGTTCTACGGCCTGAGCGAG 720
gag_beta_B1     TTCTGGCAGAACCCCCGGAACCACTTCAGATGCCAGGTGCAGTTCTACGGCCTGAGCGAG 528
gag_beta_B2     TTCTGGCAGAACCCCCGGAACCACTTCAGATGCCAGGTGCAGTTCTACGGCCTGAGCGAG 576
                ************************************************************

beta            AACGACGAGTGGACCCAGGATAGAGCCAAGCCCGTGACCCAGATCGTGTCCGCCGAGGCC 780
```

```
gag_beta_B1     AACGACGAGTGGACCCAGGATAGAGCCAAGCCCGTGACCCAGATCGTGTCCGCCGAGGCC 588
gag_beta_B2     AACGACGAGTGGACCCAGGATAGAGCCAAGCCCGTGACCCAGATCGTGTCCGCCGAGGCC 636
                ************************************************************

beta            TGGGGCAGAGCCGACTGTGGCTTCACCAGCGAGAGCTACCAGCAGGGCGTGCTGTCCGCC 840
gag_beta_B1     TGGGGCAGAGCCGACTGTGGCTTCACCAGCGAGAGCTACCAGCAGGGCGTGCTGTCCGCC 648
gag_beta_B2     TGGGGCAGAGCCGACTGTGGCTTCACCAGCGAGAGCTACCAGCAGGGCGTGCTGTCCGCC 696
                ************************************************************

beta            ACCATCCTGTACGAGATCCTGCTGGGCAAGGCCACACTGTACGCCGTGCTGGTGTCCGCC 900
gag_beta_B1     ACCATCCTGTACGAGATCCTGCTGGGCAAGGCCACACTGTACGCCGTGCTGGTGTCCGCC 708
gag_beta_B2     ACCATCCTGTACGAGATCCTGCTGGGCAAGGCCACACTGTACGCCGTGCTGGTGTCCGCC 756
                ************************************************************

beta            CTGGTGCTGATGGCTATGGTGAAGCGGAAGGACAGCAGGGGCTGATAGTCGA-------- 952
gag_beta_B1     CTGGTGCTGATGGCTATGGTGAAGCGGAAGGACAGCAG--GCTGATAGCGG--------- 757
gag_beta_B2     CTGGTGCTGATGGCTATGGTGAAGCGGAAGGACAGCAGGGGCTGATAGTCGATGAGCAGC 816
                ************************************  *******  *

beta            -----------
gag_beta_B1     -----------
gag_beta_B2     AGGCTGAGAGT 827
```

Appendix 5: Summary of TCR Vα and Vβ antibodies.

Name	Immunogen	Fluorescence	Brand
Anti-TCR Vα24	Human T-cell clone	FITC	Beckman Coulter
Anti-TCR Vβ1	Rat cell line RBL-2H3 transfected with the human TCR-Vβ1 gene	FITC	Beckman Coulter
Anti-TCR Vβ2	Human T-cell line	FITC	Beckman Coulter
Anti-TCR Vβ5.1	Murine T cell hybridoma transfected with human Vβ5.1 gene segment	FITC	Beckman Coulter
Anti-TCR Vβ5.2	1C1 Vβ5.2 positive cell line	FITC	Beckman Coulter
Anti-TCR Vβ7	Murine T-cell hybridoma transfected with Vβ7 gene segment	FITC	Beckman Coulter
Anti-TCR Vβ7.2	Murine T-cell hybridoma 58αβ, transfected with the human TCR-Vβ7.2 gene	PE	Immunotech (Coulter)
Anti-TCR Vβ8	MX3 positive cell line	FITC	Beckman Coulter
Anti-TCR Vβ12	Murine T-cell hybridoma transfected with human Vβ12 gene segment	FITC	Beckman Coulter
Anti-TCR Vβ13.1	Murine T-cell hybridoma transfected with human Vβ13.1 gene segment	FITC	Beckman Coulter
Anti-TCR Vβ13.2	Murine T-cell hybridoma DS23-27.4 transfected with human TCR-Vp13.2 gene	PE	Immunotech (Coulter)
Anti-TCR Vβ13.2	Murine T-cell hybridoma DS23-27.4 transfected with human TCR-Vp13.2 gene	PE	Immunotech (Coulter)
Anti-TCR Vβ13.6	Human T-cell clone	FITC	Beckman Coulter
Anti-TCR Vβ14	Murine T-cell hybridoma transfected with human Vβ14 gene segment	FITC	Beckman Coulter
Anti-TCR Vβ16	Murine T-cell hybridoma transfected with human Vβ16 gene segment	FITC	Beckman Coulter
Anti-TCR Vβ17	Murine T-cell hybridoma transfected with Vβ17 gene segment	FITC	Beckman Coulter
Anti-TCR Vβ18	Human T-cell clone	PE	Beckman Coulter
Anti-TCR Vβ20	Murine T cell hybridoma transfected with human Vβ20 gene segment	FITC	Beckman Coulter
Anti-TCR Vβ20	Murine T cell hybridoma transfected with human Vβ20 gene segment	PE	Beckman Coulter
Anti-TCR Vβ21.3	Murine T-cell hybridoma transfected with human Vβ21 gene segment	FITC	Beckman Coulter
Anti-TCR Vβ22	Murine T-cell hybridoma transfected with Vβ22 gene segment	FITC	Beckman Coulter
Anti-TCR Vβ23	Human T-cell line	PE	Beckman Coulter
Anti-TCR Vβ3	Human T-cell clone A2	FITC	Immunotech (Coulter)
Anti-TCR Vβ5.3	Human T cell clone	PE	Immunotech (Coulter)
Anti-TCR Vβ9	Murine T-cell hybridoma transfected with human Vβ9 gene segment	PE	Immunotech (Coulter)
Anti-TCR Vβ11	Human T-cell clone	FITC	Immunotech (Coulter)
Anti-TCR Vβ5(a)	Human T-cell clone	FITC	Thermo Scientific
Anti-TCR Vα2	Human T-cell clone	FITC	Thermo Scientific